

AD-A222 910

FTD-ID(RS)T-0202-88

FOREIGN TECHNOLOGY DIVISION

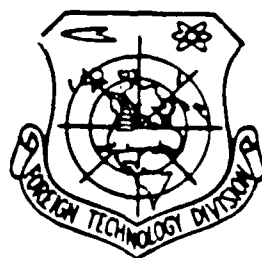
DTIC  
ELECTE  
JUN 15 1990  
S D D



GEOLOGIC INTERPRETATION OF GRAVITY ANOMALIES

by

B.A. Andreyev, I.G. Klushin.



Approved for public release;  
Distribution unlimited.



## PARTIALLY EDITED MACHINE TRANSLATION

FTD-ID(RS)T-0202-88

19 May 1988

MICROFICHE NR: FTD-88-C-000423L

GEOLOGIC INTERPRETATION OF GRAVITY ANOMALIES

By: B.A. Andreyev, I.G. Klushin

English pages: 900

Source: Geologicheskoye Istolkovaniye Gravitatsionnykh  
Anomaliy, Publishing House "Nedra", Leningrad,  
1965, pp. 1-495; 5 Un. Nr.

Country of origin: USSR

This document is a machine translation.

Input by: Mary K. Bemis, Pamela A. Bricker, Donna L. Goode,  
Michelle R. Kelley, Lynda J. Lightner, Young H. Perry,  
Barbara A. Royster, Twila J. Slaughter, Vicky L. Tipton

Merged by: Ruth A. Bennette, Eva R. Johnson

Requester: DMA Aerospace Center/DSMCC

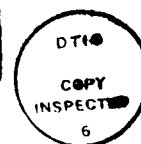
Approved for public release; Distribution unlimited.

THIS TRANSLATION IS A RENDITION OF THE ORIGINAL FOREIGN TEXT WITHOUT ANY ANALYTICAL OR EDITORIAL COMMENT. STATEMENTS OR THEORIES ADVOCATED OR IMPLIED ARE THOSE OF THE SOURCE AND DO NOT NECESSARILY REFLECT THE POSITION OR OPINION OF THE FOREIGN TECHNOLOGY DIVISION	PREPARED BY  TRANSLATION DIVISION FOREIGN TECHNOLOGY DIVISION WPAFB OHIO
---	--

PAGE 1

## GEOLOGIC INTERPRETATION OF GRAVITY ANOMALIES.

B. A. Andreev, I. G. Klushin.

[illegible]

Page 1.

The book is a textbook for students of the geologic and geophysical specialties of VUZ [Institute of Higher Education] and faculties. It can be used as a practical manual by geological engineers and geophysicist-workers.

In the book a sufficiently complete and systematic illumination of physico-geologic and mathematical aspect of complex problem of interpretation of gravity anomalies is given. The rational methods of localization of anomalies (their liberation/precipitation from the common anomalous picture) are examined in detail. Described are all methods of the interpretation of gravity anomalies which found successful application in practice; criticism is given insufficient the substantiated methods. Are presented the ideas of some new methods of the interpretation of the gravity anomalies, the prospects for further development and industrial testing, of which are favorable. The numerous practical examples to interpretation are given.



## TABLE OF CONTENTS

U.S. Board on Geographic Names Transliteration System .....	ii
Preface .....	3
Introduction .....	6
Chapter I. Bases of the Gravitational Field Theory .....	18
Chapter II. Physico-Geologic Bases of Gravitational Prospecting .....	81
Chapter III. Principles of the Geologic Interpretation of Gravity Anomalies .....	141
Chapter IV. Conversions and Calculations of Anomalies .....	209
Chapter V. Interpretation of Gravity Anomalies for Bodies of Correct Geometric Form .....	396
Chapter VI. Interpretation of Gravity Anomalies for the Bodies of Arbitrary Form .....	645
Chapter VII. Geologic Interpretation of the Results of Regional Gravitational Photographings .....	726
Chapter VIII. Searches and Prospecting of Oil- and Gas-Bearing Structures .....	782
Chapter IX. Searches and Prospecting of the Deposits of Ore and Nonmetalliferous Useful Minerals .....	821
Conclusion .....	873
References .....	876

# U. S. BOARD ON GEOGRAPHIC NAMES transliteration SYSTEM

Block	Italic	Transliteration	Block	Italic	Transliteration
А а	<i>А а</i>	A, a	Р р	<i>Р р</i>	R, r
Б б	<i>Б б</i>	B, b	С с	<i>С с</i>	S, s
В в	<i>В в</i>	V, v	Т т	<i>Т т</i>	T, t
Г г	<i>Г г</i>	G, g	У у	<i>У у</i>	U, u
Д д	<i>Д д</i>	D, d	Ф ф	<i>Ф ф</i>	F, f
Е е	<i>Е е</i>	Ye, ye; E, e*	Х х	<i>Х х</i>	Kh, kh
Ж ж	<i>Ж ж</i>	Zh, zh	Ц ц	<i>Ц ц</i>	Ts, ts
З з	<i>З з</i>	Z, z	Ч ч	<i>Ч ч</i>	Ch, ch
И и	<i>И и</i>	I, i	Ш ш	<i>Ш ш</i>	Sh, sh
Й й	<i>Й й</i>	Y, y	Щ щ	<i>Щ щ</i>	Shch, shch
К к	<i>К к</i>	K, k	Ъ ъ	<i>Ъ ъ</i>	"
Л л	<i>Л л</i>	L, l	Ы ы	<i>Ы ы</i>	Y, y
М м	<i>М м</i>	M, m	Ь ь	<i>Ь ь</i>	'
Н н	<i>Н н</i>	N, n	Э э	<i>Э э</i>	E, e
О о	<i>О о</i>	O, o	Ю ю	<i>Ю ю</i>	Yu, yu
П п	<i>П п</i>	P, p	Я я	<i>Я я</i>	Ya, ya

\*ye initially, after vowels, and after Ъ, Ь; e elsewhere.  
When written as ѣ in Russian, transliterate as yѣ or ѣ.

## RUSSIAN AND ENGLISH TRIGONOMETRIC FUNCTIONS

Russian	English	Russian	English	Russian	English
sin	sin	sh	sinh	arc sh	sinh <sup>-1</sup>
cos	cos	ch	cosh	arc ch	cosh <sup>-1</sup>
tg	tan	th	tanh	arc th	tanh <sup>-1</sup>
ctg	cot	cth	coth	arc cth	coth <sup>-1</sup>
sec	sec	sch	sech	arc sch	sech <sup>-1</sup>
cosec	csc	csch	csch	arc csch	csch <sup>-1</sup>

Russian English

rot curl  
lg log

## GRAPHICS DISCLAIMER

All figures, graphics, tables, equations, etc.  
merged into this translation were extracted  
from the best quality copy available.

Pages 2-4. No Typing.

Page 5.

#### PREFACE.

Intensive development of exploration geophysics in our country is expressed not only in industrial indices, in increase in geologic efficiency of geophysical methods, but also in constant refinement of their theory and methods of geologic interpretation of geophysical data.

In recent years the Leningrad division of publishing house "Nedra" together with general/common courses according to geophysical methods, released on series/number of methods special managements/manuals on geologic interpretation of geophysical data (seismic survey, electrical prospecting, methods of trade geophysics), in which this important question is stated very thoroughly; for example, volume of management/manual on interpretation of waves (Puzyrev, 1959) reflected data of seismic survey by method comprises more than 40 publisher's sheets. The managements/manuals indicated extensively are used both during the instruction of students and in the practical work of engineer-geophysicists.

On interpretation of results of gravitational prospecting there was up to now only monograph of O. A. Swank and Ye. N. Lyustikh, written even before patriotic war and published in 1947. This book,

naturally, does not contain a presentation of the numerous methods of interpretation, which obtained development during the subsequent years. Furthermore, the book is written not in the plan of the manual or textbook, but represents faster theoretical treatise with the detailed derivation of different formulas, used with the interpretation.

In this book authors attempted to give systematic and at contemporary level presentation of all questions, connected with geologic interpretation of results of gravitational prospecting, with examination, as far as possible, all methods of interpretation, which found practical application. During the writing of the book the many-year pedagogical and industrial experience of the authors and their comrades in work is taken into consideration.

Page 6.

Authors strove more thoroughly and correctly, than this was done in previously released managements/manuals on gravitational prospecting, to throw light very essence of problem of geologic interpretation of gravity anomalies, special feature and possibility of its resolution under different physico-geologic conditions, for different anomalous elements of gravitational field, taking into account possibility of examination of distribution of these elements not only on surface of observations, but also in space - as it is above, so also it is lower than this surface. This approach is justified now by the level of the development of the theory of

calculation of spatial distribution of potential fields reached, by the development of mine/shaft gravimetry, by the established/installed at present prospects for the development of air gravimetric surveys and by other achievements in theory and practice of gravitational prospecting.

Some questions in book are presented in more detail than this is possible to do within the framework of training course. These questions, however, are very important for the workers in their practical work; they can be used also in VUZ for the construction of facultative additional courses, for the course and thesis planning, etc.

Chapter IV and 5 49 of Chapter VI are written by I. G. Klushin; remaining sections are written by B. A. Andreyev.

Authors are very grateful to reviewers A. S. Semenov, V. S. Mironov, R. M. Demenitskaya, and also to scientific editor N. N. Mikhaylov for numerous valuable councils, which promoted improvement in the quality of the book. The authors express large gratitude for help in preparation of the manuscript of Ye. M. Andreyeva and L. Ye. Shustova.

All observations according to book authors request to direct into Leningrad division of publishing house "Nedra" (Leningrad, Lomonosov Street, 22).

Page 7.

#### INTRODUCTION.

Gravimetry, i.e., the science about the measurement of gravitational force, was conceived in the 17th century on the basis of remarkable experiments and theoretical studies of Galileo, Newton, Huygens and other scientists. Initially it was developed as a branch of geodesy - the science about the study of the form of the Earth. The first gravimetric measurements, together with data of astronomy and geodesy, made it possible to establish that the Earth with the sufficiently high approximation/approach can be likened to spheroid, i.e., to the ellipsoid of revolution with a small compression, flattened along the rotational axis. further the same data made it possible to determine the value of the compression of terrestrial spheroid.

In the middle of the 18th century French mathematician Clairauts created bases of the calculation of a normal gravitational field, i.e., gravitational field on the surface of a terrestrial spheroid, which consists of uniform in density concentric layers. This made it possible to introduce into the examination the concept about the gravity anomaly, understood as a difference in the observed value of gravitational force, normalized by the introduction of the corresponding corrections to the surface of geoid, and its theoretical normal value. The first interpretation of gravity anomalies as the

values, which characterize the mutual arrangement of geoid and spheroid, gave English mathematician Stokes. In 1849 they proved the theorem, which expresses the distance between the geoid and the spheroid at the particular point in the function of the distribution of the anomaly of gravitational force on the surface of geoid around this point. Thereby there was established the beginning of geodetic gravimetry - to interpretation of gravitational field from the point of view of geodesy and to the utilization of given gravitational photographings during the solution of different geodetic problems. This direction of the utilization of gravimetry was subsequently very developed, especially recently in connection with the works of Soviet (F. N. Krasovskiy, M. S. Molodenskiy, I. D. Zhongolovich et al.) and foreign (F. Vening-Meinesz, W. Heiskanen, etc.) scientists.

Page 8.

Emergent in middle of the 19th century the hypothesis of isostasy had as its direct goal solution of a purely geodetic problem, namely, the calculation of deviations of vertical line under effect of the masses which generate relief. During the solution of this problem it seemed that besides the masses indicated during the calculations it is necessary to allow also the effect/action of the deep masses, in a certain measure the compensating action of relief. Other words, it seemed that some geodetic problems can be solved only on the basis of one or the other hypotheses about the deep structure of the earth's crust and its effect on the gravitational field, i.e., the problem of the geodetic interpretation of gravity anomalies in this case was

connected with their geologic interpretation.

At the end of the 19th century during investigation of the Moscow anomaly of gravitational force Russian geodesist and mathematician F. A. Sludskiy (1841-1897) made an attempt, by combining gravimetric and astrogeodetic data, to solve the question about the depth of bedding of the masses which cause this anomaly. At the very beginning of the 20th century the Hungarian physicist R. Eotvos (Eotvos, 1848-1919), the inventor of the torsion balance, or gravitational variometer, performs with this instrument, and also from pendulums and magnetic instruments field work in the Hungarian plain and makes an attempt at the geologic interpretation of the results of these works.

Immediately after the great October Socialist Revolution (since 1919) on the initiative of V. I. Lenin, the systematic study by geophysical methods of region of the Kursk Magnetic Anomaly (KMA) in connection with assumption about presence in this region of large deposits of iron ores begins. Gravitational method in the form of the variometric and pendulum photographings is used here since 1921 (P. M. Nikifor, A. A. Mikhaylov). In 1923 drilling opened ferruginous quartzite of the KMA, while subsequently there was explained the structure of iron-ore thickness, which gave basis for the geologic interpretation of geophysical data of this region. Being based on these data, O. Yu. Schmidt in 1926 indicated the method of the geologic interpretation of gravity anomalies, which obtained subsequently development and wide practical application with the works



of P. M. Nikiforov et al. in the KMA, Krivoy Rog and other iron-ore regions.

Thus, the first significant step/pitch in geologic interpretation of gravity anomalies was done in our country in connection with definite prospecting and exploratory geologic mission, which has high national-economic value. In 1960 there entered into the system the first stage of the Lebedinskiy mine of the KMA - one of the objects of the seven-year plan/layout of the development of the national economy of the USSR, and several years ago was begun the industrial mastery/adoption of Kremenchug iron-ore region in the Ukraine, moreover in prospecting of the ore regions indicated to gravitational method belonged the most important role. One should note that the procedure of the interpretation of the results of detailed variometric gravitation prospecting works on the sheet iron-ore deposits was developed and applied in the USSR, while on the analogous iron-ore deposits of the foreign capitalist countries this effective methodology, apparently, until this time it did not find use.

Page 9.

Another geologic problem, in solution of which gravitational method with great success was applied both in USSR and abroad even in the 1920's, consisted in searches for salt dome oil bearing structures. The solution of this problem for this method proved to be sufficiently simple, since in the majority of regions the salt dome structures were noted by characteristic and intensive gravity

anomalies. Thus, for example, in the territory of the Caspian basin, where the salt domes have large dimensions and are almost deprived of cap rocks (i.e. covers from the dense gypsum-anhydrite rocks), the local minimum of gravitational force corresponds to each dome, and to each such minimum - a salt dome. With the shallow bedding of salt/hydrochloric dome on the outline of gravity anomaly directly are defined the form and the sizes/dimensions of dome in the plan/layout, i.e., this problem as the problem of the detection of salt/hydrochloric dome, it is elementarily simple, not requiring any special methods of the processing and interpretation of data of gravitational prospecting.

Hundreds of salt dome structures in the USSR and a number of foreign countries at the present time have been opened up by this method. The problem of the investigation of the configuration of steep/abrupt bort of salt domes proved to be much more difficult for gravitational prospecting. For this the application of sometimes sufficiently complex receptions of processing/treatment and interpretation of data was required, moreover satisfactory results were obtained far from always and only under the condition of complex application and analysis of the results of two methods - gravitational prospecting and seismic survey.

Beginning of the development of petroleum gravitational prospecting in the USSR was established with group of geophysicists of geologic committee (now VSEGEI - Leningrad), which worked in the

period of 1924-1928 under Prof. B. V. Numerov's guidance. This group consisted of E. E. Fotiadi, N. N. Mikhaylov, N. N. Samsonov, N. N. Cherepanov et al.

Subsequently application of gravitational prospecting during searches for oil and gas-bearing structures underwent considerable development. In a number of regions (Caucasus, Central Asia, Sakhalin, etc.) its application for this purpose was sufficient to successful and effective. In other regions, in particular on the Russian and Siberian platforms, the application of a method met the difficulties of the two kinds: 1) by the insufficient study of the density of the rocks in the section/cut of structures; 2) by the insufficient accuracy of used while conducting of work equipment (gravimeters). Only most recently have there been noted specific ways outlined for elimination or decrease of these difficulties (see Chapter VIII).

Page 10.

During the solution of the prospecting problems indicated is necessary to be limited greater partly only to qualitative interpretation the character of gravitational field, i.e., by the approximate indication of the location of the predicted structures, which subsequently is checked and is made more precise by seismic survey.

Beginning of application of this method together with other geophysical methods with resolution of so-called problem of large

Donbass (N. N. Samsonov since 1929) was an important stage in the development of gravitational prospecting. For the resolution of this problem, advanced by Acad./Academician noted for geologist. By P. I. Stepanov, it proved to be necessary to investigate the deep geologic structure of large/coarse region - Donets geosynclinal region, to explain the position of its boundary with the Russian platform, to study hypsometry of the surface of the productive carboniferous thickness (average/mean Carboniferous period), closed on the periphery of Donbass with the thickness of younger depositions.

Solution of these difficult problems required complex application and analysis of all given geophysical methods on the basis of a detailed study of physical properties of rocks and laws governing change in these properties in territory of Donbass and adjacent regions. The deepened qualitative and quantitative interpretation of the results of gravitational prospecting was required, thanks to which this method proved to be one of the bases with the resolution of the problem of large Donbass.

Works in Donbass were used as beginning of systematic utilization of gravitational prospecting in complex with other geophysical methods during regional geologic studies of different regions of our country, which obtained special development in postwar period. These regional investigations have a very high value and a development in connection with the searches for oil and gas, since the arrangement of local oil and gas-bearing structures in the majority of the cases is completely

distinctly controlled by the arrangement of regional structures. The example of the Donbass and other carboniferous tanks showed that the same occurs also for the carbon deposits. Subsequently the development of works in the region of metallogenic zoning showed that also in this business the very high, frequently decisive importance has a study of the history of development and deep structure of ore regions. In connection with this the problem of the interpretation of regional gravity anomalies under different geologic conditions in the platform and geosynclinal regions arose. Key/wrench to the resolution of this difficult problem proved to be in combined analysis of the gravitational and seismic methods, utilized in structural geology, in the detailed analysis of the special features of a historic-geologic development of the regions being investigated and arrangement in their boundaries of structural-metallogenic zones.

Page 11.

First investigations in this direction were carried out in prewar years by A. D. Arkhangel'skiy, I. M. Gubkin, V. V. Fedynskiy.

In postwar period Yu. N. Godin, E. E. Fotiadi, S. I. Subbotin, B. A. Andreyev and a number of other researchers continued these investigations. In this direction much work still is in prospect, but it is already now clear that the analysis of regional gravity anomalies presents first-rate importance during the study of the deep structure of the earth's crust and laws governing the arrangement/position in it of useful minerals.

Above we spoke about works on gravitational prospecting on iron-ore deposits; subsequently this method was successfully applied with searches and prospecting of chromites (A. A. Yun'kov, B. A. Andreev), pyritic ores (M. I. Anchugov, A. Ya. Jaros, A. I. Katskov), lead-zinc ores, etc. For this was required the study of the density of the rocks and ores and further development of theory and technology of the geologic interpretation of gravity anomalies, for example, during prospecting and calculating the reserves of ore deposits, with the analysis of the results of gravitation prospecting works in mine workings (Ye. A. Mudetsova et al.), etc. Special problem presented the complex interpretation of the results of several geophysical methods, including gravitational prospecting, the used during the searches ore deposits.

At present gravitational prospecting successfully is used during solution of wide circle of geologic problems under most different physicogeographical conditions. In the majority of the cases photographing with the gravimeters presents its technical basis, variometers or gradiometers sometimes are used. The efficiency of the application of gravitational prospecting during the solution of these problems is conditioned on the combination of the following basic conditions:

- 1) by the presence of high-accuracy and highly productive equipment;
- 2) by the correct selection of objects and regions;

- 3) by the application of a correct procedure of field works.
- 4) by the correct geologic interpretation of the results of gravitational prospecting.

Problem of geologic interpretation of gravity anomalies is not only very important, but also very difficult. The difficulty of problem is connected with its following special features:

1. Problem has two sides - physico-geologic (account of real physicogeographical and geologic conditions, density of rocks and laws governing its change in the space, etc.) and mathematical (calculations according to the gravity anomalies, connected with the solution of the interesting geologic problem).

Page 12.

An account of physico-geologic conditions makes it possible to correctly pose the problem and select the correct initial data during the subsequent mathematical analysis of gravity anomalies, which has the geologic of bodies as a goal to establish the location and character of those conditioning these anomalies. A one-sided approach to the resolution of problem - both purely geologic taking into account of some visual associations, primitive comparisons of gravitational field with the geologic map/chart, etc. and speculative-mathematical without the interrelationship initial data and obtained results with the specific geologic conditions of the region being investigated - is completely insufficient and usually does not give correct results.

2. Results of gravitational prospecting can be, as a rule, interpreted more reliably upon consideration of other given geophysical methods, utilized in the complex during solution of one or the other geologic problem. During the solution of different structural problems the data of seismic survey usually have special importance besides the data of gravitational prospecting, during the searches for ore deposits - data of magnetic prospecting, electrical prospecting, metallometric photographing.

3. Method of gravitational prospecting possesses very large depth of penetration. Besides the local anomalies, which are of direct interest during the solution of the majority of geologic problems, on the gravitational maps/charts are developed, sometimes very vividly, the regional anomalies, caused by the deep structure of the earth's crust. It is necessary to use different methods of the liberation/precipitation of local anomalies or localization of anomalies. Of interest is sometimes inverse problem - liberation/precipitation of regional anomalies in the presence of the associated local anomalies.

4. Theory of interpretation of gravity anomalies is not simple. For its mastery/adoption are necessary sufficiently solid mathematical preparation, knowledge not only of the bases of analysis, but also some of its special sections - integration of partial differential equations (equation of Laplace and Poisson), principles of the theory of analytic functions, some sections of mathematical statistics and information theory, etc.

5. For correct geologic interpretation of gravity anomalies is



required detailed study of density of rocks and ores and laws governing its change within limits of region being investigated.

Sufficiently numerous errors and incorrect interpretations with its resolution can serve as an index of difficulty of problem of interpretation of gravity anomalies. Some erroneous views and opinions, voiced in the geophysical literature and sometimes utilized in the practice of the interpretation of the results of gravitation prospecting works, are examined in this book.

Page 13.

Practice of contemporary utilization of gravitational prospecting puts forth new requirements for more reliable geologic interpretation of given gravimetric photographings. Much more frequently than earlier, the analysis of gravity anomalies is finished to the quantitative estimations (depth of the bedding of crystalline basement, the thickness of the Earth's crust, mass and the sizes/dimensions of different geologic objects). Possibilities to this gives an improvement in the quality of gravimetric equipment, an improvement in the procedure of field works, and, finally, the substantial development of the theory of gravitational prospecting. We attempted to reflect this last moment in our book.

Page 14.

Chapter I.

## BASES OF THE GRAVITATIONAL FIELD THEORY.

### § 1. Basic concepts and definitions. Gravitational force.

Basic concepts of gravitational-field theory are already known to reader. Nevertheless, taking up the systematic study of the theory of the interpretation of gravity anomalies, we must examine some concepts, which lie at the basis of this theory. This must be done because these concepts allow/assume, as let us see below, somewhat different interpretations and approaches from the positions of geodetic and prospecting gravimetry, moreover this fact remains insufficient to those made clear in the existing textbooks on the course "Gravitational prospecting" and sometimes it leads to the misunderstandings and even errors with the practical work.

Gravitational force is called force, which acts on any body, which is located on earth's surface or near it, that conditions trajectory of free fall in bodies and representing sum of two forces - attraction of Earth and centrifugal force, which appears as a result of rotation of Earth around axis. centrifugal force is small in the value in comparison with force of gravity (it does not exceed 1/300 fractions/portions of the latter). From the Latin name the gravity - gravitas - proceeds and the name of gravitational method.

Gravitational field is characterized by vector of intensity/strength of gravitational force, which presents the gravitational force, which acts on the mass equal to one. The strength of the gravitational force is designated by letter  $g$ . For brevity it is usually called gravitational force.

Page 15.

The gravitational force which acts on certain moving/driving mass, according to second Newton's law is equal to the product of this mass for acceleration. In order to numerically obtain the strength of field, we divide gravitational force into the mass. Consequently,

$$|g| = \frac{L}{T^2},$$

i.e. the strength of gravitational field has the same dimensionality, as acceleration, and it can be expressed in the same physical units. Such a unit in the CGS system is the gal - acceleration in  $1 \text{ cm/s}^2$ , which obtained its name in honor of Galileo (G. Galileo, 1564-1642), who for the first time investigated the law of the incidence/drop in the bodies under the effect/action of gravitational force. In the gravimetry usually is examined the thousandth of a gal ( $1 \cdot 10^{-3}$  CGS), named milligal ( $m_j$ ).

FOOTNOTE<sup>1</sup>. Since 1961 in the USSR is predicated the international system of the units (SI) of GOST 9867-61, in which the unit of mass  $1 \text{ kg} = 10^3 \text{ g}$  and the unit of length  $1 \text{ m} = 10^3 \text{ cm}$ . ENDFOOTNOTE.

Gravitational field is potential, i.e., there is always certain

function of space coordinates  $W$ , named potential, which possesses the property that its partial derivative in any direction  $s$  represents component of vector  $g$ , in this direction:

$$\frac{\partial W}{\partial s} = g_s = g \cos(g, s), \quad (1, 1)$$

$s$ , in particular, can represent any of right angled coordinates  $x$ ,  $y$ ,  $z$ .

Surface, at each point of which is satisfied condition

$$W(x, y, z) = c, \quad (1, 2)$$

where  $c$  - certain constant, carries name of equipotential surface, or equipotential surface.

Let us assume in formula (1, 1)  $\cos(g, s) = 0$ , then we will have

$$\frac{\partial W}{\partial s} = 0, \quad W = \text{const.}$$

Geometrically this indicates the fact that, moving perpendicular to vector  $g$ , we prove to be in plane, tangent to equipotential surface. Consequently, the gravitational force acts along the normal to equipotential surface also in the direction of a positive increase in the potential, i.e., it is directed along the internal normal to the level surface, i.e.

$$g = -\frac{\partial W}{\partial n}, \quad (1, 3)$$

where  $n$  - direction of internal normal to the surface of level.

This direction is frequently called the direction of the plumb

bob, since precisely on it, obviously, bob of any geodetic or astronomical instrument is directed.

Page 16.

If we have two contiguous equipotential surfaces

$$\begin{aligned} W(x, y, z) &= c, \\ W(x, y, z) &= c + \Delta W, \end{aligned}$$

arranged/located on certain small distance of  $\Delta n$ , counted along the normal to one of surfaces indicated, then from formula (I, 3)

$$\Delta n = \frac{\Delta W}{g}. \quad (I, 4)$$

Obviously, the undisturbed equilibrium surface of seas and oceans is one of the equipotential surfaces. This surface is located horizontal and perpendicular to gravitational force, which acts on the vertical line. The wave perturbations of this surface, caused by the effect/action of the wind, by lunisolar attraction, etc., are not connected with the effect of the gravitational force. The undisturbed surface of seas and oceans can be visualized continued also within the limits of continents. Its this continuation is "sea level", from which is conducted the calculation of heights on the rigid surface. The level surface, which coincides with the undisturbed surface of seas and oceans and with sea level within the limits of continents, is called geoid. This surface in geodesy is accepted for the characteristic of the actual form of the Earth.

A simple approximate analytical expression for gravitational

force can be obtained, if we assume that Earth presents body of spherical form, which consists of concentric layers uniform in density, which rotates around polar axis with constant angular velocity.

The force of gravity  $g$  on surface of Earth we define as vector sum

$$g = F_1 + C,$$

where  $F_1$  - intensity/strength of attracting force of Earth;

$C$  - centrifugal force, which acts on earth's surface to material point with a mass equal to one.

Law of universal gravitation, brought out by Isaac Newton from experimental data in 1687, can be formulated as follows. The force of interaction of two masses  $m$  and  $m_1$  at a distance of  $r$  is expressed by the relationship/ratio

$$F = f \frac{mm_1}{r^2}, \quad (I, 5)$$

where  $f$  - the gravitational constant, which presents the force (expressed in the dynes) of the attraction of two mass points with a mass of 1 g each, located at a distance 1 cm.

Page 17.

Numerical value of gravitational constant in system CGS

$$f = 66,7 \cdot 10^{-9} = \frac{2}{3} \cdot 10^{-7}$$

and dimensionality

$$[f] = \text{cm}^3 \cdot \text{g}^{-1} \cdot \text{sek}^{-2}.$$

In given formulation the law is valid for mass points, and also for bodies of spherical form of uniform density, or which consist of concentric layers of uniform density, moreover in the latter case of  $r$  in formula (I, 5) represent distance between centers of spherical bodies, and  $m$  and  $m_1$  - their total masses.

Let us designate total mass of Earth through  $M$  and its radius through  $R$ . The strength of the gravitational field, i.e., the attracting force, which acts on mass point  $m_1=1$ , on the spherical surface of the Earth is equal from the formula (I, 5)

$$F_1 = \frac{1M}{R^2}, \quad (\text{I.6})$$

this force acting along the radius of the Earth and directing toward its center. Taking into account the relative smallness of centrifugal force, it is possible in the first approximation, to consider that the same direction has gravitational force on the spherical surface of the Earth.

Centrifugal force is directed perpendicularly to rotational axis of Earth. Its total value, as is known from the mechanics (Fig. 1),

$$C = \omega^2 \rho = \omega^2 R \cos \varphi,$$

while its projection on the sense of the vector  $F_1$

$$C_{F_1} = \omega^2 R \cos^2 \varphi.$$

Hence we obtain the approximate value of the force of gravity

$$g \approx \frac{kM}{R^2} + \omega^2 R \cos^2 \varphi. \quad (I, 7)$$

In theory of figure of Earth (see, for example, Mikhaylov, 1939) is given considerably more accurate conclusion of expression of gravitational force on the basis of assumption that Earth presents spheroid i.e. ellipsoid of revolution (Fig. 2) with small compression

$$\alpha = \frac{a - c}{a},$$

where  $a$  - semimajor (equatorial) axis of meridional ellipse;

$c$  - semiminor (polar) axis of meridional ellipse.

In this case, as before it is assumed that Earth consists of concentric ellipsoidal layers uniform in density.

Page 18.

Value of gravitational force on spheroid under conditions indicated, named normal value of gravitational force, is expressed by following formula

$$\gamma_0 = g_0 (1 + \beta_1 \sin^2 \varphi - \beta_2 \sin^2 2\varphi). \quad (I, 8)$$

where  $\gamma_0$  - normal value of gravitational force on latitude  $\varphi$ ;

$g_0$  - value of gravitational force at equator;

$\beta_1, \beta_2$  - constant coefficients, whose value depends on compression  $\alpha$ .

Since coefficient  $\beta_2$  - low value in expression (I, 8) is



sometimes considered  $\beta_1=0$ ,  $\beta_1=\beta$  and they accept it in the form of following formula of Clairauts:

$$\gamma_\varphi = \gamma_\alpha (1 + \beta \sin^2 \varphi). \quad (1.8a)$$

In the USSR formula (1, 8) is used with coefficients, determined by F. Helmert in 1901-1909 for normal spheroid with compression  $\alpha=1/298.2$ . In the west since 1930 the formula of Kassinis for the spheroid with the compression  $\alpha=1/297.0$  is used. In the USSR since 1946 in the carrying out of geodetic works is accepted the spheroid of F. N. Krasovskiy with the compression  $\alpha=1/298.3$ , for which the coefficients  $\beta_1$  and  $\beta_2$  have values, a little different from those, which are accepted in the formula of Kassinis (see Table 1).

Basic difference in formulas indicated consists in value  $\gamma_\alpha$ . In Helmert's formula this value on  $0.019 \text{ g/l}$ , i.e., on  $19 \text{ mg/l}$ , is less than in other formulas of Kassinis and Krasovskiy.

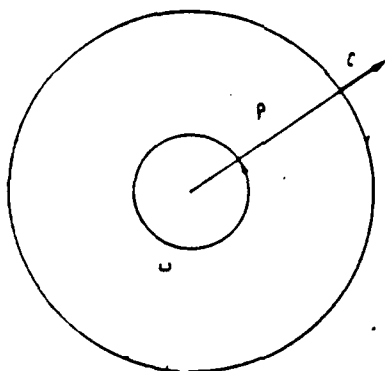


Fig. 1.

Fig. 1. Determination of centrifugal force.

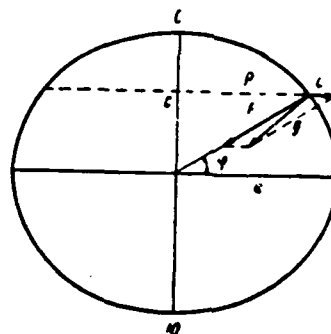


Fig. 2.

Fig. 2. Determination of gravitational force.  $a$  - semimajor axis of meridional ellipse;  $c$  - semiminor axis of meridional ellipse.

Page 19.

## § 2. The second derivatives of gravitational potential.

As has already been stated in § 1, the gravitational force is the first derivative of gravitational potential taken on the internal normal to level surface. In the gravimetry they are measured and are examined also the second derivatives of the gravitational potential in the direction of the coordinate axes. Let us examine the physical and geometric sense of these values.

In gravimetry, in an examination of second derivatives of potential following arrangement of system of right angled coordinates is always accepted: origin of coordinates is located on equipotential

surface, z axis coincides with internal normal to this surface, in other words, with direction of bob, x and y axes are arbitrarily located in tangential plane to equipotential surface (Fig. 3).

With arrangement of coordinate axes indicated, obviously, we will have

$$g = \frac{\partial W}{\partial z} \quad (1, 9)$$

Relative values g are determined by gravimeters.

With the help of gravitational variometer (or gradiometer) it is possible to determine following values, named force gradients of gravity:

$$\left. \begin{aligned} W_{xz} &= \frac{\partial^2 W}{\partial x \partial z} \\ W_{yz} &= \frac{\partial^2 W}{\partial y \partial z} \end{aligned} \right\} \quad (1, 10)$$

Table 1. Values of coefficients in formula (1, 3) for the normal value of the force of gravity (according to different authors).

(1) Автор	(2) Год	$\epsilon_a, \frac{\Delta a}{a}$	$\beta_1$	$\beta_2$
Гельмерт . . . . .	1901—1909	978.030	0.005302	0.000007
Кассинис . . . . .	1930	978.049	0.0052884	0.0000059
Красовский . . . . .	1946	978.049	0.00530029	0.0000059

Key: (1). Author. (2). Year. (2a). main. (3). Helmert. (4). Kassinis. (5). Krasovskiy.

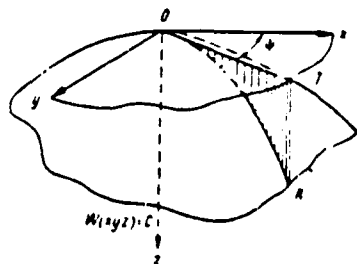


Fig. 3. Determination of second derivatives of gravitational potential.

Page 20.

Furthermore, by the same instrument there are measured still following values, conditionally named curvatures:

$$\left. \begin{aligned} W_{\Delta} &= \frac{\partial^2 W}{\partial y^2} - \frac{\partial^2 W}{\partial x^2} \\ 2W_{xy} &= 2 \frac{\partial^2 W}{\partial x \partial y} \end{aligned} \right\} \quad (1.11)$$

In order to explain physical and geometric sense of these values, let us note following. At the arbitrary point of space with coordinates  $(x, y, z)$  the vector which represents the total amount of gravitational force, is directed, generally speaking, not parallel to

any of the coordinate axes, i.e., has along these axes nonzero components  $X$ ,  $Y$ ,  $Z$ , determined by the following expressions, which ensue from the formula (I, 1):

$$\left. \begin{aligned} X &= g \cos(g, x) = \frac{\partial W}{\partial x}, \\ Y &= g \cos(g, y) = \frac{\partial W}{\partial y}, \\ Z &= g \cos(g, z) = \frac{\partial W}{\partial z}. \end{aligned} \right\} \quad (I, 12)$$

Considering values  $X$ ,  $Y$ ,  $Z$  for continuous functions of coordinates, it is possible by differentiation of left and right sides (I, 12) to obtain values of nine derivatives

$$\frac{\partial X}{\partial x}, \frac{\partial X}{\partial y}, \frac{\partial X}{\partial z}, \frac{\partial Y}{\partial x}, \frac{\partial Y}{\partial y}, \frac{\partial Y}{\partial z}, \frac{\partial Z}{\partial x}, \frac{\partial Z}{\partial y}, \frac{\partial Z}{\partial z}.$$

These derivatives characterize changeability force component of gravity along appropriate coordinate axes, i.e., it is numerical, in system CGS, value of change in that or another component on 1 cm of distance along appropriate coordinate axis. The positive sign of the corresponding derivative shows that the component is increased in the value in the direction of this coordinate axis; minus sign shows that in this direction the value of the component is reduced. As can be seen from (I, 12), the derivatives indicated are expressed as the second derivatives of gravitational potential, for example, the latter from the equations (I, 12) give

$$\begin{aligned} \frac{\partial Z}{\partial x} &= \frac{\partial^2 W}{\partial x \partial z}, \\ \frac{\partial Z}{\partial y} &= \frac{\partial^2 W}{\partial y \partial z}, \\ \frac{\partial Z}{\partial z} &= \frac{\partial^2 W}{\partial z^2}. \end{aligned}$$

Such relationships/ratios are valid and make sense for any point of space, in particular, and for origin of coordinates. Taking into account that at this point in accordance with the accepted by us above arrangement of the coordinate axes  $Z=g$ , we will have finally

$$\left. \begin{aligned} \frac{\partial g}{\partial x} &= \frac{\partial^2 W}{\partial x \partial z} = W_{xz}, \\ \frac{\partial g}{\partial y} &= \frac{\partial^2 W}{\partial y \partial z} = W_{yz}, \\ \frac{\partial g}{\partial z} &= \frac{\partial^2 W}{\partial z^2} = W_{zz}. \end{aligned} \right\} \quad (1.13)$$

Page 21.

First two of formulas (1, 13) show physical sense of force gradients of gravity. They characterize the changeability of gravitational force on the level surface. This is evident from the fact that the coordination plane  $xoy$  is tangent to the level surface.

Gradients  $W_{xz}$  and  $W_{yz}$  can be considered as components along  $x$  and  $y$  axes of vector  $G$  - total horizontal gradient of force of gravity (Fig. 4), value and direction of which can be expressed by following relationships/ratios:

$$\left. \begin{aligned} G \cos \alpha &= W_{xz}, \\ G \sin \alpha &= W_{yz}, \\ |G| &= |\sqrt{W_{xz}^2 + W_{yz}^2}|, \\ \operatorname{tg} \alpha &= \frac{W_{yz}}{W_{xz}}. \end{aligned} \right\} \quad (1.14)$$

Physical meaning of vector  $G$  consists in the fact that its direction shows direction of greatest increase of gravitational force

on level surface, and the value is the value of this increase per unit of length, i.e., - in system CGS - on 1 cm.

In geodetic gravimetry it is proven (Mikhaylov, 1939, pg. 366-368) that in meaning of the vector  $G$ , an osculating plane of line of force of gravitational field is placed, i.e., that line, as tangent to which direction of bob serves, in other words, sense of the vector of force of gravity  $g$ . Gravitational field is generally nonhomogeneous, i.e., gravitational force varies at the different points of space in the value and the direction, and line of force of gravitational field is curvilinear. Let  $\rho$  - radius of curvature of line of force, then its total curvature  $1/\rho$  be expressed by the following relationship/ratio:

$$\frac{1}{\rho} = \frac{G}{g}, \quad (I, 15)$$

i.e., the ratio of the value of the total horizontal gradient of gravitational force to the amount of gravitational force. Relation (I, 15) is used in geodesy for reducing of astronomical latitudes and longitudes/lengths, determined on the earth's surface, to sea level.

Latter from formulas (I, 13) represents analytical expression of vertical force gradient of gravity, i.e., characterizes a change in gravitational force on a vertical line. This very important for the gravimetry value instrument/tool thus far is not measured; it can be calculated through other derivatives of the potential (see below).

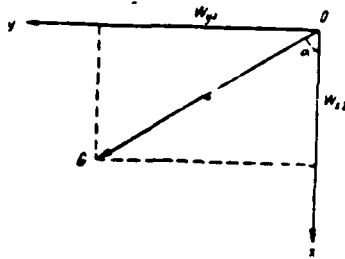


Fig. 4. Determination of total horizontal gradient of gravitational force.

Page 22.

We turn to an examination of curvatures determined by formulas (I, 11). Being congruent/equating formulas (I, 11) and (I, 12), we see that the curvature can be expressed through the gradients of the horizontal components of the force of gravity X and Y

$$\left. \begin{aligned} W_{\Delta} &= \frac{\partial Y}{\partial y} - \frac{\partial X}{\partial z}, \\ 2W_{xy} &= 2 \frac{\partial Y}{\partial z} = 2 \frac{\partial X}{\partial y}. \end{aligned} \right\} \quad (I.16)$$

Let us note that derivatives, which stand in right sides of formulas (I, 16), generally speaking, are not equal to zero in the beginning of coordinates, although at this point, in accordance with arrangement accepted by us of coordinate axes, condition  $X=Y=0$  occurs.

$W_{\Delta}$  and  $2W_{xy}$  can be expressed also through curvatures of main normal sections of level surface, i.e., those normal sections, which have at the particular point maximum and minimum curvature (by precisely this fact it is explained designation of indicated values).



In gravimetry following relations are proven:

$$R = g \left( \frac{1}{\rho_1} - \frac{1}{\rho_2} \right) = \frac{W_{\Delta}}{\cos 2\psi_0}, \quad (I, 17)$$

$$\operatorname{tg} 2\psi_0 = - \frac{2W_{xy}}{W_{\Delta}}, \quad (I, 18)$$

where  $g$  gravitational force;

$1/\rho_1$  and  $1/\rho_2$  - respectively maximum and minimum curvature of normal sections in the beginning of coordinates, i.e., at the particular point of level surface;

$\psi_0$  - azimuth of plane of normal section with maximum curvature; it is possible to demonstrate that section with minimum curvature in this case will be located in plane with azimuth  $\psi_0 + \pi/2$ .

Value  $R$  in formula (I, 17), undertaken in specific scale, determines length of certain segment, which in gravimetry is conditionally named vector of difference in curvatures (or simply by vector of curvature). The conditionality of this designation is clear from that fact that the equation (I, 18) gives for the angle, which determines the direction of this segment, two values  $\psi_0$  and  $\psi_0 + \pi$ . The "Vector" of curvature is graphically represented as follows: is noted the direction, which consists of angle  $\psi_0$  with the positive direction of  $x$  axis, and in this direction is deposited on the scale accepted value  $R$  in such a way, that this segment would be placed up to the equal distances on both sides from observation point (Fig. 5).

Page 23.

From formulas (I, 17) and (I, 18) ensue also following relationships/ratios:

$$\left. \begin{aligned} R \cos 2\psi_0 &= W_{\Delta}, \\ R \sin 2\psi_0 &= -2W_{xy}, \\ R &= \sqrt{(W_{\Delta})^2 + (2W_{xy})^2}. \end{aligned} \right\} \quad (I, 19)$$

As we see, there is formal-geo similarity of relationships/ratios (I, 17) (I, 18), (I, 19) and (I, 14) for force gradients of gravity.

In practice of gravitational prospecting curvature is investigated very rarely. The latter from the instruments used (gradiometer GRB) is virtually adapted only for measuring the force gradients of gravity. As we see further (see § 3), there is a possibility in certain cases to obtain the values of curvature by calculation in terms of the values of the force gradients of gravity.

Horizontal gradient of gravitational force presents derivative of  $g$  on horizontal coordinate, i.e., numerically gives change  $g$  per unit of length. Taking into account the physical dimensionality of the force of gravity (see § 1), we find the dimensionality of the horizontal gradient

$$|G| = \frac{1}{r^2}.$$

Corresponding unit CGS will be equal to  $1 \cdot \text{sek}^{-2}$ . One, equal to  $1 \cdot 10^{-8} \text{ sek}^{-2}$ , is called Eotvos (E) from the name of the inventor of

variational method of Hungarian physicist Roland Eotvos (R. Fotvos, 1848-1919). In these units all second derivatives of potential usually are expressed.

If the force of gravity  $g$  on the surface of Earth is changed with distance according to the linear law, then 1 E corresponds to a change in  $g$  at 0.1 mg/ per 1 km.

§ 3. The bond between the derivatives of potential. Concept about the analytical continuation.

There is formal bond between derivatives of gravitational potential. for the point, arranged/located out of the perturbing masses, Laplace's theorem

$$\Delta W = \frac{\partial^2 W}{\partial x^2} + \frac{\partial^2 W}{\partial y^2} + \frac{\partial^2 W}{\partial z^2} = 0 \quad (1, 20)$$

occurs.

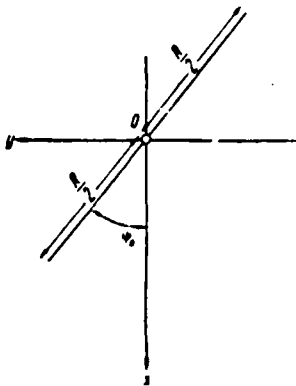


Fig. 5. To determination of "vector" of curvature.

Page 24.

For the point located within perturbing masses, is valid Poisson's theorem

$$\Delta W = \frac{\partial^2 W}{\partial x^2} + \frac{\partial^2 W}{\partial y^2} + \frac{\partial^2 W}{\partial z^2} = -4f\sigma\pi, \quad (I, 21)$$

where  $\sigma$  - density at attracted/tightened point.

Formula (I, 20) represents, obviously, special case of formula (I, 21) with  $\sigma=0$ .

Functions, which satisfy equations (I, 20) and (I, 21), are called harmonics. Such functions are gravitational and magnetic potentials, and also any derivatives of them on any space coordinates. In the case of the magnetic potential  $f\sigma$  in the formula (I, 21) are substituted by the intensity of magnetization  $J$ .

We see now that second derivatives of potential are not independent variables and can be expressed some through others. For example, at the point, arranged/located out of the perturbing masses, the derivative, which represents the vertical force gradient of gravity, on the basis of formulas (I, 13) and (I, 20) can be expressed in the following way:

$$\frac{\partial g}{\partial z} = W_{zz} = -(W_{xx} + W_{yy}). \quad (I, 22)$$

Thus, vertical gradient of force of gravity, not directly measured by instruments, can be calculated, if are known horizontal

gradients  $W_x$  and  $W_y$ .

The bond of force of gravity and gradient of force of gravity presents a great practical importance. This bond can be formulated as follows. Let on the level surface segment AB (in the general case curvilinear) be arranged/located. Let us designate as before through  $n$  the direction of internal normal to the level surface, and through  $l$  - direction of tangent to segment AB (in the general case variable). Then, obviously,

$$\int_{AB} \frac{\partial^2 W}{\partial n \partial l} dl = \left( \frac{\partial W}{\partial n} \right)_B - \left( \frac{\partial W}{\partial n} \right)_A \quad (I, 23)$$

or for the usually considered/examined special case, when level surface in this territory can be taken for the horizontal coordination plane xoy,

$$\int_{AB} \frac{\partial^2 W}{\partial z \partial l} dl = (g)_{x_2 y_2} - (g)_{x_1 y_1} = \Delta g, \quad (I, 24)$$

where  $x, y$ , and  $x_1, y_1$  - coordinates of the end and initial points of segment AB.

Page 25.

In the case of closed outline end and initial points of curve AB coincide, and

$$\oint \frac{\partial^2 W}{\partial z \partial l} dl = 0. \quad (I, 24a)$$

Element of integral (I, 24) in small rectilinear segment  $\Delta l$  easily is calculated, if we assume that in this segment gradient

$\partial^2 W / \partial z \partial l$  varies with distance according to linear law. Let us introduce the following designations:

$$p_1 = G \cos(G, \Delta l)$$

for the initial point of segment  $\Delta l$ ,

$$p_2 = G \cos(G, \Delta l)$$

for the end point of segment  $\Delta l$ ,  $p_1$  and  $p_2$  in this case presenting the projection of the total horizontal gradient  $G$  on the direction of segment  $\Delta l$  (Fig. 6). In this case an increase in gravitational force in the segment  $\Delta l$  is easily calculated from the trapezoid rule

$$\Delta g = \frac{p_1 + p_2}{2} \Delta l. \quad (1.25)$$

Let us examine following example. Let  $p_1 = 20E$ ,  $p_2 = 30E$ ,  $\Delta l = 100$  m, then from the formula (1, 25) obtain

$$\Delta g = \frac{20 \cdot 10^{-9} + 30 \cdot 10^{-9}}{2} \cdot 10^4 \text{ CGS} = 25 \cdot 10^{-5} \text{ CGS} = 0.25 \text{ mgl}.$$

Integration of horizontal gradient gives possibility to compute relative increases in gravitational force between observation points. Natural to raise the question: will agree in this sense the data obtained by the utilization of gravimetric and variometric photographings. Experiment of the comparison of this type of data shows that they, as a rule, are located in the good agreement, if works are carried out in the plains region with small relative oscillations/vibrations of heights. Under similar conditions can be completely realized the worthy complex of gravimetric and variometric (gradiometric) photographings, for example, according to the diagram, proposed by author (1959). In the regions with the large relative

oscillations/vibrations of heights the conformity of data of gravimetric and variometric photographings is disturbed<sup>1</sup>.

FOOTNOTE<sup>1</sup>. Possibly, the approximate reduction of the anomalous values of gradients to one level is true, which reduces the disagreement of the data of gravimetric and variometric photographings (Andreev, 1948, pg. 65). ENDFOOTNOTE.

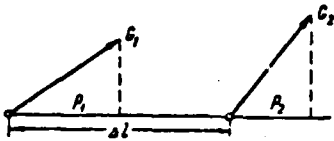


Fig. 6. Integration of horizontal gradient of gravitational force.

Page 26.

In the majority of the cases of this type of the nonconformity of proper to be caused by the following two reasons:

1) by the significant deviation of the physical earth's surface from single equipotential surface, i.e., that condition, which was assumed during the derivation of formulas (I, 23) and (I, 24);

2) the nonfulfillment of the condition of the linearity of a change in the gradient in the interval of integration (for example, due to the thin network/grid of variometric observations), i.e., the condition, which was being assumed during the derivation of formula (I, 25).

There is set of other formulas, which show bond of some of derived gravitational potential with other derivatives. In principle any derivative of potential can be calculated through any other derivative, if the distribution of this another derivative on the level surface is known. For simplification of this type of calculations it is possible in many instances without the large error to assume that the level surface coincides with the infinite plane. Below we give (in the polar coordinates) the formulas, which express the gravitational potential  $W$  and its second derivatives through the



distribution of gravitational force on the infinite level plane S.

$$\left. \begin{aligned} W(0) &= \frac{1}{2\pi} \int_S \frac{g dS}{r}, \\ W_{xx}(0) &= \frac{3}{2\pi} \int_S \frac{g \cos \alpha dS}{r^3}, \\ W_{yy}(0) &= \frac{3}{2\pi} \int_S \frac{g \sin \alpha dS}{r^3}, \\ W_{\Delta}(0) &= -\frac{3}{2\pi} \int_S \frac{g \cos 2\alpha dS}{r^3}, \\ 2W_{xy}(0) &= \frac{3}{\pi} \int_S \frac{g \sin 2\alpha dS}{r^3}. \end{aligned} \right\} \quad (I, 26)$$

Here  $(r, \alpha)$  - polar coordinates of flowing point of plane,  $dS$  - element of plane. The values of functions in the left sides relate at the beginning of coordinates. In these values are obtained in the form of integrals. If we take into account that  $W_{xx}$  and  $W_{yy}$  - derivatives of  $g$  (see §1), then we come to the conclusion that in this case the calculation of derivatives can be reduced to the integration.

Page 27.

Formulas (I, 26) can be brought out by different methods. One of the methods of the conclusion/derivation of the first of them is indicated by B. V. Numerov (1930). The following formulas are obtained from the the per by the differentiation of its left and right sides on the appropriate coordinates.

In a similar manner, i.e., by integration for level surface or any other surface, situated out of perturbing masses, it is possible for potential and any derivatives of it to solve first boundary-value

problem of theory of potential (or Dirichlet problem). It can be formulated as follows: knowing the distribution of harmonic function on the surface (consisting its sources), to find the value of this function in the space out of this surface, or as they speak, to analytically continue the function through the surface indicated. The solution of boundary-value problem is called also the analytical continuation of harmonic function.

The problem in question is especially simply solved in that case important for prospecting geophysics when initial surface presents infinite horizontal plane, which separates lower half-space, which consists sources of potential, and is upper, free from perturbing masses. Let us take the plane indicated for the coordination plane xoy, and x axis it is directed vertically downward. Then the value of the arbitrary harmonic function U at point A (0, 0, h), arranged/located on height h above the plane in the upper half-space, will be (formula of Poisson)

$$U(0,0, -h) = \frac{h}{2\pi} \int_S \frac{U dS}{r^3}, \quad (1,27)$$

where U - under the integral designates the value of harmonic function at the flowing point M on plane S;

r - radius-vector of this point, i.e.,  $r = \sqrt{x^2 + y^2 + h^2}$ ;

dS - element of plane S (Fig. 7).

Integration is produced along entire infinite plane S.

By direct integration it is possible to ascertain that in the particular case, when  $U=1$  on entire plane  $S$ , then

$$\frac{h}{2\pi} \int_S \frac{dS}{r^3} = 1.$$

Hence follows that formula (I, 27) can be converted to following form:

$$U(0, 0, -h) - U(0, 0, 0) = \frac{h}{2\pi} \int_S \frac{U - U(0, 0, 0)}{r^3} dS. \quad (I, 28)$$

Page 28.

In formulas (I, 27) and (I, 28)  $U$  can represent any harmonic function, i.e., not only gravitational or magnetic potential itself, but also any derivative of them on Cartesian coordinates.

Analytical continuation is possible not only into upper, but also into lower half-space, which consists sources of potential. The appropriate calculations in any case it is possible to produce in the space between plane  $z=0$  and plane  $z=h_0$ , where  $h_0$  are lower than the depth of the singular point of field nearest to plane  $z=0$ , i.e., the points, at which suffer discontinuous change any of the derivatives of potential.

Let us assume that  $U$  represents distribution of harmonic function in plane  $z=h$  of lower half-space. According to the property of the

uniqueness of potential (Idel'son, 1936, pg. 35) this distribution is singular. Then it is analogous with formula (I, 27) it is possible to write the relation

$$U(x, y, 0) = \frac{h}{2\pi} \int_S \frac{U dS}{r^2}, \quad (I, 29)$$

where  $(x, y, 0)$  - the flowing point of plane  $z=0$ , on which  $U$  is assigned, and  $U$  under the integral represents the distribution of harmonic function on plane  $z=h$ .

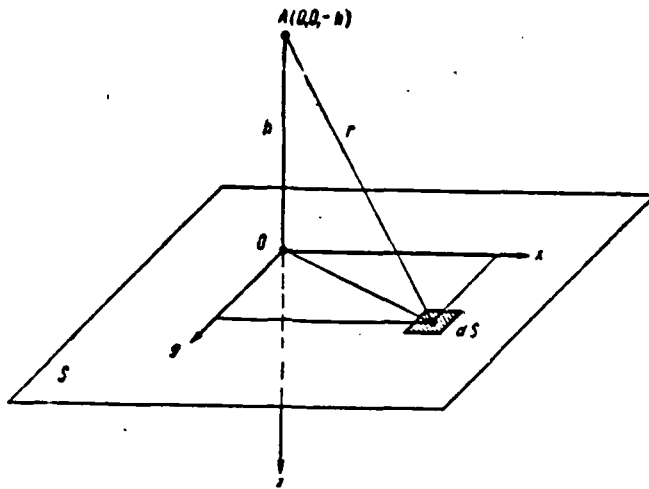


Fig. 7. To Poisson's formula.

Page 29.

Formula (I, 29) can be considered as integral equation, which is used for determining  $U$  on plane  $z=h$ . Solution of equation (I, 29) - one of the methods of the analytical continuation  $U$  into the lower half-space. In Chapter IV we will be introduced to the different methods of analytical continuation.

#### § 4. Corrections (reductions) and the anomaly of gravitational force.

We turn to question, which in method of gravitational prospecting is developed, until now, insufficiently, in spite of its fundamental importance. This is indicated by the contradictory interpretations of separate positions relating to this question available in the literature and some practical conclusions/derivations of them, which

are doubtful, and sometimes also by simply incorrect.

The main reason for this consists, in our opinion, in the fact that concepts of gravity anomaly, reduction and so forth are transferred into method of gravitational prospecting from geodetic gravimetry mechanically, without taking into account specific special features of these two regions - related on physical bases, but different in subjects of investigation.

Object of geodetic gravimetry - figure of Earth as planets, been surface of geoid (see § 1) or introduced by M. S. Molodenskiy (1947) surface of quasi-geoid, determined of some geodetic measurements, in oceans of that coinciding accurately with geoid, but on continents in limits of high-mountain regions of that stepping back from geoid is not more than on 2-3 m. The position of geoid, or quasi-geoid, is determined with respect to the figure of reference, i.e., to the surface of terrestrial spheroid (also called reference ellipsoid). According to Stokes's theorem (Stokes, 1849) the distance between the geoid and the spheroid can be calculated, if is known distribution on the surface of the geoid of the anomaly of gravitational force, determined by the following relationship/ratio:

$$\Delta g = g_0 - \gamma_0. \quad (I, 30)$$

where  $\Delta g$  - anomaly of gravitational force;

$g_0$  - corrected from observation point on the physical surface of the Earth to the appropriate point on the surface of geoid value of gravitational force;

$\gamma_0$  - normal value of gravitational force for the surface of the spheroid (see § 1).

Page 30.

Reduction in the gravitational force to surface of geoid is achieved by introduction to observed values of force of gravity of some corrections, or reductions (from Latin reductio - lowering). So that the obtained similarly of the anomaly of force of gravity would satisfy the requirements of the theorem of Stokes and would characterize the deviation of geoid from the spheroid, the corrections, utilized during the calculation of the corrected value of  $g_0$ , must satisfy the following conditions:

- 1) the complete removal/distance of masses out of the geoid;
- 2) retention of the invariable total mass of the Earth;
- 3) retention invariable surface geoid;
- 4) the smooth changeability of anomaly; the possibility of interpolating its values between the points during the calculations.

Object of prospecting gravimetry - internal structure of Earth and earth's crust, characterized by mass distribution of different density. The anomalous gravitational field, which characterizes this mass distribution, we should know not for the level of geoid, but for the real earth's surface, on which are produced gravimetric measurements. Therefore the expression of anomaly  $\Delta g$  in this case must take the form

$$\Delta g = g - \gamma_0$$

(I, 30a)

where  $g$  - observed value of gravitational force;

$\gamma$  - normal value of gravitational force, led from the surface of spheroid to the level of observation point.

Let us examine methods now basic from those used in practice of calculating anomalies of gravitational force.

Anomalies of Faye. These anomalies are occasionally referred to as also complete anomalies or anomalies in free air. Calculation  $g$  in the formula (I, 30) in this case is conducted according to the formula

$$g_0 = g + \Delta_1 g, \quad (I, 31)$$

where  $g$  - observed value of gravitational force;

$\Delta_1 g$  - correction for the height, computed from the approximation formula, which presents a difference in the attraction for the surface of the spherical mass  $M$  of radius  $R$  and at point at height  $H$  above this surface,

$$\begin{aligned} \Delta_1 g = g_0 - g_H &= \frac{1M}{R^2} - \frac{1M}{(R+H)^2} = \frac{1M}{R^2} \left[ 1 - \left( 1 + \frac{H}{R} \right)^{-2} \right] \approx \\ &\approx \frac{2g_0}{R} H \text{ (поскольку } H \ll R). \end{aligned}$$

Key: (1). since.

If we take  $R=6371200$  m for Earth  $g_0=979.77$ , we obtain then

$$\Delta_1 g = 0.3086 H, \quad (I, 32)$$

where  $\Delta_1 g$  is expressed in milligals,  $H$  - in meters.

During calculation of anomalies of Faye is considered only spot



height of observations and attraction of interlayer between surface of Earth and level of geoid is not allowed, i.e., reduction is produced "in free air" so, as if observation point was found in virtually weightless atmosphere at height H above surface of geoid.

Page 31.

This approach from the point of view of geodetic gravimetry can be justified by the consideration, which during the calculation of the anomalies of Faye of masses of interlayer, whose effect/action is not reduced and, consequently, enters into the value of anomaly  $\Delta g$ , seemingly it is condensed on the surface of geoid in the form of infinitely thin spherical layer and thereby is achieved the satisfaction of first two of the most important conditions indicated above of Stokes's theorem - the removal/distance of masses out of the geoid and the retention/maintaining of the total mass of the Earth.

Utilization of anomalies of Faye, completely permitted for purposes of geodetic gravimetry, proves to be at the same time impossible for purposes of our object/subject - prospecting gravimetry. This is evident from the following reasoning. Substituting formula (I, 31) into (I, 30), we will obtain

$$\Delta g = g - (\gamma_0 - \Delta_1 g).$$

So that this expression would correspond (I, 30a),  $\gamma$  must be equal to  $\gamma - \Delta_1 g$ , i.e., to normal value  $g$ , transferred from spheroid to earth's surface only with correction "in free air". In actuality

this not so, since values  $g$  at the levels indicated depend sloping between the levels (Fig. 8) indicated. As we will see further, this disregarded effect can be considered proportional to spot height of observations and, consequently, the anomaly of Faye deep structure will independent of vary from one point to the next with change in altitude  $H$  (or the depth of the bottom of sea during maritime photographing). The anomaly of Faye includes, it is understood, the effect of the deep structure of the earth's crust, different in the different places. For this reason in the examination of the intensity of the anomalies of Faye for different regions the bond of the latter with the height distinctly is not revealed (Fig. 9), but it is revealed very vividly in the examination of the anomalies of Faye on the profile or on the map/chart of any region (Fig. 10).

Bouguer's anomalies. During the calculation of anomalies Bouguer  $g_0$  is calculated from the formula

$$g_0 = g + \Delta_1 g + \Delta_2 g, \quad (1.33)$$

where  $g$  and  $\Delta_1 g$  - the same values, as in the formula (1, 31);

$\Delta_2 g$  - correction for the attraction of interlayer, i.e., the layer, which slopes between the level of the station of observation and the level of geoid.

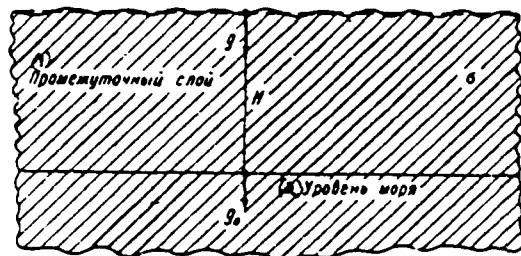


Fig. 8. Determination of reductions of Faye and Bouguer.

Key: (1). Interlayer. (2). Sea level.

Page 32.

Correction  $\Delta g$  is calculated from formula

$$\Delta g = -2\pi\sigma H = -0,0418\sigma H, \quad (I, 34)$$

where  $\sigma$  - density of rocks, which generate interlayer;

$H$  - spot height of observation, m.

During calculation according to formula (I, 34) are assumed that interlayer represents plane-parallel horizontal plate of constant density, i.e., surface of Earth is considered not spherical or ellipsoidal, but plane. This assumption simplifies problem and at the same time it does not introduce any substantial errors into the results of calculations.

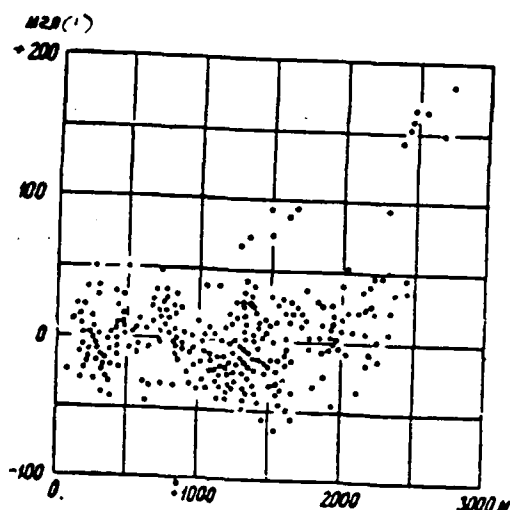


Fig. 9. Correlation diagram, which expresses dependence of value of anomalies of Faye ( $\Delta\epsilon_F$ ) from height (H) of observation point.

According to G. Woollard (1959).

Key: (1). mg|.

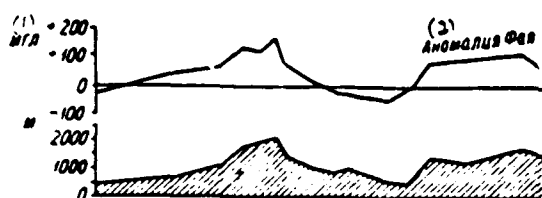


Fig. 10. Example of gravitational profile in anomalies of Faye ( $\Delta\epsilon_F$ ) in high-mountain region.

Key: (1). mg|. (2). Anomaly of Faye.

Page 33.

With maritime gravimetric survey correction of Bouguer makes other sense. By it is considered not the excess of the masses above the geoid, but a deficiency in the density under the geoid in the

layer, whose thickness is equal to the depth of the bottom of sea under the station of observations, but the density is equal to a difference in the density of sea water ( $1.03 \text{ g/cm}^3$ ) and average density of lithosphere ( $2.67 \text{ g/cm}^3$ ).

If earth's surface in region of station of observations has significant inequalities, its relief has noticeable effect on gravitational force. In this case during calculation  $g$ , is introduced additionally the correction for the effect of relief  $\Delta g$  (Nettleton, 1940; Lukavchenko, 1951). That obtained in this case according to the formula (I, 30) the refined value of the anomaly of Bouguer Ye. N. Lyustikh (1948) proposed to call topographic anomaly.

Value of  $g$ , calculated according to formula (I, 33), represents amount of gravitational force, led to surface of geoid with removal/distance of gravitational effect/action of masses, arranged/located between geoid and physical surface of Earth. During the calculation of Bouguer's anomalies the total mass of the earth's crust is reduced on the continents and is increased in the oceans, which, obviously, disturbs the actual position of geoid and cannot be considered acceptable from the point of view of geodetic gravimetry. Therefore Bouguer's anomalies are not usually used by geodesists.

At the same time, Bouguer's anomalies, as we will see below, to best degree correspond to conditions of prospecting gravimetry and now everywhere they are used in all cases, when gravitational method is

used for studying geologic structure of earth's crust <sup>1</sup>.

FOOTNOTE <sup>1</sup>. On the erroneous conclusions of some researchers on this to a question in the past see in § 15 of Chapter III. ENDFOOTNOTE.

We already noted that in practice of prospecting gravimetry should be examined anomalies, in reference to physical surface of Earth, on which is made measurement of gravitational force, and to consider these anomalies as those caused by mass distribution of earth's crust, arranged/located both above, and it is lower than level of the geoid. As an example let us examine the case of the anomaly, caused by a certain geologic body of positive excess density, arranged/located above the geoid - case completely real, for example, for the high-mountain regions. It is completely clear that on the surface of the Earth this body must create the positive anomaly of the force of gravity (this and it will be the real interesting us case), while on the surface of geoid it must create the negative anomaly of gravitational force, since the perturbing mass in this case was located above the geoid and vertical component of its attraction must be directed not downward, but upward.

Reduction of Bouguer considers not only height, but also attraction of interlayer, i.e., effect of both factors acting during transfer of normal value  $g$  from spheroid to earth's surface. The substitution of (I, 33) in (I, 30) gives

$$\Delta g = g_0 - \gamma_0 = g + \Delta_1 g + \Delta_2 g - \gamma_0 = g - (\gamma_0 - \Delta_1 g - \Delta_2 g). \quad (I, 35)$$

Page 34.

Expression, which stands in parentheses, can be considered as normal value of gravitational force normalized from the level of geoid to level of station of observations. Bouguer's anomaly can be, consequently, considered as a difference in the measured value of the force of gravity and his theoretical value, led to the physical surface of the Earth - in complete agreement for problems and purposes of prospecting gravimetry.

Until now, debatable is following important question: with what value of density  $\sigma$  should be calculated correction  $\Delta g$  during determination of Bouguer's anomaly? Below the question is stated in the way as authors of the book understand it. This question has theoretical and practical side. The fundamental aspect of business, as if, is not caused the doubts: value  $\sigma$  about the formula (I, 34), apparently, must correspond to the actual density of interlayer. However, this conclusion/derivation can be considered correct only when the density of interlayer is everywhere constant, i.e.,  $\sigma = \text{const.}$  In actuality this condition, obviously, does not occur, and  $\sigma$  represents the value, which, generally speaking, varies from one region to the next and even from one observation point to another, moreover the introduction of this variable value  $\sigma$  to calculations is inadmissible. Actually, as we already indicated, anomaly  $\Delta g$  was caused by mass distribution, arranged/located both below, and higher

than surface of geoid, moreover the presence of anomalies is the result of density variations in the horizontal direction, which occur both below, and it is higher than the level of geoid and connected with different geologic factors: by the presence of the contacts of the rocks, the lithofacies change in the special features of species/rocks and in the degree of their metamorphism, etc.

Recommended by some authors calculation of correction  $\Delta g$  at variable/alternating density  $\sigma$  presents attempt to introduce a "correction for geologic structure of interlayer", i.e., completely illegal operation, which distorts real distribution of gravity anomalies. It is most expedient to calculate correction  $\Delta g$  with the constant value  $\sigma$ , equal to the average density and the rocks of lithosphere, i.e., with the value of  $\sigma = 2.67 \text{ g/cm}^3$ . It is clear that the average/mean value of the density of layer will be most suitable for reducing the normal values of gravitational force from sea level to the earth's surface.

Let us examine now purely practical side of the same question. The rocks which generate the interlayer, as a rule, are nonhomogeneous on the density and the speech it can in actuality go only about a certain average density of interlayer. Reliable determination of this average/mean value of density when of complex section/cut and significant thickness of interlayer is a problem, as a rule, that is unattainable. Therefore, from this point of view it is necessary to put to use the value single for the large/coarse regions of the



density of interlayer. Thus, during the composition of the compound gravitational map/chart of Western Europe and North Africa the author of this map/chart of De-Bruin (1955) all values of Bouguer's anomalies computed with the constant value of the density of interlayer  $\sigma=2.67$  g/cm<sup>3</sup>, being guided by the following consideration: for the mountain regions this value it corresponds sufficiently well to the average density of species/rocks, that generate mountain masses, and for the plains regions of correction  $\Delta g$  they are small and their value in the absolute value very little they vary with the different values of the density of interlayer.

Page 35.

Thus, and theoretical and practical consideration speaks, that Bouguer's anomaly one should calculate with constant value of density of interlayer and as this constant value it is expedient to take average density of lithosphere  $\sigma=2.67$  g/cm<sup>3</sup>.

Proposition about account of variable/alternating density of interlayer during photographings of large/coarse scale deserves attention in version, proposed by Hungarian geophysicist Vajk (R. Vajk, 1956). In this version variable/alternating density is allowed in the horizontal layer, situated between the level of the quite upper and quite lower of the points of relief within the limits of the section being investigated (latter it is assumed to be small according to the sizes/dimensions, i.e., speech it goes about large-scale photographings). For the remaining part of interlayer the density is

received as constant ( $\sigma=2.67$  g/cm<sup>3</sup>).

If there is necessity for calculation of topographic correction, then this operation, of course, it is expedient to produce, accepting density of species/rocks, that generate relief, that corresponds to its actual value.

Data of gravimetric surveys by USSR it is accepted to treat at constant density of interlayer  $\sigma=2.3$  g/cm<sup>3</sup>. This value sufficiently closely corresponds to the average density of the sedimentary rocks, which slope for the majority of the stations between sea level and physical surface of the Earth.

Isostatic anomalies. isostatic anomalies are obtained in such a case when with computation of  $\Delta g$  instead of the correction for the attraction of interlayer correction for the isostasy is introduced.

Isostatic anomalies until this time are extensively used by foreign geophysicists. As the examples it is possible to indicate the monograph of F. Vening-Meinesz (1940), a number of articles in the collection "Questions of contemporary foreign tectonics" (1960), the map/chart of the isostatic anomalies of Europe scale 1:5000000 (De-Bruin, 1955). In a number of cases the calculation of isostatic anomalies practiced also in the USSR.

Below we are limited to short presentation of principle of

calculation of isostatic corrections and anomalies [more detailed presentation of this question can be found in L. V. Sorokin (1953)].

The word isostasy originates from two Greek layers ισωστας —  
(isostasy), which indicates equal pressure or equal state. At the basis of the hypothesis of isostasy lies/rests the assumption about a certain regular conformity of the relief of surface and internal structure of the upper layer of the earth/ground, as a result of which the lower surface of this layer, situated in parallel to the surface of geoid, presents isostatic surface, i.e., the surface, at each point of which the pressure of layer has constant value, independent of the relief of its external surface. In this case it is assumed that the pressure of any element or vertical block of isostatic layer on its lower surface is defined according to the law of hydrostatics as the value, equal to the weight of the corresponding block.

Page 36.

If layer is decomposed into the vertical blocks with the identical cross section, then the weight of each such block, and, consequently, the exerted by it pressure on the isostatic surface must be equal to constant value. As a certain basis/base for the assumption indicated serves the fact that the substance of deep layers of the Earth under the effect of the constant or slowly varying in the time forces behaves similarly to liquid, i.e., it obeys the law of hydrostatics (Magnitskiy, 1957; Andreyev, 1960).

If the earth's surface everywhere coincided with the geoid, and Earth up to surface would consist of concentric layers uniform in density, then it is obvious that principle of isostasy would be implemented automatically. In actuality the earth's surface has significant inequalities, and the earth's crust is nonhomogeneous in the density; therefore for the real Earth isostatic structure strongly differs from horizontal laminar structure.

Fig. 11 shows isostatic structure of earth's crust different authors. By Pratt-Hayford (Fig. 11a) isostatic compensation, i.e., the balancing of the equidimensional according to the cross sizes/dimensions of blocks, is caused by the fact that these blocks have different density - smaller in the blocks of large vertical sizes/dimensions and larger in blocks of small vertical sizes/dimensions. In this case conditionally it is assumed that density indicated variation occurs evenly in the part of the block, arranged/located between the surface of geoid and the surface of isostatic compensation. On the hypothesis of Airy-Heiskanen (Fig. 11b) the compensation is achieved due to the fact that the blocks of the earth's crust have different vertical sizes/dimensions and to different degree are submerged into the heavier subcrustal layer in accordance with the law of hydrostatics. The surface of isostatic compensation is passed within the subcrustal layer through the basis/base of the highest block of the earth's crust. According to the hypothesis of Vening-Meinesz (Fig. 11c), isostatic compensation is realized without the separation of the earth's crust into the blocks

due to the elastic bend of bark.

In spite of apparent contradiction of isostatic hypotheses indicated above, these hypotheses in actuality are not so/such different and contradictory. For example, entire difference in the hypotheses of Pratt-Hayford and Erie-Heiskanen consists only under the assumption about how the average density of substance in the layer between the surface of geoid and the surface of isostatic compensation in connection with the presence of the inequalities of topographic relief varies. According to the Pratt-Hayford hypothesis the density varies under the geoid evenly throughout entire volume of each of the equilibrium blocks of this layer, while according to the Airy-Heiskanen hypothesis changes in the average density of layer occur due to a change in the relationship/ratio of the thickness of bark and subcrustal layer, that form part of equilibrium block.

Thus, between different isostatic hypotheses in the closest examination by no means are there revealed great fundamental differences. The corrections for the isostasy, calculated in accordance with one or the other hypothesis, also prove to be sufficiently close in the value. Below we take apart the sense of calculating operations during the determination of correction for the isostasy in accordance with Pratt-Hayford hypothesis, until now, that of widely utilized by geophysicists and geodesists abroad.

Correction for isostasy in accordance with Pratt-Hayford

hypothesis represents value of gravitational effect/action, caused by such displacement/movement of masses, as a result of which earth's crust is converted into plane-parallel plate with lower surface, which coincides with surface of isostatic compensation, that has with realization in actuality of those conditions, which are assumed hypothesis of isostasy, constant density, i.e., not generating gravity anomalies.

Page 37.

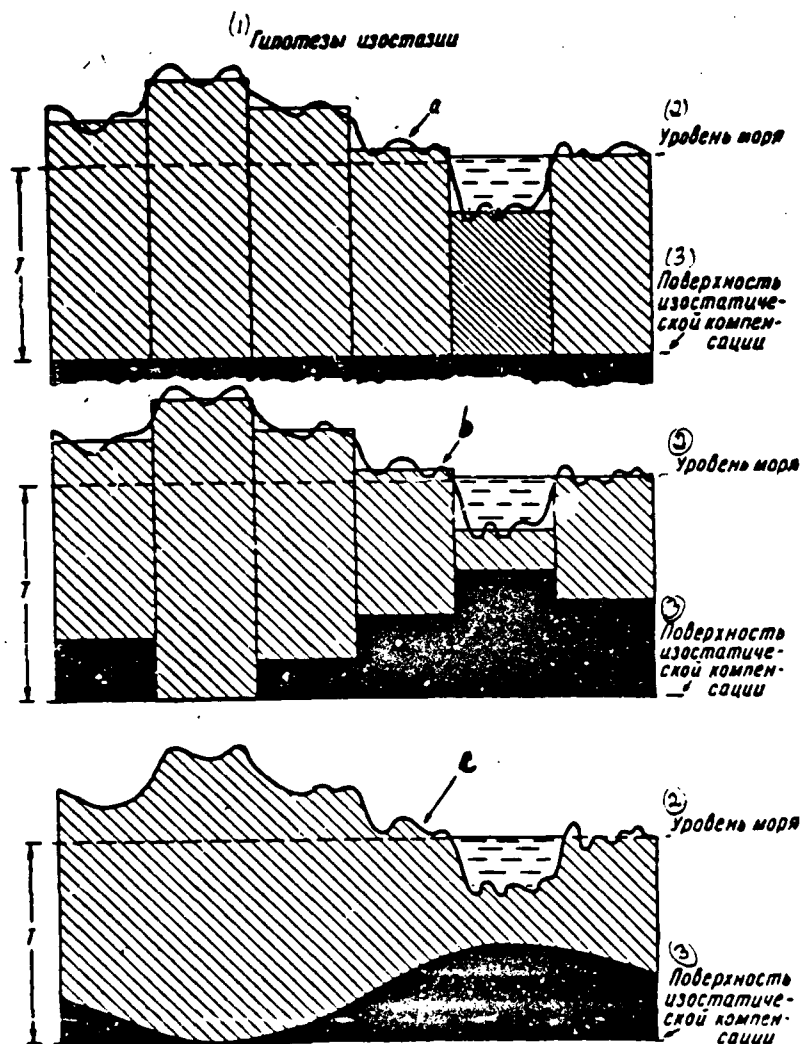


Fig. 11. Isostatic structure of earth's crust according to Pratt-Hayford (a), Airy-Heiskanen (b), Vening-Meinesz (c).

Key: (1). Hypotheses of isostasy. (2). Sea level. (3). Surface of isostatic compensation.

Page 38.

If isostatic equilibrium at any place is broken, then as a result of

the described displacements/movements of masses in this place plate density will be either more than normal (overload - positive isostatic anomaly), or it is less than the normal (underloading - negative isostatic anomaly). Isostatic correction for mass distribution in the block, projecting above the geoid, for any point A (Fig. 12), is obtained as follows:

1) from observed at point A of the value of the force of gravity  $g$  it is subtracted vertical component  $F_1$ , attraction, caused by the effect/action on the unitary mass at point A of mass of the I block, which protrudes above the geoid;

2) to the obtained difference  $g - F_1$ , we add now vertical component of  $F_2$ , of the attraction, caused by the effect/action on the unitary mass at point A of the same mass I, evenly distributed in the volume of block II, arranged/located between geoid and surface of isostatic compensation.

This calculation is done for all blocks of earth's crust, moreover effect/action of distant blocks is determined taking into account curvature of terrestrial spheriod. Complete isostatic correction will be

$$\Delta_1 g = -\sum F_1 + \sum F_2, \quad (1, 36)$$

where the summation is produced along the entire surface of the Earth.

Value corrected to sea level of gravitational force in this case is found from relation

$$g_0 = g + \Delta_1 g + \Delta_2 g. \quad (1, 37)$$



We already noted that value and sign of isostatic anomalies can characterize degree of isostatic steadiness of earth's crust and character of deviations from mass distribution, which corresponds to equilibrium (overload or underloading). Isostatic compensation can be developed only on the regional scale, i.e., real judgment about the degree of isostatic compensation can be obtained only for the significant on the area territories, examining for them average/mean values isostatic of anomalies.

Calculation of isostatic anomalies is connected with large volume of calculating work. This difficulty can be considerably decreased, using for the appropriate calculations electronic computers. Nevertheless, for many regions the calculation of isostatic anomalies remains difficult or even impossible due to the absence of the proper information, for example, about hypsometry of external and under-ice relief in the regions, covered with glaciers, about hypsometry of submerged relief in the oceans, etc.

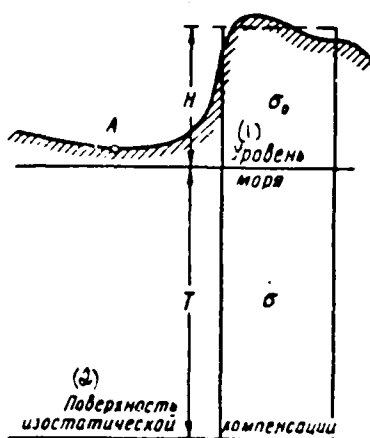


Fig. 12. Explanation of derivation of isostatic correction of gravitational force.

Key: (1). Sea level. (2). Surface of isostatic compensation.

Page 39.

For this reason the researchers of isostasy instead of the isostatic anomalies frequently examine the anomalies of Faye, accepting (without the special proofs), that the average/mean values of the anomalies of Faye and isostatic must coincide or be close ones for the regions large in the area.

By author is recently shown (Andreyev, 1961), that difference in anomalies of Faye  $\Delta g_f$  and isostatic  $\Delta g_i$  has close correlation with height of relief for continental stations and with depth of bottom of sea for maritime, revealing very significant changeability with change in altitude and depths (Fig. 13). In certain cases (the high altitudes of relief, the large depths of the bottom of sea) a

difference in average/mean values  $\Delta g_r - \Delta g_l$ , can be very great (hundreds of milligals). Any reliable judgment about average/mean value  $\Delta g_l$  for any of region in terms of average/mean value  $\Delta g_r$ , possibly only in such a case, when for this region the height of relief or the depths of the bottom of sea are changed not very considerably and are known the average/mean values of heights (or depths), in terms of which in this case with the help of the graph, shown in Fig. 13, it is possible to switch over to average/mean values  $\Delta g_l$ .

Correction of Bruns. With the examination of a question about the corrections and the anomalies we, until now, assumed that the theoretical value of gravitational force and its observed value, reduced to the level of geoid, relate to one and the same surface. In actuality theoretical values relate to the surface of terrestrial spheroid, with which the surface of geoid coincides only on the average, differing to it in some places sufficiently considerably - approximately to  $\pm 100$  m, as show the appropriate calculations.

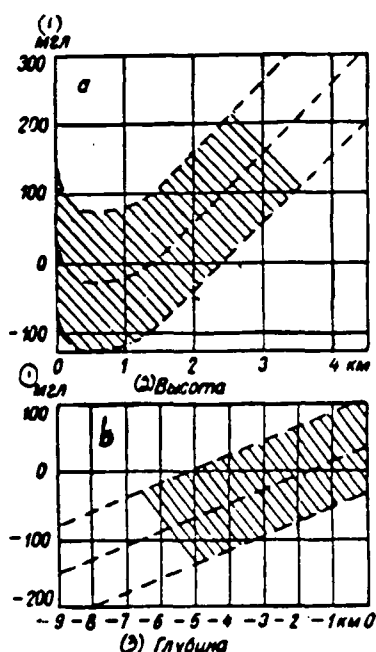


Fig. 13. Correlation graph/diagram of dependence of difference in anomalies of Faye and isostatic  $\Delta g_F - \Delta g_I$  on height of relief for maritime stations. According to B. A. Andreyev (1961). The regions of confident correlation are shaded.

Key: (1). mgal. (2). Height. (3). Depth.

Page 40.

Therefore, strictly speaking, the gravitational force should be reduced to the surface of spheroid, on that even at the end of the past century indicated German astronomer Bruns (Bruns, 1848-1919). For this it is necessary to introduce the additional correction, which considers the distance between the geoid and the spheroid, named the mount/mandrel of Bruns. However, the large deviations of geoid from the spheroid are observed in the limited on the area sections, which

gravitate predominantly to the equatorial part of the Earth (Jeffreys, 1960). On the significant part of the territory of the USSR the deviations of geoid from the spheroid are of the order of a total of  $\pm 10$  m (Sorokin, 1953), i.e., for this entire territory the correction of Bruns is of the order of a total of  $\pm 3$  mgf. During the practical calculations, in view all of reasons indicated above, the correction of Bruns is not introduced.

In geodetic gravimetry there were attempts at utilization of series/number of other corrections (according to method of inversion, Poincare-Prey, Boui, etc.). For the prospecting gravimetry the examination and the use of these corrections does not have a sense.

In gravitational measurements, produced in motion (on drifting ice, surface boats, submarines, on aircraft), high value has introduction of correction for eastwestern component of motion of instrument, named also correction for Eotvos's effect or simply by correction of Eotvos.

A sense of this correction consists of following. gravitational force, as we know, represents the sum of two forces - attraction of the Earth and the centrifugal force, caused by the daily rotation of the Earth (see §1). The centrifugal force depends on the speed of rotation of the Earth and for any fixed material point, arranged/located on the earth's surface, it can be considered as the constant value. Since the Earth is rotated from the west to the east,

for the material point, which moves over the earth's surface, centrifugal force increases/grows, if eastwestern component of motion is directed toward the east, and it is reduced if this component is directed toward the west; respectively varies the amount of gravitational force. The correction of Eotvos removes the effect of the motion of instrument on gravitational force. Formula for determining this correction (Sorokin, 1953, pg. 296-297) takes the following form:

$$\Delta g_E = 0,00405 v \cos \varphi \sin A, \quad (I.38)$$

where  $v$  - speed of the motion of instrument in the kilometers;

$\varphi$  - latitude;

$A$  - azimuth of direction of motion.

Correction of Eotvos reaches very high values (hundred milligal) in conditions for aircraft photographing.

Page 41.

With high-accuracy gravimetric survey (with error of measurement in less than 0.1 mg|) into results of measurements it is necessary to introduce correction for changes in the gravitational force, caused by lunisolar attraction. The value of these changes in the course of twenty-four hours is of the order  $\pm 0.10$ ;  $\pm 0.15$  mg|. To account for these changes it is necessary to know geographical reference of observation point and moment/torque of observation. The tables of corrections (with an accuracy to  $\pm 0.01$  mg|) systematically, for year forward, are published in the form of application/appendix to the

journal "Geophysical Prospecting".

During subterranean gravitational photographing it is necessary to consider effect on measured amount of force of gravity or second derivatives of gravitational potential of mine workings (Heiland, 1940; Zagorac, 1953; Kazinskiy, 1956; Mudretsova, 1960).

In conclusion let us underscore following fact. We measure gravitational force, i.e., the sum of the attraction of the Earth and the centrifugal force, caused by the daily rotation of the Earth. During the calculation of anomaly we from the measured value of gravitational force is subtracted its normal value, into which enters the same value of centrifugal force. Consequently, the anomalies of gravitational force present the anomalies of attraction, caused by the nonhomogeneous density of the Earth and the earth's crust.

We in detail explained above that it is understood in gravimetry under anomalies of gravitational force and sense of those calculating operations, as a result of which are obtained numerical values of anomalies. We established that for purposes of prospecting gravimetry it follows, as a rule, to use Bouguer's anomalies or topographic in such regions, where the relief has a noticeable effect on the force of gravity (with the development of high-accuracy detailed gravimetric surveys a number of such regions it will prove to be, undoubtedly, sufficiently significant). Further we will see, that determined thus anomalies are in the majority of the cases only "semi-finished

product" during the solution of the majority of the practical problems of gravitational prospecting. For the solution of these problems is frequently necessary the additional transformation of anomalies (localization, averaging, etc.) - those operations, which are in detail examined by us in Chapter IV.

§ 5. Corrections and the anomaly of the second derivatives of gravitational potential.

Introduction of corrections and calculation of anomalies for second derivatives of gravitational potential - problem, unambiguously determined and considerably simpler than calculation of anomalies of gravitational force.

Page 42.

No corrections for height, for attraction of interlayer and so forth into values of second derivatives it is introduced. The normal values of the second derivatives in limits of accuracy of their measurement can be considered identical for the surface of terrestrial spheroid, geoid and for the physical surface of the Earth. Into the measured values of the second derivatives it is necessary to introduce correction only for the effect of nonhorizontality of the relief of the earth's surface, moreover for the values indicated this correction almost always has vital importance, and in many instances it proves to be very large.



Anomalous values of second derivatives, for example  $W_{xx}$ , are calculated according to this diagram:

$$[W_{xx}]_{ан} = [W_{xx}]_{набл} + \left[ \overset{(1)}{\text{Поправка на рельеф}} \right] - [W_{xx}]_{норм},$$

Key: (1). Correction for the relief.

where the indices relate respectively to anomalous, observed and normal values  $W_{xx}$ , and the second term to the right presents correction for the effect of relief or as they speak, correction for the topography.

We do not concern question about account of correction for effect of relief, which presents separate section of gravimetry, to which is dedicated vast specialized literature (Andreyev, etc., 1941; Sorokin, 1953). Let us briefly clarify the principle of the determination of the normal values of the second derivatives of gravitational potential only.

Normal values are calculated in coordination system, whose horizontal axes in a specific manner are oriented relative to geographical meridian. With the calculation of the tables of normal values usually x axis they direct on the meridian to the north, and y axis - to the east in the direction of prime vertical. Z axis is as before considered directed vertically downward. In this case it is considered that the normal geoid coincides with the terrestrial spheroid. For the spheroid directions indicated above of x and y axes coincide with the planes of main normal sections: in the meridional

plane is arranged/located the section with the the maximum (1/M), and in the plane of prime vertical - with the minimum (1/N) curvature. Radii of curvature as follows are expressed as semimajor axis  $a$  and eccentricity  $e$  of the meridian ellipse:

$$\left. \begin{aligned} M &= \frac{a(1-e^2)}{(1-e^2 \sin^2 \varphi)^{3/2}} \\ N &= \frac{a}{(1-e^2 \sin^2 \varphi)^{1/2}} \end{aligned} \right\} \quad (I, 39)$$

Page 43.

Since under the assumptions accepted, the gravitational force does not vary along parallel (and, consequently, any of its components does not vary), two of four normal values of second derivatives, formed by differentiation with respect to coordinate  $y$ , become zero

$$\begin{aligned} (2W_{xy})_n &= 0, \\ (W_{yz})_n &= 0. \end{aligned}$$

Hence, taking into account formulas (1.17) and (I, 19),

$$(W_{xx})_n = R = \gamma_0 \left[ \frac{1}{M} - \frac{1}{N} \right].$$

Further, using formulas (I, 8) and (I, 39) and disregarding in obtained expressions low values, we obtain working formula for calculation  $(W_{xx})_n$

$$(W_{xx})_n = \frac{ga^2}{a} \cos^2 \varphi. \quad (I, 40)$$

Expression  $(W_{xx})_n$  will be

$$(W_{xx})_n = \frac{\partial \gamma_0}{\partial x} = \frac{1}{M} \cdot \frac{\partial \gamma_0}{\partial \varphi}.$$

Since  $dx = Md\varphi$ , in form converted for practical calculations, taking into account formula (I, 8a), formula for  $(W_{xz})_n$  finally is obtained in the following form:

$$(W_{xz})_n = \frac{ga\beta}{a} \sin 2\varphi. \quad (I, 41)$$

As we see from Table 2, values  $(W_{xz})_n$  and  $(W_{\Delta})_n$  are low in value and very they vary smoothly with change in latitude  $\varphi$ .

Table 2. Normal values  $(W_{xz})_n$  and  $(W_{\Delta})_n$ 

$\varphi^\circ$	$(W_{xz})_n \cdot 10^{+9} \text{ CGS}$	$(W_{\Delta})_n \cdot 10^{+9} \text{ CGS}$
35	7.6	6.9
40	8.0	6.0
45	8.1	5.1
50	8.0	4.2
55	7.6	3.4
60	7.0	2.6
65	6.2	1.8
70	5.2	1.2

Page 44.

If the x axis does not coincide with geographical meridian and azimuth of its positive direction is equal to  $\alpha$ , then normal values of second derivatives are obtained of values corrected above with the help of formulas of conversion known from gravimetry:

$$\left. \begin{aligned} (W_{xz})'_n &= (W_{xz})_n \cos \alpha, \\ (W_{yz})'_n &= (W_{yz})_n \sin \alpha, \\ (W_{\Delta})'_n &= (W_{\Delta})_n \cos 2\alpha, \\ (2W_{xy})'_n &= (2W_{xy})_n \sin 2\alpha, \end{aligned} \right\} \quad (1.42)$$

where  $(W_{xz})'_n$  and so forth - converted normal values of second derivatives.

Anomalous values of second derivatives of gravitational potential and force of gravity (see pg. 41), coincide with anomalous values of corresponding derivatives of potential of attraction.

§ 6. Connection between derivatives of gravitational and magnetic potential.

In mathematical physics there is derived the Poisson's theorem (Ideal'son, 1936, pg. 397), formulated as follows:

$$P = \frac{J}{f\sigma} \cdot \frac{\partial V}{\partial i}, \quad (I, 43)$$

where  $P$  - magnetic potential of body;

$V$  - potential of its attraction;

$J$  - intensity of magnetization (constant for entire volume of body);

$i$  - direction of magnetization.

Component of magnetic field strength along any direction  $s$  will be expressed by derivative in this direction:

$$\frac{\partial P}{\partial s} = \frac{J}{f\sigma} \cdot \frac{\partial^2 V}{\partial i \partial s} = \frac{J}{f\sigma} \cdot \frac{\partial}{\partial s} \left[ \frac{\partial V}{\partial x} \cdot \frac{\partial x}{\partial i} + \frac{\partial V}{\partial y} \cdot \frac{\partial y}{\partial i} + \frac{\partial V}{\partial z} \cdot \frac{\partial z}{\partial i} \right].$$

Page 45.

Introducing components of intensity of magnetization  $J$  along axis,  $x, y, z$ :

$$\alpha = J \frac{\partial x}{\partial i} = J \cos(i, x),$$

$$\beta = J \frac{\partial y}{\partial i} = J \cos(i, y),$$

$$\gamma = J \frac{\partial z}{\partial i} = J \cos(i, z)$$

and accepting  $s$  consecutively/serially coinciding with reference direction, we find expressions of components

$$\left. \begin{aligned} X &= \frac{\partial P}{\partial x} = \frac{1}{f\sigma} [\alpha V_{xx} + \beta V_{vx} + \gamma V_{zx}], \\ Y &= \frac{\partial P}{\partial y} = \frac{1}{f\sigma} [\alpha V_{yx} + \beta V_{yy} + \gamma V_{yz}], \\ Z &= \frac{\partial P}{\partial z} = \frac{1}{f\sigma} [\alpha V_{zx} + \beta V_{zy} + \gamma V_{zz}], \end{aligned} \right\} \quad (I, 44)$$

where  $V_{xx} = \frac{\partial^2 V}{\partial x^2}$  and so forth - abbreviations of second derivatives of potential of attractions, whose anomalous values, as it is noted above (pp. 41, 44), are identical with values of corresponding derivatives of gravitational potential  $W$ .

Keeping this in mind and taking into account that us interests relationship/ratio between anomalous values of derivatives of gravitational and magnetic potential, we we can in relationships/ratios written above replace  $V$  by  $W$ , that also is implied subsequently.

In theory of interpretation case, when perturbing masses have form of cylinders, elongated to an infinitely long distance in parallel to axis  $y$  (two-dimensional problem), frequently is examined. In this case the gravity anomaly does not vary along  $y$  axis, i.e.,  $W_{yx} = W_{yy} = W_{yz} = 0$ , and we obtain from the formula (I, 44) (substituting here  $V$  by  $W$ ):

$$\left. \begin{aligned} X = H &= \frac{1}{j_0} (\alpha W_{xx} + \gamma W_{zz}), \\ Z &= \frac{1}{j_0} (\alpha W_{xx} + \gamma W_{zz}), \end{aligned} \right\} \quad (I, 45)$$

and the component  $Y$  becomes zero.

In the examined by us case Laplace's equation (1.20)

$$W_{xx} + W_{zz} = 0, \quad (I, 46)$$

and expression (I, 11) for  $W_A$  is obtained in the form

$$W_{\Delta} = -W_{\Sigma} = W_{\Pi}. \quad (I, 47)$$

Taking into account latter/last two relationships/ratios (I, 45) it is possible to rewrite in the form

$$\left. \begin{aligned} H &= \frac{1}{j\sigma} (-\alpha W_{\Delta} + \gamma W_{\Sigma}), \\ Z &= \frac{1}{j\sigma} (\alpha W_{\Sigma} + \gamma W_{\Delta}). \end{aligned} \right\} \quad (I, 48)$$

Page 46.

Especially simple correlation of values in question is obtained in the case of two-dimensional problem with vertical intensity of magnetization, i.e., with  $\alpha=0$ ,  $\gamma=J$ . Then

$$\left. \begin{aligned} H &= \frac{J}{j\sigma} W_{\Sigma}, \\ Z &= \frac{J}{j\sigma} W_{\Delta}. \end{aligned} \right\} \quad (I, 49)$$

Taking into account formulas (I, 22), (I, 46) and (I, 47), latter from formulas (I, 49) can be rewritten in the form

$$Z = \frac{J}{j\sigma} W_{\Pi}. \quad (I, 50)$$

With  $J=\text{const}$  and  $\sigma=\text{const}$ , i.e., for uniform magnetized bodies of constant density, which compose magnetic field strengths  $H$  and  $Z$  prove to be respectively proportional in value to second derivatives of the gravitational potential  $W_{\Sigma}$  and  $W_{\Delta}$ . Furthermore, the component of  $Z$  in this case it is possible to consider the proportional to vertical force gradient of gravity  $W_{\Pi}$ .

The fact that for finite body this potential mass-free, is a special feature of magnetic potential, which distinguishes it from gravitational, : total magnetic mass of body is always equal to zero, i.e., positive magnetic mass  $+m$  in one pole is compensated by negative magnetic mass  $-m$  in the other pole of magnetized body. Therefore, formal analogy in the expressions of the gravitational and magnetic fields composing intensities/strength is obtained only in such cases, when we assume that one end and, consequently, one of the poles) of the magnetized body is distant to infinity, and the body, which causes gravity anomaly, has, conversely, finite dimensions. For example, the magnetic action of the infinitely long magnetized rod, whose one end is located at infinite depth, can be formally identical with the gravitational effect/action of mass point, which coincides with the upper pole of the magnetized rod.



Page 47.

Chapter II.

## PHYSICO-GEOLOGIC BASES OF GRAVITATIONAL PROSPECTING.

### § 7. Generalities.

Gravity anomalies exist in presence of following two conditions:

- 1) difference in the density of rocks and ores;
- 2) nonhorizontality of bedding of interfaces of density, connected with presence of geologic structures, ore bodies, etc.

Basis of setting gravitation prospecting works and correct geologic interpretation of their results is possible, if is carried out analysis of following two questions:

- 1) about density of rocks and ores and laws governing its change in geologic of section/cut;
- 2) about forms of bedding, sizes/dimensions and depth of bedding of geologic bodies, which cause gravity anomalies.

Of this type it is necessary to analyze separately for each concrete region and object, intended for performing of gravitation prospecting work, since each such region, or object, one way or another possesses, as a rule, by individual physico-geologic characteristics, which must be taken into account while conducting and during analysis of results of gravitational prospecting. At the same time, basic physico-geologic conditions are general/common in the regions with

similarly the history of geologic development, in the limits of same-type structural-facies and metallogenic zones, etc. The study of these regularities makes it possible in the first approximation, to explain the prerequisites/premises of the application of gravitational prospecting and interpretation of its results for solving the definite geologic missions in this or another region, if the general/common geologic characteristic of this region is known. Subsequently, it is understood, it is necessary the obtained conclusions/derivations to make more precise and to supplement, using data of the study of the density of the rocks of this region, the results of the carried out in the region geological exploration works, etc. The basic content of this chapter presents the examination of physico-geologic conditions and prerequisites/premises of setting and interpretation of the results of gravitation prospecting works. Let us initially examine a question about the density of the rocks and ores.

Page 48.

#### § 8. Density.

Density  $\sigma$  of any uniform substance is defined as ratio of its mass  $m$  to volume  $V$ , i.e.

$$\sigma = \frac{m}{V}. \quad (11.1)$$

For an ideally uniform rock with any sizes/dimensions of  $m$  and  $V$  specimen one and the same value of density  $\sigma$  is obtained. Also one

value  $\sigma$  is obtained also for any two specimens, used for determining the density.

#### Dimensionality of density in CGS units

$$[\sigma] = g/cm^3.$$

Specific weight/gravity is ratio of weight of body to its volume, i.e., it can be expressed by formula, analogous (II, 1), if we by  $m$  understand weight of body, expressed in weight grams. Strictly speaking, the specific weight of body, in contrast to the density, value the variable, which depends on gravitational force. However, since maximum changes in gravitational force relative to its complete mean value do not exceed 0.003, and the value of density is usually expressed by the first units, virtually it is possible to count the density of the numerically equal to specific weight/gravity.

Rocks and ores of general case consist of three phases - solid, liquid and gaseous, each of which is of different mass, volume and density. In this case

$$\sigma = \frac{m_1 + m_2 + m_3}{V_1 + V_2 + V_3} = \frac{M}{V}, \quad (II, 2)$$

where  $m_1$  and  $V_1$  relates to the solid,  $m_2$  and  $V_2$  - to the liquid,  $m_3$  and  $V_3$  - to vapor phase, and  $M$  and  $V$  represent mass and volume of specimen.

In contrast to density of uniform substance, density of rocks and ores, determined according to formula (II, 2), is different for

different M and V, and also for any two specimens as a result of discontinuity and composition of rock or ore.

For this very reason density (as other physical properties) rocks possible to consider only in terms of average/mean values from series of results of definitions, which relate to significant number of specimens. In this case the sizes/dimensions and the mass of specimens must not be very small - to avoid the sharp oscillations/vibrations, caused by their nonhomogeneous composition. Practice shows that the minimum mass of the specimens, utilized for determining the density, must be order 100-200 g.

Bulk density represents ratio of mass of solid phase to total volume of specimen

$$\sigma_V = \frac{m_1}{V} = \frac{m_1}{V_1 + V_2 + V_3} \quad (11, 3)$$

Page 49.

Density of mineral hexagonal base of rock

$$\sigma_{\text{min}} = \frac{m_1}{V_1} \quad (11, 4)$$

is called mineralogical density.

Ratio of the total volume of pores in the specimen to total volume of specimen

$$k_n = \frac{V_2 + V_3}{V_1 + V_2 + V_3} \quad (11, 5)$$

( $k_n$  is expressed in the fractions of one, or in percent) is called

porosity.

If the specimen is dried out, i.e., moisture found in it is distant, then its density will be

$$\sigma_{\text{cyl}} = \frac{m_1 + m_2}{V_1 + V_2 + V_3} \quad (\text{II, 6})$$

Density of dry specimen can be expressed through its mineralogical density and porosity. For this let us take into account first of all that in (II, 6)  $m_1 \ll m_2$ , and, consequently,

$$\sigma_{\text{cyl}} \approx \frac{m_1}{V_1 + V_2 + V_3} = \frac{m_1}{V_1} \cdot \frac{V_1}{V_1 + V_2 + V_3} = \frac{m_1}{V_1} \left[ 1 - \frac{V_2 + V_3}{V_1 + V_2 + V_3} \right],$$

whence, taking into account (II, 4) and (II, 5), we obtain

$$\sigma_{\text{cyl}} \approx \sigma_{\text{min}} (1 - k_n).$$

Density usually is determined in dried out state of specimen. If in this case the porosity of specimen is known, then from the latter/last relationship/ratio its mineralogical density

$$\sigma_{\text{min}} \approx \frac{\sigma_{\text{cyl}}}{1 - k_n} \quad (\text{II, 7})$$

is determined.

Directly for purposes of gravitational prospecting determination of specimen density under conditions of natural humidity is basic problem. If the porosity of specimen is small (not higher than the first units of percentages), as it takes place for the majority of the eruptive and metamorphic rock and some sedimentary (see below), then it is possible without the large error to take

$$\sigma \approx \sigma_{\text{cyl}}. \quad (\text{II, 8})$$

Matter concerning specimens, which have high porosity and moisture absorption capacity is much more complex, the majority of sedimentary rocks is such. Usually in this case they consider that all pores of specimen under the natural conditions are filled with water.

Page 50.

From the formulas (II, 2) and (II, 6) we find

$$\sigma \approx \sigma_{\text{cyl}} + \frac{m_1 + m_2}{V_1 + V_2 + V_3}$$

or taking into account that with the complete filling of all pores with water  $m_1 + m_2$  is numerically equal  $V_1 + V_2$ , and taking into account (II, 5), we find

$$\sigma \approx \sigma_{\text{cyl}} + [k_a] \text{ g/cm}^3. \quad (\text{II, 9})$$

Let, for example,  $\sigma_{\text{cyl}} = 2,20 \text{ g/cm}^3$ ,  $k_a = 0,15$ , then

$$\sigma \approx 2,20 + 0,15 = 2,35 \text{ g/cm}^3.$$

Assumption about filling of all pores with water, however, is not completely correct. In actuality by water and with other liquids is saturated not entire pore volume of species/rock, but only its part. the ratio of the volume of pores filled with liquid to the total volume of specimen is called apparent porosity  $k_{a.n.}$  moreover always  $k_{a.n.} < k_n$ .

Relation  $k_{a.n.} : k_n$  is called coefficient of water saturation or

simply by saturation coefficient designate  $k_s$ , so that

$$k_s = \frac{k_{0,n}}{k_n}. \quad (II, 10)$$

This coefficient depends on special features of structure of pore space of rock, precisely, from relative content in pore space of pore channels permeated for liquid. Some species/rocks are characterized by the broad band of change  $k_s$  (Table 3).

If it is known  $k_{0,n}$ , then it would be possible to determine  $\sigma$  from following refined formula:

$$\sigma \approx \sigma_{cyl} + k_{0,n}.$$

It is understood, however, that this formula is approximate, since in accuracy it is unknown, water did occupy entire permeated pore volume under deep conditions. And what is more, it is deliberately known that in many instances and this part of the pore volume is not completely occupied with water.

Sometimes during calculation of  $\sigma$  it is conditionally accepted that water occupies 50% of entire pore volume, i.e.,  $k_{0,n} = 0.50 k_n$ , whereas more frequent they consider that  $k_{0,n} \approx k_n$ .

Table 3. Values  $k_s$  for different rocks (according to the different authors).

(1) Наименование горных пород	$k_s$ , %
(2) Большинство нефтяных коллекторов (США) . . . . .	90-95
(3) Аргиллиты (Тат. АССР) . . . . .	22-45
(4) Песчаники . . . . .	30-100
(5) Карбонатные породы . . . . .	20-80

Key: (1). Designation of the rocks. (2). Majority of petroleum collectors (USA). (3). Argillites (Tatar ASSR). (4). Sandstones. (5). Carbonate rocks.

Page 51.

The uncertainty with correction for water saturation of the rock is extremely undesirable, but one ought not to overestimate role of errors connected with it in determination of density. In gravitational prospecting are essential not the absolute values of density, but its difference or excess values. Using formula (II, 9), we deliberately somewhat exaggerate the values of density, moreover for the rocks with the close values of porosity and moisture absorbtion capacity approximately to the identical value. During the calculation of the excessive (difference) density in this case the error, obviously, will be small. Large errors are possible only during the calculation of the difference of the density of the rocks, which are considerably distinguished by the porosity and the moisture absorbtion capacity.

Requirements for methodology of study of density of rocks and



ores. The generally accepted technology and the methodology of the study of density is assumed to be the known to reader from the courses "Physics", the "Physical properties of the rocks" and "Gravitational prospecting". However, the completeness and quality of the data about the density of the rocks and ores of the region being investigated require estimation in connection with the geologic interpretation of gravity anomalies; moreover it is here necessary to examine the following questions:

1. Completeness of data. the practice of gravitational prospecting shows that the systematic mass study of specimen density of all typical varieties of species/rocks and ores of region, which generate structural-facies zones is necessary and to the bed, whose effect caused the interesting us gravity anomalies. Each such typical variety must be described as the minimum of several ten determinations of specimen density.

2. Quality of specimens. First of all it is necessary to investigate the core of the drill holes lower than zone of wind erosion. It characterizes normal unchanged rocks and, furthermore, it usually has a good geologic documentation. Samples from the natural exposures also are used under the condition of their reliable geologic documentation and absence of the explicit signs of a supergene change in the rock. However, in certain cases, for example during the searches for some ore deposits, the density of supergene-changed rocks undergoes special study. The petrographically nonhomogeneous specimens of near-contact zones are unconditionally eliminated from

the examination.

3. Quality of measurements. The generally accepted technique of the volume determination by Archimedes principle of specimens with the utilization either of usual counterbalances or special instruments (densitometer of Samsonov, the weights of Bykhover-Knyupfer) gives the accuracy of the measurements of order  $0.01-0.02 \text{ g/cm}^3$ , which is completely sufficient for gravitational prospecting. The density of the porous specimens, from which during their subsidence into the water is observed the intensive liberation/precipitation of the air bubbles, accompanied during the prolonged finding in the water by the damage of normal structure or by the decomposition of specimen, must be determined with the application of a paraffin coating or with the cover/occultation of specimen with water-and-moisture-proof sheeting of another type.

Page 52.

This requirement should be satisfied especially strictly with the weighing of specimen in the water on usual counterbalances. Of the doubtful cases one should be convinced of the possibility of measurement without the paraffin coating via the comparison of the values of the density of one and the same specimens, determined with the paraffin coating and without the paraffin coating.

Density of loose rocks should be determined via their weighing in assigned volume; also one should enter, also, during determination of

density of drifts (during variometric photographing). It is necessary to keep in mind that the density of the rocks can be determined also from the observations with the high-accuracy gravimeters or the variometers during the observations either on the earth's surface (Nettlestone, 1940), or in the mines/shafts and the drill holes (Poletayev, 1958). The values of the density of the rocks can be evaluated according to the data of a gamma-gamma-logging (Ochkur, 1957), but this methodology still requires refinement and refinement. In the series/number the case sufficiently confident judgment about the density of the rocks can be obtained, knowing other their physical properties (see pg. 55-60). One should approach, using one of the methods indicated, to obtain the control of those estimations of the density of the rocks, which are done by measuring the specimens.

4. Data processing. The investigated specimens of the rocks and ores must be decomposed into the groups, on the basis of the single petrographic composition, identical position in the stratigraphic section/cut, identical location in the region, the presence or the absence of secondary changes, types of mineralization and others of a similar kind of signs. On each of such groups, in the presence in it not less than 30-50 specimens, is built the variation curve of density variation. One should approach that so that each group would be characterized by variation curve with one maximum. The value of density typical for this group is determined not on the point of the maximum of variation curve (frequently encountered in the industrial organizations error), but in terms of arithmetic mean value of

density. values arithmetic mean coincide with the value of the abscissa of the maximum of variation curve only in such a case, when this curve is ideally symmetrical with respect to the ordinate of maximum; whereas in actuality the variation density curves do not usually have strictly symmetrical form (Fig. 14). If the group being investigated is clearly nonhomogeneous, variation curve for it is obtained with several maximums. Average/mean value for this group is determined by the accidental relationship/ratio of nonhomogeneous components and its calculation does not have a sense. It is necessary to try to decompose this group according to any additional signs (lithologic, stratigraphic, etc.) into the uniform subgroups.

Page 53.

Special sense has a separation for the vast groups, which join the determinations of the density of the sedimentary rocks of one or the other region from the sign of single position in the stratigraphic section/cut and the identical lithological composition into the subgroups according to the sign of the identity of structural position, keeping in mind the investigation of the laminar zonality of density and its bond with the local and regional structures (see § 11).

Bond of density with different physico-geologic factors. The density of the rock is caused by both the primary conditions for its formation and by secondary conditions, which acted during entire period of its existence. Of special features and the property of the

rock, including density, can be considered as the objective indices of a historico-geologic process:

a) the geotectonic and petrological conditions of forming the rock;

b) all conditions and the factors of its further existence: metamorphism, oscillatory and folding motions, supergene processes, etc.

These conditions and factors in set determine following special features of rock:

a) composition and structure of its mineral hexagonal base;

b) its porosity, character and degree of filling of pore space.

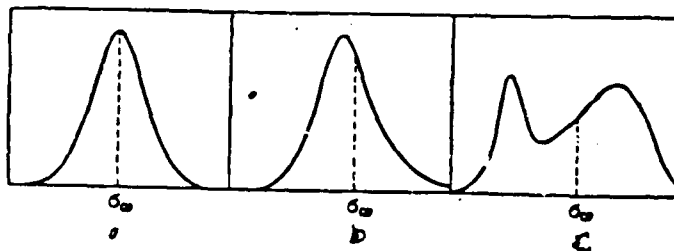


Fig. 14. Types of variation density curves: a) symmetrical curve of group of specimens (normal distribution) uniform in composition and very large in quantity; b) usually obtained type of curve of not completely symmetrical form: value  $\sigma_0$  in this case does not correspond to point of maximum; c) curve with two maximums, that indicates explicit heterogeneity of group - calculation  $\sigma_0$  does not have sense: group must be according to any signs decomposed into two separate groups.

Page 54.

These special features are basic, determining density and many other physical properties of rock. In this case it is important to have in mind the fact that the special features indicated are connected with the density (and by other physical properties) differently, namely:

a) composition and structure of mineral hexagonal base are connected with the density ambiguously/problematically - the species/rocks of completely different composition can have and they actually frequently have dissimilar or very close density;

b) porosity is connected with the density unambiguously - the

DOC = 88020203

PAGE

~~18~~ 95

species/rocks of different porosity (with the identical composition) compulsorily are distinguished by the density, we can in certain cases quantitatively take into account these differences.

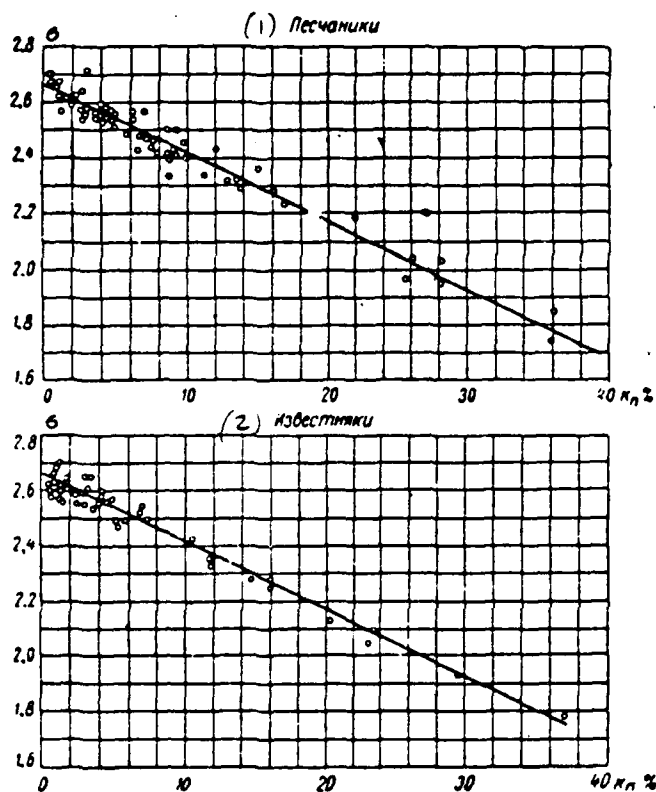


Fig. 15. Bond of density and porosity for sandstone and limestones.

L. Ya. Nesterov (1940).

Key: (1). Sandstones. (2). Limestone.

Page 55.

Majority of geologic processes, effect of which undergoes rock, one way or another affects its composition, porosity and density. In a number of cases the effect/action of these processes on the density is systematically investigated and proves to be very significant. Both on formation conditions and on the density the rocks it is expedient to examine subsequently, after decomposing them into two



groups: a) magmatic and metamorphic rock; b) sedimentary rocks.

Bond of density with other physical properties. Geologic factors and processes affect not only the density of the rocks, but also their other physical properties. In this sense it is possible to speak about the bond of different physical properties. We already clashed with this above and noted the bond of density and porosity, they indicated that this bond is simple in the volume sense, that any change in porosity of the rock in a specific manner is connected with a change in its density. The bond of density and porosity for some types of the rocks is shown by curves in Fig. 15.

Question about bond of density and elastic properties of rocks is very important. This bond exists, but it is not so defined and simple as the bond examined above of density and porosity. It is possible to assume that the reasons for this consist of the following:

1. The rocks according to their properties are not ideally elastic and they possess plasticity (different species/rocks - in different measure). Depending on this, apparently, varies the relationship/ratio of density and elastic properties.

2. Velocity of propagation of elastic waves in contrast to density - value vector and depends not only on special features of composition and structure of rock, but also on some other conditions, for example, for foliated rocks from direction of propagation of wave with respect to plane of lamination, etc.

For uniform ideally elastic infinitely extended body we have following approximate relationship/ratio (B. A. Andreev, 1960):

$$v_p = 1,095 \sqrt{\frac{E}{\sigma}}, \quad (11, 11)$$

where  $v_p$  - velocity of propagation of longitudinal waves;

$E$  - modulus of elasticity of Young;

$\sigma$  - density.

For majority of rocks with an increase in  $\sigma$  there also increases  $E$ , moreover, to a greater degree, than  $\sigma$ , so that there is an increase in speed  $v_p$ . With the decrease in  $\sigma$  we have opposite phenomenon - decrease in  $v_p$ .

Let us clarify aforesaid by following example. Let us compare two specimens of limestone with the different values of porosity  $\lambda$ , and in accordance with this with the different values of the modulus/module of elasticity  $E$  and density  $\sigma$  (Table 4).

Page 56.

As can be seen from table, with decrease of porosity 5 times modulus of elasticity is increased more than 3 times, and density increases/grows only by 32%; therefore  $v_p$ , that depends on ratio  $E/\sigma$ ; also it is increased one and a half times more than.

N. N. Puzyrev (1959), by using data based on data of laboratory of physical properties of VNIIGeofiziki, indicated that for sandy-clay

and some carbonate rocks dependence of speed  $v_p$  on density  $\sigma$  is, in the first approximation, linear function of form

$$v_p = 6\sigma - 11, \quad (II, 12)$$

where  $v_p$  is expressed in km/sec and  $\sigma$  - in g/cm<sup>3</sup>.

According to data of American researchers (Talvani, Sutton, Worzel, 1959), studied greater quantity types of rocks with respectively greater range of change  $v_p$  and  $\sigma$ , dependence between these two parameters proves to be nonlinear and is represented as curve of sufficiently complex form (Fig. 16). Fig. 16 shows also the linear dependence, represented by equation (II, 12). As we see, both graphs more or less will be coordinated in the interval of the variation in the density of 2.4-3.0 g/cm<sup>3</sup>.

Bond of density and elastic properties for separate petrographic types of rocks proves to be much more definition, moreover, as can be seen from Fig. 17, this bond is characterized by graphs of virtually linear form.

"Anomalous" character has relationship/ratio of density and speed for halogen rocks, that, probably, it follows to explain by their high plasticity. Rock salt has relatively low density ( $\sigma=2.15$  g/cm<sup>3</sup>) and it is at the same time characterized by the relatively high velocity of propagation of elastic vibrations ( $v_p = 4600$  m/s).

Table 4. Comparison of porosity  $k_n$ , modulus of elasticity  $E$  and density  $\sigma$  of two specimens of limestone. Data of K. P. Belikov (1952).

Образцы (1)	$k_n$ , %	$E \cdot 10^{11}$ , дин/см <sup>2</sup> (2)	$\sigma$ , г/см <sup>3</sup> (3)	$V_p$ , м/сек, по формуле (II, 11) (4)
(5) Первый . . . . .	30	1.86	1.96	3400
(6) Второй . . . . .	8	6.43	2.59	5450

Key: (1). Samples. (2). dyne/cm<sup>2</sup>. (3). g/cm<sup>3</sup>. (4). m/s, according to formula (II, 11). (5). The first. (6). The second.

Page 57.

Even more striking example of similar relationships/ratios gives the comparison of density and speed of elastic waves for the substances in different states of aggregation, for example for the water with  $t=0^\circ$

( $\sigma = 1.0 \text{ g/cm}^3$ ;  $v_p = 1430 \text{ m/sec}$ ) and for ice with  $t=-5^\circ\text{C}$

( $\sigma = 0.9 \text{ g/cm}^3$ ;  $v_p = 3800 \text{ m/sec}$ ).

Bond of density with specific electrical resistance is planned for some varieties of sedimentary rocks under necessary condition of homogeneity of hydrochemical characteristic of section/cut.

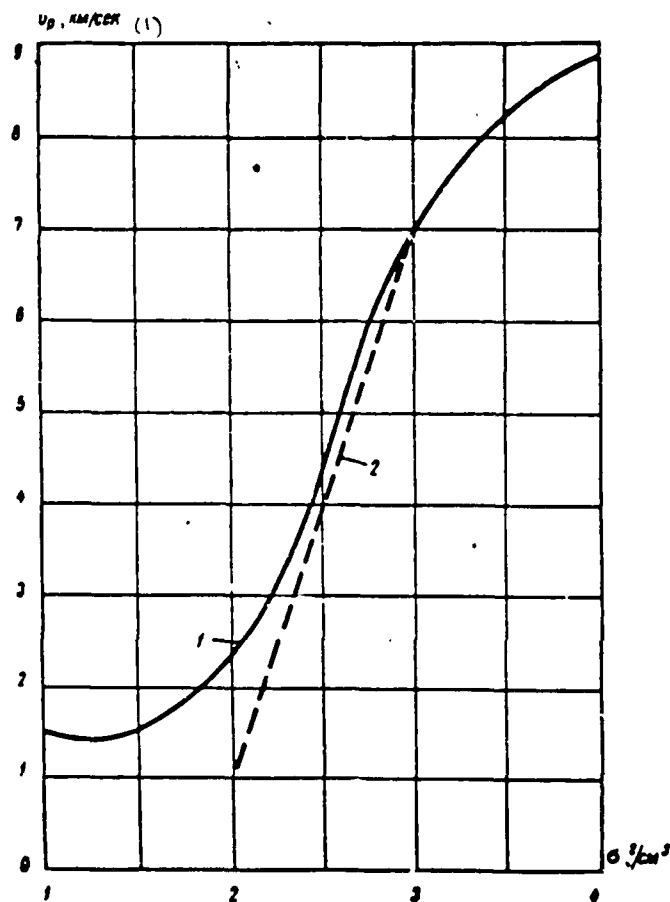


Fig. 16. Curves of dependence speed ( $v_p$ ) - density ( $\sigma$ ) for different rocks. 1 - after Naife and Drake (Talvani, Sutton, Worzel, 1959); 2 - according to N. N. Puzyrev (1959).

Key: (1). km/s.

Page 58.

This bond it is possible to consider not as a straight line, but indirect line - through the porosity and the moisture absorption capacity. Lighter rocks have a larger porosity and a moisture

absorbtion capacity, and respectively, smaller resistivity and vice versa. The density of different varieties of the crystalline rocks varies depending on the special features of their composition and structure (see below), these special features, with rare exceptions, barely affecting the value of their resistivity.

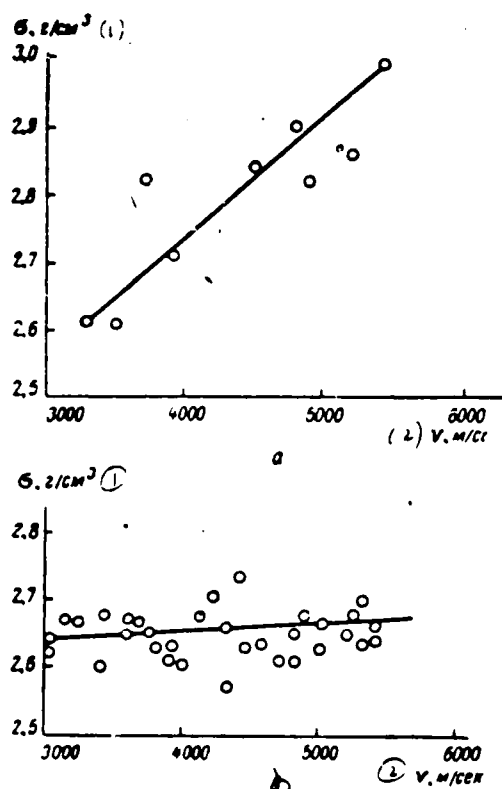


Fig. 17. Curves of dependence speed ( $v_p$ ) – density ( $\sigma$ ) for diabbases (a) and granitoids (b). According to M. L. Ozerskaya (1955).

Key: (1).  $\text{g/cm}^3$ . (2).  $\text{m/s}$ .

Page 59.

We reveal the opposite position during a comparison of density and magnetic properties of rocks. Almost all sedimentary rocks are virtually nonmagnetic, although many of them considerably are distinguished by the density (see below). The special features of the composition of the crystalline rocks are fairly often accompanied by a change in the content in them of magnetically active iron-ore

minerals. In all these cases the conformity of changes in the density and magnetic properties occurs, moreover, as a rule denser crystalline rocks prove to be more magnetic. This relationship/ratio we have, for example, in the normal series/number of magmatic ultrabasic, basic and acid rocks. At the same time, some crystalline rocks, which have a comparatively high density, are virtually nonmagnetic (crystalline carbonate rocks, the separate varieties of crystalline schists), and some magnetically active crystalline rocks have relatively low density (serpentinous ultrabasic rocks).

Bonds indicated above it is possible in a number of cases to use for judgment about density of rocks according to their other physical properties, and also during combined analysis of results of gravitational prospecting with data of other geophysical methods.

#### § 9. Density of the deep layers of the earth's crust.

According to seismological data earth's crust is separated into two layers - upper, conditionally called granite, with velocity of propagation of elastic waves of  $v_p$  about 5.5 km/s, and lower, i.e., basalt, with speed of  $v_p$  about 6.5 km/s. To the lower surface of the earth's crust corresponds the so-called boundary or the Moho surface, on which boundary speed is approximately 8 km/s. Subcrustal layer is named peridotite layer. The names indicated, which characterize the geologic sense of these words, are justified by the following facts:

1. Speed  $v_p$  actually comprises (with the appropriate values of pressure and temperature) about 5.5 km/s and the acid rocks, which



predominate in the upper zone of lithosphere, about 6.5 km/s - in the basic rock of the type of gabbro and basalt and about 8 km/s - in the ultrabasic rocks.

2. In oceans where according to seismological data granite layer usually is absent and solid earth's crust begins almost immediately from basalt layer, almost general/universal development of basic rock actually is revealed (on islands, also, during study of oceanic bottom). Furthermore, in the regions of ancient platforms are observed the vast outflows of the basic rock (on the Siberian platform they there are traprocks), which left on the surface on the faults.

Page 60.

3. With deep faults of geosynclinal and platform regions are associated intrusions of ultrabasic rocks, whose magmatic sources are connected with large depths - into several ten kilometers.

Set of facts indicated, as we see, sufficiently reliably justifies given separation and geologic interpretation of deep layers of earth's crust and subcrustal layer. Based on this, it is possible to indicate the sufficiently reliably following probable values of the average density of these layers: granite layer -2.7 g/cm<sup>3</sup>, basalt layer -2.9 g/cm<sup>3</sup>, peridotite layer -3.3 g/cm<sup>3</sup>.

Seismology shows that in regions of different geologic structure, the thickness and composition of earth's crust prove to be sharply

different. We already indicated that in the oceanic regions the upper granite layer is absent and is observed in the section/cut of the earth's crust only of continental regions. The total power of bark varies from 70 and more than kilometers in the high-mountain tectonic-active regions of continents up to 10 km in the oceanic regions (including here and the thickness of the layer of sea water). The intensive regional anomalies of gravitational force are connected with the deep structure of the earth's crust.

§ 10. Density of the crystalline rocks.

Crystalline (magmatic and metamorphic) species/rocks are characterized by low porosity (usually not exceeding by 1-2%) and significant diversity of density of entering into their composition of minerals (Table 5). Therefore, the density of the crystalline rocks virtually depends only on their chemical-mineralogical composition and structural special features.

Table 5. Density of the typical and rock-forming minerals of magmatic and metamorphic rock.

(1)	Минералы	Плотность, (2) г/см <sup>3</sup>
(3)	Амфиболы	2.9-3.6
(4)	Гранаты	3.2-4.3
(5)	Кварц	2.6
(6)	Магнетит	5.0-5.2
(7)	Нефелин	3.6
(8)	Оливины	3.0-4.4
(9)	Пироксены	2.8-3.7
(10)	Полосые шпаты (главнейшие минералы)	2.5-2.8
(11)	Серпентины	2.5-2.6
(12)	Слюда	2.7-3.2
(13)	Хлориты	2.6-3.0
(14)	Эпидоты	3.1-3.5

Key: (1). Minerals. (2). Density, g/cm<sup>3</sup>. (3). Amphibole. (4). Garnets. (5). Quartz. (6). Magnetite. (7). Nepheline. (8). Olivine. (9). Pyroxene. (10). Feldspar (principal minerals). (11) Serpentine. (12). Mica. (13). Chlorites. (14). Epidotes.

Page 61.

In majority of cases density of crystalline rocks in essence is determined by content in them, on one hand, relative to lungs of minerals (quartz, feldspar, nepheline, etc.), on the other - heavy ferro-magnesia minerals (amphibole, olivine, pyroxenes, mica). This is clearly evident on the accompanying diagram, which characterizes composition and density of different magmatic rock - alkaline, acid, basic and ultrabasic (Fig. 18).

Metamorphic rock, which present products of conversion of magmatic and sedimentary rocks, are very different - depending on parent rocks and degree of effect/action of factors of metamorphism.

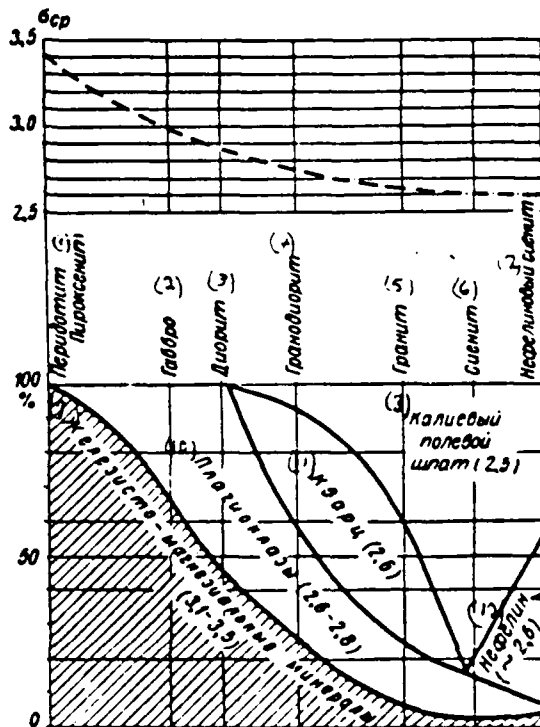


Fig. 18. Dependence of density of eruptive rocks on their mineralogical composition (diagram of mineralogical composition). According to V. P. Luchitskiy (1949). It is simplified.

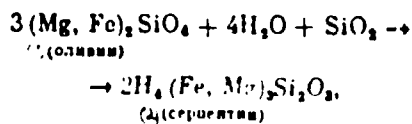
Key: (1). Pyroxenite Periodotite. (2). Gabbro. (3). Diorite. (4). Granodiorite. (5). Granite. (6). Syenite. (7). Nephelinitic syenite. (8). Potash feldspar. (9). Ferro-magnesia minerals. (10). Plagioclases. (11). Quartz. (12). Nepheline.

Page 62.

To the latter, as is known, belong pressure, temperature, the introduction or removal of one or the other mineral components. In the process of metamorphism both the increase and decrease in density

can occur. Thus, with an increase in the pressure and recrystallization connected with this there acts the law of volumes, in accordance with which the pressure increase causes the reactions, connected with the decrease of volume, i.e., with an increase in the density.

As example let us point out that deep analog of gabbro ( $\sigma=2.9 - 3.1 \text{ g/cm}^3$ ) is eclogite, in essence not differing from it by chemical composition, but which is characterized by more tight packing of molecules in crystal and in accordance with this considerably greater density ( $\sigma=3.3 - 3.6 \text{ g/cm}^3$ ). Eclogite are encountered together with the diamonds in the kimberlitic volcanic pipes. Diamond itself ( $\sigma=3.5 \text{ g/cm}^3$ ) presents the polymorphic modification of carbon, which is generated under high-pressure conditions (them are obtained now artificially with  $P=50000$  by atm.). Another, characteristic for the lower pressures, modification of carbon presents graphite ( $\sigma=2.1 \text{ g/cm}^3$ ). The conversion of the ultrabasic rocks under the effect of auto-metamorphism with the introduction of volatile components (water, silicic acids), called serpentization, very strongly reduces their density. Thus one of occurring in this case reactions



Key: (1). olivine. (2). serpentine.

As a result of which olivine ( $\sigma=4.1 - 4.4 \text{ g/cm}^3$ ) it changes into the serpentine ( $\sigma=2.5 - 2.6 \text{ g/cm}^3$ ). The process of serpentization usually is sufficiently intensively showed in the masses of the

ultrabasic rocks, which prove to be converted into serpentinites or serpentines - species/rock of relatively low density.

Supergene change of rocks in their crust of wind erosion is a special case of metamorphism, moreover, and in these conditions most significant possible change of density, usually to side of its decrease. In the majority of the cases this process conducts the effects of water and vital activity of organisms, new minerals of relatively low density to the significant decrease of density in the crust of the wind erosion of the crystalline rocks due to the formation in it, as a result of oxidation. As the example let us examine the Mesozoic crust of the wind erosion of Volynskiy gabbro-labradoritic massif (Zhitomir region of UkrSSR [Ukrainian SSR]). The crust of wind erosion is represented here by kaolinized rocks, and it is developed everywhere over the area of mass and has a thickness from 10 to 40 m. Within the limits of the crust of wind erosion the density of species/rocks (Fig. 19) is reduced (from bottom to top) from 2.8 to 1.5 g/cm<sup>3</sup>, and porosity is increased from 2 to 50% (Kondrachuk, 1958).

Page 63.

In the given example the thickness of the crust of wind erosion proved to be relatively greater <sup>1</sup>.

FOOTNOTE <sup>1</sup>. The vertical sizes/dimensions of the zone of the decrease of the density, connected with the crust of wind erosion, for

crystalline schists of Timan sometimes reach 100 m and more (Kalinin, 1959). Here, most likely, we encounter the interstitial crust of wind erosion. ENDFOOTNOTE.

Usually its value is less. Thus, during the investigation of the numerous boring wells, which opened the Precambrian crystalline basement of Russian platform, it seemed that the thickness of the crust of wind erosion comprises average/mean 8-10 m.

As has already been said above, in some comparatively rare cases processes of changing rocks in crust of wind erosion lead not to decrease, but to increase in density. As the example it is possible to indicate a change of the ferruginous quartzite in the crust of wind erosion with the debris/efflux of them of silicic acid, the oxidation of magnetite and the formation of martite-hematitic rich iron ores. The rich iron ores of the region of the Kursk Magnetic Anomaly (KMA) have specifically this origin.

We indicated above that to density of crystalline rocks besides composition structural special features affect also. Effect on the density of structure variations, connected with a difference in the degree of the crystallinity of the rocks, is especially noticeable.



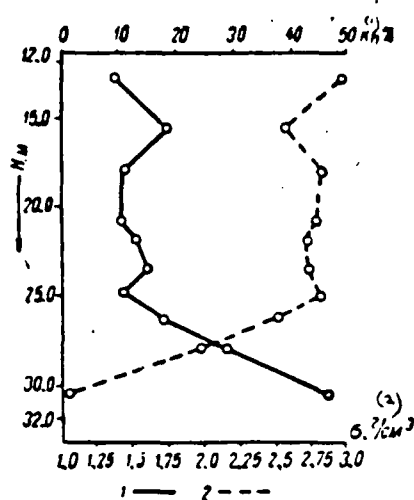


Fig. 19. Graph of change with depth of density and porosity of species/rocks in crust of wind erosion of mass of gabbro-norites. According to V. Yu. Kondrachuk (1958). 1 - density, g/cm<sup>3</sup>; 2 - porosity, %.

Key: (1). KP. (2). g/cm<sup>3</sup>.

Page 64.

Species/rocks deep with the characteristic for them holocrystalline structural have a density higher (Table 6), than their analogs with the semicrystalline or completely by glass wool by structure, since in the crystal is always obtained more tight packing of atoms and molecules than in glass. Differences in the density of minerals and glass corresponding to them in a number of cases reach 15-20% and more. For the rocks these differences also reach 7-10% (Birch, etc., 1947).

## § 11. Density of sedimentary rocks.

Basic rock differ from crystalline usually higher in terms of porosity (with exception of hydrochemical precipitation - Table 7) and in terms of smaller diversity of density of entering their composition rock-forming minerals (Table 8). Therefore, the density in the majority of sedimentary rocks to the different degree depends on their porosity and composition.

As can be seen from Table 7 porosity of many sedimentary rocks not only is great, but also varies in significant limits.

Table 6. Density of crystalline rocks.

(1) Горные породы	(2) Плотность, г/см <sup>3</sup>	
	(3) Средняя	(4) Пределы изменений
Граниты и гранито-гнейсы (типичные для древних щитов) (5)	2.7	2.4-3.0
Граниты (со слабой метаморфизацией) (6)	2.6	2.4-2.7
Гранодиориты, кварцевые диориты (7)	2.7	2.7-2.8
Анортозиты (8)	2.7	2.6-2.9
Диориты (9)	2.8	2.7-2.9
Сyenиты (10)	2.8	2.6-2.9
Диабазы, габбро, габбро-диабазы (11)	2.9	2.7-3.3
Базальты (12)	3.0	2.6-3.3
Ультрабазические породы - дуниты, перидотиты, пироксениты (слабо измененные) (13)	3.2	2.8-3.6
Серпентиниты (14)	2.6	2.4-3.0
Амфиболиты (15)	2.9	2.7-3.2
Альбитофиты (16)	3.2	2.8-3.6
Порфириты (17)	2.8	2.7-2.9
Гнейсы (18)	2.7	2.6-3.2
Кварциты аркозовые (19)	2.7	2.5-2.8
Кварциты железистые (20)	3.5	3.2-4.3
Известняки кристаллические, мраморы (21)	2.7	2.3-3.0
Сланцы глинистые (22)	2.3	3.0-2.8
Сланцы кварцевые, слюдяные (23)	2.8	2.5-2.8
Сланцы роговообманковые (24)	3.0	2.8-3.4

Key: (1). The rocks. (2). Density, g/cm<sup>3</sup>. (3). Average/mean. (4). Limits of changes. (5). Granites and gneissoids (typical for ancient shields). (6). Granites (with weak metamorphization). (7). Granodiorite, quartz diorite. (8). Anorthosites. (9). Diorite. (10). Syenite. (11). Diabase, gabbro, gabbro-diorite. (12). Basalts. (13). Ultrabasic rocks - dunites, peridotites, pyroxenites (weakly changed). (14). Serpentinites. (15). Amphibolites. (16). Albitophytes. (17). Porphyrite. (18). Gneiss. (19). Quartzite, arkosic. (20). Quartzite, ferruginous. (21). Limestone, crystalline, marbles. (22). Slates, clayey. (23). Slates, quartz, micaceous. (24). Slates, hornblende.

limits of the separate regions (see below). by this, apparently, is explained the fact that the numerous authors, according to the data of which is comprised Table 7, almost never they bring the average/mean values of porosity, but the limits of its change indicate only.

Majority of types of sedimentary rocks (with exception in essence only of hydrochemical precipitation) has close mineralogical density, although it differs sometimes very considerably in bulk density.

Table 7. Porosity of sedimentary rocks (about to the different authors).

(1) Породы	(2) Пористость, % (пределы из- менений)
Пески, алевролиты (3) . . . . .	2-42
Песчаники (4) . . . . .	0-55
Галечники (5) . . . . .	25-38
Глины (6) . . . . .	1-63
Аргиллиты (7) . . . . .	4-34
Мергели (8) . . . . .	2-31
Известняки, доломиты (9) . . . . .	1-37
Мел (10) . . . . .	17-43
Гидрохимические осадки (ангидриты, гипсы, камен- ная соль) (11) . . . . .	0-5
Кремнистые породы (диатомиты, трепелы и т. д.) (12) . . . . .	59-92
Донные осадки океанические (глинистые) (13) . . . . .	49-56
Почвы разные (14) . . . . .	23-69

Key: (1). Rocks. (2). Porosity, % (limits of changes). (3). Sands, aleurcolites. (4). Sandstones. (5). Pebbles. (6). Clays. (7). Argillite. (8). Marls. (9). Limestone, dolomite. (10). Cretaceous. (11). Hydrochemical precipitation (anhydrite, gypsum, rock salt). (12). Siliceous rocks (diatomite, tripoli/tripolites, etc. (13). Benthic sedimentations oceanic (clayey). (14). Soils, different.

Table 8. Density of the typical rock-forming minerals of sedimentary rocks (according to the different authors).

(1) Минералы	(2) Плотность, г/см <sup>3</sup>
Группа каолинита (3) . . . . .	2.6
Группа галлуазита (4) . . . . .	2.0-2.5
Группа монтмориллонита (5) . . . . .	2.1-2.6
Гидроксиды (лимонит, гетит и др.) (6) . . . . .	3.8-4.4
Группа кварца (7) . . . . .	2.3-2.8
Кальцит (8) . . . . .	2.7
Доломит (9) . . . . .	2.9
Ангидрит (10) . . . . .	2.9
Гипс (11) . . . . .	2.3
Галит (11a) . . . . .	2.1-2.2
Тяжелая фракция терригенных пород (пирит, магнетит, гранат и др.) (12) . . . . .	3-5

Key: (1). Minerals. (2). Density, g/cm<sup>3</sup>. (3). Group of kaolinite. (4). Group of halloysite. (5). Group of montmorillonite. (6). Hydroxides (limonite, goethite, etc.). (7). Group of quartz. (8). Calcite. (9). Dolomite. (10). anhydrite. (11). Gypsum. (11a). Halite. (12). Heavy fraction of terrigenous species/rocks (pyrite, magnetite, garnet, etc.)

Page 66.

For all these species/rocks changes in their density both between the different petrographic groups and within the separate petrographic groups are caused first of all by a change in the porosity of the rocks (see Fig. 15). Porosity and also density depend, first of all, on the conditions of forming the species/rocks. Data interesting in this respect are cited in work of E. A. Prozorovich (1956). He indicates that the clays of continental origin are denser than the clay of maritime tanks. He perceives the reasons for this in the considerably smaller electrolytic coagulation of clays, they are

deposited/postponed under the continental conditions. Difference in the density of the clays of continental and maritime origin, which directly change each other in the section/cut, judging by two brought E A. Prozorovich to examples, can reach  $0.1 \text{ g/cm}^3$ .

Furthermore, the surface and density of sedimentary rocks affect different geological factors, the effect of which the rock underwent within entire period of its existence. A number of these factors includes:

1. The load of overlying layers (geostatic pressure) under the conditions of platform regime/conditions leads to the decrease in porosity to values close to the zero. This limit of diagenetic consolidation usually is reached at the total power of the cap rock of the order of 3 km. The decrease of porosity is accompanied by the particle recrystallization of species/rock and by an increase in its density. Rate of change in the porosity and density with the depth is retarded. Especially graphic and typical the character has a change in the density and porosity with the depth for the clays, which in this sense can be considered peculiar "geologic barometer" (Fig. 20). The diagenetic consolidation of the majority of the rocks, apparently, has the irreversible character, i.e., it is retained during the removal of geostatic load for example during the washout of the covering thicknesses.

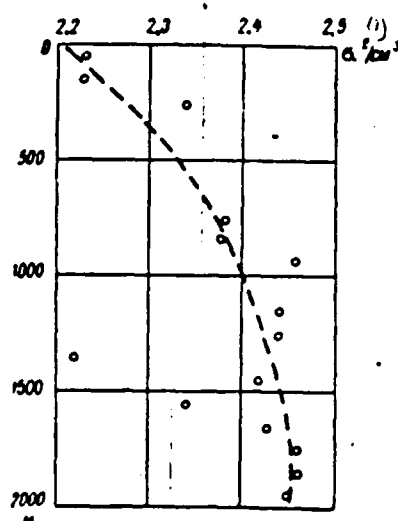


Fig. 20. Increase in density with depth for clays of Karagan stage in the Grozny region. According to O. A. Swank (1947).

Key: (1). g/cm³.

Page 67.

Widespread, but clearly erroneous is opinion about direct bond of density of sedimentary rocks with their geologic age, i.e., about the fact that more ancient species/rocks are denser. This bond, however, is straight line, but indirect - through the depth of bedding. The sedimentary rocks on the slopes of Precambrian shields, which were being placed near the surface during their entire geologic history, are characterized by frequently relatively low density, although they sometimes have very ancient age. As the example let us point out the Cambrian clays of Leningrad region, which slope on the surface and having very low density  $\sigma=2.15$  g/cm³ (Andreyev, 1938). In the regions with great thickness of sedimentary rocks the petrographically



same-type species/rocks of different age, for example the clays, opened by blowholes at the same depths, frequently have very close density (Prozorovich, 1954).

2. Folding, which leads in geosynclinal regions to intensive decrease in porosity and, respectively, to increase in density of species/rocks. By example can it serves the change in the density of the productive carboniferous thickness of the average/mean Carboniferous period from the periphery to the center of the Hercynian geosynclinal region of Donbass, established by N. N. Samosonov and A. T. Donabedov by means of the comparison of the average/mean values of the density of species/rocks on the cores of the numerous blowholes of this region (Fig. 21). In this case it seemed that in the central regions of the folding region of Donbass as a result of metamorphism the species/rocks of the middle Carboniferous period underwent so intensive a consolidation, that their porosity throughout entire section/cut was close to zero and in them density variations with the depth, characteristic for the sedimentary rocks of platform regions (Fig. 22), is not observed.

3. Oscillatory motions, which are accompanied by formation of intensively expressed tectonic susceptibility to cracking of sedimentary rocks. Tectonic susceptibility to cracking appears in all species/rocks, but it is retained well, apparently, only in the layers it is sufficient rigid "competent" rocks. The same are the carbonate rocks (limestones, dolomites), marls, sandstones, etc. In the plastic

rocks, for example in clays, tectonic susceptibility to cracking is retained poorly and, after arising, it can in the course of time vanish (coverage of cracks). However, in such species/rocks tectonic susceptibility to cracking can be sufficiently showed in the geosynclinal regions, in the presence of the repeating until recently tectonic shifts.

Tectonic susceptibility to cracking is developed in presence both macrojoints of significant width, expressed by centimeters, noted with geological surveying works and microcracks (millimeters, share of millimeter), studied in ground joints under magnifying glass and microscope.

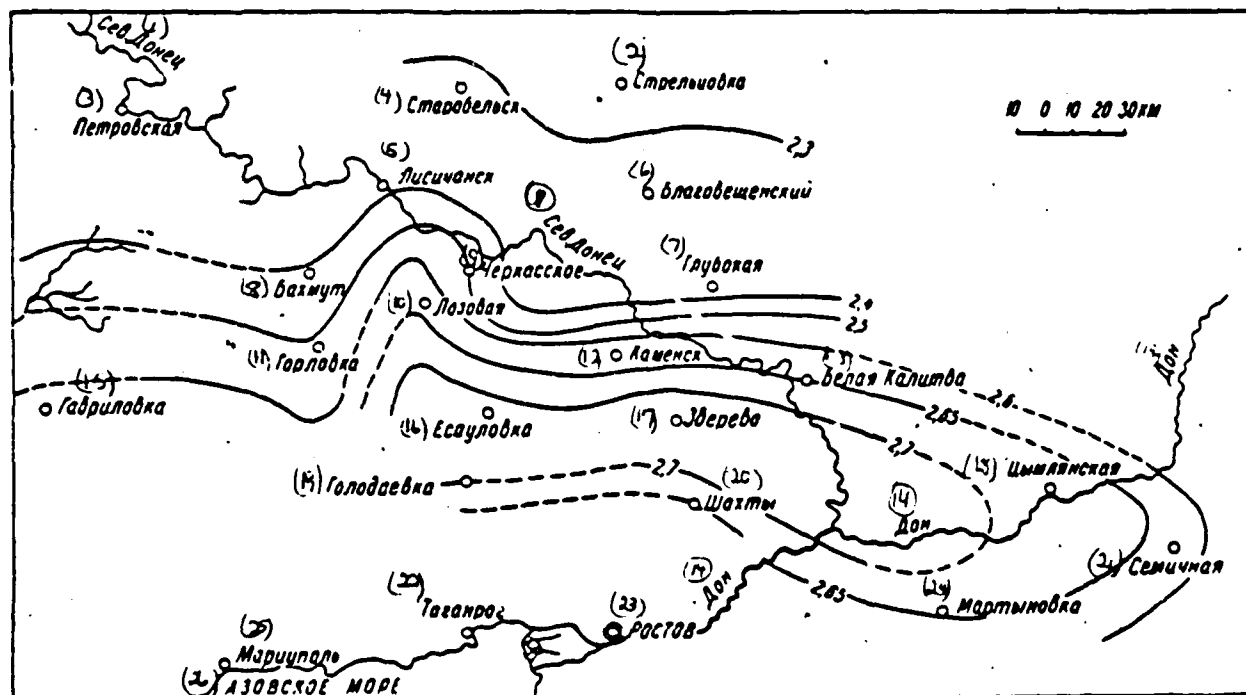


Fig. 21. Diagram of isodensities of rocks of the Carboniferous period of Donbass. According to A. T. Donabedov.

Key: (1). Northern Donets. (2). Strel'tsovka. (3). Petrovskiy. (4). Starobel'sl. (5). Lisichansk. (6). Blagoveshchenskiy. (7). Gluboka. (8). Bakhmut. (9). Cherkasskoye. (10). Loavaya. (11). Gorlovka. (12). Kamensk. (13). White Kalitva. (14). Don. (15). Gavrilovka. (16). Yesaulovka. (17). Zverevo. (18). Tsymlyanskaya. (19). Goladayevka. (20). Shakhty. (21). Semichnaya. (22). Taganrog. (23). Rostov. (24). Martynovka. (25). Mariupol'. (25). Azov Sea.

Page 69.

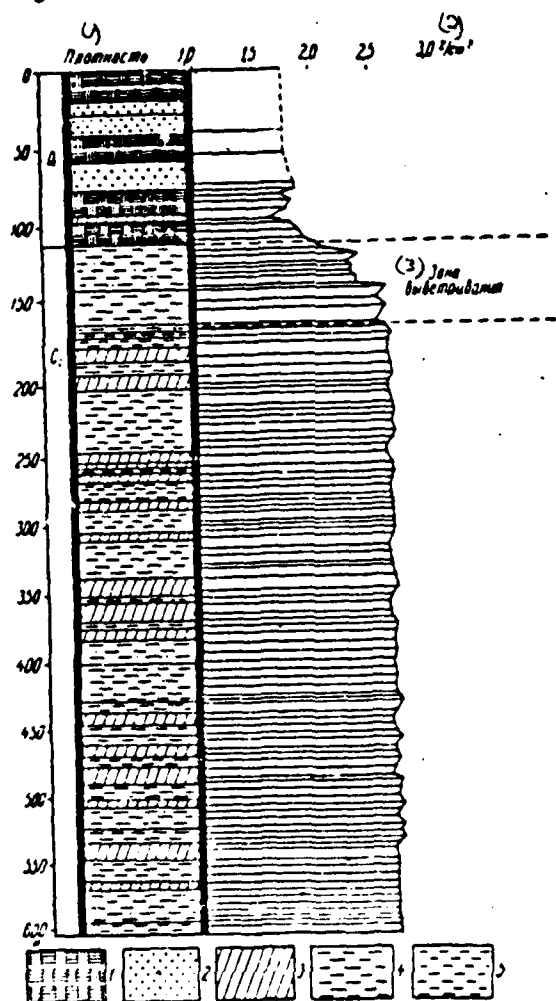


Fig. 22. Graph of density of rocks on Razdorsk blowhole in Donbass (according to N. N. Samosonov). Below the zone of the crust of wind erosion the density practically and does not vary with depth. 1 - clay; 2 - sands; 3 - sandstones; 4 - slates; 5 - sandstone schist. Key: (1). Density. (2). g/cm<sup>3</sup>. (3). zone of wind erosion.

Page 70.

Only the part of the tectonic cracks proves to be that filled with

cement, another part (frequently significant) is open, gaping, filled with gas, water or oil. This is how D. V. Nalivkin describes the tectonic susceptibility to cracking of the carbonate rocks of Russian the platform: "Vacuums take the form of the network/grid of the cracks, which communicate. Most frequently they are formed on the spot of the bend of dense limestone. Such vacuums contain the large quantities of gas, oil and water" (Nalivkin, 1958, Vol. I, pg. 141).

Bond of increased tectonic susceptibility to cracking with sections of greatest bending of layers of carbonate rocks can be confirmed by many examples. Thus, A. G. Mileschina (1953), in studying the ground joints more than 2700 samples of the carbonate rocks of Samarskay Luka and Saratov region, studied the distribution of the coefficient of susceptibility to cracking, i.e., the ratio of the summary area of cracks in the limits of ground joint to the area of ground joint. It seemed that the maximum values of the coefficient of susceptibility to cracking correspond to steep/abrupt limbs and arches of the local oil bearing structures of these regions, i.e., to the sections of the greatest bending of the layers of the carbonate rocks. Interesting is the example described by V. I. Smirnov (1957, pg. 106), the stockwork zones of polymetallic ores in the zone of crushing the carbonate rocks, confined to the place of the flexure-shaped bend of layers.

4. Conversion of sedimentary rocks in the crust of wind erosion, which is propagated frequently to tens of meters is lower than level

of denudation shear/section, it is characterized, as a rule by reduction in density of species/rocks. About this testifies the presence of the "zone of low speeds" (ZMS), isolated everywhere with seismic survey works ( $v_p = 300-1000$  m/s), to which from the point of view of gravitational prospecting undoubtedly corresponds the "zone of low density". As N. N. Puzyrev notes, the "highest efficiency of ZMS is most frequently observed for the sandy formations by pi of the weak water saturation of the latter" (Puzyrev, 1960). In these conditions the power/thickness ZMS can reach 100 and more than meters. In Fig. 22 it is given the thickness of the wind-blown zone in the condensed sandy-clay depositions of the average/mean Carboniferous period of Donbass.

From physicommechanical side process of wind erosion is characterized by strong crushing of species/rocks, by increase in their susceptibility to cracking and porosity, by intensive penetration of ground water in is increased pore space of species/rocks.

From geochemical point of view well defined crust of wind erosion of sedimentary and other rocks is characterized by the formation and wide development in it of dispersed-colloidal systems with enormous specific surface ( $6 \cdot 10^4 - 1 \cdot 10^5$  cm<sup>2</sup> on 1 cm<sup>3</sup> of substance), i.e., with very large microporosity and low density.

Very interesting from point of view of gravitational prospecting

growth, connected with processes of erosion, accompanied by dissolution and hydrolysis of silicate sedimentary rocks and by emergence of colloidal and metacolloidal forms of silica, is formation of silicified rocks, which have usually very high porosity (see Table 8) and low density.

Page 71.

In the presence of consedimentary (formed in the process of the formation of their component/term precipitation) dome-shaped folds in the thicknesses of terrigenous species/rocks, the crest parts of these folds, which were being always expressed (after their successive "renovation" by oscillatory motions) by convex relief forms and, consequently, the undergoing the intensive effect of agents wind erosion, can be characterized by increased thickness of the siliceous rocks. This phenomenon in actuality is observed in the crest parts of the series/number of the local structures of the southwestern part of the western-Siberian lowland, than, apparently, and is explained the significant (to 0.5 g/cm<sup>3</sup>) reduction in the average density of tertiary species/rocks, observed in the crest parts of the structures (Umantsev, 1959) indicated.

Set of factors indicated above leads to the fact that under varied conditions density of one and the same sedimentary rocks can be very different (this position we develop below in the concept about laminar zonality of density). We thus far note this fact in order to explain the large range of changes of the density of sedimentary rocks

in Table 9.

From Table 9 we see that different sedimentary rocks frequently sufficiently considerably differ in their density. The high density of anhydrites and carbonate rocks and the very low density of the siliceous rocks (silicifites according to G. I. Teodorovich) turns attention respectively.



Table 9. Density of sedimentary rocks (generalization of the given numerous authors).

(1) Породы	(2) Плотность, г/см <sup>3</sup>	
	(3) Средняя	(4) Пределы изменений
Глины, аргиллиты (5) . . . . .	2.3	1.6—2.8
Пески, алевролиты (6) . . . . .	2.1	2.0—2.4
Песчаники (7) . . . . .	2.3	2.1—2.8
Мергели (8) . . . . .	2.2	2.0—2.6
Известняки, доломиты (9) . . . . .	2.5	2.1—2.9
Мел (10) . . . . .	2.2	1.8—2.6
Каменная соль (11) . . . . .	2.2	2.1—2.3
Гипсы (12) . . . . .	2.3	2.1—2.5
Ангидриты (13) . . . . .	2.8	2.4—3.0
Кремнистые породы (диатомиты, трепелы, опоки и т. д.) (14) . . . . .	1.2	0.8—1.6
Донные осадки океанические (глинистые) (15) . . . . .	1.8	1.7—1.8
Почвы разные (16) . . . . .	2.0	1.5—2.4

Key: (1). Rocks. (2). Density, g/cm<sup>3</sup> (3). It is average/mean.

(4). Limits of changes. (5). Clays, argillite. (6). Sands, aleurolites. (7). Sandstones. (8). Marls. (9). Limestone, dolomite. (10). Cretaceous. (11). Rock salt. (12). Gypsum. (13). Anhydrite. (14). Siliceous rocks (diatomite, tripoli/tripolites, argillaceous clay, etc.). (15). Benthic sedimentations oceanic (clayey). (16). Soils, different.

Page 72.

The low density of species/rocks is connected with their high porosity and low density of their mineral skeleton. The relatively small content of the siliceous rocks in the section/cut of the thicknesses of sedimentary rocks can noticeably decrease the average density of this thickness.

Laminar zonality of density of species/rocks. Yet so had long

ago been it not considered that for the thickness of sedimentary rocks from the point of view of exploration geophysics completely acceptable physical model is the model of the "laminated medium", when this thickness is consisting of the layers; physical properties of which are assumed to be constants (in the limits of entire layer) or varying very gradually. Specifically, from these assumptions, until now, usually is satisfied the geologic interpretation of the given geophysical methods, including gravimetric prospecting. However, the practice of geological-geophysical investigations and corresponding factual data about the physical properties of sedimentary rocks show that in many instances the model of laminated medium is insufficient for the complete and correct interpretation of the results of methods. In actuality separation of the thickness of sedimentary rocks to the layers or to the separate complexes in the section/cut on the vertical line gives only first approximation to a correct physical model of this thickness. In many cases it is necessary this approximation/approach to make more precise and to introduce the second approximation/approach taking into account the phenomenon of the laminar zonality of physical properties - their change on the lamination, caused by the set of tectonic and facies conditions.

During oscillatory motions, bending and warping/buckling of layers of sedimentary rocks in them appears tectonic susceptibility to cracking, is most which intensively develops in arches/summaries and on steep/abrupt edges of structures. In the crest parts of the consedimentary folds the intensive development of secondary siliceous

rocks as a result of the effect of ancient erosion processes for the silicate terrigenous rocks can, as is explained above, be developed. Frequently in the thickness of sedimentary rocks, in the limits of the similar/analogous lithologic-stratigraphic complexes, considered it uniform in the model of the "layered medium", there is observed a facial zonality, regularly connected with the structures and which is developed, for example, in an increase in the total power of sandy layers in the arch of the structure composed by sandy-clay species/rocks.

All these examples show that with structures in many instances can be connected reductions in average density in thickness of sedimentary rocks, which can serve as a reason appearance of minima of gravitational force, this fact can be used during searches for structures method of gravitational prospecting (see Chapter VIII).

Page 73.

## § 12. Density of useful minerals.

Table 10 gives values of density of different ore and nonmetalliferous useful minerals, in connection with searches for which is used or can be used method of gravitational prospecting.

The table shows those useful minerals, which not only differ in density from their accomodating rocks, but also occupy sufficiently large volumes, i.e., their effect/action under favorable conditions

can directly affect gravitational field.

§ 13. Basic problems and the objects of gravitation prospecting works.

Study of plutonic structure of the earth's crust. This problem is solved in essence by the complex of two geophysical methods - gravitational and seismic.

Table 10. Density of useful minerals (according to the different authors).

(1) Полезные ископаемые	(2) Плотность, г/см <sup>3</sup>	
	(3) Средняя	(4) Пределы изменения
(5) Рудные		
Железные руды (6) . . . . .	~4	—
Хромит (7) . . . . .	~4	—
Колчеданные руды (8)		
медные (9) . . . . .	~5	—
серные (10) . . . . .	~4	—
Полиметаллические руды (свинца, цинка) (11)		
первичные (12) . . . . .	~4	—
окисленные (13) . . . . .	—	0.8—2.0
Шеелит (14) . . . . .	~6	—
(15) Нерудные		
Газ (16) . . . . .	—	0.001—0.002
Нефть (17) . . . . .	0.9	0.7—1.1
Уголь (18)		
антрацит (19) . . . . .	—	1.4—1.5
каменный (20) . . . . .	—	1.3—1.4
бурый (21) . . . . .	—	0.8—1.2
Торф (22) . . . . .	0.7	—
Минеральные соли (23)		
галит (24) . . . . .	—	2.1—2.2
сильвин (25) . . . . .	2.0	—
карналлит (26) . . . . .	1.6	—
Корунд и алмаз (27) . . . . .	—	3.0—4.0
Флюорит (28) . . . . .	~3	—
Барит (29) . . . . .	~4	—

Key: (1). Useful minerals. (2). Density g/cm<sup>3</sup>. (3). Average/mean. (4). Limits of change. (5). Ore. (6). Iron ores. (7). Chromite. (8). Pyritic ores. (9). copper. (10). sulfuric. (11). Polymetallic ores (lead, zinc). (12). primary. (13). Oxidized. (14). Scheelite. (15). Nonmetalliferous. (16). Gas. (17). Oil. (18). Coal. (19). anthracite. (20). rocky. (21). brown. (22). Peat. (23). Mineral salts. (24). halite. (25). sylvite. (26). carnallite. (27). Corundum and emery. (28). Fluorite. (29). Barite.

Page 74.

The interpretation of gravity anomalies with the solutions of this

problem is conducted as before setting of seismic works, and in this case it is used for the subsequent planning/gliding of the latter, after all after their setting - for explaining the structure of the earth's crust in the sections, situated between the seismic profiles, for most substantiated interpolation of the depths of section in the limits of these sections.

As we saw in § 9, the structure of earth's crust is very heterogeneous and is characterized by sharply pronounced relief of deep interfaces of density; it causes the presence of very intensive regional changes in gravitational field, which are expressed in some places hundred milligal. The same are the sections of transition from continental type earth's crust to oceanic type of crust, which is located usually in the zone of the transition of edge/boundary epicontinental seas into the deep-water oceanic tanks and partially appearing sometimes in the littoral land sections.

In these sections occurs gradual tapering of granite layer and uplift to Mohorovicic's discontinuity to side of the ocean, which in gravitational field causes an increase of average/mean level of gravity anomalies from close to zero values above continent to 350-450 mgal above ocean. This increase occurs in the strip with a width of 200-300 km (for the example see the edge/boundary parts of the gravitational profile in Fig. 212).

Within limits of both continents and oceans average/mean level of

gravity anomalies in different sections also proves to be different, moreover these changes are correlated with changes in power/thickness of terrestrial crust, established/installed deep to seismic soundings. This gives the possibility to use data of gravimetry, together with seismic data, with the study of the deep structure of the earth's crust.

For interpretation of gravity anomalies during the study of deep structure of earth's crust data of photographings of scale 1:1000000-1:5000000 or strip surveys with step/pitch of 5-10 km are necessary.

Page 75.

Tectonic zoning of geosynclinal and platform regions. Tectonic zoning is, according to V. V. Belousov, the "classification of the sections of the earth's crust according to the signs of their structure and history of structural development" (matgrass, 1953, pg. 521). Such sections they present: in the geosynclinal regions - large troughs and uplifts, and in their limits - separate large/coarse anticlinorium and to anticline, the zone of faults, magmatic complexes and so forth; in the platform regions - structures of the first order (arches and of basin/depression) and the second order (arches and of basin/depression) and the second order (rises and troughs) on different horizons/levels in the limits of sedimentary cover and over the surface of basement; within the basement - sections of different age, and in the limits of the latter - basic folded zones, magmatic

complexes, large/coarse zones of faults, etc. Gravitational prospecting - leading from the geophysical methods, used with the tectonic zoning of geosynclinal regions; it is great the value of this method and with the tectonic zoning of platform regions.

Large area of anomalies connected with these structures, commensurate with area of structures, is a common special feature of manifestation of regional structures indicated above in gravitational field. By the sign, the intensity and other signs these anomalies are distinguished between themselves. The largest/coarsest structural elements of geosynclinal regions (uplift/rise, downwarps/troughs) usually have "negative" expression in the gravitational field, i.e., uplifts/rises are expressed by minima, and downwarps/troughs - by relative maximums of gravitational force, moreover the intensity of these anomalies is expressed by many by ten milligal.

These special features of anomalies are caused by deep structure of earth's crust. First-order structures in the limits of platform regions more frequently have not inverse, but straight/direct expression in the gravitational field (uplift they are expressed by maximums, downwarps/troughs - by minima), moreover the intensity of anomalies is less than in the geosynclinal regions. In many instances both in the geosynclinal and in the platform regions in the gravitational field sufficiently distinctly are noted separate large/coarse structural elements - anticline, zones of faults, etc. The intensity of corresponding to these structures anomalies is



usually expressed by the milligals, sometimes first by ten milligal. These structures have in certain cases straight line, in others - "negative" expression in the gravitational field, moreover in each specific case these relationships/ratios find the necessary explanation under the specified physico-geologic conditions. The analysis of these conditions and a number of examples of regional anomalies is given in § 52-53 of Chapter VII.

With tectonic zoning gravitational maps/charts of scale 1:200000-1:1000000 are used.

Searches for oil and gas-bearing structures. In many oil and gas-bearing regions gravitational prospecting widely and successfully is used for the straight/direct searches for structures (geosynclinal regions, deep basins/depressions of platform regions). Some structures (salt/hydrochloric domes, steep/abrupt anticlinal folds) are separated/liberated by very characteristic and intensive (many milligals, ten milligal) gravity anomalies. During the searches of this type of structures gravitational prospecting comes forward "out of the competition" with other geophysical methods.

Page 76.

The matter concerning the searches for standard platform dome-shaped structures is more complex. These structures are not always distinguished as gravimetric prospecting, but even if they are separated/liberated, then by the anomalies of weak intensity (one

milligal), the character of the anomalies observed above them indicating that they are frequently caused by the not so much structural relief of layers, as by laminar zonality of the density of species/rocks. In more detail these questions are presented in Chapter VIII, where there are given numerous examples of the gravity anomalies above hods.

Cross dimensions of such anomalies, commensurate with dimensions of structures, comprise usually from 5-10 to 20-30, sometimes more than kilometers. The sign of anomalies occurs both positive and negative; intensity - from ones milligal to several ten milligals. Utilized scales of gravitational photographings - 1:100000 - 1:200000.

Investigation of carboniferous tanks. In the carboniferous tanks gravitational prospecting is used commonly for the purpose of the solution of structural-geologic problems: the refinement of the boundaries of tanks, the study of the relief of the surface of productive thickness, the determination of its power/thickness, liberation/precipitation and contour mapping of separate structural elements, zones of tectonic disturbances/breakdowns, etc. In certain cases gravitational prospecting was used sufficiently successfully for the straight/direct searches for powerful/thick lignitic beds.

Gravity anomalies, which characterize entire as a whole structure of carboniferous tank, have in number of cases significant amplitude (ten milligal) and sizes/dimensions, which correspond to area of tank.

Folding type tanks are usually characterized by maximums, and the graben-shaped basins/depressions, filled with the slightly dislocated sedimentary rocks, which enclose lignitic beds, by minima of gravitational force. With structural-erosion forms of the relief of folding carboniferous thicknesses they are connected comparatively small in the intensity (milligal several) local variations in gravitational force, which are sometimes developed very it is distinct on the force gradient of gravity. With thick lignite deposits there are connected relative minimums of gravitational force with intensity to several milligal. The examples of gravity anomalies in the carboniferous tanks are given in § 64 of Chapter IX. During the study of carboniferous tanks gravitational photographings of scale 1:200000 extensively are used.

Searches and prospecting of ore deposits. Together with the solution of those structural problem indicated above, gravitational prospecting successfully solves direct prospecting and prospecting problems on the deposits of different ore useful minerals: gland, chromite, pyritic ores, etc.

Page 77.

With the utilization of gravitational prospecting in the ore regions are solved the different structural-geologic problems:  
liberation/precipitation and contour mapping of ore-bearing intrusions, study of their planform and in the section/cut,  
liberation/precipitation and the tracking of contacts and zones of

tectonic disturbances/breakdowns, etc.

Anomalies connected with ore-bearing structures, have high intensity (many milligals, the first ten milligal) with significant area sizes/dimensions in many instances. ore gravity anomalies have very small intensity on the anomaly of the force of gravity (tenth and hundredths of milligal) with small cross sizes/dimensions (first tens of meters) usually. At the same time the intensity of many ore anomalies on the horizontal gradient of the gravity force is very great (to many ten and the first hundred Eotvos). The number of the examples of ore gravity anomalies is given in § 60-62 of Chapter IX.

In the ore search gravitational prospecting are used gravimetric and variometric photographings of large/coarse scales - from 1:25000 to 1:5000, sometimes even 1:2000.

Thus, the range of geologic problems, decided with application of gravitational method, is exceptionally/exclusively great, and character of gravity anomalies being investigated differs in terms of very great variety - in intensity, area of propagation and other special features. These different anomalies are observed, as a rule not in the "pure form", but in complex combinations; the directly interesting us anomaly usually is developed against the background of the associated anomalies.

Page 78.

Chapter III.

## PRINCIPLES OF THE GEOLOGIC INTERPRETATION OF GRAVITY ANOMALIES.

### § 14. Generalities.

Geologic interpretation of gravitational anomalies includes an analysis of laws governing their distribution on earth's surface (and near from it), bonds of regularities with geologic factors and utilization of these bonds for solution of geologic problems. In each specific case it is connected with the specific stage of the geologic study of one or the other region.

Essence of geologic interpretation of gravity anomalies usually can be formulated thus: being based on data of gravitational photographing, on given earlier carried out geological-geophysical works, on experiment of gravitational photographings in similar concerning geologic structure regions, to solve specific problems and questions, which stand in this stage of studies of geologic structure of region being investigated.

During geologic interpretation of gravity anomalies business in many instances is limited only to establishment of probable location in plan/layout of one or the other structural elements, for example domes, rip masses, anticlines, zones of fault or separate faults, ore bodies, etc. They usually name this geologic interpretation

qualitative. In other cases, besides the establishment of the location of one or the other geologic bodies, is determined the depth of bedding, form and sizes/dimensions of these bodies by executing quantitative mathematical calculations, initial data for which present these or other the special features of the distribution of the gravity anomalies being investigated. This there will be the quantitative geologic interpretation of gravity anomalies.

Very frequently in exploration geophysics instead of the term "geologic explanation" there is used the term "geologic interpretation" or simply "interpretation" (from Latin inter-pretatio - explanation, interpretation).

Page 79.

In the latter version this term, in view of its brevity and wide use, can be acknowledged completely acceptable, especially with the additional determination - qualitative interpretation or quantitative interpretation of anomalies.

Let us note now following fact, which must be always had in mind during evaluation of results of gravimetric prospecting: the conclusions based on geologic interpretation of gravity anomalies have, as a rule, not an absolute, but conditional-probable sense, just as conclusions made according to other geophysical methods and according to geologic observations.

Actually, we build geologic map/chart (or geologic section/cut) on measuring of elements of bedding of rock on exposures, we do make any conclusion according to gravitational or other geophysical data, we always construe factual data, assuming the validity of some conditions, with observance of which our constructions and conclusions/derivations are most probable, close to authenticity. during the geological-geophysical constructions a number of such conditions includes: the possibility of interpolating the elements of the bedding of the lithologic and stratigraphic boundaries used between the exposures or the productions/consumptions under the assumption of the absence between them of tectonic disturbances/breakdowns; the real existence of tectonic disturbances/breakdowns under the assumption of their presence and so forth; conformity to the reality of the predicted physical model of geologic medium and assumptions done during the construction of this model during the interpretation of gravitational and others geophysical data.

Let us examine now principles and basic content of qualitative and quantitative geologic interpretation of gravitational anomalies with proper circumstance.

§ 15. Qualitative geologic interpretation of gravity anomalies.

Qualitative geologic interpretation of gravity anomalies is realized in all cases - with respect to results of gravitational

photographings of any scale, any ultimate purpose. It must be realized via the joint operation of geophysicists and geologists, who investigate one or another region, who decide one or the other geological problem.

Page 80.

During qualitative geologic interpretation they are established: 1) probable geologic factors, which affect anomalous gravitational field, and also to results of other geophysical methods, if same were used in region being investigated; 2) location of geologic structural elements or ore bodies, whose presence can be assumed according to results of gravitational prospecting; 3) regions or sections, in limits of which, in connection with one or the other geologic task, is required setting more detailed gravitation prospecting and other geophysical works; 4) point and sections for laying of drill holes and mine workings, which have as a goal check and refinement of drawn according to data of gravitational prospecting conclusions; 5) possibility, worthwhileness, condition and degree of detail of quantitative interpretation (interpretation) of gravity anomalies.

In general case it is possible to indicate following four basic varieties of geologic factors which cause the presence and character of gravity anomalies:

1. Structure the thickness of sedimentary rocks. Everywhere, with exception of the regions of crystalline shields, above the



substructure will lie the stratum of sedimentary rocks. This stratum, as a rule, is nonhomogeneous in the density, the interfaces of density within the thickness frequently lying non-horizontally; the laminar zonality of the density (see § 11, Chapter II) occurs also. In view of these facts nonhomogeneous geologic structure the thickness of sedimentary rocks frequently conditions on the earth's surface the presence of one or the other gravity anomalies. In the regions, where there is great thickness of sedimentary rocks, differentiated on the density, which is characterized by the presence of the sharply pronounced structural forms with the large amplitude, these structures can condition intensive (ten milligal) gravity anomalies. In certain cases sufficiently intensive anomalies can be connected with the laminar zonality of density, for example, with significant changes in the lithofacies composition of sedimentary rocks.

2. Relief of surface of crystalline basement. The fact that the crystalline rocks into the general/common denser than sedimentary, conducts to the fact that the relief of the surface of basement has a noticeable, sometimes significant effect on gravitational field. This effect is developed more clearly and definitely in such cases, when basement is complex by rocks by comparatively uniform dense, and its covering sedimentary thickness - by uniform lighter.

3. Internal structure of crystalline basement. The rocks of basement considerably are distinguished by the density (see § 10, Chapter II); therefore, the internal structure of basement in many

regions it conditions on the earth's surface the presence of numerous intensive gravity anomalies.

Page 81.

The effect of the petrographic and density heterogeneity of basement appears very sharply in those regions, where the basement will lie on the relatively small depth (to 2-3 km) and is the ancient rocks (Precambrian, the lower Paleozoic era), as a rule, intensively dislocated. This effect considerably is weakened/attenuated and it becomes relatively small in the regions, where the basement will lie on the large depth and is middle- and upper-Paleozoic or younger rocks, comparatively little dislocated and more uniform in density.

4. Deep structure of earth's crust. As it will be in detail presented in chapter of the VII, the effect nonhomogeneous deep structure of the earth's crust is very intensively showed in the tectonically active regions (geosyncline, activated/promoted platform sections). Here it is the basic factor, which determines the character of anomalous gravitational field. In the typical platform regions the effect of the deep structure of the earth's crust appears comparatively weakly, also, in the most stable sections, for example on the Precambrian shields, almost completely it is absent in the anomalous gravitational field.

Gravitational effect of each of factors examined depends substantially on general geologic conditions of region being

investigated. Under some conditions the effect of any of these factors proves to be very large, in others - by very small. These general geologic conditions for the regions investigated by gravitational prospecting are usually known, that also allows to even before setting of gravitation prospecting works have in the majority of the cases the sufficiently reliable general/common judgment about anomaly-forming factors basic in terms of the value in this or another region. However, this question certainly should be made more precise, possessing the data of gravitational photographing, comparing their results with the available geologic maps/charts and the tectonic diagrams, which relate to the territory being investigated.

A comparison of gravitational and geologic maps/charts is always made during qualitative interpretation of gravity anomalies. One ought not, however, to think that this comparison always gives the strong/durable basis of this interpretation; it can seem that the gravitational map/chart shows the arrangement of anomalies, which is not completely coordinated with the outlines of structures, adjusted along the geologic map/chart.

Is feasible another case - anomalies on location are linked with structures, but sign of anomalies is not bound to character of structures, for example, to uplift/rise of compact rocks corresponds not maximum, but minimum of force of gravity, etc. In all similar cases the basic character of gravitational field is determined by the structure not of close to the surface of the horizons/levels rocks,

shown on the geologic map/chart, but by the structure of deeper horizons/levels of the earth's crust.

*page 82.*

In initial development period of gravitational method effect on anomalous gravitational field of deep structure of earth's crust usually was underestimated, that frequently they led to different misunderstandings and errors. Representative in this respect is the work of Academician A. D. Arkhangel'skiy, "Geology and Gravimetry", which was published in 1933, in which the geologic sense of gravity anomalies was investigated only via the comparison of gravitational and geologic maps/charts. In this book A. D. Arkhangel'skiy stated/established that in the mountain regions of Bouguer's anomaly they systematically give the picture which is not compatible with the geologic structure of the upper layers: in the places of uplifts/rises the minima usually are observed; in the places of downwarps/troughs - maximums gravitational force. At the same time the anomalies of Faye by nature usually are linked well with the geologic map/chart, showing maximum on the uplifts/rises and minima in the downwarps/troughs. From this A. D. Arkhangel'skiy did the conclusion that during the geologic interpretation of gravity anomalies the latter should be examined in the reduction of Faye, but not Bouguer. Now we know that this conclusion/derivation, which in the course of a number of summers/years followed some geologists geophysics and which was reflected and in educational literature on gravitational prospecting (Sorokin, 1953) he is erroneous: the nonconformity of Bouguer's anomalies to geologic map/chart in the

mountainous regions is explained by the fact that here the basic effect on the gravitational field proves to be the deep structure of the earth's crust. However, conformity of the anomalies of Faye to geologic map/chart in actuality not straight line, but indirect. These anomalies first of all are connected with the relief (see S4), and with the geologic map/chart they are bound in essence only inasmuch as, since in the tectonically active regions the large/coarse positive structural forms (anticlinorium) are frequently expressed by the uplifts/rises of relief, and downwarps/troughs - by reductions in the relief.

As it will be shown in Chapter VII, structural relief of deep interfaces of earth's crust is connected with paleotectonic special features of geosynclinal regions; to a certain extent this conformity is revealed also in platform regions. Therefore necessary element during the qualitative geologic interpretation of the results of regional gravitational photographings is familiarization with the history of geologic development and comparison of gravitational map/chart with the paleotectonic diagrams of the region (in the presence their) being investigated.

Gravimetric prospecting works are usually preceded or accompanied by works on magnetic prospecting, sometimes and according to other geophysical methods (electrical prospecting, seismic survey, etc.). The results of these works must be considered during the geologic interpretation of gravity anomalies. If work according to other

methods is carried out after gravitation prospecting, then in their this case one should draw for the critical overestimation of those conclusions/derivations, which in their time were done according to the data of gravitational prospecting. Let us point out some facts, which must be had in mind during the joint geologic interpretation of the results of gravitational prospecting and other geophysical methods.

Most frequently it is necessary to conduct joint examination of given gravitational and magnetic surveys. in this case it is necessary to, first of all, have the fact in mind that if the gravitational and magnetic anomalies are caused by one and the same geologic object, then they usually completely do not coincide in the location, the dimensions, etc., but they sometimes differ very considerably. The reason for a similar nonconformity is explained by different analytical nature also of each anomalies.

Page 83.

Above, in § 13 of Chapter II, we saw that in the case of two-dimensional task during vertical magnetizing, when between elements of magnetic and gravitational anomalous field especially simple correlations are obtained, the vertical component of  $Z$  of magnetic field is expressed not through gravitational force, but through its lapse. Based on this already it is possible to assume that the magnetic anomalies have more complex character and more clearly they react on the part of the geologic structure of the upper

part of the section than gravity anomalies. Subsequently, presentation this idea will be reinforced by the theoretical calculations and the practical examples, from which it will possibly explain the interrelations of gravitational and magnetic anomalies in such a case, when they are caused by effect/action of one and the same geologic body; in the first approximation, it is possible to consider (for the linearly elongated anomalies) that this interrelation is the same as between the anomaly of gravitational force and its lapse  $W_{\Delta}$ , or "curvature"  $W_{\Delta}$ .

Comparison of data of gravitational and magnetic surveys makes it possible in many instances to do confident conclusions about geologic nature of gravity anomalies. For example, in the platform regions conformity to the intensive gravitational and intensive magnetic anomaly testifies, as a rule, about the fact that the gravity anomaly, just as magnetic, is caused by the internal structure of basement. Actually, intensive magnetic anomaly under similar conditions cannot be connected with the structure of sedimentary rocks, since these rocks in the platform conditions usually are in practice nonmagnetic, and it cannot be connected with the deep structure of the earth's crust, since it generally sufficiently weakly is developed in the magnetic field, and in the platform conditions in practice in no way it is developed; the relief of the surface of the foundation in the platform conditions does not usually form the such sharp forms, which could serve as a reason intensive gravitational and magnetic anomalies.

If gravitational and magnetic anomalies have in plan/layout linearly elongated form they present part of regularly arranged/located system of anomalies, then it is possible to completely confidently consider that these anomalies usually characterize folding structures within basement. At the same time, as shows the comparison of gravitational and magnetic cards with the structural maps/charts on the horizons/levels in the sedimentary cover of platform regions, the distribution of the anomalies of the type indicated and linear structures of the second order reveals the explicit interrelation, which is developed in the coincidence of the course and location of many anomalies and structures. the detailed study of this problem shows that the conformity - not straight line indicated, but an oblique one: anomalies are connected with the structure of basement, but the latter proves to be connected with the regime/conditions of the oscillatory motions, as a result of which linear structures in the thickness of the sedimentary rocks of the platform regions (we let us return to this question in Chapter VII) were formed. Large with the magnetic anomalies in such cases, when gravitational prospecting is placed in connection with the searches for the ore deposits (examples of this analysis we we bring in Chapter IX).

Page 84.

Significantly makes more precise presentations/concepts about geologic nature of gravity anomalies their comparison with results of



seismic survey or electrical prospecting, conducted in territory of gravimetric prospecting works. They indicate in many instances completely definitely the bond of gravity anomalies with one or the other structures - uplifts/rises or downwarps/troughs on the horizons/levels in the thickness of sedimentary rocks or over the surface of basement, with the tectonic disturbances/breakdowns, with the ore deposits (for example, according to the data of the method of the combined electroprofiling or natural field).

Cases occur, when presence of straight/direct geologic information according to very limited number of sections almost or even entirely without utilization of other geophysical methods is sufficient for explaining geologic nature of vast set of gravity anomalies, which possess one or the other characteristic features.

As example let us point out gravity anomalies above the salt-dome structures of the Caspian Sea region basin. The experimental works, set as early as 1925 by V. B. Numerov (1931) on some known structures, showed that above them are obtained the characteristic minima of gravitational force, that, after obtaining such anomalies in the territory of the Caspian Sea region basin, it is possible without any doubt to indicate the sections of finding salt domes. In this case the relationship/ratio is one-to-one: each characteristic anomaly - salt dome. In this way at the present time in the territory of Caspian basin/depression opened more than 500 salt/hydrochloric domes, from which only very small part is thus far

investigated by other geophysical methods and drilling. For the searches for solar domes in the Caspian basin/depression actually it is required no other geophysical methods.

In other regions above salt/hydrochloric domes characteristic gravity anomalies also are observed, but greater partly not so/such definitely and unambiguously expressed and construed as in the Caspian Sea region basin. For the confident liberation/precipitation of salt dome structures in such cases besides gravitational prospecting other geophysical methods, for example seismic survey are used.

During a qualitative geologic interpretation there is given a systematic description of revealed by gravitational photographing of anomalous zones and separate characteristic anomalies, probable geologic nature of described anomalies is indicated. Necessary element of geologic interpretation - the recommendation of further (detailization) gravitation prospecting, geophysical regarding other methods and testing mine-drilling works. One should always approach that so that it would be possible to do the part of these recommendations and to implement already in the process of the flowing field works in order on the basis of the realized recommendations at the end of field season to give the more substantiated and complete geologic interpretation of the results of gravitational prospecting.

Page 85.

Such of strands is completely necessary and it is more easily realized.

during the utilization of large-scale gravitational prospecting for the searches for ore deposits, but it follows as far as possible to put into practice both during the searches for oil and with the regional works. Should be generally underscored the fact that the geologic interpretation of gravitation prospecting and others geophysical data in any way cannot be considered as the certain operation, realized on one and the same material only one time - in the process of laboratory processing/treatment and composition of the flowing report to the party or to the expedition. Accumulation by the region of the new given geologic and geological exploration works being investigated must not only stimulate setting new field works, but also work on the repeated more detailed geologic interpretation of old geophysical data, including data of gravitational prospecting.

As is known, majority of reports of gravitation prospecting parties/batches are completed only by qualitative geologic interpretation of anomalous gravitational field. Nevertheless in a number of cases it proves to be possible the results of gravitation prospecting works to subject also to quantitative geological interpretation. The fundamental bases of quantitative geologic interpretation of the results of gravitation prospecting works are further stated.

§ 16. On the possibility of executing the quantitative geologic interpretation of gravity anomalies.

Physical model of geologic medium.

Possibility of executing quantitative interpretation of gravity anomalies is limited in practice to a number of conditions. Principal of these conditions:

1. The presence is sufficient detailed geologic information about the region of investigation, which allows, with the observance other of conditions indicated below, to formulate the physical model of geologic medium, suitable for the interpretation of gravity anomalies.

2. Sharp preponderance of effect of any one of geologic factors on anomalous gravitational field above effect of other factors. For satisfaction of this condition in practice frequently it is necessary to resort to the methods of transformation of the anomalies, which will be described in Chapter IV. Observance of this condition gives the possibility to do an assumption about the fact that the anomaly being investigated in the specific section is caused by the effect/action only of one geologic body in a number of cases with the interpretation.

3. Consistency of physico-geologic conditions (density distribution, condition of bedding of rocks, etc.), which allows for all same-type anomalies in limits of territory being investigated to use identical methods of interpretation.

4. Large detail and high accuracy of gravitational photographing. In the theory of interpretation it is usually implied that the gravity anomaly being investigated is known how conveniently accurately and besides at any point of its intersecting profile. With the interpretation, as a rule are used the horizontal coordinates of the points of zero values, maximum, minimum and so forth of anomalous curve, the numerical values of maximum and minimum, etc. during the utilization of data of photographing, conducted through the finite interval, it is necessary that this interval would be sufficiently small, as a rule several times of less than the depth of the bedding of the body causing anomaly. The high accuracy of photographing is required also. Therefore,, data of photographings, carried out on the thin network/grid of observations with the old gravimeters of the type SN-3 or GAK-3M, in the majority of the cases are not profitable for the quantitative geologic interpretation. The interpretation in this respect can represent only the very intensive smoothly varying anomalies.

5. The presence of the high-quality theory of interpretation of gravity anomalies, well fitted out to real geologic conditions and tasks, which are placed before gravitational prospecting. To the present time we have only elements of this type of theory in the form of a number of general considerations and particular methods, some of them are very successful and virtually active. As the example it is possible to indicate the method of O. Yu. Schmidt - P. M. Nikiforov

to the interpretation of gravity anomalies on the horizontal gradient of gravitational force for the sloping beds, already several decades very successfully using in the iron-ore regions of type of KMA and Krivoy Rog. A number of such successful methods, unfortunately, until now, is small. For some conditions and tasks of such methods this significantly thus far not at all developed, and limits the possibilities of applying the quantitative interpretation of gravity anomalies.

We mentioned above about utilized with interpretation physical model of geologic medium. Let us pause now at the elucidation of this concept.

Theoretical studies of any phenomenon in geophysics and physics generally prove to be possible if this phenomenon is examined in a somewhat simplified form - if only essential features of this phenomenon, its only essential bonds with other phenomena and processes are allowed. This idealization in the majority of the cases is unavoidable in connection with this that the corresponding mathematical analysis of phenomenon can be carried out in the final form and it is sufficiently simple only with the known simplifying assumptions.

Page 87.

Entire mathematical interpretation of the results of seismic survey is conducted, for example, under the assumption that investigated by this

method elastic waves are propagated into an ideally elastic medium, although some rocks with great approximation only satisfy this assumption. Let us recall another assumption in the electrical prospecting - about finding of one of the electrodes "at infinity", whereas in actuality this electrode it is referred only on 50-100 m of the measuring unit (for example, in the method of electroprofiling). Similar assumptions geophysics it is necessary to make literally at each step/pitch, it is understood, developing in this case a natural feeling of measure.

Thus, physical model of geologic medium - this is certain of its simplified diagram, which makes it possible to produce interpretation of geophysical data, done during its construction simplifying assumptions, by themselves although presenting frequently essential deviation from actual conditions, but nevertheless do not cause the large errors with interpretation. With the interpretation of gravity anomalies most frequently are done the following simplifying assumptions:

1. On the possibility of reducing of the task of interpretation to two-dimensional, i.e., assumption about the fact that the anomalies being investigated are caused by infinitely long bodies with the constant cross section. Below we in the series/number of reasonings and examples will be able to be convinced of the fact that this assumption, at first glance capable of leading with the interpretation to the large errors, in actuality much is more inoffensive - like the

assumption about the infinite electrode in the electrical prospecting. At the same time this assumption leads to enormous simplification in all calculating operations with interpretation, without which very interpretation frequently not of mole to be actually maintained.

2. On constant excess density of causing gravity anomalies geologic bodies. This condition in certain cases completely satisfactorily corresponds to actual conditions, it is sometimes only very rough approximatic to reality. Assumption about the constant excess density considerably simplifies and covers interpretation. However for some bodies it is possible without the special complications to introduce assumption about a linear change in the excess density of bodies with the depth (usually occurring case of density variation in the sedimentary rocks).

3. With interpretation of anomalies of force gradient of heaviness in the case of two-dimensional task assumption about infinite propagation of disturbing bodies at depth frequently is done. This assumption simplifies the interpretation and does not lead to the large errors. In the presence of the interpretation of the anomalies of the force of gravity  $\Delta g$  of this type the assumption in the case of the two-dimensional task of making is impossible (under these conditions  $\Delta g$  it goes to infinity).

Page 88.

4. Assumption about the fact that causing gravity anomalies of



body have correct geometric form, is frequently made, which approximately correspond to real. In certain cases such likenings do not draw significant errors with the interpretation; in other cases these errors are essential, but with them nevertheless it is necessary to reconcile itself, since the interpretation virtually can be carried out only when making these assumptions. As we will see below, with the interpretation, as a rule, the examination of the complex geometric forms of the perturbing masses does not have a sense, although in some such cases the formalism of interpretation is developed.

Interpretation of gravity anomalies is satisfied on the basis of previously manufactured presentation/concept about physical model of geologic medium, with special features of structure of which is joined existence of gravity anomalies being investigated. The selection of the model, as a rule, is based on the geologic data about the region being investigated or about the adjacent region, whose structure can be considered of one type with the region being investigated. Two examples of the selection of physical model for the interpretation of gravity anomalies are examined below.

1. KMA region. Already in the first years of the investigation of the region of the Kursk Magnetic Anomaly (KMA) was here established existence, together with magnetic, also gravity anomaly. The position of separate gravitational maxima completely did not coincide with the position of the maximums of magnetic, but those, etc. definitely

gravitated to the points of emergence to the surface of the crystalline basement of the iron-ore rocks (ferruginous quartzite), which possess higher density and magnetic susceptibility, than their accomodating barren shales. Corresponding calculations, produced for the first time by O. Yu. Schmidt (1926) and by A. I. Zaborovskiy (1926), showed that the gravitational and magnetic anomalies of the region indicated are explained by the effect/action of the sheetlike bodies of ferruginous quartzite.

By physical model of such bodies it proved to be possible to take body in the form of sloping bed (Fig. 23) with horizontal upper edge AB, situated on level of erosion shear/section of basement, and as lower edge CD, located in parallel to AB on certain, usually significant, to depth from earth's surface (plane of observations), or even distant downward at infinite depth. The complex anomalous zones, which consist of several magnetic and gravitational maximums, are explained by the effect of such several sheetlike bodies, position and elements of bedding of which are determined on the anomalous curves.

2. Region of Solikamsk potassic deposit. By the drilling, produced at the isolated points of this region before setting of gravitation prospecting works, here there was established at a comparatively small depth from the surface (ten and first hundreds of meters) in the complex of sedimentary rocks the presence of powerful/thick (many hundreds of meters) sheetlike bed of the halogen rocks (Fig. 24). The halogen rocks have a density smaller than the

density of their covering sandy-clay rocks. After the conducting in this region of gravitation prospecting works the comparison of depths  $H$  of up to the surface of the halogen rocks with the signs of the anomalies of the force of gravity  $\Delta g$  for the drilled sections was produced. It seemed that values  $\Delta g$  and  $H$  are regularly connected: decrease corresponds to approximation/approach to a surface of lighter halogen rocks, and to subsidence - increase in the values of anomalies, the dependence between  $\Delta g$  and  $H$  having approximately linear character (further we learn, that this approximately linear dependence can be explained theoretically).

Page 89.

The facts indicated showed that in the region being investigated the character of the anomalies of gravitational force in the first approximation, is explained by the behavior of the surface of the thickness of the halogen rocks, moreover the relief of this surface in the sections, situated between boreholes, can be investigated according to gravitational data with the help of the appropriate correlation graph, which shows bond  $\Delta g$  and  $H$ . With this interpretation we disregard the effect of the relief of the deeply sloping sole of halide thickness.

Both examples examined higher than are typical for many cases of applying gravitational prospecting during solution of different geologic problems.

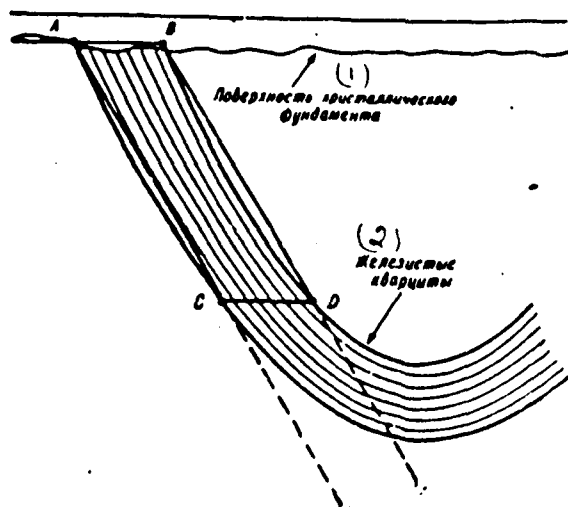


Fig. 23. Model of disturbing body in the form of sloping bed during the study of laminated iron-ore structures of type of KMA and Krivoy Rog.

Key: (1). Surface of crystalline basement. (2). Ferruginous quartzite.

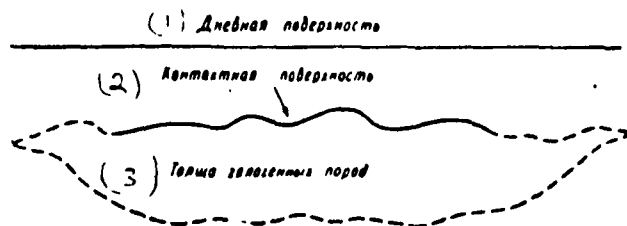


Fig. 24. Model of contact surface, which presents upper bound of disturbing body of - plastic-like bed of significant power/thickness. With the interpretation they disregard the effect/action on the gravitational field of the lateral and lower boundaries of body shown by a dot.

Key: (1). Topographic surface. (2). Contact surface. (3).

Thickness of halogenous rocks.

Page 90.

Thus, the model, examined in the first example, is usually accepted with the interpretation of gravitational and magnetic anomalies not only above the iron-ore rocks, but also in many other cases, when anomalies are caused by the internal structure of folding basement. The model, examined in the second example, is accepted in many regions, where gravity anomalies are caused by the effect/action of the sharply pronounced interface of density in the thickness of sedimentary rocks or on the boundary of basement; the same proves to be possible to make in the examination of the regional anomalies, caused first of all by a change of the thickness of the Earth's crust. To the reader must be clear that in each of the given examples, reducing entire diversity of the anomaly-forming factors to any one of them and disregarding the effect/action of the remaining ones (for example, connected with the deep structures), we go to the fact that with the interpretation the element of doubtfulness and uncertainty/indeterminacy will appear, and quantitative conclusions/derivations will be distorted by errors. It is natural to call these unavoidable errors the errors of modeling. The possibility is not excluded that in the separate cases the model accepted with the interpretation can be improved, i.e., it is given to the greater conformity with the real geologic conditions. It is clear that in this case can be reduced (sometimes very substantially) and the errors of modeling. The examples of this type of an improvement in the

physical model of interpretation will be given subsequently.

Each model in gravitational prospecting represents certain distribution of perturbing masses. In order to find corresponding to this distribution anomalous field, they put to use the formulas, which we is concluded in the following paragraph.

§ 17. Anomalous gravitational potential and its derived as functions of the distribution of the perturbing masses.

as we already noted in § 12-13 of Chapter II, if these or other elements of anomalous gravitational field are examined, then, keeping in mind, that effect of centrifugal force completely is considered during introduction of corrections for normal field of Earth, these elements can be identified with appropriate elements of gravitational field, which cause anomalies of geologic bodies. In this sense the theory of the interpretation of gravity anomalies is built on the basis of the theory of attraction. Anomalous gravitational potential and its derivatives we identify henceforth with the potential of attraction and its derivative.

Page 91.

Let us introduce rectangular coordinate system  $xyz$  into examination. Let us designate through  $x_1, y_1, z_1$  coordinates of the external point A, and through  $x, y, z$  - coordinates of elementary mass point  $dm$  at point M (Fig. 25). The intensity/strength of the

gravitational field of this mass at point A will be (see formula 1.6)

where

$$dF = \frac{f dm}{r}, \quad (III, 1)$$

$$r = \sqrt{(x-x_1)^2 + (y-y_1)^2 + (z-z_1)^2}.$$

Components of strength along coordinate axes will be

$$\begin{aligned} dF_x &= dF \cos(dF, x), \\ dF_y &= dF \cos(dF, y), \\ dF_z &= dF \cos(dF, z), \end{aligned}$$

moreover

$$\cos(dF, x) = \frac{x-x_1}{r},$$

$$\cos(dF, y) = \frac{y-y_1}{r},$$

$$\cos(dF, z) = \frac{z-z_1}{r},$$

consequently,

$$\left. \begin{aligned} dF_x &= f dm \frac{x-x_1}{r^2}, \\ dF_y &= f dm \frac{y-y_1}{r^2}, \\ dF_z &= f dm \frac{z-z_1}{r^2}. \end{aligned} \right\} \quad (III, 2)$$

Hence for solid extended body, blockaded volume  $v$ . composing intensities/strength gravitational fields will be expressed by following integral formulas:

$$\left. \begin{aligned} F_x &= f \int_V \frac{x-x_1}{r^2} dm, \\ F_y &= f \int_V \frac{y-y_1}{r^2} dm, \\ F_z &= f \int_V \frac{z-z_1}{r^2} dm. \end{aligned} \right\} \quad (III, 3)$$

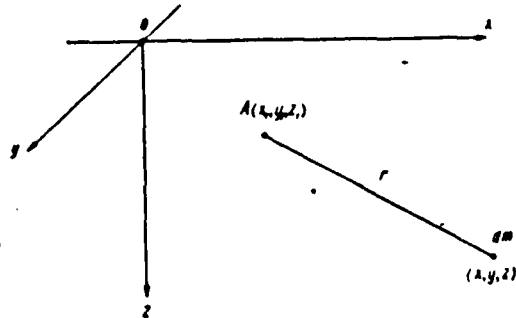


Fig. 25. To derivation of value of components of strength of gravitational field of the elementary point mass.

Page 92.

If we introduce into examination function

$$W = k \int_V \frac{dm}{r}, \quad (\text{III, 4})$$

then we will have

$$\left. \begin{aligned} F_x &= \frac{\partial W}{\partial x_1} \\ F_y &= \frac{\partial W}{\partial y_1} \\ F_z &= \frac{\partial W}{\partial z_1} \end{aligned} \right\} \quad (\text{III, 5})$$

This follows from possibility of differentiation (III, 4) under integral sign (Smirnov, V. IV, 1960) and factual execution of each of written equalities. Actually we have, for example,

$$\frac{\partial W}{\partial x_1} = \frac{\partial W}{\partial r} \frac{\partial r}{\partial x_1},$$

but

$$\frac{\partial W}{\partial r} = - \int_V \frac{dm}{r^2}; \quad \frac{\partial r}{\partial x_1} = - \frac{x - x_1}{r},$$

consequently,

$$\frac{\partial W}{\partial x_1} = \int_V \frac{x - x_1}{r^3} dm = F_x.$$



Analogously are proven corresponding equalities for  $F_y$  and  $F_z$ .

Thus,  $W$  represents potential or potential function of gravitational field of anomalous masses, i.e., potential of anomalous gravitational field.

If we as before consider that  $z$  axis of coordination system is directed along vertical line downward, then anomaly of gravitational force will be

$$\Delta g = \frac{\partial W}{\partial z_1} = \gamma \int_V \frac{z - z_1}{r^3} dm. \quad (III, 6)$$

By differentiation (III, 4) on appropriate coordinates are obtained expressions of second derivatives of gravitational potential

$$\left. \begin{aligned} W_{xz} &= \frac{\partial^2 W}{\partial x_1 \partial z_1} = 3\gamma \int_V \frac{(x - x_1)(z - z_1)}{r^5} dm, \\ W_{yz} &= \frac{\partial^2 W}{\partial y_1 \partial z_1} = 3\gamma \int_V \frac{(y - y_1)(z - z_1)}{r^5} dm, \\ W_{\Delta} &= \frac{\partial^2 W}{\partial y_1^2} - \frac{\partial^2 W}{\partial x_1^2} = 3\gamma \int_V \frac{(y - y_1)^2 - (x - x_1)^2}{r^5} dm, \end{aligned} \right\} \quad (III, 7)$$

$$\left. \begin{aligned} 2W_{xy} &= 2 \frac{\partial^2 W}{\partial x_1 \partial y_1} = 6\gamma \int_V \frac{(x - x_1)(y - y_1)}{r^5} dm, \\ W_{zz} &= \frac{\partial^2 W}{\partial z_1^2} = \gamma \int_V \frac{3(z - z_1)^2 - r^2}{r^5} dm. \end{aligned} \right\} \quad (III, 7)$$

Usually with interpretation of gravity anomalies assumption about

uniform density of perturbing masses is done. Then in expression  $dm = \sigma dv = \sigma dx dy dz$  constant multiplier  $\sigma$  can be carried out as the integral sign, and volumetric integral can be represented in the form of triple integral. finally, for the simplification it is possible to place the external point A, for which are comprised integral expressions, into the origin of coordinates, i.e., to assume  $x_1=0$ ,  $y_1=0$ ,  $z_1=0$ . Then from (III, 6) and (III, 7) we obtain:

$$\left. \begin{aligned} \Delta g &= f \sigma \iiint \frac{1}{r^3} dx dy dz, \\ W_{xx} &= 3f \sigma \iiint \frac{x^2}{r^5} dx dy dz, \\ W_{yy} &= 3f \sigma \iiint \frac{y^2}{r^5} dx dy dz, \\ W_{zz} &= 3f \sigma \iiint \frac{z^2}{r^5} dx dy dz, \\ 2W_{xy} &= 6f \sigma \iiint \frac{xy}{r^5} dx dy dz, \\ W_{xz} &= 6f \sigma \iiint \frac{xz}{r^5} dx dy dz, \\ W_{yz} &= 6f \sigma \iiint \frac{yz}{r^5} dx dy dz, \end{aligned} \right\} \quad (\text{III, 8})$$

where

$$r = \sqrt{x^2 + y^2 + z^2}.$$

Page 94.

If horizontal cylindrical coordinate system, connected with right angled with relationships/ratios, is used:

$$\begin{aligned} x &= \rho \cos \theta, \\ z &= \rho \sin \theta, \\ x^2 + z^2 &= \rho^2, \\ dx dy dz &= \rho d\rho dy d\theta. \end{aligned}$$

then there are obtained following expressions for derivatives of potential:

$$\begin{aligned}
 \Delta g &= f \int \frac{Q \sin \theta}{(Q^2 + y^2)^{3/2}} dm = f \sigma \iiint \frac{Q^2 \sin \theta}{(Q^2 + y^2)^{3/2}} dQ dy d\theta, \\
 W_{xz} &= \frac{3f}{2} \int \frac{Q^2 \sin 2\theta}{(Q^2 + y^2)^{3/2}} dm = \\
 &= \frac{3f \sigma}{2} \iiint \frac{Q^2 \sin 2\theta}{(Q^2 + y^2)^{3/2}} dQ dy d\theta, \\
 W_{yz} &= 3f \int \frac{Q y \sin \theta}{(Q^2 + y^2)^{3/2}} dm = \\
 &= 3f \sigma \iiint \frac{Q^2 y \sin \theta}{(Q^2 + y^2)^{3/2}} dQ dy d\theta, \\
 W_{\Delta} &= 3f \int \frac{y^2 - Q^2 \cos^2 \theta}{(Q^2 + y^2)^{3/2}} dm = \\
 &= 3f \sigma \iiint \frac{y^2 - Q^2 \cos^2 \theta}{(Q^2 + y^2)^{3/2}} dQ dy d\theta, \\
 2W_{xy} &= 6f \int \frac{Q y \cos \theta}{(Q^2 + y^2)^{3/2}} dm = \\
 &= 6f \sigma \iiint \frac{Q^2 y \cos \theta}{(Q^2 + y^2)^{3/2}} dQ dy d\theta, \\
 W_{zz} &= f \int \frac{Q^2 (3 \sin^2 \theta - 1) + y^2}{(Q^2 + y^2)^{3/2}} dm = \\
 &= f \sigma \iiint \frac{Q^2 (3 \sin^2 \theta - 1) + Q y^2}{(Q^2 + y^2)^{3/2}} dQ dy d\theta.
 \end{aligned}
 \tag{III, 9}$$

Let us examine now case, when gravity anomalies are caused by effect/action of bodies, which have infinite course/strike, parallel to y axis, and constant cross section (two-dimensional problem) (Fig. 26).

Integral formulas for this case are obtained, if we produce integration for y from  $-\infty$  to  $+\infty$  in formulas (III, 8) or (III, 9). The examination of these formulas shows that the discussion deals with the calculation of the following integrals:

$$I_1(y) = \int \frac{\partial y}{(y^2 + Q^2)^{3/2}}, \tag{III, 10}$$

$$I_2(y) = \int \frac{dy}{(y^2 + Q^2)^{3/2}} \tag{III, 11}$$

with the subsequent examination of the limiting values

$$\lim_{y \rightarrow \infty} \int_{-y}^y I_1(y) = \lim_{y \rightarrow \infty} \int_{-y}^y I_2(y)$$

(i.e. by computation of the corresponding definite integrals in the sense of principal value). All the remaining integrals, which contain the variable  $y$  in the formulas (III, 8) or (III, 9), easily are reduced to two indicated or to their linear combination.

Page 95.

For calculation of  $I_1(y)$  according to formula (III, 10) we replace variable (Euler's substitution) in it

$$t = y + \sqrt{y^2 + q^2}$$

and we find after some conversions

$$I_1(y) = \int \frac{4t \, dt}{(t^2 + q^2)^2} = -\frac{2}{t^2 + q^2}.$$

whence, returning to with variable  $y$  and supplementing to value of indefinite integral  $\frac{1}{q^2}$ , we find

$$I_1(y) = \frac{y}{q^2 \sqrt{y^2 + q^2}} \quad (\text{III, 12})$$

and limiting value

$$\lim_{y \rightarrow \infty} \int_{-y}^y I_1(y) = \frac{2}{q^2}. \quad (\text{III, 13})$$

During calculation  $I_2(y)$  in formula (III, 11), integrating in parts and using previously calculated integral  $I_1(y)$ , we find

$$I_2(y) = \frac{I_1(y)}{y^2 + q^2} + 2 \int \frac{I_1(y) \, dy}{(y^2 + q^2)^2}.$$

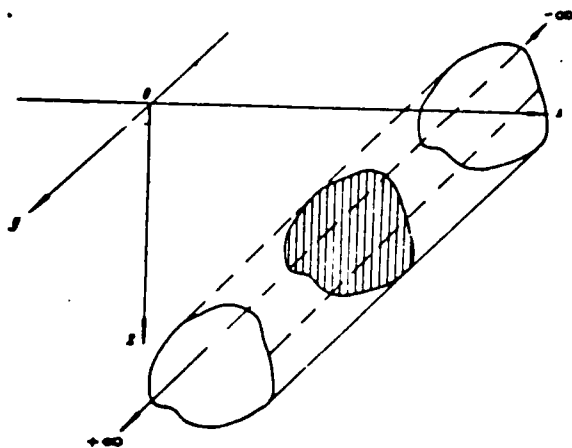


Fig. 26. Body of infinite course (two-dimensional problem).

Page 96.

Secondary integration in parts gives

$$2 \int \frac{I_1(y) y dy}{(y^2 + q^2)^{3/2}} = \frac{2}{q^2} \int \frac{y^2 dy}{(y^2 + q^2)^{3/2}} - \frac{1}{q^2} \int \frac{2y dy}{(y^2 + q^2)^{3/2}} =$$

$$= \frac{2I_1(y)}{q^2} - 2I_2(y) + \frac{1}{q^2(y^2 + q^2)}.$$

Substituting this result into preceding equation and solving it relative to  $I_1(y)$ , we find after conversions

$$I_1(y) = \frac{1}{q^2} \left[ \frac{y}{\sqrt{y^2 + q^2}} - \frac{1}{3} \frac{y^3}{(y^2 + q^2)^{3/2}} \right] \quad (\text{III, 14})$$

and limiting value

$$\lim_{y \rightarrow \infty} \int_{-y}^y I_1(y) = \frac{2}{3q^2}. \quad (\text{III, 15})$$

In the derivation of integral formulas for two-dimensional task of interpretation let us take, first of all, following fact into consideration. All derivatives on by the variable  $y$ , i.e., along the direction of the course/strike of disturbing bodies, in this case must be equal to zero, since anomalous field, obviously, does not vary in the direction indicated. Thus,

$$W_{yx} = W_{xy} = W_{yy} = 0.$$

Consequently, in this case

$$W_{\Delta} = -W_{xx}. \quad (\text{III}, 16)$$

Laplace's equation (II.20) in the case of two-dimensional task contains only two variables

$$\frac{\partial^2 W}{\partial x^2} + \frac{\partial^2 W}{\partial z^2} = 0$$

or in other designations

$$W_{xx} + W_{zz} = 0. \quad (\text{III}, 17)$$

From formulas (III, 16) and (III, 17) it follows that in the case of two-dimensional task of value  $W_{\Delta}$  and  $W_{zz}$  identically they are identical

$$W_{\Delta} = W_{zz}. \quad (\text{III}, 18)$$

Page 97.

Integral formulas for case of two-dimensional task will be obtained directly from formulas (III, 8) and (III, 9) taking into

account relationships/ratios (III, 10), (III, 11), (III, 13), (III, 15) in the following form:

$$\left. \begin{aligned} \Delta g &= 2f\sigma \iint \frac{z}{q^3} dx dz, \\ U_{xx} &= 4f\sigma \iint \frac{zx}{q^3} dx dz, \\ W_{\Delta} = W_{xx} &= 2f\sigma \iint \frac{z^2}{q^3} dx dz. \end{aligned} \right\} \quad (\text{III}, 19)$$

Formulas (III, 8), (III, 9) and (III, 10) relate to usually considered/examined case, when excess density of bodies, which cause anomalies, is received as constant. In a more complex case  $\sigma$  is left under the integral sign and is considered as a function of one or several of the space coordinates.

Formulas (III, 10) of two-dimensional task can be rewritten in the form:

$$\begin{aligned} \Delta g &= 2f\sigma \iint \frac{\partial}{\partial z} (\ln q) dx dz = -2f\sigma \iint \frac{\partial \varphi}{\partial x} dx dz = \\ &= -2f\sigma \iint \frac{\partial}{\partial \varphi} (\cos \varphi) d\varphi dq, \\ W_{xx} &= -2f\sigma \iint \frac{\partial}{\partial z} \left( \frac{z}{q^3} \right) dx dz = -2f\sigma \iint \frac{\partial}{\partial x} \left( \frac{z}{q^3} \right) dx dz = \\ &= -f\sigma \iint \frac{\partial}{\partial \varphi} \left( \frac{\cos 2\varphi}{q} \right) d\varphi dq, \\ W_{\Delta} = W_{xx} &= -2f\sigma \iint \frac{\partial}{\partial z} \left( \frac{z}{q^3} \right) dx dz = \\ &= 2f\sigma \iint \frac{\partial}{\partial x} \left( \frac{z}{q^3} \right) dx dz = -f\sigma \iint \frac{\partial}{\partial \varphi} \left( \frac{\sin 2\varphi}{q} \right) d\varphi dq. \end{aligned}$$

According to the theory of line integrals (see, for example, the following presentation/concepts:

$$\left. \begin{aligned} \Delta g &= 2f\sigma \oint \ln q dx = 2f\sigma \oint \varphi dz = -2f\sigma \oint \cos \varphi dq, \\ W_{xx} &= -2f\sigma \oint \frac{z}{q^3} dx = 2f\sigma \oint \frac{z}{q^3} dz = -f\sigma \oint \frac{\cos 2\varphi}{q} dq, \\ W_{\Delta} = W_{xx} &= 2f\sigma \oint \frac{z}{q^3} dz = -2f\sigma \oint \frac{z}{q^3} dx = \\ &= -f\sigma \oint \frac{\sin 2\varphi}{q} dq, \end{aligned} \right\} \quad (\text{III}, 20)$$

where integration is produced along closed outline of cross section of body.

Page 98.

§ 18. Special features of the two-dimensional task of interpretation and the region of its practical application.

Basic special feature of two-dimensional task of interpretation consists in the fact that it is reduced to examination of harmonic functions only from two space coordinates, and theory of these functions it coincides with theory of analytic complex variable functions - one of remarkable in its methods and results of deeply investigated regions of contemporary mathematics.

Usually complex variables are designated  $z = x + iy$  ( $i = \sqrt{-1}$ ), however, in accordance with designations utilized by us we will complex variable write in the form  $\xi = x + iz$ , identifying  $x$  and  $z$  with above space coordinates accepted. Complex variable  $\xi$  in that case it is possible to represent by the point coordination of plane  $xoz$ , which is the cross-sectional flow of the bodies, which cause the anomalous field being investigated.

Complex variable function

$$f(\xi) = \varphi(x, z) + i\psi(x, z) \quad (\text{III, 21})$$

is called analytical in region, if at each point  $\xi = \xi_0$  of this region it an unlimited number of times is differentiated and can be decomposed in convergent exponential Taylor series

$$f(\xi) = f(\xi_0) + (\xi - \xi_0) \frac{f'(\xi_0)}{1} + (\xi - \xi_0)^2 \frac{f''(\xi_0)}{1 \cdot 2} + \dots \quad (\text{III, 22})$$



In theory of analytical functions it is proven (Smirnov, 1956, Vol. III), that conditions of analyticity of functions  $f(\zeta)$  presented can be substituted by some conditions, assigned on function real variable/alternating  $\phi(x, z)$  and  $\psi(x, z)$ . These variables must be also differentiated in the region of analyticity  $f(\zeta)$  and satisfy the following differential equations:

$$\left. \begin{aligned} \frac{\partial \phi}{\partial x} &= \frac{\partial \psi}{\partial z}, \\ \frac{\partial \phi}{\partial z} &= -\frac{\partial \psi}{\partial x}. \end{aligned} \right\} \quad (III, 23)$$

Differentiating left and right sides of the first of written equations for  $x$ , and the second - on  $z$  and by storing/adding up their left and right sides, let us find

$$\frac{\partial^2 \phi}{\partial x^2} + \frac{\partial^2 \phi}{\partial z^2} = 0.$$

Differentiating left and right sides of first equation for  $z$ , and the second - on  $x$  and subtracting their left and right sides, we obtain

$$\frac{\partial^2 \psi}{\partial x^2} + \frac{\partial^2 \psi}{\partial z^2} = 0.$$

Consequently, for analyticity  $f(\zeta)$  it is sufficient, in order to  $\phi(x, z)$  and  $\psi(x, z)$  be represented as harmonic functions of two variables  $x$  and  $z$ , connected with condition (III, 23).

Such functions are called conjugated harmonic functions. Example of the conjugated harmonic functions:

$$W_{xx} = \frac{\partial g}{\partial x},$$

$$W_{zz} = \frac{\partial g}{\partial z}.$$

Actually,

$$\frac{\partial}{\partial x} W_{xx} = \frac{\partial}{\partial z} W_{xz} = \frac{\partial^2 g}{\partial x \partial z},$$

$$\frac{\partial}{\partial z} W_{xx} = \frac{\partial^2 g}{\partial z^2}; \quad \frac{\partial}{\partial x} W_{xz} = \frac{\partial^2 g}{\partial x^2}.$$

and since we have (Laplace's equation)

$$\frac{\partial^2 g}{\partial x^2} + \frac{\partial^2 g}{\partial z^2} = 0,$$

that

$$\frac{\partial}{\partial z} W_{xx} = - \frac{\partial}{\partial x} W_{xz},$$

i.e. occur equations (III, 23).

After leading analogous calculations or using bond of derivatives of magnetic and gravitational potential (see § 6 of Chapter I), it is possible to demonstrate that components of  $H$  and  $z$  of magnetic field are also conjugated harmonic functions. As the conjugated harmonic function for the anomaly of gravitational force, i.e., for derivative  $\frac{\partial W}{\partial z}$  of gravitational potential, serves derivative  $\frac{\partial W}{\partial x}$ , not directly thus far measured in gravitational prospecting, but which can be computed, knowing distribution on the plane of the observations  $\frac{\partial W}{\partial z}$  or any other derivative of the gravitational potential (see § 27 of Chapter IV).

Thus,  $f(z) = W_{xx} + iW_{xz}$ ,  $f_1(z) = \frac{\partial W}{\partial z} + i \frac{\partial W}{\partial x}$  and so forth represent in certain part of the plane  $xoz$  analytic complex variable functions  $z = x + iz$ . Above, in § 17, we saw that  $\Delta z = \frac{\partial W}{\partial z}, W_{xz}$  and so forth can be represented in the form of line integrals on the outline of the cross section of the body, which causes the gravity anomaly being investigated. Consequently, and the corresponding analytic function can be represented in the form of the same integral.

In theory of analytic functions an important role is played by a study of singular points - those points, at which is disturbed analyticity of function, i.e., its continuity, uniqueness, etc. Singular point defines the boundaries of region, in limits of which the most analytical possible continuation of function, i.e., its determination beyond the limits of that set of points (for example segment of certain curve), for which to us is known its distribution.

The singular points  $f(\zeta)$  in (III, 21) are special and for the conjugated harmonic functions  $\phi(x, z)$  and  $\psi(x, z)$ , i.e., in particular, and for the interesting us derivatives of gravitational potential.

Page 100.

This points are placed either within the outline of the section of disturbing body (if this outline is smooth, not having salient points), or on the outline itself, moreover in the latter case of the point of the analytical special features of harmonic functions they coincide with the points of the geometric special features of the outline of the cross section of body, precisely, with those points, at which the direction of tangent to the outline varies intermittently (salient points, angular points).

From aforesaid it is clear that the theory of analytic functions it can have fundamental importance in development of theory of two-dimensional task of interpretation of gravitational and magnetic anomalies. In this direction we have a number of investigations of the Soviet and foreign scientists (Zamorev, 1941, 1942; Kh'yug, 1943; Andreyev, 1949, 1954, 1955; Shalayev, 1958; Klushin, 1959; Strakhov, 1957, 1960, et al), some results of which have at present direct practical value, we are briefly presented in Chapters IV-V.

Besides fundamental special feature indicated two-dimensional of tasks of interpretation has still the essential advantage over three-

dimensional task, about which we above already mentioned, large simplicity of calculations, which is decisive in practice. It is at the same time completely clear that the two-dimensional model far from always can be used for the interpretation. Subsequently we will in more detail examine a question about the region of the practical utilization of a two-dimensional task of interpretation.

Geologic objects, investigated with the help of gravitational prospecting, frequently have elongated planform and frequently significant sizes/dimensions on course/strike: are such linear folding forms in sedimentary cover and in basement, zone of faults, separate faults, sheet intrusions, etc. In all these cases during the analysis of gravity anomalies it is usually completely possible to use a calculating apparatus of the two-dimensional task of interpretation. Even if the sizes/dimensions of body are small in the course in comparison with the depth of its bedding, then the application of methods of localization of anomalies, for example transition from  $\Delta g$  to  $\delta \Delta g$  or  $W_{xx}$  (see Chapter IV), it very sharply reduces the errors in the interpretation, which appear due to the utilization of a two-dimensional model of interpretation. Of this we repeatedly will be convinced subsequently based on different examples. Finally, such methods of the transformation of the anomalies (one of them it is examined below), are possible, whose application makes it possible to correctly determine some elements of the bedding (for example, depth) of bodies isometric in the plan/layout with the utilization of methods of interpretation for the case of two-dimensional task.

Page 101.

Let us write the general expression of anomaly  $\Delta g$  in the case of three-dimensional task for point  $y=y_1$ :

$$\Delta g = f \sigma \iiint \frac{z \, dx \, dy \, dz}{[q^2 + (y - y_1)^2]^{3/2}}.$$

Let us multiply the right and left sides of this relation by  $dy_1$  and let us take from both parts integrals within limits from  $-\infty$  to  $+\infty$ . If we in this case designate the coordinates of the ends of the body causing anomaly along  $y$  axis through  $y_1$  and  $y_2$  and to place

$$\sigma' = \int_{y_1}^{y_2} \sigma \, dy_1,$$

that, taking into account of formula (III, 10) and (III, 13), it is possible to write

$$\int_{-\infty}^{+\infty} \Delta g \, dy_1 = \sigma' \iint \frac{z \, dx \, dz}{q^2},$$

i.e. is obtained the formula of two-dimensional task.

Thus, it is possible three-dimensional task of reducing to two-dimensional, examining at each point of  $x$  axis instead of  $\Delta g$  value

$$\int_{-\infty}^{+\infty} \Delta g \, dy_1.$$

If anomaly  $\Delta g$  is caused by effect/action of cylindrical body of final course/strike, arbitrary, but constant section, situated in parallel to  $y$  axis, then the interpretation of converted thus anomaly gives real elements of bedding of body, but in this case gives

distorted (reduced against actual) value  $\sigma$ . The latter is evident, in particular, from the following fact. If we in the formula (III, 13) instead of limits of  $y$  and  $-y$  take  $y$  and  $0$ , then instead of  $\frac{2}{\rho^2}$  in the right side we will obtain  $\frac{1}{\rho^2}$ . the curve  $\Delta g$  along the profile through the end of the semi-infinite body of density  $\sigma$  corresponds  $\Delta g$  infinite body with density  $\sigma/2$ .

To a decrease of error in interpretation, connected with utilization of two-dimensional model, can contribute also to correct selection of utilized for interpretation profiles.

Let us clarify this by following elementary example. Let us assume we have the anomaly of the form depicted in Fig. 27, which is represented as the combination of the anomalies of two types - by basis of  $\pi$  of the intensity of linear, sustained in the course, which well corresponds to the requirements of two-dimensional task, and additional less in the intensity, the almost isometric on the area anomalies, which are placed along the "ridge/spine" of the first anomaly (this combination it is very frequently observed in actuality).

Page 102.

Where should be selected the profiles, along which it is necessary to construct curves for the interpretation of anomalies with the utilization of calculating methods of two-dimensional task? Many they would prefer to lead the profile through the sections of the greatest

in the value maximums, keeping in mind to obtain curves for the case of the most sharply pronounced anomaly. In actuality it is most correct to lead

the profiles through the sections with the values of anomalies average/mean in the intensity, since for these average/mean values, obviously, to the best degree is justified the basic assumption of the two-dimensional task about the invariability of sizes/dimensions and shape of body, and, consequently, the intensity of the corresponding to it anomaly on the course of the body.

With the correct approach to question region of practical application of two-dimensional task of interpretation of gravity anomalies proves to be extremely large. During the correct utilization of booster calculating agents the transformations of anomalies, the worthwhile selection of profiles for calculations and so forth of the rules of calculations, valid formally only for the ideal infinitely extended bodies, can be without great error applied in the interpretation of the significant part of all gravity anomalies being investigated.



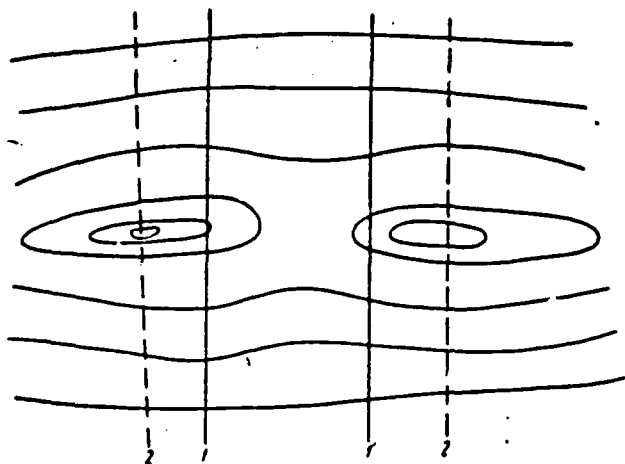


Fig. 27. Selection of profile for interpretation according to formulas of two-dimensional task. 1 - correct; 2 - incorrect.

Page 103.

§ 19. Direct and reverse problems of the gravitational-field theory. Conditions for uniqueness and stability of the solution of inverse problem.

With interpretation are distinguished direct (auxiliary) problem - determination of anomaly from specified distribution of perturbing masses - and inverse (basic) problem - determination of the form and depth of bedding of perturbing masses from after this anomaly. If by the form of the disturbing body with the interpretation they are assigned (which under the known physico-geologic conditions is completely possible to make), then the analysis of the solution of direct problem makes it possible to lay down the rules of the solution

of inverse problem for the case, when anomaly is caused by the effect/action of the body of the assigned form.

We illustrate this fact based on numerous examples in Chapters V and VI. If the shape of disturbing body is selected in the process of interpretation, then this type selection is realized via the comparison of the anomaly being investigated with the group of the solutions of inverse problem. In this case that of the solutions of direct problem, which in the best way corresponds to the assigned anomalous field, is accepted for the solution of direct problem. Thus, in many instances for solving the inverse problem is required solution or the group of the possible solutions of direct problem and the subsequent analysis of these solutions. Below we will see (Chapter VI), what some questions, connected with the solution of inverse problem, can be explained directly, without the turning to the solution of direct problem.

Basis for solving direct problem present calculating apparatus, described in § 17 of present chapter - integral formulas (III, 8), (III, 9), (III, 19), (III, 20), expressing derivatives of gravitational potential in function of distribution of perturbing masses. The solution of direct problem is reduced to the substitution of integration limits for the assigned form and the sizes/dimensions of disturbing body and to the calculation of the corresponding integrals. The solution, which characterizes the distribution of anomaly on the plane of observations, is obtained in this case

completely determined and simple.

It is a different matter concerning solution of inverse problem.  
If anomalous potential out of the disturbing body

$$W_e = \int_V \frac{\sigma dV}{r}, \quad (\text{III}, 24)$$

is uniquely determined according to the distribution of excess density  $\sigma$  in volume  $V$  of the body, then, by knowing  $W_e$ , it is not possible to unambiguously determine the distribution of excess density  $\sigma$ . It is possible to change distribution  $\sigma$  within volume of the  $V$  body, without varying its external potential  $W_e$ .

Page 104.

This ensues from that fact, established/installed in the theory of potential, that within volume of the  $V$  body are possible density distributions, which create extra- $w$  of its surface zero anomalous potential, i.e., in other words, not varying its external gravitational field. Let us assume that this density distribution to us is known; let us designate it through  $\sigma_0$ . Then, obviously,

$$W_e = \int_V \frac{\sigma dV}{r} = \int_V \frac{(\sigma + \sigma_0) dV}{r}. \quad (\text{III}, 25)$$

Let us give idea about how it is possible to determine distribution of density  $\sigma_0$  of zero potential. Let us introduce, first of all, the following determination. Let  $F_1$  and  $F_2$  - functions of space coordinates, specific within the assigned volume  $V$ . If in this

case

$$\int_V F_1 F_2 dV = 0,$$

then functions  $F_1$  and  $F_2$  are called orthogonal within volume  $V$ .

Albeit now  $U_i$  — any harmonic function determined within volume  $V$  of a disturbing body, i.e., in particular, the gravitational potential or any of its derivatives on one of space coordinates. It proves to be that for region  $V$  within the disturbing body

$$\int_V U_i \sigma_0 dV = 0, \quad (\text{III}, 26)$$

i.e. density distribution of zero external potential is orthogonal within the disturbing body to any harmonic function.

Factual determination of  $\sigma_0$  proves to be possible as follows. Let us introduce into the examination the level surface of  $S$  of anomalous potential, for which  $W_0 = \text{const.}$

From set of harmonic functions, determined within this surface, let us select that, which is subordinated on  $S$  to condition

$$\frac{dW}{dn} = 0,$$

where  $n$  — direction of internal normal to the surface of  $S$ .

In that case, on the basis of equation of Poisson (II, 21), we obtain

$$\sigma_0 = \frac{\Delta W}{4\pi}, \quad (\text{III}, 27)$$

where it is marked

$$\Delta W = \frac{\partial^2 W}{\partial x^2} + \frac{\partial^2 W}{\partial y^2} + \frac{\partial^2 W}{\partial z^2}.$$

Page 105.

Functions of  $W$  and corresponding to them distributions  $\sigma$ , can not exist, i.e., the inverse problem can have unique solution. However, cases are possible when there exists even an infinite number of functions  $W$  and corresponding to them distributions  $\sigma$ , i.e., infinite of the equal in the purely mathematical sense solutions of inverse problem. This is evident from the following example. Newton's law is applicable to the attraction of the point or spherical mass, which consists of concentric layers uniform in the density, but with an arbitrary change in the density from one layer to the next [see formulas (1, 5) and (1, 6)] The gravitational field of this spherical body in the external space does not depend on that how density along the radius of sphere varies; the intensity/strength of the gravitational field of this body depends only on its mass and on distance from the attracted/tightened point to the center of sphere.

Thus, a simple solution to the inverse problem is ensured only by presence of additional conditions, assigned or to shape of disturbing body. The possibility of the assumption of these conditions in each specific case must be substantiated by the account of real physico-geologic conditions, other given geophysical methods, etc.

13

Degree of uniqueness in solving the inverse problem sharply is raised with knowledge of density of rocks of region being investigated. In many instances it is possible without the large error to do an assumption about the constant density of the body, which causes anomaly. Soviet mathematician P. S. Novikov in 1938 for this case proved the remarkable theorem, which in the simplified formulation can be presented as follows: if two bodies, convex relative to a certain common internal point, have general/common constant excess density willow external space they condition identical anomalous gravitational field, then these bodies coincide one with another. An analogous theorem is proved by P. S. Novikov, also, in the more general/more common formulation, considering density the positive variable quantity, whose variation on any straight line does not exceed its minimum value, and body - not convex, but by a star with respect to the common internal point. On the whole, with respect to smooth bodies it is possible to consider that the knowledge of their density characteristic almost removes the uncertainty/indeterminacy, connected with the ambiguity of the solution of inverse problem.

As let us see in Chapter VI, some important characteristics of disturbing body are theoretically determined completely uniquely, independent of its form: excess mass, volume or cross-sectional area (at known excess density) of body, coordinate of its center of gravity, etc.

Many geologic bodies are limited by surfaces which have sharp breaks, angular bends, gaps and other inaccuracies in section/cut. Above, in § 18, we noted that the type indicated the geometric special features of the outlines of the cross section of bodies represent, at the same time, singular points for the appropriate harmonic and formed by them analytic functions.

Page 106.

At these points the derivatives of gravitational potential intermittently vary their value, go to infinity, etc. The position of these singular points or sources, which determine the very structure of anomalous potential field, is in principle determined unambiguously. Thereby there is indirectly determined the surface of disturbing body, moreover it is determined without the knowledge of its excess density, which is determined, together with elements of the bedding of bodies, on the quite gravity anomaly. Fig. 28 gives the typical sections/cuts of bodies with the angular section and the position of the singular points of anomalous gravitational field. Inverse problem for all of this type of bodies is solved theoretically unambiguously.

Until now, of limitation and possibility of interpretation we examined thus far purely theoretically, lowering many moments/torques, connected with actual conditions, which have high, sometimes decisive importance for obtaining reliable, geologically reliable results of interpretation. Target of interpretation - not only obtaining of one

or the other numerical result, for example the depth of the bedding of the causing anomaly body, but also estimation, at least approximated, accuracy and authenticity this result for one or the other physico-geologic conditions.

For this purpose practice developed the concept about the stability of the solution of inverse problem. Concept close in meaning already is long ago introduced in physics (capacity of system to reduce its original steady state after the stop of the short-time effect/action of the perturbing factor), in construction business (capability of buildings for the retention/maintaining of equilibrium state under the effect of external forces), etc. In mathematical physics similar presentation/concept is contained in the determination of correctly stated problem, i.e., the task, whose solution little depends on errors under the initial and boundary conditions (otherwise task it is considered as the incorrectly set). We will consider the solution of inverse problem stable in such a case, when the relative small change in the position, form or sizes/dimensions of the causing anomaly body, determined with the interpretation, produces an already completely noticeable change in the anomalous field (of what it is possible to be convinced, for example, solving direct problem for the changed section/cut of body).

Concept of stability is frequently expedient to use individually to determination of different elements of body, keeping in mind, that each of these elements is determined with different reliability, for



example, position of upper edge of body is determined usually much more reliable than depth of bedding of lower edge.

Page 107.

The values of some elements frequently affect the accuracy of the determination of other elements, for example, the shape of the body is determined stably only when the depth of its bedding is relatively small, it is more accurate, that the dimensions of body are sufficiently great in comparison with the depth of its bedding. For example the reliable determination of the horizontal power/thickness of sheetlike body is possible only when the power/thickness is more than the depth of the bedding of its upper edge.

Stability of process of interpretation should be understood also in sense of its "freedom from interference".

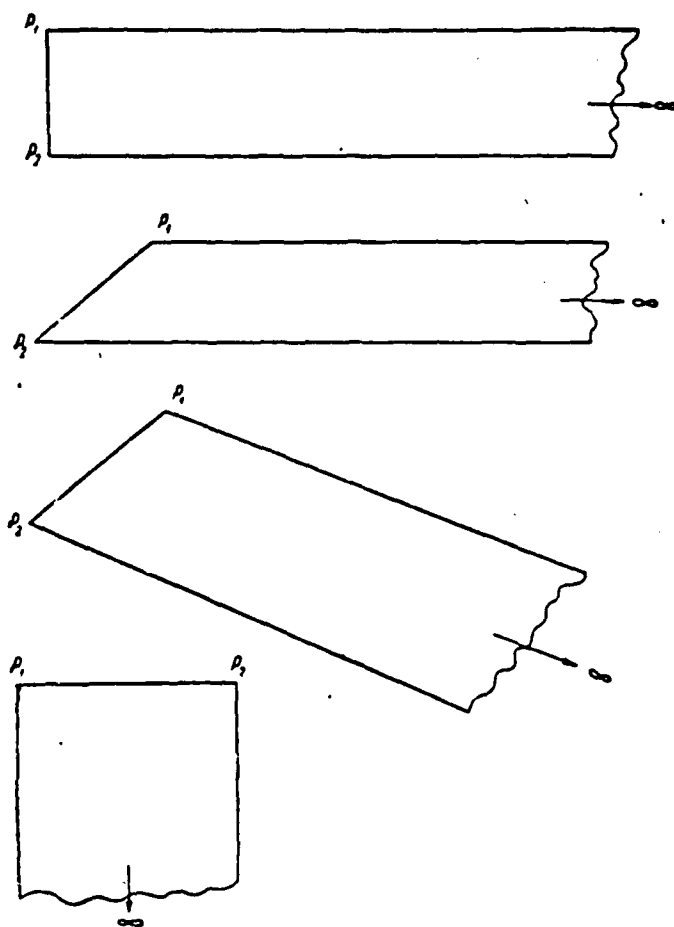


Fig. 28. Typical sections/cuts of two-dimensional bodies with angular section and position of singular points ( $P_i$ ) of anomalous field.

Page 108.

By interference we will understand all that which distorts the anomaly interesting to us: error of observation, error in the account of the effect of the relief and other interfering factors, the effect of dimensions of the network of observations, the effect of adjacent anomalous objects, etc. In the theory of interpretation the

interference effect usually is not considered and anomaly is assumed to be that determined "in the pure form" and it is absolutely accurately. The "freedom from interference" of interpretation in certain cases can be decreased by the special methods of perfecting the observations (see Chapter IV) that it makes sense especially in the relatively small relation the signal: interference (understanding under the signal the anomaly being investigated). Another way of combatting the interference is to increase the accuracy of equipment and an increase in the detail of gravitational photographing. A question about an increase in the relation the signal: interference is examined via special calculating methods in Chapter IV.

Interpretation will be most reliable in presence of conditions, which ensure sufficient degree of uniqueness and stability of its results. Fig. 29a shows the cross section of the body, located near the earth's surface, while in Fig. 29b - the section of the same body, whose one end is found at significant removal/distance from the earth's surface. as we already indicated, the cross section of any two-dimensional body of the assigned density can be unambiguously determined on the gravity anomaly; but the stability of the solution of this problem in different cases is different. In the case, shown in Fig. 29a, since entire body is located near the earth's surface, any, even small, a change of its sizes/dimensions it will affect the character of gravity anomaly, i.e., cross section is determined stably. But in the case shown in Fig. 29b, a change of the position of the lower end of the body, far distant from the plane of

observations, obviously, it little affects the character of gravity anomaly, i.e., the cross section of body in this case it is determined unstably.

Estimation of efficiency of interpretation of gravity anomalies. From the content of Chapter III in the reader an impression can be created, that the reliable geologically reliable interpretation of gravity anomalies is realized only in the exceptional cases, whereas in the majority the efficiency of our interpretation is very small and even it is equal to zero. Actually, at the way of interpreter appears the set of limitations and difficulties. Task itself, proves to be, allows/assumes only the conditionally probable solution, which moreover, generally speaking, is by no means only, it is on top of that and not always stable. All this at first glance confirms the conclusion given above.

In actuality, however, matter is otherwise. all the limitations indicated higher than and the difficulties, it is understood, they are essential, they decrease authenticity and reliability of the analysis of gravity anomalies, but in the majority of the cases this analysis nevertheless gives the additional geologic information required from the results of gravitational prospecting.

Page 109.

To the help come, as a rule, two facts: 1) the fact that the required information is additional to that geologic information, which we

already have available, beginning the interpretation; 2) the presence of other given geophysical methods, which also render aid during the solution of our problem. Furthermore, it is necessary to have in mind that the task, which is placed before gravitational prospecting, is frequently sufficiently narrow and simple. More complex problems is placed before gravitational prospecting only in those comparatively rare cases when it comes forward in the role of the detailization prospecting method, but these are exactly those cases when we have available the vast additional geological- geophysical information, which substantially simplifies and which facilitates the task of the interpretation of gravity anomalies, which raises the degree of the authenticity of the latter.

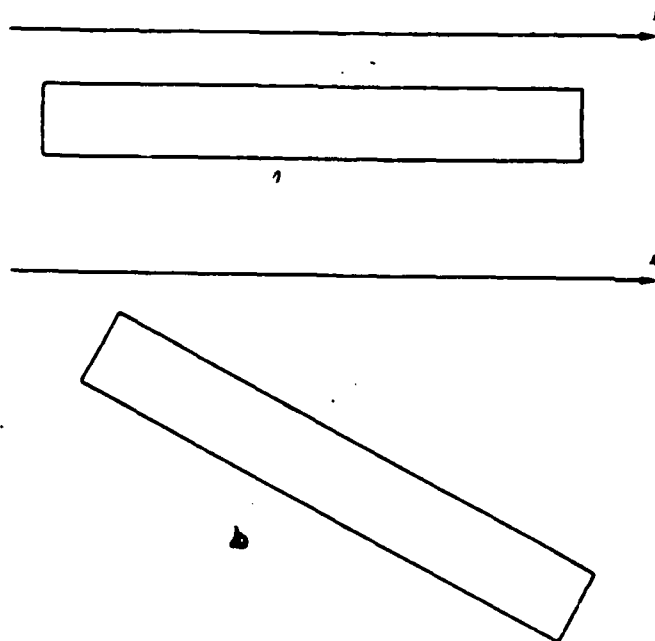


Fig. 29. Determination of stability of solution of inverse problem.

Page 110.

Complexity of problem of interpretation leads to the fact that we must decisively forego attempts at estimation of reliability of one or the other methods of interpretation on the basis of some speculative theoretical considerations. The real estimation of efficiency and reliability of the methods of interpretation is possible only for the specific physico-geologic conditions and the tasks via the comparison of the results of interpretation with the data of the mine-drilling works and other geophysical methods. In certain cases of this type the analysis can be done very thoroughly, also, in these cases, projecting/designing performing gravitation prospecting work in this

or another region, we can assuredly say what precisely additional geologic information can be obtained as a result of their setting and reliably consider the degree of reliability of the interpretation of data of gravitational prospecting to that how these data are acquired. These will be the cases when gravitational prospecting is placed in the well mastered by it territories, on which already there is a many-year successful experience of its application for solving those geologic tasks, which prove to be accessible for this method at the contemporary stage of its development. In the overwhelming majority of such cases gravitational prospecting is used in the complex with other geophysical methods and this complex sufficiently detailed.

As example it is possible to indicate those regions and tasks, majority of which has already been mentioned above: searches and prospecting of salt dome structures in regions of type of Caspian basin, prospecting of deposits of potassic salts of type of Solikamsk, the study of surface of folding basement in regions of type of Donbass, prospecting iron-ore regions of type of KMA and Krivoy Rog, searches and prospecting of chromite and pyrite ores, etc. In all cases indicated (but their list it would be possible to continue) usually very successfully and reliably is conducted not only the qualitative, but also quantitative geologic interpretation of the results of gravitational prospecting.

Efficiency of interpretation of data of gravitational prospecting - concept, which must be examined not only in connection with concrete

regions and geologic tasks, but also for concrete development stage of method. Conclusions about the possibilities of method require systematic review and refinement in connection with an improvement in the equipment, procedure and geologic interpretation of the results of gravitation prospecting works, in connection with an improvement in entire complex of methods, in composition of which is used gravitational prospecting.

Page 111.

§ 20. Promising trends in further development of the theory of the interpretation of gravity anomalies.

In contemporary physics and technology are examined two kinds of tasks:

1. The determined tasks, whose solution is completely and uniquely determined by the system of initial data, each of these data can be by us accurately measured and taken into consideration. The solution of problem is obtained in the form of definite functional dependence or in the form of a number, i.e., the particular value of function for the interesting us value of its argument.

2. Stochastic tasks, initial data for solution which we know only partially or insufficiently accurately, owing to this the solution is not derived/concluded unambiguously from known to us data. As writes I. A. Poletayev in his book about basic concepts of



cybernetics, "... the result of the solution of the problems of this type is not a number and not the function, but the probability distribution, assigned above the possible values of result. It is natural that in the initial data of task the negligible accurately factors of accidental character also must be assigned by the probability distribution" (Poletayev, 1958, pg. 332).

We repeatedly underscored above the conditional-probabilistic sense of solution of problem of interpretation of gravity anomalies. This task, examined/considered in general form, must be, consequently, it is added to the category stochastic tasks of physics and technology. At the same time separate particular questions, which relate to the interpretation, under the favorable for gravitational prospecting physical-geological conditions the being all-inclusive almost completely essence entire problems of interpretation, they can have and they actually have a character of the determined tasks, which allow/assume the specific unique solution.

In connection with this it is possible to indicate two basic promising trends in further development of theory of interpretation of gravity anomalies:

1. Systematic utilization of newest mathematical disciplines - information theory, theory of games, operations research and so forth (Poletayev, 1958; Ross-Ashby, 1959; collection: "Contemporary mathematics for engineers", 1958; Morse and Kimbell, 1956), keeping in

mind the development of algorithms (rules of the transformation of information) for the contemporary high speed computers, which give the solution complete in a theoretical-probable sense of the problem of interpretation.

2. Analysis of particular, but very important geologic tasks, whose solution under favorable physico-geologic conditions can be with high degree of probability achieved/reached by utilization of calculating apparatus of corresponding particular task of determined type interpretation.

Page 112.

Below, by necessity very briefly and schematically, we give some examples of thematics, which relates to two directions indicated.

Attempt at production/consumption of algorithm for sufficiently widely formulated task of interpretation of geophysical (not only gravimetric-prospecting) data from point of view of information theory was undertaken by .. A. Khalfin (1958). Very task of interpretation by them is formulated thus: on assigned geophysical field  $\varphi_0(r)$  (to signal) to determine the appropriate source distribution of this field  $q$  (communication/report), assuming one-to-one bond of the sources of the field

$$\varphi_0(r) \rightleftharpoons q.$$

(III. 28)

In given designations  $r$  - generalized symbol of space

coordinates. The concept of the source of field can be considered coinciding with that examined above in § 18-19 by the concept of the singular point of potential field. Thus, is examined the interpretation of potential field when the latter is reduced to the determination of its sources or singular points. We already know that real sense the task of interpretation in this setting makes for the bodies, limited by the uneven surfaces (beds, faults, etc.).

L. A. Khalfin examines the case when in the measured field  $\psi(r)$  besides useful information  $\varphi_0(r)$  interfering information  $n(r)$ , caused by interference effect, is contained. In this case in the concept of interference are included not only instrument errors, but also the noncontrollable effect of all remaining (except those investigated  $\varphi$ ) information sources. Thus,

$$\psi(r) = \varphi_0(r) + n(r). \quad (III, 29)$$

It is clear that under condition (III, 29) one-to-one character of relationship/ratio of measured field  $\psi(r)$  and sources  $\varphi$  no longer occurs. There appears, according to L. A. Khalfin, the task of the interpretation of this kind: to produce above the measured field  $\psi(r)$  a certain irreversible conversion, which destroys the interfering  $n$ -information and which retains, as far as possible, the interesting us  $\varphi$ -information. Such transformations will be examined in chapter IV.

If interfering information remained not removed, then measured

field  $\psi(r)$  and communication/report  $\varphi$  prove to be connected not functionally, but stochastically. In this case, as we already noted in the beginning of this paragraph, it is possible to investigate the probability of communication  $\varphi$  in the measured field  $\psi(r)$ , designated below through  $p_\varphi(q_i)$ . In the work of L. A. Khalfin given explicitly expression  $p_\varphi(q_i)$  under the assumption that the interference are uniform, i.e., that values  $n(r_k)$  with the different values of index  $k$  (making sense number of observation point) are not statistically dependent and the distribution of probability of interference  $p_1(n(r_k))$  is equal with different  $k$ . Is examined also the case, when distribution  $p_1(n(r_k))$  in the accuracy is not known, but are known only some statistical characteristics of the distribution of interference, precisely, the so-called moments/torques of distribution  $p_1(n)$ :

$$\left. \begin{aligned} \int_{N_1}^{N_2} p_1(n) dn &= 1, \\ \int_{N_1}^{N_2} n p_1(n) dn &= e_1, \\ \int_{N_1}^{N_2} n^2 p_1(n) dn &= e_2 \end{aligned} \right\} \quad (III. 30)$$

and so forth.

Page 113.

For this case is also obtained corresponding expression, which represents result of interpretation  $p_\varphi(q_i)$  in the following form:

$$p_\varphi(p_i) = ap(q_i) \exp \left\{ \sum_k \lambda_k [\psi(r_k) - \varphi_{0k}(r_k)] + \lambda_2 \times \right. \\ \left. \times [\psi(r_k) - \varphi_{0k}(r_k)]^2 + \dots + \lambda_m [\psi(r_k) - \varphi_{0k}(r_k)]^m \right\}. \quad (III. 31)$$

where  $a$  - constant;

$P(e_i)$  - a priori probability of communication, i.e., probability of communication/report  $e_i$  before application of this geophysical method, which characterizes the preliminary geologic concepts or results of interpretation of other geophysical methods;

$\lambda_1, \lambda_2, \dots, \lambda_m$  - constants, determined from (III, 30);

$\exp N$  - makes here sense

L. A. Khalfin brought out also complicated modifications of formula (III, 31) for that case when results of interpretation of different methods are interlocked (complex of methods), and also for cases when with interpretation are considered data about appropriate physical properties of rocks of region being investigated.

The second of promising trends indicated above is very vast in its content. To it can be attributed much of the fact that already long ago there was developed in the theory of the interpretation of gravity anomalies, namely methods of interpretation for the bodies of the correct geometric form, in detail examined/considered in Chapter V, and fitting these methods to the real geological conditions. Here there belong methods of the straight/direct determination of mass, cross section and coordinates of the center of gravity of the disturbing body, the beginning of development of which is established by G. A. Gamburtsev and M. I. Polikarpov as early as 1926. On these methods we already mentioned above, in § 19, and their detailed presentation will be given in Chapter VI.

To the same direction belongs the method of maximum distributions (Andreev, 1954, 1955), whose idea is reduced to following:

1. Is realized the analytical continuation of the anomalous field (gravitational or magnetic) being investigated into the lower half-space, i.e., into that part of the space, which includes the perturbing masses, whose effect/action caused the anomalies being investigated (general/common concept about the analytical continuation was given in § 10, and the corresponding calculations technique it will be in detail described in Chapter IV).

Page 114.

2. Depth of upper surface of perturbing masses according to characteristic limiting distribution of anomalous field at level of this surface is determined. Such kind of limiting distributions exists for some of the derived gravitational and magnetic potentials in such a case, when on the upper surface of the perturbing masses the singular points of the anomalous field (see § 18-19) are located.

As example Fig. 30 shows limiting distribution of vertical force gradient of gravity  $w_z$  for the case when gravity anomaly being investigated is caused by effect/action of bed with infinite propagation on incidence/drop on depth. It is possible to find it by direct calculation, if limiting distribution indicated above is

expressed by a certain final function.

S. V. Shalayev (1958) indicated the method of transformation of anomalous field with utilization of theory of complex variable functions, with the help of which it is possible to determine position of points on upper surface of disturbing body and in which derivative of potential being investigated goes to infinity. I. G. Klushin (1958) indicated the method of determining the intensity of a change in the anomalous density and power of the sources (singular points) of anomalous potential field with the depth. All these methods, which in Chapter V will be described in more detail in connection with special cases of interpretation, can be used for determining the depth of the surface of the basement of platform regions from the gravitational and magnetic anomalies. This particular, but very important task it proves to be possible to solve in many instances virtually unambiguously.

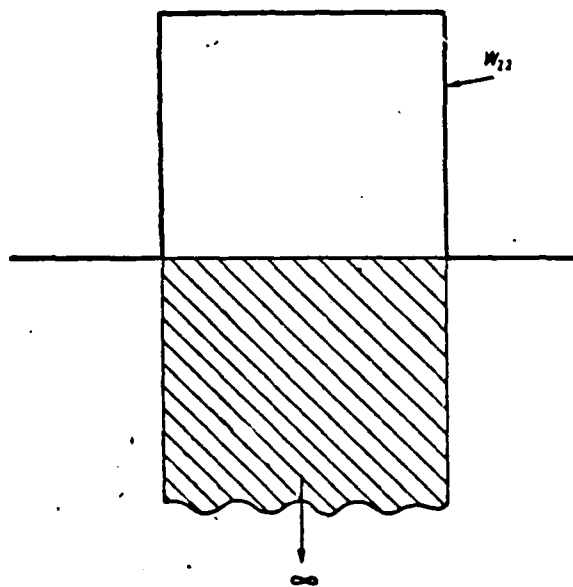


Fig. 30. Limiting distribution  $w_{11}$  on the level of upper edge of the vertical bed.



Page 115.

Chapter IV.

## CONVERSIONS AND CALCULATIONS OF ANOMALIES.

### § 21. General considerations.

In practice of geologic interpretation of results of gravitation prospecting works separation and conversions of gravity anomalies extensively are used. The need for such operations is caused by the fact that the observed anomalous field reflects the effects of many geologic reasons. Most important of them are power/thickness, composition and the structural special features of sedimentary formations, the relief of surface and the petrographic heterogeneity of crystalline basis/base, in particular, the presence of the intrusion bodies of acid and basic composition, and the deep structure of the earth's crust.

The solution to different prospecting and exploratory problems connected with detection and study of deposits of useful minerals, is facilitated, if we there is possibility at least approximately isolate components with different geologic nature from observed field. The same problem appears also in the case of applying other geophysical methods, in particular magnetic prospecting. However, the distribution of gravity anomalies depends on the wider circle of reasons, in particular, the effect of deep factors on anomaly  $\Delta g$  in many regions more noticeable than on the anomaly  $\Delta T$ . Therefore the

methods of separation and converting the anomalies the first were applied in gravitational prospecting, and subsequently - in magnetic prospecting.

By forces of superposition principle (superposition), which is valid for potential physical fields of Earth, effects, caused by different geologic factors, algebraically are summarized. This indicates, for example that the gravity anomaly from the complex geologic structure has accurately this form and intensity, such as we will obtain as a result of composing the anomalies, caused by each separate element of this structure.

Page 116.

Possibilities for interpretations, which are opened up by this principle, are limited to fact that for finding of any one component of anomaly it is necessary to know all the remaining components of complete anomaly. However, the attraction of different geologic and geophysical data makes it possible in the yard of the cases to do a similar separation of anomalous field. Thus, in the generalizing work of E. E. Fotiadi (1958), dedicated to deep geologic structure Russian platform, for the characteristic of the structure of basement and deeper zones were drawn the maps/charts of the transformed anomalies  $\Delta g$ , obtained after subtraction from the observed anomalies of Bouguer of the gravitation effects, caused by the structure of the basic structural-facies complexes of sedimentary cover.

Practical possibility of separation of anomalies in the absence of independent data and minimum of previously made assumptions is based on what sharply distinct in their scales and character of special feature of geologic structure create changes in anomalous field with different correlation, i.e., with different degree of changeability, observed during motion along profile or on area.

By A. K. Malovichko (1956) and some other authors assume that conversions of anomalies are not compatible with solution of so-called "inverse problem" of gravitational prospecting. One of the basic proofs of this assertion is reduced to the fact that in the case of applying different conversions the fictitious anomalies (mainly negative sign), which do not reflect real mass distribution, appear. It is easy to show the groundlessness of this position based on the following examples.

Anomaly of the gravitational force above extended body of type of horizontal circular cylinder takes form of symmetrical maximum, if body density exceeds density of enclosing rocks. The anomaly of horizontal gradient  $W_x$  has one maximum and one minimum (Fig. 31). Both for the curves  $\Delta g$ , obtained during the observations with the gravimeters, and for curved  $W_x$ , constructed according to the results of measurements with the variometers or the gradiometers, are developed the simple methods, which make it possible to find the depth of the bedding of the center of the body (see Chapter V).

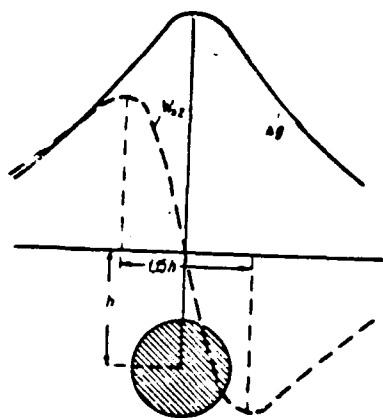


Fig. 31. Curves  $\Delta g$  and  $W_{\Delta g} \approx \frac{1}{a} \times [\Delta g(x+a) - \Delta g(x)]$  for horizontal circular cylinder.

Page 117.

Curve  $W_{\Delta g}$  can be constructed not only according to the direct results of measurements, but also by conversion (differentiation) curved  $\Delta g$  with the help of the numerical methods of mathematical analysis (Krylov, 1954; Mikeladze, 1953).

For a number of points  $x=a; 2a; 3a; \dots; na$  they calculate finite first-order difference

$$\Delta g(x+a) - \Delta g(x). \quad (\text{IV.1})$$

With small  $a$  curve  $\Delta g(x+a) - \Delta g(x)$  is completely similar to curve  $W_{\Delta g}$ , at the same time difference curve has dimensionality  $\Delta g$  (in order to obtain dimensionality of gradient, it is necessary to divide finite difference into length of interval  $a$ ).

Does this indicate that the interpretation of curve  $\Delta g(x+a) - \Delta g(x)$  is incompatible with solution of inverse problem, since converted curve does have "false" minimum, equal in magnitude to maximum? Of course, not. The distance between the minimum and the maximum directly enters into formula for determining the depth of the bedding of the body, which causes the anomaly being investigated.

Fig. 32 depicts map/chart of anomalies  $\Delta g$  for one of deposits of oil in the USA, while in Fig. 33 - its constructed on basis map/chart of second force derivative of gravity  $w_{xx} = \frac{\partial^2 g}{\partial x^2}$ . On the last map of isoline the deposit clearly is contoured. Meanwhile the interpretation of this map/chart from the point of view, presented Malovichko (1956), is incompatible with the solution to the "inverse problem".

It would be erroneous to think that application of transformations converts "unsuitable" for geologic targets map/chart  $\Delta g$  into map/chart, at which suddenly appear special features interesting researcher and regularities. The maps/charts of the transformed anomalies not cannot contain anything fundamentally new in comparison with the fact that it is noted during the photographing in the initial map  $\Delta g$ .

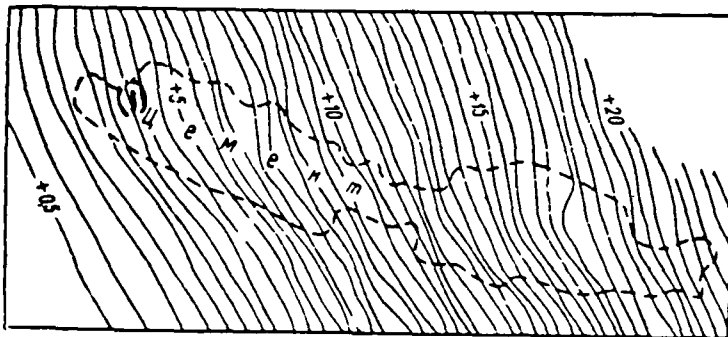


Fig. 32. Map of Bouguer's anomalies for deposit of Cement, Oklahoma. Section of the isolines through 0.5 mgal (from the work of Hammer, 1956).

Key: (1). Cement.

Page 118.

They only underscore, are separated/liberated some special features of initial map/chart and they depress, eliminate others. From the point of view of information theory (Goldman, 1957) any transformation of initial data leads to the decrease of a quantity of information, which are contained in the parent substance. Entirely this position relates also to the transformations of gravity anomalies. Localizing anomalies in the example of Fig. 33, we eliminate regional background and information containing in it about the deep structure of territory. In other cases the information about the fine/small structural special features is eliminated.

Let us note that question about decrease of quantity of information during processing of geophysical maps/charts does not

stand as sharply as during transfer of communication/report in theory of bond. Actually, the initial map/chart of anomalies physically is not destroyed. Entire/all imprinted in it geologic remains whole. This information partially disappears only on the transformed maps/charts. The latter fact indicates only that the maps/charts of local and regional anomalies never will be replaced initial map/chart and they must be considered as application/appendix to material. However, they substantially facilitate analysis and understanding of the latter, since they show in the underscored form, and sometimes consciously simple, first some, then other lines of the complete picture.

Most effective, from point of view of geologic interpretation, are transformations, based not on decrease of available, but during attraction additional information, i.e., transformations, which use independent geologic and geophysical data. We find the excellent examples of this approach in the works of Yu. N. Godin (1957, 1958). One of them is shown in Fig. 34.

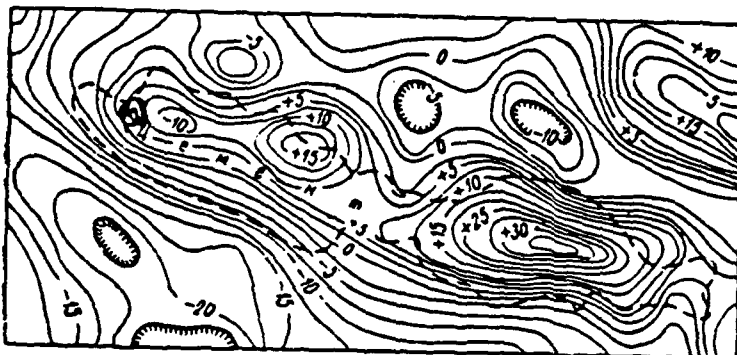


Fig. 33. Map/chart of second vertical force derivative of gravity, constructed on the basis Fig. 32. Section of the isolines  $2.5 \cdot 10^{-11}$  of CGS (from the work of Hammer, 1956).

Key: (1). Cement.

Page 119.

Let us note that preliminary construction of maps/charts of transformed anomalies completely does not eliminate attraction of other given methods of study at subsequent stages of interpretation, during combined analysis of all available material.

Concept of correlation of anomalies above has already been mentioned. The correlation of anomalies statistically characterizes the degree of the changeability of the latter during the motion along the profile or the areas of observations.



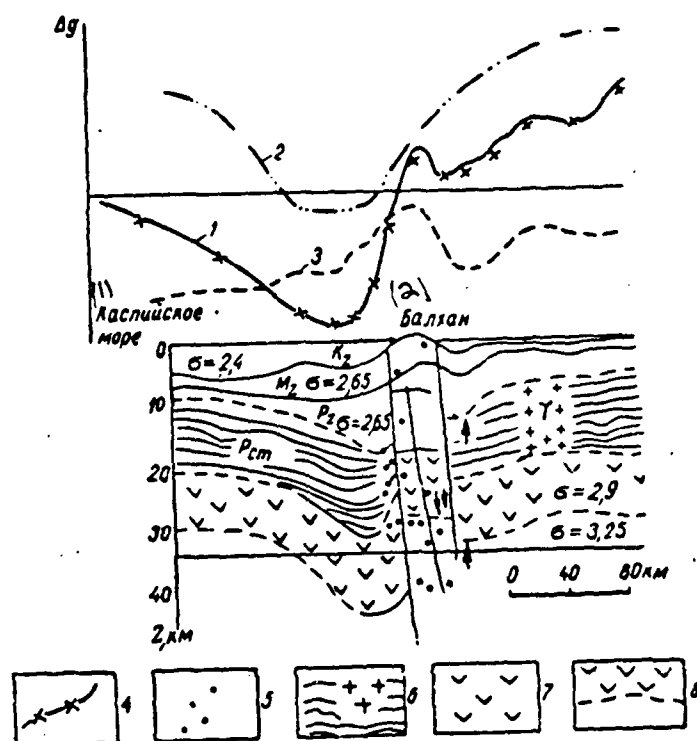


Fig. 34. Example of separation of summary field  $\Delta g$  to components caused by the effect of deep and surface factors, geological-geophysical section/cut of earth's crust along profile of Caspian Region-Bol'shoy Balzhan-Tuarkyr. 1 - curve of the observed anomaly  $\Delta g$ ; 2 - curve of anomaly  $\Delta g$ , which characterizes the effect of the deep factors (it is calculated according to the section/cut of the earth's crust); 3 - curve of anomaly  $\Delta g$ , caused by the effect of the weakly-metamorphized sedimentary rocks; 4 - computed values of anomaly  $\Delta g$  for represented section; 5 - seismic centers, which are grouped in the zones of deep faults; 6 - "granite layer" (predominantly gneiss with the separate zones of the development of granites); 7 - "basalt layer"; 8 - base of the earth's crust - boundary M.

Key: (1). Caspian Sea. (2). Balkhan.

Page 120.

The quantitative estimation of correlation can be done with the help of the so-called radius of autocorrelation. If are examined statistically uniform changes in a certain function, for example change in anomalies  $\Delta g(x)$  above the series of the similar in general terms geologic structures, crossed by one or several profiles, then the integral

$$\lim_{L \rightarrow \infty} \frac{1}{L} \int_{-\frac{L}{2}}^{+\frac{L}{2}} \Delta g(x) \Delta g(x + \tau) dx, \quad (IV, 2)$$

will determine autocorrelation function  $R(\tau)$  (Goldman, 1957). Here  $L$  - summary length of profiles, along which are considered the statistical properties of anomalies;  $\tau$  - distance between the starting point and the point of comparison, with respect to which is considered the changeability of anomaly.

When  $\tau = 0$   $R(\tau) = \overline{\Delta g^2}$ , i.e. during displacement, equal to zero, integral (IV, 2) determines average/mean value of square of anomaly.

Ratio  $R(\tau)$ :  $R(0)$  they call normalized autocorrelation function  $R_n(\tau)$  or coefficient of correlation (Chernov 1958). The correlation coefficient vary within the range of 1 to 0. In the case when the starting point and the point of comparison coincide,  $R_n(0) = 1$ . With an increase  $\tau$  value  $R_n(\tau)$  unavoidably is reduced, since the further we go

away from the starting point, the more the new parts contains the curve  $\Delta g$ .

Distance, at which statistical bond to a considerable extent is lost - correlation coefficient is reduced from 1.0 approximately to 0.3, it is called radius of autocorrelation (Chernov, 1958). In the complete absence of any bond  $R_{\Delta}(\tau) = 0$ . If anomaly variations along the profile do not contain latent periodicity,  $R_{\Delta}(\tau)$  monotonically decreases with an increase of displacement  $\tau$ , independent of direction of motions along the profile. The form of curve  $R_{\Delta}(\tau)$  and the value connected with it of the radius of autocorrelation give the possibility to judge the degree of the changeability of the distribution of anomalies. With the small correlation curve  $R_{\Delta}(\tau)$  rapidly decreases. In the case of the propagation of statistical long-range communication  $R_{\Delta}(\tau)$  it is changed smoothly (Fig. 35).

In the presence of latent periodicity in changes  $\Delta g$  curve is of alternating sign. The distance between the transition points through zero approximately corresponds to half of the period of oscillations (Fig. 36).

Page 121.

Virtually specific graph  $R_{\Delta}(\tau)$  for anomalies of one of ancient platforms is constructed in Fig. 37. As we see, in essence is noted the independent from each other distribution of anomalies with the linear dimensions of the order of several ten kilometers. The

transition of function  $R_*(\tau)$  through zero during displacement on the order of 110 km indicates that occurs also a certain periodicity, probably, caused by the oscillations/vibrations of the structural relief of deep interfaces of the earth's crust, by the generatrices of fold with linear dimensions on the order of 200 km and more. Approximately the same sizes/dimensions have structures, surfaces of basement expressed in the relief, arches/summaries and vast basins/depressions first-order.

Statistical uplifts/rises and definitions, given above, extensively are used in technical literature. Unfortunately, in the works from exploration geophysics they did not find an even proper propagation. The question can arise: wouldn't it be simpler to directly proceed in all calculations from the dimensions of anomalies. This simplicity, however, is apparent.

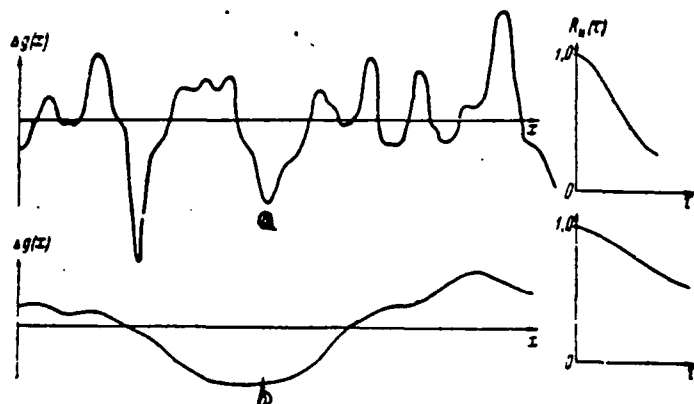


Fig. 35. Typical statistically uniform sequences of anomalies and corresponding to them graphs of correlation coefficient as function of displacement: a) distribution of anomalies, which is characterized by small radius of autocorrelation; b) distribution of anomalies, which is characterized by significant radius of autocorrelation.

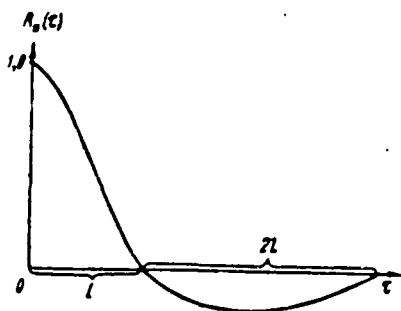


Fig. 36. Form of graph  $R_g(\tau)$  in presence of latent periodicity in distribution of anomalies  $4L$  is the approximate value of the period.

Page 122.

It is reached by the value of rigid holding of conditions. In the statistical description we in the considerably smaller measure are connected with the form and the sizes/dimensions of each concrete anomaly. The radius of autocorrelation relates not to any one

anomaly, but to a whole set of the anomalies, which differ from each other and by form and by sizes/dimensions, just as they are distinguished, for example, in the value the casual errors of the series/number of the measurements, which are characterized by one rms error.

Correlation of anomalies is closely related to graphic scales of change in geologic conditions. The regional special features of anomalous field express the general/common lines of the deep structure of large/coarse areas. The radius of the autocorrelation of regional anomalies composes many ten or first hundreds of kilometers. The local special features of anomalous field substantially change their view of the distances of the order of several kilometers, and in a number of cases, for example, in the limits of ore deposits, at the distances into ten and hundreds of meters.

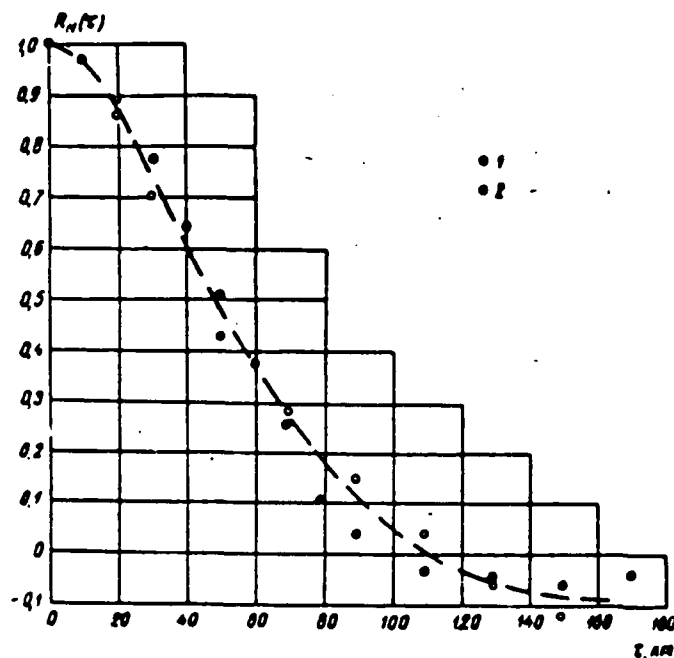


Fig. 37. Virtual determinations of graphs/curves  $R_n(\tau)$ , statistically characterizing distribution of anomalies in platform conditions. According to V. N. Kalashnikov (1959). 1 - points determined along the first profile; 2 - the same, on the second.

Page 123.

There is a known similarity of the order of anomalies and order of geologic structures. It correctly virtually in the very broad band of conditions. The disturbance/breakdown begins in that relatively rare for gravitational prospecting case, when the deeply sloping sources of anomalies with small linear dimensions have large intensity. In this case the linear dimensions of anomalies can considerably exceed the sizes/dimensions of structures and bodies, their creating. (In magnetic prospecting this relationship/ratio it is disseminated in

view of the broad band of a change in the magnetic properties of the rocks).

Presence of simple conformity of order of anomalies and order of structures allows on basis of quite schematic presentations/concepts about special features of geologic structure for area to graphically separate observed anomalies into regional and local components (Fig. 38). This separation is based on the assumption that regional field component within the limits of the profile of observations possesses very large correlation it either it is constant on the magnitude or approximately equally it is changed in the entire interval.

In a number of cases it is useful to establish the very observation system in such a way that regional background would remain approximately constant within limits of profile. Fig. 39 shows the typical banded anomaly, caused by large/coarse linear tectonic dislocation. With similar disturbances/breakdowns in the basement - the separational surfaces between the sections with different structure of crystalline basis/base in many regions of Russian platform, Central Asia and Siberia (Godin, 1958) - there are connected "networks" of the buried structures of sedimentary cover. The local anomalies of gravitational force, the reason for which there are structural uplifts/rises and change of the physical properties of sedimentary rocks within the limits of similar/analogous complexes, have insignificant value. From Fig. 39 it follows that their liberation/precipitation is facilitated, if basic profiles are



arranged/located on the course/strike of isolines  $\Delta g$ . Usual rule is to place the line of the observations transversely of course/strike, is understood, remains valid if the main target of photographing consists in the study of dislocation itself, and not connected with its structures of higher order.

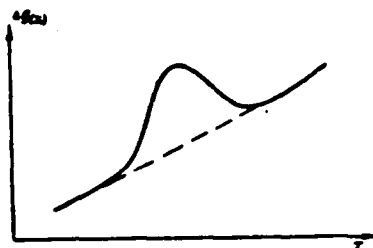


Fig. 38. Graphic separation of local anomaly and smoothly changing regional anomaly.

Page 124.

Autocorrelation function and radius of correlation remain invariable only under relatively uniform geologic conditions. In particular, the radius of autocorrelation can depend substantially on the direction of displacement. Such geologic units, as narrow trenches and trenches in the basement, and also linear folding zones, create the intensive anomalies, the radius of autocorrelation of which in the direction along the structures composes many ten and hundreds of kilometers, and in the perpendicular direction - kilometers or first tens of kilometers. In this case it is possible to speak about the sharp anisotropy of the radius of autocorrelation.

Such objects as the positive and negative structures of basement, and distribution connected with them of powers and composition of sedimentary formations are most frequently reason for anomalies, whose correlation in different directions is approximately identical, i.e., radius of autocorrelation is isotropic.

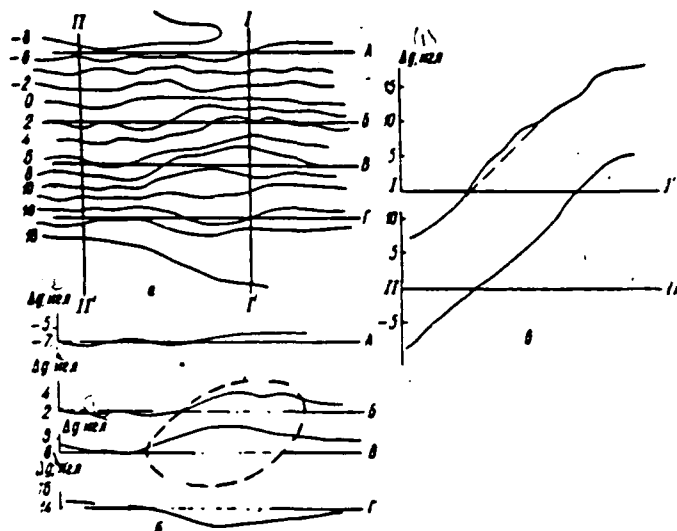


Fig. 39. Liberation/precipitation of local anomalies in zones of intensive "gravitational stages". a) the diagram of isoanomaly  $\Delta g$ , combined with the layout of profiles for the localization of anomalies; b) graphs  $\Delta g$  along the profiles, arranged/located on the course/strike of "gravitational step/stage"; the position of the local anomaly (shown by dotted line) is determined easily; c) graphs  $\Delta g$  along the profiles, which intersect "step/stage"; the liberation/precipitation of local anomaly is hindered/hampered by the intensive background, which in such cases frequently is changed according to the nonlinear law.

Key: (1). mg/.

Page 125.

Almost all methods of separation of anomalies are based on account of differences in sizes/dimensions of radius of autocorrelation. However, the transformations of anomalies can lean

also on another sign - the direction of preferred correlation.

General considerations, presented in first paragraph of present chapter, are defined concretely in § 22, 23, 24, 25, 26.

§ 22. Circular measuring grid for the "isotropic" transformation of the anomalous field.

At present there is developed a significant number of methods of separation of anomalies into regional and local components, and also methods of localization, in the case of applying which local special features of field are underscored and "is taken" a regional background. They are almost all based on the assumption that the picture of anomalous field remains invariable in one direction in this case it is examined two-dimensional model and the corresponding to it linear measuring grids or it is considered that any courses/strikes are possible, and then circular measuring grids are used.

Template is drawing, prepared on sheet of tracing paper, on which is depicted series of concentric circles/circumferences. At the isolated points of circles/circumferences the knots (Fig. 40) are noted. During calculations the center of measuring grid is placed into the selected point on the map/chart. The interpolating between the isolines of map/chart, at central point and in the knots of measuring grid the values of anomalous field are counted off. Then calculations according to the formula, which corresponds to this measuring grid, are produced.

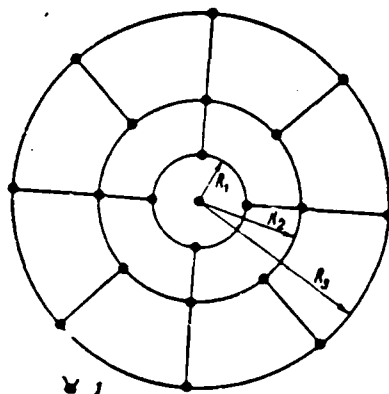


Fig. 40. Overall diagram of circular measuring grid for isotropic transformation of gravitational field. 1 - knots of the measuring grids, in which is removed/taken from the map/chart field value;  $R_1, R_2, \dots$  - radii of measuring grid.

Page 126.

Analytical expression of transformation, realized with the help of circular measuring grid, takes form

$$\Delta g(0)_{\text{transf}} = \Delta g(0) k_0 + \sum_{i=1}^n k_i \overline{\Delta g}(R_i), \quad (\text{IV}, 3)$$

where  $\Delta g(0)_{\text{transf}}$  - value of transformed anomaly, in reference to central point;

$\Delta g(0)$  - value of observed anomaly at central point of measuring grid;

$\overline{\Delta g}(R)$  - average/mean value of observed anomaly on ring of radius  $R$ , obtained after account of values, counted off in separate knots;

$k_0, k_i$  - coefficients, which depend on type of measuring grid.

It is known that anomaly at selected point can be represented by its values over entire area with the help of equality

$$\Delta g(0) = \int_0^{\infty} a da \int_0^{\infty} \overline{\Delta g}(q) J_0(aq) q dq. \quad (IV, 4)$$

Here  $J_0(aq)$  — function of Bessel of the first zero-order order. Let us recall that function  $J_0(x)$  is represented in the form of the sum

$$\sum_{k=0}^{\infty} \frac{(-1)^k \left(\frac{x}{2}\right)^{2k}}{(k!)^2} = \left(1 - \frac{x^2}{2^2} + \frac{x^4}{2^4 \cdot 2^2} - \dots\right). \quad (IV, 5)$$

Plotted functions  $J_0(x)$  and  $J_1(x)$  are constructed in Fig. 41. Functions  $J_0(a, x)$  and  $J_1(ax)$  differ from  $J_0(x)$  and  $J_1(x)$  approximately just as functions  $\cos(a, x)$  and  $\sin(a, x)$  from  $\cos x$  and  $\sin x$ , i.e., parameter  $a$  plays the same role as angular frequency in the case of trigonometric functions.

It is analogous with equality (IV, 4)

$$\overline{\Delta g}(R) = \int_0^{\infty} J_0(aR) a da \int_0^{\infty} \overline{\Delta g}(q) J_0(aq) q dq. \quad (IV, 6)$$

consequently,

$$\Delta g(0)_{\text{transf}} = \int_0^{\infty} \left[ k_0 + \sum_{i=1}^n k_i J_0(a R_i) \right] a da \int_0^{\infty} \overline{\Delta g}(q) J_0(aq) q dq. \quad (IV, 7)$$

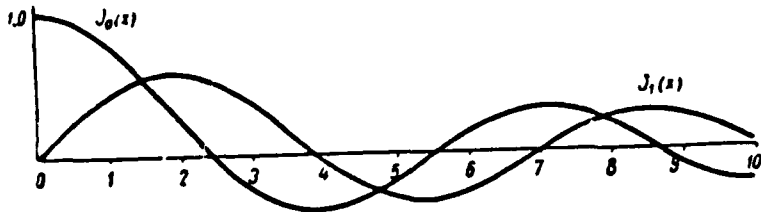


Fig. 41. Plotted functions of Bessel  $J_0(x)$  and  $J_1(x)$ . Explanation to formula (IV, 5).

Page 127.

Function  $\Psi(\alpha) = k_0 + \sum_{i=1}^n k_i J_0(\alpha R_i)$  is characteristic of transformation, on which depend basic special features of circular measuring grid [transparency].

Depending on number and dimensions of radii, value and sign of coefficients transformed anomaly expresses regional or local special features of observed gravitational field. The physical dimensionality of the transformed anomalies can be the same as in initial, or differ. This is determined by the dimensionality of the coefficients of measuring grid.

During utilization of one or the other measuring grid it is important to know its filter discrimination and sensitivity to errors in initial data. The filtering effect of the measuring grid can be considered with the help of several criteria, not not completely which are coordinated with each other, since they are based on different approach to this problem. The measuring grid can be considered on how

the value of anomalies of different types will be changed as a result of its application. It is most simple to fulfill this estimation, after tracing a change in the anomaly of the unitary sharpened source, arranged/located on depth  $z$ .

In normal case (with characteristic of transformation, equal to one) value of this anomaly, as sensitivity in question to masses  $M(z)$ , depend on depth as follows:

$$\begin{aligned} M(z)_{\text{norm}} &= \int_0^{\infty} 1a da \int_0^{\infty} \Delta g(q) J_0(aq) q dq = \\ &= \int_0^{\infty} 1a da \int_0^{\infty} \frac{z}{(z^2 + q^2)^{3/2}} J_0(aq) q dq = \int_0^{\infty} 1e^{-az} a da = \frac{1}{z^2}. \quad (\text{IV}, 8) \end{aligned}$$

For transformed anomaly we obtain, respectively,

$$\begin{aligned} M(z) &= \int_0^{\infty} \left[ k_0 + \sum_{i=1}^n k_i J_0(a R_i) \right] e^{-az} a da = \frac{k_0}{z^2} + \\ &+ \sum_{i=1}^n \frac{k_i z}{(z^2 + R_i^2)^{3/2}}. \quad (\text{IV}, 9) \end{aligned}$$

Relative sensitivity to masses as function of depth of up to sources or relative deep characteristic  $N(z) = M(z): M(z)_{\text{norm}}$ . Determines more clearly the filter discrimination of measuring grid. Taking into account that  $R_0 = 0; J_0(a R_0) = 1$ , will obtain

$$N(z) = \sum_{i=0}^n k_i \frac{z^2}{(z^2 + R_i^2)^{3/2}}. \quad (\text{IV}, 10)$$



Equality (IV, 10) can be used for comparison with each other of different concrete diagrams of measuring grid, and also for approximate estimate of interval of depths, within limits of which are included sources of chosen anomalies. This estimation will be maximum, since it is based on the presentation/concept about a maximally abrupt change in the density. In all other cases the anomaly-forming bodies can be nearer to the surface of the Earth, since the correlation of anomalies depends not only on the depth of bedding, but also on the horizontal gradient of the density of the rocks.

Anomaly variation with this correlation can serve as the more general criterion for evaluating effect/action of measuring grid. During this estimation nature of the observed changes  $\Delta g$  completely is not examined and therefore a question is eliminated, is connected this anomaly with a gradual change in the density of the rocks at the small depth or with an abrupt change in the density at the large depth.

Let us designate average/mean value of square of amplitude of observed anomaly  $\bar{A}^2$ , after transformation with measuring grid —  $\bar{A}_{\text{транс}}^2$ . Let us represent  $\bar{A}^2$  in the form of integral on separate components (Bartlett, 1958)

$$\bar{A}^2 = 2\pi \int_0^{\infty} G(\alpha) \alpha d\alpha, \quad (\text{IV, 11})$$

where

$$G(\alpha) = \frac{1}{2\pi} \int_0^{\infty} \bar{A}^2 H_0(\tau) J_0(\alpha\tau) \tau d\tau. \quad (\text{IV, 12})$$

Investigation of many processes of nature shows that dependence of coefficient of correlation of random function on displacement  $r$  is satisfactorily described by equality

$$R_{\alpha}(r) = \exp\left(-\frac{r^2}{r^2}\right), \quad (\text{IV}, 13)$$

where  $r$  - radius of autocorrelation.

Hence we find that

$$G(\alpha) = \frac{\bar{A}^2}{4\pi} r^2 \exp\left(-\frac{\alpha^2 r^2}{4}\right). \quad (\text{IV}, 14)$$

To transformation of anomalous field all components remain invariable. The integral (IV, 12), as has already been stated above, gives the average/mean value of the square of the amplitude of the observed anomalies

$$2\pi \int_0^{\infty} G(\alpha) \alpha d\alpha = 2\pi \int_0^{\infty} \frac{\bar{A}^2}{4\pi} r^2 \exp\left(-\frac{\alpha^2 r^2}{4}\right) \alpha d\alpha = \bar{A}^2$$

in this case.

Page 129.

After filtration of anomalies with the help of measuring grid effect of different components will be changed in accordance with characteristic  $\Psi(\alpha)$

$$\begin{aligned} G(\alpha)_{\text{transf}} &= G(\alpha) \Psi^2(\alpha), \\ \bar{A}_{\text{transf}}^2 &= 2\pi \int_0^{\infty} G(\alpha)_{\text{transf}} \alpha d\alpha = \\ &= \frac{2\pi \bar{A}^2 r^2}{4\pi} \int_0^{\infty} \exp\left(-\frac{\alpha^2 r^2}{4}\right) \left[ \sum_{i=0}^n k_i J_0(\alpha R_i) \right]^2 \alpha d\alpha. \quad (\text{IV}, 15) \end{aligned}$$

Opening the brackets in equality (IV, 15), we determine relative change in mean square of anomaly with this correlation (radius of autocorrelation  $r$ )

$$\begin{aligned} \frac{\bar{A}_{\text{транс}}^2}{\bar{A}^2} = & \sum_{i=0}^n k_i^2 P\left(\frac{R_i}{r}\right) + 2k_0 \sum_{i=1}^n k_i S\left(\frac{R_i}{r}\right) + \\ & + 2k_1 \sum_{i=2}^n k_i P\left(\frac{\sqrt{R_1 R_i}}{r}\right) S\left(\frac{R_i - R_1}{r}\right) + \\ & + 2k_2 \sum_{i=3}^n k_i P\left(\frac{\sqrt{R_1 R_i}}{r}\right) S\left(\frac{R_i - R_2}{r}\right) + \dots \quad (\text{IV, 16}) \end{aligned}$$

Analytical expression and numerical values of functions  $P$ ,  $S$  are given in Table 11.

Let us examine practical example, which elucidates utilization of formula (IV, 16) and Table 11.

Liberation/precipitation of local anomalies is realized with the help of measuring grid, which has parameters (to scale of map/chart)  $R_0=0$ ;  $k_0=0$ ;  $R_1=1$  cm;  $k_1=1$ ;  $R_2=4$  cm;  $k_2=-1$ . Transformation consists in the fact that is counted the average/mean value of anomaly on the rings with radii 1 and 4 cm, then from the first average/mean value the second is subtracted

$$\Delta g(0)_{\text{транс}} = \bar{\Delta g}(1) - \bar{\Delta g}(4). \quad (\text{IV, 17})$$

In more detail this method of localization is examined in § 24, here we will pay primary attention to illustration of positions presented.

Obviously, fine/small variations in observed field, anomaly with radius of autocorrelation smaller than radius of internal ring, will not affect transformed anomalies. In exactly the same manner the anomalies with the large correlation, which are not changed substantially during the displacement, equal to the radius of external ring, they will prove to be excluded during the transformation.

Page 130.

Table 11. Numerical values of functions P, S.

$\frac{R}{r} = z$	$S(z) = e^{-z^2}$	$P(z) = e^{-2z^2} J_0(2z^2)$	$z$	$S(z)$	$P(z)$
0.00	1.000	1.000	1.00	0.368	0.308
0.02	1.000	0.999	1.02	0.353	0.301
0.04	0.998	0.997	1.04	0.339	0.294
0.06	0.996	0.993	1.06	0.325	0.288
0.08	0.994	0.987	1.08	0.312	0.281
0.10	0.990	0.980	1.10	0.298	0.275
0.12	0.986	0.972	1.12	0.285	0.270
0.14	0.981	0.962	1.14	0.273	0.264
0.16	0.975	0.951	1.16	0.260	0.259
0.18	0.968	0.938	1.18	0.249	0.254
0.20	0.961	0.925	1.20	0.237	0.249
0.22	0.953	0.910	1.24	0.215	0.240
0.24	0.944	0.894	1.28	0.194	0.231
0.26	0.935	0.878	1.30	0.185	0.227
0.28	0.925	0.860	1.34	0.166	0.220
0.30	0.914	0.842	1.38	0.149	0.213
0.32	0.903	0.823	1.40	0.141	0.209
0.34	0.891	0.804	1.44	0.126	0.203
0.36	0.878	0.785	1.48	0.112	0.197
0.38	0.866	0.765	1.50	0.105	0.194
0.40	0.852	0.745	1.54	0.093	0.189
0.42	0.838	0.725	1.58	0.082	0.184
0.44	0.824	0.705	1.60	0.077	0.181
0.46	0.809	0.685	1.64	0.068	0.176
0.48	0.794	0.665	1.68	0.060	0.172
0.50	0.779	0.645	1.70	0.056	0.170
0.52	0.763	0.626	1.74	0.048	0.166
0.54	0.747	0.607	1.78	0.042	0.162
0.56	0.731	0.588	1.80	0.039	0.160
0.58	0.714	0.570	1.84	0.034	0.156
0.60	0.698	0.552	1.88	0.029	0.153
0.62	0.681	0.535	1.90	0.027	0.151
0.64	0.664	0.518	1.94	0.023	0.148
0.66	0.647	0.502	1.98	0.020	0.145
0.68	0.630	0.486	2.00	0.018	0.143
0.70	0.613	0.471	2.05	0.015	0.140
0.72	0.596	0.456	2.10	0.012	0.136
0.74	0.578	0.443	2.20	0.008	0.130
0.76	0.561	0.429	2.30	0.005	0.124
0.78	0.544	0.416	2.40	0.003	0.119
0.80	0.527	0.404	2.50	0.002	0.114
0.82	0.510	0.392	2.60	0.001	0.110
0.84	0.494	0.381	2.70	0.001	0.105
0.86	0.477	0.371	2.80	0.000	0.101
0.88	0.461	0.360	3.00	0	0.095
0.90	0.445	0.351	3.50	0	0.081
0.92	0.429	0.341	4.00	0	0.071
0.94	0.413	0.333	5.00	0	0.057
0.96	0.398	0.324	7.00	0	0.040
0.98	0.383	0.316			

Page 131.

After averaging on external and internal rings and subtraction these close values will give small difference. Consequently, from entire range of the observed anomalies after transformation will remain only those, whose correlation is not too great and it is not too small.

After substituting parameters of measuring grid into formula (IV, 16), we will obtain

$$\begin{aligned} \frac{\bar{A}_{\text{транс}}^2}{\bar{A}^2} &= 1P\left(\frac{1}{r}\right) + 1P\left(\frac{4}{r}\right) + 2 \cdot 0 + \\ &+ 2 \cdot 1 \cdot (-1) P\left(\frac{\sqrt{1 \cdot 4}}{r}\right) S\left(\frac{4-1}{r}\right). \end{aligned} \quad (\text{IV}, 18)$$

Graph  $\sqrt{\frac{\bar{A}_{\text{транс}}^2}{\bar{A}^2}}$  for distributions of anomalies with different value of radius of autocorrelation is given in Fig. 42. For the concrete value of  $r=2$  cm (to scale of map/chart) we find, putting to use Tables 11,  $\bar{A}_{\text{транс}}^2 : \bar{A}^2 = 0,645 + 0,143 - 2 \cdot 0,308$   
 $\times 0,105 = 0,723$ ;  $\sqrt{\frac{\bar{A}_{\text{транс}}^2}{\bar{A}^2}} = 0,85$ .

The large part of the statistical distribution of anomalies, which is characterized by this radius of autocorrelation, remains invariable after processing/treatment. With

$$r = 20 \text{ cm} \quad \sqrt{\frac{\bar{A}_{\text{транс}}^2}{\bar{A}^2}} = 0,1.$$

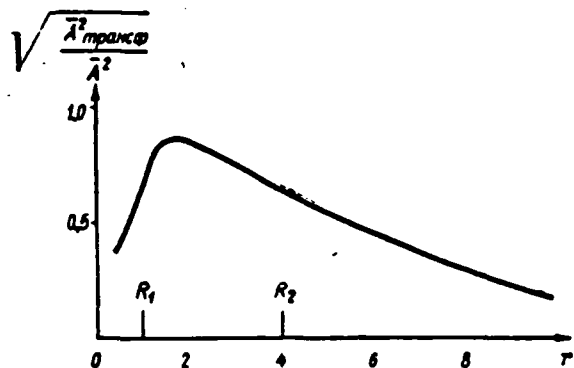


Fig. 42. Relative change in anomalies of different correlation after their transformation according to formula (IV, 17).

Page 132.

Considering the sensitivity of the measuring grid to errors in initial data, it is possible to consider errors in measuring as anomalies, but not geologic, but technical origin. For calculations according to the formula (IV, 16) it is necessary to know root-mean-square annoyance value and their correlation. The latter depends on the denseness of network/grid, methodology of the observation and other factors.

Maximum, smallest distance, at which disappear couplings between errors, is equal to distance between observation points. Factual errors in the contiguous points of profile are not independent variables. The utilization of common graphs of the displacement of zero point, the leveling of errors while conducting of isolines and other factors lead to the fact that the radius of autocorrelation can

exceed the smallest possible value, equal to the step of the network, 1.5-2 times.

### § 23. Methods of averaging.

After examining overall diagram of circular measuring grid, we change to presentation of separate methods of separation of anomalies. The most known and virtually disseminated method of separation of field to the components is the method of the averaging, whose theoretical basis was for the first time done in the work of A. N. Tikhonov and Yu. D. Boulangers (1945).

Anomaly  $\Delta g$  at each point is in the form of sums of regional  $\Delta g_{per}$  and local  $\Delta g_{lok}$  of components, which are subject to determination. The observed anomalous afterward is neutralized in the limits of the circle of radius  $R$ . Size/dimension  $R$  is selected by such so that it would considerably exceed the radius of the autocorrelation of the anomalies being isolated.



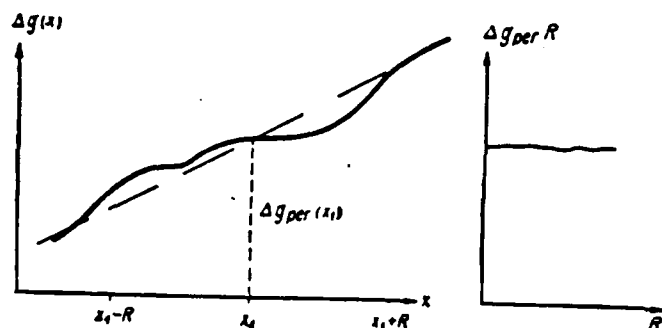


Fig. 43. Value of regional anomaly, isolated using method of averaging, at the particular point barely depends on radius of averaging, if regional field is changed according to linear law.

Page 133.

If this condition is observed, then with the averaging local positive and negative anomalies to a considerable extent compensate each other, whereas regional comprising, possessing greater correlation, weakly depend on averaging. Dependence completely disappears in the case of changing the regional field according to the linear law (Fig. 43).

Regional field component  $\Delta g$  at point  $x$ , coincides with arithmetic mean value of this component at all points of interval of averaging (with averaging on area point  $x$ , it is central point of circle)

$$\Delta g_{\text{per}}(x_0) = \frac{1}{2n+1} \sum_{i=-n}^{+n} \Delta g_{\text{per}}(x_i). \quad (\text{IV}, 19)$$

If the interval of averaging is selected correctly, then

$$\begin{aligned} \frac{1}{2n+1} \sum_{i=-n}^{+n} \Delta g(x_i) &= \frac{1}{2n+1} \sum_{i=-n}^{+n} \Delta g_{\text{per}}(x_i) + \\ &+ \frac{1}{2n+1} \sum_{i=-n}^{+n} \Delta g_{\text{non}}(x_i) \approx \frac{1}{2n+1} \sum_{i=-n}^{+n} \Delta g_{\text{per}}(x_i) \approx \Delta g(x)_{\text{per}}, \quad (\text{IV}, 20) \end{aligned}$$

since in the condition the average/mean value of local anomalies is close to zero.

Averaging is such operation, which eliminates sharply variable part of field, leaving invariable smoothly varying part. Therefore, the effect of the deeply arranged/located masses with the averaging is retained regardless of the fact how these masses are distributed, and the effect of the density heterogeneity of the rocks near the surface of the Earth is eliminated. The gravitation effect of the horizontally sloping layers of approximately constant composition and thickness will enter into the regional background, even if these rocks lie comparatively shallow.

Change (as a result of averaging of anomalies) in sensitivity to masses, arranged/located on different depths, is convenient to trace based on example of point source. Thus,

$$\Delta g(0)_{\text{per}} = \frac{1}{\pi R^2} \int_0^{2\pi} d\varphi \int_0^R \overline{\Delta g}(r) r dr = \frac{2}{R^2} \int_0^R \overline{\Delta g}(r) r dr, \quad (\text{IV}, 21)$$

where  $\overline{\Delta g}(r)$  - value  $\Delta g$  on the circle/circumference of radius  $r$  after averaging on the angle  $\varphi$ .

Taking into account expression  $\overline{\Delta g}(r)$  according to equality (IV, 6), we find

$$\Delta g(0)_{\text{per}} = \int_0^\infty \left[ \frac{2}{R^2} \int_0^R J_0(\alpha r) r dr \right] \alpha d\alpha \times \int_0^\infty \overline{\Delta g}(\varrho) J_0(\alpha \varrho) \varrho d\varrho. \quad (\text{IV}, 22)$$

Page 134.

Consequently, characteristic of transformation, realized with averaging, takes form

$$\frac{2}{R^2} \int_0^R J_0(ar) r dr = \frac{2J_1(aR)}{aR}. \quad (\text{IV}, 23)$$

Hence we find sensitivity  $M(z)$  to sources as function of depth of bedding

$$M(z) = \int_0^\infty \frac{2J_1(aR)}{aR} e^{-az} a da = \frac{2}{\sqrt{z^2 + R^2} (z + \sqrt{z^2 + R^2})}. \quad (\text{IV}, 24)$$

Relative sensitivity to be defined as

$$N(z) = \frac{M(z)}{M(z)_{\text{ном}}} = \frac{2z^2}{\sqrt{z^2 + R^2} (z + \sqrt{z^2 + R^2})}. \quad (\text{IV}, 25)$$

With  $z \rightarrow 0$   $N(z) \rightarrow 0$  with  $z \rightarrow \infty$   $N(z) \rightarrow 1$ .

Graph  $N(z)$  is constructed in Fig. 44. Along the vertical axis the depth, expressed in the units of the radius of averaging, is plotted. As we see, the effect of the masses, arranged/located on the depth, equal to the interval of averaging ( $z=2R$ ) and greater it, it remains almost invariable.

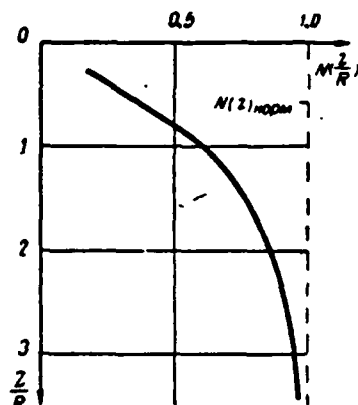


Fig. 44.

Fig. 44. Relative deep characteristic  $N(z)$  of method of averaging.

Explanation to the formula (IV, 25).

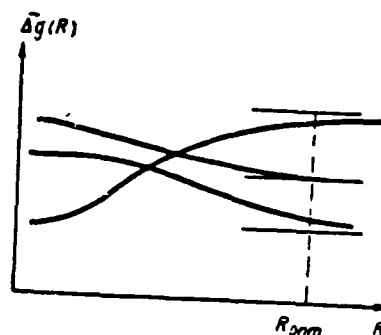


Fig. 45.

Fig. 45. Change in curves  $\Delta g(R)$  in presence of linearly changing regional background. (Case of the anomalies of two orders).

Page 135.

This position is important from a methodic point of view while conducting of gravimetric photographings. If there is studied a certain geologic surface, on which the density of the rocks (for example, the surface of crystalline basement) sharply is changed, then with the average depth of up to the boundary of the order of several kilometers being investigated the distance between observation points also can be several kilometers. Interpolation will satisfactorily show anomaly value in the gaps/intervals between the points. The greater thickening of observation points within the limits of entire area can prove to be technically and economically not justified. The at the same time separate interpretation profiles, which occupy the

insignificant part of the overall volume of works, must be conducted with the step/pitch, considerably less than the average depth of the bedding of objects of study, since further decrease of the step/pitch of network/grid slowly affects an improvement in the quality of material.

For determining the optimal radius of averaging they select on initial map/chart  $\Delta g$  several points, arranged/located in different sections. At these points the average/mean values of anomalies count, increasing consecutively/serially the size/dimension of the area of averaging. According to graphs  $\Delta g_{\text{average}}(R)$  it is possible to establish/install such value of  $R$ , whose excess unessentially affects the value of regional anomalies. In the case of linear "regional background" graphs  $\Delta g_{\text{average}}(R)$  go out to the asymptote (Fig. 45). Under such favorable conditions local anomalies are separated/liberated without the essential distortions, almost in the "pure form" (Fig. 46).

Feasible is such a version that after certain increase in radius  $R$  shape of the curve  $\Delta g_{\text{average}}(R)$  again sharply will be changed. This is indicated by the presence of anomalies of several orders. For the selection of optimal radius under these conditions is used not the asymptotic branch of the curve  $\Delta g_{\text{average}}(R)$ , and point of inflection (Fig. 47).

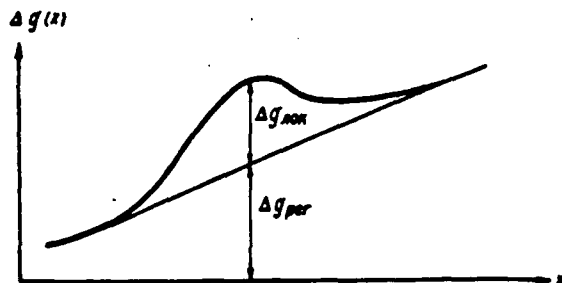


Fig. 46. Local anomaly is separated/liberated with minimum distortions, if regional background is changed according to linear law.

Page 136.

A. N. Tikhonov and Yu. D. Boulanger (1945) for explanation of physical sense of averaged anomalies and selection of radius of averaging introduce concept of measure of averaging. Proves to be that the averaged anomalous field can be considered as the observed field, but that caused by averaged, smoothed mass distribution. The total value of anomalous mass in this case is retained. Thus, if the anomaly is created by the mass concentrated at one point at depth  $z$ , the effect/action of averaging with the measuring grid of radius  $R$  is equipollent to the "flaring" of mass in the flat/plane disk, arranged/located on the same depth and the having radius, equal to the radius of averaging, i.e., on the area equal to measuring grid. The measure of averaging is defined as the ratio of the anomaly of that averaged to the anomaly, observed for the epicentral point.

It fundamentally does not differ from the circular measuring grid

for averaging measuring grid quadratic (Fig. 48). During the utilization of a quadratic measuring grid readings of anomalies  $\Delta g$  are taken at the points, distant behind each other at the equal distances. The practical advantage of quadratic measuring grid consists into the somewhat smaller volume of calculations. The analyzed map/chart immediately entire/all is divided/marked off by the system of vertical and horizontal lines into the squares of intended size. (Within the limits of the side of measuring grid must be stacked the integer of such squares). At the points of intersection of lines are written out values  $\Delta g$ , which are used during the calculations of average/mean values.

The distance between adjacent lines is established/installed after that how optimal dimension of side of square is selected. The latter is determined analogously with the radius of circle.

---

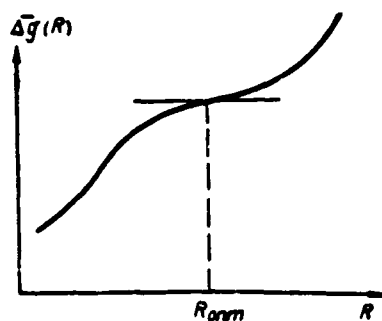


Fig. 47.

Fig. 47. Change in curve  $\overline{\Delta g}(R)$  in presence of nonlinearly changing regional background. (Case of anomalies of three and more than orders).

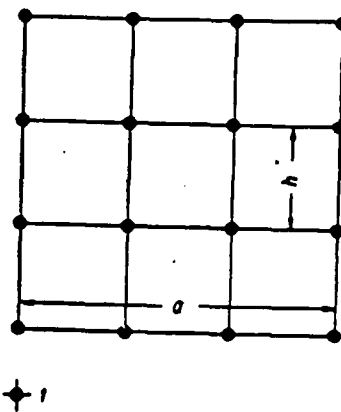


Fig. 48.

Fig. 48. Quadratic measuring grid for separation of anomalies according to method of averaging. 1 - knots of measuring grid; a) the size/dimension of the side of square; h) the distance between the knots.

Page 137.

Keeping constant the size/dimension of measuring grid and gradually increasing the step/pitch between the knots, is found this distance of  $h$ , and, consequently, a number of fiducial marks, with which the average/mean value of anomaly, in reference to the central point, still remains constant. Usually within the limits of one side of square 4-6 knots are located.

Maps of regional anomalies, constructed according to the



averaging method, extensively are used during tectonic zoning of closed territories and solution of other geologic problems. According to experiment, the radius of averaging in such cases can compose several ten kilometers. This means that the processing/treatment by the method of the averaging of the separate maps/charts, which contain the small area (for example, ten or hundreds of quadratic kilometers), can prove to be ineffective, since for the part of the area, which adjoins the boundaries of plane table, the values of regional anomalies cannot be determined will be. The width of this "empty zone" (Fig. 49) is approximately equal to radius of circular measuring grid or to half of the side of the square of averaging.

Drawing gravimetric data on adjacent areas, even if there were conducted less detailed photographings, it is possible to construct map/chart of local and regional anomalies for entire area of observation.

#### § 24. Method of variations.

The method of variations, proposed by B. A. Andreyev in 1938, is one of simple in application technique. This method is very effective with the localization of anomalies, however, in contrast to the method of averaging, it does not make it possible to obtain the map/chart of regional field. The very name of the method indicates that it has as a goal to underscore changes, variations in the observed distribution of anomalies, i.e., to isolate those components which are

characterized by a small correlation.

According to B. A. Andreyev, function

$$\delta U(x, l) = U(x) - \frac{U(x+l) + U(x-l)}{2}, \quad (\text{IV}, 26)$$

is called variation in anomaly  $U(x)$ .

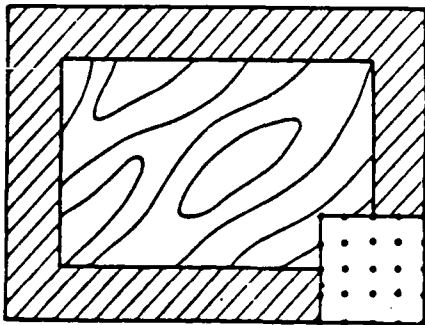


Fig. 49. Relationship of dimensions of the measuring grid and area for which it is not possible to construct a map of regional field (shaded).

Page 138.

Placing origin of coordinates into point of calculation of variation, we will obtain into somewhat simpler form analogous equality for case of assignment of initial data with respect to area

$$\delta U(0, l) = U(0) - U(l). \quad (\text{IV}, 27)$$

In this form formula was independently proposed by American geophysicist Griffin (Griffin, 1949).

As we see, for calculating variation in anomaly at the particular point it is necessary from observed value to subtract average/mean value of anomaly on circle/circumference of radius  $l$ . during this processing/treatment the anomalies with a small correlation will remain constant and will be excluded the anomalies, which are unessentially changed at a distance  $l$ , i.e., the distribution of anomalies with the radius of autocorrelation considerably larger than  $l$ .

Just as template of method of averaging is determined only by one parameter, properties of template of method of variations uniquely determines parameter value of transformation  $l$ .

Let us examine filter discrimination of template as function of this parameter. From the equality (IV, 27) follow that with  $k_0=1$ ,  $k_1=-1$ ,  $R_1=1$  the characteristic of transformation  $\psi(a)$  satisfies the relationship/ratio

$$\psi(a) = 1 - J_0(a l). \quad (\text{IV}, 28)$$

Relative sensitivity to masses is changed with depth according to the law

$$N(z) = 1 - \frac{z^2}{(z^2 + l^2)^{3/2}} \quad (IV, 29)$$

Graph  $N(z)$  is constructed in Fig. 50. The scale of depths is selected in ones  $l$ .

The fact that effect of objects, arranged/located in interval of depths from 0 to 0.5 $l$ -0.7 $l$ , remains virtually invariable, is one of remarkable properties of method of variations. The effects, caused by the fine/small manifestations of density heterogeneity, are not underscored excessively.

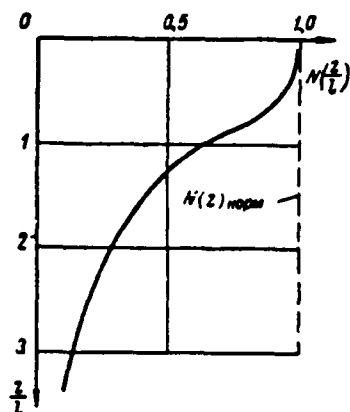


Fig. 50. Relative deep characteristic  $N(z)$  of method of variations.  
Explanation to the formula (IV, 29).

Page 139.

The latter, as it shows below, is characteristic for other methods of localization, in particular, the methods, based on the transition from anomalies  $\Delta g$  to anomalies  $W_{xyz}$ .

as shows Fig. 50, effect of masses, arranged/located more deeply than interval of localization  $l$ , virtually in all cases it becomes negligible regardless of the fact how these masses are distributed. In § 22 of the present chapter it was underscored that this estimation is maximum.

Filtering effect/action of template with respect to anomalies with different correlation illustrates Fig. 51. From the formula (IV, 16) follow that

$$\bar{A}_{\text{template}}^2: \bar{A}^2 = 1P(0) + 1P\left(\frac{l}{r}\right) + 2 \cdot 1(-1)S\left(\frac{l}{r}\right). \quad (\text{IV}, 30)$$

If  $(l)/(r)$  order of one and more, anomalies during transformation remain virtually invariable. Anomalies with the large correlation  $r \geq 2/$  are eliminated almost completely.

Let us pause at practical questions of calculation  $\delta U$ . If the specified distribution of anomalies  $U(x)$  along the profile, variation  $\delta U(x)$  easily is calculated graphically. For this it suffices to connect the straight/direct point  $U(x+l)$  and  $U(x-l)$  and to measure the segment of ordinate, intercepted by a straight line (Fig. 52). During calculation  $\delta \Delta g$  on the map/chart of anomalies  $\Delta g$  is conveniently to preliminarily draw the grid of vertical and horizontal lines with a step/pitch less  $l$  into the integer of times. At the points of intersection of lines (junctions) the values of anomaly  $\Delta g$  are written out. The average/mean value  $\overline{\Delta g(l)}$  is determined by p four, eight or to another number of readings.

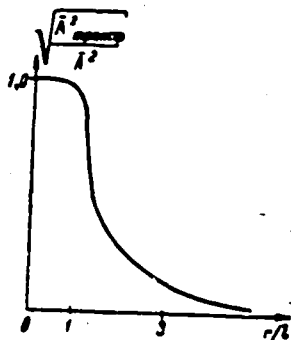


Fig. 51.

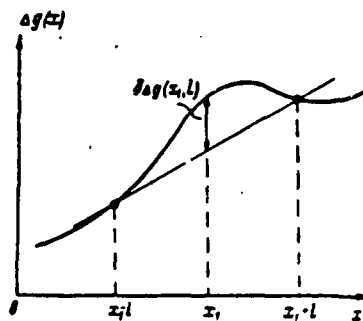


Fig. 52.

Fig. 51. Relative change in anomalies of different correlation after their transformation according to formula (IV, 27).

Fig. 52. Graphic calculation of  $\delta\Delta g(x, l)$ .

Page 140.

If  $l$  great and on external ring fall eight and more than points, appears certain nonconformity in "weight" of central point and points, located on the periphery. The casual errors of measurement, reading, etc. during calculation  $\overline{\Delta g}(l)$  to a considerable extent are compensated, whereas error in central point is manifested  $\delta\Delta g$  entirely. In these cases there is useful to define  $\Delta g(0)$  as  $\overline{\Delta g}(0)$ , neutralizing readings  $\Delta g$  at the nearest four points and carrying result to the center of square. They sometimes go still further, increasing internal ring to the sizes/dimensions, close to one third or half of external. The anomalies, localized thus, in the essence are a difference in two variations with the low and high values  $l$ . Actually, variations with radii of  $l_1$  and  $l_2$  are expressed, respectively as



$$\delta \Delta g(0, l_1) = \Delta g(0) - \overline{\Delta g}(l_1),$$

$$\delta \Delta g(0, l_2) = \Delta g(0) - \overline{\Delta g}(l_2).$$

Subtracting from the second equality the first, we find

$$\delta \Delta g(0, l_2) - \delta \Delta g(0, l_1) = \overline{\Delta g}(l_1) - \overline{\Delta g}(l_2). \quad (\text{IV, 31})$$

Transformations, similar (IV, 31), are recommended by some foreign geophysicists. Thus, Saskso and Nygard (1953) recommend for the localization of anomalies (but thereby also their causing objects) to calculate according to maps/charts  $\Delta g$  the function

$$F(\Delta g) = \frac{\overline{\Delta g}(R_1) - \Delta g(R_1)}{R_2 - R_1}. \quad (\text{IV, 32})$$

As we see, right sides of equalities (IV, 31) and (IV, 32) are characterized by only multiplier  $(1)/(R_2/R_1)$ . Since working initial maps/charts occurs with the templates, which have the fixed values of  $R_1$  and  $R_2$ , the effect of multiplier  $(1)/(R_2/R_1)$  will affect only the dimensionality of the calculated anomalies and the general/common level of numerical values. Somewhat will be increased and the volume of calculations. The configuration of isolines, position and relative value of maximums and minima will be completely identical, if the radii of the external and internal ring of such templates coincide.

Consequently, identical will be geologic efficiency of such maps/charts.

As already mentioned above, difference transformations of form (IV, 31) from entire set of anomalies separate/liberate only part,

with correlation of not too great and not too small. The radius of the autocorrelation of such anomalies lies/rests within the limits between the radii of the internal and external ring of template.

Page 141.

Therefore difference transformations are characterized by peculiar relative sensitivity to the depth of the bedding of sources. With an increase  $z$  the sensitivity initially is increased to a certain limit, and then it decreases, forming the gently sloping maximum (Fig. 53). The analytical expression of function  $N(z)$  gives equality (IV, 33)

$$N(z) = \frac{z^2}{(z^2 + l_1^2)^{3/2}} - \frac{z^2}{(z^2 + l_2^2)^{3/2}} \quad (\text{IV, 33})$$

Method of variations and other with it connected finite-difference transformations allow with successive increase in parameter of transformation to dismember observed field to groups of anomalies of different order.

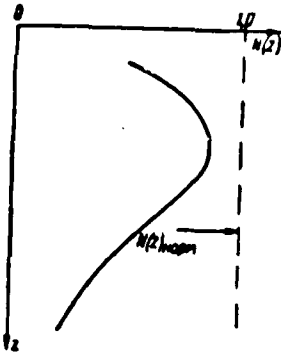


Fig. 53. Transformations which are described by formulas (IV, 31), (IV, 32) correspond to the relative deep characteristic with maximum in  $z > 0$ .

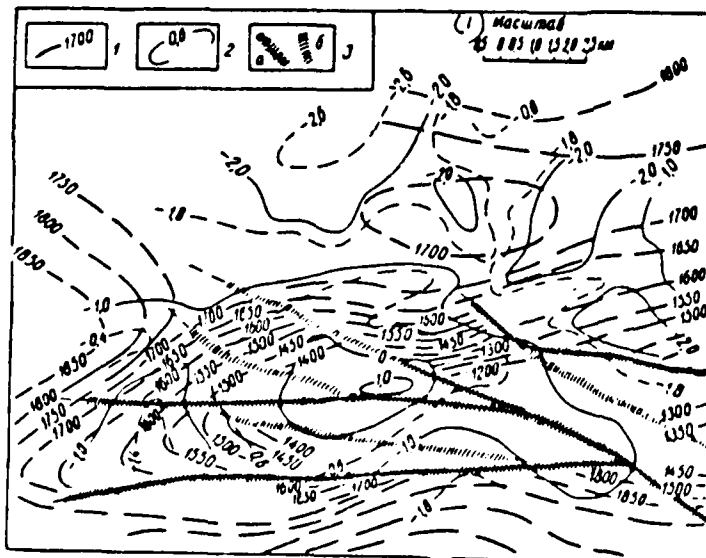


Fig. 54. Example to local anomaly  $\delta\Delta g$  above oil bearing structure.

On F. A. Arest et al. 1 - stratoisohypses of the seismic horizon; 2 - isoline  $\delta\Delta g$ , mgal; 3 - drives of tectonic disturbances/breakdowns; a) established; b) predicted.

Key: (1). Scale.

Page 142.

Usually such groups there can be two-three. In contrast to the method of averaging calculations are satisfied also on comparatively small plane tables. The sizes/dimensions of the "empty zone", situated along the boundaries of plane table, for which it is not possible to compute the localized anomalies, are comparatively small, several times less than with the averaging. This is the result of in principle different approach to the task.

Transformation of gravitational field according to method of averaging is calculated for the fact that from observed picture set of local anomalies of different sign is eliminated as a result of mutual compensation. Only in the second development stage local anomaly is defined as difference  $\Delta g - \Delta g_{per.}$

Method of variations is designed for direct liberation/precipitation of each local anomaly individually. The example to the local anomaly  $\delta \Delta g$  above the oil bearing structure is shown in Fig. 54.

§ 25. Methods of the recount of anomalies  $\Delta g$  in the anomaly of the vertical force gradient of heaviness  $W_{..}$

Localization of anomalies by transition from observed field distribution to field distribution of vertical force gradient of gravity is based on the fact that the effect of masses, located at

different depths, and also differently distributed at one depth, in this case is sharply underscored or is weakened/attenuated.

Rocks, which generate in the first approximation, uniform layers, whose thickness is substantially changed only at distances into ten and hundreds of kilometers, are reason for anomalies with very large correlation. The value of these anomalies, itself sufficiently large - ten milligal, it depends first of all on the vertical extent of species/rocks and their excess density, to the much smaller degree - from the depth of bedding and order of alternating separate layers. Since the dependence on the depth in this case plays secondary role, the anomalies of lapse  $W_{\text{II}}$ , similar masses barely will affect.

Masses concentrated, with linear dimensions of the same order, that also depth of bedding, creates anomalies, which sharply depend on depth. In the case of point sources the intensity of anomalies is inversely proportional to the square of distance. Transition from anomalies  $\Delta g$  to anomalies  $W_{\text{II}}$ , even more (to one degree) strengthens this dependence. As a result it proves to be that the intensity and the position of anomalies  $W_{\text{II}}$  are wholly determined by the special features of geologic structure, which contain the interval of depths from 0 to 2-5 km, and a preferred effect have the sources, arranged/located on the depths into ten and hundreds of meters.

Page 143.

Hence follows that a recount of anomalies  $\Delta g$  in anomaly  $\frac{\partial g}{\partial z} = W'_{\text{II}}$  can be

realized only on the detailed maps/charts, as a rule scale 1:100000-1:50000 it is larger/coarser. General maps with a cross-section of isoanomaly of 5 mgal are not completely suitable for the kind of recounts, since they do not reflect the parts, which determine the anomalies of the vertical force gradient of gravity.

All diagrams of calculation of anomalies  $W_{\Delta}$  on anomalies  $\Delta g$  are based on utilization of integral of Poisson (IV, 34). From the point of view of exploration geophysics this integral is important fact that gives the value of the potential function  $U$  (including anomaly of gravitational force) in the upper half-space in terms of its values, measured at the initial level - the surface of the Earth.

Let us take cylindrical coordinate system,  $z$  axis it is directed downward, towards anomaly-forming objects. Let us designate the specified distribution of potential function on surface of  $z=0$  through  $U(\delta, \varphi, 0)$ . With these designations the formula determines integral of Poisson

$$U(0, 0, -z) = \frac{1}{2\pi} \int_0^{2\pi} d\varphi \int_0^{\infty} U(\varphi, \rho, 0) \frac{\rho}{(z^2 + \rho^2)^{3/2}} \rho d\rho. \quad (IV, 34)$$

Neutralizing value of function  $U(\varphi, \rho, 0)$  on ring of radius  $\rho$ , let us exclude dependence on angle  $\varphi$

$$U(0, 0, -z) = \int_0^{\infty} \bar{U}(\rho, 0) \frac{\rho}{(z^2 + \rho^2)^{3/2}} \rho d\rho. \quad (IV, 34a)$$

The difference  $U(0, -z) - U(0, 0)$  shows a change in function  $U$  with

the recount upward to the height  $-z$ . Differentiating difference in  $z$ , we find

$$\begin{aligned} \frac{\partial [U(0, -z) - U(0, 0)]}{\partial z} &= \frac{\partial}{\partial z} \left[ \int_0^\infty \frac{\bar{U}(q, 0) - U(0, 0)}{(z^2 + q^2)^{3/2}} z q dq \right] = \\ &= \int_0^\infty [\bar{U}(q, 0) - U(0, 0)] \frac{q^2 - 2z^2}{(z^2 + q^2)^{5/2}} q dq. \end{aligned} \quad (IV, 35)$$

Page 144.

Taking into account that

$$\frac{\partial [U(0, -z) - U(0, 0)]}{\partial z} = \frac{\partial U(0, -z)}{\partial z} = - \frac{\partial U(0, z)}{\partial z},$$

and directing  $z \rightarrow 0$ , we will obtain

$$\begin{aligned} \frac{\partial U(0, 0)}{\partial z} &= - \int_0^\infty [U(q, 0) - \bar{U}(0, 0)] \frac{dq}{q^3} = \\ &= \int_0^\infty [\bar{U}(0, 0) - U(q, 0)] \frac{dq}{q^3}. \end{aligned} \quad (IV, 36)$$

Integral (IV, 36) is improper with  $\rho=0$ . However, the anomalies actually observed on the surface of the Earth always possess final correlation, they do not contain jumps and breaks, being smoother (Fig. 55). This means that rate of change in the horizontal gradient (not gradient itself), and, consequently, and limit  $\lim_{q \rightarrow 0} \frac{U(0, 0) - \bar{U}(q, 0)}{q^3}$  they will be always final.

The form of formula (IV, 36) shows that transformation described by it does not depend on parameters. This means that this method of localization can be used for the minimum preliminary (a priori) presentations/concepts about the character of the isolatable and eliminated anomalies. Virtually dependence on the parameter exists,

although not so/such strong as in the methods of averaging and variations. This dependence appears during the numerical calculations.

For executing latter integral (IV, 36) is divided/marked off into three parts

where

$$\frac{\partial U(0,0)}{\partial z} = I_1 + I_2 + I_3$$

$$I_1 \int_0^{R_0} [U(0,0) - \bar{U}(q,0)] \frac{dq}{q^2}, \quad (IV, 37)$$

\*  $I_2$  and  $I_3$  represent analogous integrals within limits from  $R_0$  to  $R$  and from  $R$  to  $+\infty$ .



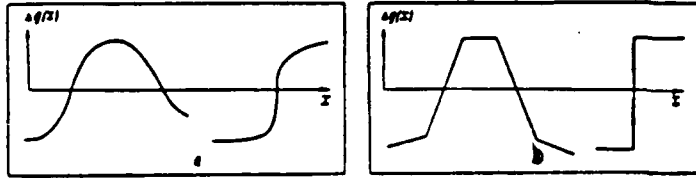


Fig. 55. Examples of anomalies with different correlation: a) anomaly, in which rate of change in horizontal gradient between adjacent points is final; b) anomaly, in which rate of change in horizontal gradient, between adjacent points can be infinite.

Page 145.

The first radius  $R_0$  is selected so/such small that within circle, described by it, it would be possible to consider function  $U$  constant.

If

$$U(0,0) - \bar{U}(q,0) \approx 0.$$

integral  $I_1$  can be disregarded/neglected.

Integral  $I_1$  is divided/marked off into sum of integrals of form

$$\int_{q_n}^{q_{n+1}} [U(0,0) - \bar{U}(q,0)] \frac{dq}{q^3}. \quad (IV.3b)$$

According to law of mean, each such integral can be represented in the form of product of interval  $q_{n+1} - q_n$  at value of integrand at certain point, included between  $q_n$  and  $q_{n+1}$ . The smallest error is reached, when they assume/set

$$\int_{q_n}^{q_{n+1}} [U(0,0) - \bar{U}(q,0)] \frac{dq}{q^3} =$$

$$= [U(0,0) - \bar{U}(\sqrt{q_n q_{n+1}}, 0)] \frac{q_{n+1} - q_n}{q_n q_{n+1}}. \quad (IV, 39)$$

Thus,  $I_1$  is represented in the form of sum

$$I_1 = \sum_{n=0}^m [U(0,0) - \bar{U}(\sqrt{q_n q_{n+1}}, 0)] \frac{q_{n+1} - q_n}{q_n q_{n+1}} =$$

$$= \sum_{n=0}^m \delta U(R_n) \frac{\Delta R_n}{R_n^3}. \quad (IV, 40)$$

If initial map/chart represents map/chart of anomalies  $\Delta g$ , whose isolines are enumerated in milligals, and radii  $R_n$  have dimensionality in kilometers, then for expression of anomaly of lapse in Eotvos (E) it is necessary coefficients  $k_n = \frac{\Delta R_n}{R_n^3}$  to increase ten times.

Theory of template for calculating anomalies  $W_n$  on anomalies  $\Delta g$  is presented by K. Ye. Veselov (1954). The circular template proposed by them in the case of the map/chart of scale 1:100000 has the following radii and the coefficients (Table 12) corresponding to them.

The last radius is selected so that it would be possible to disregard/neglect integral  $I_1$ . If initial map/chart is constructed on the larger/coarser scale, coefficients  $k_n$  one should increase proportional to the relation of scales, and in the case of lower range - decrease.

On each ring it suffices to take 8 fiducial marks. Further increase in the number of assemblies does not lead to the essential

refinement of calculations  $W_{ii}$ .

Investigations carried out by O. A. Swank (1960), virtually showed that account of integrals  $I_1$  and  $I_2$  unessentially affects numerical value of coefficients in Table 12.

Page 146.

For the elimination of the effect of the random errors it is useful to increase radius  $R_0$ . For this purpose calculations are begun directly with  $R=0.57$ . Naturally, in this case the error in the analytical concept is increased; however, general/common error, as a rule, is reduced.

In work of O. A. Swank it is shown that for refining results  $\Delta g(0,0)$  to define as  $\overline{\Delta g}(0,0)$ , neutralizing anomaly value within first circle of template.

In Fig. 56, 57 diagram of isoanomaly  $\Delta g$  and diagram of isoanomaly  $W_{ii}$  calculated on it are constructed by section 5E. The positive anomaly of the vertical force gradient of gravity clearly contours the zone of the uplift/rise of paleozoic species/rocks.

In the case of bivariate distribution of masses circular template is substituted by linear. Basic equality for calculating the lapse takes the form

$$\frac{\partial U(0,0)}{\partial z} = \frac{1}{\pi} \int_{-\infty}^{+\infty} [U(0,0) - U(x,0)] \frac{dx}{x^3}. \quad (IV, 41)$$

This means that coefficients of linear template in  $\pi$  times less than the coefficients indicated in Table 12. The distances of the assemblies of template from the central point are numerically equal to radii  $R_n$ .

Table 12. Radii of template for the calculations of anomalies.

$R_n, \text{km}$	0.2	0.57	1.06	1.76	2.74	4.12	5.85	7.72	10.2	13.7	18.6
$k_n = \frac{10\Delta R_n}{R_n^2}$	75	12.5	5.35	2.60	1.60	0.94	0.53	0.34	0.29	0.21	0.18

Fig. 56. Diagram of isoanomaly  $\Delta g$ . According to O. A. Swank (1960).

Page 147.

Formally through distribution of anomalies  $\Delta g$  we find anomalies of lapse  $\frac{\partial \Delta g}{\partial z}$ . However, taking into account that  $g$  differs from  $\Delta g$  by the value of the normal field, led to photographing conditions, one should recognize that gradients  $\frac{\partial g}{\partial z}$  and  $\frac{\partial \Delta g}{\partial z} = W_{zz}$  coincide.

B. A. Andreyev (1957) proposed method of calculating anomalies of vertical force gradient of gravity and any other potential function  $U$ , based on direct study of distribution  $U$  on vertical line. As the basis of the method the utilization of a Poisson integral lies. As noted above, the latter allows according to the distribution of function  $U$  on plane  $z=0$  to compute values of  $U$  at the points of upper half-space located at heights  $-z=h, 2h, 3h, \dots, nh$ . Value  $(\partial U)/(\partial z)$  in the beginning of coordinates is expressed as the finite differences

(Fig. 58)

$$\frac{\partial U(0,0)}{\partial z} \approx -\frac{1}{h} \left[ \Delta U - \frac{1}{2} \Delta^2 U + \frac{1}{3} \Delta^3 U - \dots \right], \quad (\text{IV}, 42)$$

where

$$\left. \begin{aligned} \Delta U &= U(0, -h) - U(0, 0), \\ \Delta^2 U &= U(0, -2h) - 2U(0, -h) + U(0, 0), \\ \Delta^3 U &= U(0, -3h) - 3U(0, -2h) + 3U(0, -h) - U(0, 0). \end{aligned} \right\} \quad (\text{IV}, 43)$$



Fig. 57. Diagram of isoanomaly  $W_m$ , constructed on the basis Fig. 56. Section of isoanomaly of 5E. According to O. A. Swank (1960). 1 - axial zone and the apex/vertex of the uplifts/rises of the Paleozoic era.

Page 148.

Substituting expression (IV, 43) into formula (IV, 42), we find, being limited respectively to differences 1, 2 and the 3rd of orders,

$$\left. \begin{aligned} \frac{\partial U}{\partial z} &\approx \frac{1}{h} [U(0, 0) - U(0, -h)], \\ \frac{\partial U}{\partial z} &\approx \frac{1}{2h} [3U(0, 0) - 4U(0, -h) + U(0, -2h)], \\ \frac{\partial U}{\partial z} &\approx \frac{1}{2h} [11U(0, 0) - 18U(0, -h) + \\ &\quad + 9U(0, -2h) - 2U(0, -3h)]. \end{aligned} \right\} \text{(IV, 44)}$$

Formulas (IV, 44) are valid for cases of assignment of initial data both with respect to area and with respect to profile.

Accuracy analysis of these formulas, carried out by B. A. Andreyev (1957), showed that error, caused by inaccuracy in analytical presentation/concept  $(\partial U)/(\partial z)$ , depends substantially on

relationship/ratio of interval of  $h$  and average depth of bedding of sources of anomalies. The effect of errors in the initial data proves to be inversely proportional  $h$ .

Experiment shows that with low quality of initial data (error in anomalies  $\Delta g$  it composes several the tenths of milligal) more acceptable prove to be two first formulas (IV, 44).



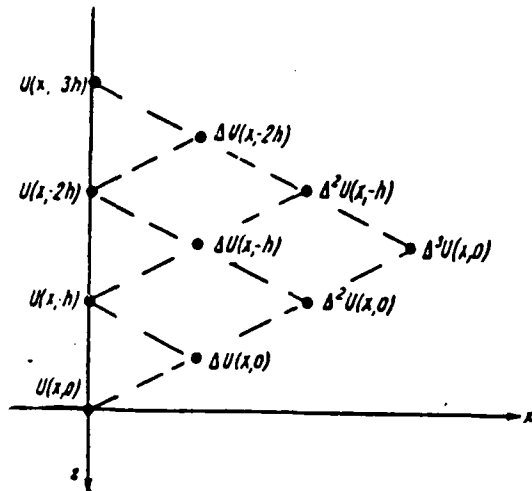


Fig. 58. Explanation to formula (IV, 42).

Page 149.

Detailed description of templates for numerical determination of  $U(-z)$  from values of  $U$  on initial level  $z=0$  is given in § 27 of this chapter.

Let us turn again to Poisson integral. Formula (IV, 34a) can be represented in a somewhat different form

$$U(0, z) = \int_0^\infty e^{-az} a da \int_0^\infty J_0(aq) \bar{U}(q, 0) q dq, \quad (IV, 45)$$

since

$$\int_0^\infty e^{-az} J_0(aq) a da = \frac{z}{(z^2 + q^2)^{3/2}}. \quad (IV, 46)$$

Differentiating expression (IV, 45) on  $z$  and assuming/setting  $z=0$ , we obtain

$$\frac{\partial U(0,0)}{\partial z} = \int_0^\infty a^2 da \int_0^\infty \bar{U}(q,0) J_0(aq) q dq. \quad (\text{IV}, 47)$$

By comparing the right sides of equalities (IV, 47) and (IV, 4), we are convinced, that characteristic of transformation, realized upon transfer from anomalies  $U$  to anomalies  $(\partial U)/(\partial z)$ , takes simple form

$$\psi(a) = a. \quad (\text{IV}, 48)$$

This gives possibility to easily consider filtering effect of transformation, order of anomalies  $W_{in}$ , which correspond to initial anomalies  $\Delta g$ , and also relative change in errors in initial data.

Substituting formula (IV, 48) into equality (IV, 15), we find

$$\left. \begin{aligned} \bar{A}_{\text{trapucf}}^2 &= \frac{\bar{A}^2 r^2}{2} \int_0^\infty \exp\left(-\frac{a^2 r^2}{4}\right) [a]^2 a da = \bar{A}^2 \frac{4}{r^2}, \\ \bar{A}_{\text{trapucf}}^2 : \sqrt{\bar{A}^2} &= \frac{2}{r}. \end{aligned} \right\} \quad (\text{IV}, 49)$$

Let us examine the following example. The intensity of the chosen anomalies in the initial map/chart  $\Delta g$  is 2-3 mgal. In the absence of the regional background of anomaly they would take the form of maximums with linear dimensions on the order of 6-8 k. . It means, the radius of autocorrelation somewhat less or is equal to 3-4 km. Anomalies  $W_{in}$  in this case will have an intensity of the order of

$$(2+3) \cdot 10^{-3} \cdot \frac{2}{(3+4) \cdot 10^3} \approx (10+20) \cdot 10^{-9} \text{ ClC} = 10+20 \text{ E.}$$

Page 150.

Let us assume that error of measurement  $\Delta g$  is 0.4 mgal and

observations were conducted with step/pitch of 2 km. A relative error in the local anomalies  $\Delta g$  is equal to approximately 13-20%. After transformation the level of an error in the initial data there will be the order

$$0,4 \cdot 10^{-3} \cdot \frac{2}{2 \cdot 10^4} \text{CFC} \approx 4E.$$

Relative error in local anomalies  $W_{\text{L}}$  will be increased to 20-40%. Phenomenon this is completely regular. The transformation of anomalies  $\Delta g$  in anomaly  $W_{\text{L}}$  eliminates or it substantially reduces the effect of the regional special features of field  $\Delta g$  with the intensity into ten milligal only because the correlation of these components is too great. In exactly the same manner fine/small variations, with a small radius the autocorrelations, including of changes, caused by the random errors, become significant.

In effect certain decrease of effect of random errors is achieved by preliminary leveling of anomalies  $\Delta g$  and by increase in radius  $R$ , of first ring of template. Those components of the complete error in anomaly  $\Delta g$ , which have the large correlation (error in the base net, etc.), anomalies  $W_{\text{L}}$  will affect insignificantly.

#### § 26. Methods of the recount of anomalies $\Delta g$ in anomaly

Effect of weakly correlated special features of anomalous field underscores the secondary differentiation of anomalies  $\Delta g$  on  $z$  in even greater measure. In the case of the sharply concentrated masses the

slope of curve  $W_{III}$  stronger than in curves  $W_{II}$ ; this characterizes the increased resolution. Fig. 59 depicts curves  $\Delta g, W_{II}, W_{III}$  for the set of two circular cylinders, which imitate anomalous bodies. The curve  $\Delta g$  has one overall maximum, a certain hint to the presence of two sources gets underway by curve  $W_{II}$  and only in curve  $W_{III}$  relief are separated/liberated the maximums above each body.

To practical utilization of transformations of anomalies  $\Delta g$  and to anomaly  $W_{III}$  contributed the fact that formulas for calculating second vertical gradient of the force of gravity are much simpler than for the first. This of formula directly they follow from Laplace's equation

$$\left. \begin{aligned} \frac{\partial^2 U}{\partial z^2} + \frac{\partial^2 U}{\partial x^2} + \frac{\partial^2 U}{\partial y^2} &= 0, \\ \frac{\partial^2 U}{\partial x^2} &= - \left( \frac{\partial^2 U}{\partial z^2} + \frac{\partial^2 U}{\partial y^2} \right). \end{aligned} \right\} \quad (IV, 50)$$

Page 151.

Calculation of horizontal gradients  $\frac{\partial U}{\partial x^2}$  and  $\frac{\partial^2 U}{\partial y^2}$  in terms of values of function  $U(x, y)$  at discrete/digital points - junctions of right angled grid is realized sufficiently simply with the help of equalities

$$U''(a) \approx -\frac{1}{h^2} [2U(a) - U(a+h) - U(a-h)], \quad (IV, 51)$$

$$\begin{aligned} U''(a) \approx & -\frac{1}{h^2} \left[ \frac{5}{2} U(a) - \frac{4}{3} U(a+h) - \frac{4}{3} U(a-h) + \right. \\ & \left. + \frac{1}{12} U(a+2h) + \frac{1}{12} U(a-2h) \right], \quad (IV, 52) \end{aligned}$$

where  $(a+nh), \dots, (a+h), a, (a-h), \dots, (a-nh)$  - points, arranged/located on one

straight line and distant behind friend at a distance of  $h$ ;  $U''(a)$  - second derivative of function  $U$  on horizontal coordinate at point  $a$  (Fig. 60).

In simplest case

$$\frac{\partial^2 U(0,0)}{\partial z^2} \approx \frac{4}{h^2} [U(0) - \bar{U}(h)], \quad (IV, 53)$$

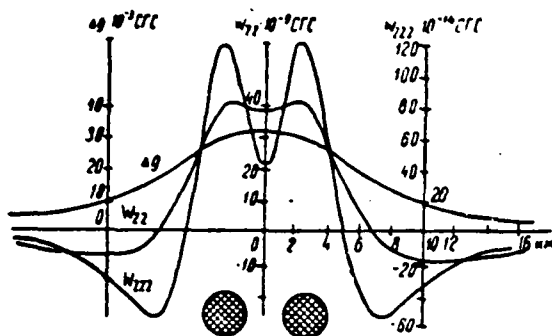


Fig. 59. Illustration on theoretical model of high resolution of method  $W_{222}$ . According to M. U. Sagitov (1960).

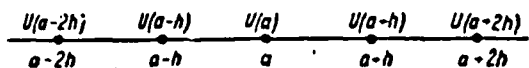


Fig. 60. Explanation to formulas (IV, 51) and (IV, 52).

Page 152.

Is analogous, for system of coordinates  $x', y'$ , turned relative to  $(x, y)$  on  $45^\circ$ , we will obtain

$$\frac{\partial^2 U(0,0)}{\partial z^2} \approx \frac{4}{2h^2} [U(0) - \bar{U}(h\sqrt{2})]. \quad (\text{IV}, 54)$$

Since the right sides of equalities IV, 53) and (IV, 54) approximately determine  $\frac{\partial^2 U}{\partial z^2}$ , then their any linear combination will also determine  $\frac{\partial^2 U}{\partial z^2}$ . In this case will be changed in front the coefficient confronting, inversely proportional to the square of the distance between the network points. On this position are based the numerous formulas, described in the geophysical literature (Malovichko, 1955; Elcins 1951; Rosenbach, 1953). Some of them are given below

$$\frac{\partial^2 U}{\partial z^2} \approx \frac{1}{h^2} [6U(0) - 8\bar{U}(h) + 2\bar{U}(h\sqrt{2})] \quad (\text{формула Розенбаха}), \quad (1) \quad (IV, 55)$$

$$\frac{\partial^2 U}{\partial z^2} \approx \frac{1}{h^2} [0,71 U(0) + 0,26 \bar{U}(h) - 0,20 \bar{U}(h\sqrt{2}) - 0,77 \bar{U}(2h)] \quad (\text{формула Элцина}), \quad (IV, 56)$$

$$\frac{\partial^2 U}{\partial z^2} \approx \frac{1}{h^2} [5U(0) - 5,33 \bar{U}(h) + 0,33 \bar{U}(2h)] \quad (\text{формула Маловичко}), \quad (2) \quad (IV, 57)$$

$$\frac{\partial^2 U}{\partial z^2} \approx \frac{1}{h^2} [3,47 U(0) - 2,27 \bar{U}(h) - 3,07 \bar{U}(h\sqrt{3}) + 1,87 \bar{U}(2h)] \quad (\text{формула Шарпа}). \quad (4) \quad (IV, 58)$$

Key: (1). Rosenbach formula; (2). Elcins formula; (3). Malovichko formula; (4). Sharp formula.

One of the simple formulas for determination of  $\frac{\partial^2 U}{\partial z^2}$  is based on utilization of variation anomaly  $\delta U$ . Taking into account equalities (IV, 27) and (IV, 53), we find that

$$\frac{\partial^2 U}{\partial z^2} = \lim_{l \rightarrow 0} \frac{46 U(l, 0)}{l^2}. \quad (IV, 59)$$

Determination of limit (IV, 59) is easy to fulfill graphically (Fig. 61) on variation anomaly at two-three values of parameter  $l$ . Formula (IV, 59) is more pliable than formula (IV, 54-58), it better calculates the relationship/ratio changing on the basis of area of the radius of the autocorrelation of anomalies and mesh sizes, but it requires additional constructions.

Calculation of second lapse and gradients of higher order possibly also according to diagram, already described in preceding paragraph, using distribution of anomaly on vertical line. For calculating the finite difference in the second order it is necessary to have a minimum of three values of function  $U$ .

Page 153.

One value -  $U(0, 0)$  directly is removed/taken from the map/chart;  $U(0, h)$  and  $U(0.2h)$  are calculated with the help of the templates described in S 27. The approximation formula for calculation  $\frac{\partial^2 U}{\partial z^2}$  takes the form

$$\frac{\partial^2 U}{\partial z^2} \approx \frac{1}{h^2} [U(0, 0) + U(0, -2h) - 2U(0, -h)]. \quad (\text{IV}, 60)$$

Formula (IV, 60) has accuracy greater than formula (IV, 53); however, it requires much greater calculations.

Let us consider sensitivity of method  $\frac{\partial^2 U}{\partial z^2}$  to anomalies with different correlation, independent of concrete calculating formulas. Twice differentiating equality (IV, 45) on  $z$  and by assuming  $z=0$ , we will obtain

$$\frac{\partial^2 U}{\partial z^2}(0, 0) = \int_0^\infty \alpha^3 d\alpha \int_0^\infty J_0(\alpha, \varrho) \bar{U}(\varrho, 0) \varrho d\varrho. \quad (\text{IV}, 61)$$

Comparing formula (IV, 61) with formula (IV, 4), we find that transformation of anomalies  $\Delta g$  in anomaly  $W_{\text{int}}$  has characteristic

$$\psi(\alpha) = \alpha^2. \quad (\text{IV}, 62)$$

Hence

$$\begin{aligned} \bar{A}_{\text{тпассф}}^2 &= \frac{\bar{A}^2 r^2}{2} \int_0^\infty \exp\left(-\frac{\alpha^2 r^2}{4}\right) [u^2]^2 \alpha d\alpha = \frac{\bar{A}^2 \cdot 32}{r^4}, \\ \sqrt{\bar{A}_{\text{тпассф}}^2} : \sqrt{\bar{A}_2} &= \frac{5.65}{r^2}. \end{aligned} \quad (\text{IV}, 63)$$

Amplitude of anomalies  $W_{\text{int}}$  is proportional to amplitude of initial anomalies  $\Delta g$  is inversely proportional to square of radius of autocorrelation.



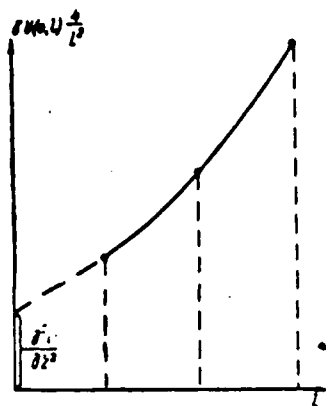


Fig. 61.

Fig. 61. Graphic calculation  $W_m$  in terms of values of  $\delta \Delta g$ .

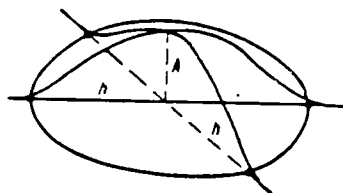


Fig. 62.

Fig. 62. Explanation to formula (IV, 64). A - amplitude of anomaly;  
h - distance between the assemblies of template.

Page 154.

For illustration of equality (IV, 63) let us give following simple example. Let us assume that the template for calculation  $W_m$  stands in the center of anomaly with an amplitude of A (Fig. 62). The assemblies of template are arranged/located on such distance, that the anomaly at these points is in effect equal to zero. Then approximately  $r=h$

$$W_m \approx \frac{4}{h^2} [\Delta g(0) - \bar{\Delta g}(h)] \approx \frac{4A}{r^2}. \quad (\text{IV, 64})$$

Equality (IV, 63) is correct for case, when transformation realized in accuracy corresponds to transition from anomalies  $\Delta g$  to anomalies  $W_m$ . The in practice utilized for calculations formulas (IV, 53-59), etc. are characterized by one or the other error in the

analytical approximation/approach  $\epsilon$ , which depends mainly on the relationship/ratio between the radius of autocorrelation  $r$  of the distributions of anomalies and the distance between the assemblies of template  $h$ . Let us designate  $[\overline{A^2}_{\text{трансф}}]$  the accurate value of  $\overline{A^2}$  after transformation,  $\overline{A^2}_{\text{трансф}}$  — the same, calculated with the help of the template. Then

$$\epsilon = 1 - \sqrt{\frac{\overline{A^2}_{\text{трансф}}}{[\overline{A^2}_{\text{трансф}}]}} \quad (\text{IV}, 65)$$

it will determine an error in the analytical approximation/approach. In the first part Table 13 are given the values  $\epsilon$  for one of the formulas of the recount of anomalies  $\Delta g$  in anomaly  $W_{\text{из}}$  as the function of ratio  $h/r$ . A gradual increase  $\epsilon$  with increase in  $h$  is common for all formulas. With  $h/r$  of the order of one and more, the error consists already tens of percent, and it has a systematic character. Calculated values  $W_{\text{из}}$  as a whole prove to be lowered, since with the large mesh size abrupt changes in the anomaly are passed.

With very large  $h$  we calculate not second vertical derivative of anomalies of gravitational force, and the value which only remotely resembles it, having identical physical dimensionality.

Based on the example of formula (IV, 53), let us show how error  $\epsilon$  was determined. The template, which corresponds to formula (IV, 53), has parameters

$$k_0 = \frac{4}{h^3}, \quad R_0 = 0, \quad k_1 = -\frac{4}{h^2}, \quad R_1 = h.$$

In accordance with equality (IV, 16) we find

$$\bar{A}_{\text{transf}}^2 = \bar{A}^2 \left( \frac{4}{h^2} \right)^2 \left[ P \left( \frac{0}{r} \right) + P \left( \frac{h}{r} \right) - 2S \left( \frac{h}{r} \right) \right]. \quad (\text{IV}, 66)$$

Page 155.

Taking into account that

$$[\bar{A}_{\text{transf}}^2] = \frac{32\bar{A}^2}{r^4}, \quad P(0) = 1,$$

we find

$$\begin{aligned} \bar{A}_{\text{transf}}^2 &= [\bar{A}_{\text{transf}}^2] \frac{1}{2 \left( \frac{h}{r} \right)^4} \left[ 1 + P \left( \frac{h}{r} \right) - 2S \left( \frac{h}{r} \right) \right], \\ \varepsilon &= 1 - \sqrt{\frac{1 + P \left( \frac{h}{r} \right) - 2S \left( \frac{h}{r} \right)}{2 \left( \frac{h}{r} \right)^4}}. \end{aligned} \quad (\text{IV}, 67)$$

With small  $h/r$  are valid expansions

$$P \left( \frac{h}{r} \right) = e^{-2 \left( \frac{h}{r} \right)^2} I_0 \left( 2 \left( \frac{h}{r} \right)^2 \right) \approx 1 - 2 \left( \frac{h}{r} \right)^2 + 3 \left( \frac{h}{r} \right)^4 \dots,$$

$$S \left( \frac{h}{r} \right) = e^{-\left( \frac{h}{r} \right)^2} \approx 1 - \left( \frac{h}{r} \right)^2 + \frac{1}{2} \left( \frac{h}{r} \right)^4 - \dots,$$

i.e.

$$1 + P \left( \frac{h}{r} \right) - 2S \left( \frac{h}{r} \right) \approx 2 \left( \frac{h}{r} \right)^4, \quad \varepsilon \approx 0.$$

With increase in  $h/r$  error increases/grows, as can be seen from Table 13A.

Taking into account only data of Table 13A, it is possible to arrive at the conclusion that for increasing accuracy of calculations should be used templates with small distance between assemblies.

However, this estimation is one-sided. It does not take into consideration a relative increase of the errors initial data with the decrease of interval of  $h$ . Just as the amplitude of the anomalies being isolated, magnitude of error in the initial data after transformation are inversely proportional to the square of the distance between the assemblies.

Table 13. Effect of the length of interval  $h$  between the assemblies of template on an error in the calculation of anomalies  $W_{int}$

A. In the case of applying formula (IV,53).

(1) Отношение расстояния между узлами палетки к радиусу автокорреляции, $h/r$ . . . . .	0.1	0.2	0.4	0.6	0.8	1.0	1.2
(2) Относительная погрешность аналитического представления $\epsilon$ , % . . . . .	0	3	11	23	35	42	57

B. In the case of applying the formula (IV,55).

(3) Расстояние между узлами палетки $h$ , км	(4) Относительная погрешность представления палетки, %	(5) Относительная погрешность за счет качества исходных данных, %	(6) Полная относительная погрешность определения $W_{int}$ , %
1	0	58	58
2	3	45	46
4	25	17	30
6	54	8	55

Key: (a). In the case of applying the formula (IV, 53). (1). Ratio of the distance between assemblies of template to radius of autocorrelation,  $h/r$ . (2). Relative error in analytical concept.

(3). Distance between assemblies of template. (4). Relative error in impressiveness of template. (5). Relative error due to quality of initial data. (6). Complete relative error in determination.

Page 156.

Since the errors are characterized by smaller correlation than the anomalies being isolated, it is possible to select such interval of  $h$ , with which an error in the analytical presentation/concept will be yet very great, and an error in the initial data is not excessively underscored, so that the square of the common relative error will have minimum value.

14

Let us examine example, typical for practice of liberation/precipitation of local anomalies. The map/chart of the anomalies of Bouguer of scale 1:200000 are treated with the help of the template of Rosenbach (1953), which has the parameters

$$k_0 = \frac{6}{h^2}, \quad R_0 = 0, \quad k_1 = -\frac{8}{h^2}, \quad R_1 = h, \\ k_2 = \frac{2}{h^2}, \quad R_2 = h\sqrt{2}.$$

Local anomalies being isolated in initial map/chart have amplitude  $1/\sqrt{4}$  on the order of 4 mgal and radius of autocorrelation, close to 4 km. (This means that the maximums of anomalies  $\Delta g$  reach 4-6 mgal, and cross dimensions - 7-10 km). A root-mean-square error of measurement is 0.6 mgal, and the radius of autocorrelation is approximately equal to 2 km. Complex regional background has an intensity many ten milligal, which substantially is changed at the distances into many tens of kilometers.

Putting to use formula (IV, 63), we find that after recount intensity of regional background will compose only several units of  $10^{-11}$  CGS, local anomalies - many tens of  $10^{-11}$  CGS and errors in initial data - tens of  $10^{-11}$  CGS. Varying the distance between assemblies of the template, we will change the complete relative error in anomalies  $W_m$  within the limits indicated in Table 13B.

Page 157.

As we see, the relative error the smallest under given typical conditions is such that quantitative interpretation of map/chart cannot be reliable. If the conversion sets as its goal only the liberation/precipitation of the anomalies, connected with the unknown geologic objects, the determination of their position in the plan/layout, then the problem considerably is simplified. Formulas (IV, 53-59) can be examined only as formulas for the liberation/precipitation of the local anomalies, expressed in units of  $10^{-11}$  CGS. The relative change in the sensitivity to the masses, located at depth  $z$ , depends substantially on sizes/dimensions of  $h$ .

Actually, according to equality (IV, 10), transformation with transparency of Rosenbach has relative deep characteristic

$$N(z) = \frac{1}{h^3} \left[ 6 - \frac{8z^3}{(z^2 + h^2)^{3/2}} + \frac{2z^3}{(z^2 + 2h^2)^{3/2}} \right], \quad (\text{IV}, 68)$$

In ideal case this characteristic must be changed according to the law

$$N(z) = \frac{\int_0^\infty e^{-\alpha z} \alpha^2 d\alpha}{z^3} = \frac{6}{z^3}. \quad (\text{IV}, 69)$$

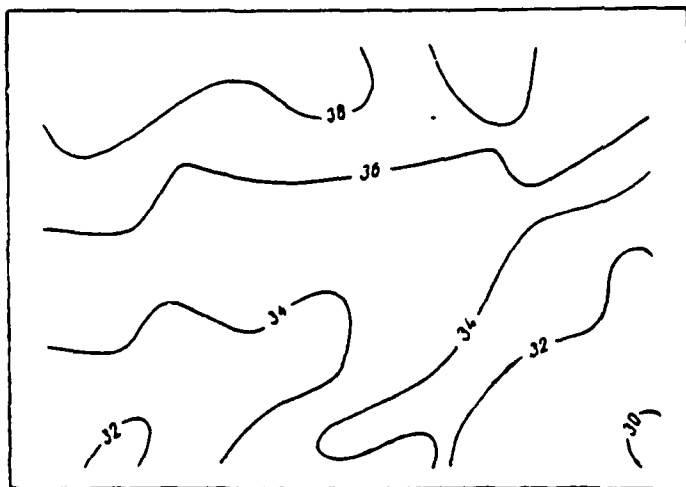


Fig. 63. Diagram of isoanomaly  $\Delta g$ . According to L. N. Yelanskiy and S. V. Pavel'yev (1960).



Page 158.



Fig. 64. Diagram of isoanomaly  $w_{\text{iso}}$  constructed on the basis Fig. 63 with the help of formula (IV, 55). Step between nodes of transparency is 2 km. According to L. N. Yelanskiy and S. V. Pavel'yev (1960).

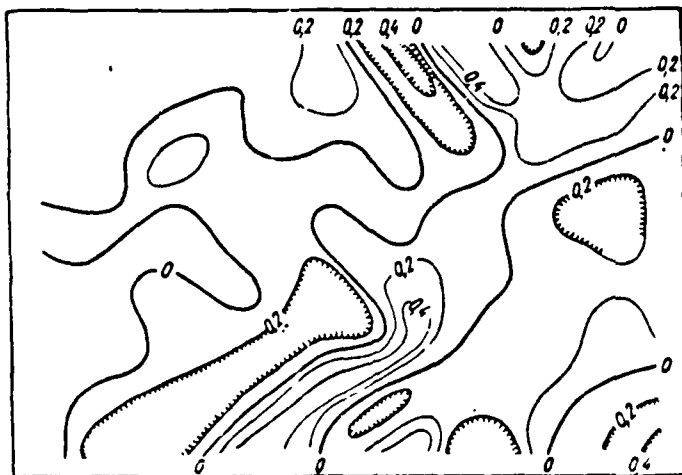


Fig. 65. Diagram of isoanomaly  $w_{\text{iso}}$  constructed on the basis of Fig. 63 with the help of formula (IV, 55). Step/pitch between the nodes of transparency 4 km. According to L. N. Yelanskiy and S. V. Pavel'yev (1960).

Page 159.

With increase in distance between nodes sharply is reduced sensitivity to mass, concentrated at small depth. Since sensitivity to the deeply submerged masses remains invariable, as a whole this leads to the significant decrease of the intensity of anomalies  $W_{\dots}$ .

Fig. 63-66 depicts for one and the same area initial map/chart  $\Delta g$  and maps/charts  $W_{\dots}$  with  $h=2; 4$  and  $8$  km, constructed by L. N. Yelanskiy and S. V. Pavel'yev (1960). With an increase in the mesh size of map/chart considerably are simplified. The authors (Yelanskiy, 1960) draw hence the conclusion that at depth on the order of  $6-8$  km and more the sources of anomalies are absent. Actually, as shown in Fig. 67, where represented are the curves  $N(z)$ , anomalies  $W_{\dots}$  are simply insensitive to the masses located deeper than  $7-8$  km, regardless of the fact how in what quantity are distributed the sources of anomalies.

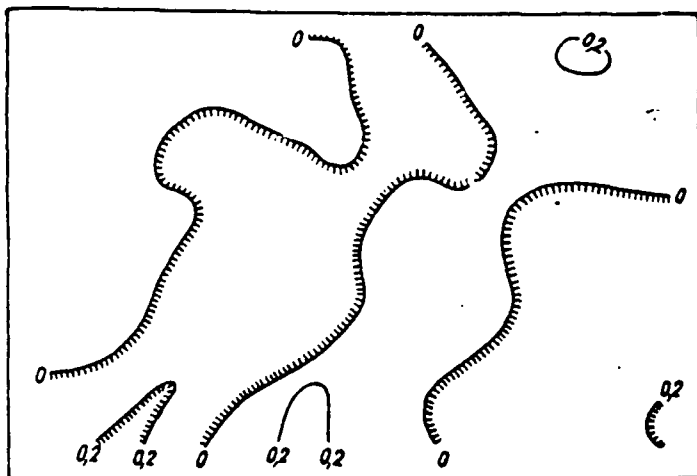


Fig. 66. Diagram of isoanomaly  $w_m$ , constructed on the basis Fig. 63 with the help of formula (IV, 55). Step between the nodes of transparency is 8 km. According to L. M. Yelanskiy and S. V. Pavel'yev 1960).

Page 160.

Summing up that presented, let us again note that anomalies comparatively simply are calculated from anomalies  $\Delta g$ , clearly is determined position of shallow sloping objects, it is very sensitive to errors initial data, with contemporary quality gravimetric materials (map  $\Delta g$  of a scale of 1:200000, 1:100000) can have a relative error at tens of a percent. the maps/charts of anomalies  $\Delta g$  of a scale smaller than 1:200000 to use for calculating the anomalies  $w_m$  it is completely cannot.

§ 27. Calculations of three-dimensional distribution of anomalies.

As is shown in preceding of chapters, many tasks of interpretation are simplified, if we know distribution of anomalies not only on plane of observations, but also at points of space, arranged/located above and below of surface of Earth. The important practical and theoretical value of the study of the three-dimensional/space picture of field repeatedly was underscored in the work of Soviet researchers (Malkin, 1934; Zamorev, 1939, 1941; Andreev, 1947-1954; Strakhov, 1959, 1960, etc.) and geophysicists of the foreign countries (Reynbow, 1933; Hugh, 1942; Pearson, 1945, etc.).

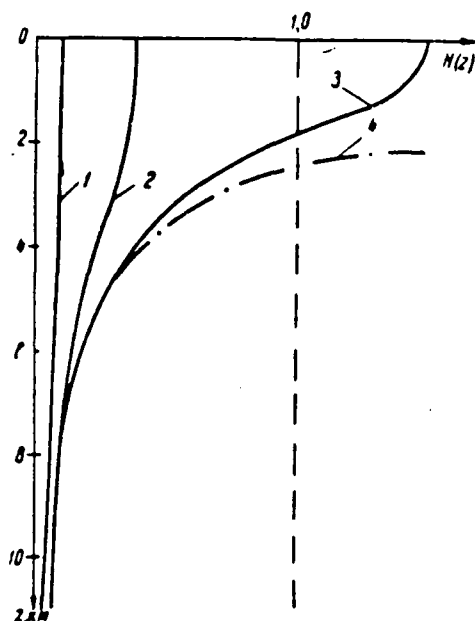


Fig. 67. Relative deep characteristic, which corresponds to transformation of anomalies  $\Delta g$  in anomaly  $w_{\text{m}}$  according to formula of Rosenbach. The step of the grid: 1-8 km; 2-4 km; 3-2 km; 4 - ideal case (error in the analytical presentation/concept it is equal to zero).

Page 161.

Sharpest shift/shear with respect to of practical study and utilization for purposes of interpretation of three-dimensional/space picture of anomalous field was done on border of 40th and 50's. Specifically, at this time the general theoretical positions, known from Laplace's times, found wide application/appendix to the tasks of exploration geophysics. Great merit in this question belongs to B. A. Andreyev (1947, 1948, 1949, 1950, 1950, 1950, 1952, 1954, 1955).

At present calculations of spatial distribution of potential fields it is very powerful apparatus of quantitative interpretation. At the same time, on the recount of field one of the methods of separation of anomalies, remarkable in the sense that it introduces the minimum "distortions" in the anomaly - it makes it possible to examine the sources of the observed anomalies from a new point of view. The recount of field upward to a certain height leads to such changes in the anomalies, which was observed at the initial level during the subsidence of masses at the same depth.

Being congruent/equating distribution of anomalies on different of level, it is possible to note, what parts of original picture effaced, they became poorly expressed, such as remained virtually constant.

Let us examine Fig. 68, which elucidates separation of anomalies into regional and local components. Curve 1 - the observed anomaly of gravitational force, caused by cumulative effect of two bodies, one of which has large mass and will lie on the significant depth. Curve 2 - the anomaly converted to height. The position of masses, noted by dotted line, corresponds to it. Curve 3 - the difference of that observed and that converted in the anomalies. It indicates the position of local object to tap hole. the effect of the major mass, arranged/located on the significant depth, substantially weakened, since, first, the large part of the mass proved to be "cut out" during

the subtraction, secondly, the effect of positive and negative masses to a considerable extent it is compensated.

Numerical diagrams for executing calculations  $U(z, 0)$  and  $U(-z, 0)$  were proposed by many authors (Reynbow, 1933; Andreyev, 1947-1954; Strakhov, 1959-1960, etc.). Let us examine some of them, first in connection with the case of the assignment of initial data on the profile, and then - over the area. In the two-dimensional of the case the value of potential function at level  $z$  is determined through the values on the surface of observation with the help of the integral equality.

$$U(0, z) = \frac{1}{\pi} \int_0^{\infty} e^{-\alpha z} d\alpha \int_{-\infty}^{+\infty} U(x, 0) \cos \alpha x dx. \quad (IV, 70)$$

Page 162.

For calculations at points, in arranged/located higher than observation level, i.e., in case of negative  $z$ , formula is simplified

$$\begin{aligned} U(0, -z) &= \frac{1}{\pi} \int_0^{\infty} e^{-\alpha z} d\alpha \int_{-\infty}^{+\infty} U(x, 0) \cos \alpha x dx = \\ &= \frac{1}{\pi} \int_{-\infty}^{+\infty} \frac{U(x, 0) z}{z^2 + x^2} dx. \end{aligned} \quad (IV, 71)$$

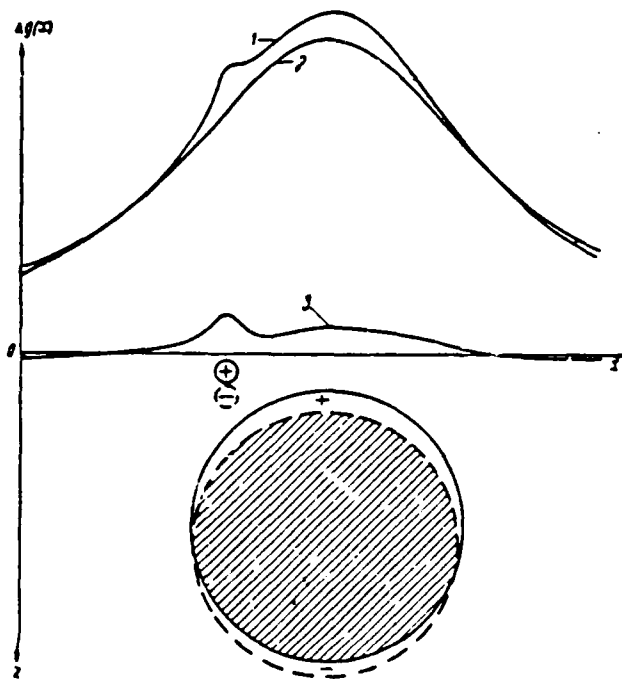


Fig. 68. Example which elucidates the separation of local and regional components by method of recount of field to height. 1 - initial curve  $\Delta g$ , reflection the summary effect of two bodies (outlines of the section of bodies are shown by solid lines; 2 - curve  $\Delta g$ , converted to the height (recount to the height it is equivalent to the additional subsidence of masses; the outlines of the section of bodies are shown by dotted line; 3 - difference of that observed and that converted the anomalies (shaded area determines the masses, which do not affect difference curve; signs + and - indicate the sign of the density of the masses, which affect the shape of the curve 3).

Page 163.

We obtained known integral of Poisson. The mentioned above



formula (IV, 34) is generalization (IV, 71) to the case of the two-dimensional assignment to function  $U$ . For the numerical determination of  $U(0, -z)$  L. V. Kantorovich and V. I. Krylov (1941, 1952) recommends the following method. New variable (Fig. 69) is introduced

$$\varphi = \operatorname{arctg} \frac{x}{z}, \quad d\varphi = \frac{z}{z^2 + x^2} dx.$$

Equality (IV, 71) takes in this case following simple form:

$$U(0, -z) = \frac{1}{\pi} \int_{-\frac{\pi}{2}}^{+\frac{\pi}{2}} U(\varphi, 0) d\varphi. \quad (\text{IV, 72})$$

As we see value of  $U(-z, 0)$  at height  $z$  is defined as average/mean inecarbon tetrachlorideal  $U(\varphi, 0)$  on angle of visibility  $\varphi$ . Dividing/marking off entire half-plane by a system of rays/beams occurring from one point  $(0, -z)$  and being deflected from each other at a constant angle  $\Delta\varphi = \frac{\pi}{n}$  ( $n$  - the integer, a sufficiently large number, for example, 20) we find

$$U(0, -z) \approx \frac{1}{n} \sum_{k=1}^n \bar{U}_k,$$

where  $\bar{U}_k$  - average/mean value of anomaly in the  $k$  interval, which is visible from point  $(-z, 0)$  at angle of  $\pi/n$ , and is limited by the points of intersection of rays/beams with  $x$  axis.

Formula (IV, 73) is the basis of two versions of transparency, described by B. A. Andreev (1950, 1954). The transparency, depicted

in Fig. 70, can be used (without the rearrangement curved U) for calculation of field at the different levels. The height of recount is equal to the length of plumb ray/beam, expressed in units of the horizontal scale of the graph. The practical example of calculation of anomaly at the height is shown in Fig. 70.

For facilitating calculation of average/mean values  $\bar{U}_x$  frequently previously is conducted on transparency system vertical of lines. In this case become unnecessary the rays/beams, which diverge from the point  $(-z, 0)$ . The transparency takes the form depicted in Fig. 71. In this form the transparency is suitable for the recalculation of field only to one level, usually equal to 5 cm. For calculating the anomaly at another height it is necessary to change the horizontal scale of the curve.

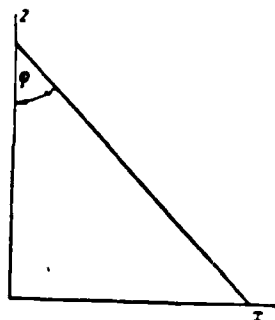


Fig. 69. Explanation to formulas (IV, 71-72).

Page 164.

After this, the 5 cm along the horizontal axis of the graph will be equal to the new level of recount.

Analogously it is realized calculations of anomalous field at overlying level in magnetic prospecting (Logachev, 1955).

V. N. Strakhov proposed somewhat different transparency (Fig. 72). Basic special feature during calculations with it consists in the fact that the determination of the average/mean values of anomaly within the intervals is substituted by readings on the scales, which is less tiresome, it is simpler and it is more rapid. So as during calculations with the help of the transparency, depicted in Fig. 71, the curve  $U(x, 0)$  is drawn on the tracing paper on the appropriate horizontal scale (level of recount it is noted on the transparency in the form of the segment of the specific length), vertical scale can be arbitrary, but it is desirable so that anomaly variation would comprise not less than 10-15 cm. The projection currents, in which is

calculated  $U(0, -z)$ , it is combined since the beginning of the transparency. For each scale the reading, which they summarize, is taken, and the sum, divided on  $\pi$ , is equal to value of  $U(0, -z)$  in the millimeters of the ordinates of drawing.

During construction of transparency integral (IV, 70) with infinite limits was decomposed into series/number of particular integrals in final limits and remainders, which can be disregarded/neglected. Each of the partial integrals is calculated with the help of the quadrature formulas of Gauss, which with the given number of ordinates are most accurate (Krylov, 1954).

Templates for calculation  $U$  in upper half-space according to specified distribution of anomalies on plane  $z=0$  are constructed in a similar manner. Poisson's integral is represented in the form of the sum

$$U(0, -z) = \sum_{i=0}^n \bar{U}(R_i, 0) k_i. \quad (IV, 73)$$

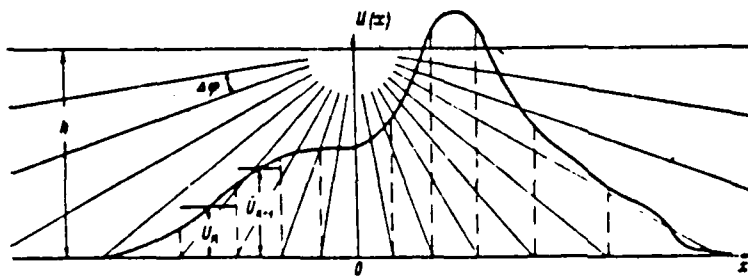


Fig. 70. Ray transparency of B. A. Andreev for recount of potential physical field to overlying level. The height of recount  $h$  is equal to the length of the vertical ray/beam, intercepted/detached from below by the horizontal axis of the graph of anomaly.

Page 164a.

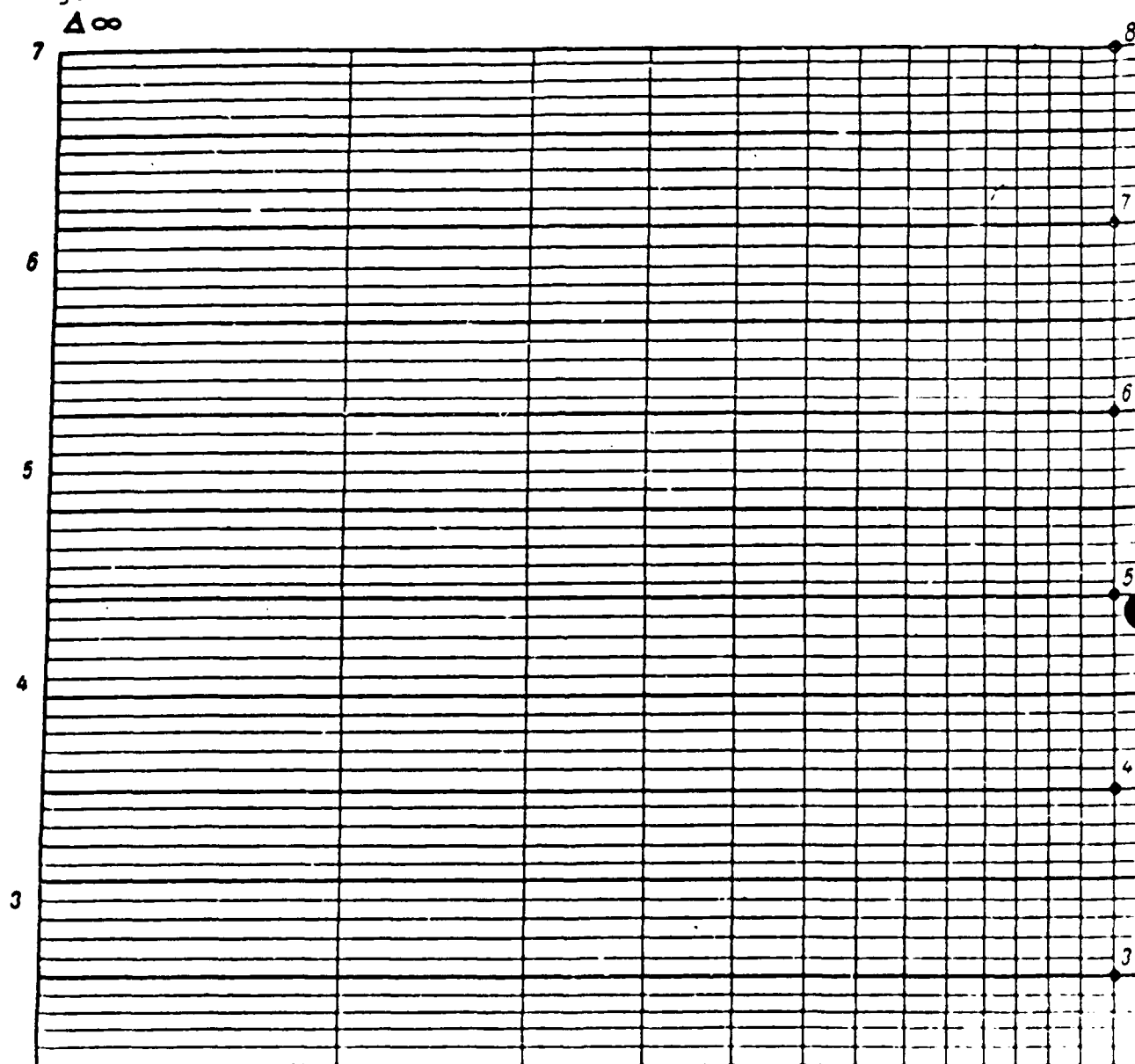


Fig. 71. Top Left.

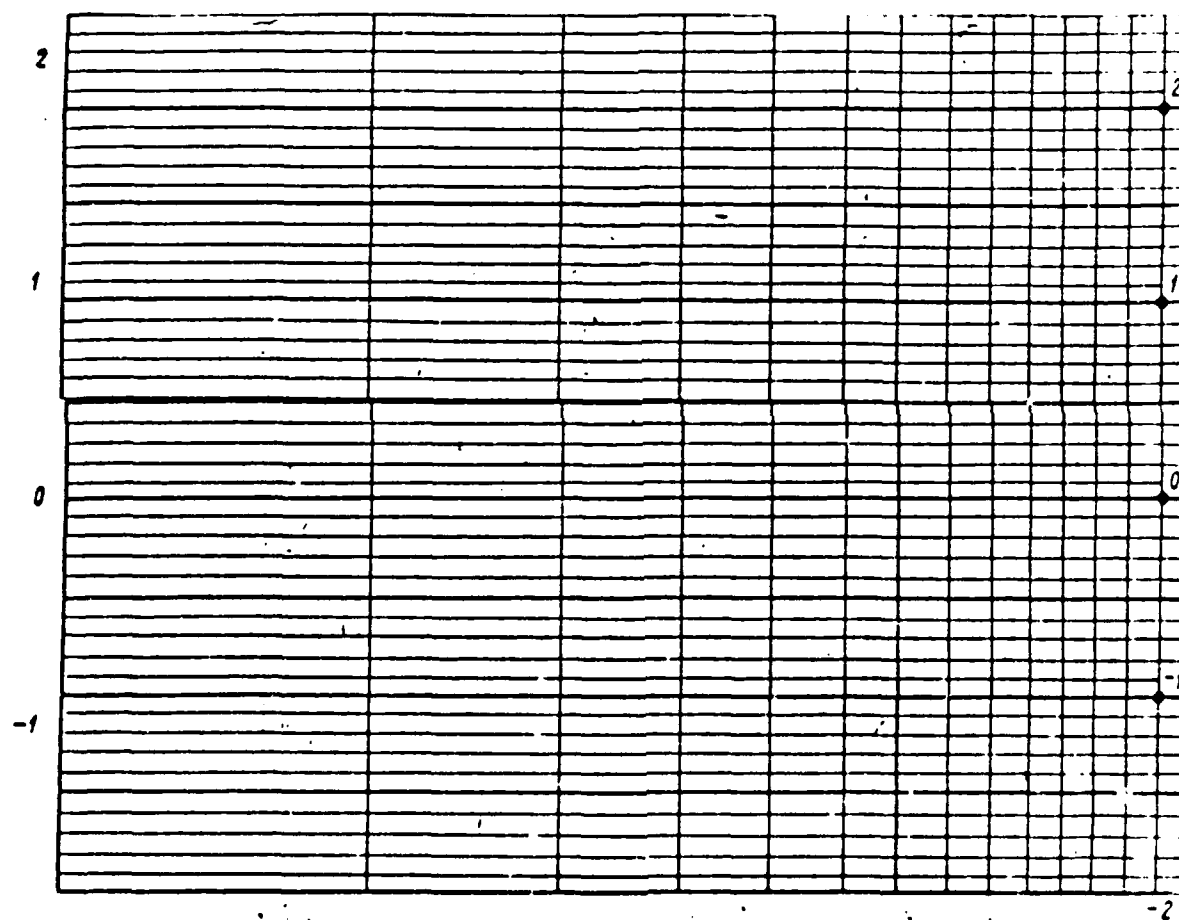


Fig. 71. Bottom Left.

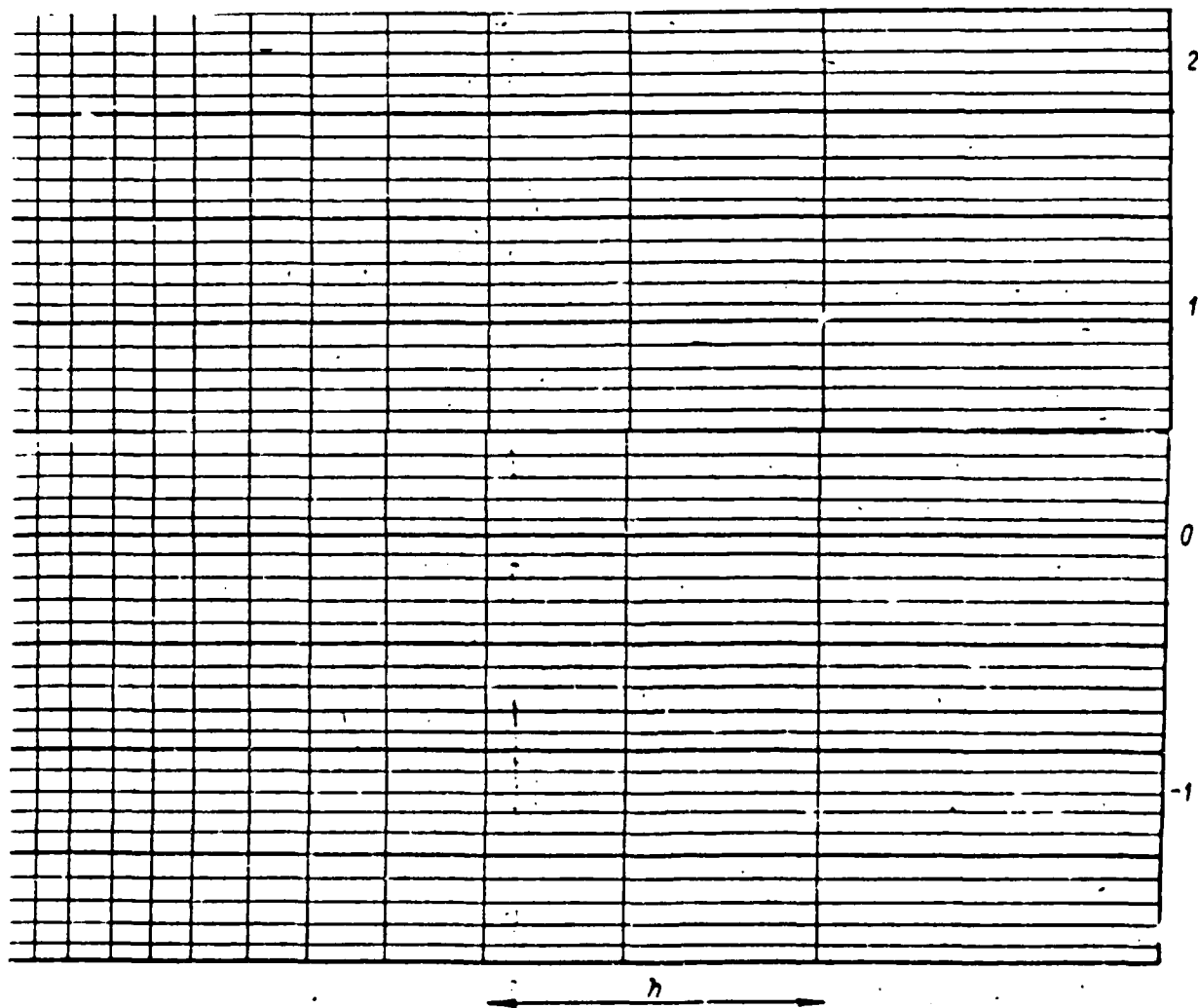


Fig. 71. Top Right.



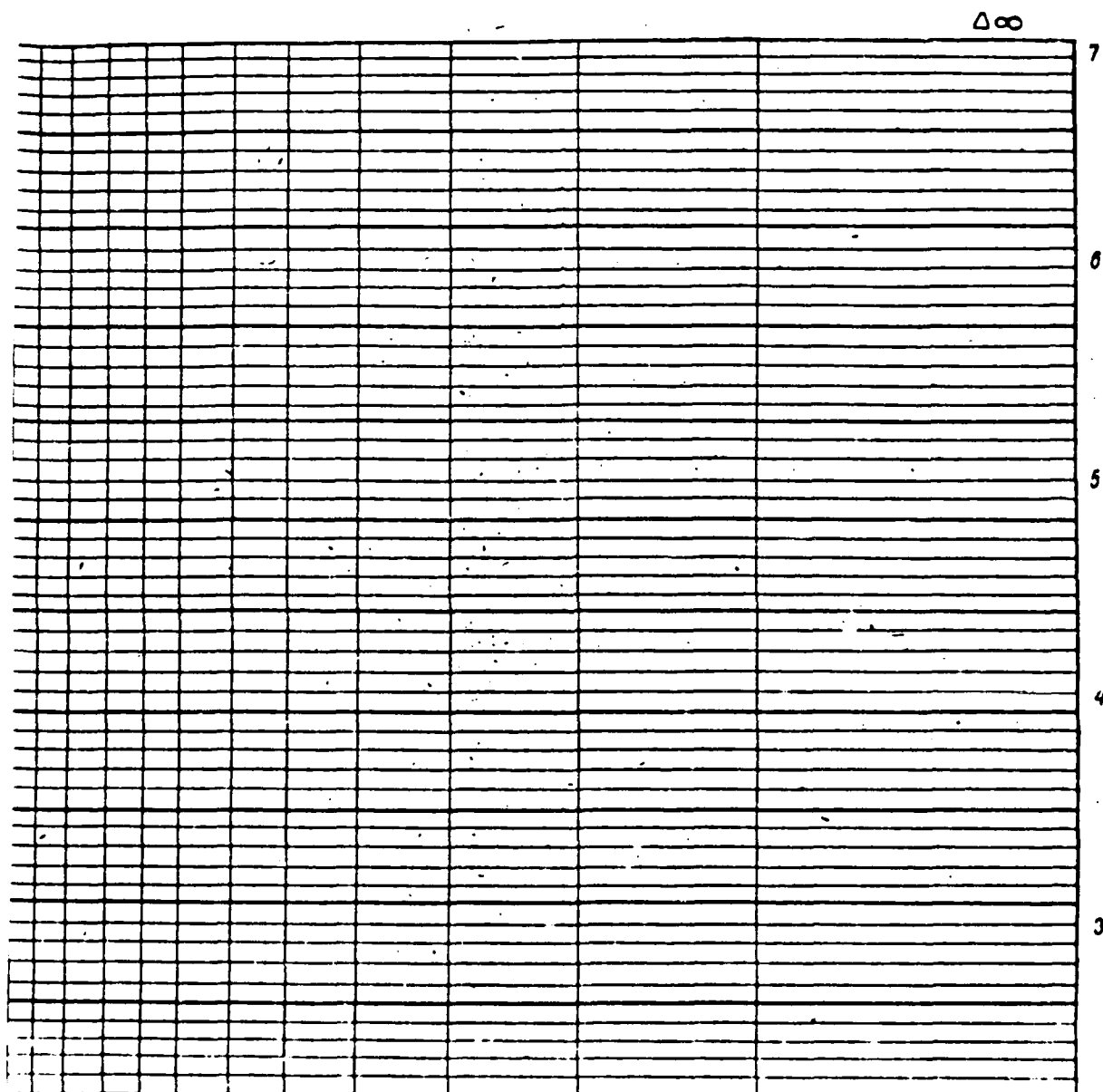


Fig. 71. Bottom Right.

Fig. 71. B. A. Andreev's transparency for recount of potential physical field to overlying level (height of recount is equal to 5 cm of the horizontal scale of the graph).



Fig. 72. V. N. Strakhov's transparency for recount of potential physical field to overlying level. The height of recount is  $h=1$  cm. With a change in the scale of transparency, i.e., with the nonconformity of the interval, indicated on transparency, to one centimeter, the calculated value of the anomaly should be reduced  $1$  cm/ $h$  cm times.



Fig. 72a. V. N. Strakhov's transparency for calculating the field in the lower half-plane according to the formula (IV, 88). The sum of the readings of curve  $u$  on the scales gives  $\Sigma u$ .

Page 165.

Basic difference in published transparencys consists in the fact that some authors assume invariable coefficients  $k_i$ , in consequence of which radii  $R_i$  are increased nonlinearly; others - previously select system of radii, which are consecutively/serially increased by constant of value, in this case coefficients  $k_i$  are variables.

As first type transparency let us examine transparency of N. R. Malkin (1934), depicted in Fig. 73, whose description is given in A. A. Logachev's book (1955). By the system of the rays/beams divergent at an angle of  $36^\circ$ , and concentric circles/circumferences with the radii, equal to 0.48; 0.75; 1.02; 1.33; 1.73; 2.28; 3.17; 4.91; 9.8 cm, entire/all plane it is divided/marked off on 100 pads. Ten areas/sites from a total number are placed within the circle with  $R=0.48$  cm, and ten more areas/sites - beyond the limits of circle with  $R=9.8$  cm.

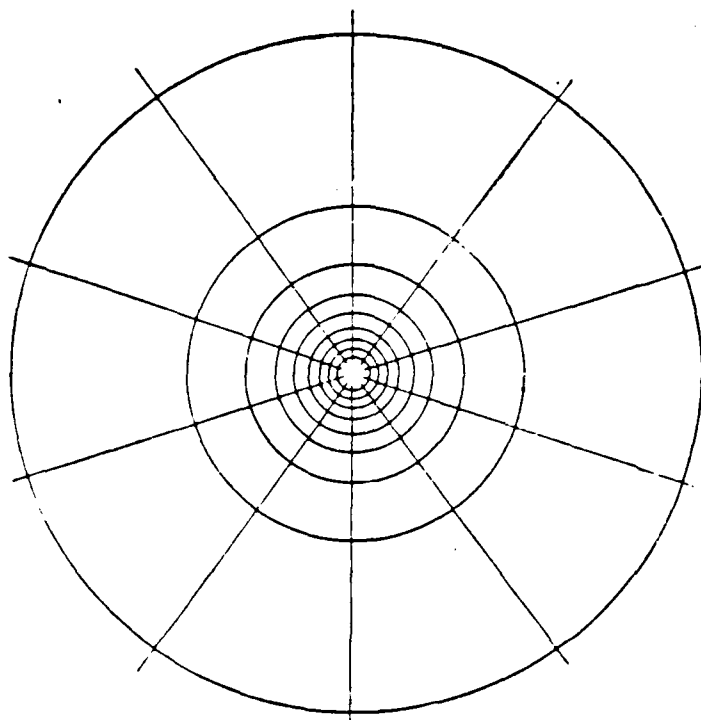


Fig. 73. Circular transparency for calculating potential physical field at overlying level.

Page 166.

From each of the areas the average value of the anomaly is determined. The sum of average/mean values, divided into 100, determines anomaly value at the height, equal to scale of map/chart 1 cm. The anomaly is calculated in the same units in which the numbering of the isolines of initial map/chart is given.

For calculating the anomaly at another level, it is necessary to proportionally change radii of a circle.

Transparency of A. K. Malovichko (1956) is an example of a transparency based on the other approach. Table 14 shows the values of radii  $R_i$  and corresponding coefficients.

Calculating formula, realized with the help of transparency, takes form

$$U(0, -z) = \bar{U}(R_0, 0) + \sum_{i=0}^5 k_i [\bar{U}(R_i) - \bar{U}(R_0)]. \quad (IV, 74)$$

Average/mean value of anomaly on ring of given radius is determined in terms of 8 values. The height of recount is equal to the radius of the first ring.

So as in the case of other transformations, let us examine filtering effect of transparencys and sensitivity to errors in initial data.

Above we noted that recount of field upward to height  $h$  was equipollent to subsidence of masses at the same depth, if we examine transformed field on surface of  $z=0$ . Therefore the relative deep characteristic of transformation has the simple analytical expression

$$N(z) = \frac{z^2}{(z+h)^2}. \quad (IV, 75)$$

Graph  $N(z)$  is constructed in Fig. 74. Depth is expressed in units of the level of recount. As we see, recomputation of the field

upward substantially affects the anomalies, caused by the deeply submerged masses. Even with the depth, ten times which exceeds the level of recount,  $N(z)$  differs from one ( $N(z)=0.83$ ). In Fig. 74 is additionally constructed curve  $N(z)$ , which corresponds to one concrete transparency - the transparency of A. K. Malovichko, which has radii and coefficients, indicated in Table 14.



Table 14. Values  $R_i$  and  $k_i$  for the transparency of A. K. Malovichko.

$\frac{R_i}{z}$	0	1	2	3	4	5
$k_i$	0.146	0.276	0.195	0.102	0.060	0.039

Page 167.

The curves  $N(z)$  coincide, beginning with  $z/h=1$ . With small  $z$  a considerable disagreement is planned. This special feature is general/common for all transparencys. The recount of field is upward with the satisfactory accuracy feasible only for the heights, greater than a certain limiting value, usually equal to 0.5-0.8 cm to scale of map/chart. Recalculation of anomalies to the small height - unstable operation.

Calculated distribution of anomalies at any level in upper half-space can be used, together with distribution of averaged anomalies. for characteristic of regional special features of field, observed on surface of Earth. It is useful to establish/install, with what relationship/ratio of the radius of averaging  $R$  and level of recount  $h$  similar results are obtained, in the first approximation. Business in the fact that the operation of the recount of anomalous field to the overlying level makes visual physical sense, but requires comparatively bulky calculations, whereas averaging is satisfied much more simply.

K. V. Gladkiy (1961) established, on the basis of analysis of

characteristics of transformation in two-dimensional case, that  $\frac{R}{\lambda} \approx 1/3$ . The obtained relationship/ratio is not completely convincing, since it does not find confirmation in the practice. Actually, this relationship/ratio is brought out under the assumption that the greatest objectivity will be achieved/reached, if we consider the spectral distribution of anomalies equiprobable in the limits of the entire frequency band. Meanwhile, the observed anomalous field is always correlated in the finite intervals. One of the reasons for correlation consists in the fact that the anomalies in the surface of the Earth reflect a nonuniform distribution of masses in the large range of depths. The case, actually examined by K. V. Gladky, is equipollent to the chaotic source distribution of anomalies on the very surface of the Earth.

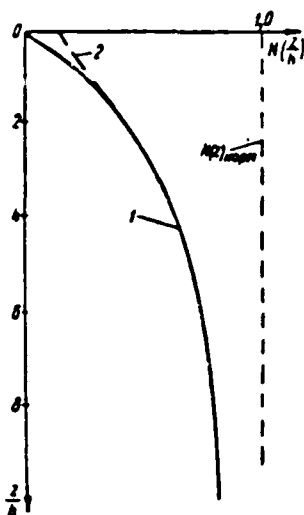


Fig. 74. Relative deep characteristic of the method of recount to height. 1 - theoretical dependence; 2 - for the transparency of A. K. Malovichko (Table 15).

Page 168.

Theory of filters in the application to the transformations of anomalies it must consider that smoothly changing components of anomalous field always have large intensity.

We will obtain more reliable relationship/ratio of averaging and recount of anomalies to height during analysis of results of these transformations. In Fig. 75 there are plotted curves  $N(z)$ , which correspond to recount to height  $h=0.2R, 0.3R, 0.4R, 0.5R, R/\sqrt{3}$  and to averaging with a radius of  $R$ . As a comparison of the curves shows, the greatest proximity is reached at  $R \approx 3.5h$ . This relationship/ratio is confirmed by practice. Thus, in the work of Yu. I. Nikol'skiy

(1960), that generalizes experiment of the interpretation of anomalies  $\Delta g$  in the limits of the geologically closed territories of the west of Central Asia, are cited the data which show that the optimum height of recount ( $h=5-7$  km) remains invariable for the vast regions. The comparable picture of regional field is reached at the averaging, if the radius not less than 20 km.

Local anomalies, isolated with method of averaging and with recount into height, also reveal similarity only with relationship/ratio  $R/h \geq 4$ . As the example in Fig. 76 there are constructed the diagrams of the isolines of the local anomalies above one brachianticlinial structural for cases of  $R=4$ ; 8 km and  $h=1$  km. The configuration and intensity of the chosen anomalies in all cases they indicate the presence of the large/coarse fold, whose eastern pericline is complicated by additional uplift/rise. If we consider the diagrams of isolines as the results of one type transformation with the consecutively/serially increased parameter, should be placed diagram  $\Delta g_{\text{anom}}|_{h=1}$  following diagram  $\Delta g_{\text{anom}}|_{R=4}$ .

We will obtain anomaly variation with a different correlation after recount to height, substituting characteristic of transformation into equality (IV, 15). The comparison of Poisson's integral (IV, 45) with the integral (IV, 4) shows that the characteristic of the transformation, realized with the recount of anomalies into the upper half-space to the level -  $z=h$ , takes the form

$$\psi(\alpha) = e^{-\alpha h}.$$

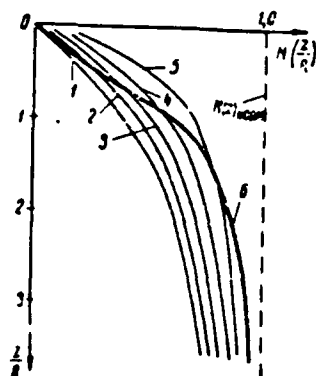


Fig. 75. Comparison of relative deep characteristics  $N(z)$  by method of averaging and recount to height. 1 - curve  $N(z)$  for the recount to the height with  $h=R/\sqrt{3}$ ; 2 - the same,  $R=2.00h$ ; 3 - the same,  $R=2.50h$ ; 4 - the same,  $R=3.33h$ ; 5 - the same,  $R=5.00h$ ; 6 - curve  $N(z)$  for the method of averaging.

Page 169.

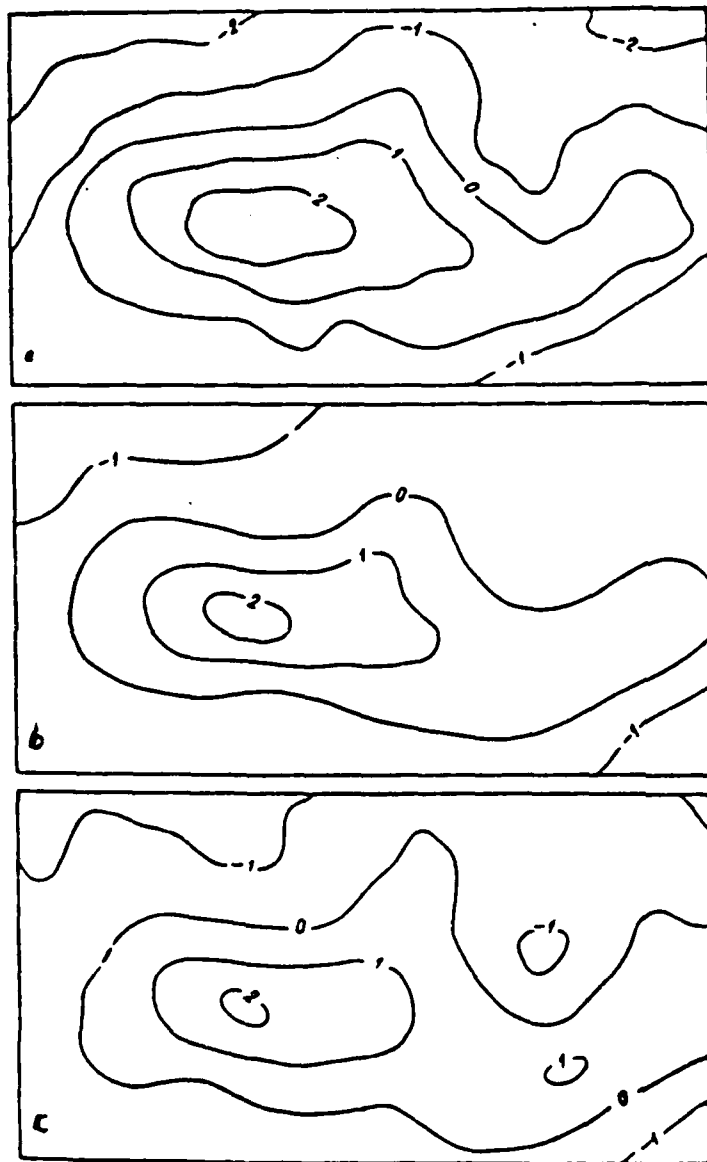


Fig. 76. Diagrams of isolines of local field  $\Delta g$  above anticlinal structure: a) method of averaging,  $R=8$  km; b) method of recount to height,  $h=1$  km; c) method of averaging,  $R=4$  km.

Page 170.

Hence

$$\begin{aligned}\bar{A}_{\text{transc}}^2 &= \bar{A}^2 \frac{r^2}{2} \int_0^{\infty} \exp\left(-\frac{a^2 r^2}{4}\right) [e^{-a h}]^2 a da = \\ &= \bar{A}^2 \varphi^2\left(\frac{r}{h}\right).\end{aligned}\quad (\text{IV}, 76)$$

Graph/curve of relative change of amplitude of anomalies as function of relationship/ratio of height of recount and radius of autocorrelation it is given in Fig. 77. Those components of the anomalous field, which are correlated on the large of distance, with the recount remain almost invariable. If the radius of autocorrelation is considerably lower than the level of recount, is observed the approximate equality

$$\sqrt{\bar{A}_{\text{transc}}^2} \approx \sqrt{\bar{A}^2} \frac{r}{h_2 \sqrt{2}}. \quad (\text{IV}, 77)$$

Recount of field upward reduces effect of accidental errors of observation and effect of anomalies of high order, conditioned by small dense heterogeneity of geologic bodies. Taking into account this, many researchers recommend the calculating of the anomalies of the vertical force gradient of gravity  $W_{\text{v}}$  and anomaly  $W_{\text{v}}$ , not a certain level higher than surface of the Earth in order to weaken/attenuate the distorting effect/action of interference.

Analytical continuation of anomalies, measured on surface of Earth, into lower half-space or half-plane is more interesting and at the same time more complex problem. Data about field distribution of the force of gravity or higher derivatives of the gravitational

potential  $W$  are of practical use during the study of the relief of contact surface, during the determination of the depth of the bedding of the singular points of the anomaly-forming bodies.

Proposition of American geophysicist Pearson (1945), who examined construction of field on auxiliary plane between earth's surface and perturbing masses as effect/action of optical lens, which focuses image of object of study, is widely known.

One of the first problems about the analytical continuation of field downward was examined by Reynbow (1933).



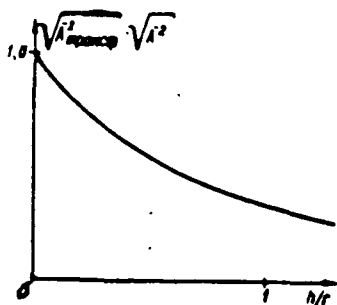


Fig. 77. Relative change in anomalies of different correlation after a recount to height.  $h/r$  - ratio of the height of recount to the radius of autocorrelation.

Page 171.

Brought out by it formula, which gives value of  $U(0, z)$  in terms of values of  $U(x, 0)$ , can be obtained from the equality (IV, 70).

Let us decompose integral in the right side of equality (IV, 70) to two terms

$$\begin{aligned} \int_0^\infty e^{-\alpha z} d\alpha \int_{-\infty}^{+\infty} U(x, 0) \cos \alpha x dx = \\ = \int_0^B e^{-\alpha z} d\alpha \int_{-\infty}^{+\infty} U(x, 0) \cos \alpha x dx + I(B). \end{aligned} \quad (\text{IV, 78})$$

In view of the fact that actually observed anomalies always possess terminal radius of autocorrelation, integration can be replaced with summation, after taking readings of anomaly in isolated point. In information theory (Goldman, 1957) it is proven, that the behavior of continuous function is completely described by the

discrete/digital readings, undertaken at the points, distant behind each other at a distance of  $h$ , if function does not contain components with the frequencies of more than the certain boundary  $\alpha = \pi/h$ .

Therefore, selecting the interval between the points by such so that would not be smoothed out the essential features of the curve  $U(x, 0)$ , it is possible to place  $B = \frac{\pi}{h}$ ,  $z = h$ ,  $x = nh$  ( $n$  integer).

After using trapezoid rule, we will obtain

$$U(0, h) = \frac{1}{\pi} \sum_{n=-\infty}^{+\infty} U(nh, 0) \frac{(-1)^n (e^{\pi} - 1)}{1 + n^2}. \quad (\text{IV, 79})$$

Formula (IV, 79) was derived by Reynbow in 1933, when yet there was no information theory and it was not widely known to one of its fundamental theorems - sampling theorem, proved by V. A. Kotelnikov (1933). Is to a considerable extent intuitively for Reynbow selected the best ratio of step  $h$ , depth of recount and boundary of cutting  $\alpha = \pi/h$ . O. A. Swank, S. V. Shalayev et al. investigated formula (IV, 79). Its strict basis (1959) belongs to S. V. Shalayev.

Graph of relative error, constructed in Fig. 78, shows that calculations according to formula (IV, 79) give satisfactory results, if depth of recount  $h$  does not exceed half of depth of bedding of sources.

Simple formulas for calculating any potential function in lower half-plane and half-space escape/ensue from law of mean. Under the

DOC = 88020209

PAGE *31 323*

conditions of the two-dimensional problem the value of function in the center of circle is equal to the integral average of its values taken on a circle.

Page 172

Substituting integral average arithmetic mean of four readings, we will obtain

$$U(0, h) = 4U(0, 0) - [U(0, -h) + U(-h, 0) + U(h, 0)]. \quad (IV, 80)$$

Position of points is shown in Fig. 79.

In the case of three-dimensional field distribution integral average over surface of sphere is substituted arithmetic mean of six values

$$U(0, 0, h) = 6U(0, 0, 0) - [U(0, 0, -h) + U(0, -h, 0) + U(0, h, 0) + U(-h, 0, 0) + U(h, 0, 0)]. \quad (IV, 81)$$

Formulas (IV, 80) and (IV, 81) are the basis net point method. Let us examine the latter based on the example of two-dimensional problem. The vertical plane  $xoz$  is divided/marked off by the system of the vertical and horizontal lines, distant in the equal intervals. The points of intersection of lines form nodes. In those nodes, which are arranged/located on level  $z=0$ , the values of anomaly are written out directly according to the results of measurements. At the points, in arranged/located above the lines of observation, anomalies are calculated with the help of the templates [measuring grids] of B. A. Andreyev, V. N. Strakhov et al. Thus, with the help of the relation (IV, 80) it is possible to compute values of  $U(x, z)$  at any point at level  $z=h$  (Fig. 80), and then in a similar manner to compute values of  $U$  at level  $z=2h$  and so forth, including the entire, interesting to us, part of the lower half-plane. This region must not include the singular points of anomalous field.

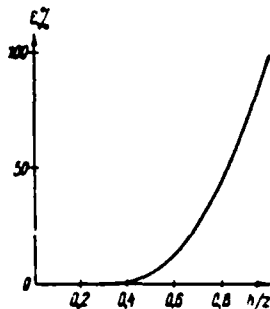


Fig. 78.

Fig. 78. Graph of relative error in calculation  $\epsilon$ , caused by rejection of components with  $\alpha > \pi/h$ . Case of the line source, located on depth  $z$ . According to S. V. Shalayev (1959).

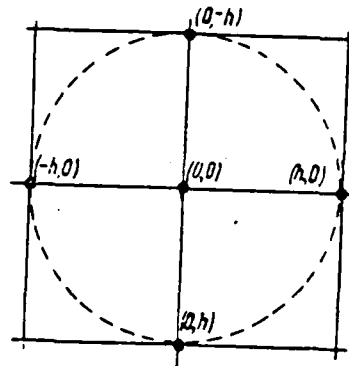


Fig. 79.

Fig. 79. Explanation to formula (IV, 80).

Page 173.

Unfortunately, it is impossible to go down lower than to 2-3 steps usually due to errors, which unavoidably accompany process of calculation (round-off error, observation error, etc.). On the basis of the formula (IV, 80), it is easy to find that the error  $\epsilon$  at the point  $(0, x)$  of the initial profile  $z=0$  engenders on the lower profiles the whole "field of the errors", whose numerical values increase very rapidly (Fig. 81): at point  $(x, h)$  the error is equal to  $4 \epsilon$ ; at point  $(x, 2h)$  -  $17 \epsilon$  and at point  $(x, 3h)$  -  $80 \epsilon$ .

This instability can be to high degree weakened/attenuated, if calculations  $U(x, z)$  are implemented on periphery of anomalous zone and function  $U(z, x)$  along any vertical profile has general/common

special features of distribution at identical levels. Thus, for example, if  $U(x, z)$  reaches maximum value or it becomes zero on the same level, it is possible to find the latter summarizing the values, calculated by the net point method according to several points located at one depth<sup>1</sup>.

FOOTNOTE<sup>1</sup>. Proposition of B. A. Andreyev. It is published for the first time. ENDFOOTNOTE.

The general/common special features of field in this case are retained, for example the sum of maximum values will give maximum. These special features will be even underscored, they appear in the clearer form than along the single vertical profiles, and errors substantially compensate for, since they always have different signs at contiguous points.

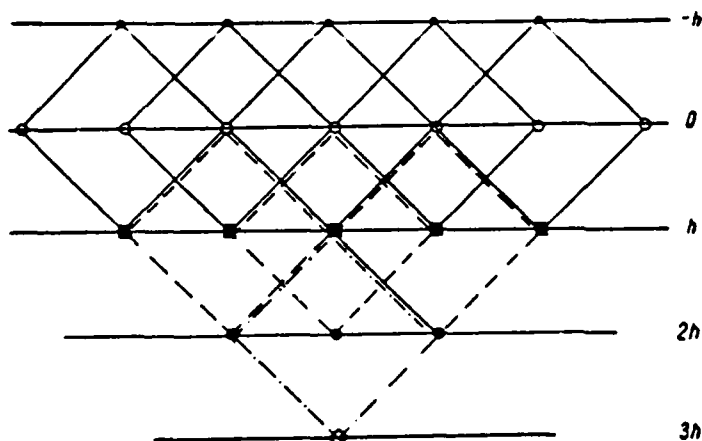


Fig. 80. Diagram of successive recount to underlying levels according to net point method.

Page 174.

Actually, the sum of the errors, generated by error in one point, has the following values along the profiles:  $z=h-2e$ ,  $z=2h-3e$ ,  $z=3h-4e$ , i.e., these values are relatively low and slowly they increase with the transition to the lower levels.

Fig. 82 gives examples of practical determination of special feature of distribution of anomalous field with depth - transition point through zero. With a similar problem they are encountered with the interpretation of anomalies  $W_{II}$ , and also anomalies  $Z$ , in magnetic prospecting. On the vertical profiles assigned in the side from the anomalous body, the transition point through zero is placed at the level of the upper edge of body. (Course/strike at the depth it is assumed to be significant, so that the effect of the lower edge of

body can be disregarded/neglected).

Fig. 83 shows specific on theoretical models and practical curve  $\Delta g$  distribution of anomalies  $\Delta g$  and  $W_{zz}$  in the case, when course/strike of body at depth not many times exceeds depth of up to upper edge. At the level of recount, which corresponds to the position of upper edge and equal for the practical example 3.5-4.0 km, total variation in the anomaly satisfies the equality

$$(W_{zz})_{\text{max}} - (W_{zz})_{\text{min}} \approx 2\pi f \Delta\sigma. \quad (\text{IV}, 82)$$

Hence we find the drop/jump in density on contact of anomaly-forming body and enclosing rocks

$$\Delta\sigma \approx \frac{40 \cdot 10^{-9}}{6.28 \cdot 67 \cdot 10^{-9}} \approx 0.1 \overset{(1)}{z/\text{cm}^3}. \quad (\text{IV}, 83)$$

Key: (1).  $\text{g/cm}^3$ .



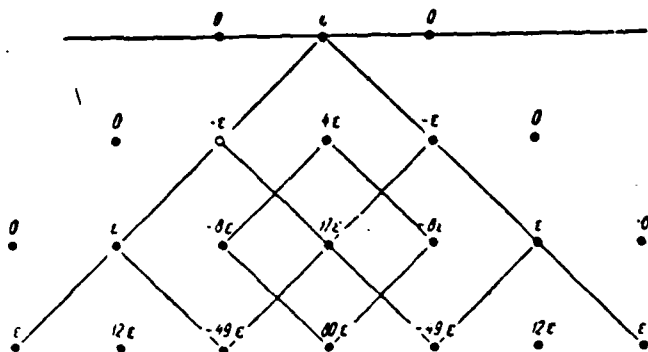


Fig. 81. "field of errors", engendered by error in initial point.  
According to B. A. Andreev.

Page 175.

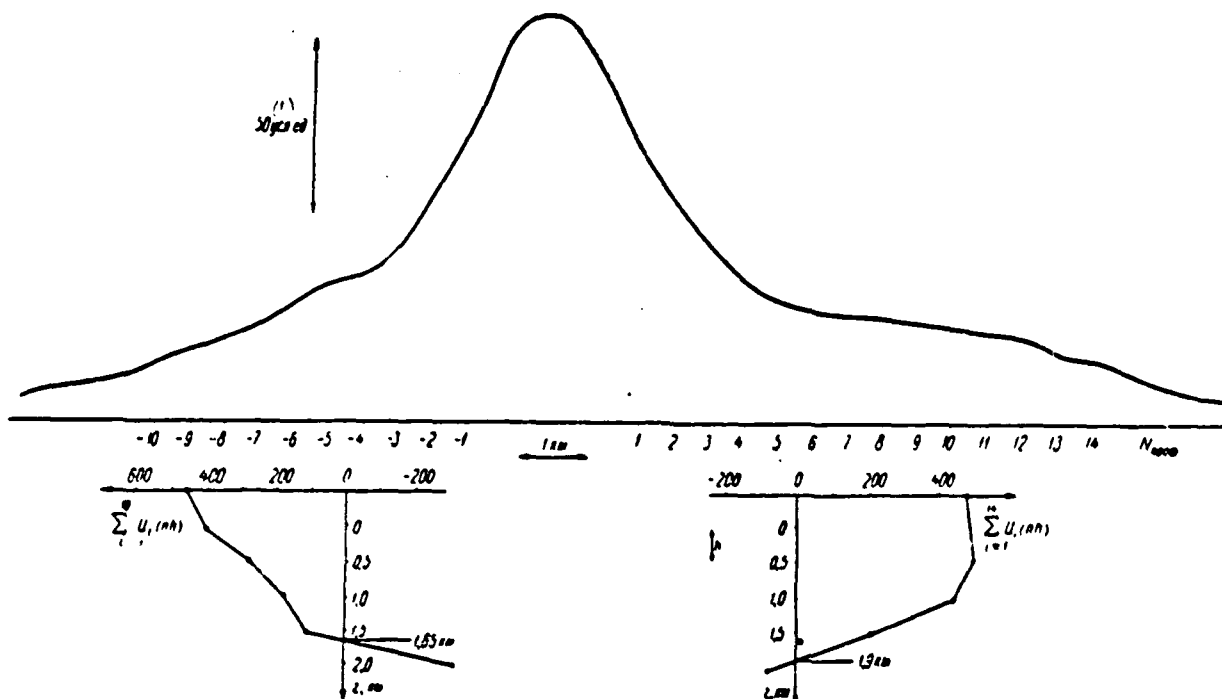


Fig. 82. Example of calculation of potential field in lower half-plane according to net point method. The conversion step  $h$  is equal to 0.5 km.

Key: (1). 50 conv. unit.

Pages 176-177.

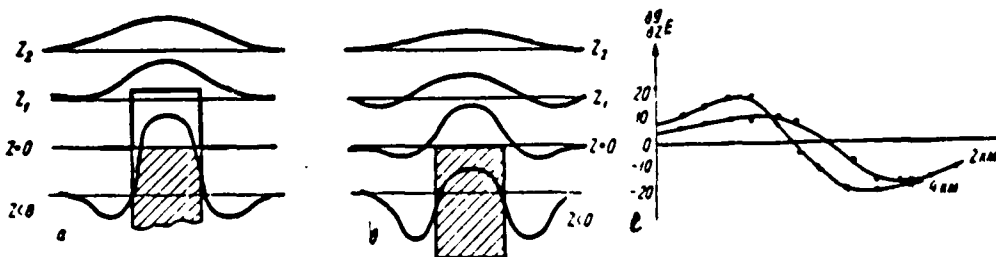
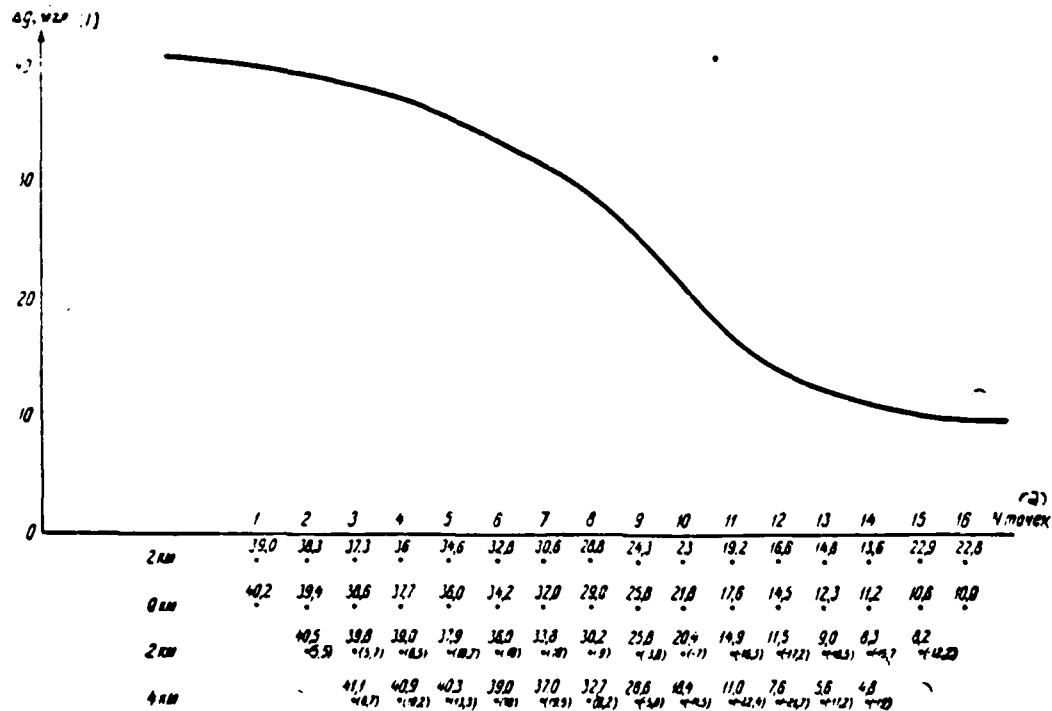


Fig. 83. Example of calculation in lower half-plane of anomalies  $\Delta g$  and  $\frac{\partial g}{\partial z} = w'$ . Step/pitch between the network points 2 km. the numeral above the network point - anomaly  $\Delta g$  in the milligals, numeral in the parentheses - anomaly  $w'$  in Eotvos: a) theoretical curves  $w'$  above the body of infinite course/strike at the depth; b) the same, of final course/strike at the depth; c) practical curves.

Key: (1).  $\Delta g$ , mgal. (2).  $N$ , points.

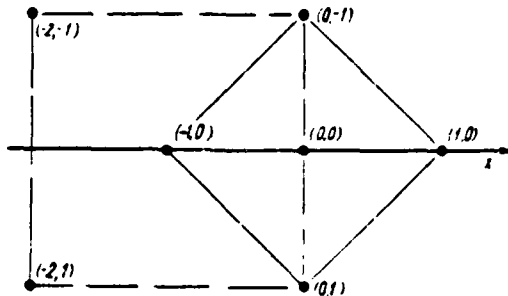


Fig. 84. Explanation to formulas (IV, 84-85).

Page 178.

In each specific case of applying net point method can be used different methods, which make it possible to make more precise calculated values of  $U(z, x)$ . Thus, with an abrupt change in the anomalous field near the body the calculated value  $U(x, z)$  can be controlled, after including the point interesting in the new set of points (Fig. 84). Value  $U(0, 1)$  in the first version is determined by the equality

$$U(0, 1) \approx 4U(0, 0) - U(-1, 0) - U(1, 0) - U(0, -1). \quad (\text{IV}, 84)$$

To check this value is possible, using points  $(-2, -1)$ ;  $(0, -1)$ ;  $(-2, 1)$ ;  $(-1, 0)$ :

$$U(0, 1) \approx 4U(-1, 0) - U(-2, -1) - U(0, -1) - U(-2, 1). \quad (\text{IV}, 85)$$

In this case the operation of analytical continuation of field to side controls analytical continuation downward.

Original template for analytical continuation of potential field into lower half- plane is proposed by V. N. Strakhov (1961). Taking into account finite differences in the third order anomaly value at point  $U(0, h)$  can be expressed through its values at the points of upper half- plane by the equality

$$U(0, h) = 4U(0, 0) - 6U(0, -h) + 4U(0, -2h) - U(0, -3h). \quad (\text{IV}, 86)$$

Taking into account integral of Poisson (IV, 71), we find

$$U(0, h) = -\frac{1}{\pi} \int_{-\infty}^{+\infty} U(x, 0) \left[ \frac{6h}{h^2 + x^2} - \frac{8h}{4h^2 + x^2} + \frac{3h}{9h^2 + x^2} \right] dx + 4U(0, 0). \quad (\text{IV}, 87)$$

Integral in (IV, 87) is divided into a number of particular integrals, each of which is calculated with the help of quadrature formulas of Gauss. For calculation  $U(0, h)$  the template is laid under graph  $U(x, 0)$ , traced on the sheet of tracing paper. The projection of the point, at which is calculated  $U(h)$ , it is combined with the center of template. In the points of the intersection with the curve  $U(x, 0)$  with the scales are taken the readings, whose sum composes value  $\Sigma U$ . Anomaly  $U(0, h)$  (in the millimeters of the ordinates of drawing) is found by the formula

$$U(0, h) = 4U(0, 0) - \Sigma U, \quad (\text{IV}, 88)$$

where  $U(0, 0)$  - the value of field at the center of template in the millimeters.

Level of recount is equal to 1 cm and usually it is indicated on template in the form of segment of specific length.

Page 179.

S. V. Shalayev downward fulfilled significant investigations on analytical continuation of field. Referring reader after the details in his works (1959, 1960), let us write out the brought out by it formula for the finding

$$\begin{aligned}
 U(0, h) + U(0, -h) &= \\
 &= k_0 U(0, 0) + \sum_{n=1}^{\infty} k_n [U(nh, 0) + U(-nh, 0)]. \quad (\text{IV}, 89) \\
 k_0 &= 6,665; \quad k_1 = -3,015; \quad k_2 = 0,8935; \quad k_3 = -0,2710; \\
 k_4 &= 0,07918; \quad k_5 = -0,02104; \quad k_6 = 0,004921; \quad k_7 = -0,0009929.
 \end{aligned}$$

Formula (IV, 89) is analog of formula to Reynbow, possessing more rapid convergence.

§ 28. Comparison of the different methods of the separation of anomalies.

After laying aside methods of separation of anomalous field of based on attraction additional geologic data (methods most reliable and at the same time expensive - cost of additional information can exceed cost of gravimetric survey), it is summed up most important special features of those methods, which are based on account of different correlation of anomalies.

Isolation of regional anomalies is realized by the method of

averaging or via recount of anomalous field to height. Both methods give stable results. On the basis of the theoretical positions, the recount of anomalies into the upper half-space is more acceptable. The conversion, realized with the recount, is equipollent to simple removal/distance from the sources of anomalies. In exactly the same manner in the museum or to picture gallery we make step/pitch back/ago from the picture in question in order with one view to contain its composition.

Mass calculations for purpose of construction of maps/charts of regional field by this method are impossible without application of special technical equipment - computers (Klushin, Nicol, 1959), etc.

Method of averaging is considerably more simple in a technical sense. On the relationship/ratio of averaging and recount of anomalies to the height it spoke above.

Maps/charts of regional field are built with section, equal to section of initial map/chart or which exceeds it.

Liberation/precipitation of local anomalies is realized without large additional calculations with liberation/precipitation of regional anomalies. At the same time are used the special methods of localization - calculation of the variation anomalies  $\delta\Delta g$ , the recount of anomalies  $\Delta g$  in anomaly  $W_{11}$  and  $W_{12}$  and so forth.

Results of calculations to a considerable extent depend on parameter of conversion also to a lesser degree - from form of conversion. This position is widely confirmed by the practice of working the maps/charts of anomalies. As the obvious case let us examine Fig. 85-90, in which are consecutively/serially represented the following maps/charts:

- 1) the map/chart of Bouguer's anomalies, with the section of isoanomaly through 1 mgal, for one of the regions in the coast of Mediterranean (Soliani, 1954);
- 2) the map/chart of the vertical force gradient of gravity (section of isoanomaly through 10 E);
- 3) the map/chart of the local anomalies, isolated with the method, similar to the calculation of variation anomalies ( $l=1.12$  km, the section of isoanomaly through 0.2 mg/).
- 4) the map/chart of the local anomalies, isolated analogously with  $l=2.24$  km;
- 5) the map/chart of anomalies  $W_{int}$  calculated with the help of the template of Rosenbach (distance between the network points 1 km, the section of isoanomaly  $1 \text{ mg/km}^2 = 100 \cdot 10^{-11}$  CGS);
- 6) the map/chart of anomalies  $W_{int}$  calculated with the help of the template of Elkins, the section of isoanomaly is the same.

Basic conclusion/derivation, which follows from analysis of maps/charts indicated, is reduced to the fact that anomalies, isolated with different methods, approximately retain their form and position.



They are such intensive positive anomaly in the center of plane table, the anomaly of complex form in northwestern angle, etc. Are kept constants also many parts of local anomalies.

If localization is produced for territory with proved confinement of gravity anomalies of small value to objects interesting geologists, for example, for the purpose of determination of structures of sedimentary formations all enumerated methods can prove to be suitable. The geologic efficiency of each of them will be approximately identical. At the same time the laboriousness for calculations depends substantially on the method of the liberation/precipitation of anomalies. Together with the labor expense important value has a relative increase in the level of errors in the initial data.

In contemporary accuracy of gravimetric surveys and absence of special calculating means, the most acceptable method of localization is calculation of variations in anomalous field  $\delta\Delta g$ . Virtually recommended themselves the different modifications of the method of variations, including liberation/precipitation of anomalies on a difference in the variations

$$\delta\Delta g(i_2) = \delta\Delta g(i_1) = \bar{\Delta g}(i_1) - \bar{\Delta g}(i_2).$$

Page 181.

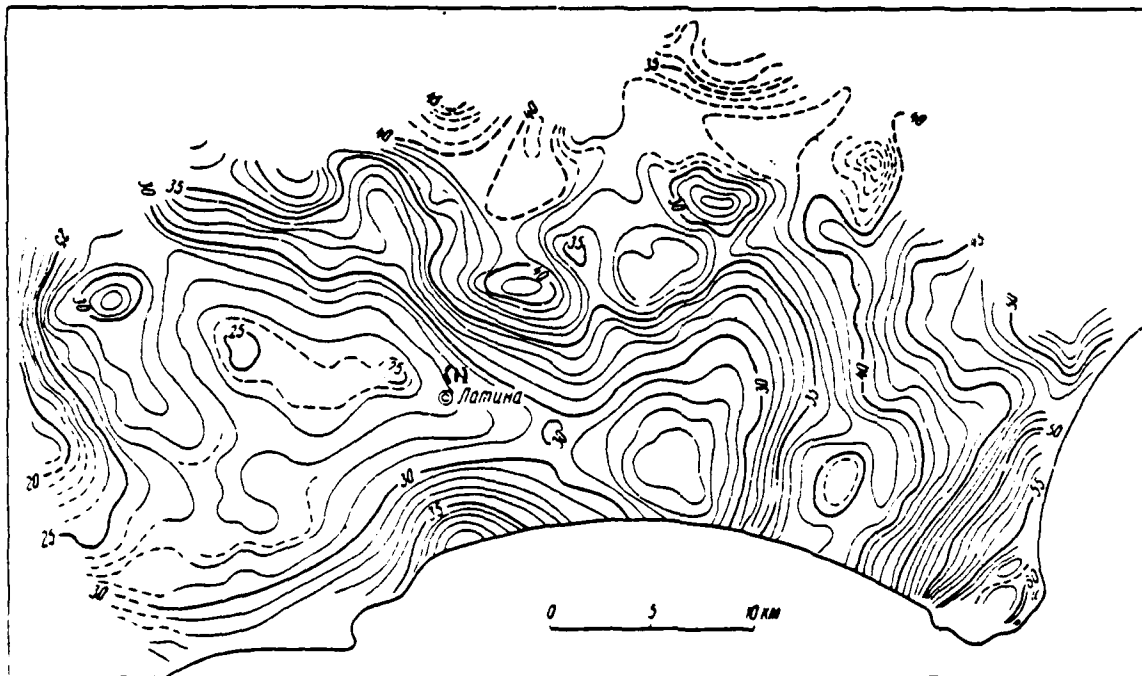


Fig. 85. Map/chart of Bouguer's anomalies one of regions Mediterranean coast. Section of isoanomaly of 1 mgf. (Fig. 85-90 according to Soliani, 1954).

Key: (1). Latina.

Page 182.

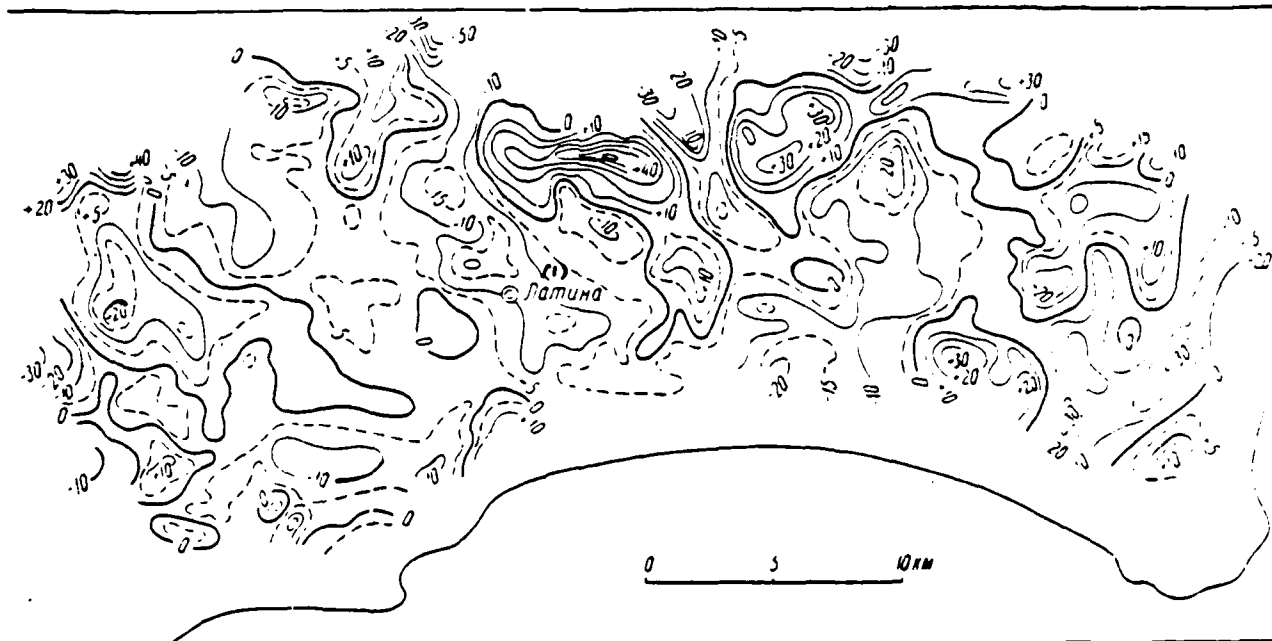


Fig. 86. Map of anomalies  $W_m$ , constructed on the basis Fig. 85.

Section of isoanomaly of 10 E.

Key: (1). Latina.

Page 183.

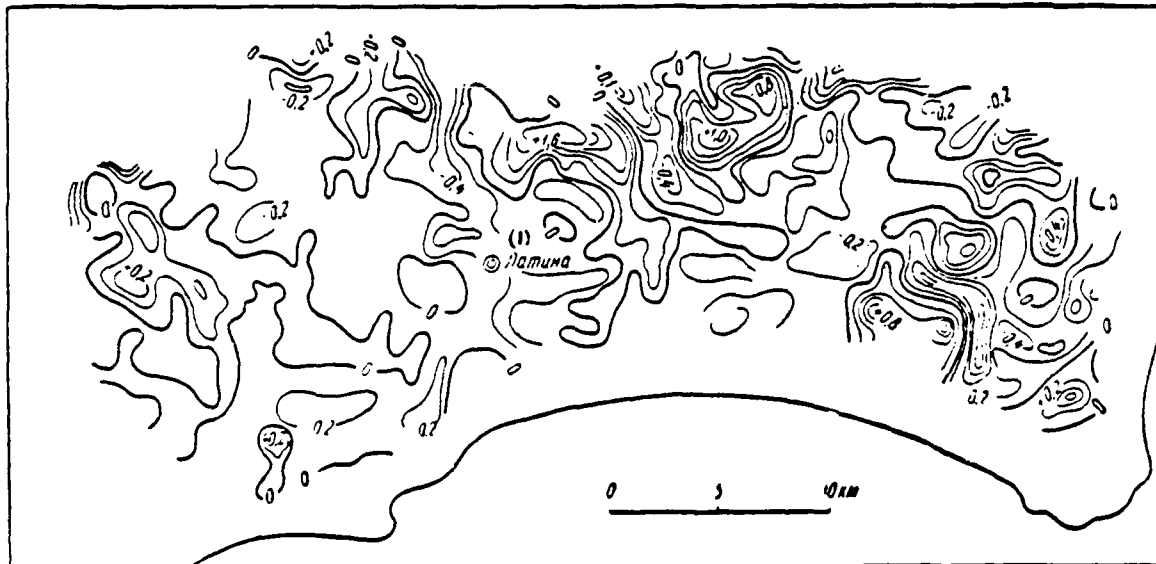


Fig. 87. Map of local anomalies  $\delta Ag$  ( $l=1.12$  km). Section of isoanomaly of 0.2 mg/l.

Key: (1). Latina.

Page 184.

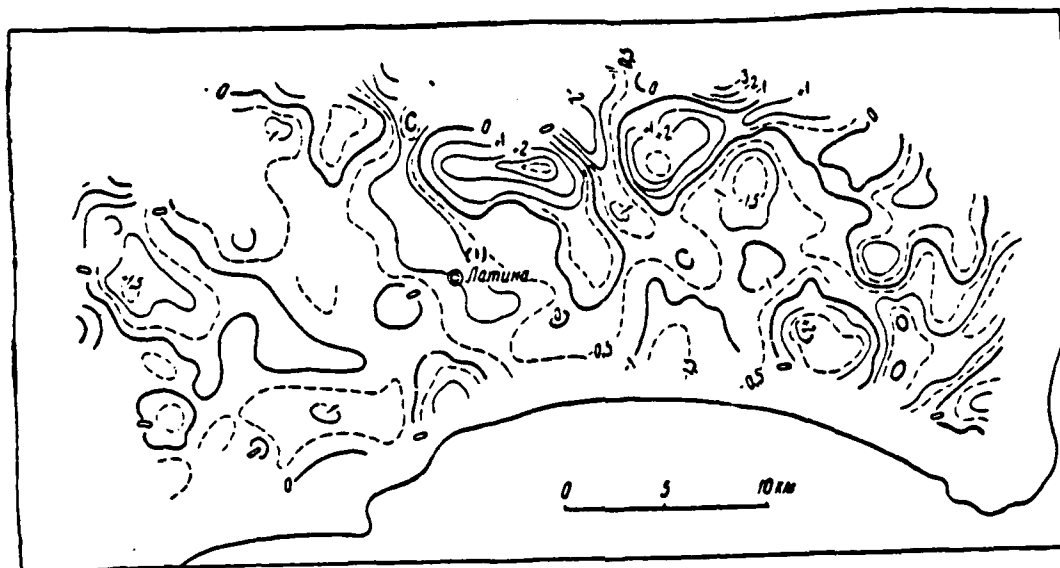


Fig. 88. Map of local anomalies  $\delta\Delta g(l=2.24 \text{ km})$ . Section of isoanomaly 1 mg/.

Key: (1). Latina.

Page 185.

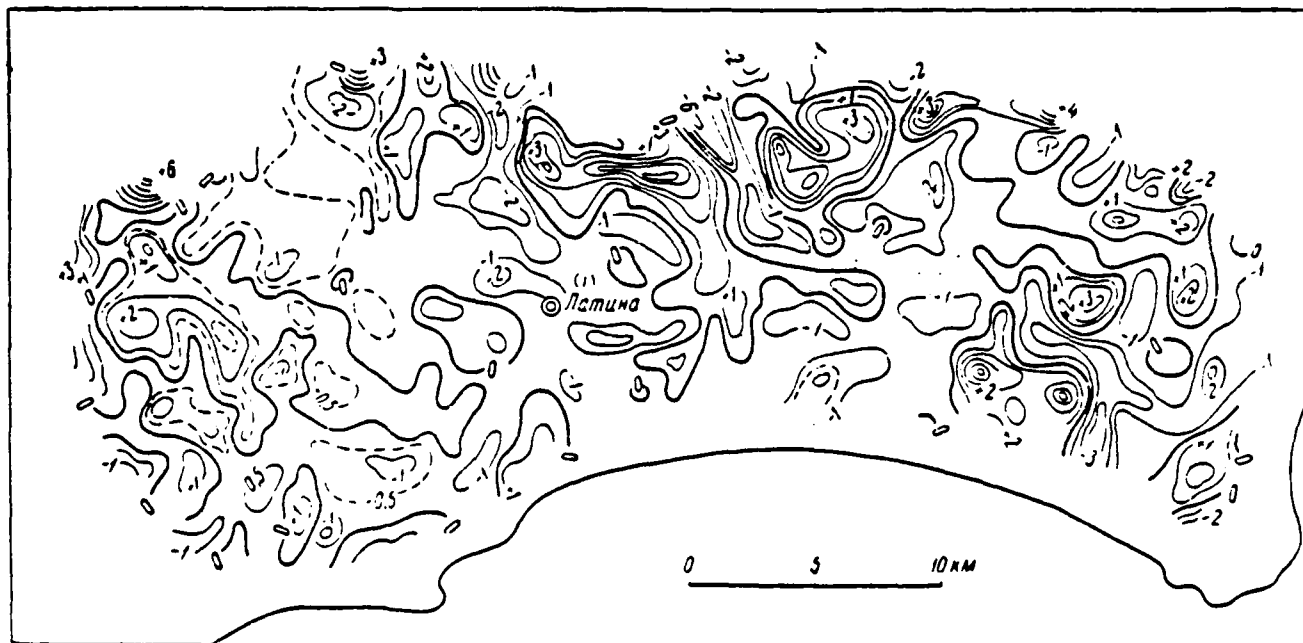


Fig. 89. Map of anomalies  $w_m$  calculated according to formula of Rosenbach. Dimension of the first radius of 1 km. Section of the isolines  $1 \cdot 10^{-11}$  CGS.

Key: (1). Latina.

Page 186.

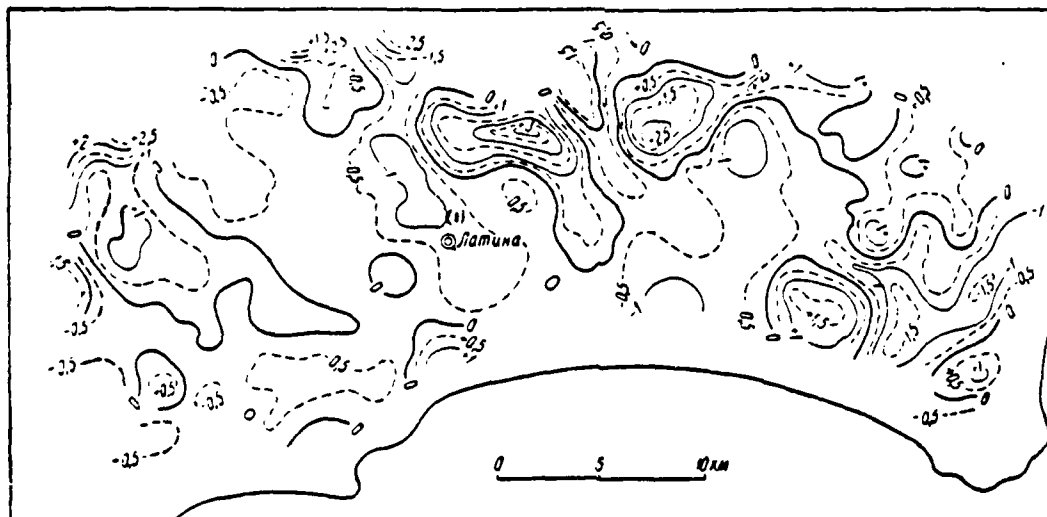


Fig. 90. Map of anomalies  $W_m$ , calculated according to formula of Elkins. Dimension of the first radius of 1 km. Section of isoanomaly  $1 \cdot 10^{-11}$  CGS.

Key: (1). Latina.

Page 187.

Anomalies isolated with method of variations have similar configuration with anomalies  $W_m$ . In many respects Above was examined the method, which makes it possible calculate  $W_m$  on  $\delta\Delta g$ . At the same time, the operation of calculation  $\delta\Delta g$  is not accompanied by a sharp increase in the level of errors in the initial data, which is characteristic for anomalies  $W_m$ . Convenient is the fact that anomalies  $\delta\Delta g$  have a dimensionality of the initial anomalies  $\Delta g$ .

The laborious calculation of anomalies of vertical force gradient of gravity  $W_{\text{v}}$  is justified only in those comparatively rare cases,

when quantitative interpretation is assumed. The major advantages of method  $W_{11}$ : weak dependence on the parameter of conversion, and thereby - simple tastes to the completeness of preliminary presentations/concepts, the sufficiently effective exception/elimination of regional background at the moderate increase in the interference level.

---





Fig. 91. Diagram of results of processing map/chart  $\Delta g$ . The zones relative to positive anomalies, which supposedly coincide with the uplifts/rises of sedimentary cover, are shaded. According to Yu. I. Nikol'skiy (1960). 1 - boundary of the predicted uplifts/rises; 2 - boundary of the predicted downwarps/troughs; remaining lines designate the position of the zero isolines of the local anomalies, isolated with different methods (averaging with  $R=40$  and  $20$  km, variation with  $l=10, 16, 30$  and  $40$  km).

Page 188.

Table 15. Recommendations regarding the application of transformations.

(1) Характеристика исходных данных		(2) Применяемая трансформация					
(3) Масштаб карты аномалий	(4) Сечение изоаномал. мгг	(5) Осреднение аномалий $\Delta g$	(6) Пересчет аномалий $\Delta g$ на высележа- щий уровень	(7) Вычисление вариаций аномалий $\delta \Delta g$ по Б. А. Андре- еву	(8) Вычисление аномалий $\frac{\partial g}{\partial z} = W_{12}$	(9) Вычисление аномалий $\frac{\partial^2 g}{\partial z^2} = W_{22}$	(10) Вычисле- ние оста- точных ано- малий по Саксову и Ниггарду
1:10 000 000—1:2 500 000	5—10	+	— +	—	—	—	—
1:1 000 000—1:500 000	5	++	+	— +	—	—	—
1:200 000—1:100 000	2—1	++	++	+	— +	—	+
1:100 000—1:50 000	1—0.5	++	++	++	+	+	—
1:50 000—1:25 000	0.5—0.2	++	++	++	++	+	—
1:25 000—1:10 000 и крупнее (10)	0.2—0.1	++	++	++	++	++	—

Note. The quality of the initial data: ++ completely corresponds to the transformation used; + corresponds; — + completely it does not correspond; — does not correspond.

Key: (1). Characteristic of initial data. (2). Transformation used. (3). Map scale of anomalies. (4). Section of isoanomaly, mgal. (5). Averaging of anomalies  $\Delta g$ . (6). Recount of anomalies  $\Delta g$  to overlying level. (7). Calculation of variations in anomalies  $\delta \Delta g$  according to B. A. Andreev. (8). Calculation of anomalies. (9). Calculation of residual anomalies on Saksov and Nyggard. (10). and larger.

Page 189.

If at the disposal of the interpreter productive calculating means are located, an undoubted sense has utilization of two-three methods of liberation/precipitation of anomalies, at condition of variation of parameter of conversion. The work consuming assignment of initial data will be general/common for all calculations. Comparing the maps of the transformed anomalies, it will be possible to make more precise the outlines of the anomalies of different order and, consequently, the boundaries of geologic structures (Fig. 91). Table 15 gives recommendations regarding the application of different transformations depending on initial data.

§ 29. Diagrams of working out maps of anomalies with the application of computers and computers.

Conversions and recounts of anomalies of gravitational force require significant volume of calculations. For facilitation and accelerating this work both abroad and in the Soviet Union are conducted experiments in the application of the specialized computers and universal computers (Hear, 1955; Klushin, Nicol, 1959; Shalayev, 1961; Kogbetliantz, 1956). In all cases it is necessary to transfer the distribution of anomalous field from map/chart  $\Delta g$  into the diagram of input of initial data. For this purpose the map/chart of the anomalies of gravitational force is divided/marked off by the system of the lines, which generate quadratic grid with the distance between the nodes, usually equal to 1 cm. In certain cases is divided/marked

off the triangular grid (Fig. 92), which is more convenient during the replacement of circles by the system of points.

As follows from paragraphs examined above, overall diagram of calculations takes form

$$U(0, \lambda)_{\text{triangle}} = \int_0^{\infty} \bar{U}(\rho) P(\rho, \lambda) \rho d\rho, \quad (\text{IV}, 90)$$

where  $P(\rho, \lambda)$  - nucleus of conversion, which depends on parameter  $\lambda$ .

With quadratic grid with step/pitch of  $a$  can be accepted, for example, following system of radii, which sufficiently fully considers values of field at points, which surround central (Henderson, 1960):

$$\frac{0}{1}; \frac{a}{1}; \frac{a\sqrt{2}}{4}; \frac{2a}{3}; \frac{a\sqrt{5}}{8}; \frac{a\sqrt{8}}{8}; \frac{a\sqrt{13}}{8}; \frac{5a}{12};$$

$$\frac{a\sqrt{10}}{12}; \frac{a\sqrt{136}}{8}; \frac{a\sqrt{274}}{8}; \frac{25a}{12} \dots$$

Numerals in denominator indicates number of fiducial marks on a circle of given radius.

Page 190.

Integral (IV, 90) is represented in the form of sum of particular integrals

$$U(0, \lambda)_{\text{triangle}} = \sum_{i=0}^{\infty} \int_{\rho_i}^{\rho_{i+1}} \bar{U}(\rho) P(\rho, \lambda) \rho d\rho \approx$$

$$\sim \sum_{i=0}^{\infty} \bar{U}(\bar{\rho}_i) \int_{\rho_i}^{\rho_{i+1}} P(\rho, \lambda) \rho d\rho \sim \sum_{i=0}^{\infty} \bar{U}(\bar{\rho}_i) k_i(\lambda), \quad (\text{IV}, 91)$$

where  $\bar{U}(\bar{\rho}_i)$  - average/mean value  $\bar{U}(\rho)$  in range from  $\rho_i$  to  $\rho_{i+1}$

$$k_i(\lambda) = \int_{q_i}^{q_{i+1}} P(q, \lambda) q dq. \quad (IV, 92)$$

Transformed anomaly is calculated with some discrete/digital values of parameter of conversion, usually multiple to step/pitch of grid

$$\lambda = ma; \quad m = 1, 2, 3, \dots, n.$$

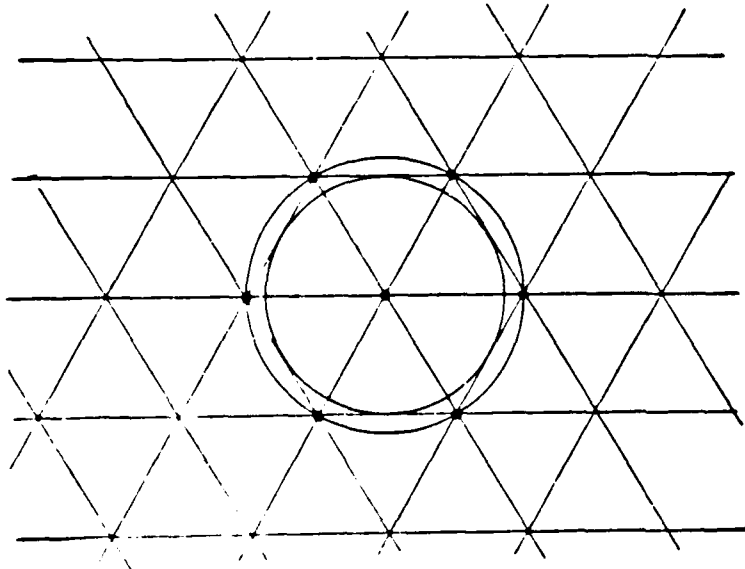


Fig. 92. Triangular grid of assignment of initial data.

Page 191.

Continuous function of parameter of conversion, and also continuous function of coordinates is calculated with the help of interpolated polynomials. Most frequently is used the interpolated polynomial of Lagrange - polynomial  $L(x)$  of degree  $n$ , which in  $n+1$  the given points

$$x_0, x_1, x_2, \dots, x_n$$

takes, respectively, the given values

$$y_0, y_1, y_2, \dots, y_n.$$

Polynomial  $L(x)$  is built with the help of expression

$$L(x) = \sum_{m=0}^n y_m \frac{(x-x_0) \dots (x-x_{m-1})(x-x_{m+1}) \dots (x-x_n)}{(x_1-x_0) \dots (x_m-x_{m-1})(x_m-x_{m+1}) \dots (x_m-x_n)} \quad (IV, 93)$$

With  $n=2$  we obtain

$$\begin{aligned}
 U(0, \lambda)_{\text{транс}} = & U(0, a)_{\text{транс}} \left[ \frac{1}{2} \cdot \frac{\lambda^3}{a^3} - \frac{5}{2} \cdot \frac{\lambda}{a} + 3 \right] + \\
 & + U(0, 2a)_{\text{транс}} \left[ -\frac{\lambda^3}{a^3} + 4 \frac{\lambda}{a} - 3 \right] + \\
 & + U(0, 3a)_{\text{транс}} \left[ \frac{1}{2} \cdot \frac{\lambda^3}{a^3} - \frac{3}{2} \cdot \frac{\lambda}{a} + 1 \right]. \quad (\text{IV}, 94)
 \end{aligned}$$

It is easy to ascertain that if  $\lambda=a$ , in the right side of the equality (IV, 94) remains only term  $U(0, a)_{\text{транс}}$ .

During calculations with the help of computers of anomaly value, taken/removed in network points, are transferred to punched card or punched tape. A special device with the passage of maps/charts with the openings sends electric signals into the machine. For each point the average value of anomaly on its surrounding rings (in effect it is located not average/mean value, but the sum of values at the  $n$  points, which lie on the ring) is calculated by machine. Multiplier  $1/n$  is joined with coefficient  $k_i$ . Average/mean values or sums on the rings are written/recorded on the magnetic tape and are transmitted to the memory of machine, just as the sequence of coefficients  $k_i$ , which correspond to this transformation.

Machine produces multiplication of sums by coefficients and issues result.

Attained accuracy of calculations can be illustrated by example (Fig. 93). The graphs of the gravity anomalies above the complex

theoretical model are here constructed. the anomalies, assigned at level  $z=0$ , are analytically continued into the lower half-space and are compared with the actual values. Calculation formula uses  $\bar{U}(0, \rho)$  with 10 values  $\rho$ . (Interpolated polynomial of Lagrange of the 5th order).

Page 192.

During estimation of possibilities of contemporary computers, which found use in the USSR, should be taken into account volume of their active or working storage. Thus, the disseminated machine "Ural", which belongs to the class of the small machines of universal designation/purpose, has core storage capacity 1024 number (Kitov, 1961). (External accumulator/storage of machine; that not directly connected with the arithmetic unit, it has with capacity 40000 numbers). The significant volume of working storage must be used for the memorization of routine and coefficients, which correspond to different conversions.

Electronic computer "Strela", which belongs to class of large machines, has doubly large working storage - 2048 numbers (Kitov, 1961). External accumulator/storage is calculated for 200000 numbers, which are written/recorded on the magnetic tape.

Speed of machine computation "Ural" composes 100 commands per second, in machine "Strela" - 2-3 thousand commands.



Together with universal calculators for working of maps/charts of anomalies narrowly specialized simulators are used. Such devices, which execute the limited circle of operations, have small clearance and small cost/value, only several times the exceeding cost/value of gravimeter.

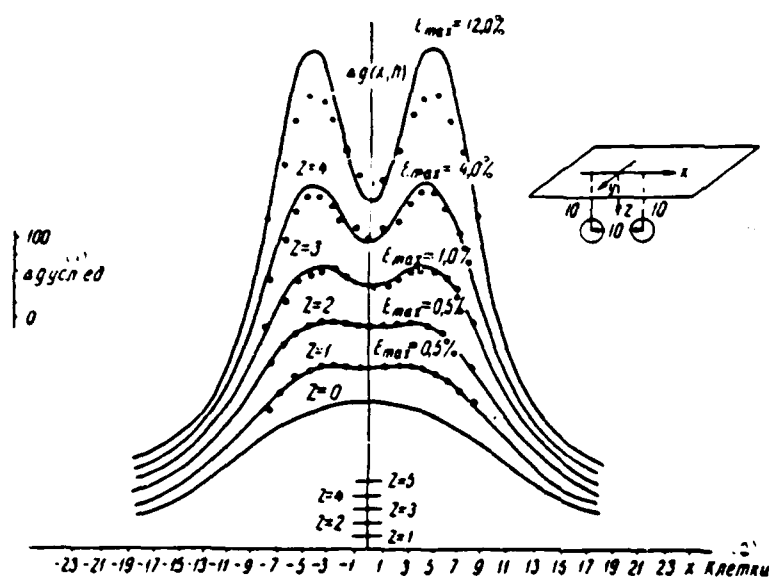


Fig. 93. Illustration of accuracy, attained during calculations with the help of electronic digital computer. According to Henderson (1960). Complex anomaly from two bodies analytically is continued into the lower half-space.

Key: (1).  $\Delta g$  conv. unit. (2). Cells.

Page 193.

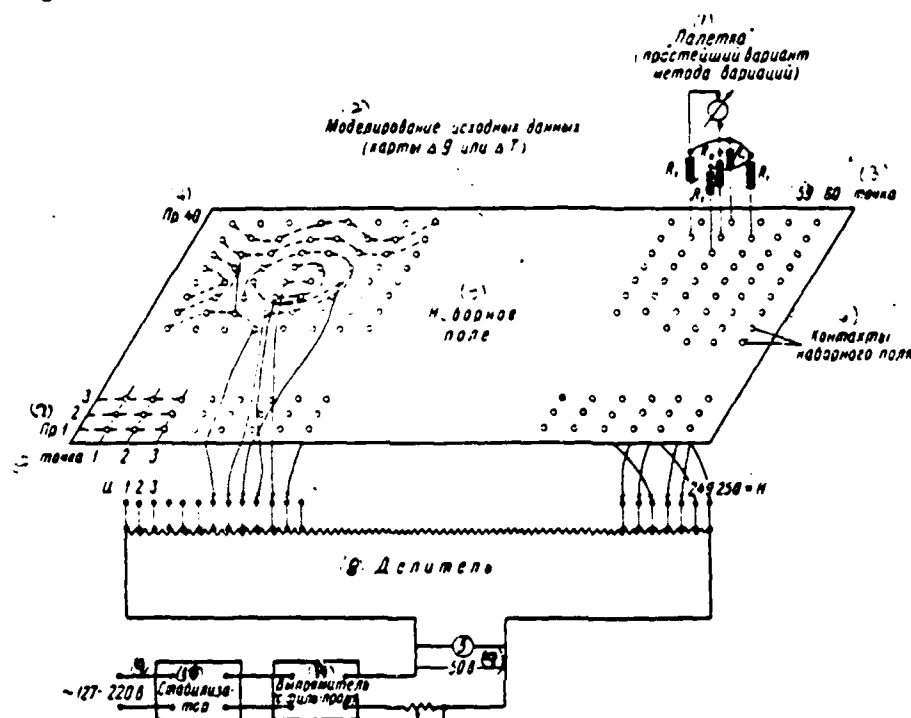


Fig. 94. Schematic diagram of computer for separation of anomalous fields. The assignment of initial data is realized from the common divisor. According to I. G. Klushin and Yu. I. Nikol'skiy (1959). Key: (1). "Template" (simplest version of the method of variations). (2). Modeling of initial data (map/chart  $\Delta g$  or  $\Delta T$ ). (3). point. (4). The rest 40. (5). setting field. (6). Contacts of setting field. (7). The rest 1. (8). Divider/denominator. (9). V. (10). Stabilizer. (11). Rectifier (with filter).

Page 194.

Distribution of anomalous field is modeled by distribution of electric potentials. Different practical methods of solution of this problem are possible: voltage is supplied immediately to entire set

of points from one common divisor of stress/voltage (Fig. 94), or independent dividers/denominators are connected to the series of those points, which participate at the present moment/torque in calculations (Fig. 95). The dynamic range of similar devices, depending on type, is from 200 to 500. If we take the latter number, then in the case of changes  $\Delta g$  within the limits from 0 to 50 mgal of anomaly they can be assigned with the accuracy 0.1 mgl.

A constant component of anomalous field with all of conversion either remains invariable or completely it is eliminated; therefore it is possible to preliminarily take into account it, after rounding off to ten milligals in order to ensure more detailed assignment to variable component.

System of rings of template with nodes or fiducial marks is substituted by system of electrical resistance and contacts. The electric current, recorded by accurate microammeter, is determined by the equality

$$I = \sum_{i=1}^n I_i(q_i) k_i \quad (IV.95)$$

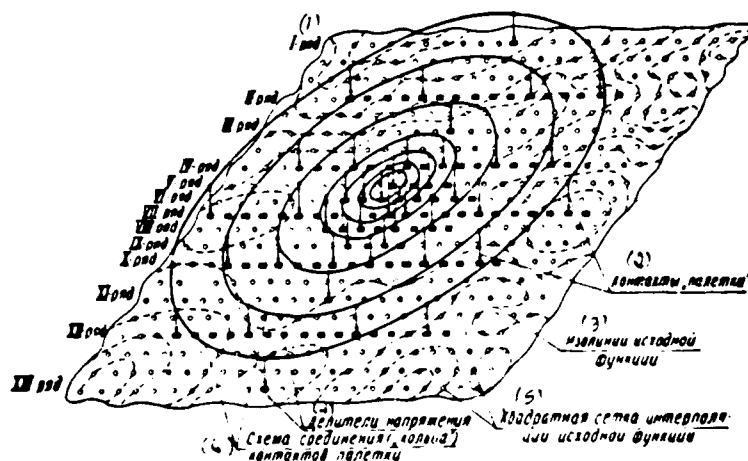


Fig. 95. Schematic diagram of assignment of initial data with autonomous dividers. According to Yu. I. Nikol'skiy (1960).  
Key: (1). series/number. (2). Contacts of "template". (3). Isolines of original function. (4). Voltage dividers. (5). Quadratic grid of interpolation of original function. (6). Diagram of averaging ("Kol'tsa") of contacts of template.

Page 195.

As we see, this equality in perfect analogy with equality (IV, 91), if we place in it:  $V(0,1)$  - potential of point relative to zero;  $k_1$  - conductivity;  $\bar{I}(0, \lambda)_{\text{трансф}}$  - recorded current.

Fig. 96, 97 show appearance and electric circuit of device, developed by Yu. I. Nikol'skiy et al. and prepared by OKB [Special Design Office] of Geolkom of USSR and plant "Geologorazvedka" for All-Union Scientific Research Geological Institute (VSEGEI). Device executes transformations of the type of averaging, recount to the

height, localizations according to the method of variations, etc. There is a universal template with the variable coefficients, which can be used for executing such operations as the calculation of anomalies in the case of three-dimensional bodies, etc.

Practical expenditures of time for conversions and recounts of anomalies are reduced 5-10 times. The application of simulator makes it possible to build the different maps/charts of the transformed anomalies for the vast geologic regions.

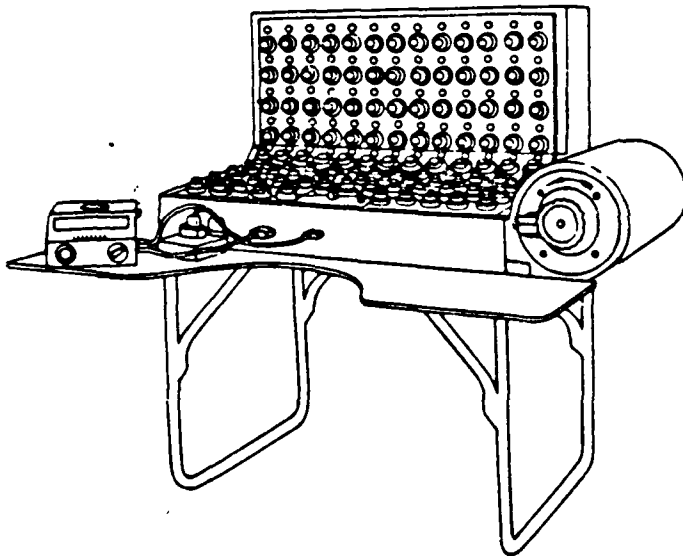


Fig. 96. General view of computer, prepared by OKB of Geolkom of USSR for VSEGEI.

Page 196.

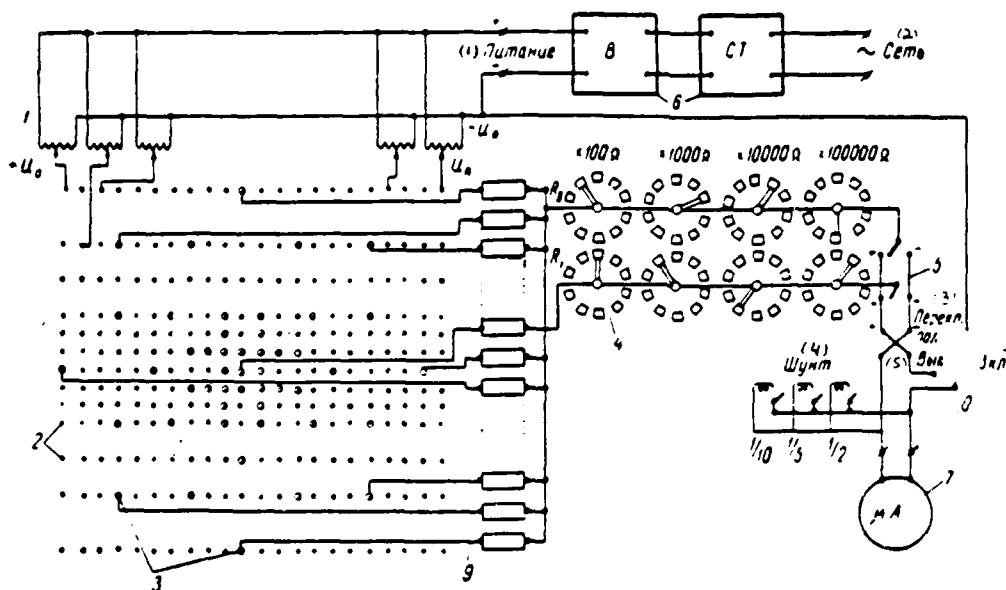


Fig. 97. Electric circuit of computer, depicted in Fig. 96.

According to Yu. I. Nikol'skiy (1960). 1 - voltage divider; 2 - contacts of setting field; 3 - contacts of template; 4 - resistance box (the "coefficient of the knot of template"); 5 - change-over switch; 6 - power supply unit, which includes rectifier B and stabilizer CT; 7 - recording instrument.

Key: (1). Power feed. (2). Network. (3). Polar switch. (4). Shunt. (5). Off. (6). On.



Page 197.

S30. Analysis of transformations on the basis of Fourier integral.

In the case of bivariate distribution of field convenient apparatus for analysis of transformations represents integral of Fourier

$$U(x) = \frac{1}{2\pi} \int_{-\infty}^{+\infty} e^{i\alpha x} d\alpha \int_{-\infty}^{+\infty} U(S) e^{-i\alpha S} dS. \quad (\text{IV, 96})$$

Integral formula (IV, 96) expresses nonperiodic function in the form of infinite sum of harmonic functions. At first glance can seem by strange, why occur physical field relatively invariable in the time (depending only on the geologic scales) in the form of the sum of alternating sign harmonic functions. But the fact is that we examine not fluctuations in the time, but change along the line of profile. In this case the oscillations/vibrations of anomaly make completely real sense.

Basic convenience in utilization of integral formula (IV, 96) consists in the fact that it makes it possible to examine different transformations from point of view of filter theory. This opens/discloses completely real ways for the automation of calculations. Converting the curve  $U(x)$  into the electric signal  $U(t)$ , i.e., by substituting graphic scale with time scale, it is possible with the help of the collection of the filters, which play

the role of usual templates, to obtain the graphs of the transformed anomalies (as they obtain, for example, well curves with different probes). Investigations in this direction are carried out by K. V. Gladkiy (1960).

It is possible to indicate one more aspect, which imparts to utilization of Fourier's integral physical sense for decomposition of anomalies. Any anomaly  $\Delta g$  can be considered as the thickening track of motions and caused by the latter real changes, which were being developed in this section of the Earth during the entire geologic history and in particular in those stages, when observed mass distribution stored/added up. With the tectonic motions the downwarps/troughs and the uplifts/rises of deep interfaces of the earth's crust, which are structural boundaries, are directly connected. Almost in the same measure this relates to structural-erosion surface of crystalline basement, and thereby - to the total power of sedimentary cover.

Indirectly tectonic motions determine lithologic composition of sedimentary formations, manifestation of magmatism, etc.

Separating on maps/charts of gravity anomalies vast maximums and minima, it is possible to consider latter/last as sections, which are characterized by general/common directionality of tectonic oscillating processes.

The practice of geologic interpretation confirms this, such anomalies, connected with the large/coarse anticlinal structures of Central Asia (Mangyshlak, Bol'shoy Balkhan, Tuarkyr, etc.), Russian platform (Pilyuginsko-Buzuluksiy, Balakovskiy, etc. anticlines), Siberia, etc. As an example is presented anticline geolog-geophysical section/cut along r. Yenisey (Fig. 98), constructed by D. B. Tal'virskiy and Ye. M. Khakhalev.

In whole series of cases sign of regional anomalies and sign of tectonic motions, which were being developed in this territory during latter/last stages of geologic history, can not coincide. Thus, for example, in the limits of the geosynclinal regions of the zone of negative gravity anomalies on the location usually correspond to deepest downwarps/troughs, and the zones of positive anomalies - to sections of the most significant uplifts/rises of pre-inversion cycle (Andreyev, 1960).

In this sense the expansion into components, analysis of gravitational field can have the same value for analysis of tectonic motions as gravimetric method as a whole for studying tectonics.

If formula of transformation, realized with the help of template, takes form

$$U(x)_{\text{transform}} = k_0 U(x) + \sum_{i=1}^n k_i [U(x + R_i) - U(x - R_i)], \quad (IV, 67)$$

characteristic of transformation depends on coefficients  $k_i$  and position of fiducial marks  $x \pm R_i$  relative to central point  $x$  as follows:

$$\Psi(\alpha) = k_0 + 2 \sum_{i=1}^n k_i \cos \alpha R_i. \quad (IV, 98)$$

Actually,

$$\begin{aligned} U(x+R) + U(x-R) &= \frac{1}{2\pi} \int_{-\infty}^{+\infty} (e^{i\alpha(x+R)} + e^{i\alpha(x-R)}) d\alpha \times \\ &\times \int_{-\infty}^{+\infty} U(S) e^{-i\alpha S} dS, \\ e^{i\alpha(x+R)} + e^{i\alpha(x-R)} &= e^{i\alpha x} [e^{i\alpha R} + e^{-i\alpha R}]. \end{aligned}$$

Taking into account that

$$e^{i\alpha R} = \cos \alpha R + i \sin \alpha R, \quad e^{-i\alpha R} = \cos \alpha R - i \sin \alpha R, \quad (IV, 99)$$

we find

$$\begin{aligned} &U(x+R) + U(x-R) \\ &= \frac{1}{2\pi} \int_{-\infty}^{+\infty} e^{i\alpha x} 2 \cos \alpha R d\alpha \int_{-\infty}^{+\infty} U(S) e^{-i\alpha S} dS. \quad (IV, 100) \end{aligned}$$

Page 199.

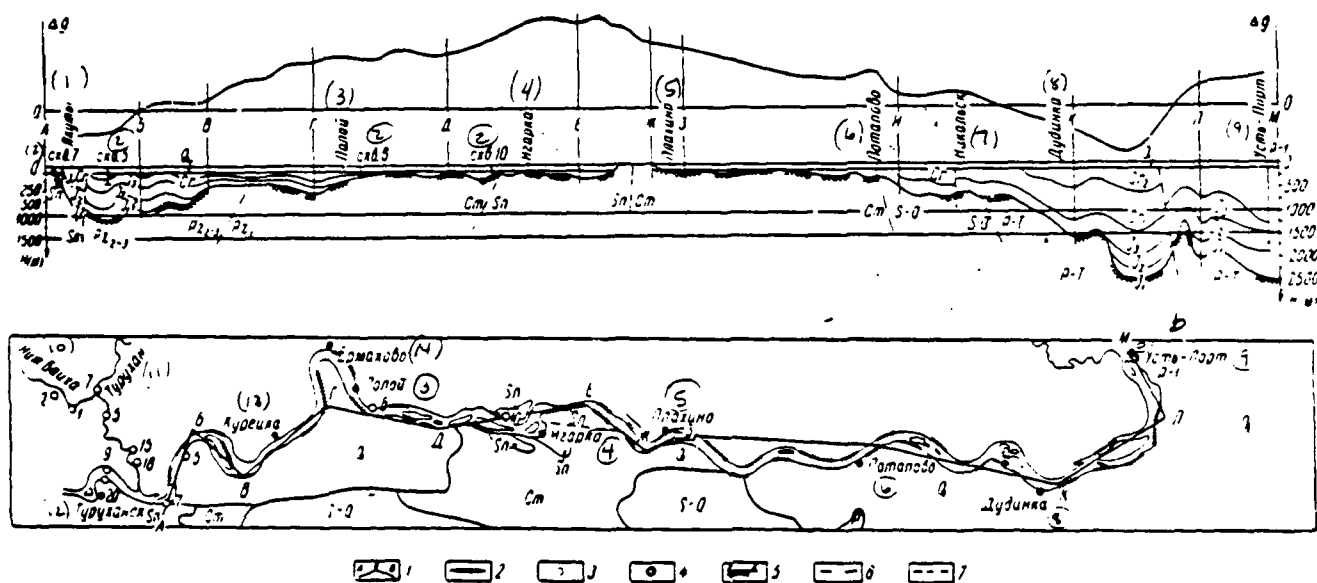


Fig. 98. Geological-geophysical section/cut along r. Yenisey, which illustrates conformity of regional anomalies and regional structures. According to D. B. Tal'virskiy and Ye. M. Khakhalev (1961). 1 - line of compound section/cut; 2 - seismic profiles (soundings KMPV [- correlation method of refracted waves]); 3 - structural-prospecting blowholes (on the plan/layout); 4 - deep blowhole (on the plan/layout); 5 - surface of the pre-Jurassic basement: a) according to the data of seismic survey and drilling, b) predicted; 6 - predicted boundaries within the Paleozoic complex of rocks; 7 - disjunctive disturbances/breakdowns.

Key: (1). Yakuts. (2). Hole. (3). Hollow. (4). Igarka. (5). Plakhinc. (6). Lotapovo. (7). Nikol'sk. (8). Dudinka. (9). Ust'-Port. (10). Lower Baikha. (11). Turukhan. (12). Turukhansk. (13). Kureyka. (14). Yermakovo.

Page 200.

Hence, taking into account equality (IV, 96), we obtain formula (IV, 98).

From theory of spectra (Charkevich, 1954) it is known that spectrum of transformed function  $S_{\text{транс}}(\alpha)$  is equal to product of spectrum of original function  $S(\alpha)$  to characteristic of transformation  $\Psi(\alpha)$

$$S_{\text{транс}}(\alpha) = S(\alpha) \Psi(\alpha). \quad (\text{IV, 101})$$

In general case spectra  $S_{\text{transform}}(\alpha)$  and  $S(\alpha)$  are complex. Function  $\Psi(\alpha)$ , that describes the transformations of form (IV, 97), is real and acts only on the amplitudes of separate components, but not on their phases. Analytical expression  $\Psi(\alpha)$  for some transformations is indicated in Table 16.

During correlation of anomalies of gravitational force with data of other geophysical methods can arise need for transformations with complex characteristic  $\Psi(\alpha)$ . Such transformations are the more general case in comparison with those particular versions, which extensively are used in practice. Let us clarify this, changing from the simple to the more complex case.

Seismic profile of considerable range (many tens or first hundreds of kilometers) intersects area of gravimetric survey. Comparing changes in the anomaly of gravitational force with the relief of the surface of the reference seismic horizon/level, we are convinced that between them there is an approximate dependence of the form

$$\Delta g(x_1) - \Delta g(x_2) \sim 2\pi f \Delta \sigma [z(x_1) - z(x_2)], \quad (\text{IV, 100})$$

where  $\Delta g(x)$  - anomaly value at point  $x$ ;

$x_1, x_2$  - points of profile, sufficiently distant from each other;

$f$  - gravitational constant;

$\Delta \sigma$  - excess density;

$z(x)$  - depth of the bedding of the reference horizon/level.

Table 16. Values of functions  $\Psi(\alpha)$  during different transformations.

(1) Преобразования	$\Psi(\alpha)$
(2) Осреднение на интервале $2R$	$\frac{\sin \alpha R}{\alpha R}$
(3) Пересчет на высоту $h$	$e^{-\alpha h}$
(4) Вычисление $k$ -й вертикальной производной	$\alpha^k$

Key: (1). Transformations. (2). Averaging in interval  $2R$ . (3). Recount to height  $h$ . (4). Calculation of  $k$  vertical derivative.

Page 201.

This dependence can be used for study according to gravimetric data of part of territory, which directly adjoins profile.

Putting to use established/installed bond, we will transform map/chart  $\Delta g$  into map/chart of surface of geologic horizon/level. The characteristic of transformation follows from the equality (IV, 102)

$$\Psi(\alpha) = k \cdot \text{const.} \quad (\text{IV, 102})$$

where  $k = -2\pi f \Delta \sigma$  (minus sign indicates that an increase in the depth is accompanied by the decrease of anomaly).



Models of all components, independent of frequency, are multiplied to constant coefficient, phases of oscillations of anomaly and excesses of relief of surface of reference horizon/level completely coincide, for example, maximum of anomaly corresponds to maximum uplift of horizon/level.

Similar bond is very idealized, although virtually it can have important value, even if it is satisfied in rough approximation and in limited intervals.

In certain cases it is possible to establish/install formal conformity of anomalies  $\Delta g$  to behavior of one of interfaces of density with factual effect on anomalous field of several approximately agreeing boundaries. It is obvious that the excess density, entering coefficient  $k$  of equality (IV, 103), will differ from a real difference in the density by the studied boundary. (The numerical ratios, which relate to this case, are in more detail examined in 548). However, this does not change the general character of bond.

Extrapolation of data of seismic survey, obtained along profile, to adjacent area can be done with the help of map/chart of anomalies of gravitational force, even in such a case, when sharp conformity to curve  $\Delta g$  and relief of studied boundary is absent. Actually this means that the effect of boundary is covered with the effect of other factors. Task is formulated as follows: how must be transformation, i.e., what form take frequency and phase responses, in order to

approximately transform the curve  $\Delta g$  into relief curve of the surface of the studied boundary.

Representing curve  $\Delta g$  along profile in the form

$$\Delta g(x) = \frac{1}{2\pi} \int_{-\infty}^{+\infty} e^{i\alpha x} S_g(\alpha) d\alpha, \quad (\text{IV, 104})$$

where

$$S_g(\alpha) = \int_{-\infty}^{+\infty} \Delta g(t) e^{-i\alpha t} dt, \quad (\text{IV, 105})$$

and analogously curve of relief of surface of boundary

$$z(x) = \frac{1}{2\pi} \int_{-\infty}^{+\infty} e^{i\alpha x} S_z(\alpha) d\alpha, \quad (\text{IV, 106})$$

we find

$$S_z(\alpha) = S_g(\alpha) \Psi(\alpha), \quad (\text{IV, 107})$$

$$\Psi(\alpha) = \frac{S_z(\alpha)}{S_g(\alpha)} = A(\alpha) + iB(\alpha) = |\Psi(\alpha)| e^{i\varphi(\alpha)}, \quad (\text{IV, 108})$$

Modulus/module of characteristic of transformation (strictly frequency characteristic of transformation) is determined by equality

$$|\Psi(\alpha)| = \sqrt{A^2(\alpha) + B^2(\alpha)}. \quad (\text{IV, 109})$$

Page 202.

Argument (phase response of transformation) is found by formula

$$\varphi(\alpha) = \arctg \frac{B(\alpha)}{A(\alpha)}. \quad (\text{IV, 110})$$

Hence

$$z(x) = \frac{1}{2\pi} \int_{-\infty}^{+\infty} e^{i\alpha x} [A(\alpha) + iB(\alpha)] S_R(\alpha) d\alpha. \quad (\text{IV, 111})$$

For calculations of integrals (IV, 105) and (IV, 111), i.e., for analysis and synthesis of curves, can be used general/common means of harmonic analysis, including tables, described in work of F. M. Holzman and T. B. Kalinina (1958).

It is natural that characteristic  $\psi(\alpha)$  determined experimentally makes statistical sense and only under conditions, uniform with those that are established/installed by seismic profile. Its utilization is lawfull to the same degree and with the same limitations as constant coefficients in the empirical bonds, for example, between the velocity of propagation of elastic waves and the density for some types of species.

Similar approach to interpretation was developed and used by I. S. Vol'vovskiy, V. Z. Ryabyy and V. I. Shraybman for interpretation of gravitational field in Bukharo-Khivin oil and gas-bearing province on basis of materials of deep seismic soundings.

§31. Separation of anomalies at the interference level.

One of basic criteria of perfection of each geophysical method of prospecting is its resolution, i.e., capacity to isolate against the background of common picture these or other parts, which can be used

for solution of geologic problems.

Utilized at present geophysical equipment does not always possess necessary accuracy, which is serious obstacle during solution of many problems of ore and structural geophysics. However, a straight/direct increase in the accuracy of measurements compulsorily does not lead to the desired results, since in this case ever more obvious becomes the role of the interference of geologic origin, not visible in the rough measurements. The anomalies of high order, caused by a nonuniform distribution of the physical properties of the rocks of identical petrographic characteristic, are frequently these interferences.

Accuracy of geophysical works can be increased due to strict account of correlation of interference and their subsequent filtration.

Separation of anomalies at interference level is analogous with separation of signal, strongly distorted by noise. Latter/last task obtained the being all-inclusive solution in information theory (Goldman, 1957). Questions of the mathematical processing of the results of geophysical observations are examined in the series/number of the works, among which should be noted the especially important work of L. A. Khalfin (1958).

Page 203.

Some gravimetric analysts (Malovichko, 1961) made the attempts to

demonstrate the strictly substantiated in the contiguous regions of scientific knowledge positions with the help of the specially selected examples.

Taking into account important and ever increasing role of information theory and great interest in its conclusions/derivations, we consider it necessary at least in short form to present positions of linear minimal-quadratic theory of leveling, developed in classical works of A. N. Kolmogorov (1941), N. Wiener (1949), K. Shannon and G. Bode (1950).

Basic question is formulated as follows. The results of measurements along the profile represent the sum of anomaly  $A(x)$  and its complicating interference  $a(x)$

$$U(x) = A(x) + a(x). \quad (IV, 112)$$

It is desirable so to treat  $U(x)$  in order to obtain anomaly  $A(x)$ , maximally "purified" from interference.

Theory is based on following positions:

- 1) distribution of anomalies and interference in limits of profile is statistically uniform;
- 2) filtration of interference is realized in such a way as to ensure smallest possible under given conditions for photographing standard deviation of true and chosen anomalies.

Thus, function  $a(x)$  is distribution of technical and geologic interference on profile with length  $L$ . The length of profile must be sufficiently large so that the average/mean value  $\bar{a}$  would be equal to zero. Therefore subsequently by  $\bar{a}^2$  we will understand the average/mean value of the square of interference, which is obtained in the limit

$$\bar{a}^2 = \lim_{L \rightarrow \infty} \frac{1}{L} \int_{-\frac{L}{2}}^{+\frac{L}{2}} a^2(x) dx. \quad (IV, 113)$$

For calculations it is necessary to know not only interference level, but also their correlation, i.e., correlation coefficient as function of displacement -  $R_H(\tau)$ .

Page 204.

According to Khinchin-Wiener equality

$$\bar{a}^2 R_H(\tau) = \int_0^{\infty} G(\alpha) \cos \alpha \tau d\alpha. \quad (IV, 114)$$

$$G(\alpha) = \frac{2}{\pi} \int_0^{\infty} \bar{a}^2 R_H(\tau) \cos \alpha \tau d\tau. \quad (IV, 115)$$

where  $G(\alpha)$  - "energy" interference spectrum  $\bar{a}^2$ , which shows value of its separate components

$$\bar{a}^2 = \int_0^{\infty} G(\alpha) d\alpha. \quad (IV, 116)$$

Total value  $\bar{a}^2$  is obtained by integration for all components.

After processing/treatment the annoyance value is decreased and it will comprise

$$\int_0^{\infty} G(\alpha) |\Psi(\alpha)|^2 d\alpha. \quad (IV, 117)$$

where  $\Psi(\alpha)$  - characteristic of unknown transformation.

Transformation will introduce specific distortions, also, into anomaly  $A(x)$ . The error, caused by the filtration of anomaly in the process of processing/treatment, let us find from the equality (IV, 118)

$$\int_0^{\infty} |1 - \Psi(\alpha)|^2 \Phi(\alpha) d\alpha. \quad (IV, 118)$$

where  $\Phi(\alpha)$  - the "energy" spectrum  $\bar{A}$ .

Accumulated error after transformation of curve  $U(x)$  will be represented in the form

$$\int_0^{\infty} [G(\alpha) |\Psi(\alpha)|^2 + \Phi(\alpha) |1 - \Psi(\alpha)|^2] d\alpha. \quad (IV, 119)$$

Characteristic of transformation  $\Psi(\alpha)$  must ensure minimum of integral (IV, 119).

Determination  $\Psi(\alpha)$  is facilitated by the fact that perfecting geophysical observations begins at moment, when field observations are completed. There is curve  $U(x) = A(x) + a(x)$  along entire profile  $L(L \rightarrow \infty)$ .

Requirement  $L^{-\infty}$  means that both to the right, and to the left of the point, where is calculated the "purified" from the interference value of anomaly, must be placed the sufficiently large section of profile. Since the anomalies and interference enter into equality (IV, 119) in the form of the "energy" spectra, which consider only the amplitudes of components, but not their phase, characteristic  $\Psi(\alpha)$  in this case must be real function.

Let us designate for brevity  $\Psi(\alpha) = \Psi$ ,  $\Phi(\alpha) = \Phi$ ,  $G(\alpha) = G$ . Supplementing and subtracting under the integral sign in the formula (IV, 119) value  $\frac{\Phi^2}{\Phi+G}$ , we will obtain

$$\int_0^{\infty} \left[ G |\Psi|^2 + \Phi |1 - \Psi|^2 + \frac{\Phi^2}{\Phi+G} - \frac{\Phi^2}{\Phi+G} \right] d\alpha =$$

$$= \int_0^{\infty} \left( \left[ \Psi + \frac{\Phi}{\Phi+G} - \frac{\Phi}{\Phi+G} \right]^2 + \frac{\Phi G}{\Phi+G} \right) d\alpha. \quad (\text{IV, 120})$$

Page 205.

Term in bracket is square of real number; therefore it is positive or equal to zero. For the decrease (IV, 120) it should be made equal to zero

$$\Psi + \frac{\Phi}{\Phi+G} - \frac{\Phi}{\Phi+G} = 0.$$

Hence

$$\Psi(\alpha) = \frac{\Phi(\alpha)}{\Phi(\alpha) + G(\alpha)}. \quad (\text{IV, 121})$$

It is known that

$$U(x) = \frac{1}{2\pi} \int_0^{\infty} e^{i\alpha x} d\alpha \int_{-\infty}^{\infty} U(t) e^{-i\alpha t} dt.$$



After the processing/treatment

$$[U(x)]_{\text{транс}} = \frac{1}{2\pi} \int_{-\infty}^{+\infty} e^{i\alpha x} \Psi(\alpha) d\alpha \int_{-\infty}^{+\infty} U(t) e^{-i\alpha t} dt. \quad (\text{IV, 122})$$

Usually function  $\Psi(\alpha)$  is such, which ensures uniform convergence of integral (IV, 123)

$$\int_0^{\infty} \Psi(\alpha) d(\alpha). \quad \cdot (\text{IV, 123})$$

This makes it possible to change order of integration in right side of equality (IV, 122)

$$[U(x)]_{\text{транс}} = \frac{1}{2\pi} \int_{-\infty}^{+\infty} U(t) k(x-t) dt, \quad (\text{IV, 124})$$

where

$$\begin{aligned} k(x-t) &= \int_{-\infty}^{+\infty} e^{i\alpha(x-t)} \frac{\Phi(\alpha)}{\Phi(\alpha) + G(\alpha)} d\alpha = \\ &= 2 \int_0^{\infty} \cos \alpha(x-t) \frac{\Phi(\alpha)}{\Phi(\alpha) + G(\alpha)} d\alpha. \end{aligned} \quad (\text{IV, 125})$$

Application of formula (IV, 124) is illustrated by example (Fig. 99). Distribution of anomalies is complicated by interference, moreover level of anomalies and interference is identical

$$\bar{A}^2 = \bar{a}^2.$$

Anomalies are correlated at a distance, 5 times greater than

interference:  $r_A = 5$ ;  $r_a = 1$ . Assuming that

$$R_B(\tau) = \exp\left(-\frac{\tau^2}{r^2}\right).$$

let us find, following equalities (IV, 114), and (IV, 115),

$$\Phi(\alpha) = \bar{A}^2 r_A \frac{1}{\sqrt{\pi}} \exp\left(-\frac{\alpha^2 r_A^2}{4}\right). \quad (\text{IV, 126})$$

$$G(\alpha) = \bar{a}^2 r_a \frac{1}{\sqrt{\pi}} \exp\left(-\frac{\alpha^2 r_a^2}{4}\right). \quad (\text{IV, 127})$$

Page 206.

Characteristic of optimal transformation for filtering interference will take form

$$\begin{aligned} \Psi(\alpha) &= \frac{\Phi(\alpha)}{\Phi(\alpha) + G(\alpha)} = \frac{1}{1 + \frac{G(\alpha)}{\Phi(\alpha)}} = \frac{1}{1 + \frac{1}{5} \exp\left(-\frac{\alpha^2 \cdot 1}{4} - \frac{\alpha^2 \cdot 25}{4}\right)} \\ &= \frac{1}{1 + \frac{1}{5} \exp(6\alpha^2)}. \end{aligned} \quad (\text{IV, 128})$$

$$[U(x)]_{\text{trap}} = \frac{1}{2\pi} \int_{-\infty}^{+\infty} U(t) k(x-t) dt, \quad (\text{IV, 124})$$

where

$$k(x-t) = 2 \int_0^{\infty} \frac{\cos(\alpha(x-t))}{1 + \frac{1}{5} \exp(6\alpha^2)} d\alpha \quad (\text{IV, 129})$$

After determining  $k(x-t)$  according to formulas of numerical integration and after using trapezoid rule for calculating integral (IV, 124), after some transformations we will obtain approximation working formula

$$[U(x)]_{\text{транс}} \approx \frac{1}{\pi} \int_{-\infty}^{+\infty} U(t) \left[ 0.293 \frac{\sin 0.8(x-t)}{0.8(x-t)} + 0.172 \frac{\sin 0.4(x-t)}{0.4(x-t)} \right] dt,$$

$$[U(n)]_{\text{транс}} \approx 0.148 U(n) + 0.136 [U(n+1) + U(n-1)] +$$

$$+ 0.107 [U(n+2) + U(n-2)] + 0.060 [U(n+3) + U(n-3)] +$$

$$+ 0.033 [U(n+4) + U(n-4)] + \dots, \quad (\text{IV. 130})$$

where  $n$  - ordinal number of point of profile.

Results of processing of curve  $U(x)$  are also shown in Fig. 99.

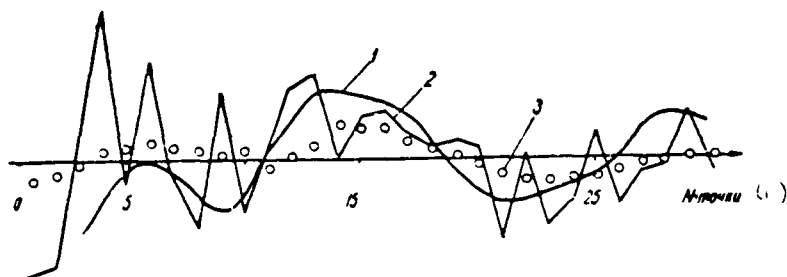


Fig. 99. Example, which elucidates application of theory of minimal-quadratic leveling (filtration of interference). 1 - specified distribution of anomalies; 2 - distribution of anomalies, complicated by interference; 3 - distribution of anomalies, "purified" of interference.

Key: (1). N-points.

Page 207.

Methods of processing materials of geophysical observations, based on correlation of observed and expected distribution of anomalies, deserve serious attention. We will consider as before that

$$r = A(x) + a(x),$$

where  $A(x-x_0)$  - expected distribution of anomaly; point  $x_0$  is the coordinate of the epicenter of anomaly, which should be determined.

Let us compute integral

$$\lim_{L \rightarrow \infty} \int_{-\frac{L}{2}}^{+\frac{L}{2}} U(x) A(x-x_0+\tau) dx = \lim_{L \rightarrow \infty} \int_{-\frac{L}{2}}^{+\frac{L}{2}} A(x) \times A(x-x_0+\tau) dx + \lim_{L \rightarrow \infty} \int_{-\frac{L}{2}}^{+\frac{L}{2}} a(x) A(x-x_0+\tau) dx. \quad (IV.131)$$

If distributions of anomaly  $A(x)$  and interference  $a(x)$  are independent, second integral in right side of equality (IV. 131) will be close to zero. The integral

$$\int_{-\frac{l}{2}}^{+\frac{l}{2}} A(x) A(x - x_0 + \tau) dx \quad (IV. 132)$$

attains maximum value during displacement  $\tau = x_0$ .

Virtually calculations are reduced to determination of sums of form

$$\left. \begin{aligned} \sum_{n=1}^k U(n) A(n), \\ \sum_{n=1}^k U(n) A(n+1), \\ \sum_{n=1}^k U(n) A(n+2), \end{aligned} \right\} \quad (IV. 133)$$

where 1, 2, 3, ..., k - points of profile.

Expected anomaly  $A(x)$  is shifted each time to one step/pitch and the process of correlation, comparison again is repeated. The application of this method (the "method of reverse probability") is in detail presented in the work of A. G. Tarkhov and A. A. Sidorov (1960). Fig. 100, 101 give the examples of its application on the theoretical model and the practical materials.

Let us note that task of separation of anomalies at interference level is closely related also to task of levelling or smoothing of observed values. Latter/last operations have long since been used in the statistic studies. The essence of leveling consists in the approximation of the observed values of anomaly, which correspond to the equidistant points of profile, by the polynomial of the form

$$U(x) = a + bx + cx^2 + \dots + kx^n.$$

Approximation is most extensively used by polynomial of second power. In this case, depending on a number of points, which participate in the leveling, can be used the following formulas (Whittaker and Robinson, 1935):

$$\begin{aligned} [U(n)]_{\text{transf}} &= \frac{17}{35} U(n) + \frac{12}{35} [U(n+1) + U(n-1)] - \\ &- \frac{3}{35} [U(n+2) + U(n-2)], \quad (\text{IV}, 134) \end{aligned}$$

$$\begin{aligned} [U(n)]_{\text{transf}} &= \frac{1}{3} U(n) + \frac{6}{21} [U(n+1) + U(n-1)] + \\ &+ \frac{1}{7} [U(n+2) + U(n-2)] - \frac{2}{21} [U(n+3) + U(n-3)], \quad (\text{IV}, 135) \end{aligned}$$

$$\begin{aligned} [U(n)]_{\text{transf}} &= \frac{59}{231} U(n) + \frac{54}{231} [U(n+1) + U(n-1)] + \\ &+ \frac{39}{231} [U(n+2) + U(n-2)] + \frac{14}{231} [U(n+3) + U(n-3)] - \\ &- \frac{21}{231} [U(n+4) + U(n-4)], \quad (\text{IV}, 136) \end{aligned}$$

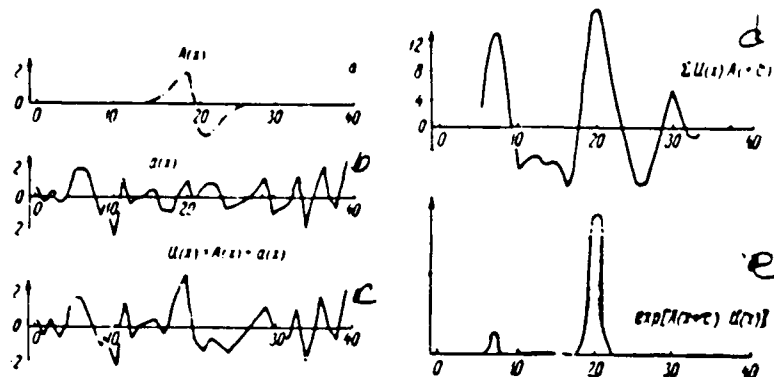


Fig. 100. Theoretical example, which illustrates application of method of "reverse probability". According to A. G. Tarkhov and A. A. Sidorov (1960). a) theoretical signal; b) the distribution of interference; c) the sum of signal and interference; d) the function, which characterizes the correlation of theoretical signal and observed curve, complicated by interference; e) the curve of function  $\exp[\lambda(x-c) U(x)]$

Page 209.

The greater the number of points is drawn in for obtaining smoothed value of anomaly at central point, the greater correlation we assume in anomaly being isolated.

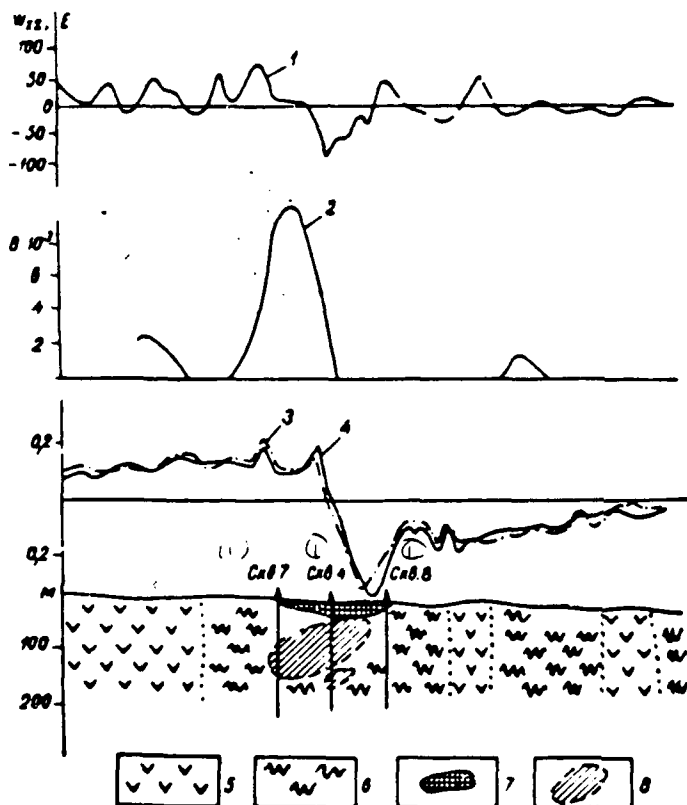


Fig. 101. Practical example of application of method of "reverse probability". (One of the central Kazakhstan deposits, the materials of A. K. Auzin, 1961). 1 - observed curve; 2 - function of the correlation of theoretical curve (curve "a" Fig. 100) and observed (are constructed only positive values); 3 - curve of potential gradient with the charge of body in hole 4; 4 - the same, in hole 7; 5 - porphyrite; 6 - secondary quartzite; 7 - iron cap; 8 - ore body. Key: (1). Hole.



For facilitating calculations according to formulas (IV, 134-136) can be constructed templates with scales, which consider values of coefficients before brackets.

§32. The "anisotropic" transformations of anomalies with the separation of linear tectonic dislocations.

All transformations examined above of anomalies for purpose of separation of regional and local components or for purpose of filtration of interference are based on differences on correlation. The average/mean value of the square of anomaly and the radius of autocorrelation (or autocorrelation function itself) = the basic parameters, which we used in all calculations. The radius of autocorrelation was considered as a number, but not as a vector.

Together with "isotropic" transformations (such transformations actually were only and examined until recently in geophysical literature) important practical application can have "anisotropic" transformations, i.e., such transformations, which have different sensitivity to anomalies, which are correlated in this or another direction. First of all "anisotropic" transformations can be used in such cases, when against the background of the variegated picture of the physical field being investigated, which reflects the local heterogeneities of geologic section/cut, it is necessary to isolate the relatively narrow linear zones, caused by the deep dislocations (Klushin, Tolstikhin, 1961). These zones can have the most different,

previously unknown courses/strikes. Their objective separation using the geophysical materials is of special interest, since they are the reflection of tectonic disturbances/breakdowns of the type of faults, to which are coordinated frequently the deposits of useful minerals.

As usual, before working of map/chart of physical field (or structural relief) it is necessary to visualize probable bonds of observed changes in anomalies with that part of information, which we wish to isolate. In particular, the edge dislocations, whose effects interest us, are characterized by the following signs:

1) by considerable range, several times exceeding cross sizes/dimensions;

2) by the unknown, but invariable within the limits of the limited sections course/strike.

Radius of autocorrelation of anomalies, connected with edge dislocations, is sharply anisotropic value. It is sufficiently great on the course/strike and is small transverse to course/strike.

Page 211.

Relative to background of interference, which shades picture interesting us, it is possible to make assumption that it contains components with different correlation, radius of autocorrelation not depending on direction. This can be the sharp anomalies, which generate complex "mosaic" design, and the smooth changes in the fields, which have different courses/strikes.

For exception/elimination of sharply variable, "mosaic" component of anomalous field transformation must have character of averaging or recount to height. For the emphasis of field variations in the zones of dislocations the transformation must have a character of differentiation. The simultaneous execution of these operations is realized with the help of the template, depicted in Fig. 102. Template has a form of the elongated rectangle, divided into four strips. In its center the dividing dial through  $45^\circ$  is replaced. The center of template is combined with the calculation point on the map/chart. Thus, on each point template is set in four positions. The rotation of template is equivalent to the change in the direction, in which is ensured the greatest sensitivity to the extended changes in the anomalies.

Calculations are reduced to the fact that in limits of each of four strips average/mean value of anomalous field, taken/removed from map/chart of isolines, is counted. A number of fiducial marks within each longitudinal strip can vary from 10 to 20 depending on complexity and changeability of anomalies. Average/mean values  $\bar{f}_i$  for each strip are used for calculating the differences

$$\Delta_1 = \bar{f}_1 + \bar{f}_2 - \bar{f}_3 - \bar{f}_4, \quad (\text{IV, 137})$$

$$\Delta_2 = \bar{f}_2 + \bar{f}_3 - \bar{f}_1 - \bar{f}_4, \quad (\text{IV, 138})$$

Calculations according to formula (IV, 135) will give maximum value in presence of edge dislocations, whose cross section is

represented in the form relative to symmetrical maximum (with negative sign of result of calculations - minimum). Analogously, during the calculations according to the formula (IV, 134) maximum values will testify about the presence of skew-symmetric changes - anomaly of the type of "step/stage".

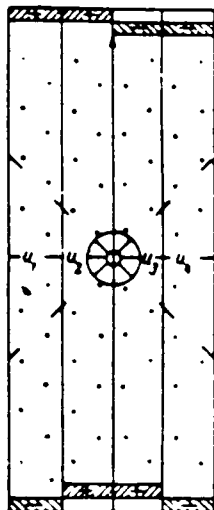


Fig. 102. General view of template for anisotropic transformation of anomalous field.

Page 212.

If template is placed on map/chart out of zone of edge dislocations, then fine/small variations in picture being investigated, which are repeatedly changed in interval, equal to length of template, will be excluded from calculations only due to their averaging in limits of each strip. Smooth, correlated changes, which characterize general/common regional background, after the calculation of differences will give small or zero values. Analogous result will be obtained in the case, if template is placed in the limits of the zone of edge dislocation, but the axis of template is directed approximately perpendicular to basic course/strike.

Consecutively changing direction of axis of template in each of calculation points and taking into account value of differences  $\Delta_1$  and  $\Delta_2$ , it is possible to establish/install course/strike of unknown edge dislocations, their position in plan/layout and form of cross section of anomalies connected with them. If course/strike is established according to independent data, it is possible to be bounded to one position of template at each calculation point, which accelerates processing/treatment.

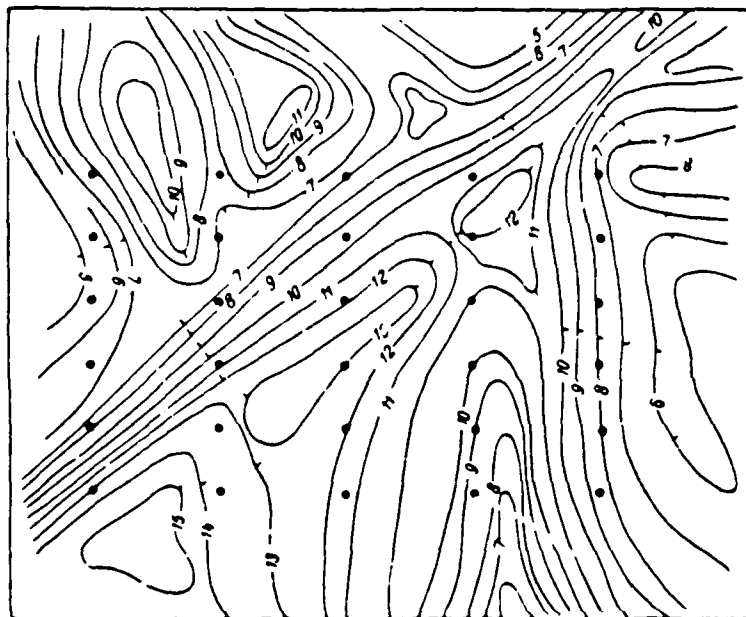


Fig. 103. Diagram of isolines of anomalous field above theoretical model. 1 - isoanomalies; 2 - points, at which was produced the calculation of vectors.

Page 213.

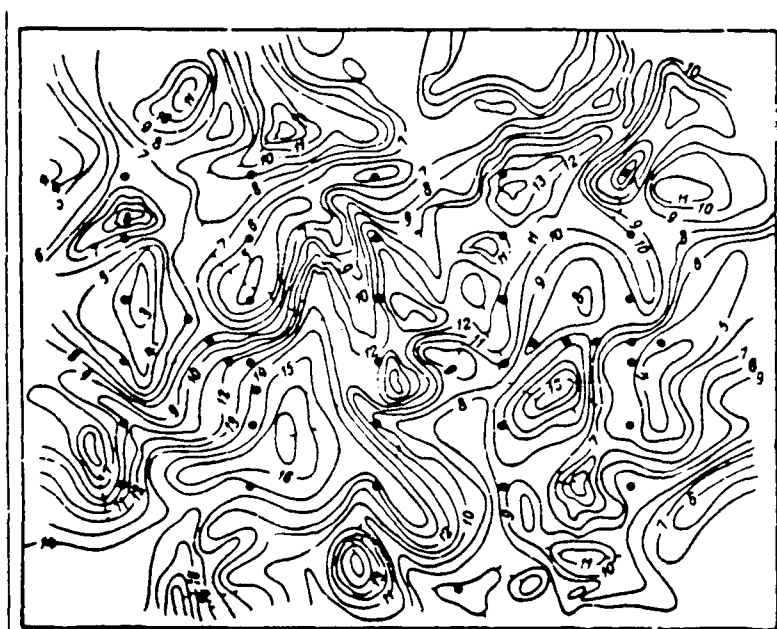


Fig. 104. Diagram of isolines of anomalous field above theoretical model, complicated by interference (conventional designations the same as in Fig. 103).

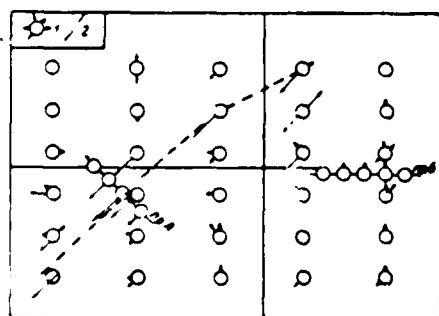


Fig. 105. Plan/layout of vectors, obtained during processing/treatment of initial field, complicated by interference. 1 - calculation points with the vectors calculated according to the formula (IV, 134) (solid lines) and to formula (IV, 135) (dotted lines); 2 - line of abrupt change in the field.



Page 214.

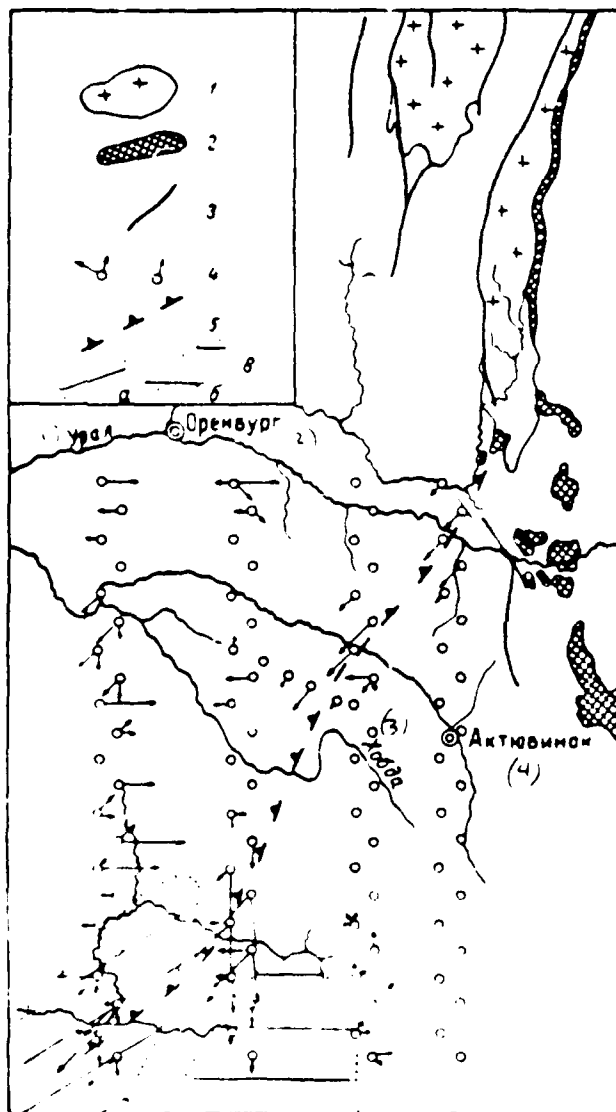


Fig. 106. Practical example of determination of position of edge dislocation according to schematic of vectors  $\Delta_1$  and  $\Delta_2$ . According to I. G. Klushin and I. N. Tolstikhin (1961). 1 - emergences/outcrop of Precambrian metamorphic rock; 2 - intrusion of the ultrabasic rocks; 3 - faults, established/installed according to geologic data; 4 -

vectors, obtained during processing/treatment of the diagram of isolines  $\Delta T$ ; 5 - axis of the predicted edge dislocation of crystalline basement, which is developed in structure of sedimentary cover and, partially, geomorphology of region; 6 - gently sloping structures of the Mesozoic complex: a) Sagiz uplift/rise; b) Emba-Sagiz downwarp/trough. According to M. P. Zazakov.

Key: (1). Urals. (2). Orenburg. (3). Khobda. (4). Aktyubinok.

Page 215.

Sizes/dimensions of template depend on sizes/dimensions of predicted linear zones and anomaly-interference. Its width to scale of map/chart must be close to the sizes/dimensions of separate "spots", but not less than the width of the zone being isolated. With an increase in the length of template azimuthal sensitivity is improved and interference suppression is strengthened. However, for the safeguard of the independent conducting of the zones being isolated at different points of map/chart it is necessary that the length of template was at least two times less than the minimum extent of edge dislocations. Therefore on the high level of the correlated interference it is possible to separate/liberate only the very extended zones of dislocations. In Fig. 103 is constructed the diagram of the isolines of the anomalous field above the theoretical model, while in Fig. 104 - the diagram of the isolines of the anomalous field, complicated by interference. Root-mean-square annoyance value is approximately equal to the intensity of anomalies.

Position of banded zones of abrupt change in field, distinctly visible in Fig. 103, is considerably shaded in Fig. 104. The results of the transformation of latter/last diagram are shown in Fig. 105 in the form of the vectors, whose direction corresponds to the direction of the axis of template, and value is proportional to difference  $\Delta_1$  (solid lines) and  $\Delta_2$  (dotted lines). In each calculation point the circle, which corresponds to interference level, is replaced.

Schematic of vectors clearly indicates position of linear zone of abrupt change in field, which has northeastern course/strike. The zone of meridian course/strike proved to be expressed less clearly, the intensity of vectors only insignificantly exceeds interference level; however, in this case attention is drawn to the stable repetition of the sense of the vector on many contiguous points. For logging of zones profiles A and B are calculated additionally.

In Fig. 106 practical example of processing/treatment of diagram of isoanomalies is given.

Page 216.

Chapter V.

INTERPRETATION OF GRAVITY ANOMALIES FOR BODIES OF CORRECT GEOMETRIC FORM.

§33. Generalities.

During quantitative geologic interpretation of gravity anomalies assumption about the fact that the causing these anomalies geologic bodies have correct geometric form, frequently is made. In such cases, when this likening closely corresponds to reality, for example in the case of step, bed, etc., the corresponding methods of interpretation give the possibility to sufficiently accurately determine the elements of bedding, and sometimes also the excess density of geologic bodies on the gravity anomalies. In other, more numerous cases, when one or the other geologic body, which causes gravity anomaly, only very approximately can be likened to the geometric solid of simple correct form, the application of the corresponding methods of interpretation frequently nevertheless proves to be useful. In these cases we, naturally, do not obtain from gravitational data the accurate characteristic of body, but frequently we can sufficiently reliably consider some quantitative data, which characterize the object of anomaly, for example the order of the depth of its bedding, possible mass, volume, etc. Having such data, during the searches for structures or ore bodies it is possible with respect to one or the other anomaly to make the conclusion about that, does

deserve this anomaly attention from the point of view by decided gravitational photographing of the prospecting task, such as must gravitational photographing of prospecting task, what must be the depth of the drill hole or bore pit, assigned for the purpose of the check of anomaly, etc.

For each of bodies of correct geometric form in question first is solved straight/direct problem, i.e. formulas, which express gravitational effect/action of body on these or other derivatives of potential, are found. For some cases such formulas are brought out and for the converted forms of anomaly, for example for the variation anomaly of the force of gravity  $\delta\Delta g$ , whose determination is given in Chapter IV, for derivative  $W_{ii}$  and so forth.

Page 217.

Further there are two ways of the construction of apparatus for solving the inverse problem (for some shapes of bodies they are used both ways).

First path is such: investigating formulas, which represent solution of direct problem for one or the other derivative of potential, we determine coordinates of characteristic points of this derivative - points of maximum and minimum, half-maximum, zero values, etc., we find also values of anomaly at points of maximum and minimum. This gives us the system of equations, from which the elements of the bedding of body directly are determined, i.e., the solution of inverse

problem is obtained.

Alternate path consists in the fact that, using formulas of solution of direct problem, are built atlases of theoretical curves (template) : corresponding derivatives of gravitational potential for different sizes/dimensions, depths of bedding and values of other parameters of disturbing body of this geometric form; such constructions are done for profile, which passes above body.

FOOTNOTE 1. Term "template" (by analogy with the electrical prospecting) we relate below to the atlases of the theoretical curves, constructed, first of all, on the logarithmic or semilogarithmic scales. ENDFOOTNOTE.

The comparison of these curves with that obtained from the observations actually gives the possibility to select the theoretical curve, which most corresponds to observed, and thereby to obtain the solution of inverse problem; in this case the degree of confidence of this comparison gives the possibility to consider the degree of reliability of the obtained solution. As we will see below, even for some bodies of simple geometric form the analytical solution of direct problem in the final form is not obtained, however this solution can be obtained approximately to any degree of accuracy and it is possible to depict it in the form of the series of theoretical curves.

During construction of atlases of theoretical curves relative

scale usually is used, i.e., along horizontal axis are deposited not absolute values of horizontal coordinate, but its relation to any linear parameter on vertical line, for example to depth of bedding of body. In a number of cases is used (but in the practice of gravitational prospecting thus far wide application it did not obtain) the construction of theoretical curves on the logarithmic or semilogarithmic scale; such constructions make sense during the analysis of the single or very well localized anomalies. The first of the methods of solution of inverse problem indicated we will briefly call analytical, the second - graphic (measuring grid).

Page 218.

Important value with interpretation can have utilization of space patterns of anomalous field in the form of curves along system of vertical and horizontal profiles or in isolines of values of corresponding derivative of potential. In this book we propagandize this method, until now, barely used in gravitational prospecting, and we show in a number of examples its practical value. The special importance of such kind of approach to examination and investigation of anomalies can gain with the development of subterranean and air gravitational prospecting.

Debatable in gravitational prospecting is question about worthwhileness of examination with interpretation, besides simplest elementary bodies of correct geometric form, also more complex forms, for example ellipsoid and so forth majority of specialists in region

of gravitational prospecting (both theoreticians and practitioners) is considered worthwhile to be bounded with interpretation to examination only of simplest shapes of bodies. The same point of view is accepted also in the program on the course of gravitational prospecting, predicated by the Ministry of Highest and Special secondary Education of the USSR for geological exploration VUZ [ - Institute of Higher Education]. Different is the point of view of the collective of geophysicists, led by Prof. A. A. Yun'kov (Dnepropetrovski mining institute), and some individual researchers (I. S. Gelfand, L. I. Gavrilov, N. N. Pariyskiy) - by them are systematically published works on the solution of straight/direct and inverse problem for the bodies of complex form (general ellipsoid and ellipsoid of revolution, paraboloid and parabolic cylinder, hyperbolic dome, etc.). This question is examined purely theoretically - without the reduction of practical examples.

Opinion of authors on question indicated is reduced to following. Practice requires certain increase in the number of models of the bodies of correct geometric form, utilized with the interpretation against their small number, which is examined in the textbooks, especially for the three-dimensional task. At the same time the solution of straight/direct and in particular the reverse tasks almost for each of such complicated models is connected, as a rule, with the calculation according to the unusually bulky formulas. If we take into account that the conformity of the models in question to real geologic bodies nevertheless approximated, and initial data for the



calculations are also approximated, then for such cases the solution of inverse problem analytically is unstable and, apparently, it is inexpedient. However, for some of such more complex cases is expedient the construction of the atlases of theoretical curves, and also space patterns of anomalous fields for solving the inverse problem of interpretation by graphic (measuring grid) method.

On the basis of all these consideration, in the present work we somewhat increased number of models of bodies of correct geometric form against usually those examined/considered, but in number of cases solutions of direct problem of interpretation were bounded to reduction only of formulas.

Page 219. <sup>71</sup> For the important from the point of view of practice cases of the bodies of correct geometric form the examination of the methods of solving direct and reverse problems in this book is conducted by us very thoroughly - in much more detail, than this was done in the previously released manuals.

The examined below methods of interpretation it is possible to divide into two following groups:

1) accurate methods, i.e., methods, specially fitted out for investigation of one model or the other and which give for it exact solution of inverse problem.

2) the approximate (asymptotic) methods, i.e., the methods, which only under some boundary conditions - with respect to sizes/dimensions and form of the perturbing masses, with respect to the very procedure

of calculations and so forth - can give results, more or less being adequate/approaching for this model.

Application of accurate methods further is clarified based on some practical examples, application of approximation methods, as a rule, based on examples of theoretical, which correspond to assigned model.

#### §34. Material point and sphere.

As we already indicated in §1 of Chapter I, attraction of body of spherical form of uniform density, or consisting of concentric layers uniform in density, identical to attraction of material point, located in center of spherical body, whose mass was equal to mass of this body. This is correct for any point of the space, external with respect to this spherical body. Therefore the anomaly of gravitational force, which presents the attraction of spherical body, under conditions indicated above will coincide with the anomaly of the force of gravity, caused by the effect/action of material point.

Geologic bodies, more or less isometric form, whose cross sizes/dimensions in all measurements of one order, can be during calculation of their gravitational effect/action likened to spherical or mass points. Accuracy of this likening is greater, the greater the distance from the body to the attracted/tightened point. The geologic bodies of this type are very different: ore shoots of boss-shaped and

nest-shaped form, salt/hydrochloric domes, karst holes, etc. Furthermore, it is necessary to have in mind that if we examine the summary gravitational effect/action of several spherical bodies or material points, arranged/located correspondingly, then it is possible with the approximation/approach sufficient for practice to present the gravitational effect/action of the bodies of very complex form. In this case is completely possible the solution not only of straight line, but also the inverse problems of interpretation - true no longer analytical, but only graphic method.

Page 220.

Hence is clear great practical value of this case, in detail taken apart below.

Let us examine uniform body of spherical form with center C, which lies at plane xoz (Fig. 107). The coordinates of the center of sphere let us designate as follows:  $x_C = x$ ;  $y_C = 0$ ;  $z_C = h$ .

Let us designate total mass of sphere through M.

Instead of spherical body for space, external to its surface, we can examine material point with mass M, located in center of body. Consequently, in this case the formulas, which express the gravitational effect/action of body, can be obtained without the calculation of the corresponding volumetric integrals - directly from the integrands of formulas (III,8), if we in them write instead of x,

y, z the corresponding values of the coordinates of the center of sphere, and instead of dm - total mass of sphere M. For the origin of coordinates we obtain the following expressions:

$$\left. \begin{aligned} \Delta g &= fM \frac{h}{r^3}, \\ W_{xz} &= 3fM \frac{xh}{r^5}, \\ W_{\lambda} &= -3fM \frac{x^2}{r^5}, \\ W_{xx} &= fM \frac{3h^2 - r^2}{r^5} = fM \frac{2h^2 - x^2}{r^5}, \\ W_{yz} &= 2W_{xy} = 0. \end{aligned} \right\} \quad (V, 1)$$

where  $r = \sqrt{x^2 + h^2}$ .

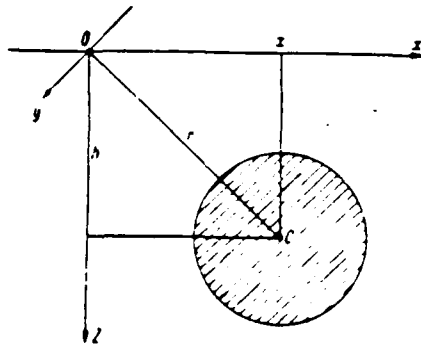


Fig. 107. For determination of gravitational effect/action of spherical body

Page 221.

After obtaining these formulas, to us it is more convenient to somewhat convert them, precisely, to place center of sphere under origin of coordinates to extra-mobile point  $(0, 0, h)$ , and observation point - into flowing point with coordinate  $x$ . It is easy to see that this is equipollent simply to a change in the sign in coordinate  $x$  in the formula (V, 1). We obtain:

$$\left. \begin{aligned} \Delta g &= fM \frac{h}{r^3}, \\ W_{xx} &= -3fM \frac{rh}{r^5}, \\ W_{\Delta} &= -3fM \frac{x^2}{r^5}, \\ W_{zz} &= fM \frac{2h^2 - x^2}{r^5}, \\ W_{xy} &= 2W_{yz} = 0, \end{aligned} \right\} \quad (V, 2)$$

where, as before:

$$r = \sqrt{x^2 + h^2}.$$

Advantage of formulas (V, 2) over (V, 1) is the fact that they

correspond to natural state of affairs: disturbing body is motionless, and moves in plane  $z=0$  (plane of observations) along axis  $x$  (line of observations) point  $x$ , for which formulas (V, 2) give values of derivatives of gravitational potential, i.e. observation point. In such cases, when they investigate a change in one or the other derivative of gravitational potential on the vertical line, in the formulas (V, 2) instead of  $h$  they write  $h-z$ , where  $z$  characterizes the position of the point in question relative to the plane of observations  $z=0$ . We will conduct simultaneously research of the form of the curves of derivatives of potential with the examination of the methods of solving the inverse problem of interpretation.

Let us begin from anomaly of force of gravity

$$\Delta g \approx fM \frac{h}{r^3}.$$

Corresponding curve  $\Delta g$  is everywhere positive, <sup>1</sup> moreover

$$\Delta g(-x) = \Delta g(+x).$$

FOOTNOTE <sup>1</sup>. It is assumed, as it is everywhere further, if there are no special stipulations, that the excess mass  $M>0$  and excess density  $\sigma>0$ . Otherwise  $\Delta g$  - everywhere negative function. ENDFOOTNOTE.

From condition  $\frac{d}{dx}(\Delta g) = 0$  we find  $x_{\max} = 0$ , i.e., the maximum of curve is arranged/located above the center of spherical body. Anomaly  $\Delta g$  becomes zero with  $x=\pm\infty$ . The form of the curve  $\Delta g$  is shown in Fig.

Assuming/setting  $x=0$  in formula for  $\Delta g$ , we find value of maximum

$$\Delta g_{\max} = \frac{fM}{h^3}. \quad (V.3)$$

Page 222.

Let us find abscissa of curve, for which  $\Delta g = \frac{1}{2} \Delta g_{\max}$  (Fig. 108); let us designate its value through  $x_{1/2}$ . It is determined by the condition

$$fM \frac{1}{(x_{1/2}^2 + h^2)^{3/2}} = \frac{fM}{2h^3}.$$

Whence after abbreviations and reductions we find

$$x_{1/2} = h \sqrt{\frac{3}{4} - 1} = 0,766 h. \quad (V.4)$$

Depth of center of sphere  $h$  and its excess mass  $M$  are unknowns in the case of inverse problem. Determining these values from the formulas (V, 4) and (V, 3), we obtain:

$$\left. \begin{aligned} h &= 1,31 x_{1/2}, \\ M &= \frac{\Delta g_{\max} h^3}{f}, \end{aligned} \right\} \quad (V.5)$$

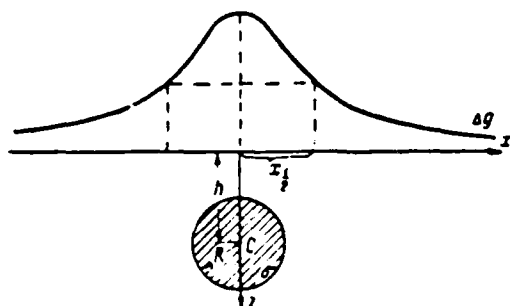
where  $x_{1/2}$  and  $\Delta g_{\max}$  directly are determined on the curve  $\Delta g$ .

If excess density  $\sigma$  of spherical body is known, then it is possible to determine its volume  $V$  and radius  $R$  from relationship/ratio

$$M = V\sigma = \frac{4}{3} \pi R^3 \sigma \quad (V.6)$$

and depth  $H$  of upper surface of sphere from plane of observation

$$H = h - R. \quad (V.7)$$

Fig. 108. Curve  $\Delta g$  above body of spherical form.

Page 223.

Since measuring system of gravimeter is arranged/located close to earth's surface,  $H$  it is possible to take as equal to depth of upper surface of spherical body, counted from this surface. Generally depth from the earth's surface is equal to  $H - I$ , where  $I$  - height of instrument.

Let us write now  $\Delta g$  in more general view

$$\Delta g = fM \frac{h - z}{[x^2 + (h - z)^2]^{3/2}} \quad (V, 8)$$

and we investigate change  $\Delta g$  with change in vertical coordinate  $z$  of observation point.

Let us examine first the case, when  $x = 0$ , i.e., change of  $\Delta g$  along side vertical profile. Condition  $\frac{d}{dz} (\Delta g) = 0$  gives the values

$$\left. \begin{aligned} z_{\max} &= h - \frac{|x|}{\sqrt{2}}, \\ z_{\min} &= h + \frac{|x|}{\sqrt{2}}. \end{aligned} \right\} \quad (V, 9)$$



Anomaly  $\Delta g$  becomes zero with

$$z = z_0 = 0,$$

(V, 10)

and also, obviously, with  $z = z_0 = \pm\infty$ .

Character of change  $\Delta g$  along lateral vertical profile is shown in Fig. 109.

Conditions (V, 9) or (V, 10) determine  $h$ , and substitution of the first of equations (V, 9) in (V, 8) gives equation for determining of  $M$ .

With  $x=0$  formula (V, 8) gives

$$\Delta g = \frac{fM}{(h-z)^2} \quad (V, 11)$$

from which it is clear that  $\Delta g$  on one vertical line with material point continuously increases with increase in  $z$  from 0 to  $h$ , while with  $h = z$   $\Delta g = \pm\infty$ .

Point with coordinates  $x=0$ ,  $z=h$  - singular point of anomalous field.

On lateral vertical profile, as we saw above, level of this singular point is noted by zero value of  $\Delta g$ .

At this point goes to infinity value  $\Delta g$  for material point, and

also value  $\Delta g$  for material sphere, analytically continued through its surface with the help of formula (V, 11).

Page 224.

Does correspond, however, this value to actual value  $\Delta g$  for center of material sphere? Basis/base to setting of a similar question is the following consideration: formula (V, 11), unconditionally, is real out of the perturbing masses, there where the potential field is subordinated to Laplace equation, but it, apparently, is ineffective within the perturbing masses - there where the potential field is subordinated to the equation of Poisson (about these equations see in §3 of Chapter I).

Similar study of problem shows that formula (V, 11) for points, arranged/located within sphere, does not correspond to actually existing there gravitational field. In order of this to be convinced, let us take into consideration the following theorem of the theory of the attraction: attraction of uniform spherical material layer to the material point, arranged/located within the layer, is equal to zero. Let us give elementary purely geometric proof of this theorem, given already by I. Newton (1687). Let there be the material point M, arranged/located somewhere within the uniform infinitely thin spherical layer; let us examine the effect/action on this point of the mutually inverse elements of layer AB and CD, arranged/located within the elementarily small solid angle  $\theta$  (Fig. 110).

DOC = 88020212

PAGE

~~17~~ 411

FOOTNOTE 1. Let us recall that the solid (spherical) angle is measured by the surface area of the sphere of unitary radius, arranged/located within this angle, with the center at the point (vertex of angle) in question. ENDFOOTNOTE.

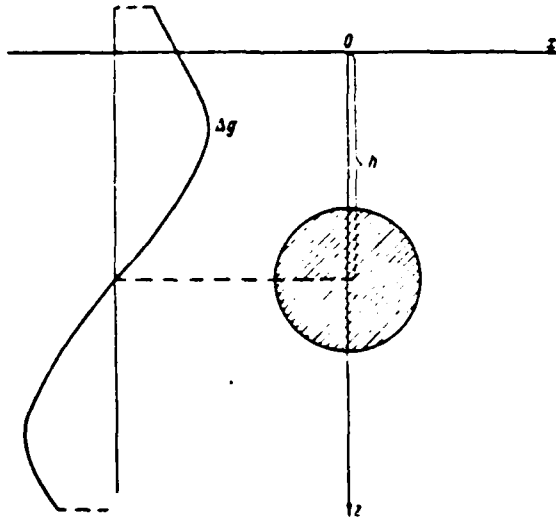


Fig. 109. Curve  $\Delta g$  for body of spherical form along lateral vertical profile.

Page 225.

These elements can be replaced respectively by spherical elements  $AB'$ , described radius  $MA$  and  $C'D$ , described radius  $MD$ . The areas of these elements, and consequently, their mass are proportional to the squares of these radii, and their attractions, in accordance with Newton law, are inversely proportional to the squares of these radii; since these elements are mutually contradictory, their cumulative effect on point  $M$  is equal to zero. Material spherical layer represents the set of such mutually inverse elements; consequently, it as a whole does not affect the internal point.

Infinitely thin spherical layer can be considered as element of

uniform spherical layer of finite thickness. It is hence obvious that also for the uniform layer of finite thickness the given theorem is also real. And what is more, theorem, obviously, retains force for the spherical layer and the solid material sphere, that consist of concentric spherical layers different in the density.

If we have material point with mass, equal to one, arranged/located within solid uniform material sphere of density  $\sigma$  and radius  $R$  at a distance  $q$  from center of sphere (Fig. 111a) ( $q < R$ ). then effect/action of this sphere on unitary material point is equal to effect/action of sphere of radius  $q$ . since external spherical layer with thickness of  $R - q$ . as we explained, does not act on point in question.

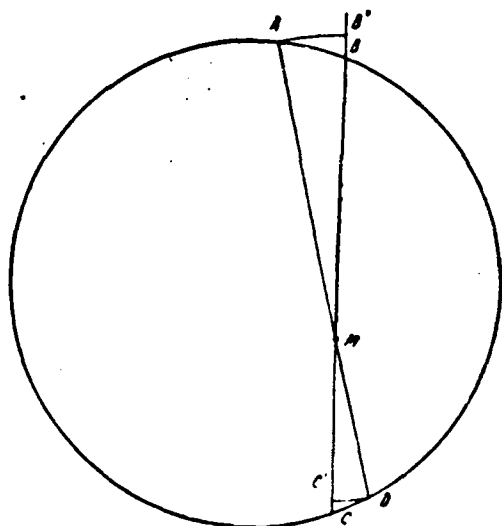


Fig. 110. For determination of attraction of material spherical layer to internal point.

Page 226.

Thus,

$$\Delta g = \frac{\frac{4}{3} \pi \rho' \sigma}{\rho^2} = \frac{4}{3} \pi \rho \sigma (\rho - R). \quad (V, 12)$$

Consequently, real law of change in anomaly of force of gravity  $\Delta g$  for case of material sphere is such: with approximation/approach to surface of sphere on vertical line  $\Delta g$  it increases/grows, on surface of sphere it reaches maximum value

$$\Delta g = \frac{4}{3} \pi R \sigma, \quad (V, 13)$$

but further it decreases according to linear law in accordance with (V, 12) and it becomes zero when  $\rho = 0$ , in center of sphere (Fig.

111b). Thus, actual value  $\Delta g$  for the center of material sphere entirely is different, than for the material point. Their effect/action is equivalent only in the space, external with respect to the surface of spherical mass.

Formula (V, 12) shows change  $\Delta g$  within sphere of uniform density. If density varies along the radius of sphere, then  $\Delta g$  varies according to the more complex nonlinear law, but also it becomes zero in the center of sphere. The example of this body is our planet the Earth; in this case very force of gravity  $g$  plays the role of anomaly  $\Delta g$ . Within the Earth gravitational force virtually is unchanged to the depth of 2900 km, and then it begins rapidly to decrease and it becomes zero in its center (Andreyev, 1960).

Consideration developed above about three-dimensional/space change of  $\Delta g$  has common sense in two cases: 1) during calculation of  $\Delta g$  along lateral vertical profiles, for example with utilization of net point method (see Chapter IV); 2) during subterranean gravitational photographing. We will have these two possibilities in mind also in the following presentation.

We change to examination of horizontal gradient of force of gravity

$$W_{xx} = -3/M \frac{x^h}{r^5}.$$

Curve for this function is positive with  $x < 0$  and is negative with

$x > 0$ , moreover  $W_{xz}(-x) = -W_{xz}(+x)$ . With  $x=0$  and also when  $x = \pm \infty$   $W_{xz} = 0$  (Fig. 112).

Condition  $\frac{d}{dx} [W_{xz}] = 0$  gives

$$\left. \begin{aligned} x_{\max} &= -\frac{h}{2}, \\ x_{\min} &= +\frac{h}{2}. \end{aligned} \right\} \quad (V, 14)$$



Page 227.

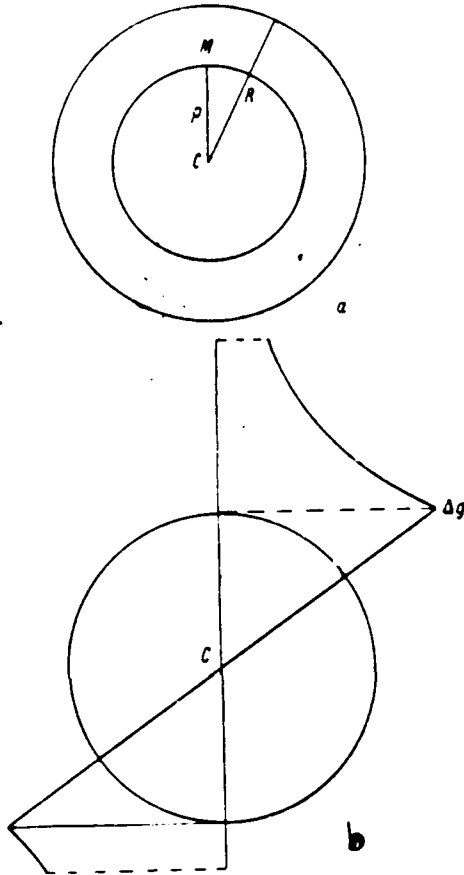


Fig. 111. For determination of attraction of material sphere to external and internal point. a) construction to the determination of the attraction of sphere to the internal point; b) curve  $\Delta g(q)$  when  $q = h$  and  $q < h$ .

Page 228.

Thus, if we designate distance along profile between points of minimum and maximum  $W_{\alpha} l$ , then, it is obvious,

$$l = x_{\min} - x_{\max} = h, \quad (V, 15)$$

which immediately and very simply determines depth of center of sphere

h.

Assuming/setting in general formula for  $W_{xz} x = -\frac{h}{2}$ , we find

$$[W_{xz}]_{\max} = 3/M \frac{h^2}{2 \left( \frac{5h^2}{4} \right)^{3/4}} = 0,858 \frac{fM}{h^2}, \quad (V, 16)$$

whence excess mass of sphere M is determined.

Let us examine now value

$$W_{\Delta} = -3/M \frac{x^2}{r^3}.$$

This value is everywhere negative with exception of point  $x=0$ , at which  $W_{\Delta} = 0$ . In this case  $W_{\Delta}(-x) = W_{\Delta}(+x)$ . Further investigation of the corresponding equation shows that

$$x_{\min} = \pm h \sqrt{\frac{2}{3}}, \quad (V, 17)$$

$$(W_{\Delta})_{\min} = -0,558 \frac{fM}{h^2}. \quad (V, 18)$$

From latter/last equations are also determined h and M during solution of inverse problem. Knowing  $\sigma$ , it is possible to determine also radius R of sphere and depth of the bedding of its upper surface (see pg. 222).

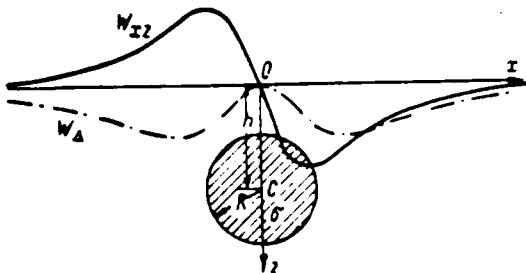


Fig. 112. Curves  $W_{xz}$  and  $W_{\Delta}$  above spherical body.

Page 229.

Singular point in center of sphere is developed also in second derivatives of potential. Thus, from general formula for  $W_{xz}$  and the condition (V, 15) ensues the following character of change in this derivative along the profile at level  $z = h$ :  $W_{xz}$  turns into  $+\infty$  with the approach to the singular point to the left and into  $-\infty$  with the approach to it to the right.

If line of observation ( $x$  axis) passes above center of sphere, then  $W_{yz} = 0$ , consequently,  $W_{xz} = G = \sqrt{(W_{xt})^2 + (W_{yt})^2}$  at all observation points. If the line of observations does not pass above the center of spherical body, but away from it, then  $W_{yz}$  is generally nonzero and the vectors of total horizontal gradient take the form, shown in Fig. 113; they intersect at the point, arranged/located above the center of the sphere higher than point O. This gives the possibility to reduce the form of the curve of gradient on the epicentral profile: role  $x$  play in this case distances from the point of intersection of vectors to appropriate observation point, and role  $W_{xz}$  - the value of the total

horizontal gradient G.

Vertical gradient of force of gravity

$$W_{zz} = fM \frac{2h^3 - x^3}{r^5}$$

is positive with  $x^3 < 2h^3$ , it is negative with  $x^3 > 2h^3$  and becomes zero with

$$x = x_0 = \pm h\sqrt[3]{2}. \quad (V, 19)$$

Reaches maximum value  $W_{zz}$  with  $x=0$ , moreover

$$W_{zz} = \frac{2fM}{h^3}. \quad (V, 20)$$

Formulas (V, 19) and (V, 20) determine unknowns M and h.

At level  $z=h$

$$W_{zz} = \frac{-fM}{x^3},$$

but at singular point  $(0, h)$   $W_{zz} = -\infty$ .

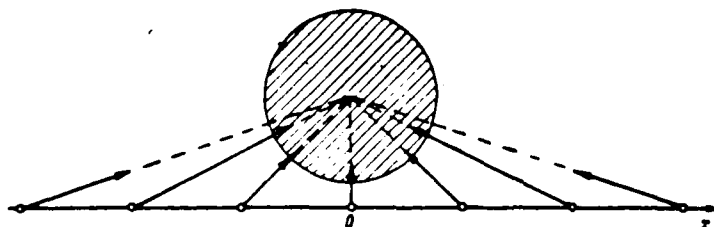


Fig. 113. Vectors of total horizontal gradient  $G$  in horizontal plane  $z=0$  in the case, when  $x$  axis (line of observations) does not pass above center of spherical body.

Page 230.

Based on example of sphere and material point it is clearly evident that solution of inverse problem actually is reduced to position finding of singular point (source) of anomalous field, situated in this case in center of sphere, and anomalous mass of body (source power). The real surface of sphere does not affect the character of field out of the sphere and directly it is not determined; it is possible to determine it only in the presence of additional information - knowledge of the value of the excess density of sphere.

So is the matter in the case of any body, limited by smooth surface, on which are not located singular points of anomalous gravitational field.

§ 35. Vertical material rod, circular disk and vertical circular

cylinder.

It is possible to liken to vertical material rod the different geologic bodies, elongated on vertical line, more or less isometric section in such cases, when their cross sizes/dimensions are small in comparison with depth of bedding and their vertical sizes/dimensions. Such bodies can be the salt domes of small cross sizes/dimensions and wide distribution to the depth, some types of intrusive bodies, for example diamond-bearing kimberlitic tubes, the ore bodies of column-like form, etc.

We will be bounded to examination of direct and reverse problem of interpretation for vertical rod on anomaly of force of gravity  $\Delta g$ , by assuming that distribution of anomaly is assigned along profile (x axis), passing through projection of upper end of rod on earth's surface. The horizontal coordinate of this point let us designate through x, depth of upper end of the rod - through  $z_1$ , lower end - through  $z_2$ . The mass of rod with the length, equal to one, let us designate through  $\lambda$ , so that

$$dm = \lambda dz.$$

With these conditions the first of formulas (III.8) gives

$$\Delta g = f\lambda \int_{z_1}^{z_2} \frac{dz}{(x^2 + z^2)^{3/2}} = f\lambda \left[ \frac{1}{\sqrt{x^2 + z^2}} \right]_{z_1}^{z_2} = f\lambda \left( \frac{1}{\sqrt{x^2 + z_1^2}} - \frac{1}{\sqrt{x^2 + z_2^2}} \right). \quad (V.21)$$

In the particular case with  $z_2 = \infty$  we will have

$$\Delta g = \frac{f\lambda}{V \sqrt{z^2 + z_1^2}} \quad (V.22)$$

Page 231.

On the basis of physical sense of task, radicals in formulas (V, 21) and (V, 22) should be implied with plus sign.

Since into formulas (V, 21) and (V, 22)  $x$  enters only squared, their form remains invariable, if rod is counted located under origin of coordinates, and we by coordinate  $x$  note position of observation point on profile.

Inverse problem for rod (with  $z_1 = \infty$ ) is solved so simply, as in the case of sharpened mass. The maximum value of  $\Delta g$  we have at point  $x=0$ , arranged/located above the rod

$$\Delta g_{\max} = \frac{f\lambda}{z_1} \quad (V.23)$$

We will obtain second equation for determining unknowns  $z_1$  and  $\lambda$ , after determining position of abscissa of half-maximum  $x_{1/2}$ , in which

$\Delta g = \frac{1}{2} \Delta g_{\max}$ . We find

$$x_{1/2} = z_1 \sqrt{3} \quad (V.24)$$

and obtain  $z_1$  and  $\lambda$  from the formulas (V, 23) and (V, 24).

Let us examine change  $\Delta g$  on vertical line, for which let us represent formula (V, 22) in more general form

$$\Delta g = \frac{f\lambda}{\sqrt{x^2 + (z_1 - z)^2}}. \quad (V.23)$$

Let us allow first that  $x \neq 0$ , i.e., that we are found on lateral vertical profile. If  $z$  increases from 0 to  $z_1$ , then  $\Delta g$  increases/grows and with  $z = z_1$  it reaches the maximum value

$$\Delta g_{\max} = \frac{f\lambda}{|x|} \quad (V.24)$$

and gradually it decreases with further increase in  $z$  (Fig. 114)

with

$$z = z_{1,2} = z_1 \pm x \sqrt{3}. \quad (V.25)$$



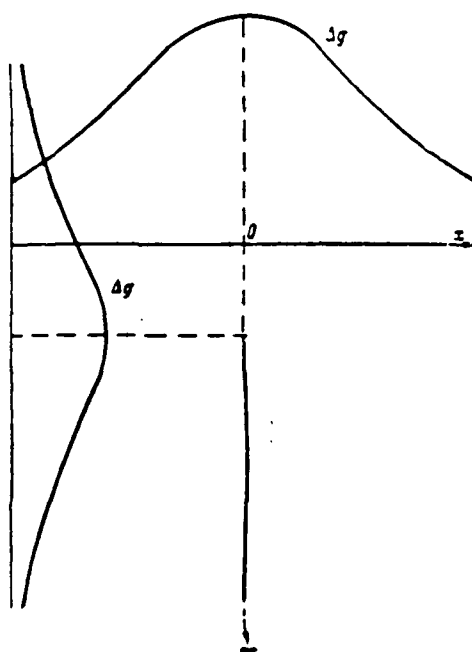


Fig. 114. Change of  $\Delta g$  on horizontal and on lateral vertical profiles in the case of vertical semi-infinite rod.

Page 232.

If  $x$  is known, then formulas (V, 24) and (V, 25) make it possible to determine  $\lambda$  and  $z_1$ .

But if  $x=0$ , then  $\Delta g$  increases/grows with increase in  $z$  from 0 to  $z_1$ , moreover with  $z=z_1$ ,  $\Delta g=+\infty$ . Thus, upper end of the rod represents the singular point of anomalous field.

Analogous research can be conducted, also, for formula (V, 21), i.e., case of limited on incidence/drop rod. Since here are not two,

but three unknowns, it is possible to examine three values of  $\Delta g$

$$\begin{aligned} \Delta g_{\max} \overset{(1)}{\text{при}} x = 0, \\ \frac{1}{2} \Delta g_{\max} \overset{(1)}{\text{при}} x = x_{1/2}, \\ \frac{1}{4} \Delta g_{\max} \overset{(1)}{\text{при}} x = x_{1/4}. \end{aligned}$$

Key: (1). with.

which gives the system of equations, necessary for solving the inverse problem. In this case it is necessary to have in mind that if  $z_1 \gg z_2$ , then, as can be seen from formula (V, 21), effect of  $z_2$  on  $\Delta g$  is much less than effect  $z_1$ , and consequently,  $z_2$  with the interpretation will be determined considerably less accurately than  $z_1$ .

Let us examine now question about attraction of uniform flat/plane horizontal layer, limited by arbitrary outline. The density of plane layer, i.e., the mass of the element of layer, with the area, equal to one, let us designate through  $\mu$ . Let us take infinitesimal element of layer  $dS$  with the center at point M (Fig. 115). Attraction  $dF$  of the element of layer to the external point O (with the unitary mass), according to Newton's law, will be equal to

$$dF = \frac{\mu dS}{R^2} (R - \vec{OM}).$$

Z axis let us direct downward along the normal to plane of layer and let us designate angle between axis  $g$  and  $OM$  through  $\psi$ . In that case vertical component of the attraction of the element of layer will be registered in the following form:

$$dF_z = \frac{\mu dS \cos \psi}{R^2}.$$

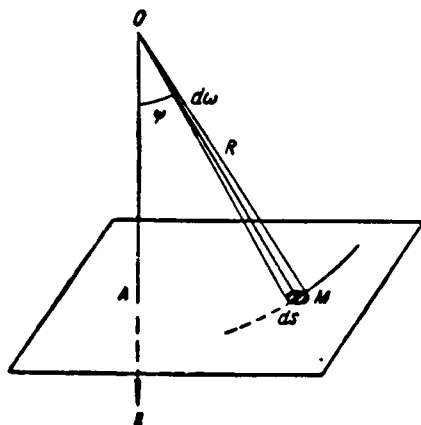


Fig. 115. For conclusion/derivation of expression of anomaly  $\Delta g$  for horizontal plane layer.

Page 233.

Let us lead surface of sphere of radius  $R$  with center in  $O$  through point  $M$ . Let us designate through  $d\omega$  the elementary solid angle, at which is visible element  $dS$  from point  $O$ . Corresponding to this angle element of the surface of auxiliary sphere will be, obviously, equal to  $R^2 d\omega$ . It is easy to see that

$$R^2 d\omega = dS \cos \psi$$

and, consequently,

$$dF_z = f \mu d\omega.$$

Hence total value  $F_z$ , which presents anomaly  $\Delta g$  for entire layer, will be expressed as follows:

$$F_z = \Delta g - f \mu \omega, \quad (V.26)$$

where  $\omega$  - total solid angle of visibility of layer from point  $A$ .

In the case of infinite material plane  $\omega = 2\pi$  and

$$\Delta g = 2f\pi\mu. \quad (V, 26a)$$

The same result, obviously, will be obtained also for layer of finite horizontal dimensions in the extreme case, when point A approaches up to infinitesimal distance plane of layer, proving to be within outline of its section. If point A approaches plane of layer out of its outline, then in this case limiting value  $\omega$  is equal to zero, and consequently,  $\Delta g = 0$ .

Above we examined gravitational effect/action of horizontal plane layer, limited by arbitrary outline, and we were limited by examination of vertical component of attraction, which acts along the normal to plane of layer. In connection with the tasks of mine/shaft gravimetry the calculation of the gravitational effect/action of arbitrarily arranged/located plane layer (leaflet) is of interest; about this will be described in Chapter IX.

Formula (V, 26) gives, in particular, value of anomaly  $\Delta g$  for horizontal flat/plane circular disk. As its geologic analogs can serve the dome-shaped platform structures of a small amplitude, arranged/located on the significant depth from the surface, laccolite-like intrusion bodies, some ore shoots, etc.

Case in question is investigated in works of L. Nettleton (1942),

I. S. Ogarinov (1958) and other authors. Value  $\Delta g$  for the case in question is expressed only approximately and besides by the very complex bulky formula, whose direct analysis for the conclusion/derivation of the rules of the solution of inverse problem so, as this is done usually and as we did above for the case of sphere, is clearly unsuitable.

Page 234.

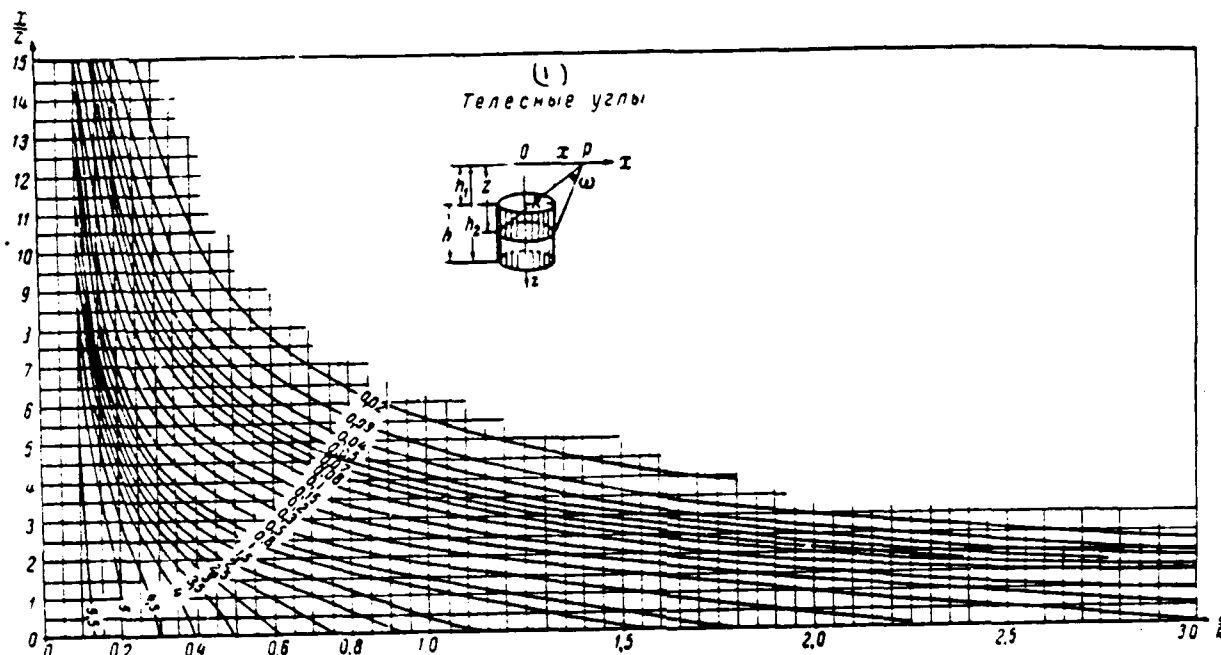


Fig. 116. Nomogram for determining solid angle of visibility  $\omega$  in the case of horizontal circular disk. According to L. Nettleton (1942) with the addition of I. S. Ogarkov (1958).

Key: (1). Solid angles.

Page 235.

Instead of this L. Nettleton constructed the convenient nomogram, which gives value  $\omega$  for the circular disk in the form

$$\omega = f\left(\frac{x}{z}, \frac{R}{z}\right),$$

where  $x$  - horizontal distance from point A to the center of disk.

$z$  - depth of bedding of disk.

$R$  - radius of disk.

This nomogram was checked, reconstructed in another form and somewhat supplemented by I. S. Ogarinov; in this form it was given in Fig. 116. Putting to use nomogram and formula (V, 26), it is possible to construct the series of the theoretical curves, whose comparison with the curve, obtained from the observations, makes it possible to determine probable values of  $z$ ,  $R$  and  $\mu$  for the body, which causes the anomaly being investigated.

Gravitational effect/action of body of revolution with arbitrary generatrix can be approximately computed, substituting this body by system of material disks (Fig. 117).

Following important model - vertical circular cylinder. With the relatively small vertical sizes/dimensions of cylinder (in comparison with the depth of its bedding) this cylinder can be approximately replaced with the circular horizontal material disk, arranged/located in the middle between the upper and lower bases.

With this likening one should assume

$$\mu = \sigma \Delta z,$$

where  $\sigma$  - volumetric density.

$\Delta z$  - low height of cylinder.

However, during this replacement errors in determination of value  $\Delta g$  can be significant, in particular with low values of  $x$ , reaching

15-25%. Therefore the direct calculation  $\Delta g$  for the vertical cylinder is of interest. Anomaly  $\Delta g$  for the case indicated so, as in the case of circular disk, is not determined in the final form and is expressed in the form of the so-called elliptical integrals. The numerical value  $\Delta g$  in this case can be determined only approximately, true with any desired degree of accuracy.

Initial integral expression  $\Delta g$  for vertical material circular cylinder of radius  $R$  with centerline along  $z$  axis, depth of upper end/face  $z_1$  and lower end/face of  $z_2$ , (Fig. 118) in horizontal cylindrical coordinate system  $(l, \alpha, z)$ :

$$\Delta g = f \sigma \int_0^R \int_0^{2\pi} \int_{z_1}^{z_2} \frac{l \, dl \, d\alpha \, dz}{(z^2 + x^2 + l^2 - 2xl \cos \alpha)^{3/2}}, \quad (V. 27)$$

where  $x = l \cos \alpha$ .



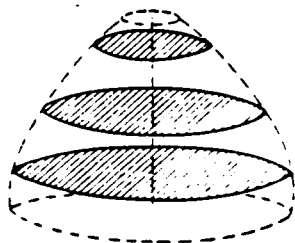


Fig. 11.7. Approximate presentation/concept of body of revolution with arbitrary generating system of material disks.

Page 236.

In work of I. S. Ogarev (1958) it is expressed in the following form:

$$\Delta g = 2f\sigma R [\Phi(\bar{x}, \bar{z}_1) - \Phi(\bar{x}, \bar{z}_2)], \quad (V. 28)$$

where

$$\bar{x} = \frac{x}{R}; \quad \bar{z}_1 = \frac{z_1}{R}; \quad \bar{z}_2 = \frac{z_2}{R};$$

$$\begin{aligned} \Phi(\bar{x}, \bar{z}_1) = & \sqrt{\bar{z}_1^2 + (\bar{x} + 1)^2} E(k) + \\ & + \left[ \frac{2\bar{z}_1^2}{\sqrt{\bar{z}_1^2 + \bar{x}^2 + 1} \sqrt{\bar{z}_1^2 + (\bar{x} + 1)^2}} - \frac{\bar{z}_1^2 + \bar{x} - 1}{\sqrt{\bar{z}_1^2 + (\bar{x} + 1)^2}} \right] K(k) + \\ & + \frac{\pi \bar{z}_1}{2} [\lambda_0(\theta, \beta) + \lambda_0(\theta, \beta_1)]; \end{aligned}$$

$$k = \sqrt{\frac{4x}{\bar{z}_1^2 + (\bar{x} + 1)^2}}; \quad \theta = \arcsin k;$$

$$\beta = \arcsin \frac{\sqrt{\bar{z}_1^2 + \bar{x}^2} - 1}{\sqrt{\bar{z}_1^2 + (\bar{x} - 1)^2}}; \quad \beta_1 = \arcsin \frac{\sqrt{\bar{z}_1^2 + (\bar{x} + 1)^2}}{\sqrt{\bar{z}_1^2 + \bar{x}^2 + 1}};$$

$$\begin{aligned} \lambda_0(\theta, \beta) = & \frac{2}{\pi} \sqrt{(1-n) \left(1 - \frac{k^2}{n}\right)} \pi(n, k); \\ n = & - \frac{2x}{x + \sqrt{\bar{z}_1^2 + x^2}}; \end{aligned}$$

$K(k)$ ,  $E(k)$ ,  $\pi(n, k)$  - respectively complete elliptic integrals of the first, second and third kinds, and  $\Phi(\bar{x}, \bar{z}_1)$  and  $\Phi(x, z_1)$  are expressed analogously with appropriate replacement of  $\bar{z}_1$  for  $\bar{z}_2$ .

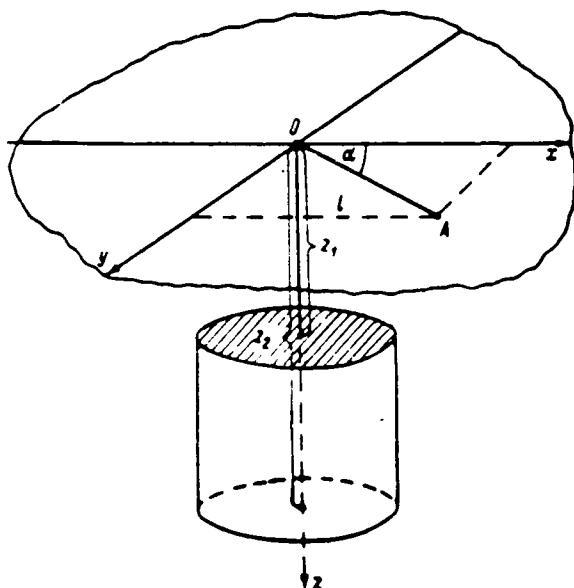


Fig. 118. To formula, which expresses gravitational effect/action of vertical cylinder.

Page 237.

There Are elliptical integrals of form  $\int R(x, \sqrt{P(x)}) dx$ , which are not expressed in the final form, where  $R$  - the rational integral function of its arguments, but  $P(x)$  - polynomial of the third or fourth power. In more detail about these integrals see in V. I. Smirnov (1958, Vol. 3).

For calculation  $\Phi(\bar{x}, \bar{z}_1)$  and  $\Phi(\bar{x}, \bar{z}_2)$  in formula (V, 28) I. S. Ogarev compiled the nomogram given in Fig. 119, on vertical axis of which is deposited value  $x$ , and on horizontal -  $z_1$  or  $z_2$ ; on point of intersection of corresponding coordination tracks of interpolation

between enumerated isolines is located unknown value  $\Phi(x, z_1)$  or  $\Phi(x, z_2)$ . With the help of the nomogram and the formula (V, 28) can be calculated the theoretical curves  $\Delta g$  for the vertical cylinders, whose comparison with the factual curve makes it possible to determine probable values of  $z_1$ ,  $z_2$ ,  $R$  and  $\sigma$  the cylindrical body, by effect/action of which can be caused the anomaly being investigated.

It is necessary to note that at points, arranged/located above axis of vertical cylinder, i.e., points of maximum of anomaly, value  $\Delta g$  is determined by simple final expression. Actually, assuming/setting  $x=0$  in the initial formula and implementing integration, we obtain

$$\begin{aligned}\Delta g(0) &= f\sigma \int_0^R \int_0^{2\pi} \int_{z_1}^{z_2} \frac{z l dl d\alpha dz}{(z^2 + l^2)^{3/2}} = 2f\pi\sigma \int_0^R \int_{z_1}^{z_2} \frac{z l dl dz}{(z^2 + l^2)^{3/2}} = \\ &= 2f\pi\sigma \int_{z_1}^{z_2} \left(1 - \frac{z}{\sqrt{z^2 + R^2}}\right) dz = \\ &= 2f\pi\sigma [z_2 - z_1 - \sqrt{z_2^2 + R^2} + \sqrt{z_1^2 + R^2}]. \quad (V, 29)\end{aligned}$$

With the help of formula (V, 29) it is possible to compute distribution of anomaly  $\Delta g$  along centerline of cylinder above its upper end/face. The anomalous field above the cylinder, obviously, possesses the property of axial symmetry. From the theory of potential it is known that in this case, knowing field distribution along the centerline, it is possible to determine its distribution along the line, perpendicular to axis, using the series/number, as coefficients of which serve Legendre's polynomials (Idel'son, 1936, pg. 205-208).

Page 238.

This gives another method of calculation  $\Delta g$  for the vertical cylinder according to the profile which intersects its centerline, which can be considered the independent testing of calculations using the method described above. This method of calculation  $\Delta g$  also approximated, since it is necessary to be limited to the determination of several first terms of series/number.

Let us note two special cases of formula (V, 29). With  $R=\infty$  we have

$$\Delta g(0) = 2f \pi \sigma (z_2 - z_1), \quad (V, 30)$$

since two latter/last members in the formula (V, 29) can be converted to the following expression:

$$1 \sqrt{z_1^2 + R^2} - \sqrt{z_2^2 + R^2} = \frac{z_1 - z_2}{\sqrt{z_1^2 + R^2} + \sqrt{z_2^2 + R^2}},$$

which becomes zero with  $R=\infty$ .

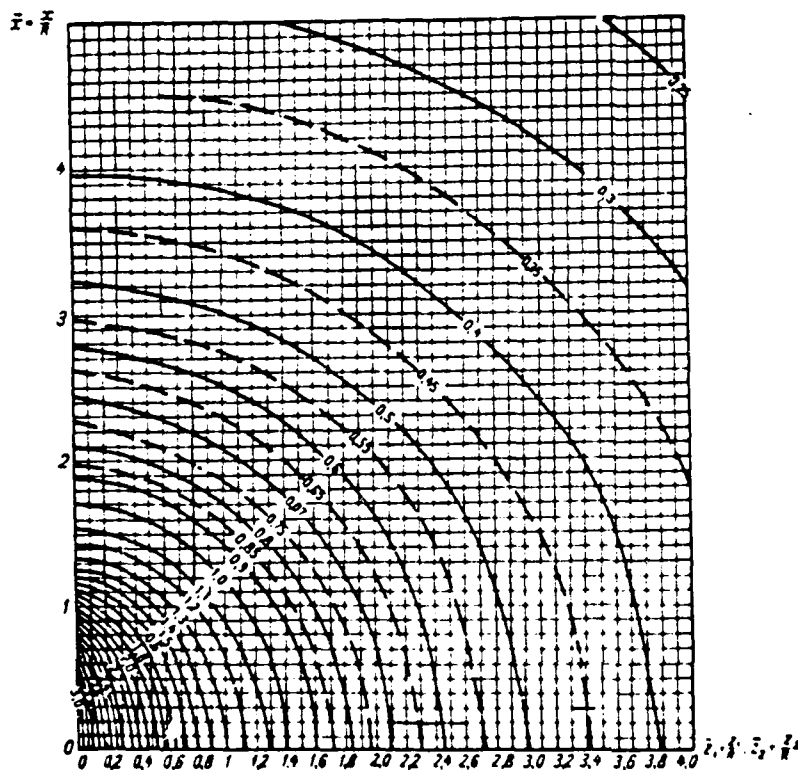


Fig. 119. I. S. Ogarinov's nomogram for determining auxiliary functions  $\Phi(\bar{x}, \bar{z}_1)$  and  $\Phi(\bar{x}, \bar{z}_2)$  during calculation of anomaly  $\Delta g$ , caused by effect/action of vertical cylinder.

Page 239.

Comparison (V, 30) (V, 26a) shows that the attraction of infinite material plane is equivalent to the attraction of infinite plane layer of bulk density  $\sigma$  and power/thickness  $(z_2 - z_1)$ , if the density  $\mu$  of material plane taken in the form

$$\mu = \sigma (z_2 - z_1). \quad (V. 31)$$

With  $z_2 = \infty$  we have

$$\Delta g(0) = 2/\pi \sigma \left[ \sqrt{z_1^2 + R^2} - z_1 \right], \quad (V. 32)$$

since terms with  $z_1$ , they are converted to the expression

$$z_1 - \sqrt{z_1^2 + R^2} = \frac{-R^2}{z_1 + \sqrt{z_1^2 + R^2}},$$

which becomes zero with  $z_1 = \infty$ .

As we already indicated, expression  $\Delta g(0)$  represents maximum value of  $\Delta g$ , caused by effect/action of vertical cylinder. Formulas (V, 23) and) V, 32) show that  $\Delta g$  remains final both in the case of vertical material rod and in the case of the vertical cylinder of the terminal radius, when the lower end of the rod or of cylinder is found at infinite removal/distance from the plane of observations.

Formula (V, 32) can be converted also to following form:

$$\Delta g(0) = \frac{2f \pi \sigma R}{\sqrt{z_1^2 + R^2} + z_1} \quad (V, 32a)$$

### § 36. Rectangular prism.

As geologic analogs of rectangular prism can serve block structures of type of horsts or grabens, some ore shoots, whose form in final form is determined by the fault-shift displacement, etc. The examination of this case is of interest, also, in other respects: during the construction of measuring grids for calculating the gravitation effect of the three-dimensional bodies of the arbitrary form (see Chapter VI), during the calculation of gravitation effect of mine workings under the conditions of subterranean gravitational

prospecting (Mudretsova, 1960). Of the formulas of the gravitational effect/action for the parallelepiped we below will obtain how a special case, formula for the step and the vertical bed.

Analytical solution of inverse problem for case in question is not developed, the reason for which is the complexity of the corresponding formulas. Below we are limited to the solution of direct problem of interpretation for  $\Delta g$ ,  $W_{xx}$ ,  $W_y$  and  $W_{xz}$  and by graphical solution of inverse problem on  $W_{xz}$  for one special case.

Let us examine rectangular prism, limited by planes  $x = x_1$ ,  $x = x_2$ ,  $y = y_1$ ,  $y = y_2$ ,  $z = z_1$  and  $z = z_2$ , (Fig. 120).

Page 240.

Let us designate the excess density of the parallelepiped by  $\sigma$ . The first of the formulas (III, 8) under the conditions indicated gives the following expression  $\Delta g$ :

$$\Delta g = -f\sigma \left[ x \ln(y + R) + y \ln(x + R) + z \arctg \frac{zR}{xy} \right]_{x_1, y_1, z_1}^{x_2, y_2, z_2} \quad (V, 33)$$

Let us transfer origin of coordinates from observation point to center of rectangle, which represents projection of parallelepiped on plane xoy (i.e. let us change sign in x and y) and will designate length of this rectangle along x axis by 2a, and the length along y axis - by 2b. Then



$$\Delta g = f\sigma \left[ x \ln(R-y) + y \ln(R-x) - z \operatorname{arctg} \frac{zR}{xy} \right]_{-a, -b, -c}^{a, b, c} =$$

$$= 2f\sigma \left[ a \ln \frac{r-b}{r+a} + b \ln \frac{r-a}{r+b} - 2z \operatorname{arctg} \frac{zr}{ab} \right]_{z_1}^{z_2}, \quad (V, 34)$$

where

$$r = \sqrt{a^2 + b^2 + z^2}.$$

Formulas (V, 33) and (V, 34) are fairly complicated: (V, 33) present result of successive substitution of six limiting values into trinomial, i.e., in expanded form are included 24 members; (V, 34) include 6 members, more complex structure than in (V, 33).

Expressions of second derivatives are much more simply obtained. The second of the formulas (III, 8) gives:

$$W_{xz} = 3f\sigma \iiint \frac{xz \, dx \, dy \, dz}{(x^2 + y^2 + z^2)^{5/2}} = -f\sigma \iint \left| \frac{z \, dy \, dz}{(x^2 + y^2 + z^2)^{3/2}} \right|_{x_1}^{x_2} =$$

$$= f\sigma \int \left| \frac{dy}{(x^2 + y^2 + z^2)^{1/2}} \right|_{x_1, z_1}^{x_2, z_2} = f\sigma \ln(y+R) \Big|_{x_1, y_1, z_1}^{x_2, y_2, z_2}, \quad (V, 35)$$

where as before  $R = \sqrt{x^2 + y^2 + z^2}$ .

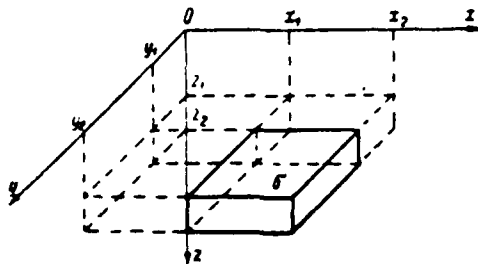


Fig. 120. Rectangular prism.

Page 241.

The third of the formulas (III, 8) gives:

$$\begin{aligned}
 W_{\Delta} &= 3f\sigma \iiint \frac{y^2 - z^2}{(x^2 + y^2 + z^2)^{3/2}} dx dy dz = \\
 &= f\sigma \iiint \frac{3y^2 - R^2}{(x^2 + y^2 + z^2)^{3/2}} dx dy dz = f\sigma \iiint \frac{3x^2 - R^2}{(x^2 + y^2 + z^2)^{3/2}} \times \\
 &\times dx dy dz = f\sigma \left[ \operatorname{arctg} \frac{yz}{xR} - \operatorname{arctg} \frac{xz}{yR} \right]_{x_1, y_1, z_1}^{x_2, y_2, z_2}. \quad (V, 36)
 \end{aligned}$$

Expression  $W_{xz}$  from appropriate formula (III, 8)

$$\begin{aligned}
 W_{xz} &= 3f\sigma \iiint \frac{2x^2 - (x^2 + y^2)}{(x^2 + y^2 + z^2)^{3/2}} dx dy dz = \\
 &= -f\sigma \left[ \operatorname{arctg} \frac{xy}{zR} \right]_{x_1, y_1, z_1}^{x_2, y_2, z_2}. \quad (V, 37)
 \end{aligned}$$

During transfer, it is analogous with the preceding, the origin of coordinates to center of horizontal projection of parallelepiped of formula (V, 35), (V, 36) and (V, 37) change into following:

$$W_{xz} = f\sigma \left[ \ln(R - y) \right]_{-a, -b, z_1}^{a, b, z_2}, \quad (V, 38)$$

$$W_{\Delta} = f\sigma \left[ \operatorname{arctg} \frac{yz}{xR} - \operatorname{arctg} \frac{xz}{yR} \right]_{-a, -b, z_1}^{a, b, z_2}, \quad (V, 39)$$

$$W_{xz} = f\sigma \left[ \operatorname{arctg} \frac{xy}{zR} \right]_{-a, -b, z_1}^{a, b, z_2}, \quad (V, 40)$$

where as before  $2a$  - length of parallelepiped along  $x$  axis;  $2b$  - along  $y$  axis.

It is known about utilization of expression (V, 40) for special case of  $z, \infty$ , i.e., virtually for case of right angled block or beam of very large vertical sizes/dimensions. In this case the formula (V, 40) is simplified and can be rewritten in the form

$$W_{xx} = -f\sigma \left| \operatorname{arctg} \frac{zy}{z_1 R} \right|_{-1, -b}^{a, b} \quad (V, 41)$$

French geophysicists (G. Shasne de Jem and A. Odi, 1957) published two log-log measuring grids for solving inverse problem of interpretation on  $W_{xx}$ , on the basis of formula (V, 41), for two cases, given in Fig. 121 and 122:

$$\begin{aligned} b &= a, \\ b &= 2a. \end{aligned}$$

Page 242.

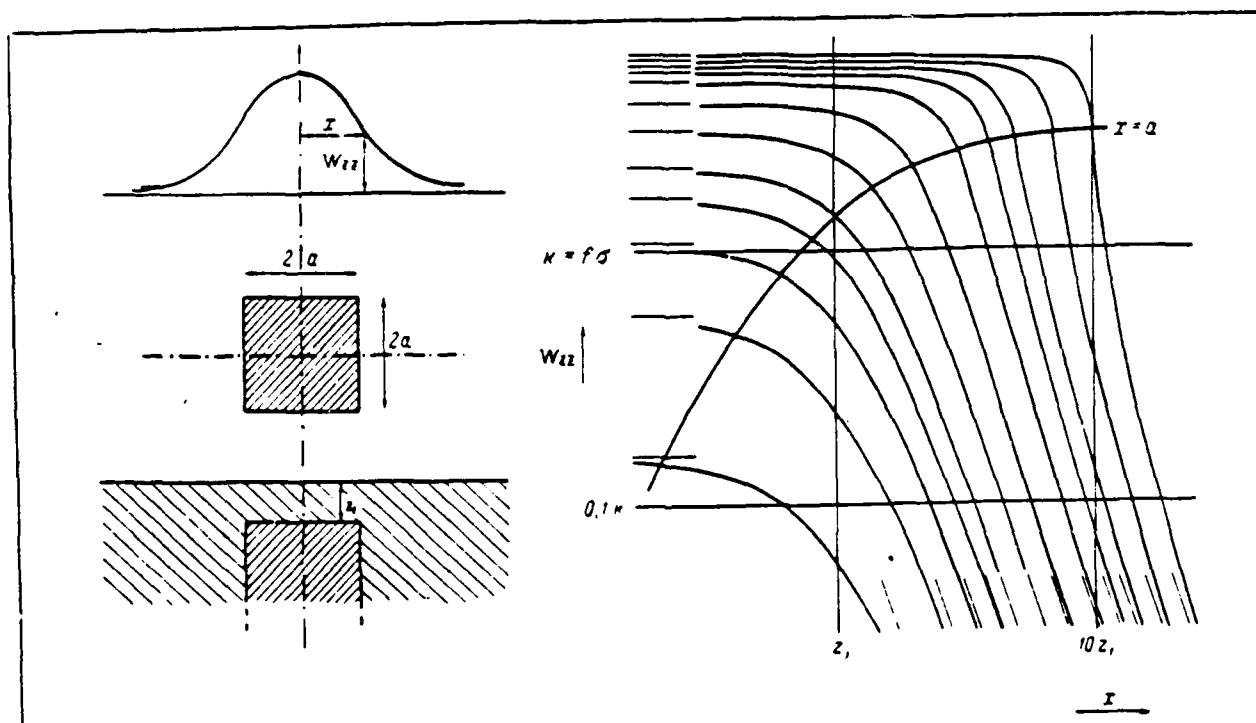


Fig. 121. Template for  $w_{12}$  in the case of right angled beam with  $z_1 = \infty$ ,  $b = a$ . According to G. Shasne de Jeri and A. Odi (1957).

Page 243.

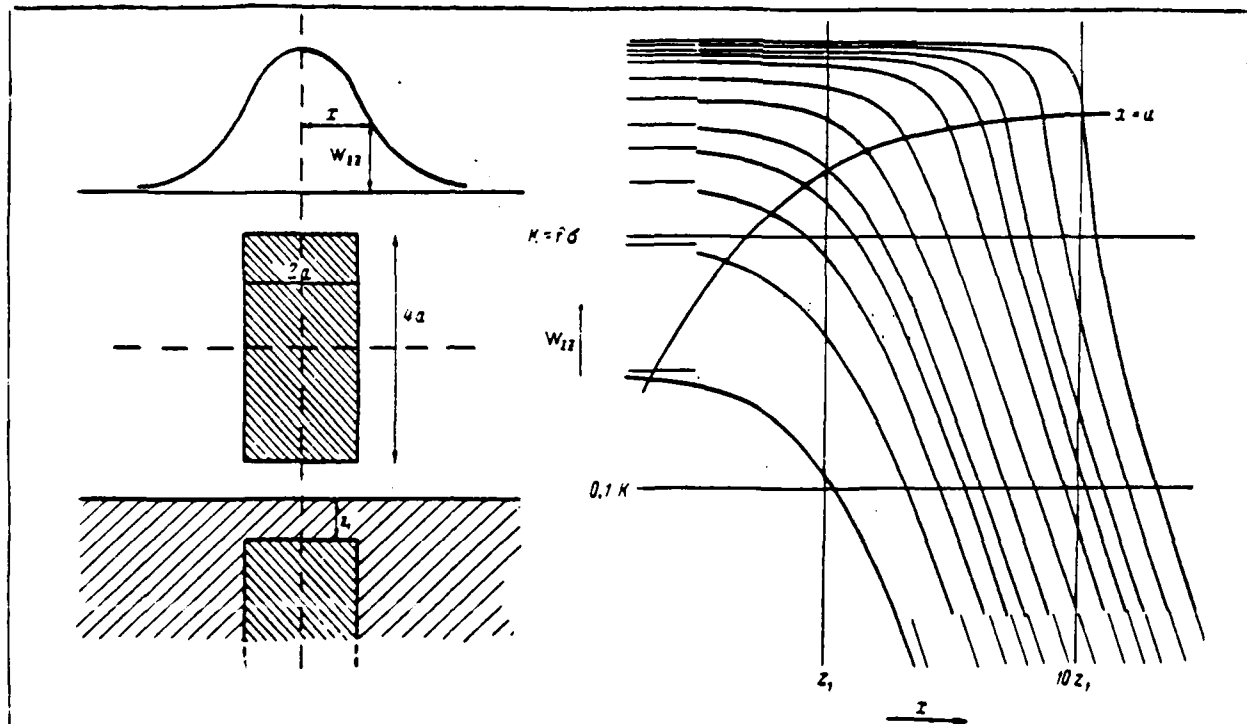


Fig. 122. The measuring grid for  $w_{12}$  in the case of right angled beam with  $z_1 = \infty$ ,  $b = 2a$ . According to G. Shasne de Jeri and A. Odi (1957).

Page 244.

According to these measuring grids, via coincidence of segment of factual curve (constructed also on the log-log scale) with most adequate/approaching theoretical curve, is determined depth  $z_1$  (on left vertical straight line), multiplier  $K = f\sigma$  (on upper horizontal line) and position of edge of block ( $x = a$ ) along secant curved line of measuring grid.

It is possible to demonstrate, on the basis of formula (V, 25), what by formula, analogous (V, 41), can be expressed also gravitational effect/action on  $\Delta g$  element of plane layer with surface density of  $\mu = \sigma \Delta z$  ( $\Delta z$  - small value) with boundary outline, which presents horizontal section of right angled block and situated on depth  $z_1$ . Thus, if we there is the basis/base assume that value  $\Delta z$  is low, that on anomaly  $\Delta g$  with the help of the given measuring grids it is possible to determine depth  $z_1$ , value  $\mu = \sigma \Delta z$  and coordinate  $x=a$ . If  $\sigma$  is assigned, then is determined  $\Delta z$ .

§ 37. Other cases of the three-dimensional problem.

Based on example of vertical cylinder we clearly saw that calculation of gravitation effect can prove to be difficult even for bodies of very simple geometric form: anomaly either not at all is expressed in final form or it is expressed by very bulky formulas, extremely inconvenient for direct utilization. In all similar cases in practice worthwhile is not the analytical, but graphic (measuring grid) method of solving the inverse problem: construction and utilization of nomograms and atlases of the theoretical curves of anomaly for the bodies of one or the other form and the comparison of these curves with anomaly curves, obtained from the field observations. Certainly, latter/last way in the majority of the cases is not simple and long, since it requires constructions for the whole class of the solutions of direct problem, that not is only connected with the large volume of calculating and drawing work, but, the main

thing, it requires the good agreement of geometric model to the real shape of geologic bodies, in what we far from always can be assured. In the absence of a similar conformity can prove to be preferable the methods of interpretation for the bodies of the arbitrary form, to presentation of which is dedicated the following chapter.

Here we give short survey/coverage of experiments, carried out according to theory of interpretation for cases of some three-dimensional bodies of correct geometric of form.

By L. I. Gavrilov (1945) and A. A. Yun'kov (1952) examined cases of paraboloid of revolution and elliptical paraboloid, elongated along vertical axis. These authors indicate the methods of solving direct and reverse problems of interpretation for the paraboloid on  $\Delta g$ ,  $W_{xx}$  and  $W_y$ . According to gravitational data they are determined the depth of focus of paraboloid and, at the known excess density  $\sigma$ , parameter  $p$  of the parabolas, which present the sections of the lateral surface of paraboloid<sup>1</sup>.

FOOTNOTE<sup>1</sup>. Without knowledge of  $\sigma$  there is determined only the product of  $\sigma p$  for the paraboloid. ENDFOOTNOTE.

Subsequently, by A. A. Yun'kov and N. A. Fedotovoy (1952) examined the case of sloping elliptical paraboloid.

By N. N. Pariyskiy (1950) is indicated the method of calculating

anomaly  $\Delta g$  for case of vertical hyperbolic dome. For this case the solution of direct problem is obtained in the final form, but it is represented by very complex expression.

Page 245.

In work I. S. Gelfand (1949) there is derived the formula which presents gravitational effect of the body in the form of hemisphere.

In works of A. A. Yun'kov (1952), A. A. Yun'kov and N. L. Afanas'yev (1952) the solution to direct and reverse problems for general ellipsoid and ellipsoid of revolution is given. The corresponding formulas are very complex and bulky. Without the knowledge of excess density  $\sigma$  are determined the depth of the center of ellipsoid, a difference in the squares of its semi-axes and excess mass; with the given one  $\sigma$  are determined the absolute sizes/dimensions of semi-axes. The point of the maximum value  $\Delta g$  and, respectively, the zero value of horizontal gradient proves to be that coinciding with the projection of the center of ellipsoid on the plane of observations. N. L. Afanas'yev (1952) examined also direct and reverse problems for the layers of elliptical paraboloid and paraboloid of revolution.

For the majority of the cases enumerated above auxiliary nomograms, which facilitate construction of corresponding theoretical anomalous curves (Yun'kov, Afamas'yev, Fedorov, 1953), are published.



§ 38. Horizontal material rod, horizontal circular cylinder.

As geologic analogs of circular horizontal cylinder can serve linear structures (anticlinal and synclinal folds), ore shoots of vein-like and lenticular form, etc.

Above (§ 34) we indicated the equivalency of gravitational effect of spherical and mass point; the same kind equivalency occurs with respect to gravitational effect/action of infinite uniform circular cylinder and infinite material rod. Cylinder conditions the same anomalous gravitational field as material linear rod with the same mass distribution per unit of length, arranged/located along the centerline of cylinder (Zhukovskiy, 1950, pp. 733-737).

Fact indicated gives possibility immediately, without any calculations, to write formulas, which express gravitational effect/action of infinite horizontal circular cylinder with utilization of integrands of formulas (III, 19). However, we will obtain the same formulas somewhat by more complex way - their immediate conclusion for the cases of first final, and then infinitely long material rod, since the comparison of formulas for the cases indicated will permit us to obtain the visual presentation/concept about the conditions and the possibilities of the assumption of the infinite course/strike of geologic bodies, which we will repeatedly make subsequently.

Thus, let us examine the first problem of final horizontal linear material rod, arranged/located symmetrically relative to coordination plane xoz (Fig. 123). For the calculation we will use horizontal cylindrical coordinate system.

Page 246.

The coordinates of the ends of the rod let us designate through  $(x, y, h)$ , and  $(x, -y, h)$ , and its linear density by  $\lambda$ . From the formulas (III, 9), assuming/setting in them  $dm = \lambda dy$ , we have for the origin of the coordinates

$$\begin{aligned}\Delta g &= f \lambda \int_{-y}^y \frac{q \sin \theta}{(y^2 - q^2)^{3/2}} dy = f \lambda q \sin \theta [I_1(y)]_{-y}^y, \\ W_{xz} &= \frac{3f\lambda}{2} \int_{-y}^y \frac{q^2 \sin 2\theta}{(y^2 - q^2)^{3/2}} dy = \frac{3}{2} f \lambda q^2 \sin 2\theta [I_2(y)]_{-y}^y, \\ W_x &= 3f\lambda \int_{-y}^y \frac{y^2 - q^2 \cos^2 \theta}{(y^2 - q^2)^{3/2}} dy = 3f\lambda \int_{-y}^y \frac{(y^2 - q^2) - q^2(1 - \cos^2 \theta)}{(y^2 - q^2)^{3/2}} dy = \\ &= 3f\lambda \left\{ [I_1(y)]_{-y}^y - q^2(1 + \cos^2 \theta) [I_2(y)]_{-y}^y \right\}, \\ W_{xz} &= 3f\lambda \int_{-y}^y \frac{q^2(3 \sin^2 \theta - 1) - q^2}{(q^2 - y^2)^{3/2}} dy = \\ &= 3f\lambda \int_{-y}^y \frac{q^2(3 \sin^2 \theta - 1) - (q^2 - y^2 - q^2)}{(q^2 - y^2)^{3/2}} dy = \\ &= 3f\lambda \left\{ [I_1(y)]_{-y}^y + q^2(2 \sin^2 \theta - 2) [I_2(y)]_{-y}^y \right\},\end{aligned}$$

where  $I_1(y)$  and  $I_2(y)$  - integrals calculated in § 17 of Chapter III.

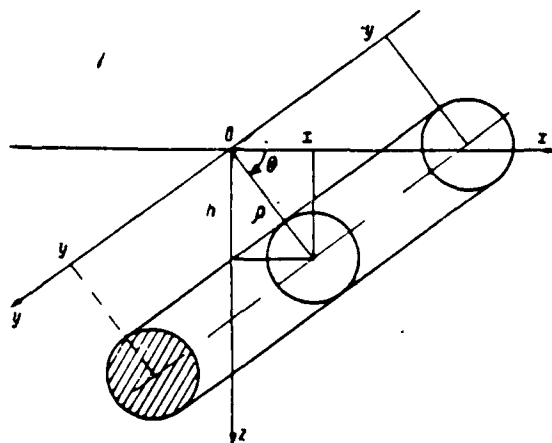


Fig. 123. Determination of gravitational effect of linear material rod.

Page 247.

Taking into account values of these integrals, making substitutions indicated and returning in basic (independent from  $y$ ) expression to right angled coordinates, connected with cylindrical relationships/ratios

$$\begin{aligned} x &= \rho \cos \theta, \\ z &= \rho \sin \theta, \\ \sqrt{x^2 + z^2} &= \rho, \\ y &= y. \end{aligned}$$

and accepting  $z=h$ , we obtain following resultant expressions

$\Delta g$ ,  $W_{xx}$ ,  $W_{yy}$  and  $W_{zz}$  for final linear rod:

$$\left. \begin{aligned} \Delta g &= 2f\lambda \frac{x}{x^2 + h^2} f_1(y), \\ W_{xx} &= 2f\lambda \frac{xh}{(x^2 + h^2)^2} [3f_1(y) - f_2(y)], \\ W_{yy} &= 2f\lambda \frac{1}{(x^2 + h^2)} [-3x^2 f_1(y) + (x^2 + \rho^2) f_2(y)], \\ W_{zz} &= 4f\lambda \frac{1}{x^2 + h^2} \left[ f_1(y) + \frac{3x^2 - 2\rho^2}{\rho^2} \left[ f_1(y) - \frac{1}{3} f_2(y) \right] \right]. \end{aligned} \right\} (V, 42)$$

where

$$\left. \begin{aligned} f_1(y) &= \frac{y}{\sqrt{y^2 + Q^2}}, \\ f_2(y) &= \frac{y^2}{(y^2 + Q^2)^{3/2}}. \end{aligned} \right\} \quad (V, 43)$$

With  $y \rightarrow \infty$   $f_1(y) = f_2(y) = 1$ , and we obtain appropriate expressions for infinite linear rod:

$$\left. \begin{aligned} \Delta g &= 2f\lambda \frac{h}{x^2 + h^2}, \\ W_{xx} &= 4f\lambda \frac{xh}{(x^2 + h^2)^2}, \\ W_{xx} = W_{\Delta} &= 2f\lambda \frac{h^2 - x^2}{(x^2 + h^2)^2}. \end{aligned} \right\} \quad (V, 44)$$

Here, as always in the case of two-dimensional problem (see S 17-18, Chapter III), we have  $W_{xx} = W_{\Delta}$ . In the following presentation we retain only the first of these designations.

Page 248.

Formulas (V, 44) express gravitational effect also of infinite circular horizontal cylinder, moreover, in this case by  $\lambda$  there should be understood the product of volumetric excess density  $\sigma$  of cylinder to area of its cross section, i.e.

$$\lambda = \sigma S = \sigma \pi R^2, \quad (V, 45)$$

where  $R$  - radius of cross section of cylinder.

Subsequently we examine series/number of cases of bodies of infinite course/strike, i.e. cases of two-dimensional problem of interpretation. All real geologic bodies have finite dimensions on

the course/strike. Above (§ 18, Chapter III) we already indicated that for many such bodies with the interpretation of the gravity anomalies caused by them it is possible to put to use the formulas of the two-dimensional problem, i.e., to accept assumption about their infinite course/strike. Now, comparing formulas (V, 42) and (V, 44), we can be convinced of the possibility of this assumption based on the example of horizontal linear rod.

Let us designate values, which stand in left sides of formulas (V, 42) and relating to crux of finite dimensions, by index  $k$ , and value in left sides of formulas (V, 35), that relate to infinitely long rod, by index  $\infty$ . Let us introduce into the examination the following relations<sup>1</sup>:

$$\left. \begin{aligned} \delta_g &= \frac{\Delta g_{\infty} - \Delta g_k}{\Delta g_{\infty}}, \\ \delta_{xz} &= \frac{(W_{xz})_{\infty} - (W_{xz})_k}{(W_{xz})_{\infty}}, \\ \delta_{\Delta} &= \frac{(W_{\Delta})_{\infty} - (W_{\Delta})_k}{(W_{\Delta})_{\infty}}, \\ \delta_{zz} &= \frac{(W_{zz})_{\infty} - (W_{zz})_k}{(W_{zz})_{\infty}}. \end{aligned} \right\} \quad (V, 46)$$

FOOTNOTE <sup>1</sup>. The examination of the relations indicated makes sense, of course, only for the different from zero values anomalous elements.  
ENDFOOTNOTE.

These values characterize relative value of disagreement of values  $\Delta g$ ,  $W_{xz}$ ,  $W_{\Delta}$  and  $W_{zz}$  upon transfer from crux of finite length to infinitely long rod. From the formulas (V, 42) and (V, 43) it is possible to see that these disagreements depend on the relation

$$r = \frac{y}{y_0}.$$

since formula (V, 43) it is possible to rewrite in the form

$$f_1(y) = \frac{1}{\sqrt{1+e^2}} = (1+e^2)^{-1/2},$$

$$f_2(y) = \frac{1}{(1+e^2)^{3/2}} = (1+e^2)^{-3/2}.$$

Page 249.

For points located near the axis of the rod, i.e., in the region of the most intensive manifestation of anomaly caused by it, in majority of cases assumption  $e < 1$  is correct. Then it is possible to write

$$\left. \begin{aligned} f_1(y) &= 1 - \frac{1}{2} e^2 + \frac{3}{8} e^4 - \dots \\ f_2(y) &= 1 - \frac{3}{2} e^2 + \frac{15}{8} e^4 - \dots \end{aligned} \right\} \quad (V, 47)$$

Being limited to terms  $e^4$  in written expressions and taking into account formula (V, 42), (V, 43), (V, 44) and (V, 46), we obtain:

$$\left. \begin{aligned} \delta_g &= \frac{1}{2} e^2 + \frac{3}{8} e^4, \\ \delta_{x_1} &= \frac{3}{8} e^4, \\ \delta_s &= 1 - \frac{1}{x^2 - x^2} [-3x^2 f_1(y) + (h^2 + Q^2) f_2(y)], \\ \delta_{11} &= 1 - \frac{h^2}{h^2 - x^2} \left[ 3 - \frac{Q^2}{h^2} f_1(y) - f_2(y) \right]. \end{aligned} \right\} \quad (V, 48)$$

As we see, errors for the noninfinity of course/strike in  $\Delta g$  and  $W_{11}$  have constant values in segment of profile, within which  $e < 1$ . At the same time, errors in  $W_s$  and  $W_{11}$  are functions  $x$  and  $h$ , i.e., by values by variables. With  $x=0$  and  $h=\rho$ , i.e., above the centerline of rod  $^1$ , error  $\delta_s$  and  $\delta_{11}$  have the following values:

$$\left. \begin{aligned} \delta_{\Delta} &= \frac{3}{2} e^2 - \frac{15}{8} e^4, \\ \delta_{zz} &= -\frac{1}{2} e^2 + \frac{9}{8} e^4. \end{aligned} \right\} \quad (V, 48a)$$

FOOTNOTE<sup>1</sup>. Below we will see, that with  $x=0$   $w_{\Delta}$  and  $w_{zz}$ ,  $\Delta g$  have the maximum values. ENDFOOTNOTE.

Formulas (V, 48) and (V, 48a) show that effect of the noninfinity of course/strike on different derivatives must be sharply different. With  $\epsilon=0.5$  ( $y=2\rho$ ) and  $x=0$  we have, for example:

$$\begin{aligned} e^2 &= 0,2500, \\ e^4 &= 0,0625, \\ \delta_g &= \frac{1}{2} \cdot 0,2500 + \frac{3}{8} \cdot 0,0625 = 0,1250 + 0,0234 = 0,1484, \\ \delta_{zz} &= \frac{3}{8} \cdot 0,0625 = 0,0234, \\ \delta_{\Delta} &= \frac{3}{2} \cdot 0,2500 - \frac{15}{8} \cdot 0,0625 = 0,3750 - 0,1170 = 0,2580, \\ \delta_{zz} &= -\frac{1}{2} \cdot 0,2500 + \frac{9}{8} \cdot 0,0625 = -0,1250 + 0,0702 = -0,0548. \end{aligned}$$

Page 250.

Thus, absolute magnitudes of error for the noninfinity of course/strike of rod for different derivatives of gravitational potential in this case comprise: for  $\Delta g$  — 15%, for  $w_{zz}$  — 2%, for  $w_{\Delta}$  — 26%, for  $w_{zz}$  — 5%.

With further decrease  $\epsilon$ , i.e., with increase in length of rod, errors for all derivatives are sharply reduced (Table 17).

Most interesting fact as results of those produced of above

calculations (not noted, until now, in the literature on gravitational prospecting) consists in sharp difference in effect of noninfinity of courses/strikes of rod on  $W_{\Delta}$  and  $W_{xx}$ , whose values, as we already know, identically coincide for infinitely long rod.

How it is possible to explain relatively great effect of noninfinity of course/strike on value  $W_{\Delta}$ ? The fact here is that into the expression

$$W_{\Delta} = \frac{\partial^2 W}{\partial y^2} - \frac{\partial^2 W}{\partial x^2}$$

directly enters the derivative  $\frac{\partial^2 W}{\partial y^2}$  in the direction of the course/strike of rod (equal to zero with  $y=\infty$  and not entering into expression  $W_{xx}$ ), most sensitive to the noninfinity of course/strike along y axis is obvious.

Let us explain now effect of noninfinity of course/strike of rod on variation anomaly

$$\delta \Delta g(x, l) = \Delta g(x) - \frac{\Delta g(x+l) + \Delta g(x-l)}{2}, \quad (V, 40)$$

where x - moving coordinate of point on axis x (line of observations of that going transversely of course/strike of rod); l - linear parameter.



Table 17. Absolute values  $\delta_g$ ,  $\delta_{xz}$ ,  $\delta_\Delta$  and  $\delta_{zz}$  (in the percentages).

$\epsilon$	$ \delta_g $	$ \delta_{xz} $	$ \delta_\Delta $	$ \delta_{zz} $
0.500	15	2	26	5
0.300	4	0	12	4
0.200	2	0	6	2
0.100	1	0	1	0

Page 251.

On the basis of those written above expressions [see first of formulas (V, 42), (V, 43), (V, 44), (V, 47)] values of anomalous elements in formula (V, 49) they can expressed as follows.

For it is infinite rod:

$$\begin{aligned}\Delta g_\infty(x) &= 2f\lambda \frac{h}{x^2 + h^2}, \\ \Delta g_\infty(x+l) &= 2f\lambda \frac{h}{(x+l)^2 + h^2}, \\ \Delta g_\infty(x-l) &= 2f\lambda \frac{h}{(x-l)^2 + h^2}.\end{aligned}$$

For final rod, half of length of which is equal to  $y$ :

$$\begin{aligned}\Delta g_h(x) &= 2f\lambda \frac{h}{x^2 + h^2} \left[ 1 - \frac{x^2 + h^2}{2y^2} + \frac{3}{8} \left( \frac{x^2 + h^2}{y^2} \right)^2 \right], \\ \Delta g_h(x+l) &= 2f\lambda \frac{h}{(x+l)^2 + h^2} \left[ 1 - \frac{(x+l)^2 + h^2}{2y^2} + \frac{3}{8} \left( \frac{(x+l)^2 + h^2}{y^2} \right)^2 \right], \\ \Delta g_h(x-l) &= 2f\lambda \frac{h}{(x-l)^2 + h^2} \left[ 1 - \frac{(x-l)^2 + h^2}{2y^2} + \frac{3}{8} \left( \frac{(x-l)^2 + h^2}{y^2} \right)^2 \right].\end{aligned}$$

Hence we find

$$\begin{aligned}\delta_A &= \frac{\Delta g_\infty - \Delta g_h}{\Delta g_\infty} \\ &= \frac{3}{8} \frac{l^2}{y^4 \left[ \frac{1}{x^2 + h^2} - \frac{1}{2} \left( \frac{1}{(x+l)^2 + h^2} + \frac{1}{(x-l)^2 + h^2} \right) \right]} \quad (V, 50)\end{aligned}$$

or in the particular case with  $x=0$ , i.e., for point, arranged/located above axis of rod:

$$\delta_0 = \frac{3}{8} \epsilon^2 \left[ \left( \frac{l}{y} \right)^2 + \epsilon^2 \right]. \quad (V, 50a)$$

where, it is analogous with preceding, is marked

$$\epsilon = \frac{h}{y}.$$

FOOTNOTE<sup>1</sup>. Below we will see, which  $\delta \Delta g(x, l)$  reaches maximum value with  $x=0$ . ENDFOOTNOTE.

Let us compare formulas (V, 50a) (V, 48). Let us assume that  $l \ll y$ , then from (V, 50a) we have

$$\delta_0 \approx \frac{3}{8} \epsilon^4,$$

i.e. in this case an effect of noninfinity of the course/strike of rod on  $\delta \Delta g(x, l)$  almost the same as on  $W_{xx}$ , it is very small (see Table 17).

Page 252.

Let us allow now that  $l=y$ . In this case we have from the formula (V, 50a)

$$\delta_0 = \frac{3}{8} (y^2 + y^4).$$

As we see, in this case  $\delta_0 \approx \delta_{xx}$ . But if

$$0 < \frac{l}{y} < 1,$$

then value  $\delta_0$  has the intermediate value between values  $\delta_{xx}$  and  $\delta_{yy}$ .

Hence follows that at calculation  $\delta \Delta g(x, l)$  parameter  $l$  it is necessary to try to take by such so that there would be  $l < y$ , where  $y$  -

distance of nearest to profile end of intersected by it banded linear anomaly (i.e. to zone of closing/shorting those contouring anomaly of the isoanomaly).

Conclusions about the effect of noninfinity of course/strike (based on example of horizontal material rod) it is possible to do similar:

1. It proves to be that even without resorting to the special calculating operations, which weaken the effect of the finite dimensions of geologic bodies on their course/strike, like the summation of the values of anomalous elements along the parallel profiles, described above in chapter III, it is possible in many instances of practice to disregard this effect and to put to use with the interpretation of anomalies the formulas of two-dimensional problem.

2. Difference in gravitational effect/action of final and infinite on course/strike body proves to be sharply different depending on value of ratio of length of body to depth of its bedding; it considerably increases/grows with decrease of this relation and is reduced with its increase.

3. Effect of noninfinity of course/strike proves to be sharply different for different elements of anomalous gravitational field. In the ascending order of this effect from the minimum relative values to the maximum the elements of anomalous gravitational field are placed

(approximately) in this sequence:  $W_{xx}$ ;  $W_{zz}$  and  $\delta\Delta g$ ;  $\Delta g$ ;  $W_{\Delta}$ .

Thus, for utilization of two-dimensional models of geologic bodies with quantitative interpretation most suitable (of that examined above) are following elements of anomalous gravitational field: horizontal gradient  $W_{xz}$ , lapse  $W_{zz}$  and variation anomaly  $\delta\Delta g$ .

Page 253.

Let us return now to formulas (V, 35), that expresses gravitational effect/action of horizontal circular cylinder or material crux of infinite course/strike. Let us change the sign in coordinate  $x$  in these formulas, i.e., we convert them to that case, when the origin of coordinates is placed above the centerline of cylinder, and  $x$  represents observation point on the profile ( $x$  axis), which goes transversely the course/strike of cylindrical body. We will obtain for this case the following expressions:

$$\left. \begin{aligned} \Delta g &= 2f\lambda \frac{h}{x^2 + h^2}, \\ W_{xz} &= -4f\lambda \frac{xh}{(x^2 + h^2)^2}, \\ W_{zz} &= 2f\lambda \frac{h^3 - x^3}{(x^2 + h^2)^3} = W_{\Delta}. \end{aligned} \right\} \quad (V, 51)$$

It is earlier than to turn to examination of each from written expressions of derivatives of potential individually, let us note the interesting formal bond between these derivatives, which directly escapes/ensues from formulas (V, 51)

$$\Delta g = -xU_{xz} + hU_{zz}. \quad (V, 52)$$

This bond - particular result of more general/more common

relationship/ratio, which joins derivatives of potential in the case of two-dimensional problem

$$\int \Delta g \, ds = - \int x U_{xx} \, ds + \int h U_{xz} \, ds, \quad (V, 53)$$

where  $(x, h)$  - coordinate of flowing point within section of body, and integration is produced on area  $s$  of its cross section.

Formula (V, 53) directly escapes/ensues from general integral formulas of two-dimensional problem.

If gravity anomaly, caused by effect/action of infinite rod or cylinder, is known in the form  $\Delta g$ ,  $W_{xx}$  and  $W_{xz}$  then relation (V, 52) can be used for the definition of depth  $h$  of center of rod or cylinder (as let us see below, coordinate  $x$  in this case it is possible to consider as the assigned magnitude). The equations, which determine  $h$ , we in this case will have as much, as we have observation points on the profile. If  $h$  - known value, and is also known  $\Delta g$  and  $W_{xx}$ , then from the formula (V, 52) can be determined value  $W_{xz}$  respectively for each of observation points.

Let us examine now separately each of anomalous elements investigated by us.

Anomaly

$$\Delta g = 2f \lambda \frac{h}{x^2 + h^2}$$

with  $\lambda > 0$  - everywhere positive function, which has maximum with  $x=0$ ,

i.e., above axis of cylinder; in this case  $\Delta g$  - function even, i.e.,  $\Delta g(+x) = \Delta g(-x)$ , and  $\Delta g(+\infty) = \Delta g(-\infty) = 0$ . Graph  $\Delta g$  is given in Fig. 124.

Page 254.

Maximum value

$$\Delta g_{\max} = \frac{2f\lambda}{h}. \quad (V.54)$$

Let us find value of  $x=x_{1/2}$ , with which  $\Delta g = \frac{1}{2} \Delta g_{\max}$ .

Substituting this value into the first of formulas (V, 51), we find  $x_{1/2} = \pm h$ , whence

$$h = |x_{1/2}|. \quad (V.55)$$

Formulas (V, 54) and (V, 55) give  $\lambda$  and  $h$ . If it is known  $\sigma$ , then from the formula (V, 45) is determined radius  $R$  of cylinder and the depth of its upper edge (from the horizon/level of instrument)

$$H = h - R.$$

Let us write now  $\Delta g$  in more general view

$$\Delta g = 2f\lambda \frac{h-z}{x^2 + (h-z)^2} \quad (V.56)$$

and let us examine how varies  $\Delta g$  to vertical direction, i.e., with change in coordinate  $z$ .

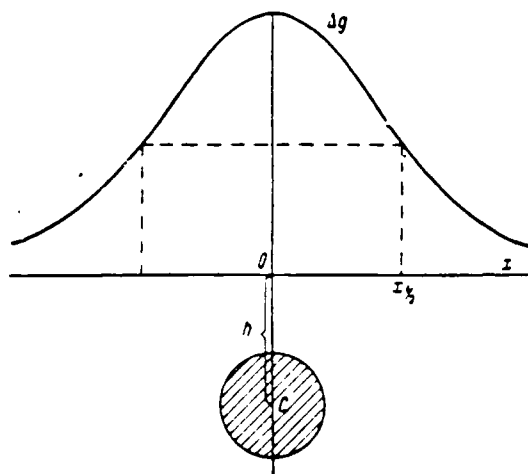


Fig. 124. Curve of anomaly  $\Delta g$  above circular horizontal cylinder.

Page 255.

Let us allow first that  $x \neq 0$ , i.e., we are found on lateral vertical profile. First of all we see that on this profile  $\Delta g > 0$  with  $z < h$  and  $\Delta g < 0$  about  $z > h$ , moreover  $\Delta g_{z=h} = 0$ . With  $z = z_0 = h$ ,  $\Delta g = 0$  (Fig. 125) thus

$$h = z_0 \quad (V, 55)$$

Differentiating formula (V, 56) through  $z$  and equalizing to zero derivative, we find

$$\frac{\partial \Delta g}{\partial z} = 0 \quad (V, 56)$$

Hence follows that  $\Delta g_{\max} = 0$  with  $x = h$ , i.e., with this value of  $x$  maximum value  $\Delta g$  is located on level of plane of observations. This gives the simple method of determination  $h$ , if distribution  $\Delta g$  is

known for several lateral vertical profiles, including that for which  $x=h$ .

Maximum value  $\Delta g$  on lateral vertical profile will be

$$\Delta g = \frac{f\lambda}{2x}. \quad (V, 59)$$

Conditions (V, 57) and (V. 59) determine values of  $h$  and  $\lambda$ . With  $x=0$  we have

$$\Delta g = \frac{2f\lambda}{h-z}, \quad (V, 60)$$

whence  $\Delta g = \infty$  with  $z=h$ . Consequently, point  $(0, h)$ , i.e., the center of rod or cylinder, represents singular point for anomaly  $\Delta g$ .



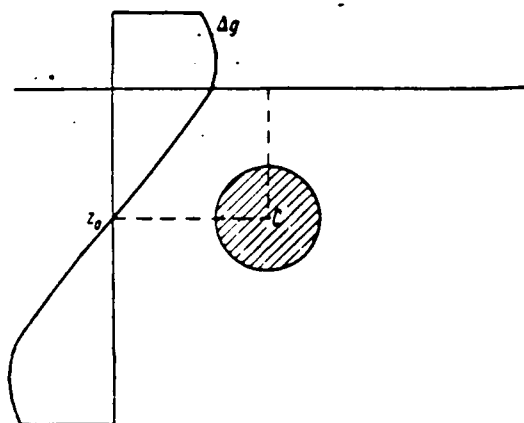


Fig. 125. Curve of anomaly  $\Delta g$  on lateral vertical profile in the case of circular horizontal cylinder.

Page 256.

Let us examine now upper segment ( $z < 0$ ) of vertical profile, passing through point  $x=0$ . From the formula (V, 60) it is evident that in this segment  $\Delta g$  gradually decreases to the zero value with  $z \rightarrow \infty$ .

Let us find point  $(0, z_{1/2})$ , at which  $\Delta g = \frac{1}{2} \Delta g|_{z=0} = \frac{f\lambda}{h}$ .

Formula (V, 60) shows that decrease  $\Delta g$  twice occurs when  $z_{1/2} = -h$ , which also gives possibility to determine depth  $h$ .

It is shown by the author (Andreyev, 1949), that analytical continuation of any potential function  $U(x, z)$ , assigned on  $x$  axis, to point  $(x', h)$  of lower half-plane ( $h > 0$ ) can be realized by summation of series

$$\text{where } SU(x', h) = \sum_{k=0}^{\infty} \Lambda_k U'(x', h), \quad (V, 61)$$

$$\Lambda_k U'(x', h) = -\frac{h}{\pi} \int_{-\infty}^{+\infty} \frac{\Lambda_{k-1} U'(x, h) - \Lambda_{k-1} U'(x', h)}{(x-x')^2 + h^2} dx, \quad (V, 61a)$$

$$\Lambda_0 U(x', h) = U(x', 0)$$

in region of convergence of this series.

Anomaly  $\Delta g$  for linear material rod is proportional to real part of analytic complex variable function  $\Psi(z) = (z_0 - z) + i(z_0 - x)$

$$\Psi(z) = \frac{1}{z} - \frac{(z_0 - z)}{(x_0 - x)^2 + (z_0 - z)^2} + i \frac{(x_0 - x)}{(x_0 - x)^2 + (z_0 - z)^2}.$$

Series, analogous to  $SU(x', h)$ , for  $\psi(\zeta)$  in case in question proves to be possible to represent in the form

$$S\psi(\zeta) = \frac{1}{\zeta_0} \sum_{k=1}^{\infty} \frac{k! h^k}{(\zeta_0 + h) \dots (\zeta_0 + kh)}. \quad (V, 62)$$

$(\zeta_0 = z_0 - iz_0).$

In analysis it is proved (Norlund, 1924) that this series, and consequently, process of analytical continuation for  $\Delta g$  descends evenly with  $h < z_0$ , and it diverges with  $h \geq z_0$ .

With  $x = x_0$ ,  $h = z_0$ , real part of  $S\psi(\zeta)$  gives

$$\frac{1}{z_0} \left\{ 1 + \frac{1}{2} + \frac{1}{3} + \dots + \frac{1}{k} + \dots \right\}.$$

(In parentheses stands the harmonic divergent series).

Thus, analytical continuation of anomaly  $\Delta g$  to horizontal profile  $z = h$  of lower half-plane is possible only to level of singular point  $(x_0, z_0)$  of anomalous field.

Page 257.

Horizontal gradient  $W_{xx}$  (the second of formulas (V, 51)) represents function positive with  $x < 0$  and negative with  $x > 0$ ,  $W_{xx}(-x) = -W_{xx}(x)$ .  $W_{xx}$  represents odd function  $x$ . With  $x = 0$ ,  $W_{xx} = 0$  becomes zero (Fig. 126). Differentiating  $W_{xx}$  through  $x$  and equalizing to zero derivative, we find

$$x_{\max} = -\frac{h}{1.3},$$

$$x_{\min} = +\frac{h}{1.3},$$

whence

$$h = 0.87 l. \quad (V.63)$$

where  $l = x_{\min} - x_{\max}$ , <sup>i.e.</sup> the distance between the points of maximum and minimum  $W_{zz}$ .

Value of maximum

$$W_{zz} = \frac{9/\lambda}{4 \sqrt{3} h^3},$$

whence

$$\lambda = 0.011 h^3. \quad (V.64)$$

Distribution  $W_{zz}$  on lateral vertical profile presents function of form

$$W_{zz} = -4/\lambda \frac{x(h-z)}{[x^2 - (h-z)^2]^2}, \quad (V.65)$$

where  $x$  constant (not equal to zero) value of horizontal coordinate.

For the

certainty we will count  $x < 0$ . Then, obviously,  $W_{zz} > 0$  with  $z < h$  and

$W_{zz} < 0$  with  $z > h$ . With  $z = z_0 = h$   $W_{zz} = 0$  (Fig. 127). At the singular point  $(0, h)$  (center of rod)  $W_{zz} = +\infty$  with the approach to the point to the left and  $W_{zz} = -\infty$  with the approach to the right.

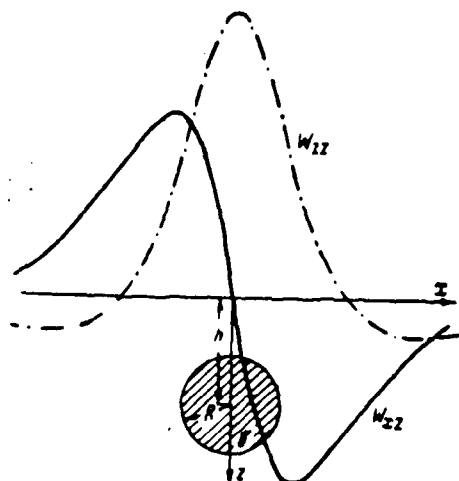


Fig. 126. Curves  $w_{zz}$  and  $w_{zx}$  above circular horizontal cylinder.

Page 258.

Differentiating expression (V, 65) on  $z$  and assuming/setting to zero obtained derivative, we find

$$\left. \begin{aligned} z_{\max} &= h - \frac{x}{\sqrt{3}}, \\ z_{\min} &= h + \frac{x}{\sqrt{3}} \end{aligned} \right\} \quad (V, 66)$$

and value of maximum

$$W_{zz} = \frac{3V\lambda}{10} \cdot \frac{1\lambda}{x^2}. \quad (V, 67)$$

Depth  $h$  is determined on position on lateral vertical profile either of zero point or point of maximum  $W_{zz}$  on the basis of formula (V, 66). From the equation (V, 67) is determined the value  $\lambda$ .

Lapse  $W_{zz}$  and curvature  $W_{\lambda}$  identically are indentical for rod, cylinder and for any body with infinite course/strike in  $y$  axis.

Since subsequently we examine only the bodies of infinite course/strike, we introduce for the values indicated single designation  $W_{xx}$  implying everywhere  $W_{xx} = W_{\Delta}$ .

If

$$W_{xx} = 2f\lambda \frac{h^2 - x^2}{(x^2 + h^2)^2},$$

then  $W_{xx}$  is function of positive in interval of  $|x| < h$  and negative with  $|x| > h$ .  $W_{xx}$  is equal to zero with  $|x| = h$ , and also with  $x = \pm\infty$ .

Hence

$$h = |x_0|, \quad (V, 68)$$

where  $x_0$  - abscissa of zero value  $W_{xx}$ .

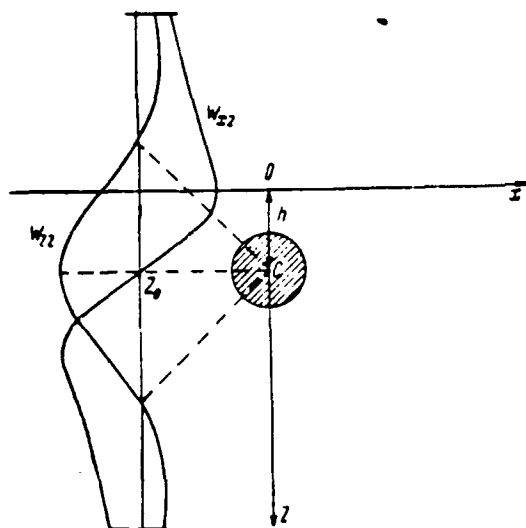


Fig. 127. Curves  $W_{zz}$  and  $W_{zz}$  on lateral vertical profile in the case of circular horizontal cylinder.

Page 259.

Investigation of derivative  $\frac{\partial}{\partial x} W_{zz}$  shows that  $W_{zz}$  has maximum when  $x_{max} = 0$  and two minima when  $x_{min} = \pm h/3$ . From the latter/last condition we have

$$h = C |x_{min}|. \quad (V, 69)$$

This is second equation, which determines  $h$ .

Form of curve  $W_{zz}$  is shown in Fig. 126.

Substituting the value  $x_{max}$  and  $x_{min}$  into general formula for we obtain

$$\left. \begin{aligned} |W_{zz}|_{max} &= \frac{2/\lambda}{h^2}, \\ |W_{zz}|_{min} &= -\frac{1/\lambda}{4h^2}. \end{aligned} \right\} \quad (V, 70)$$

Each of these relationships/ratios gives possibility to determine  $\lambda$ .

Let us represent now  $W_{zz}$  in the form

$$W_{zz} = 2f\lambda \frac{(h-z)^2 - x^2}{[x^2 + (h-z)^2]^2} \quad (V, 71)$$

and we investigate change in this value in vertical direction. Let us begin from the examination of lateral vertical profile, i.e., the case, when  $x$  in the formula (V, 71) has the constant value, not equal to zero. The investigation of formula (V, 71) shows the following. We have zero values  $W_{zz}$  with  $z = z_0 = h \pm x$ .

Thus,

$$h = (z_0)_{\text{max}} + |x| = (z_0)_{\text{min}} - |x|. \quad (V, 72)$$

Condition  $\frac{\partial}{\partial z} W_{zz} = 0$  gives ordinates of maximum and minimum:

$$\left. \begin{aligned} z_{\text{max}} &= h \pm x \sqrt{3}, \\ z_{\text{min}} &= h, \end{aligned} \right\} \quad (V, 73)$$

whence we have:

$$\left. \begin{aligned} |W_{zz}|_{\text{max}} &= \frac{f\lambda}{4x^2}, \\ |W_{zz}|_{\text{min}} &= \frac{2f\lambda}{x^2}. \end{aligned} \right\} \quad (V, 74)$$

Since  $x$ , obviously, it is possible to consider as the known value, equations (V, 73) give possibility of determination of  $h$ , and (V, 74) determine  $\lambda$ . Change  $W_{zz}$  the vertical line is shown in Fig.



127.

With  $x=0$  we have

$$|W_{zz}| = \frac{2f\lambda}{(h-z)^2} \quad (V, 75)$$

Page 260.

Comparing formula (V, 75) with (V, 60), we see that character of change  $W_{zz}$  and  $\Delta g$  in this case is similar, but  $W_{zz}$  more rapidly decreases with removal/distance from rod.

Let us examine now variation anomaly of force of gravity

$$\begin{aligned} \delta \Delta g(x, l) &\approx \\ &= 2f\lambda \left[ \frac{h}{x^2 + h^2} - \frac{1}{2} \left[ \frac{h}{(x+l)^2 + h^2} + \frac{h}{(x-l)^2 + h^2} \right] \right] \quad (V, 76) \end{aligned}$$

Investigation of formula (V, 76) shows that curve  $\delta \Delta g(x, l)$  is symmetrical relative to origin of coordinates, so that  $\delta \Delta g(x, l) = \delta \Delta g(-x, l)$ . In this case  $x_{max} = 0$ , i.e.  $\delta \Delta g$  as  $\Delta g$ , has the maximum value above the axis of rod or cylinder (Fig. 128).

Maximum value will be

$$\delta \Delta g_{max} = 2f\lambda \frac{l^2}{h(l^2 + h^2)} \quad (V, 77)$$

We obtained one of equations for determining unknowns  $h$  and  $\lambda$ .

The second equation most simply is obtained, if we determine the

values of abscissa  $x$ , of the zero value  $\delta\Delta g$ . From the formula (V, 76) it follows that

$$x_0 = \pm \sqrt{\frac{h^2 + l^2}{3}}.$$

whence

$$h = \left| \sqrt{3x_0^2 - l^2} \right|. \quad (V, 78)$$

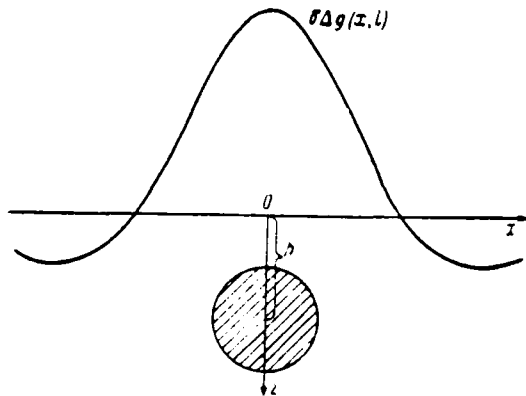


Fig. 128. Curve  $\delta\Delta g(x, l)$  above circular vertical cylinder.

Page 261.

Formulas (V, 77) and (V, 78) are published by G. D. Managadze (1957).

Varying parameter  $l$  in formula (V, 76), we obtain different curves  $\delta\Delta g$ . On each of such curves with the help of the equations (V, 77) and (V, 78) it is possible to determine parameters  $h$  and  $\lambda$  of rod or cylinder. Knowing  $\sigma$  for the cylinder, it is possible, as shown above, to determine radius  $R$  of cylinder and depth up to its upper edge.

In conclusion let us present following theoretical example, which shows possibility of applying method described above of interpretation of anomaly  $\delta\Delta g$  for cylinder. We already said above that the symmetrical anticlinal or synclinal folds can serve as the geologic analog of circular horizontal cylinder. It is clear that this type of

likenings are possible only in such cases, when amplitude and width of structures are commensurate between themselves; very narrow sharp/acute folds, and also very wide and gently sloping, obviously, no longer can serve as the analogs of horizontal cylinder. In this case, obviously, anticlinal folds better are suitable for such comparisons than synclinal, since the essential nonconformity in the section/cut of anticline and circular cylinder (with the commensurability of amplitude and cross sizes/dimensions of structure) will be observed only in the basis/base of fold, i.e., at considerable depth from the surface. For the interpretation best of all will be suitable not the anomaly of the force of gravity  $\Delta g$ , but the variation anomaly  $\delta \Delta g$ , on which near masses will act much more strongly than the masses, arranged/located on the large depth from the earth's surface. Most reliably in this case, obviously, will be determined the position of the apex/vertex of structure.

We assign the section/cut of symmetrical anticlinal fold and excess density  $\sigma$  of composed by it rocks (Fig. 129); in example in question is taken  $\sigma=0.5$  g/cm<sup>3</sup>. Having these data and putting to use the method, which will be described in §46 of Chapter VI, it is possible to calculate the curve of anomaly  $\Delta g$ , which presents the gravitational effect/action of fold. After assigning further  $l$ , on the curve  $\Delta g$  we build curve  $\delta \Delta g(x, l)$ .

Since fold is symmetrical, curves  $\Delta g$  and  $\delta \Delta g$  for it are symmetrical relative to point of maximum, similar in their form to

curves  $\Delta g$  and  $\delta \Delta g$  for circular cylinder. Let us pose this problem: to determine the depth of the bedding of the apex/vertex of structure, likening it with the interpretation to circular horizontal cylinder. In this case according to the rules described above we determine  $h$  and  $\lambda$  for the cylinder, then, knowing  $\sigma$ , we find its radius  $R$  and depth of the bedding of upper edge  $H=h-R$ ; this latter/last value is carried to the apex/vertex of structure. Calculations  $h$  and  $\lambda$  we conduct according to the curve  $\Delta g$  according to the formulas (V, 54) and (V, 55), and also along curves  $\delta \Delta g$ , constructed according to curve  $\Delta g$  with  $l=300$  m and  $l=400$  m according to the formulas (V, 77) and (V, 78). Radius  $R$  of cylinder is determined according to the formula (V, 36).

Page 262.

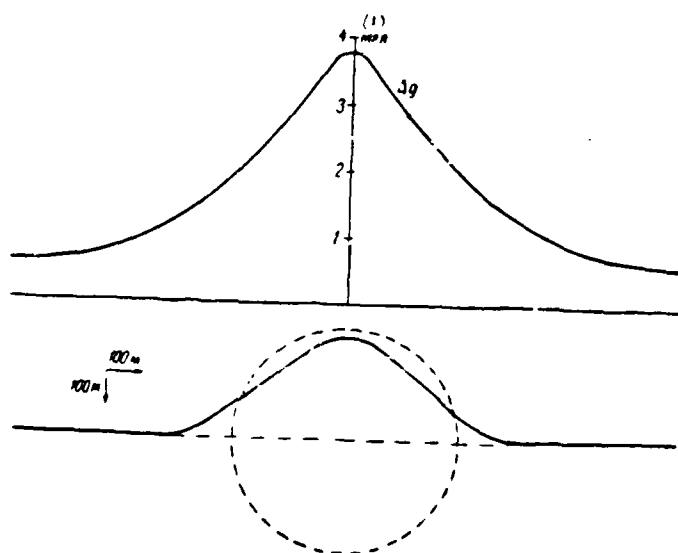


Fig. 129. Section/cut of anticlinal fold and the corresponding to it curve of anomaly  $\Delta g$ . Position of the vertical cylinder, determined on the curve  $\Delta g$  (dotted curve).

Key: (1). mg/.

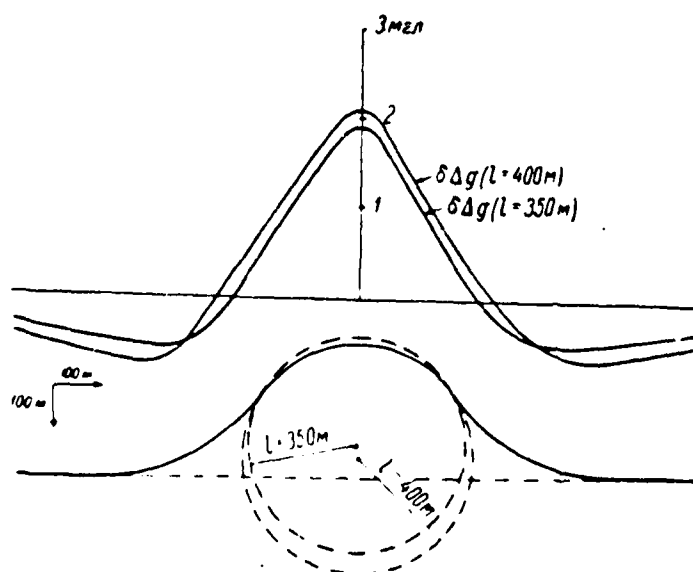


Fig. 130. Section/cut of anticlinal fold and corresponding curves of

variation anomaly  $\delta\Delta g$  with  $l=300$  m and  $l=400$  m. Position of the vertical cylinders, determined on the curves  $\delta\Delta g$  (dotted curves 1 and 2).

Key: (1). 3 mgl.

Page 263.

Finally we obtain following data about depth of bedding of apex/vertex of structure:

Depth, factual ... 100 m.

Depth on curve  $\Delta g$  ... 85 m.

Depth on curve  $\delta\Delta g$  ( $l=350$  m) ... 94 m.

Depth on curve  $\delta\Delta g$  ( $l=400$  m) ... 101 m.

As we see, best results are obtained with interpretation of anomaly  $\delta\Delta g$ . The average/mean value of depth from two versions of the curve  $\delta\Delta g$  examined is 97 m; an error in this value against the real - 3 m (3%).

Results of calculations in the form of corresponding sections/cuts of cylinders are shown also in Fig. 129 and 130.

§39. Horizontal material half-plane.

Vertical drops of small amplitude, which condition presence of ledged bedding of horizontal interface of density (for example, within horizontally layered structure), zones of tapering of horizontally

sloping beds of small power/thickness, etc, can serve as geologic analogs of horizontal material half-plane (Fig. 131).

Let us assume that half-plane with surface density  $\mu$  will lie on depth  $h$  from surface and its boundary is arranged/located in parallel to  $y$  axis. Let us designate the horizontal coordinate of the projection of the edge of half-plane through  $x$ .



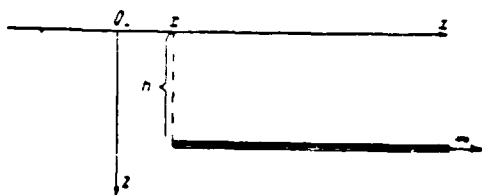


Fig. 131. Material half-plane.

Page 264.

For calculating corresponding to case in question anomalous elements we must in general formulas (III, 19) assume  $\mu = \sigma dz$ ,  $z = h$  and integration produce only on variable  $x$ , from  $x$  to  $+\infty$ . This gives for anomaly  $\Delta g$

$$\Delta g = 2f\mu h \int_x^\infty \frac{dx}{x^2 + h^2} = 2f\mu \left[ \arctg \frac{x}{h} \right]_x^\infty$$

or

$$\Delta g = 2f\mu \left( \frac{\pi}{2} - \arctg \frac{x}{h} \right). \quad (V, 79)$$

For gradient  $W_x$  we have:

$$W_x = 4f\mu h \int_x^\infty \frac{x dx}{(x^2 + h^2)^2} = 2f\mu h \left[ \frac{-1}{x^2 + h^2} \right]_x^\infty$$

or

$$W_x = 2f\mu \frac{h}{x^2 + h^2}. \quad (V, 80)$$

For  $W_z$  we have:

$$\begin{aligned}
 W_{xx} &= 2f\mu \int_{-\infty}^{\infty} \frac{h^2 - x^2}{(x^2 + h^2)^3} dx = 2f\mu \int_{-\infty}^{\infty} \frac{(x^2 + h^2 - 2x^2)}{(x^2 + h^2)^3} dx = \\
 &= 2f\mu \int_{-\infty}^{\infty} \frac{dx}{x^2 + h^2} - 4f\mu \int_{-\infty}^{\infty} \frac{x^2 dx}{(x^2 + h^2)^3} = \frac{2f\mu}{h} \left( \frac{\pi}{2} - \arctg \frac{x}{h} \right) - \\
 &\quad - 2f\mu \left\{ - \int_{-\infty}^{\infty} \frac{x}{x^2 + h^2} + \int_{-\infty}^{\infty} \frac{dx}{x^2 + h^2} \right\}
 \end{aligned}$$

or

$$W_{xx} = -2f\mu \frac{x}{x^2 + h^2}. \quad (V.81)$$

For case, when edge of half-plane is arranged/located under origin of coordinates, and  $x$  represents coordinate of observation point, reversing sign in  $x$  in preceding formulas, we have:

$$\left. \begin{aligned}
 \Delta g &= 2f\mu \left( \frac{\pi}{2} + \arctg \frac{x}{h} \right), \\
 W_{xx} &= 2f\mu \frac{h}{x^2 + h^2}, \\
 W_{xx} &= 2f\mu \frac{x}{x^2 + h^2}.
 \end{aligned} \right\} \quad (V.82)$$

As we see, all anomalous elements, including anomaly  $\Delta g$ , in case in question are expressed by very simple formulas. The sufficiently simple form in this case take the expressions of the variation anomalies  $\delta\Delta g$  and  $\delta W_{xx}$ .

Page 265.

Actually, from the general/common expression of the variation anomaly

$$\delta U(x, l) = U(x) - \frac{1}{2} [U(x+l) + U(x-l)]$$

and the first two formulas (V, 82) we have respectively:

$$\left. \begin{aligned}
 \delta \Delta g &= -2f\mu \left[ \arctg \frac{x}{h} - \frac{1}{2} \left[ \arctg \frac{x+l}{h} + \arctg \frac{x-l}{h} \right] \right], \\
 \delta W_{xx} &= f\mu h \left[ \frac{2}{x^2 + h^2} - \left[ \frac{1}{(x+l)^2 + h^2} + \frac{1}{(x-l)^2 + h^2} \right] \right].
 \end{aligned} \right\} \quad (V.83)$$

Anomaly of force of gravity  $\Delta g$  (first of formulas V, 82) in case in question is characterized by following relationships/ratios:

$$\left. \begin{array}{l} \text{при } x = -\infty \Delta g = 0, \\ \bullet \quad x = 0 \Delta g = f \pi \mu, \\ \bullet \quad x = +\infty \Delta g = 2f \pi \mu, \\ \Delta g(+x) + \Delta g(-x) = 2f \pi \mu. \end{array} \right\} \quad (\text{V. 84})$$

Key: (1). with.

Form of curve  $\Delta g$  is shown in Fig. 132.

As we see, curve  $\Delta g$  in this case does not have easily determined characteristic points and therefore its utilization for quantitative interpretation is difficult. It is possible, however, for the approximate determination  $\mu$  to use value of  $\Delta g$  at point of inflection of curve with  $x=0$ , which gives

$$\mu = \frac{\Delta g(0)}{f \pi}. \quad (\text{V. 85})$$

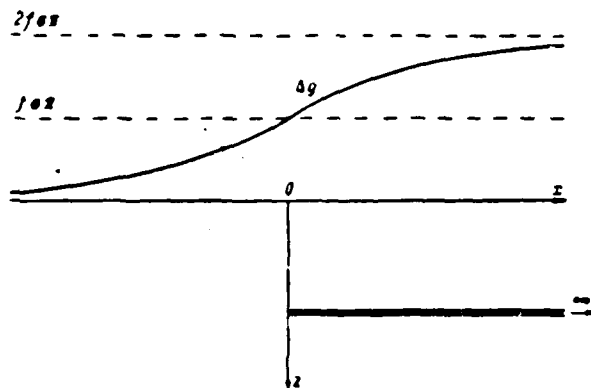


Fig. 132. Curve of anomaly  $\Delta g$  above material half-plane.

Page 266.

For approximate determination of  $h$  it is possible to determine in curve  $\Delta g$  point with coordinate  $x = x_{1/2}$ , in which

$$\Delta g = \frac{1}{2} \Delta g(0)$$

or <sup>1</sup>

$$2f\mu \left( \frac{\pi}{2} - \arctg \frac{|x_{1/2}|}{h} \right) = \frac{f\mu\pi}{2}.$$

FOOTNOTE <sup>1</sup>. Since  $\Delta g < 1/2 \Delta g(0)$  with  $x < 0$ ,  $x_{1/2}$  - negative value. For convenience its absolute value  $|x_{1/2}|$  further is examined.

ENDFOOTNOTE.

Hence

$$\arctg \frac{|x_{1/2}|}{h} = \frac{\pi}{4},$$

i.e.

$$h = |x_{1/2}|. \quad (V, 86)$$

We investigate spatial distribution of anomaly  $\Delta g$ , for this let us write its expression in the form

$$\Delta g = 2f\mu \left( \frac{\pi}{2} + \operatorname{arctg} \frac{z}{h-z} \right). \quad (V, 87)$$

With  $z=h$  from formula (V, 87) we have

$$\left. \begin{aligned} \Delta g &= 0 & (x < 0), \\ \Delta g &= \pm 2f\pi\mu (x \geq 0) \end{aligned} \right\} \quad (V, 88)$$

(sign +, if we approach half-plane on top; sign -, if we approach from below).

On lateral vertical profile (with  $x \neq 0$ ) we have from formula (V, 87) and conditions  $\partial/\partial z \Delta g = 0$ :

$$\begin{aligned} z_{\max} &= -\infty, & \Delta g_{\max} &= f\pi\mu, \\ z_{\min} &= +\infty, & \Delta g_{\min} &= -f\pi\mu. \end{aligned}$$

Finally, with  $x=0$  we have

$$\begin{aligned} \text{всюду при } z > h & \Delta g = f\pi\mu, \\ \text{•} \quad \text{•} \quad z < h & \Delta g = -f\pi\mu. \end{aligned}$$

Key: (1). everywhere with.

Fig. 133 illustrates character of spatial distribution  $\Delta g$  in the case of material half-plane.

Formula (V, 82) for horizontal gradient  $W_z$  in this case is analogous to formula  $\Delta g$  for case of vertical cylinder (V, 51), if in

latter linear density  $\lambda$  is replaced by surface density, and we center of cylinder combine with edge of half-plane.

Page 267.

$W_{xx}$  as  $\Delta g$  in formula (V, 51), represents even positive function with maximum with  $x=0$ , i.e., in this case above edge of half-plane (Fig. 134). Analogous with formulas (V, 54) and (V, 55) we have formulas for solving the inverse problem:

$$W_{xx} = \frac{2f\mu}{h}, \quad (V, 89)$$

$$h = |x_{1/2}|, \quad (V, 90)$$

where  $x_{1/2}$  - abscissas of half value  $[W_{xx}]_{0.5x}$ .

Spatial distribution  $W_{xx}$  is also analogous with distribution  $\Delta g$  for case of rod (see formulas (V, 56-V, 60) and Fig. 125), edge of half-plane representing singular point for  $W_{xx}$  at which this derivative goes to infinity.

Let us turn now to formula (V, 82) for  $W_{xx}$ :

$$W_{xx} = 2f\mu \frac{x}{x^2 + h^2}.$$

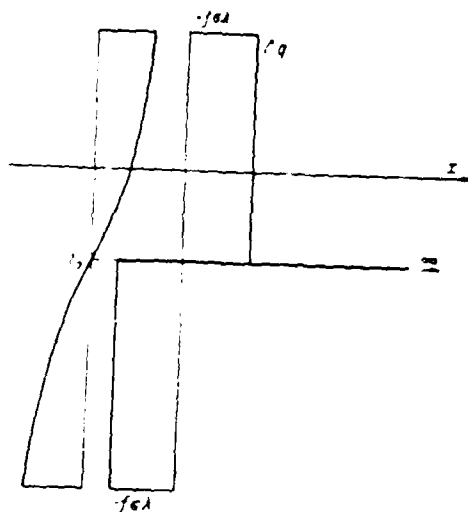


Fig. 133. Curves of anomaly  $\Delta g$  on lateral vertical profiles in the case of material half-plane.

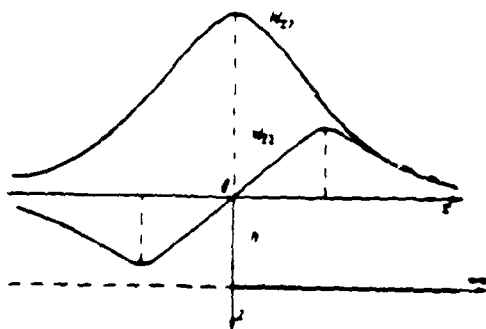


Fig. 134. Curves  $W_{xx}$  and  $W_{yy}$  above material half-plane.

Page 268.

As we see,  $W_{xx}$  -- function odd, i.e.,  $W_{xx}(-x) = -W_{xx}(x)$ . When  $x = 0$   $W_{xx} = 0$  (Fig. 134). Differentiating  $W_{xx}$  through  $x$  and equalizing derivative zero, we find

$$\left. \begin{aligned} x_{\max} &= +h, \\ x_{\min} &= -h, \end{aligned} \right\} \quad (V, 91)$$

whence is determined  $h$ . For the determination  $\mu$  we find

$$(W_{xz})_{\max} = \frac{l\mu}{h}. \quad (V.92)$$

If we write  $W_{xz}$  in more general view

$$W_{xz} = 2f\mu \frac{x}{x^2 + (h-z)^2}, \quad (V.93)$$

then it is possible to explain special features of spatial distribution of this derivative. On the lateral vertical profile extreme value  $W_{xz}$  is obtained with

$$z = z_m = h. \quad (V.94)$$

With  $x > 0$  this will be maximum, when  $x < 0$  - minimum (Fig. 135). Numerical value of the minimum

$$(W_{xz})_{\min} = -\frac{2f\mu}{x}. \quad (V.95)$$

Formulas (V, 94) and (V, 95) determine  $h$  and  $\mu$ .

At singular point  $(0, h)$  (edge of half-plane) limiting value is  $+\infty$  with approximation/approach to point indicated to the right (in region  $x > 0$ ) and  $-\infty$  with approximation/approach to the left (in region  $x < 0$ ).

Let us examine now variation anomaly

$$\delta \Delta g(x, l) = -2f\mu \left[ \operatorname{arc} \operatorname{tg} \frac{x}{h} - \frac{1}{2} \left[ \operatorname{arc} \operatorname{tg} \frac{x+l}{h} + \operatorname{arc} \operatorname{tg} \frac{-l}{h} \right] \right].$$



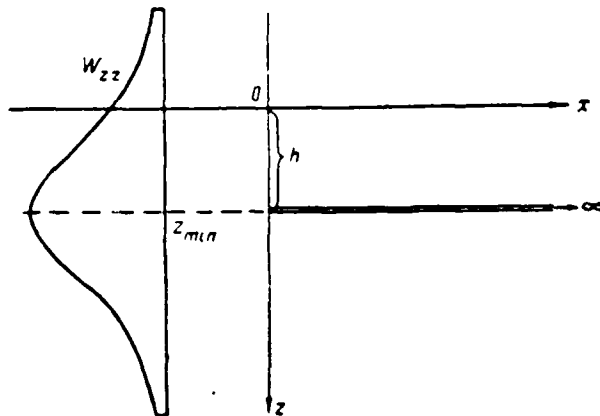


Fig. 135. Curve  $W_{zz}$  on vertical lateral profile in the case of material half-plane.

Page 269.

Investigation of this formula shows that with  $x=0$   $\delta\Delta g(x, l)=0$ . Thus, with any value the edge of half-plane is noted by the zero value of  $\delta\Delta g(x, l)$ . If  $x<0$   $\delta\Delta g(x, l)<0$ , while if  $x>0$   $\delta\Delta g(x, l)>0$ , moreover  $\delta\Delta g(x, l)=-\delta\Delta g(-x, l)$  (Fig. 136).

Further investigation of formula shows that

$$x_m^2 = \frac{h^2 \cdot l^2}{\beta}, \quad x_{\max} = +\sqrt{\frac{h^2 \cdot l^2}{\beta}},$$

$$x_{\min} = -\sqrt{\frac{h^2 \cdot l^2}{\beta}},$$

whence

$$h = \sqrt{\beta x_m^2 - l^2}. \quad (V, 96)$$

From written relationships/ratios it follows that at any level, when  $z \leq h$   $|x_m| \geq \frac{l}{\beta}$ , and when  $z > h$   $|x_m| < \frac{l}{\beta}$ . On the other hand, if  $z = x_m$ , then from the formula (V, 96) we have

$$h \approx |x_m| \sqrt{3} \quad (l < |x_m|). \quad (V.96a)$$

Substitution of value  $x = x_{\max}$  into general formula for  $\delta \Delta g(x, l)$  gives

$$|\delta \Delta g(x, l)|_{\max} = f \mu \operatorname{arctg} \frac{2h^2 x_{\max}}{x_{\max}^4 + (2A^2 - l^2) x_{\max}^2 + h^2 l^2 + h^4}. \quad (V.97)$$

whence  $\mu$  is determined.

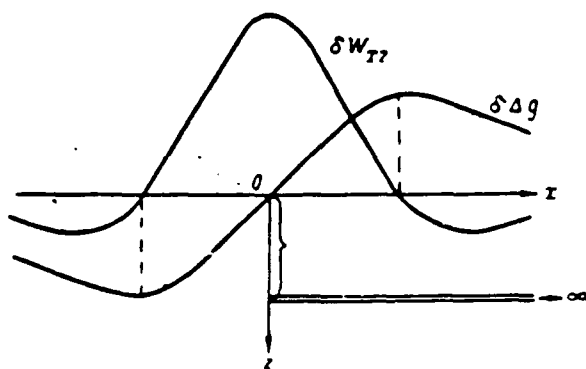


Fig. 136. Curves of variation anomaly  $\delta\Delta g$  and  $\delta W_{Tz}$  above material half-plane.

Page 270.

Let us focus attention on following fact. As we indicated above, the curve  $\Delta g$  for the half-plane does not have easily determined characteristic points and its utilization with the quantitative interpretation is difficult. On the other hand, from the analysis of curve  $\delta\Delta g(x, l)$  given above for the half-plane it follows that this curve takes the form, which is completely adequate/approach for the quantitative interpretation. It is necessary to also have in mind that we have the capability, varying the parameter  $l$ , to obtain different presentations/concepts  $\delta\Delta g(x, l)$  and for each of them to determine values of  $h$  and  $\mu$ , on the basis of the formulas (V, 96) and (V, 97).

Thus, transition from  $\Delta g$  to  $\delta\Delta g$  considerably improves possibilities of quantitative interpretation of gravity anomalies. Is hence obvious the groundlessness of the assertion of some

geophysicists about the fact that the application of methods of localization of gravity anomalies allegedly is incompatible with the solution of the inverse problem of interpretation (Malovichko, 1956, pg. 32).

Variation anomalies has sense to examine not only in the form of  $\delta\Delta g$ , but also in the form  $\delta W_{xz}$ . For this purpose let us examine formula for  $\delta W_{xz}$  (V, 83):

$$\delta W_{xz}(x, l) = f\mu h \left\{ \frac{2}{x^2 + h^2} - \left[ \frac{1}{(x+l)^2 + h^2} + \frac{1}{(x-l)^2 + h^2} \right] \right\}.$$

Investigation of formula shows that  $\delta W_{xz}$  — even function, which has maximum value when  $x = x_{max} = 0$ , which turns into zero with

$$x = x_0 = \pm \sqrt{\frac{h^2 + l^2}{3}} \quad (V, 98)$$

and proving to be negative when  $|x| > |x_0|$  (Fig. 136). For solving the inverse problem it is convenient to use point of maximum and point of zero value  $\delta W_{xz}$ . From the formula (V, 98)

$$h = \left| \sqrt{3x_0^2 - l^2} \right|, \quad (V, 99)$$

and, substituting  $x=0$  in the general formula for  $\delta W_{xz}$ , we find

$$[\delta W_{xz}]_{max} = 2f\mu \left( \frac{1}{h} - \frac{h}{h^2 + l^2} \right), \quad (V, 100)$$

whence

$$\mu = \frac{[\delta W_{xz}]_{max}}{2f \left( \frac{1}{h} - \frac{h}{h^2 + l^2} \right)}. \quad (V, 101)$$

Formulas given here for solving inverse problem of interpretation on  $\delta\Delta g$  and  $\delta W_{xx}$  for case of material half-plane are published by G. D. Managadze (1958).

Page 271.

K. V. Gladkiy (1957) published convenient auxiliary table for construction of theoretical curves of anomaly  $\Delta g$ , representing gravitational effect/action of material half-plane. Table gives the possibility to obtain values of  $\Delta g$  not for the points of profile, arranged/located through the equal intervals, as usually is done in this type tables, but the value of coordinate  $x$  (i.e. the distances along the profile, counted from the origin of coordinates), which correspond to the boundaries of the equal intervals of values  $\Delta g$ , counted in fractions/portions  $\Delta g_{max}$ . Number  $n$  of such intervals is accepted equal to 20, so that each interval composes 0.05  $\Delta g_{max}$ , with exception of the latter, that constitutes 0.01  $\Delta g_{max}$ . On the basis of the formulas (V, 82) and (V, 84):

$$\Delta g = 2f\mu \left( \frac{\pi}{2} + \arctg \frac{x}{h} \right),$$

$$\Delta g_{max} = 2f\pi\mu,$$

is determined the value

$$x_k = h \lg \left( \frac{\pi}{2} - \frac{2k - n}{n} \right) = Ph, \quad (V, 102)$$

where  $1 - \frac{k}{n} = \frac{\Delta g}{\Delta g_{max}}$ , and coefficient  $P$  is given in Table 18.

Table 18 can be used also for determining depth of value  $h$  of half-plane. Let, for example,  $\Delta g$  compose 0.15  $\Delta g_{max}$  for the anomaly, which is interpreted, counting its caused by the effect/action of

DOC = 88020214

PAGE

~~25~~ 494

material half-plane. Consequently,

$$1 - \frac{k}{n} = 0.15; \quad \frac{k}{n} = 0.85; \quad P = 1.96,$$

where the latter/last value is determined from Table 18.

Table 18. Values of coefficient P in the formula (V, 102).

$\frac{k}{n}$	P	$\frac{k}{n}$	P
0.01	-31.67	0.55	0.16
0.05	-6.31	0.60	0.32
0.10	-3.02	0.65	0.51
0.15	-1.96	0.70	0.73
0.20	-1.38	0.75	1.00
0.25	-1.00	0.80	1.38
0.30	-0.73	0.85	1.96
0.35	-0.51	0.90	3.08
0.40	-0.32	0.95	6.31
0.45	-0.16	0.99	31.67
0.50	0.00	1.00	$\infty$

Page 272.

Further we find

$$h = \frac{3.0 \text{ km}}{P} = \frac{3.0 \text{ km}}{1.96} = 2.0 \text{ km.}$$

In work indicated above of K. V. Gladkiy of analogous type auxiliary tables are given also for cases of sphere and circular horizontal cylinder.

## §40. Vertical step.

By vertical step in theory of interpretation of gravity anomalies is implied body of infinite course/strike, limited by two horizontal and one vertical plane, that has in cross section form of semi-infinite right angled strip with sides, parallel to coordination x and z axes (Fig. 137). From the comparison of Fig. 137a with Fig. 131 it follows that the vertical step presents the case, similar to

the case of horizontal material half-plane, but more general and, consequently, more complex: it is assumed that the horizontal planes, which limit body, are arranged/located not on infinitesimal, but on finite arbitrary distance.

In given definition of vertical step it is assumed that disturbing body, limited by planes indicated above (by two horizontal and by one vertical), has certain excess density  $\sigma$  relative to zero excess density of its accomodating medium. However, if we will assume that in entire half-space, arranged/located lower than the step, excess density is not zero, but different from zero constant values, equal to  $\sigma$ , then, it is obvious, the anomalous gravitational field, caused by step, will not be changed (anomalies are engendered only by density variations in the horizontal direction). Consequently, is possible following, equivalent to given above, determination of the vertical step: this is the form of the relief of interface with the excess density  $\sigma$ , which has the form of step/stage, finite vertical dimensions, limited from the side by vertical, and from above by the horizontal plane (Fig. 137b).



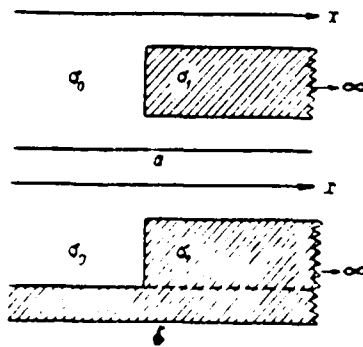


Fig. 137. Vertical step (a) and its equivalent presentation/concept (b).

Page 273.

This equivalent determination formally is suitable also for case examined above of material half-plane, but in this case it does not have visual physical sense - for us it would be necessary to speak about the step/stage of infinitesimal vertical sizes/dimensions.

After given elucidations let us point out geologic analogs of vertical step. These will be all those elements of the geologic structure, whose basic gravitational effect/action is caused by the presence of one vertical or steep contact of two media of different density: faults with the steep/abrupt drop in the plane of ejector in the thickness of the rocks, whose density varies on the vertical line, the contacts in the thickness of the steep rocks, which are distinguished by the density (for example, in the thickness of crystalline basement), the contacts of solar domes or intrusion masses with the enclosing rocks, the zone of abrupt changes in

faciles-lithologic composition of sedimentary rocks, etc. It is possible to say that the case of vertical step - one of the basic questions of theory and practice of the interpretation of gravity anomalies.

We give conclusion/derivation of formulas, which express gravitational effect/action of vertical step. Let us designate through  $x$  the horizontal coordinate of the edge of step, through  $z_1$  and  $z_2$  - depth of the bedding of the upper and lower horizontal planes, which limit step.

For calculations it would be possible to use general formulas (III, 19) for two-dimensional task. However, in this case we more rapidly will lead to the target the utilization of those already brought out above in §36 formulas for rectangular prism. By their successive simplification we will obtain first formulas for rectangular prism with the infinite course or the infinite prism (beam), which are for us of independent interest and examined/considered in §42, and then formula for the vertical step.

Assuming/setting in formulas (V, 33), (V, 35), (V, 36)  $y_2 = y_1 = y$  and then changing to limiting value of  $y \rightarrow \infty$ , we obtain following formulas for rectangular prism with infinite course/strike:

$$\left. \begin{aligned} \Delta g &= f \sigma \left[ x \ln(x^2 + z^2) + 2z \operatorname{arctg} \frac{z}{x} \right]_{x_1, z_1}^{x_2, z_2} \\ W_x &= f \sigma [\ln(x^2 + z^2)]_{x_1, z_1}^{x_2, z_2} \\ W_z &= 2f \sigma \left[ \operatorname{arctg} \frac{z}{x} \right]_{x_1, z_1}^{x_2, z_2} \end{aligned} \right\} \quad (V, 40)$$

Page 274.

Assuming/setting in formulas (V, 103)  $x_1 = x$ ,  $x_2 = \infty$ , we obtain formulas for case of vertical step:

$$\Delta g = f \sigma \left[ \pi z - 2z \operatorname{arctg} \frac{z}{x} - x \ln(x^2 + z^2) \right]_{z_1}^{z_2},$$

$$W_{xz} = f \sigma \left[ \ln(x^2 + z^2) \right]_{z_1}^{z_2},$$

$$W_{xx} = 2f \sigma \left[ \operatorname{arctg} \frac{z}{x} \right]_{z_1}^{z_2}.$$

Varying now as usually, sign for  $x$ , i.e., transferring origin of coordinates into point, arranged/located above edge of step, and making substitutions  $z_2$  and  $z_1$ , we finally obtain:

$$\left. \begin{aligned} \Delta g &= f \sigma \left[ (z_2 - z_1) \pi + 2z_2 \operatorname{arctg} \frac{z}{z_2} - 2z_1 \operatorname{arctg} \frac{z}{z_1} + \right. \\ &\quad \left. + x \ln \frac{x^2 + z_2^2}{x^2 + z_1^2} \right], \\ W_{xz} &= f \sigma \ln \frac{x^2 + z_2^2}{x^2 + z_1^2}, \\ W_{xx} &= 2f \sigma \left( \operatorname{arctg} \frac{z}{z_2} - \operatorname{arctg} \frac{z}{z_1} \right). \end{aligned} \right\} \text{(V, 104)}$$

Formulas (V, 104), especially expression for  $\Delta g$ , according to their form are more complex than formulas (V, 82) for material half-plane. Formulas (V, 82) for the half-plane are obtained from (V, 105), if we in the latter consider  $z, -z_1$  as the low value and assume  $\sigma(z, -z_1) = \mu$ . Under this condition, removing the parentheses in the formula (V, 104) for  $\Delta g$ , we can write

$$2f\sigma\left(z_2 \operatorname{arctg} \frac{x}{z_2} - z_1 \operatorname{arctg} \frac{x}{z_1}\right) \approx 2f\mu \operatorname{arctg} \frac{x}{h},$$

$$\ln \frac{z^2 + z_2^2}{z^2 + z_1^2} = \ln \left( \frac{1 + \left(\frac{z_2}{x}\right)^2}{1 + \left(\frac{z_1}{x}\right)^2} \right) \approx 0,$$

that also gives the appropriate formula (V, 82). analogously can be converted expressions for  $W_{\pi}$  and  $W_{\pi}$ .

Let us turn to examination of formula  $\Delta g$  for vertical step

$$\Delta g = f\sigma \left[ \pi(z_2 - z_1) + 2z_2 \operatorname{arctg} \frac{x}{z_2} - 2z_1 \operatorname{arctg} \frac{x}{z_1} + \ln \frac{z^2 + z_2^2}{z^2 + z_1^2} \right].$$

Page 275.

Its investigation shows that

$$\left. \begin{aligned} \text{при } x = -\infty \quad \Delta g &= 0, \\ \bullet \quad x = 0 \quad \Delta g &= f\sigma\pi(z_2 - z_1), \\ \bullet \quad x = +\infty \quad \Delta g &= 2f\sigma\pi(z_2 - z_1), \\ \Delta g(+x) + \Delta g(-x) &= 2f\sigma\pi(z_2 - z_1). \end{aligned} \right\} \quad (\text{V, 105})$$

Key: (1). with.

Curve  $\Delta g$  for step proves to be same-type with curve  $\Delta g$  for material half-plane (see Fig. 132), and expressions (V, 105) are identical to (V, 88), if we in latter take  $\mu = \sigma(z_2 - z_1)$ .

Let us take vertical step with excess density  $\sigma$  with depths of upper and lower bounds of  $z_1$  and  $z_2$  (Fig. 138) and will count for it values of anomaly of force of gravity  $\Delta g$  according to appropriate

formula (V, 104). Let us take further material half-plane with density  $\mu = \sigma(z, -z_1)$  at the depth

$$h = \frac{z_1 + z_2}{2}$$

and with the same position of left edge, as in vertical step. Let us count for it anomaly value of gravitational force according to the appropriate formula (V, 82) and designate it through  $\overline{\Delta g}$ . If we now count the values of the relative deflection

$$\varepsilon = \frac{\Delta g - \overline{\Delta g}}{\Delta g} \cdot 100\%$$

for the different values of ratio  $x/h$ , then it proves to be that the values  $\varepsilon$  on the whole are small and do not exceed in the extreme case 7.2% (Fig. 139).

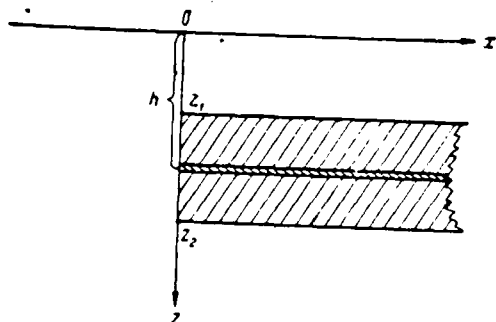


Fig. 138. Mutual arrangement of vertical step and half-plane during comparison of their gravitational effect/action.

Page 276.

We have this limiting case with  $x/h=1/4$ , when  $z_1=0$ , and  $z_2-z_1=2h$ , i.e., face side of step coincides with the plane of observations. But if  $x/h=1$ , then  $\epsilon$  composes only 3.4%. This fact, explained in the work of K. V. Gladkiy (1957), gave to its author the foundation for making the following conclusion: "... virtually in all cases during the determination of the depth of the bedding of the plane, situated halfway between the upper and lower bounds of infinite vertical step/stage, it is possible to use the relationships/ratios, brought out for real half-plane". The discussion here deals with the formula (V, 86)

$$h = |x_{1/2}|.$$

brought out above for the case of material half-plane. It proves to be that it is in practice applicable for the vertical step of finite vertical dimensions, if we by  $h$  understand average value from depths  $z_1$  and  $z_2$ .

Actually, this value is determined on position of point in that section, where corresponding curves for step and half-plane are not distinguished between themselves more than 3%.

Given conclusion/derivation is accurate only for anomaly  $\Delta g$  and only for determination from this value of average/mean value from depths  $z_1$  and  $z_2$  of step. For  $W_{xx}$  and  $W_{yy}$  in the case of step, as we see below, are required other methods of interpretation, different from the methods of interpretation for the material half-plane. However, for the anomaly  $\Delta g$  in the general case also cannot be spoken about the equivalency of the effect/action of step and material half-plane: although the difference between them is relatively small, it has systematic character, without varying on the sign on entire profile (see Fig. 139). This will be especially clearly evident below, when we will examine spatial distribution of anomaly  $\Delta g$  for the step.

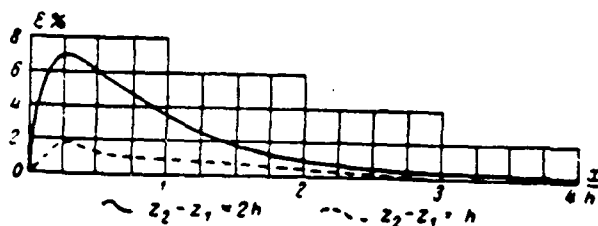


Fig. 139. Relative disagreement  $\epsilon$  (in %) of values of anomalies of force of gravity  $\Delta g$  for vertical step  $\Delta g$  for material half-plane.

$$\epsilon = \frac{\Delta g - \bar{\Delta g}}{\bar{\Delta g}} \cdot 100\% \quad (\text{according to K. V. Gladkov}).$$

Page 277.

Primary task with interpretation of gravity anomalies for step consists not in determination of average depth  $h$ , but in determination of depths themselves  $z_1$  and  $z_2$ . This task, even if it can be solved on anomaly  $\Delta g$ , then, obviously, only for the case of step. It, actually, does not make sense for the case of material half-plane.

In §42 we give tables, with the help of which it is possible to easily build theoretical curves  $\Delta g$ ,  $W_{xx}$  and  $W_{yy}$  for any bodies with rectangular cross section - including for vertical step.

Let us pause at question about special features of spatial distribution of anomaly  $\Delta g$  in the case of vertical step. Formula (V.104) for  $\Delta g$  is valid for the half-space, arranged/located above face side of step. For the half-space, arranged/located below lower bound of step, is valid the same formula, but, obviously, in this case it is necessary to take values of  $z_1$  and  $z_2$  with minus sign, and this is



equipollent to sign change in the expression for  $\Delta g$ : positive anomaly on the upper profile is converted into the negative on the lower profile, moreover, if these profiles are arranged/located symmetrically relative to step, then for one and the same  $x$  anomaly will be identical with respect to absolute value. The physical sense of sign change in  $\Delta g$  in this case is analogous to change  $\Delta g$  in the case of material half-plane and does not require new elucidations.

Let us examine now distribution  $\Delta g$  in layer between upper and lower boundary planes of step. The basic special features of distribution  $\Delta g$  in this layer can be established from the simple physical consideration. Let there be point A, arranged/located on the side from the step (Fig. 140). We conduct the horizontal plane through point A; it will separate from the step Part I - also in the form of the vertical step, arranged/located on top of the plane indicated. Let us construct step II, similar to step I and arranged/located from below from the horizontal plane, carried out through point A, i.e., representing as the mirror image of step I. It is easy to comprehend that the gravitational effect/action of steps I and II on vertical component  $\Delta g$  is equal in the value, but it is contradictory on the sign and, consequently, cumulative effect of steps I and II on  $\Delta g$  is equal to zero.

Consequently, gravitational effect/action of entire step on  $\Delta g$  at point A is reduced only to effect/action of its remaining part III, located below step II (see Fig. 140). If point A is arranged/located

on the horizontal plane, which separates step in half (point A, in Fig. 140), then the effect/action of step at this point is equal to zero, moreover with any arrangement of point with respect to the step both outside and within it.

Page 278.

From all the aforesaid the following law of change  $\Delta g$  on vertical profile, carried out through edge of step (with  $x=0$ ) above escapes/ensues:

$\Delta g = f \sigma \pi (z_2 - z_1)$  everywhere when  $z < z_1$ ;  $\Delta g$  linearly decreases when  $z_1 < z < z_2$ , becoming zero when  $z = \frac{z_1 + z_2}{2}$ ;  $\Delta g = -f \sigma \pi (z_2 - z_1)$  everywhere with  $z \geq z_2$ .

Change  $\Delta g$  with  $x=0$  as functions  $z$  is shown graphically in Fig. 141. Graphs  $\Delta g(z)$  with  $x < 0$  and with  $x > 0$  are given here.

Being congruent/equating Fig. 141 and 133, we see that character of three-dimensional/space change  $\Delta g$  is substantially various for cases of material half-plane and vertical step, what, however, is natural in view of different arrangement of singular points, which determine structure of anomalous field: in the case of half-plane this point only one (edge of half-plane), in the case of step their two - in upper and lower points of inflection of its cross section.

For case of step it is easy to investigate question, that gives analytical continuation of anomaly  $\Delta g$  along positive direction of  $z$  axis, i.e., in lower half-plane on vertical line, passing through points of inflection of step, if distribution  $\Delta g$  is known along line of observations ( $x$  axis), also, in upper half-plane along negative direction of  $z$  axis. On the basis of formula (V, 104) we have

$$\begin{aligned} \Delta g(x, 0) + \Delta g(-x, 0) &= 2f\sigma\pi(z_2 - z_1) \overset{(1)}{\text{для любого } x}, \\ \Delta g(0, -z) &= -f\sigma\pi(z_2 - z_1) \text{ для любого } z > 0. \end{aligned}$$

Key: (1). for any.

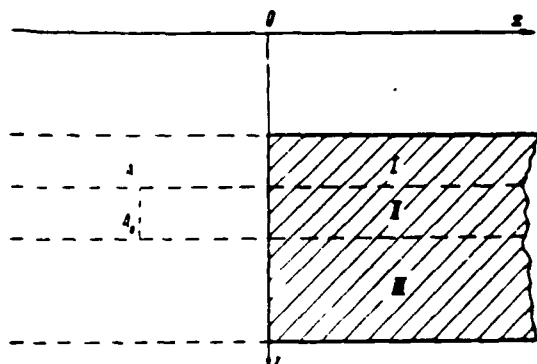


Fig. 140. Determination of gravitational effect of vertical step in layer, situated between its upper and lower boundary planes.

Page 279.

If we now use formula (IV, 80) of net point method, then, after replacing there  $z=h$ , it is possible to write:

$$\Delta g(0, z) = 4\Delta g(0, 0) - [\Delta g(z, 0) + \Delta g(-z, 0) + \Delta g(0, -z)],$$

and making appropriate substitutions, we obtain

$$\Delta g(0, z) = f\sigma\pi(z_2 - z_1) \text{ with any } z > 0.$$

This formula gives completely accurate result under condition  $z \leq z_1$ , i.e., to level of nearest singular point  $(0, z_1)$  of function  $\Delta g$ . It is lower than the singular point, i.e., with  $z < z_1$ , formula net point method gives the result, which does not correspond to the real distribution  $\Delta g$  along axis  $z$  (see Fig. 141).

Let us turn now to formula (V, 104) for gradient  $W_z$ ,

$$W_z = f\sigma \ln \frac{z^2 + z_1^2}{z^2 + z_2^2}.$$

it reaches maximum at point  $x=0$ , moreover

$$(W_{xx})_{\max} = 2f\sigma \ln \frac{z_2}{z_1}, \quad (V.106)$$

$W_{xx}$  — even positive function, are decreased with increase  $|z|$  and turning zero with  $x=\pm\infty$  (Fig. 142).

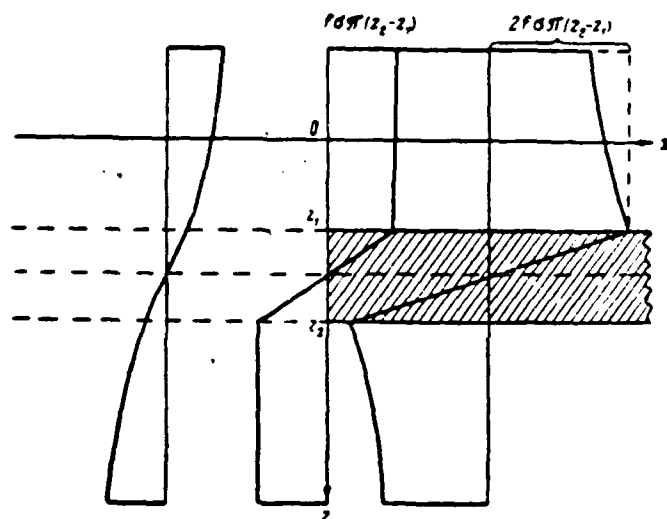


Fig. 141. Change in anomaly  $\Delta g$  on lateral vertical profiles in the case of vertical step.

Page 280.

Values  $z_1$ ,  $z_2$  and  $\sigma$  can be expressed through abscissas  $x_{1/2}$  and  $x_{1/4}$  points, where  $W_{xz}$  it reaches values  $\frac{1}{2} |W_{xz}|_{\max}$  and  $\frac{1}{4} |W_{xz}|_{\max}$ , and value  $|W_{xz}|_{\max}$  (method of P. M. Nikiforov).

For points indicated we have respectively:

$$f\sigma \ln \frac{z_2}{z_1} = f\sigma \ln \frac{z_1^3 + z_2^3}{z_1^3 + z_1^3}$$

either

$$\frac{z_2}{z_1} = \frac{z_1^3 + z_2^3}{z_1^3 + z_1^3}$$

or

or

$$\frac{1}{2} f \sigma \ln \frac{z_2}{z_1} = f \sigma \ln \frac{x_{1/4}^2 + z_2^2}{x_{1/4}^2 + z_1^2}$$

$$\frac{z_2}{z_1} = \left( \frac{x_{1/4}^2 + z_2^2}{x_{1/4}^2 + z_1^2} \right)^2.$$

The first of given relations gives

$$z_1 z_2 = x_{1/4}^2,$$

but from the second we obtain after some transformations

$$z_1 + z_2 = \frac{x_{1/4}^2 - x_{1/8}^2}{x_{1/8}}.$$

Whence, using property of square roots equation, directly we find

$$\left. \begin{aligned} z_1 &= m - \sqrt{m^2 - x_{1/8}^2} \\ z_2 &= m + \sqrt{m^2 - x_{1/8}^2} \end{aligned} \right\} \quad (\text{V. 107})$$

where it is marked

$$m = \frac{x_{1/4}^2 - x_{1/8}^2}{2x_{1/8}}. \quad (\text{V. 107a})$$

After determining  $z_1$  and  $z_2$ , and after substituting obtained values into formula (V, 106), we find value  $\sigma$

$$\sigma = \frac{\{W_{x1}\}_{\max}}{2f(\ln z_2 - \ln z_1)}. \quad (\text{V. 108})$$

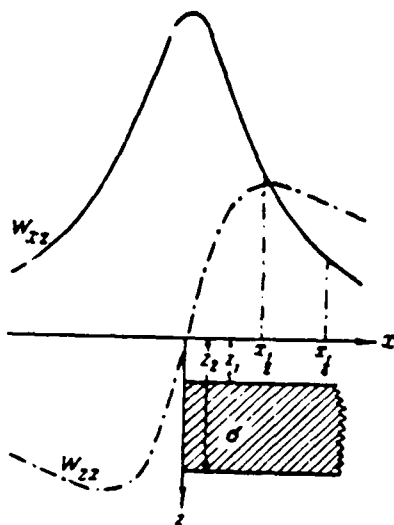


Fig. 142. Curves  $W_{xz}$  and  $W_{zz}$  above vertical step.

Page 281.

Let us focus attention to the fact that in this case we have the capability of immediate determination according to gravitational data by some of surface of disturbing body and its excess density, we did not have what in cases of sphere and circular cylinder. The reason for this was made clear above in § 19 of Chapter III: the surface of step angular, its section has the singular points of the anomalous gravitational field, situated on the body surface. Therefore in this case during the solution of the inverse problem, which gives the position of the singular points of field, we directly determine both the surface of disturbing body and its excess density.

It is here appropriate to explain this question: all parameters of step  $z_1$ ,  $z$ , and  $\sigma$  are theoretically determined unambiguously, but



does mean this that all these parameters are determined equally stably. (Question about the stability of the solution of inverse problem we already was examined in general form in § 19 of Chapter III). To this question in this case it is possible to give this answer: depth  $z_1$  (i.e. the position of the nearest to the plane of the observations of the singular point of anomalous field) most stably is determined, values  $z$ , and  $\sigma$  are determined much less stably. In this case the error in  $z$ , strongly influences the accuracy of determination  $\sigma$ , but it little affects the determination of  $z_1$ .

If instead of constant value  $\sigma=\sigma_0$ , to take linear dependence  $\sigma$  on depth in the form

$$\sigma = \sigma_0 + m(z - z_1),$$

that it is possible, after introducing this value into integral expressions  $W_{xz}$  and  $W_{zx}$ , to obtain following expressions (Berzon, 1939):

$$W_{xz} = \left(1 - \frac{mz_1}{\sigma_0}\right) W_{xz0} + \frac{mx}{\sigma_0} W_{zx0} + 2/m(z_1 - z),$$

$$W_{zx} = \left(1 - \frac{mz_1}{\sigma_0}\right) W_{zx0} - \frac{mx}{\sigma_0} W_{xz0},$$

where  $W_{xz0}$  and  $W_{zx0}$  — value of these quantities with  $\sigma=\sigma_0$ .

Comparison of curves  $W_{xz}$  and  $W_{zx}$ , constructed according to given formulas, with curves for case  $\sigma=\sigma_0$ , shows that coefficient  $m$  (gradient of excess density in depth) very strongly influences  $z$ , and little affects value of  $z_1$  (Fig. 143).

We investigate spatial distribution  $W_{xz}$ , after representing it in the form

$$W_{xz} = f \sigma \ln \frac{x^2 + (z_2 - z)^2}{x^2 + (z_1 - z)^2}. \quad (V, 109)$$

Differentiating (V, 109) on  $z$  and by equalizing zero derivative, we will obtain:

$$\begin{aligned} z_{\max} &= \frac{z_2 + z_1}{2} - \sqrt{\left(\frac{z_2 - z_1}{2}\right)^2 + x^2}, \\ z_{\min} &= \frac{z_2 + z_1}{2} + \sqrt{\left(\frac{z_2 - z_1}{2}\right)^2 + x^2}. \end{aligned} \quad (V, 110)$$

Page 282.

If

$$x^2 \ll \left(\frac{z_2 - z_1}{2}\right)^2,$$

then we have from formula (V, 110)

$$\left. \begin{aligned} z_{\max} &\approx z_1, \\ z_{\min} &\approx z_2. \end{aligned} \right\} \quad (V, 110a)$$

Consequently, structure of field in the case of step is determined by no means midpoint with depth  $\frac{z_1 + z_2}{2}$ , but by position of singular points  $(0, z_1)$  and  $(0, z_2)$  - points of inflection of step.

If we assume in formulas (V, 110)

$$\frac{z_2 + z_1}{2} = h, \quad \frac{z_2 - z_1}{2} \approx 0,$$

then we arrive at formulas (V, 58) for  $z_{\max}$  and  $z_{\min}$ , valid for  $\Pi_1$ , in the case of material half-plane (see pg. 255), and also for  $\Delta g$  in the case of linear material rod.

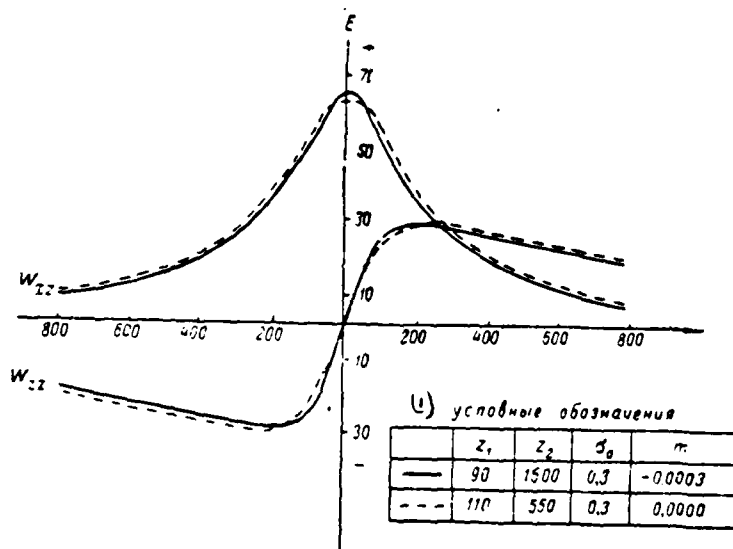


Fig. 143. Comparison of curves  $w_{zz}$  and  $w_{zz}$  in the case of vertical step with constant and variable/alternating (on vertical line) excess density. According to I. S. Berzon (1939).

Key: (1). The conventional designations.

Page 283.

Let us look, with what value  $z_{\max} = 0$  for case of step. Making this substitution in the first of the formulas (V, 110), we find

$$z = z|_{z_{\max}=0} = \pm \sqrt{z_1 z_2}. \quad (\text{V.111})$$

If we know distribution  $W_{zz}$  in series/number of lateral vertical profiles, which include that, on which maximum value  $W_{zz}$  proves to be at level of plane of observations, then this gives to us possibility to determine geometric mean from depths  $z_1$  and  $z_2$  step.

If we substitute expression  $z = z_{\max}$  from formula (V, 110) into (V, 109) and to designate for abbreviation

$$\frac{z_2 - z_1}{2} = d,$$

we will obtain that

$$(W_{xz})_{\max} = f \sigma \ln \frac{\sqrt{z^2 + d^2} + d}{\sqrt{z^2 + d^2} - d}. \quad (V, 112)$$

Zero value  $W_{xz}$  (besides obvious value of  $z = \pm \infty$ ) we have with

$$z = z_0 = \frac{z_1 + z_2}{2}. \quad (V, 113)$$

From formulas (V, 111), (V, 112), (V, 113) values  $z_1$ ,  $z_2$  and  $\sigma$  for the step can be determined.

Distribution  $W_{xz}$  on lateral vertical profile is shown in Fig. 144.

At singular point  $(0, z_1)$   $W_{xz} = +\infty$ , while at singular point  $(0, z_2)$   $W_{xz} = -\infty$ .

Theoretical values of gradient  $W_{xz}$  in the case of vertical step of intended sizes and depth for any point of profile ( $x$  axis), its going transversely course/strike, can be easily found at application of nomogram, proposed by D. M. Khramov (Ris. 145). The initial formula, which is used for its construction, is obtained as follows. Let us designate  $m = \frac{z_2}{z_1}$ ,  $n = \frac{z}{z_1}$  and then we obtain from the formula (V, 104)

$$\frac{W_{xz}}{\sigma} = f \ln \frac{n^2 + m^2}{n^2 + 1}.$$

For calculation  $W_{xz}$  in terms of given values of  $z_1$ ,  $z_2$ ,  $\sigma$  and  $x$  we enter as follows. We are assigned by values of  $m$  and  $n$  and find on the extreme scales of the nomogram of point, which correspond to values  $\xi = m$  and  $\xi = n$ . Drawing through these points straight line, let us read value  $\frac{W_{xz}}{\sigma}$  at the point of intersection with this straight line with the average/mean scale  $G$ . Multiplying this value on  $\sigma$ , we obtain unknown value  $W_{xz}$ .

Page 284.

Let us examine now curved  $W_{xz}$ , determined by appropriate equation (V, 104)

$$W_{xz} = 2f\sigma \left( \operatorname{arctg} \frac{z_2}{x} - \operatorname{arctg} \frac{z_1}{x} \right).$$

In this case  $W_{xz} = 0$  with  $x=0$  and  $x=\pm\infty$ .  $W_{xz}$  — function odd, negative with  $x<0$  and positive with  $x>0$  (see Fig. 142).

From condition  $\frac{d}{dx} W_{xz} = 0$  we find

$$x_{\min} = -\sqrt{z_1 z_2}, \quad x_{\max} = \sqrt{z_1 z_2},$$

so that

$$z_1 z_2 = x_{\max}^2 \quad (V. 114)$$

$$(W_{xz})_{\max} = 2f\sigma \left( \operatorname{arctg} \sqrt{\frac{z_2}{z_1}} - \operatorname{arctg} \sqrt{\frac{z_1}{z_2}} \right). \quad (V. 115)$$

If for step  $\sigma$  it is known, then from the last two equations it is possible to find

$$\left. \begin{aligned} z_1 &= (\sqrt{A^2 + 1} - A) x_{\max}, \\ z_2 &= (\sqrt{A^2 + 1} + A) x_{\max}. \end{aligned} \right\} \quad (V.116)$$

$$\text{where } A = \operatorname{tg} \frac{(W_{xz})_{\max}}{2f\sigma}.$$

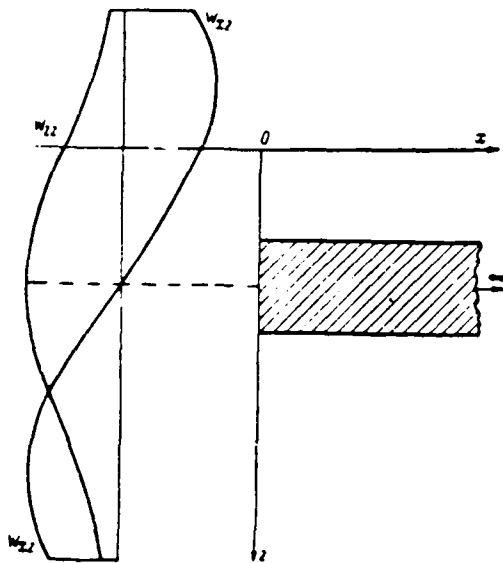


Fig. 144. Curves  $w_x$  and  $w_z$  on lateral vertical profile in the case of vertical step.

Page 285.

If  $\sigma$  is unknown, then it is possible to determine value of  $x=x_v$ , with which  $W_{xz} = \frac{1}{2} (W_{xz})_{max}$ . This, in addition to equations (V, 114) and (V, 115), gives system of equations, which determine  $z_1$ ,  $z_2$  and  $\sigma$ .

It is necessary to keep in mind that if  $\sigma$  step is known, then  $z_1$  and  $z_2$  are determined more simply and accurately on any derivatives.

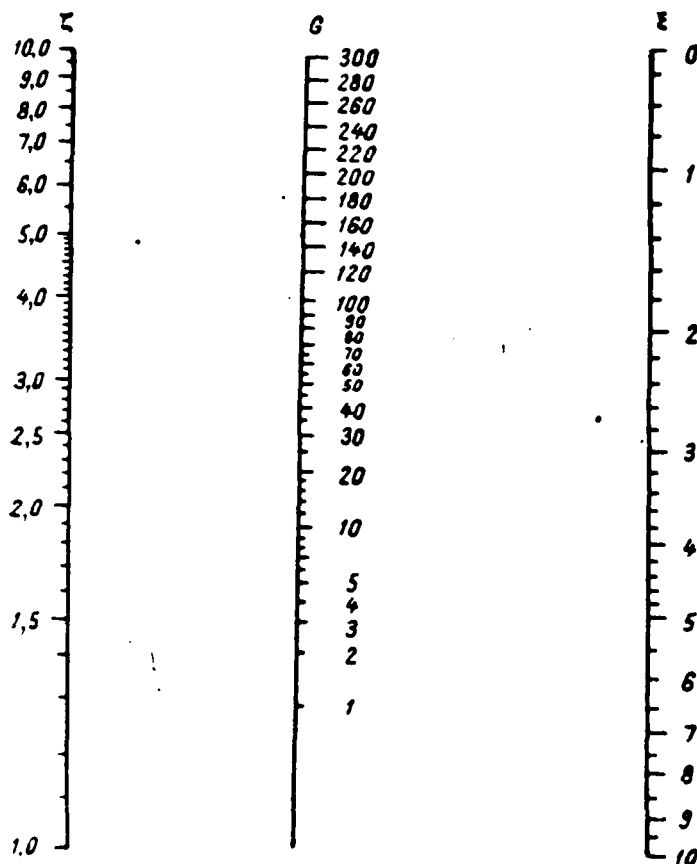


Fig. 145. D. M. Khramov's nomogram for calculation of  $W$ , in the case of vertical step.

Page 286.

Thus, with  $\sigma$  the known drops out the necessity of determination  $x_V$ , on the force gradients of gravity, and  $z_1$  and  $z_2$  easily are determined from the equation (V, 106)

$$(W_V)_{\max} = 2/\sigma \ln \frac{z_2}{z_1}$$

and the conditions

$$z_1^2 = z_2^2$$



Hence, after introducing designation

$$B = e^{\frac{(W_{xx})_{\max}}{2/\sigma}},$$

can be obtained

$$\left. \begin{aligned} z_1 &= \frac{z_{1,2}}{B}, \\ z_2 &= z_{1,1} \overline{B}. \end{aligned} \right\} \quad (V.117)$$

Let us return to  $W_{xx}$ . If besides  $W_{xx} = W_{\Delta}$  known also  $2W_{xx}$ , then, as it follows from the formulas (II, 17) and (II, 18), it is possible to construct the "vectors of curvature" having very characteristic view of the profile, which goes transversely the course/strike of the vertical step: vectors are oriented along the profile above the upper part of the step and it is perpendicular to the profile above its lower part, changing direction on  $90^\circ$  above step itself (Fig. 146).

It is possible to construct template for interpretation of anomaly  $W_{xx}$  in the case of vertical step on log-log scale. The special feature of template is the fact that curves on it they are constructed not from zero level  $W_{xx}$ , but from level  $(W_{xx})_{\min}$ . Is explained this by the fact that the point with  $W_{xx} = 0$  cannot be depicted on the logarithmic scale (since  $\lg 0 = -\infty$ ). The depicted on the template segment of a curve  $W_{xx}$  is shown in the left, template itself in the right side of Fig. 147.

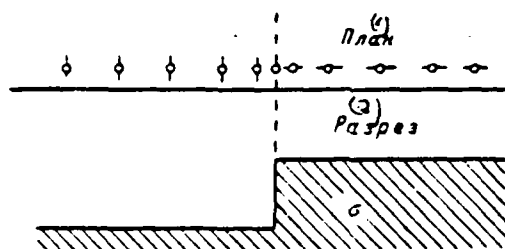


Fig. 146. Character of "vectors of curvature" along profile above vertical step.

Page 287.

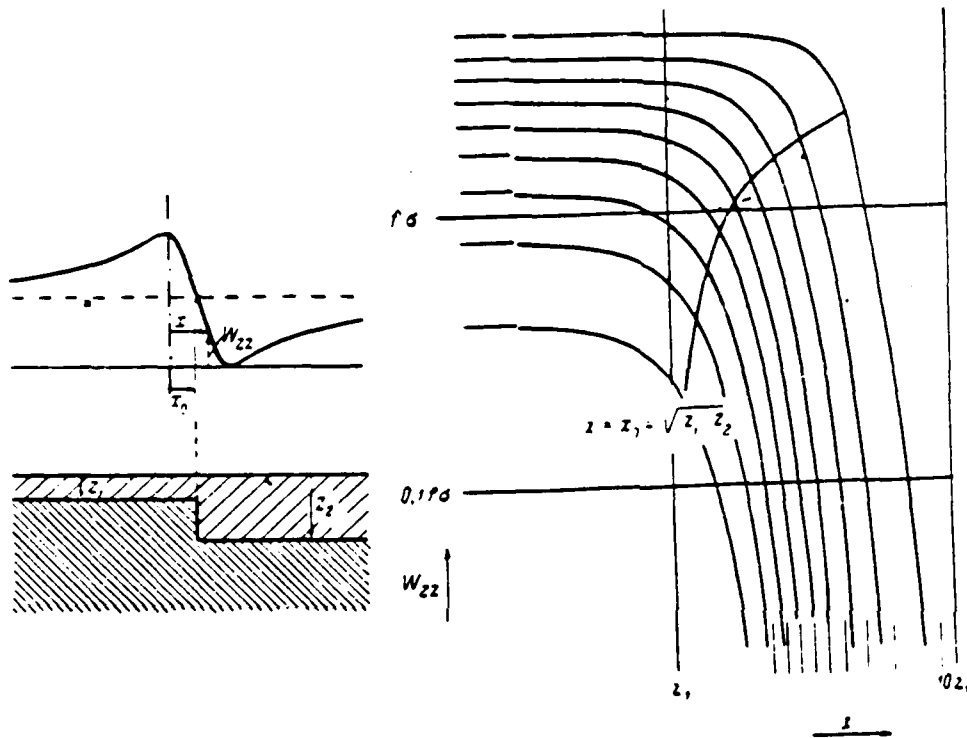


Fig. 147. Template for interpretation of curves  $W_{zz}$  in the case of vertical step. According to G. Shasne de Jeri and A. Odi (1957).

Page 288.

With the coincidence of the template observed curved with one of the theoretical curves on the vertical straight line value  $z_1$  is determined, and on the horizontal - excess density  $\sigma$  (more accurate, product  $f \sigma$ ). Along the secant curved line value  $x_0 = \sqrt{z_1 z_2}$  is further determined, whence  $z_2$  is located.

let us examine distribution  $W_{zz}$  on vertical line, for which let

us write initial equation in the form

$$W_{zz} = 2f\sigma \left( \operatorname{arctg} \frac{z_2 - z}{z} - \operatorname{arctg} \frac{z_1 - z}{z} \right). \quad (V, 118)$$

Investigation of formula gives

$$\left. \begin{aligned} z_{\min} &= \frac{z_2 - z_1}{2}, \\ (W_{zz})_{\min} &= 2f\sigma \operatorname{arctg} \frac{4zd}{4z^2 - d^2}, \end{aligned} \right\} \quad (V, 119)$$

(при  $z \neq 0$ )

Key: (1). with.

where as before

$$d = \frac{z_2 - z_1}{2}.$$

Taking into account formula (V, 118), relationship/ratio

$$W_{zz} = \frac{\partial}{\partial z} \Delta g$$

and character of distribution of anomaly  $\Delta g$  along  $z$  axis, passing through edge of step (see pg. 279-280), we come to conclusion that

$W_{zz}$  as follows is distributed along  $z$  axis:

$$\begin{aligned} W_{zz} &= 0 \text{ всюду при } z < z_1, \\ W_{zz} &= -f\pi\sigma \text{ при } z_1 < z < z_2, \\ W_{zz} &= 0 \text{ всюду при } z > z_2 \text{ (рис. 118).} \end{aligned}$$

Key: (1). everywhere with. (2). with. (3). Fig.

It is hence evident that vertical force gradient of gravity of second order

$$\frac{\partial^2}{\partial z^2} (\Delta g) = \frac{\partial}{\partial z} (W_{zz}) = W_{zzz}$$

as follows is distributed along  $z$  axis:

$W_{zz} = 0$  всюду, за исключением точек  $(0, z_1)$  и  $(0, z_2)$ ;

$W_{zz} = -\infty$  в точке  $(0, z_1)$ ;

$W_{zz} = +\infty$  в точке  $(0, z_2)$ .

Key: (1). everywhere, with exception of points ... and ... (2). at point.

All this very clearly shows determining role of singular points (in this case  $(0, z_1)$  and  $(0, z_2)$ ) in structure of anomalous field.

Page 289.

#### Variation anomaly

$$\delta \Delta g(x, l) = \Delta g(x, l) - \frac{\Delta g(x+l) + \Delta g(x-l)}{2}$$

in the case of step is determined by very bulky expression, since each of members of right side must be expressed by formula of type of appropriate of formulas  $\Delta g$  in (V, 104). This expression is presented, however, by very tame curve, similar to the curve  $\delta \Delta g$  in the case of the material half-plane (see Fig. 136).

Investigation of formula  $\delta \Delta g$  for vertical step, carried out by G. D. Managadze (1958), leads to following solution of inverse problem:

$$\left. \begin{aligned} z_1 &= \sqrt{m - \sqrt{m^2 - n}} \\ z_2 &= \sqrt{m + \sqrt{m^2 - n}} \\ n &= \frac{\delta \Delta g_{max}}{f\rho} \end{aligned} \right\} \quad (V, 120)^2$$

where

$$\left. \begin{aligned} m &= \frac{3(x_m^4 - x_m^2) - (x_m^2 l^2 - x_m^2 l^2)}{2(x_m^2 - x_m^2) - (l^2 - l^2)}; \\ n &= \frac{3x_m^4(2x_m^2 - l^2) - 3x_m^2(2x_m^2 - l^2) - l^2 l^2(x_m^2 - x_m^2) - 2x_m^2 x_m^2(l^2 - l^2)}{2(x_m^2 - x_m^2) - (l^2 - l^2)} \end{aligned} \right\}$$

$$\begin{aligned}
 p = & 2z_2 \operatorname{arctg} \frac{x_m}{z_2} - 2z_1 \operatorname{arctg} \frac{x_m}{z_1} + x_m \ln \frac{z_m^2 + z_2^2}{z_m^2 + z_1^2} - \\
 & - z_2 \operatorname{arctg} \frac{x_m + l}{z_2} + z_1 \operatorname{arctg} \frac{x_m + l}{z_1} - \\
 & - \frac{x_m + l}{2} \ln \frac{(x_m + l)^2 + z_2^2}{(x_m + l)^2 + z_1^2} - z_2 \operatorname{arctg} \frac{x_m - l}{z_2} + \\
 & + z_1 \operatorname{arctg} \frac{x_m - l}{z_1} - \frac{x_m - l}{2} \ln \frac{(x_m - l)^2 + z_2^2}{(x_m - l)^2 + z_1^2},
 \end{aligned}$$

(V, 120a)

$x'_m$  and  $x_m$  represents here abscissas of extreme values  $\delta\Delta g(x, l)$  with two values of parameter  $l'$  and  $l$  (one should take  $l' \gg l$ ).

FOOTNOTE<sup>1</sup>. In expressions  $z_1$  and  $z_2$ , the positive values of radicals are implied everywhere. ENDFOOTNOTE.

Page 290.

Method requires very precision determination  $x'_m$  and  $x_m$ . virtually let us apply with interpretation of intensive anomalies, investigated by very in detail high-accuracy gravimetric photographing. The example of the practical utilization of a method (Managadze, 1959) is published.

Subsequently, it makes sense to develop nomograms for determining values  $m$ ,  $n$  and  $p$  in formula (V, 120a).

Approximate methods of determining depth  $z_1$  of step. Until now, we examined the methods of interpretation, which give the possibility of the independent determination of depths  $z_1$  and  $z_2$ , upper and the lower bounds of step, and also its excess density  $\sigma$ . However, in a

number of cases there is special interest in the determination only of one of the elements indicated, namely, depth  $z_1$  of face side of step. As the example let us assume that we is interpreted an intensive anomaly of the type of the so-called "gravitational step/stage" in the platform region with the depth of the bedding of basement into several kilometers - under the conditions, when this anomaly can be explained by the effect/action of the steep contact (interface of density) within the basement. In such cases for us there is first-rate interest in value of  $z_1$  of step, which can be with the high fraction/portion of probability considered coinciding with the depth of the bedding of the surface of basement in the region being investigated.

Below we examine four approximate methods of determining depth  $z_1$  of vertical step, of obtained application in practice interpretations and characterizing by following special features:

1. Utilization of the variation anomaly  $\delta\Delta g$  with its subsequent recount to the height - for high-amplitude step with the unknown excess density.

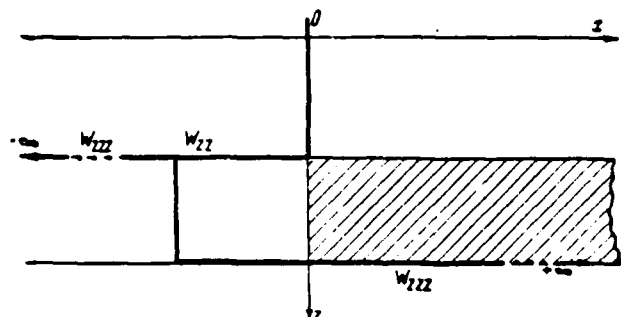


Fig. 148. Distribution  $w_{zz}$  and  $\Delta g$  on vertical profile, passing through edge of vertical step.

Page 291.

2. Interpretation on  $\Delta g$  and  $\delta \Delta g$  for material half-plane - in the case of step of small amplitude with assigned excess density  $\sigma$ .

3. Utilization of integral transform of anomaly  $\Delta g$ .

4. Joint utilization  $\Delta g$  and  $w_{zz}$ .

Method 1. For the author it was possible to adapt G. D. Managadze's formula for determining the depth  $z$ , of vertical step, (V, 96) for the case of material half-plane.

FOOTNOTE<sup>1</sup>. B. A. Andreyev - is published for the first time.

ENDFOOTNOTE.

This method, which proved to be during the practical utilization very



simple and sufficiently accurate, we described below.

The following is an interesting special feature of this method. As we already indicated above, the replacement of step by material half-plane was possible only under the condition of the relative smallness of the vertical sizes/dimensions of step. Nevertheless the described method is most acceptable precisely for those cases, when the gravity anomaly being investigated is caused by the effect/action of the vertical step of large vertical sizes/dimensions, i.e., such cases, when a difference in depths  $z_2 - z_1$  for the step high value in comparison with depth  $z_1$ . Virtually these will be anomaly of the type of the "gravitational step/stage" of large intensity, since, as we know, total variation  $\Delta g$  above the step comprises

$$\Delta g = 2f\delta\pi(z_2 - z_1),$$

i.e. it is directly proportional to difference  $(z_2 - z_1)$ . With depth  $z_1$  on the order of 2-3 km the desirable amplitude of anomaly  $\Delta g$  must compose order 10 or more milligal.

Thus, let there be curve  $\Delta g$  for vertical step with excess density  $\sigma$  and large vertical amplitude of  $z_2 - z_1$  (Fig. 149). We are assigned by the parameter  $l$  (it desirable to take small value) and change to the variation anomaly  $\delta\Delta g(x, l)$ . We count over this anomaly upward to level  $z = -z_2$ , taking value  $z_1$  of comparatively small, desirably 2-3 times of smaller than the predicted value of depth  $z_1$  of step (if this predicted value can be according to one or the other data established).

Let us examine now difference

$$\delta\Delta g(x, 0) - \delta\Delta g(x, -z_0).$$

Page 292.

It is easy to see that this difference is gravitational effect/action not  $\delta\Delta g$  of initially assigned vertical step minus gravitational effect/action on  $\delta\Delta g$  of the same step, omitted downward at depth  $z$ , from its original position, or, in other words, two vertical steps: upper - with excess density  $\sigma$  and depths of bedding of face side  $z_1$  and lower bound of  $z_1 + z_2$ , and lower with excess density  $-\sigma$  and with depths of bedding of face side  $z_1$  and lower bound  $z_1 + z_2$ . In this case if  $z_1 < z_2$ , then, obviously each of the steps indicated it is possible to take for the material half-plane: upper with a density of  $\mu = +\delta z_1$ , at depth  $h = z_1 + z_2 / 2$  and lower with a density of  $\mu = -\sigma z_2$ , at depth  $h = z_1 + z_2 / 2$ .

Since, as it is agreed, difference  $z_1 - z_2$  in value is significant,  $\delta\Delta g$  for two steps indicated is distinguished not only by sign, but also by intensity and character of distribution (this it follows from formulas (V, 96) (V, 97) for material half-plane): upper step is characterized by more intensive anomaly  $\delta\Delta g$  with relatively small value  $|x_m|$ , but lower - by anomaly  $\delta\Delta g$  of weak intensity with relatively larger value  $|x_m|$ . Under this condition  $|x_m|$  of curve  $\delta\Delta g(x, 0) - \delta\Delta g(x, -z_0)$ , obviously, it is possible without the large error to identify with value  $x_m$  for the upper from the steps indicated. Substituting this step by material half-plane, we find for it value of  $h$  from the

formula (V, 96)

$$h = \left| \sqrt{3x_m^2 - l^2} \right|,$$

and then depth  $z_1$  of the upper point of inflection of the step

$$z_1 = h - \frac{z_0}{2}. \quad (V.121)$$

It is possible within known limits to vary values  $l$  and  $z_0$ , also, for each pair of these values to calculate value of  $z_1$ , and its final value to define as average from several values.

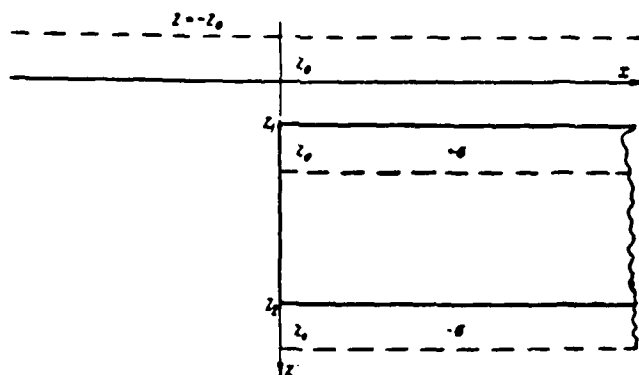


Fig. 149. Determination of depth  $z_1$  of vertical step.

Page 293.

These values can be considered more or less equally accurate.

Business in the fact that, although theoretically most accurate it is possible to consider values of  $z_1$ , which correspond to minimum values  $l$  and  $z_2$ , virtually they can and not be the same, since with the low values  $l$  and  $z_2$  it is reduced and the intensity of difference anomaly  $\delta\Delta g(x, 0) - \delta\Delta g(x, -z_0)$  and value  $x_m$  for it in connection with this virtually is determined less confidently.

Method 2. For a rough estimate of depth  $z_1$ , and also  $z_2$  step, if its excess density  $\sigma$  is known, it is possible to act then:

1) by the methods described above for the case of material half-plane on the curve  $\Delta g$  or  $\delta\Delta g$  to determine the average depth of the step

$$h = \frac{z_1 + z_2}{2};$$

2) on the curve  $\Delta g$  to determine the power/thickness of the step

$$z_2 - z_1 = \frac{\Delta g(0)}{f\sigma\pi},$$

where  $\Delta g(0)$  - value  $\Delta g$  above the step;

3) from two equations indicated to determine  $z_1$  and  $z_2$ .

Method 3. Let us examine now the method of determining the depth  $z_1$  of vertical step with the application of the integral transform  $\Delta g$ . This method is examined in the work of I. G. Klushin (1958), and the generalized presentation of method is given in the work of G. A. Troshkov and S. V. Shalayev (1961). Here we are briefly presented the essence of method in connection with the examined by us special case, keeping in mind his that version, which was used in practice with the interpretation of gravity anomalies. The general/common idea of utilization by integral of transformations is presented above in Chapter IV.

Instead of anomaly  $\Delta g$ , which is function of coordinate  $x$ , let us introduce into examination function of frequency  $\alpha$ , determined by following integral transformation:

$$I(\alpha) = \int_{-\infty}^{+\infty} \Delta g(x) \sin \alpha x dx. \quad (V, 122)$$

Page 294.

Since for the vertical step [see formula (V, 105)

$$\Delta g(-x) = 2f\sigma\pi(z_2 - z_1) - \Delta g(+x)$$

and, consequently,

$$\sin(-\alpha x) \Delta g(-x) = -2f\sigma\pi(z_2 - z_1) \sin \alpha x + \sin \alpha x \Delta g(x),$$

and

$$2f\sigma\pi(z_2 - z_1) \int_{-\infty}^{+\infty} \sin \alpha x dx = 0,$$

that  $I(\alpha)$  it is possible to rewrite in the form

$$I(\alpha) = 2 \int_0^{\infty} \Delta g \sin \alpha x dx. \quad (V, 123)$$

where anomaly  $\Delta g$  can be expressed (if we use formula (V, 82) for material half-plane and to replace in it  $\mu$  through  $\sigma dz$ , and  $h$  through  $z$ ) in the form

$$\Delta g = 2f\sigma \int_{z_1}^{z_2} \left( \frac{\pi}{2} + \operatorname{arctg} \frac{z}{z} \right) dz.$$

Substituting this expression  $\Delta g$  into formula (V, 123), we obtain

$$I(\alpha) = 4f\sigma \int_0^{\infty} \sin \alpha x dx \int_{z_1}^{z_2} \left( \frac{\pi}{2} + \operatorname{arctg} \frac{z}{z} \right) dz$$

or, varying order of integration,

$$I(\alpha) = 4f\sigma \int_{z_1}^{z_2} dz \int_0^{\infty} \left( \frac{\pi}{2} + \operatorname{arctg} \frac{z}{z} \right) \sin \alpha x dx.$$

Since

$$\frac{\pi}{2} \int_0^{\infty} \sin \alpha x dx = 0,$$

the expression  $I(\alpha)$  can be rewritten in the form

$$I(\alpha) = 4f\sigma \int_{z_1}^{z_2} dz \int_0^{\infty} \operatorname{arctg} \frac{z}{z} \sin \alpha x dx.$$

Integral on  $x$  makes sense and its value it can be calculated as follows. It is known that

$$\int_0^{\infty} \frac{e^{-ax}}{a} \sin ax \, da = \operatorname{arctg} \frac{x}{z}$$

(see, for example, saffron milk-cap and Gradstein, 1956, pg. 203, formula 3. 573).

Page 295.

On the other hand, are known inversion formulas: if

$$F(x) = \sqrt{\frac{2}{\pi}} \int_0^{\infty} f(\alpha) \sin \alpha x \, d\alpha,$$

that

$$f(\alpha) = \sqrt{\frac{2}{\pi}} \int_0^{\infty} F(x) \sin \alpha x \, dx$$

(see, for example, Ditkin and Prudnikov, 1961, pg. 16). Hence there follows

$$\frac{2}{\pi} \int_0^{\infty} \operatorname{arctg} \frac{x}{z} \sin \alpha x \, dx = \frac{e^{-\alpha z}}{\alpha}.$$

Substituting this value into the expression for  $I(\alpha)$  and integrating by  $z$ , finally we find

$$I(\alpha) = \frac{2f(\alpha)\pi}{\alpha^2} e^{-\alpha z_1} [1 - e^{-\alpha(z_2 - z_1)}]. \quad (V.12)$$

If  $\alpha$  is sufficiently great and  $z, -z$ , is great in comparison with  $z_1$ , it is possible to write approximate equality

$$I(\alpha) \alpha^2 \sim 2f(\alpha)\pi e^{-\alpha z_1}.$$

whence for two (sufficient different) values  $\alpha=\alpha_1$  and  $\alpha=\alpha_2$ , it is possible to find

$$z_1 \approx \frac{\ln I(\alpha_1) \alpha_1^2 - \ln I(\alpha_2) \alpha_2^2}{\alpha_2 - \alpha_1} \quad (V, 125)$$

and further

$$\sigma \approx \frac{I(\alpha) \alpha^2 e^{\alpha z_1}}{2j\pi}, \quad (V, 126)$$

where it is possible to take any of values  $\alpha_1$  and  $\alpha_2$ , or on succession each of them with subsequent averaging of value  $\sigma$ .

Instead of  $\sin \alpha x$  in formula (V, 122) it is possible to take many other functions, orthogonal along  $x$  axis to 1 and  $x$  (see Chapter IV). Method allows/assumes, in the principle, there are many further generalizations and modifications (see articles indicated above of I. G. Klushin and other authors).

Method 4. Let us examine now the method of determining the depth  $z_1$  of step by the joint utilization of anomaly  $\Delta g$  and gradient  $W_g$ . This method, more accurately its particular variety, is known in our literature by the name of the method of Fisher-Lyustikh. The origin of this name is such.

Page 296.

In the work of American geophysicist Fisher (Fischer, 1941) were examined some inequalities, which permit consider on the gravity anomaly maximum the value of the parameters of the structure, likened



for vertical step. Subsequently in the work of Ye. N. Lyustikh (1946) one of Fisher's inequalities was used as the approximate equality for evaluating the depth  $z_1$  of vertical step for the interpretation of anomalies of the type of "gravitational step/stage". Further appeared several works, in which discussion centered on the possibilities of the practical utilization of E. N. Lyustikh's recommendation either directly or under the condition of a certain transformation of obtained data (Salikhov 1957; Tatevosyan, 1958) and this recommendation won acceptance by the name of the method of Fisher-Lyustikh. Below we examine these recommendations.

If we take difference in values  $\Delta g(x)$  for step at points  $-\infty$  and  $+\infty$ , then from the relations (V, 105) derived above (pg. 275) it is possible to write

$$\Delta g(+\infty) - \Delta g(-\infty) = 2f\sigma\pi(z_2 - z_1).$$

On the other side of gradient  $W_{xz}$  in the case of step we have formula (V, 106)

$$|W_{xz}|_{\max} = f\sigma \ln \frac{z_2}{z_1},$$

whence

$$\frac{z_2}{z_1} = e^{\frac{|W_{xz}|_{\max}}{2f\sigma}}.$$

From written relationships/ratios follows

$$z_1 = \frac{\Delta g(+\infty) - \Delta g(-\infty)}{2f\sigma\pi \left[ e^{\frac{|W_{xz}|_{\max}}{2f\sigma}} - 1 \right]}$$

or

$$z_1 \approx \frac{\Delta \kappa(+x) - \Delta \kappa(-x)}{2f\sigma\pi \left[ e^{\frac{|W_{xz}|_{\max}}{2f\sigma}} - 1 \right]}, \quad (V, 127)$$

where  $x$  - abscissa of point, sufficient distant from edge of step, so that written approximate equality would make sense.

According to this formula is calculated depth  $z_1$  of step in method in question.

Page 297.

Itself formula (V, 127), is understood, it cannot cause objections and its utilization in practice can be considered permissible; however, with observance of following two conditions:

- 1) excess density  $\sigma$  of step is known (at least approximately;
- 2) value both  $|W_{xz}|_{\max}$  and  $\Delta g$  are known with sufficient accuracy, i.e., for example, by region of anomaly are data and variometric photographing, from which is directly known value  $|W_{xz}|_{\max}$ , but values  $\Delta g$  on profile are obtained by integrating gradient or by high-accuracy gravimetric photographing.

During practical application of method indicated usually but one of these conditions is not observed, namely:

- 1) values  $\sigma$  assign arbitrarily, for example, with interpretation of anomalies, connected with internal structure of basement, are taken by completely conditionally  $\sigma = +0.3 \text{ g/cm}^3$ , considering that anomaly being investigated compulsorily must be caused by contact of magmatic

rock of basic and acid composition. Meanwhile on the majority of density contacts within the basement of density variation, in all likelihood, there will be less than  $0.3 \text{ g/cm}^3$ , i.e., the value accepted for the appropriate anomalies will prove to be exaggerated as depth  $z_1$ , determined from the formula (V, 127).

2) For the interpretation there are used data of gravimetric photographing of a small accuracy, moreover value  $\Delta g$  is determined, taking two points into the profile, which intersects "gravitational step/stage" and after dividing a difference in the values of anomaly  $\Delta g$  at these points for the distance between the points, i.e., putting to use the following approximate relationship/ratio:

$$[W_{xx}]_{\max} \approx \frac{\Delta g(x_2) - \Delta g(x_1)}{x_2 - x_1}. \quad (\text{V, 128})$$

However, formula (V, 128) in actuality gives not maximum, but a certain average value of gradient  $W_{xx}$  in interval of  $x_2 - x_1$ . Remembering, what form takes curve  $W_{xx}$  in the case of the vertical step (see Fig. 142), we come to the conclusion that this average/mean value must be, as a rule, it is less than value  $[W_{xx}]_{\max}$ . The difference of average/mean value  $W_{xx}$  and  $[W_{xx}]_{\max}$  can be very large with the low value of  $z_1$ , when curve  $W_{xx}$  takes the form of high narrow maximum. On the basis of the given consideration, it is possible to arrive at the conclusion that the formula (V, 127) in the majority of the cases must give the systematically exaggerated value of depth  $z_1$ .

During attempt to apply this method to determination of depth of surface of crystalline basement in the Tatar ASSR according to data of

gravitational photographings it was explained that depths, determined according to formula (V, 127), exceed several times of depth of up to basement. A. G. Salikhov (1957) undertook an attempt at scheduling the correlation, with the help of which it would be possible to convert depths  $z_1$ , determined according to the formula (V, 127), into the depths of up to the surface of basement, A. G. Salikhov arriving at the conclusion that this problem is successfully solved by it.

Page 298.

In actuality success proved to be imaginary: business in the fact that the depths of up to the basement at the apex/vertex of the Tatar arch/summary, where these investigations were conducted, vary very little, so that changes in the depths are small in comparison with their average/mean value; under such conditions the calculation of depths of up to the basement with the help of the correlation graph indicated created false impression of the application of an accurate method of interpretation. The attempt to apply this graph beyond the limits of the apex/vertex of Tatar arch/summary, naturally, did not yield positive results.

In conclusion it is possible to give following estimation of method in question: itself formula (V, 127) is completely acceptable, but its practical application with utilization only of given gravimetric photographings (besides, usually, small accuracy) and determination  $W_{\text{mean}}$  from formula (V, 128) with utilization of arbitrarily selected value  $\sigma$  - operation unreliable neither in

theoretical nor in practical sense.

At the same time, under conditions, when excess density  $\sigma$  it is possible without large error to assign previously with utilization of intensive anomalies, investigated by high-accuracy detailed gravimetric photographing (or, still better, with utilization of data of complex of gravimetric or variometric photographings), application of formulas (V, 127), apparently, it is possible to consider it permissible for preliminary approximate calculations of depth  $z_1$  of step.

Let us examine two examples to interpretation of gravity anomalies for case of vertical step. The first of them - practical - for the application of an accurate analytical method, the second - theoretical - for the application of the approximate asymptotic methods.

Example 1. Fig. 150 depicts the anomaly of horizontal gradient  $W_{\alpha}$  along the profile through the oil bearing structure of Ompareti (Georgia), described by B. K. Balavadze and M. S. Abakeliya (1940). Profile intersects the buried ledged tectonic disturbance/breakdown on board the structure. As is evident on the curve of gradient, tectonic disturbance/breakdown in the first approximation, can be accepted as the vertical step.

For determining the elements of bedding of the step, let us apply

method of P. M. Nikiforov described above (see pg. 280). We determine values  $x_{1/2}$  and  $x_{1/4}$  separately on each of the wings of curve  $W_{xz}$ , and then find their average values, which we introduce into further calculations.

FOOTNOTE<sup>1</sup>. So we act because curve  $W_{xz}$  is not completely symmetrical relative to maximum ordinate. ENDFOOTNOTE.

Page 299.

We obtain:

$$x_{1/2} = \frac{1}{2} (300 + 320) = 310 \text{ } \mu,$$

$$x_{1/4} = \frac{1}{2} (500 + 660) = 580 \text{ } \mu.$$

As we see,  $x_{1/4}$  is determined on curve considerably less confidently than  $x_{1/2}$ .

We calculate auxiliary value

$$m = \frac{x_{1/4}^2 - x_{1/2}^2}{2x_{1/2}} = 388 \text{ } \mu$$

and we find through formulas (V, 107)

$$z_1 = 388 - \sqrt{388^2 - 310^2} = 155 \text{ } \mu,$$

$$z_2 = 388 + \sqrt{388^2 - 310^2} = 622 \text{ } \mu.$$

We determine on curve  $W_{xz}$

$$|W_{xz}|_{\max} = 83E = 8.3 \cdot 10^{-9} \text{ CGS}$$

and we find through formula (V, 108)

$$\sigma = \frac{8.3 \cdot 10^{-9}}{2 \cdot \frac{2}{3} \cdot 10^{-7} \ln \frac{622}{155}} = 0.45 \frac{\text{e}}{\text{cm}^2}$$

According to data of drilling depth of upper edge of step of approximately 170 m, i.e., error in determination  $z$ , in this case of approximately 9%.

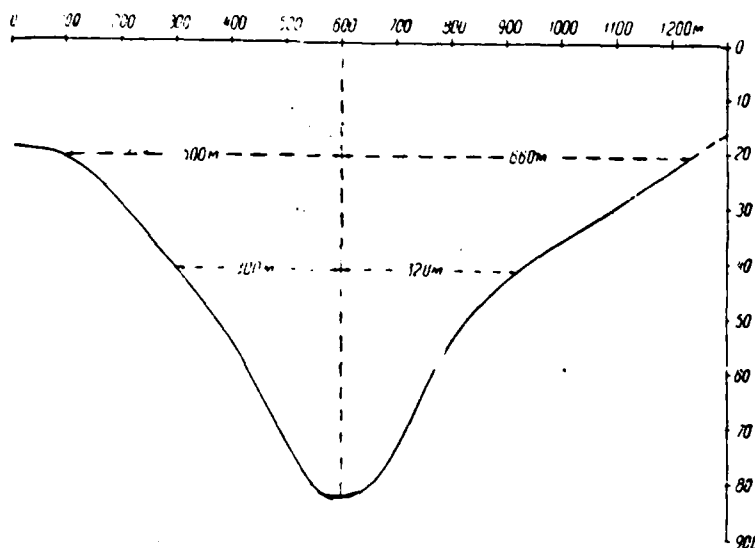


Fig. 150. Anomaly  $W_{\pi}$  above structure of Ompareti. According to B. K. Balanvadze and M. S. Abakeliya (1940).



Page 300.

The amplitude of the step is several hundred meters. Step is complex by the species/rocks of Sarmatian with a density of 2.3-2.4 g/cm<sup>3</sup>, and contact with them the species/rocks of the suite of Chauda with a density of 1.9-2.0 g/cm<sup>3</sup>, i.e. the factual excess density of the step [scarp] of approximately 0.4 g/cm<sup>3</sup>. Accuracy of determination of  $\sigma$  in this case of approximately 10%. As we see, the results of interpretation will agree well with the data of drilling, although curve  $W_n$  only approximately corresponds to the case of vertical step.

Example 2 (theoretical). Problem of anomaly  $\Delta g$  on the profile through the step with  $z_1 = 0.5$  km,  $z_2 = 1.5$  km,  $\sigma = 0.5$  g/cm<sup>3</sup> (Fig. 151). On this model we test/undergo three approximate (asymptotic) methods of interpretation (methods 2, 3, 4 on given above numbering).

Method 2. Directly from the curve  $\Delta g$  we find through the formula (V, 86)

$$h \approx \frac{z_1 + z_2}{2} = |x_{1,2}| = 0.02 \text{ km.}$$

If we consider that value  $\mu = \sigma(z_2 - z_1)$  is determined according to formula (V, 85) accurately in accordance with its theoretical value, then  $z_1$  and  $z_2$  on  $\Delta g$  are obtained with underestimation against actual values on 0.08 km (8%).

It is necessary, however, to have in mind that in practice we do

not know accurate values  $\sigma$  and  $\Delta g$  similar accuracy of interpretation, as a rule, cannot be reached.

### Method 3.

FOOTNOTE'. For the case in question the example is given in O. A. Swank's article (1961). ENDFOOTNOTE.

There were calculated values from the formula (V, 122), in which instead of the infinite limits substituted the value themselves of +15 km and -15 km and subintegral values for  $(4n+1)$  values of the period

$$T = \frac{2\pi}{\alpha}$$

were located.

It was assumed that quarter of period  $T$  contain  $n$  of intervals, equal to  $h$ , so that

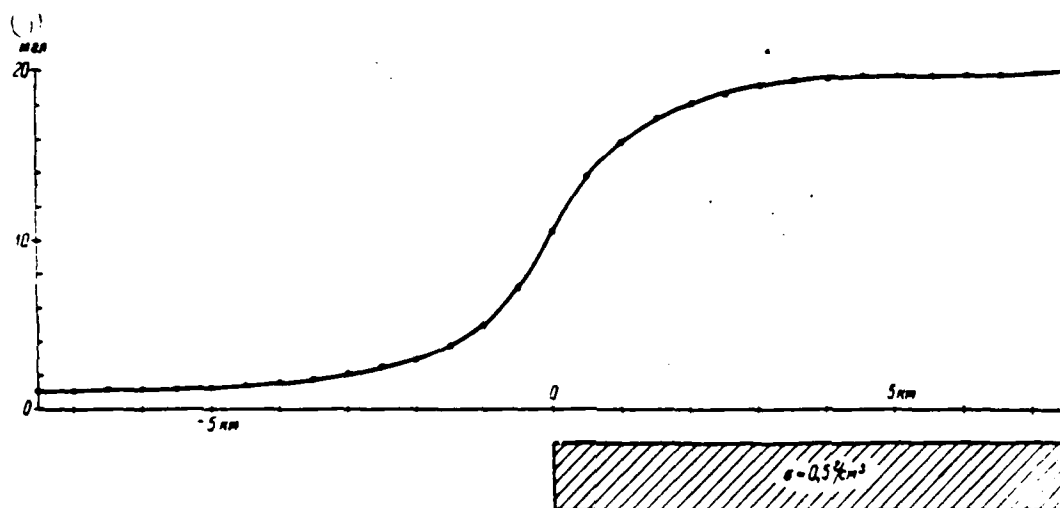
$$\alpha = \frac{\pi}{2nh}.$$

In limits of each separate interval, equal to  $nh$ , element of integral, which expresses  $I(\alpha)$ , was calculated from Stirling formula. Calculation was conducted with a gradual increase in the values  $\alpha$ , which is virtually possible only to the known limit, on achievement of which the numerator in the formula (V, 125)

$$z_1 = \frac{\ln \left[ \alpha_1^2 / (a_1) \right] - \ln \left[ \alpha_2^2 / (a_2) \right]}{a_2 - a_1}$$

is determined uncertainly due to errors in the calculations.

Page 301.

Fig. 151. Theoretical example of anomaly  $\Delta g$  above vertical step.

Key: (1). mgal.

Page 302.

Following results (Table 19) are obtained.

Taking average of four is most confidently determined values of  $z_1$ , we obtain 0.42 km instead of theoretical value of  $z_1 = 0.50$  km, i.e., error in this average is 0.08 km (16%).

It is necessary to have in mind that in given example conditions for applying method of integral transforms are distant from optimal: above we saw (pg. 293) that for reliable determination of  $z_1$  in this manner were necessary not only high values  $\alpha$ , but also high values of

difference  $z_2 - z_1$ . In the given case of  $z_2 - z_1 = 1.0$  km, and ratio  $z_2 - z_1 / z_1$  is equal to 3, i.e., it is relatively small. It is necessary to remember, finally, that in this method  $z_1$  is determined without the knowledge  $\sigma$ .

Method 4. It is checked based on the example in question the accuracy of the approximate form (V, 127)

$$z_1 = \frac{\Delta g(+x) - \Delta g(-x)}{2f\sigma\pi \left[ e^{\frac{[W_{xz}]_{\max}}{2f\sigma}} - 1 \right]},$$

considering that in this formula all values are known accurately, with exception  $W_{xz}$ , determined by the approximate relationship/ratio (V, 128)

$$W_{xz} \approx \frac{\Delta g(x_2) - \Delta g(x_1)}{x_2 - x_1}.$$

Let us place  $x_2 - x_1 = 2$  km (i.e. 1 cm to scale of map 1:200000) and let us take  $x_2 = +1$  km, and  $x_1 = -1$  km relative to point  $x=0$ , arranged/located above step. We obtain (on the curve  $\Delta g$  - Fig. 15)

$$W_{xz} \approx \frac{108 \cdot 10^{-3}}{2 \cdot 10^3} = 54 \cdot 10^{-9} \text{ CGU.}$$

Table 19. Example of calculation of depths  $z_1$  by the method of integral transforms.

$\alpha$	$I(\alpha)$	$z_1, \text{ км}$
1.257	1050	0.09
1.571	653	0.40
2.094	295	0.36
2.513	176	0.53
3.142	80.8	0.37
4.189	30.8	—

(1)  
Среднее = 0.42 км

Key: (1). Average.

Page 303.

Actual value  $[W_{xz}]_{\max}$  according to formula (V, 105) will be

$$[W_{xz}]_{\max} = 2 \cdot 66,7 \cdot 10^{-2} \cdot 0,5 \ln \frac{1,5}{0,5} = 73 \cdot 10^{-2} \text{ ГРГ.}$$

Substitution of these values into formula for  $z_1$  shows that value  $z_1$  due to inaccurate determination  $[W_{xz}]_{\max}$  in this case is obtained with exaggeration to 60% against its actual value. Let us note that this result is obtained in the theoretical example under the assumption that the excess density  $\sigma$  of step is accurately known. Is hence clear the practical inadequacy of the method in question.

#### § 41. Sloping scarp.

Body of infinite course/strike, limited by two horizontal and one inclined plane (Fig. 152), is called a sloping scarp. Sloping step is the more general/more common analog of those geologic structures, which approximately are represented in the form of the vertical step

(see pg. 272). Hence great practical value of this case. Until now, this case is insufficiently developed in the theory of interpretation for two reasons: 1) the complexity of the corresponding analytical expressions; 2) the fact that the ledged structural forms are fairly often limited by the steep lateral surface, and in these cases with the interpretation of gravity anomalies it is possible without the large error to put to use simpler model examined above of vertical step. However, in certain cases, in particular during the utilization of the second derivatives of gravitational potential, the model of vertical step is frequently clearly inappropriate, and the examination of the model of sloping step is required.

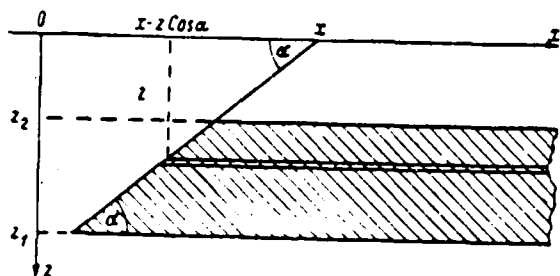


Fig. 152. Sloping step.

Page 304.

We give conclusion of analytical expressions of anomaly  $\Delta g$ ,  $W_x$ , and  $W_z$  for case of the sloping scarp. Initially, as is usual, we accept, that the origin of coordinates is arranged/located in observation point, and  $x$  represents the coordinate of the point of intersection of the lateral face of step with axis  $x$  (line of observations); let us designate the angle between the basis/base of step and the lateral plane through  $\alpha$ . Let us isolate within the step the elementary layer, limited by horizontal planes at depth  $z$  and  $z+dz$ ; its gravitational effect/action will be expressed by formulas for the material half-plane with the coordinate of the extreme point  $x-z \cos \alpha$  (see Fig. 152). Having this in mind, putting to use formulas (V, 79), (V, 80) and (V, 81) and taking into account that  $\mu = \sigma$   $dz$  and  $h=z$ , the gravitational effect of sloping scarp let us represent by the following formulas:

$$\left. \begin{aligned} \Delta g &= 2f\sigma \int_{z_1}^{z_2} \left( \frac{\pi}{2} - \operatorname{arctg} \frac{x - z \operatorname{ctg} a}{z} \right) dz, \\ W_{11} &= 2f\sigma \int_{z_1}^{z_2} \frac{z dz}{(x - z \operatorname{ctg} a)^2 + z^2}, \\ W_{12} &= -2f\sigma \int_{z_1}^{z_2} \frac{x - z \operatorname{ctg} a}{(x - z \operatorname{ctg} a)^2 + z^2} dz. \end{aligned} \right\} \quad (\text{V, 129})$$

The first of formulas (V, 129) gives

$$\begin{aligned} \Delta g &= 2f\sigma \int_{z_1}^{z_2} \left[ \frac{\pi}{2} - \operatorname{arctg} \frac{x - z \operatorname{ctg} a}{z} \right] dz = \\ &= f\sigma\pi(z_2 - z_1) - 2f\sigma \int_{z_1}^{z_2} \operatorname{arctg} \frac{x - z \operatorname{ctg} a}{z} dz, \end{aligned}$$

whence, calculating integral in parts, we obtain after conversions

$$\begin{aligned} \Delta g &= f\sigma\pi - 2f\sigma \left\{ \int_{z_1}^{z_2} z \operatorname{arctg} \frac{x - z \operatorname{ctg} a}{z} - \right. \\ &\quad \left. - \int_{z_1}^{z_2} \frac{z \frac{-\operatorname{ctg} a z - (x - z \operatorname{ctg} a)}{z^2}}{1 + \left( \frac{x - z \operatorname{ctg} a}{z} \right)^2} dz \right\} = f\sigma\pi - \\ &= 2f\sigma \left\{ \int_{z_1}^{z_2} z \operatorname{arctg} \frac{x - z \operatorname{ctg} a}{z} - x \int_{z_1}^{z_2} \frac{z dz}{z^2 (1 + \operatorname{ctg}^2 a) - 2x \operatorname{ctg} a z + x^2} \right\}. \end{aligned}$$

Page 305.

Latter from terms in parentheses represents known tabular integral of form

$$\begin{aligned} \int \frac{(m + nz) dz}{az^2 + bz + c} &= \frac{m}{2a} \ln(az^2 + bz + c) + \\ &+ \left( m - \frac{nb}{2a} \right) \frac{2}{4ac - b^2} \operatorname{arctg} \frac{2az + b}{4ac - b^2}. \end{aligned} \quad (\text{V, 130})$$

This gives



$$\Delta g = 2f\sigma \left[ z \left( \frac{\pi}{2} - \operatorname{arctg} \frac{z - x \operatorname{ctg} \alpha}{x} \right) - \frac{x \sin^3 \alpha}{2} \ln (z^2 - 2xz \cos \alpha \sin \alpha + x^2 \sin^2 \alpha) - \right. \\ \left. - x \sin \alpha \cos \alpha \operatorname{arctg} \frac{z - x \cos \alpha \sin \alpha}{x \sin^2 \alpha} \right]_{z_1}^{z_2}. \quad (\text{V, 131})$$

If we now change sign in  $x$ , i.e., to transfer origin of coordinates into point of intersection of lateral boundary plane of step with  $x$  axis, then we will obtain

$$\Delta g = 2f\sigma \left[ z \left( \frac{\pi}{2} + \operatorname{arctg} \frac{z + x \operatorname{ctg} \alpha}{x} \right) + \frac{x \sin^3 \alpha}{2} \ln (z^2 - 2xz \cos \alpha \sin \alpha + x^2 \sin^2 \alpha) - \right. \\ \left. - x \sin \alpha \cos \alpha \operatorname{arctg} \frac{z + x \cos \alpha \sin \alpha}{x \sin^2 \alpha} \right]_{z_1}^{z_2}. \quad (\text{V, 132})$$

In a similar manner, on the basis of formulas (III, 19) and also varying in final result sign in  $x$ , we obtain following expressions for  $W_{xz}$  and  $W_{zz}$ :

$$\left. \begin{aligned} W_{xz} &= f\sigma \left[ \sin^3 \alpha \ln (z^2 + 2xz \cos \alpha \sin \alpha + x^2 \sin^2 \alpha) - \right. \\ &\quad \left. - \sin 2\alpha \operatorname{arctg} \frac{z + x \cos \alpha \sin \alpha}{x \sin^2 \alpha} \right]_{z_1}^{z_2}, \\ W_{zz} &= f\sigma \left[ \sin 2\alpha \ln (z^2 + 2xz \cos \alpha \sin \alpha + x^2 \sin^2 \alpha) - \right. \\ &\quad \left. - 2 \sin^3 \alpha \operatorname{arctg} \frac{z + x \cos \alpha \sin \alpha}{x \sin^2 \alpha} \right]_{z_1}^{z_2}. \end{aligned} \right\} \quad (\text{V, 133})$$

Page 306.

As we see, formulas, which express gravitational effect/action of sloping step, prove to be sufficiently complex and bulky form. It is possible to considerably simplify them, if we make with them the

following conversions: first to be returned to that case, when the origin of coordinates is located in observation point, and coordinate  $x$  - at the point of intersection of the lateral limiting plane with  $x$  axis, i.e. to change to the opposite sign in  $x$  in the formulas (V, 131), (V, 132) and (V, 133), and then to introduce into the examination the polar coordinates  $\rho$  and  $\theta$ , connected with the right angled following relationships/ratios:

$$x - z \operatorname{ctg} \alpha = \rho \cos \theta,$$

$$z = \rho \sin \theta,$$

$$\rho^2 = (x - z \operatorname{ctg} \alpha)^2 + z^2 = \frac{z^2 - 2xz \cos \alpha \sin \alpha + x^2 \sin^2 \alpha}{\sin^2 \alpha}$$

and to designate through  $(\rho_1, \theta_1)$  and  $(\rho_2, \theta_2)$  the values of polar coordinates respectively for the upper and lower points of inflection of step (Fig. 1.53). As a result of all these conversions the formulas, which express the gravitational effect/action of step, are obtained in the following form:

$$\left. \begin{aligned} \Delta g &= 2f\sigma \left[ (z_2 \theta_2 - z_1 \theta_1) + x \left[ \sin^2 \alpha \ln \frac{\rho_2}{\rho_1} + \right. \right. \\ &\quad \left. \left. + \cos \alpha \sin \alpha (\theta_2 - \theta_1) \right] \right], \\ W_{xx} &= f\sigma \left[ 2 \sin^2 \alpha \ln \frac{\rho_2}{\rho_1} + \sin 2\alpha (\theta_2 - \theta_1) \right], \\ W_{xz} &= f\sigma \left[ \sin 2\alpha \ln \frac{\rho_2}{\rho_1} - 2 \sin^2 \alpha (\theta_2 - \theta_1) \right]. \end{aligned} \right\} \quad (V, 134)$$

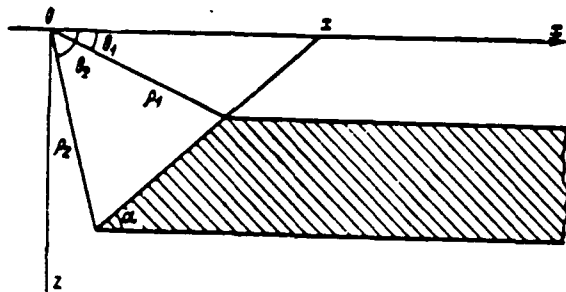


Fig. 153. Transition from right angled coordinates to polar during calculation of gravitational effect/action of sloping step.

Page 307.

As we see, these expressions are very simple and visual in comparison with formulas written above. With  $\alpha = \pi/2$ , i.e., for the case of vertical step, formula (V, 134) they give:

$$\left. \begin{aligned} \Delta g &= 2f\sigma \left[ (z_2\theta_2 - z_1\theta_1) + x \ln \frac{\rho_2}{\rho_1} \right], \\ W_{xx} &= 2f\sigma \ln \frac{\rho_2}{\rho_1}, \\ W_{zz} &= 2f\sigma (\theta_1 - \theta_2). \end{aligned} \right\} \quad (V, 135)$$

From formula (V, 131) and (V, 134) escapes/ensues following relationship/ratio between  $\Delta g$  and  $W_{xx}$  having value both for sloping and for vertical of steps:

$$\Delta g = 2f\sigma (z_2\theta_2 - z_1\theta_1) + x W_{xx}. \quad (V, 136)$$

It is necessary to remember that  $x$  in latter/last formulas considers from beginning of coordinates, adopted at observation point, to point of intersection of lateral limiting plane of step  $x$  axis.

Formulas (V, 134), with their simplicity and clarity, can have only secondary importance during calculation and investigation of distribution  $\Delta g$ ,  $W_{xx}$  or  $W_{zz}$  for sloping step. Primary meaning in this case have the nevertheless corresponding formulas in the right angled coordinates, to examination of which we return.

Analytical methods of solving the inverse problem of interpretation for the case of sloping step are not developed. For anomaly  $\Delta g$  is not developed graphic method, i.e., neither atlas of theoretical curves nor nomogram for the construction of these curves is comprised. In the literature, true, there is a description of this type of nomogram (Afanas'yev, 1952), but, unfortunately, into the basis of the construction of this nomogram was undertaken without the check formula  $\Delta g$  for the sloping step from the textbook of L. V. Sorokina (1953), who proved to be due to the slipping in misprint of erroneous<sup>1</sup>.

FOOTNOTE<sup>1</sup>. As it was explained subsequently by L. V. Petrov (1957), in L. V. Sorokin's textbook coefficient of 0.5 with natural logarithm was omitted. ENDFOOTNOTE.

Curve of anomaly  $\Delta g$  along x axis, as it follows from examination of corresponding formula (V, 131), has following special features. So, as in the case of vertical step,  $\Delta g=0$  with  $x=-\infty$  and  $\Delta g=2f\sigma\pi(z_1-z_2)$  with  $x=+\infty$ ; however, with  $x=0$ , i.e., at the point of intersection of

the lateral limiting plane of step with x axis, we have

$$\Delta g(0) = 2f\sigma(\pi - \alpha)(z_2 - z_1). \quad (V, 137)$$

Page 308.

With  $\alpha = \pi/2$ , i.e., in the case of vertical step, this gives already known relation

$$\Delta g(0) = f\sigma\pi(z_2 - z_1), \quad (V, 137a)$$

while with  $\alpha < \pi/2$  -  $\Delta g(0) > f\sigma\pi(z_2 - z_1)$ , (V, 137b)

which is physically clear, since in this case of  $\Delta g$  represents value of  $\Delta g$  above edge of vertical scarp I with amplitude of  $(z_2 - z_1)$  plus value  $\Delta g$  for prism of the same II height  $(z_2 - z_1)$  plus value  $\Delta g$  for prism of the same II height  $(z_2 - z_1)$  and with the same excess density (Fig. 1.54).

Let us designate value of  $\Delta g(0)$  with arbitrary value  $\alpha$  through  $\Delta g(0, \alpha)$ , and  $\Delta g(0)$  with  $\alpha = \pi/2$  - through  $\Delta g(0, \pi/2)$ . Table 20 shows the relations of these values for the different values  $\alpha$ .

Until now, we examined effect/action on  $\Delta g$  of sloping step with  $\alpha < \pi/2$ . From this case it is not difficult, however, to arrive also at the effect/action of step with the base angle, equal to  $(\pi - \alpha)$  (Fig. 155). As can be seen from Fig. 155, both of the indicated steps together is formed the infinite plane- parallel plate with a thickness of  $(z_2 - z_1)$ , i.e., their cumulative effect is equal  $2f\sigma\pi(z_2 - z_1)$ .

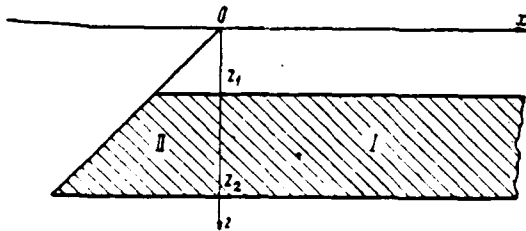


Fig. 154. Explanation to formula (V, 137) for sloping step.

Table 20 relation  $\frac{\Delta g(0, \alpha)}{\Delta g(0, \frac{\pi}{2})} = n_\alpha$  for the different values of the angle  $\alpha$  of sloping step.

$\alpha^\circ$	$n_\alpha$
90	1.00
75	1.17
60	1.33
45	1.50
30	1.67
15	1.84

Page 309.

At the same time, a change of the direction of step is equipollent in the sense of the gravitational effect/action to sign change in coordinate  $x$  in the appropriate formula, since during the derivation of this formula integration limits transpose. Taking into account these all facts, we can write the following relation:

$$\Delta g(x, \pi - \alpha) = 2f\sigma\pi(z_2 - z_1) - \Delta g(-x, \alpha). \quad (V, 138)$$

This relation makes it possible to construct curve  $\Delta g$  for step with angle  $(\pi - \alpha)$ , if curve  $\Delta g$  for step with angle  $\alpha$  is known.

Noticeable effect of angle  $\alpha$  on form of curve  $\Delta g$  for sloping step is developed only in the case, when amplitude of step  $z_1 - z_2$  is great in comparison with depth  $z_1$ ; otherwise this effect proves to be insignificant even for  $\alpha$ , considerably different from  $\pi/2$  (Fig. 156). The fact indicated allows many anomalies, caused by the effect/action of sloping step, to interpret as those caused by the effect/action of vertical step; for such anomalies the angle of the slope of the lateral face of step is determined unstably.

Until now, as it has already been said above, atlases of theoretical curves of anomaly  $\Delta g$  for structures of type of sloping step there are no. Subsequently this atlas should be constructed. Is even more expedient to construct the atlas of the theoretical curves of the variation anomaly  $\delta\Delta g$  for the case of sloping step, first, because the utilization of an atlas of theoretical curves, as already mentioned in Chapter IV, is especially effective for the localized forms of anomalies (variation, the higher derivatives), secondly, because the curves  $\delta\Delta g$  for the sloping step take the incomparably more characteristic and more indicative form, than the curves  $\Delta g$ .

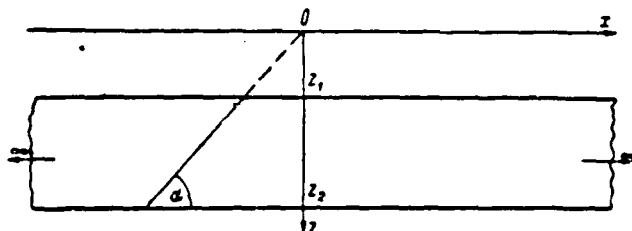


Fig. 155. Explanation to formula (V, 138) for sloping step.

Page 310.

As can be seen from Fig. 157, the sloping scarp is characterized by the asymmetric curve  $\delta\Delta g$ , the point of zero value of which is placed near the projection of the upper point of inflection of step on x axis, and smaller in the absolute value the extremum of curve is placed in the direction from the zero point in the direction of the incidence/drop in the lateral limiting plane of step.

Let us turn now to second derivatives  $W_{xx}$  and  $W_{yy}$ . For them the analytical solution of the inverse problem of interpretation in the case of sloping step also is not developed, but the possibilities of graphic method, which prove to be very favorable in view of convenience in the construction of theoretical curves and characteristic form of these curves, are investigated. Let us examine this question based on the example of gradient  $W_{xx}$ .



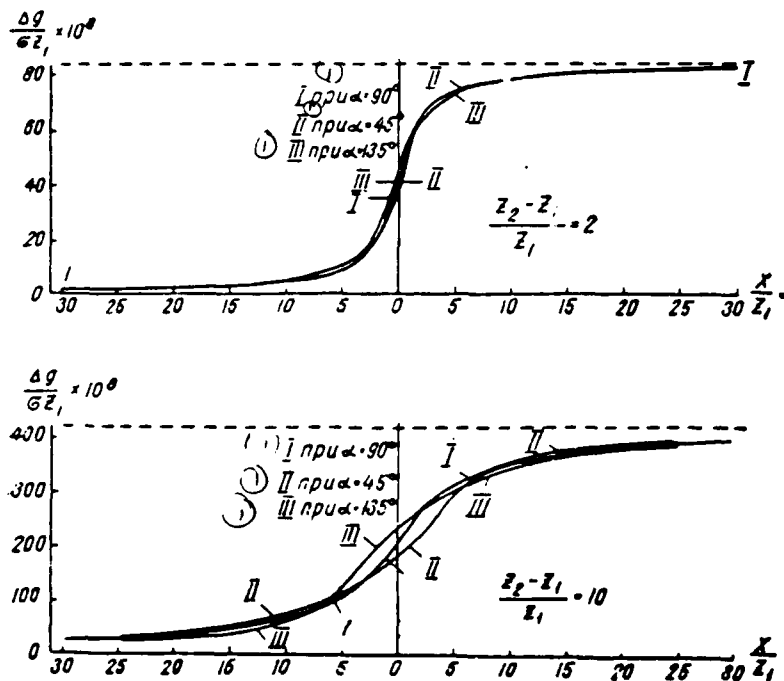


Fig. 156. Comparison of curves of anomaly  $\Delta g$  for vertical and sloping steps. According to O. A. Swank (1960).

Key: (1). with.

Page 311.

Formula (V, 132) for  $W_{xx}$  can be rewritten in the following form:

$$W_{xx} = \left[ f(\mu) + \beta \ln z \right]_{z_1}^{z_2} = f\left(\frac{x}{z_2}\right) - f\left(\frac{x}{z_1}\right) + \beta \ln \frac{z_2}{z_1}, \quad (\text{V, 133})$$

where

$$\begin{aligned} f(\mu) = & f\sigma \left[ \sin^2 \alpha \ln(1 + 2\mu \cos \alpha \sin \alpha + \mu^2 \sin^2 \alpha) - \right. \\ & \left. - \sin 2\alpha \operatorname{arctg} \left( \frac{1}{\mu} \operatorname{cosec}^2 \alpha + \operatorname{ctg} \alpha \right) \right], \\ \beta = & 2f\sigma \sin^3 \alpha, \\ \mu = & \frac{x}{z}. \end{aligned} \quad (\text{V, 134})$$

Let us assume, for example,  $\sigma=0.5$  let us assign values of relation of depths  $z_2/z_1$ , angle  $\alpha$  and argument  $\mu$ .

For values of  $z_2/z_1$  selected by us and  $\alpha$  it is possible to make table values of coefficient  $\beta$  and function  $f(\mu)$  <sup>1</sup>.

FOOTNOTE<sup>1</sup>. For calculation of tables, see in B V. Numerov (1931). In this work function  $f(\mu)$ , is designated  $g(\mu)$ , and angle  $\alpha$  - by letter  $\phi$ . ENDFOOTNOTE.

Putting to use these tables, it is possible according to the formula (V, 139) to construct tables and graphs  $W_{\alpha}$  for the different values of parameters  $z_2/z_1$  and  $\alpha$  of sloping step. The analogous calculations also of the plottings can be produced also for  $W_{\alpha}$ .

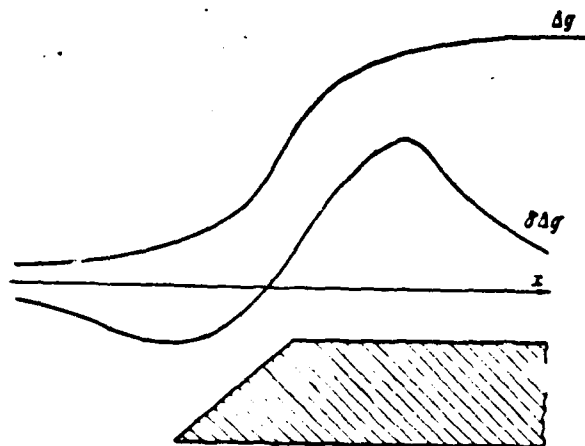


Fig. 157. Comparison of curves  $\Delta g$  and  $\delta\Delta g$  for sloping scarp.

Page 312.

With the given values of the parameters  $W_{xx}$  and  $W_{xx}$  indicated can be represented by the functions only of the one argument

$$\mu = \frac{x}{z_1},$$

i.e. by function the ratios of the horizontal distance of observation point from the point of intersection of the bevel edge of step with axis  $x$  (line of observation) to the depth of the upper boundary horizontal plane of step. Let us note that on this relative scale can be represented only second derivatives  $W_{xx}$  and  $W_{xx}$ , in contrast to them anomaly  $\Delta g$  it is necessary to represent on the usual graphic scale, for example in 1 cm of 1 km, etc.

Fig. 158 depicts four series of curves of gradient  $W_{xx}$  for sloping step, constructed according to formula (V, 139) for values of

$\sigma=0.5$  g/cm<sup>3</sup> and  $\alpha=90^\circ$  (Fig. 158a),  $\alpha=60^\circ$  (Fig. 158b),  $\alpha=40^\circ$  (Fig. 158c) and  $\alpha=20^\circ$  (Fig. 158d). Along the horizontal axis the values of  $\mu$  are plotted. For each  $\alpha$  curves  $W_{xx}$  are given for the values of the relation

$$\frac{z_2}{z_1} = 1.5; 2; 3; 5; 10; 20; 50.$$

Putting to use graphs indicated, it is possible to do analogous constructions for values  $\alpha+\pi/2$ , i.e., for angles  $\alpha$ , equal to  $60^\circ+90^\circ=150^\circ$ ;  $40^\circ+90^\circ=130^\circ$  and  $20^\circ+90^\circ=110^\circ$ . In order to be convinced of this, let us represent  $\alpha$  in the form

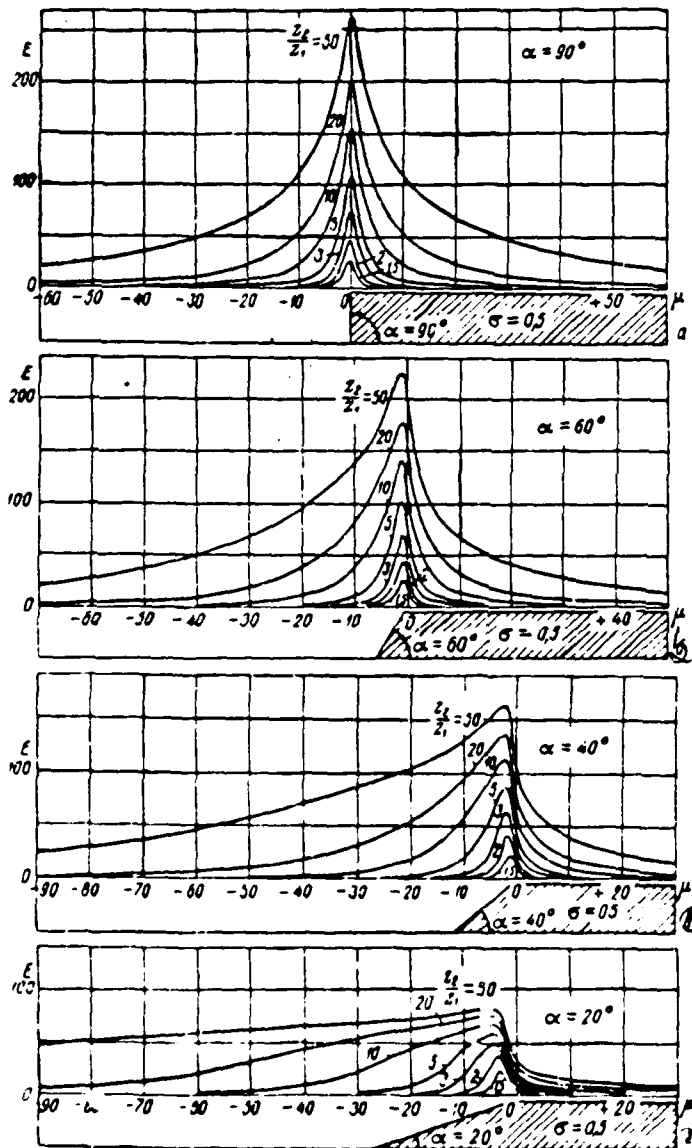
$$\alpha = \frac{\pi}{2} \pm \varphi,$$

and substituting this value in  $f(\mu)$ , we see that

$$f(+\mu, -\varphi) = f(-\mu, +\varphi).$$

Thus, in order from case  $\alpha=\pi/2-\varphi$  to switch over to case  $\alpha=\pi/2+\varphi$ , sufficient to change direction of  $x$  axis relative to step and to change curve as this is shown in Fig. 159a and 159b. But if it is necessary to construct curve for the analogous cases, but with a change in the direction of step relative to profile, then it is necessary to change sign  $W_{xx}$  to the reverse as this shown in Fig. 159c and 159d. The latter is obvious from that fact that a change in the direction of the course/strike of step is equipollent to a change of integration limits for  $x$  in the general formula for  $W_{xx}$ .

Page 313.

Fig. 158. Curves of gradient  $W_x$  for the sloping scarp.

Page 314.

Being congruent/equating between themselves series of curves for

different  $\alpha$ , we see that curves  $W_{\alpha}$  noticeably are changed with change  $\alpha$  only with sufficiently high values of ratio  $z_2/z_1$ . But if ratio  $z_2/z_1 \leq 2$  or 3, then curves are barely changed their character even with very significant changes in the angle  $\alpha$ . Hence it is possible to draw the conclusion that for the structures of the type of the sloping step/stage, whose vertical extent is relatively small ( $z_2/z_1 < 2$  with  $\sigma = 0.5$ ), the determination of the angle of the slope of the lateral face of step from curve  $W_{\alpha}$  in effect is not possible. At the same time for them the possibility of determining the depths  $z_1$  and  $z_2$  is opened up, using the methods of interpretation described above for the case of vertical step.

With  $\alpha$ , not too different from  $90^\circ$  (to  $70-50^\circ$ ), curves  $W_{\alpha}$  very differ little from appropriate curves for vertical step/stage and with high values of relative power/thickness of step ( $z_2/z_1 \leq 5-10$ ). With the high values of  $z_2/z_1$  and the decrease of angle  $\alpha$  begins noticeably to be manifested the inclination/slope of the lateral face of step. It is developed in the asymmetry of curves  $W_{\alpha}$  relative to the point of maximum and in the decrease of maximum ordinate. In this case in incident direction in the lateral face more gently sloping branch of the curve  $W_{\alpha}$  is placed

Atlas of theoretical curves for described case of sloping step can be used in many instances in practice of interpretation of results of gravitation prospecting works, carried out for purpose of analysis of geologic structures.

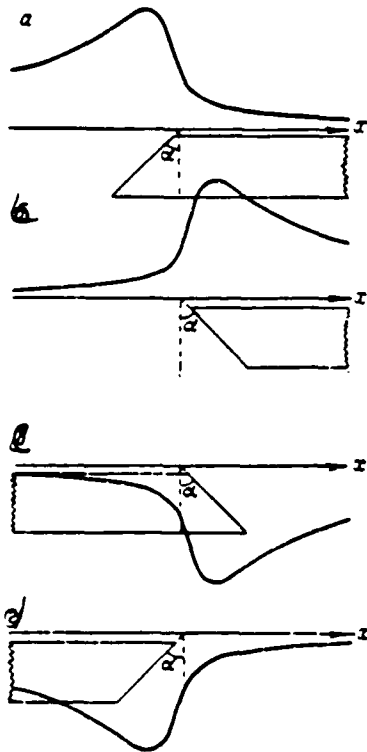


Fig. 159. Reorganizations of curve  $w_x$  (a, b, c, d) with change in incident direction in lateral face and course/strike of sloping step.

Page 315.

If structure (or its part) according to the character of curve approaches the type of sloping step/stage and to us from any data are known  $z$ , and density  $\sigma$ , then, after constructing the observed curve of gradient to scale of depth  $z$ , and by comparing it with the theoretical curves, it is possible to determine the position of the boundary of step relative to profile, depth  $z$ , and, at the sufficient vertical power/thickness of structure, the angle of the slope of lateral face

a. Depth  $z$ , is defined only approximately and besides with greater error, the more gently sloping is the incidence/drop in the lateral face, as is evident from the character of the theoretical curves, given in Fig. 158.

With the help of atlas of curves for sloping step/stage it is possible to easily construct theoretical curves also for prisms with triangular section, depicted in Fig. 160a and 160b and which correspond to structures of type of anticlines or synclines, and also for structures of more complex section, similar to that depicted in Fig. 160c, since their gravitational effect/action can be represented as equality or sum of effect/action of corresponding sloping scarps of various forms and depth.

Let us examine numerical example to interpretation of results of gravitation prospecting works on structure of type of the inclined step. Fig. 161 shows the curve of gradient the profile, which goes transversely the course/strike of structure. A difference in the density of lower and upper thicknesses is known and equal to  $+0.5$ .

Because of that fact that curve goes comparatively symmetrically relative to point of maximum, we will use formulas for case of vertical step. These formulas will permit us to find approximate values of depths  $z_1$  and  $z_2$ , which will facilitate further selection of theoretical curve for the sloping step. Let us determine values of  $x_{11}$  and  $x_{12}$  separately on the right and left wings of curve (counting from the point of maximum).



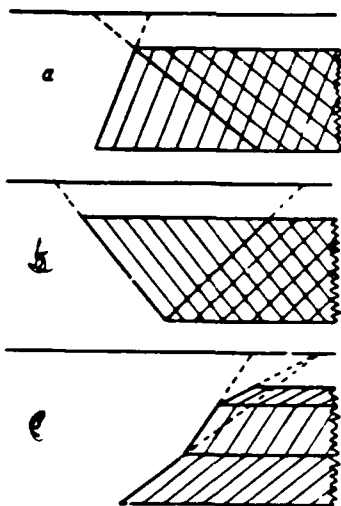


Fig. 160. Bodies with triangular section of (a, b) and step of complex form (c), whose gravitational effect/action can be represented in the form of combination of curves  $W_x$  for sloping step.

Page 316.

According to graph we find following average/mean values of  $x_{1/2}$  and  $x_{1/4}$  on both wings of curve:  $x_{1/2}=300$  m,  $x_{1/4}=570$  m, whence

$$m = \frac{x_{1/4}^2 - x_{1/2}^2}{2x_{1/2}} = \frac{570^2 - 300^2}{2 \cdot 300} = 392 \text{ m},$$

$$z_1 = m - \sqrt{m^2 - x_{1/2}^2} = 392 - \sqrt{392^2 - 300^2} = 139 \text{ m},$$

$$z_2 = m + \sqrt{m^2 - x_{1/2}^2} = 392 + \sqrt{392^2 - 300^2} = 645 \text{ m},$$

$$\frac{z_2}{z_1} = \frac{645}{139} = 4.64.$$

For a check let us find approximate value of excess density

$$\sigma = \frac{\{W_{xx}\}_{\max}}{2/(\ln z_2 - \ln z_1)} = \frac{88 \cdot 10^{-9}}{2 \cdot 66.7 \cdot 10^{-9} \cdot 2.3 (\lg 645 - \lg 139)} = 0.44 \text{ g/cm}^3$$

from these data.

As we see, it differs little from the given value of  $\sigma=0.5$  g/cm<sup>3</sup>. Selecting from the atlas theoretical curves for the sloping step with different  $\phi$  and  $z_1/z=4$  and 5, accepting  $z_1$  as included in the interval of 100-150 m and comparing these curves with that observed, we find that the best convergence gives the curve, which corresponds following to the values:  $z_1=100$  m,  $z_2=500$  m, to  $\phi=150^\circ$  with  $\sigma=0.5$  g/cm<sup>3</sup>. This curve and section corresponding to it are shown in Fig. 161.

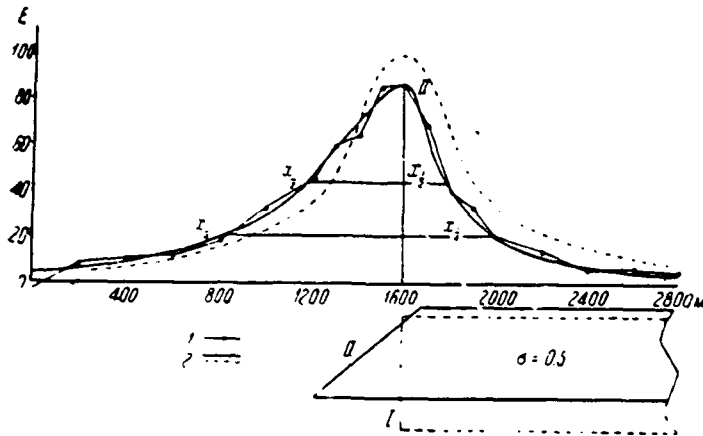


Fig. 161. Example of interpretation of anomaly  $w_{xx}$  on structure of type of sloping step/stage. 1 - observed curve; 2 - disturbing body and anomaly caused by it  $w_{xx}$ .

Page 317.

#### § 42. Rectangular infinite prism; vertical bed.

Above we already derived formulas (V, 103), that express gravitational effect/action of infinite prism with rectangular cross section. Infinite rectangular prism can serve as the prototype of real geologic bodies of the type of the vertical bed, limited on the incidence/drop, the horizontal bed, limited on the course/strike and, etc. The analytical methods of solving the inverse problem for this case in general form are not developed, which can be explained by the complexity of initial formulas, and for the second derivatives - by possibility of the examination of simpler and in many instances in practice more applicable case of the vertical bed with the infinite

incidence/drop, which is obtained from the appropriate formulas (V, 103), if in them we pass to limit  $z, \rightarrow \infty$ . However, as far as anomaly  $\Delta g$  is concerned, since into its expression the vertical coordinate  $z$  enters in absolute form, and  $e$  in the form of relation, with  $z, \rightarrow \infty$   $\Delta g \rightarrow \infty$ .

Let us examine tabular method of solving direct problem of interpretation for case of infinite rectangular prism, developed by B. V. Numerov (1931) and F. Vening-Meinesz (1940), <sup>1</sup>.

FOOTNOTE <sup>1</sup>. Letterings used below are somewhat different from those used by the authors indicated. ENDFOOTNOTE.

For applying this method of formula (V, 103) we convert to the following form:

$$\left. \begin{aligned} \Delta g &= \sigma |z A(\mu)|_{x_1, z_1}^{x_2, z_2}, \\ W_{xz} &= -\sigma |B(\mu)|_{x_1, z_1}^{x_2, z_2} = \sigma |B'(\mu)|_{x_1, z_1}^{x_2, z_2}, \\ W_{zz} &= \sigma |C(\mu)|_{x_1, z_1}^{x_2, z_2}, \end{aligned} \right\} \quad (V, 141)$$

where

$$\left. \begin{aligned} \mu &= \frac{x}{z}, \\ A(\mu) &= j \left( \mu \ln \frac{1+\mu^2}{\mu^2} + 2 \operatorname{arctg} \mu \right), \\ B(\mu) &= f \ln \frac{1+\mu^2}{\mu^2}, \\ B'(\mu) &= f \ln (1+\mu^2), \\ C(\mu) &= 2f \operatorname{arctg} \frac{1}{\mu}. \end{aligned} \right\} \quad (V, 142)$$

Tables of functions  $A(\mu)$  (Table 21) are given below <sup>1</sup>,  $B(\mu)$ ,

$B'(\mu)$  and  $C(\mu)$  (Table 22).

FOOTNOTE 1. Table 21 for  $A(\mu)$  is given to a somewhat abbreviated/reduced form. ENDFOOTNOTE.

Page 318.

Formulas (V, 103) and following of them formulas (V, 141), and also Tables 21 and 22 are brought out for that case, when origin of coordinates is located in observation point. During the calculations one should also remember that functions  $A(\mu)$  and  $C(\mu)$  are odd, i.e.  $A(-\mu) = -A(+\mu)$ ;  $C(-\mu) = -C(+\mu)$ . In contrast to them functions  $B(\mu)$  and  $B'(\mu)$  are even and are everywhere positive.

Table 21 for function  $A(\mu)$  is given with greater detail and with large number of significant places. The latter is done with calculation to that so that with the multiplication of values  $A(\mu)$  for  $z$ , in accordance with the formula (V, 141), for  $\Delta g$  concluding accuracy would be sufficient high. Table 21 gives vertical columns for the hundredths in the value  $\mu$ .

41

Table 21. Value of function  $A(\mu) \cdot 10^4$  of CGS for calculating the anomaly  $\Delta g$  in the case of infinite rectangular prism. (according to F. Vening-Meinesz, 1940).

$\pm \mu = \frac{x}{z}$	0	1	2	3	4	5	6	7	8	9
0.0	0.06	0.75	1.31	1.80	2.25	2.66	3.05	3.42	3.76	4.09
0.1	4.41	4.71	5.00	5.28	5.55	5.81	6.06	6.30	6.53	6.76
0.2	6.98	7.19	7.40	7.60	7.80	7.99	8.18	8.36	8.54	8.71
0.3	8.88	9.04	9.20	9.36	9.51	9.66	9.81	9.95	10.09	10.23
0.4	10.36	10.49	10.62	10.74	10.87	10.99	11.10	11.22	11.32	11.44
0.5	11.55	11.66	11.77	11.87	11.97	12.07	12.16	12.26	12.35	12.44
0.6	12.53	12.62	12.70	12.79	12.87	12.95	13.03	13.11	13.19	13.26
0.7	13.34	13.41	13.49	13.56	13.63	13.70	13.76	13.83	13.90	13.96
0.8	14.02	14.08	14.15	14.21	14.27	14.32	14.38	14.44	14.49	14.55
0.9	14.60	14.66	14.71	14.76	14.81	14.86	14.91	14.96	15.01	15.05
1.0	15.10	15.15	15.19	15.24	15.28	15.32	15.37	15.41	15.45	15.49
1.1	15.53	15.57	15.61	15.65	15.69	15.73	15.76	15.80	15.84	15.87
1.2	15.91	15.94	15.98	16.01	16.05	16.08	16.11	16.14	16.18	16.21
1.3	16.24	16.27	16.30	16.33	16.36	16.39	16.42	16.45	16.47	16.50
1.4	16.53	16.56	16.58	16.61	16.64	16.66	16.69	16.71	16.74	16.76
1.5	16.79	16.81	16.84	16.86	16.89	16.91	16.93	16.95	16.98	17.00
2.0	17.75	17.76	17.77	17.79	17.80	17.82	17.83	17.85	17.86	17.87
2.5	18.35	18.36	18.37	18.38	18.39	18.40	18.41	18.42	18.43	18.44
3.0	18.77	18.78	18.79	18.79	18.80	18.80	18.81	18.82	18.82	18.83
4.0	19.30	19.31	19.31	19.32	19.32	19.32	19.33	19.33	19.34	19.34
5.0	19.63									
$\frac{1}{\mu}$	0	1	2	3	4	5	6	7	8	9
0.2	19.63									
0.1	20.29	20.22	20.16	20.09	20.02	19.96	19.89	19.83	19.76	19.69
0.0	20.95	20.89	20.82	20.75	20.69	20.62	20.55	20.49	20.42	20.36

Page 319.

For calculation  $W_z$ , it is possible to put to use both function  $B(\mu)$  and function  $B'(\mu)$ , keeping in mind that great accuracy is given by utilization of  $B(\mu)$  for small values of  $\mu$  and  $B'(\mu)$  - for high values  $\mu$ .

Example to use of tables. Let for the prism  $\sigma = +0.5 \text{ g/cm}^3$ ,  $x_1 = -1.0 \text{ km}$ ,  $x_2 = +1.0 \text{ km}$ ,  $z_1 = 0.5 \text{ km}$ ,  $z_2 = +1.0 \text{ km}$  (Fig. 162). Then we

have from the formulas (V, 141)

$$\begin{aligned}\Delta g &= \sigma \left\{ z \left[ A \left( \frac{z_2}{z} \right) - A \left( \frac{z_1}{z} \right) \right] \right\}_{z_1}^{z_2} = \sigma \left\{ z_2 \left[ A \left( \frac{z_2}{z_2} \right) - A \left( \frac{z_1}{z_2} \right) \right] - \right. \\ &\quad \left. - z_1 \left[ A \left( \frac{z_2}{z_1} \right) - A \left( \frac{z_1}{z_1} \right) \right] \right\} = 0,5 \cdot 10^5 \cdot 10^{-8} [|17,75 + 15,10| - \\ &\quad - |19,30 + 17,35|] = 7,17 \cdot 10^{-3} \text{ CFC} = 7,17 \text{ mGal}, \\ W_{12} &= -0,5 (15 + 15 - 4 - 46) \cdot 10^{-9} \text{ CFC} = +10 \cdot 10^{-9} \text{ CFC} = \\ &\quad = +10E, \\ W_{11} &= 0,5 (62 - 62 - 33 + 105) \cdot 10^{-9} \text{ CFC} = \\ &\quad = +36 \cdot 10^{-9} \text{ CFC} = 36E.\end{aligned}$$

Let us turn now to the case of the vertical bed, when we assume in formulas (V, 103) that  $z_2 = \infty$ ,  $z_1 = h$ .

Table 22. Values of functions  $B(\mu)$ ,  $B'(\mu)$  and  $C(\mu)$  in Ectvoses ( $10^{-7}$  CGS) for calculation of  $w_{\pi}$  and  $w_{\pi}$  in the case of an infinite rectangular prism (according to B. V. Numerov, 1931).

$\pm \mu = \frac{x}{z}$	$+ B(\mu)$	$+ B'(\mu)$	$\pm C(\mu)$	$\pm \mu = \frac{x}{z}$	$+ B(\mu)$	$+ B'(\mu)$	$\pm C(\mu)$
0.0		0	210	6		242	22
0.1	309	1	197	7	1	262	19
0.2	218	3	184	8	1	279	17
0.3	167	6	171	9	1	295	15
0.4	132	10	159	10	1	309	13
0.5	108	15	148	20	0	401	7
0.6	89	21	138	30	0	455	4
0.7	74	27	128	40	0	493	3
0.8	63	33	120	50	0	523	3
0.9	54	40	112	60	0	548	2
1	46	46	105	70	0	568	2
2	15	108	62	80	0	586	2
3	7	154	43	90	0	602	1
4	4	189	33	100	0	616	1
5	3	218	26		0		0



Page 320.

As already said above,  $\Delta g$  in this case goes to infinity. Physically this means that the fact that anomaly  $\Delta g$  reveals so strong a sensitivity to value  $z_1$ , that for it there is no sense to examine idealized case  $z_1 = \infty$ . The second derivatives have a small sensitivity to depth  $z_1$ , and for them transition to case  $z_1 = \infty$  is completely justified. Let us assume still

$$x_2 = x + d_1,$$

$$x_1 = x - d_1,$$

where  $d_1$  - half thickness of layer, and let us change sign for  $x$  as a final result, that, as we know, is equivalent to the transfer of the origin of coordinates into the point, arranged/located above the middle of the upper edge of bed (Fig. 163). We will finally obtain the following expressions:

$$W_{xx} = f \sigma \ln \frac{(x-d_1)^2 + h^2}{(x+d_1)^2 + h^2},$$

$$W_{xz} = 2f \sigma \operatorname{arctg} \frac{2hd_1}{x^2 + h^2 - d_1^2}. \quad (V.144)$$

Let us examine gradient  $W_{xz}$  first. As can be seen from formula (V. 143)  $W_{xz}$  has zero point with  $x=0$ , i.e., above the middle of bed, being positive with  $x<0$  and negative with  $x>0$  moreover

$W_{xz}(-x) = -W_{xz}(+x)$  (see Fig. 163). Condition  $\frac{\partial}{\partial x} |W_{xz}| = 0$  gives

$$x_m = \pm \sqrt{h^2 + d_1^2}. \quad (V.145)$$

where  $x_m$  - general/common symbol of the abscissa of extreme value.

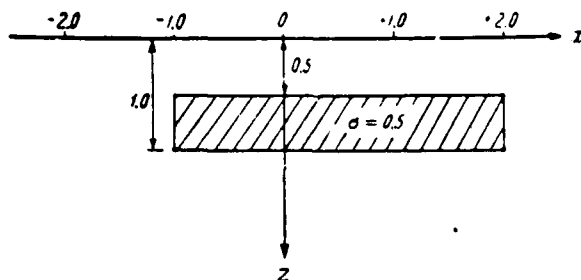


Fig. 162. Explanation for example of calculation of gravitational effect/action of rectangular prism.

Page 321.

When  $x_{\max} = -\sqrt{h^2 + d_1^2}$  we have from formula (V, 143)

$$\begin{aligned} [W_{x_1}]_{\max} &= f\sigma \ln \frac{\sqrt{h^2 + d_1^2} + d_1}{\sqrt{h^2 + d_1^2} - d_1} = \\ &= f\sigma \ln \frac{|x_m| + d_1}{|x_m| - d_1}. \end{aligned} \quad (\text{V, 145})$$

If we now find abscissa of half value of maximum of curve from obvious condition

$$\begin{aligned} \left[ \frac{(x_1 - d_1)^2 + h^2}{(x_1 + d_1)^2 + h^2} \right]^2 &= \\ &= \frac{|x_m| + d_1}{|x_m| - d_1}, \end{aligned}$$

then, solving this equation together with equation, which determines  $x_m$ , we obtain

$$d_1 = \sqrt{V - a(a + 2|x_m|)}.$$

where

$$a = \frac{x_m^2 + x_1^2}{2x_1}. \quad (\text{V, 146})$$

Whence total horizontal thickness of layer

$$d = 2d_1 = 2|\sqrt{-a(a + 2|x_m|)}|. \quad (V, 147)$$

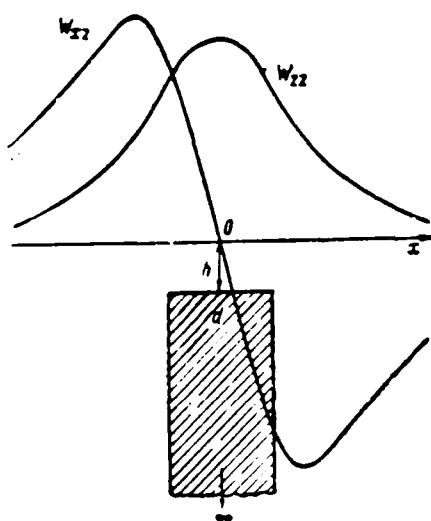
Let us note that, according to definition,  $x_{1/2}$  - negative value, i.e., is negative value  $a$  in formula (V, 147). Generally speaking, there are two values  $x_{1/2}$ , smaller in absolute value  $x_{max}$  and greater  $x_{max}$ . Into formula (V, 146) enters the first of the values of  $x_{1/2}$  indicated.

From formula (V, 144) we find further depth of upper edge of bed

$$h = |\sqrt{x_m^2 - d_1^2}|. \quad (V, 148)$$

Substituting  $d_1$  from formula (V, 147) in (V, 148), it is possible to obtain expression  $h$  also in the following form:

$$h = \frac{(x_m + x_{1/2})^2}{2|x_{1/2}|}. \quad (V, 148a)$$



Curves

Fig. 163.  $w_{xz}$  and  $w_{zz}$  above vertical bed.

Page 322.

According to formula (V, 148a) it is possible to compute  $h$  without preliminary calculation  $d_1$ .

Knowing  $d_1$ , we find from formula (V, 145) excess density of bed

$$\sigma = \frac{i W_{xz}|_{m,x}}{f \ln \frac{x_m + a_1}{x_m - d_1}} \quad (V, 149)$$

We underscore again that in this case (as in the case of step) problem of interpretation is solved to end up to definition  $\sigma$ , because of the fact that outline of bed is wholly defined by position of its points of inflection, which represent, as we now will be convinced, singular points  $W_{xz}$ . The position of the latter, as we know, is determined unambiguously.

At the same time, as in the case of step, it is necessary to have in mind that different parameters of bed, although they are determined theoretically unambiguously, virtually are obtained with different degree of reliability, precisely, depth  $h$  is determined considerably more accurately than power/thickness  $d$  and excess density  $\sigma$ . This fact is not so obvious as in the case of step, since in this case the singular points of anomalous field (i.e. the points of inflection of bed) are located on the same level. The fact here is that within known limits a change of the relative distance of singular points in the horizontal direction (i.e. in this case change of horizontal thickness of layer), as it proves to be, can be compensated by a change in the excess density of body, without varying the virtually external anomalous field, caused by the given body. This type of phenomenon is well known and is in detail investigated in the electrical prospecting and carries the name of the principle of equivalency. In this case the fact indicated is developed in the fact that in  $d < h$  and a certain  $\sigma$  anomalous field of bed corresponds virtually to the field of any other bed with  $d_1 < d$  and corresponding value  $\sigma_1 > \sigma$ , but with the same value of  $h$ . However, changes in depth  $h$  cannot be compensated by change  $\sigma$ .

Hence follows practical conclusion: if with interpretation value  $d < h$  is obtained, then it is completely unreliable, just as value  $\sigma$  of bed in case indicated. However, value  $h$  in this case is determined reliably.

Page 323.

Let us write now  $W_{xz}$  in the form

$$W_{xz} = f \sigma \ln \frac{(x-d_1)^2 + (h-z)^2}{(x+d_1)^2 + (h-z)^2} \quad (V.150)$$

and let us look how varies  $W_{xz}$  with change in vertical coordinate  $z$  of observation point. Condition  $\frac{\partial}{\partial z} |W_{xz}| = 0$  gives

$$z_m = h, \quad (V.151)$$

moreover in  $x < 0$  it corresponds to maximum, and when  $x > 0$  - to minimum  $W_{xz}$ . The extreme value

$$|(W_{xz})_m| = 2f\sigma \left| \ln \frac{x-d_1}{x+d_1} \right| \quad (V.152)$$

Knowing  $z_m$  and values  $|W_{xzm}|$  for two different given values of  $x=x_1$  and  $x=x_2$ , we can determine depth of bedding, power/thickness and excess density of bed. Curve  $W_{xz}$  on the lateral vertical profile is shown in Fig. 164.

From formula (V, 152) it is evident that at point  $(-d_1, h)$   $W_{xz} = +\infty$ , and at point  $(+d_1, h)$   $W_{xz} = -\infty$ , i.e. these points actually represent singular points  $W_{xz}$ .

Let us examine now derivative

$$W_{xz} = 2f\sigma \operatorname{arctg} \frac{2hd_1}{x^2 + h^2 - d_1^2}$$

As can be seen from this formula,  $W_{xz}$  represents even positive

function with maximum value when  $x = x_{\max} = 0$ , i.e. at point above middle of bed (see Fig. 163). In this case

$$\{W_{zz}\}_{\max} = 2f\sigma \operatorname{arctg} \frac{2h d_1}{h^2 - d_1^2}. \quad (V, 153)$$

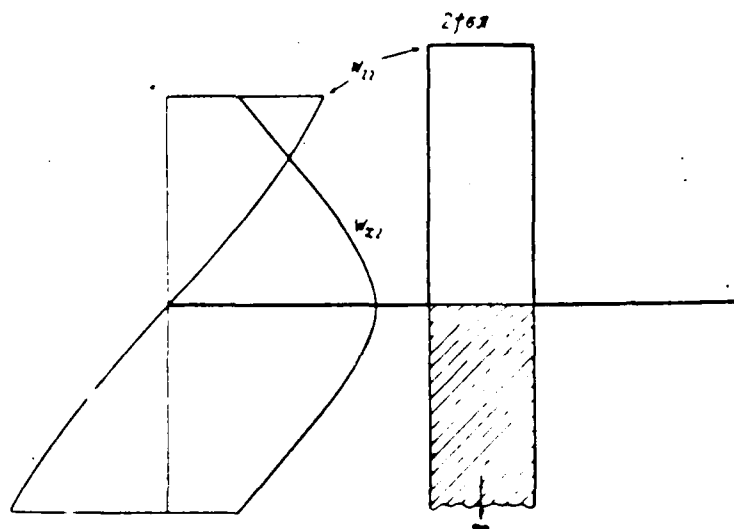


Fig. 164. Curves  $W_{xz}$  and  $W_{xz}$  on lateral vertical profile in the case of vertical bed and limiting distribution  $W_{xz}$  at level of upper edge of bed.

Page 324.

Let us find abscissas  $x_{1,2}$  and  $x_{1,4}$  in which  $W_{xz}$  is respectively equal to  $\frac{1}{2} W_{xz, \max}$  and  $\frac{1}{4} W_{xz, \max}$ .

Taking into account that

$$2 \operatorname{arctg} \alpha = \operatorname{arctg} \frac{2a}{1 - a^2},$$

and on the basis of formulas for  $W_{xz}$  and  $|W_{xz}|_{\max}$ , we obtain

$$x_{1,2} = \pm \sqrt{h^2 + d_1^2},$$

$$x_{1,4} = (h^2 + d_1^2) \pm 2h \sqrt{h^2 - d_1^2},$$

whence

$$h = \frac{x_{1,2}^2 - x_{1,4}^2}{2x_{1,2}}, \quad (V.154)$$



Further

$$d_1 = |\sqrt{x_1^2 - h^2}|$$

or

$$d = 2d_1 = 2|\sqrt{x_1^2 - h^2}|. \quad (V, 155)$$

Now we find from formula (V, 153)

$$\alpha = \frac{|W_{zz}|_{\max}}{2/\sigma \operatorname{arctg} \frac{h d_1}{h^2 - d_1^2}}. \quad (V, 156)$$

Let us represent now  $W_{zz}$  in the form

$$W_{zz} = 2/\sigma \operatorname{arctg} \frac{2(h-z)d_1}{x^2 - (h-z)^2 - d_1^2} \quad (V, 157)$$

and investigate dependence  $W_{zz}$  on  $z$ .

First of all we see that  $W_{zz} = 0$  with  $x^2 > d_1^2$  and

$$z = z_0 = h. \quad (V, 158)$$

But if  $x^2 = d_1^2$  then when  $z = h$   $W_{zz} = 2/\sigma\pi$  (see Fig. 164).

This fact is very clearly clarified by following geometric construction. Function  $\operatorname{arctg}$  in the formula (V, 157) represents the angle of the visibility  $\theta$  of the upper edge of bed from observation point. If observation point is moved to the level of the upper edge of bed, then  $\theta$ , obviously, has two limiting values:  $\theta=0$  outside of bed and  $\theta=\pi$  on the upper edge of bed.

Thus, limiting distribution  $W_{zz}$  at level  $z=h$  has very characteristic shape of right angled pulse with height  $2f \sigma \pi$  with width of  $d$  (see Fig. 164).

Page 325.

Condition  $\frac{\partial}{\partial x} (W_{zz}) = 0$  gives

$$\left. \begin{aligned} z_{\max} &= h - \sqrt{x^2 - d_1^2} \\ z_{\min} &= h + \sqrt{x^2 - d_1^2} \end{aligned} \right\} (x^2 \geq d_1^2), \quad (V, 159)$$

whence

$$[W_{zz}]_{\max} = 2f \sigma \operatorname{arctg} \frac{d_1}{\sqrt{x^2 - d_1^2}}. \quad (V, 160)$$

If  $x$  and  $\sigma$  it is possible to consider known, then from formula (V, 159) and (V, 160) it is possible to determine  $d_1$ .

Let us examine now change  $W_{zz}$  on vertical straight line, passing through point  $x = x_{\max} = 0$ , i.e. through middle of upper edge of bed. We already know that on this vertical line

$$\text{with } z = h \quad W_{zz} = 2f \sigma \pi,$$

$$\text{when } z = 0 \quad W_{zz} = 2f \sigma \operatorname{arctg} \frac{2h d_1}{h^2 - d_1^2}.$$

If we now take on the same straight line in upper half-plane point with coordinate  $z = -\sqrt{h^2 - d_1^2}$ , then, after substituting this value into formulas (V, 157) together with  $x=0$  and after taking into account already brought trigonometric relationship/ratio

$$\operatorname{arctg} \frac{2h d_1}{h^2 - d_1^2} = \operatorname{arctg} \frac{2h d_1}{h^2 - d_1^2}.$$

it is possible to obtain following:

$$\text{with } x=0, z=-\sqrt{h^2+d_1^2}=z_1,$$

$$W_{zz} = \frac{1}{2} W_{zz} \Big|_{x=0, z=0}.$$

This fact is especially simply clarified by following geometric construction. Values  $W_{zz}$  at points  $(0, 0)$  and  $(0, -\sqrt{h^2+d_1^2})$  are proportional to the angles of the visibility of the upper edge of bed AOB and  $AO_1B$  in Fig. 165. Since  $\overline{OO_1} = \sqrt{h^2+d_1^2} = \overline{O_1A} = \overline{O_1B}$ , then triangles  $AO_1O$  and  $BO_1O$  are isosceles and are similar, from which it immediately follows that  $\angle AO_1B = 1/2 \angle AOB$ .

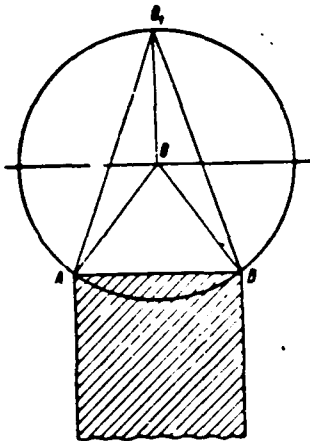


Fig. 165. For determination of  $z=z_y$ , for  $|W_{xx}|_{\max}$  in the case of vertical bed.

Page 326.

Following graphic method of determining position of upper edge of vertical bed on  $W_{xx}$  hence emerges. Let us suppose that to us is known distribution  $W_{xx}$  along the vertical profile, passing through the point of maximum  $x=0$ . This distribution  $W_{xx}$  for the upper half-plane  $z>0$  and partially for the lower half-plane  $z>0$  can be determined, knowing distribution  $W_{xx}$  on the initial profile  $z=0$  by the methods, described in Chapter IV. From the aforesaid above it follows that  $W_{xx}$  will be expressed by the monotonically decreasing curve of the type, shown in Fig. 166. We take on the vertical profile the initial point M with value  $|W_{xx}|_M$  for zero or certain positive value of  $z$ ; at a certain distance, measured from point M on the vertical line upward, equal to  $\Delta z_M$ , we find point with value  $W'_{xx} = \frac{1}{2} |W_{xx}|_M$ .

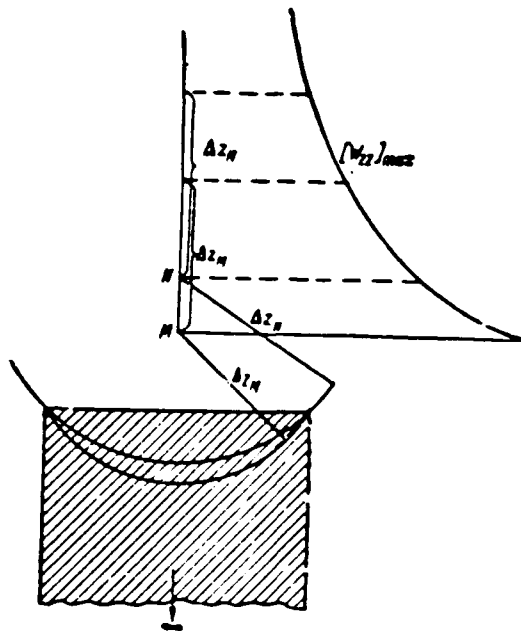


Fig. 166. For graphic method of determining position of upper edge of vertical bed on  $W_{II}$ .

Page 327.

We conduct the circular arc of radius  $\Delta z_H$  with the center in M in the lower half-plane; on this circle/circumference points of inflection A and B of bed must be located. We take on the vertical profile another point N with value  $W_{II}|_N$  and at a distance on profile from point N, equal to  $\Delta z_H$ , we find point with value  $W_{II} = \frac{1}{2} W_{II}|_N$ . We conduct now in the lower half-plane circular arc to radii  $\Delta z_H$  with the center in N. The points of intersection of two circles/circumferences indicated correspond to points of inflection A and B of bed. As we see below, this method can be applied not only for the vertical, but also for inclined bed <sup>1</sup>.

FOOTNOTE 1. Method presented above is proposed by B. A. Andreyev (it is published for the first time). ENDFOOTNOTE.

From this method great reliability of determination of depth of upper edge of bed  $h$  in comparison with determination of its horizontal power/thickness  $d$  especially is explained well, about which we already spoke above (pg. 322): on "notches" vertical coordinates of points of inflection of bed are determined more reliably than horizontal.

Besides method indicated above, it is possible to still as follows determine elements of bedding of vertical bed on curve  $W_{11}$  (Andreyev, 1950). Let us introduce the difference

$$\Delta_1(x, -z) = W_{11}(x_1, 0) - W_{11}(x, -z),$$

into the examination, where  $W_{11}(x, 0) = W_{11}$  - for the initial profile  $x=0$ ;

$W_{11}(x, -z)$  - its values, converted to height  $z$  above the initial profile.

From formula (V, 157) follows

$$\Delta_1(x, -z) = 2/\sigma \left[ \operatorname{arctg} \frac{2h \cdot d_1}{x^2 + h^2 - d_1^2} - \operatorname{arctg} \frac{2(h-z) \cdot d_1}{x^2 + (h-z)^2 - d_1^2} \right].$$

Function  $\Delta_1(x, -z)$  is depicted graphically in Fig. 167.

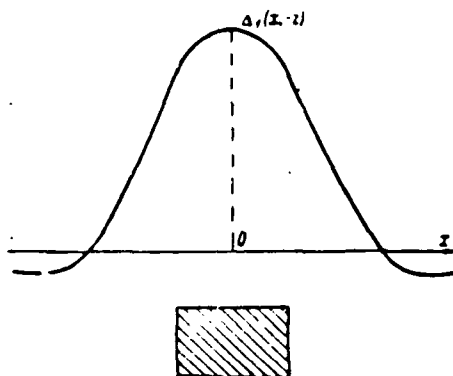


Fig. 167. Form of the function  $\Delta_1(x, -z) = W_{12}(x, 0) - W_{12}(x, -z)$  for case of vertical bed.

Page 328.

Let us find value of  $x=x_0$ , with which  $\Delta_1(x, -z)=0$ . It will be determined by the condition

$$x_0^2 = h^2 + d_1^2 - hz.$$

Let us designate  $x_0^2$  with  $z=z_1$  through  $x_{0,z_1}^2$  when  $z=z_2$  - through  $x_{0,z_2}^2$ . Then obviously,

$$h = \frac{x_{0,z_2}^2 - x_{0,z_1}^2}{z_1 - z_2}$$

(let us note that  $z_1$  and  $z_2$  - negative values).

Further we find

$$d_1 = \left| \sqrt{x_{0,z}^2 - h(z + h)} \right|,$$

where  $z$  - one of values of  $z_1$  or  $z_2$ .

For refining value of  $h$  and  $d$ , it is possible to take several different values of  $z_1$  and  $z_2$ .

For interpretation of anomalies  $W_m$ , caused by effect/action of vertical bed, it is possible to use, finally, log-log template, analogous to described above for step, right angled block and so forth (Fig. 168).

Until now, we examined case of vertical bed with lower edge, situated on large (theoretically infinite) depth. A question arises, how one should interpret anomaly for the bed with the lower edge at the relatively small depth, which, consequently, is also subject to determination.

For this purpose it is possible to use tables given in the beginning of this paragraph for calculating gravitational effect/action of rectangular prism; with the help of these tables, by trial and error, it is possible to determine probable position of both lower and upper edges of bed, and also its horizontal power/thickness.

For bed of small horizontal power/thickness ( $d < h$ ) by analogy with magnetic prospecting (Logachev, 1951, pg. 171) gradient  $W_m$  for bed with depth of upper edge  $z_1$ , and lower -  $z_2$ , will be expressed by following approximation formula:

$$W_m \sim 2f\sigma d \left[ \frac{z_2}{x^2 + z_2^2} - \frac{z_1}{x^2 + z_1^2} \right]. \quad (V.161)$$



Origin of coordinates - above middle of bed. Curve  $W_{zz}$  is depicted in Fig. 169. Depths  $z_1$  and  $z_2$  in this case are simplest to determine thus:  $W_{zz} = 0$  on the initial profile  $z=0$  with

$$x = x_{0,0} = \pm \sqrt{z_1 z_2} ,$$

and for curve  $W_{zz}$  converted to the upper profile  $z=h$ , zero value will be with

$$x = x_{0,h} = \pm \sqrt{(z_1 + h)(z_2 + h)} .$$

Page 329.

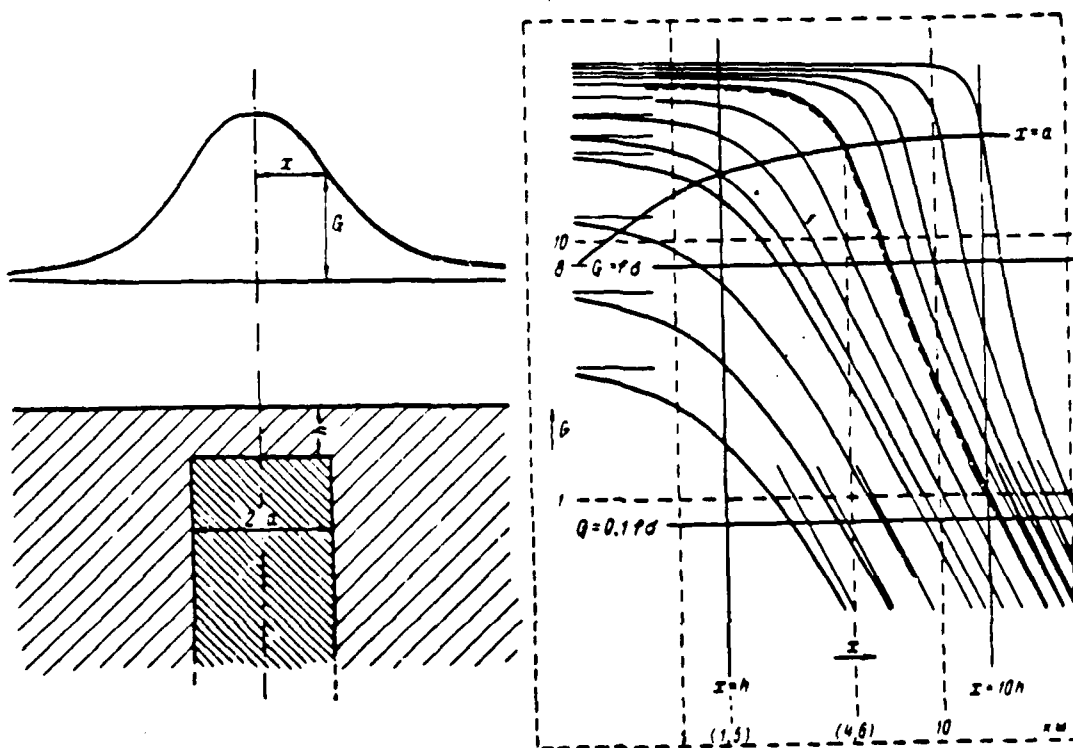


Fig. 168. Template for interpretation of curves  $G = W_{zz}$  above vertical bed. According to Zh. Shasne de Zheri and A. Odi (1957).

Page 330.

From latter/last two equations we obtain <sup>1</sup>.

$$\begin{aligned} z_1 &= m - \sqrt{m^2 - x_{0,0}^2} \\ z_2 &= m + \sqrt{m^2 - x_{0,0}^2} \end{aligned} \quad (\text{V. 162})$$

where

$$m = \frac{x_{0,h}^2 - x_{0,0}^2 - h^2}{h} \quad (\text{V. 162a})$$

FOOTNOTE <sup>1</sup>. Formulas (V, 162) are published for the first time (B. A. Andreyev). ENDFOOTNOTE.

Let us return now to case of vertical bed with  $z = \infty$  and based on this example let us explain real possibilities of utilization of analytical continuation into lower half-space during solution of inverse problem. The case of vertical bed is for this especially adequate for the following reasons: 1) it has important practical value and it is very frequently encountered with the interpretation both of gravitational and magnetic anomalies; 2) vertical bed will be characterized by especially characteristic limiting distribution both  $W_{xx}$  and  $W_{zz}$  (see Fig. 164).

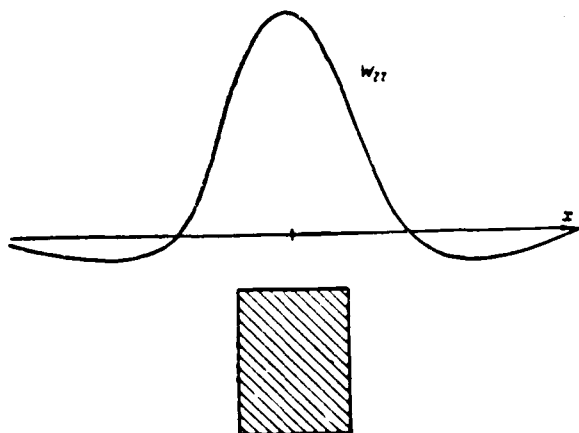


Fig. 169. Curve  $w_{11}$  for bed, limited on incidence/drop.

Page 331.

Based on theoretical example of vertical bed we investigate possibilities of both indicated in Chapter III versions methods of limiting distributions: 1) construction of vertical lateral profiles of anomalous field; 2) construction of horizontal profile of anomalous field for level of upper surface of perturbing masses. For the calculations we use the net point method, which is simplest and convenient for the case in question.

Fig. 170 shows graphs of initial data, i.e., second derivatives  $w_{11}$  and  $w_{111}$  caused by effect/action of vertical bed with  $f = 1$ . These graphs are indicated for level  $z=0$ ; values  $w_{11}$  were determined also for level  $z = -\frac{h}{2}$  and values  $w_{111}$  - for level  $z=-h$ . In the actual conditions the first level can correspond to the plane of observations, the second - to level of the recount of data into the

upper half-plane. As we know (see Chapter IV), accuracy of this recount is very high, and in the first approximation, directly measured and converted into the upper half-plane values  $W_{xx}$  and  $W_{zz}$  can be considered equally accurate. The points, at which are directly calculated according to the formulas (V, 143) values  $W_{xx}$ , on two profiles indicated are taken with the step/pitch, equal to  $h/2$  (analogous constructions for  $W_{zz}$  in the figures are not given). Power/thickness  $d$  of bed is accepted equal to  $6h$ . By the net point method, on the basis of the formula (IV, 80), we find  $U(x, z) = 4U(x, 0) - [U(x+z, 0) + U(x, -z, 0) + U(x, -z)]$ . ( $U$  - potential function being investigated).

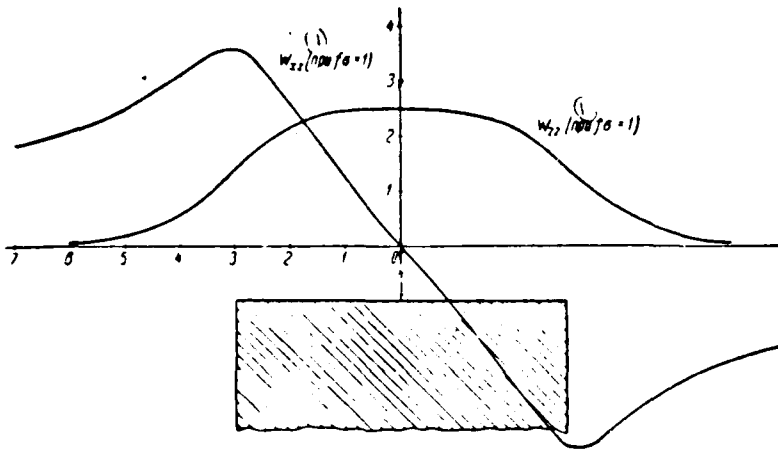


Fig. 170. Curves  $w_{xz}$  and  $w_{zz}$  along initial horizontal profile  $z=0$ . For the numerical example.

Key: (1). with.

Page 322.

Assuming/setting  $z=h/2$ , values  $W_{xz}$  are consecutively converted first for level  $z=h/2$ , then on  $z=h$  and  $z=3h/2$ . Fig. 171 (with numerals in the appropriate points) shows directly initial data and data of calculations  $W_{xz}$  net point method, on Fig. 172 - calculated by the net point method of values  $W_{xz}$  for level  $z=h$ , and also the vertical profile on the side from the bed, while in Fig. 173 - the curves of summary values along four lateral vertical profiles, arranged/located on the side from the bed. Summation was produced for decreasing the effect of the errors in the calculations, connected with rounding of data (see §27), and obtaining more indicative summary curves, since the characteristic features for each of the separate vertical profiles (point of maximum for  $W_{xz}$ ) are placed in the case of vertical bed on one and the same level,

precisely, at the level of the upper edge of bed.

As we see, level of upper edge of bed is noted completely distinctly and confidently according to following three signs:

1) on appropriate horizontal profile - characteristic  $\Pi$ -shaped pulse/momentum of curve  $W_{xx}$ ; 2) in curve summary values  $W_{xx}$  along vertical lateral profiles maximum; 3) on curve of values of gradient  $W_{xx}$  along vertical lateral profile - point of zero value. All this shows that the utilization of analytical continuation is unconditionally possible and is expedient in certain cases with the interpretation of gravity anomalies.

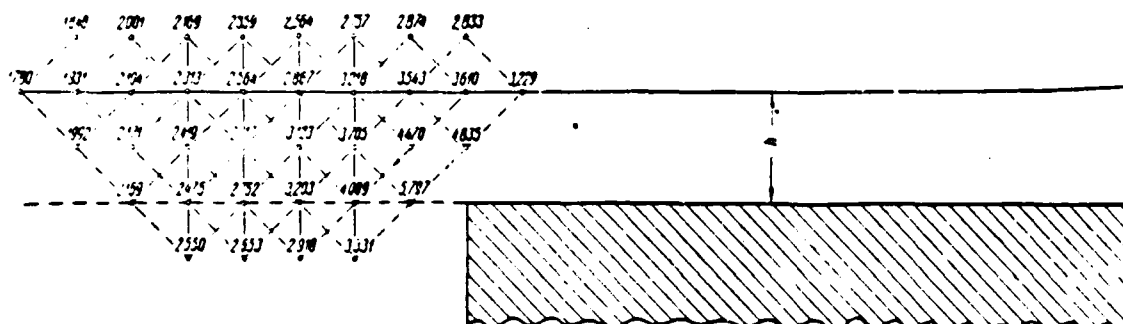


Fig. 171. Diagram, which shows distribution in vertical plane of given and calculated by net point method values  $w_x$  on the side from bed. For the numerical example.



Page 333.

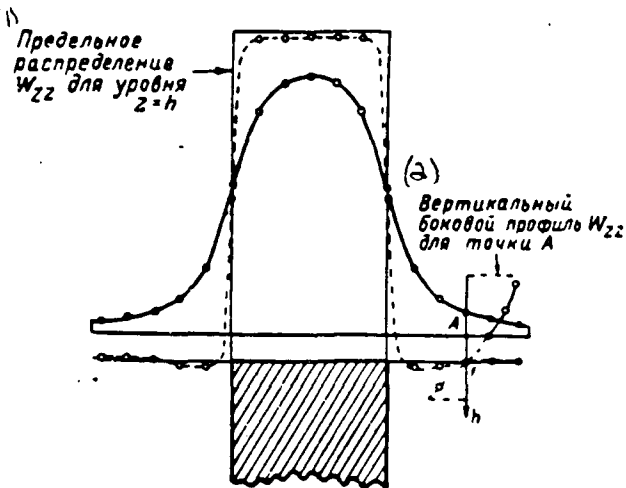


Fig. 172. Calculated by net point method distribution  $w_{zz}$  for horizontal profile at level of upper edge of bed and for vertical lateral profile on the side from bed. For the numerical example.

Key: (1). Limiting distribution ... for level  $z=h$ . (2). Vertical lateral profile ... for point A.

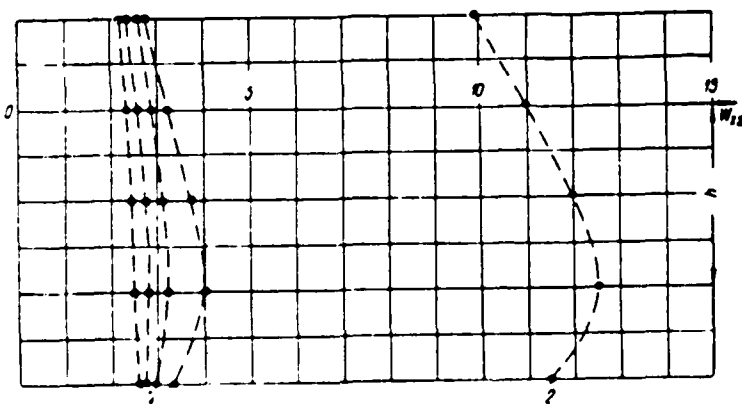


Fig. 173. Curve  $w_{zz}$  along separate lateral vertical profiles, shown in Fig. 171 (1), and curve of summary (for identical levels) values  $w_{zz}$  along these vertical profiles (2). For the numerical example.

Page 334.

Should be especially underscored the fact that methods presented above of interpretation of gravity anomalies are applicable in more complex and frequently encountered case, when these anomalies are caused by effect/action not of one, but several vertical beds, whose upper edges are arranged/located on one depth.

#### §43. Sloping bed.

By sloping bed we will imply body of infinite course/strike, bounded above horizontal, and from sides - by two parallel inclined planes (Fig. 174). Sloping bed, naturally, is more general analog of those structural elements and ore bodies, which in a number of cases can be with the interpretation of gravity anomalies accepted as the vertical beds.

In examination of anomaly  $\Delta g$  we do not have possibility to make simplifying assumption about infinite propagation of bed on incidence/drop (under this assumption  $\Delta g$  turns in  $\infty$ ). and they are forced to examine bed with lower edge, which is located on finite depth (see Fig. 174). The analytical expression  $\Delta g$  in this case can be obtained from the formula (V, 131) or (V, 134), by considering bed as "difference" in two similar sloping steps, arranged/located on the identical depth and displaced one relative to another to value  $d$ , equal to horizontal thickness of layer. Omitting the appropriate computations and being limited to expression in the polar coordinate

system, it is possible for the case in question to obtain the following formula:

$$\Delta g = 2f\sigma h \left\{ \xi(\varphi_1 - \varphi_3) - (\varphi_2 - \varphi_4) + \right. \\ \left. + \xi \sin^2 \alpha \ln \frac{Q_1}{Q_2} - (\xi - n) \sin^2 \alpha \ln \frac{Q_3}{Q_4} - \xi \cos \alpha \sin \alpha (\varphi_2 - \varphi_1) + \right. \\ \left. + (\xi - n) \cos \alpha \sin \alpha (\varphi_3 - \varphi_4) \right\}, \quad (V, 163)$$

designations in which are clear from Fig. 174.

As we see, formula takes complex form even during utilization of polar coordinates. The development of the solution of the inverse problem of interpretation for this case is very difficult business. Nevertheless we now have the original graphic method of the solution of the problem in question, whose general/common idea belongs to A. I. Zaborovskiy (1955), and development in connection with this case - Ye. A. Mudretsova (1956).

Page 335.

Essence of method consists in determination of area, bounded above curve of anomaly  $\Delta g$ , and from below - chord of this curve (see Fig. 174), and investigation of relationship/ratio of this area  $Q$  with length of chord  $a$ . The analytical expressions of area  $Q$  and chord length  $a$  are such:

$$\left. \begin{aligned} Q &= \int_{x_1}^{x_2} \Delta g dx - a \Delta g|_{x_1(x_2)} \\ a &= x_2 - x_1 \end{aligned} \right\} \quad (V, 164)$$

On the basis of formula (V, 163) and by designating through  $d$  horizontal thickness of layer, it is possible expression  $Q$  from

DOC = 88020217

PAGE ~~28~~ 604

formula (V, 164) to represent in the form

$$Q = 2f\sigma h^2 F(\sigma, \zeta, n). \quad (V, 165)$$

where

$$\sigma = \frac{a}{h}, \quad \zeta = \frac{H}{h}, \quad a = \frac{d}{h}.$$

Consequently,

$$\lg Q = \lg(2f\sigma h^2) + \lg F(\sigma, \zeta, n). \quad (V, 166)$$

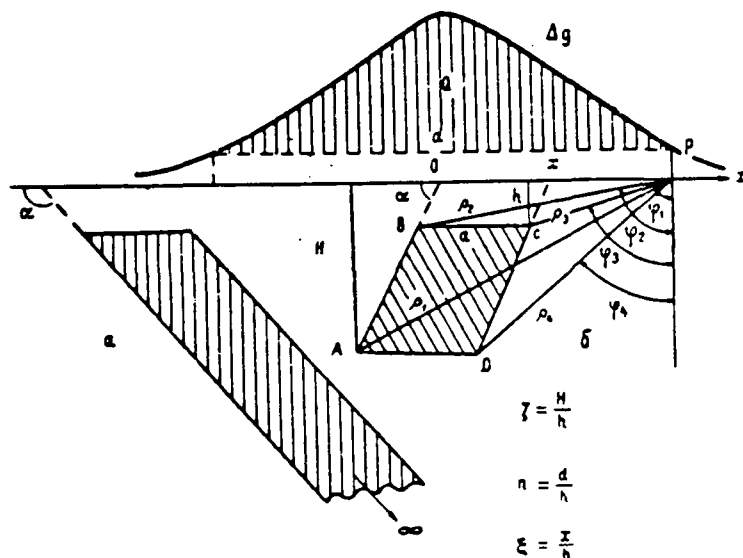


Fig. 174. Sloping bed, unconfined on incidence/drop (a) and limited on incidence/drop (b). For the limited by incidence/drop bed is shown the curve of anomaly  $\Delta g$  and the designations, which relate to the method of Ye. A. Mudretsova's interpretation (1956).

Page 336.

From formula (V, 166) we see that for one and the same bed  $lg Q$  is two terms, the first of which is constant value, and the second varies with change  $\sigma$ , i.e., with change in length of chord  $a$ .

If we have atlas of theoretical curves  $\Delta g$  for beds with different values of  $a$ ,  $n$ ,  $\xi$ , then, after measuring for each curve area  $Q$  for different  $a$ , it is possible to depict dependence  $Q=\varphi(a)$  on logarithmic scale and to obtain series of templates for interpretation of curves  $\Delta g$  for case of sloping bed. Four such templates for the values

$$\alpha = 90^\circ; 60^\circ; 45^\circ; 30^\circ;$$

$$n = \frac{d}{h} = 0.5; 1.0; 2.0; 5.0;$$

$$\zeta = \frac{H}{h} = 10; \sigma = 1.0 \text{ g/cm}^3$$

are given in Fig. 175. This template one should construct, also, for other values of  $\zeta = \frac{H}{h}$ .

Interpretation is reduced to following operations:

1. For the curve  $\Delta g$  being investigated is built on the double logarithmic scale dependence  $Q=f(a)$ . For the obtained graph, via coincidence, is selected most adequate from theoretical curves one of the templates. With the coincidence the coordinate axes of graph and template, remaining parallel, will prove to be displaced relative to one another.

2. Parameters  $n = \frac{d}{h}$  and  $\zeta = \frac{H}{h}$  on indices, inscribed on appropriate template, are determined.

3. Angle  $\alpha$  on index of corresponding curve of template is determined.

4. Are determined  $\lg h$  and  $h$  in amount of vertical displacement of axes of graph and template.

5. Are determined  $\lg \sigma$  and  $h'$ , and consequently,  $\sigma$  in amount of horizontal displacement of axes of template and graph.

Using these data, we obtain all interesting us parameters of sloping bed.

Page 337.

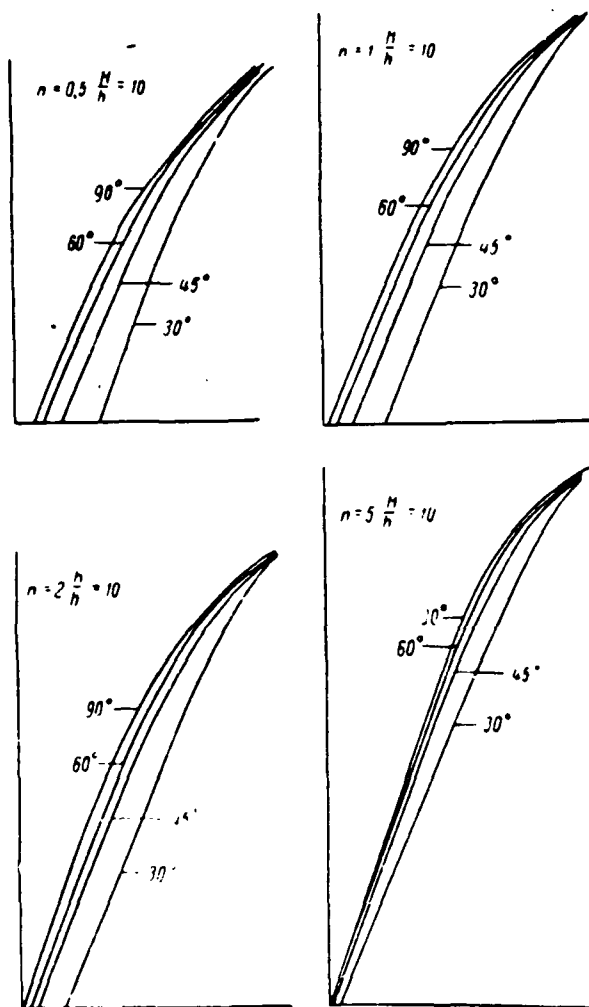


Fig. 175. Templates of curves of anomaly  $\Delta g$  for sloping beds on log-log scale. According to Ye. A. Mudretsova (1956). Modulus/module is equal to 5 cm.

Page 338.

By Ye. A. Mudretsova it is explained that change in parameter  $\xi = \frac{M}{h}$  significantly affects right (upper) part of theoretical curves

and comparatively little affects their left (lower) side. Hence he made the conclusion that in the case, when the definition of the depth of the lower edge of bed does not especially interest us, it is possible to put to use with the interpretation templates for any value  $\xi$  (for example, for  $\xi = 10$ , as accepted by Fig. 175), considering this value conventional, and to determine all the remaining elements of the bedding of bed, combining the left (lower) sides of the theoretical and factual curves, without turning attention to the disagreement of these curves in their right (upper) part.

In conclusion let us pause at position finding of bed from curve  $\Delta g$ . For the vertical bed the curve  $\Delta g$  is symmetrical relative to maximum ordinate and the latter is placed above the middle of the horizontal edge of bed. For the sloping bed the curve  $\Delta g$  becomes asymmetric and its maximum is displaced in incident direction in the bed. Ye. A. Mudretsova determined the amounts of the shift of the maximum of curve  $\Delta g$  relative to the origin of coordinates (Fig. 176) in the fractions/portions of depth  $h$  (Table 23).

With other values  $\xi$  shifts prove to be of the same order.

Let us turn now to examination of second derivatives  $W_{xx}$  and  $W_{yy}$ .



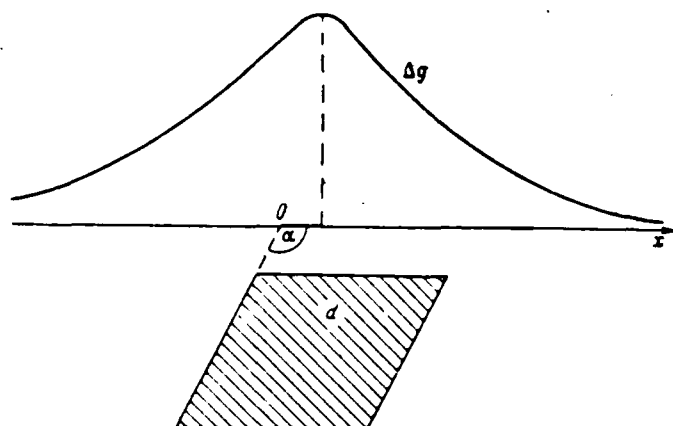


Fig. 176. For determination of position of sloping bed from curve of anomaly  $\Delta g$ .

Page 339.

During derivation of formulas, which present gravitational effect/action of sloping bed on derivatives  $W_{xx}$  and  $W_{yy}$ , is revealed interesting fact: according to their form these formulas prove to be completely identical with formulas for  $W_{xx}$  and  $W_{yy}$  in case examined above of sloping step.

This fact can be explained especially simply and clearly, if we use formulas (V, 134) for case of sloping step in polar coordinates:

$$W_{xx} = f\sigma \left[ 2 \sin^2 \alpha \ln \frac{q_2}{q_1} + \sin 2\alpha (\theta_2 - \theta_1) \right].$$

$$W_{yy} = f\sigma \left[ \sin 2\alpha \ln \frac{q_2}{q_1} - 2 \sin^2 \alpha (\theta_2 - \theta_1) \right].$$

Being based on these formulas, let us write first expressions

$W_{11}$  and  $W_{21}$  for sloping bed, limited in drop and in presenting "difference" two similar sloping steps: the first, gravitational effect/action of which is written above formulas (V, 134), and the second, similar to the first according to sizes/dimensions, located on the same depth and having the same excess density  $\sigma$ , but displaced from the first to the right up to distance of  $d$  (Fig. 177).

Table 23. Amounts of the shifts of the maximum of the curve  $\Delta g$  relative to the origin of coordinates in the fractions/portions of depth  $h$  with  $\zeta = \frac{H}{h} = 10$  for the sloping bed (according to Ye. A. Mudretsova).

$h$	$\alpha = 90^\circ$	$\alpha = 60^\circ$	$\alpha = 45^\circ$	$\alpha = 30^\circ$
0.5	+0.25	-0.30	-1.70	-2.85
1.0	+0.50	-0.55	-1.40	-2.70
2.0	+1.00	-0.25	-1.10	-2.45
5.0	+2.50	+0.75	-0.40	-1.70

Page 340.

If we designate the polar coordinates of the upper and lower points of inflection of the second step respectively through  $(\rho'_1, \theta'_1)$  and  $(\rho'_2, \theta'_2)$ , the gravitational effect/action of the second step will be expressed as follows:

$$W_{II} = f\sigma \left[ 2\sin^2 \alpha \ln \frac{\rho'_2}{\rho'_1} + \sin 2\alpha (\theta'_2 - \theta'_1) \right],$$

$$W_{II} = f\sigma \left[ \sin 2\alpha \ln \frac{\rho'_2}{\rho'_1} - 2\sin^2 \alpha (\theta'_2 - \theta'_1) \right],$$

and the gravitational effect/action of the sloping bed, limited on drop, will be

$$W_{II} = f\sigma \left[ 2\sin^2 \alpha \ln \frac{\rho_2}{\rho_1} \cdot \frac{\rho'_2}{\rho'_1} + \sin 2\alpha (\theta_2 - \theta_1 - \theta'_2 + \theta'_1) \right],$$

$$W_{II} = f\sigma \left[ \sin 2\alpha \ln \frac{\rho_2}{\rho_1} \cdot \frac{\rho'_2}{\rho'_1} - 2\sin^2 \alpha (\theta_2 - \theta_1 - \theta'_2 + \theta'_1) \right].$$

If we now make assumption about the fact that lower edge of bed is moved at infinite depth, then, as can easily be seen from Fig. 177,

during this passage to the limit  $\frac{\theta'_2}{\theta'_1} \rightarrow 1$ ;  $(\theta'_1 - \theta'_2) \rightarrow 0$ , i.e. polar coordinates of lower points of inflection of bed disappear from final expression. If we in this expression do now replacement

$\theta'_1 = \theta_2$ ;  $\theta'_2 = \theta_1$ . then we will obtain finally

$$\begin{aligned} W_{xx} &= f\sigma \left[ 2\sin^2 \alpha \ln \frac{\theta_2}{\theta_1} + \sin 2\alpha (\theta_2 - \theta_1) \right], \\ W_{xx} &= f\sigma \left[ \sin 2\alpha \ln \frac{\theta_2}{\theta_1} - 2\sin^2 \alpha (\theta_2 - \theta_1) \right], \end{aligned} \quad (V, 167)$$

i.e., as we see, formulas are actually identical with the formulas (V, 134) for the sloping step. Difference in the sense of designations in the formulas only is the fact that  $(\theta_1, \theta_2)$  relates not to the lower point of inflection of step, but to the right point of inflection of bed.

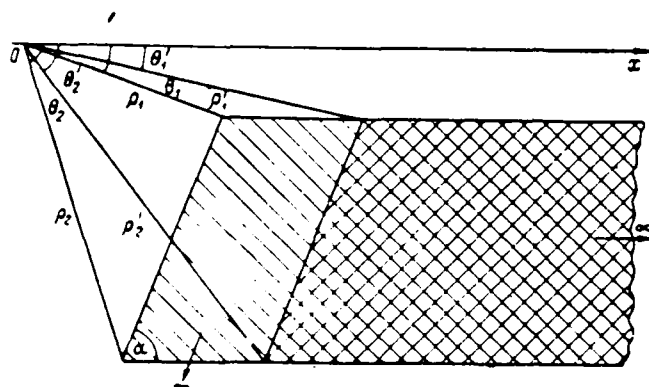


Fig. 177. For derivation of formula for  $W_{xz}$  and  $W_{yz}$  in the case of sloping bed.

Page 341.

Identity of expressions occurs, it is understood, also in the rectangular coordinate system, to which we return subsequently presentation. Let us introduce the following designations:

$$\rho_1 = \sqrt{(x - d_1)^2 + h^2},$$

$$\rho_2 = \sqrt{(x + d_1)^2 + h^2},$$

$$\theta_1 = \arctg \frac{h}{x - d_1},$$

$$\theta_2 = \arctg \frac{h}{x + d_1}$$

and let us replace angle  $\alpha$  through  $\varphi = \pi - \alpha$ , the more specific geologic sense (angle of incidence) having for the bed.

Having done substitutions indicated in formulas (V, 167) and then after changing sign in  $x$ , which is equipollent to transfer of origin of coordinates into point, arranged/located above middle of horizontal edge of bed, it is possible expressions  $W_{xz}$  and  $W_{yz}$  to represent in the following form:

$$\left. \begin{aligned} W_{xz} &= L(x) + A(x), \\ W_{zz} &= L_1(x) + A_1(x), \end{aligned} \right\} \quad (V, 168)$$

where

$$\left. \begin{aligned} L(x) &= 2f\sigma \sin^2 \varphi \ln \frac{(x-d_1)^2 + h^2}{(x+d_1)^2 + h^2}, \\ A(x) &= f\sigma \sin 2\varphi \operatorname{arctg} \frac{2hd_1}{x^2 + h^2 - d_1^2}, \\ L_1(x) &= -f\sigma \sin 2\varphi \ln \frac{(x-d_1)^2 + h^2}{(x+d_1)^2 + h^2}, \\ A_1(x) &= 2f\sigma \sin^2 \varphi \operatorname{arctg} \frac{2hd_1}{x^2 + h^2 - d_1^2}. \end{aligned} \right\} \quad (V, 169)$$

Let us focus attention on the fact that logarithmic functions  $L(x)$  and  $L_1(x)$  are proportional to  $W_{xz}$  and to function of arc tangent  $A(x)$  and  $A_1(x) = W_{zz}$  for case of vertical bed, which follows from comparison of formulas (V, 169) and (V, 143).

However, concerning derivatives themselves  $W_{xz}$  and  $W_{zz}$  as can be seen from Fig. 178, considerably are distinguished by their form in cases of vertical and sloping beds, if angle  $\varphi$  is noticeably different from  $90^\circ$ .

For quantitative interpretation of curves  $W_{xz}$  and  $W_{zz}$  it is possible to use following method, for the first time indicated by P. M. Nikiforov (1927).<sup>1</sup>

FOOTNOTE <sup>1</sup>. The work of P. M. Nikiforov preceded O. Yu. Schmidt's article (1926), in which was for the first time given the formula  $W_{xz}$  for the case of sloping bed. ENDFOOTNOTE.

Page 342.

If we determine from condition  $\frac{d}{dx} (W_{xz}) = 0$  values  $x_{\max}$  and  $x_{\min}$ , place these values into the general formula for  $W_{xz}$  and determine then the sum of maximum and minimum values  $W_{xz}$ , we will obtain that

$$[W_{xz}]_{\max} + [W_{xz}]_{\min} = f \sigma \sin 2\varphi \operatorname{arctg} \frac{2h d_1}{h^2 - d_1^2}. \quad (V, 170)$$

But if we substitute value of  $x=0$  into general formula for  $W_{xz}$ , then we will obtain

$$W_{xz}(0) = f \sigma \sin 2\varphi \operatorname{arctg} \frac{2h d_1}{h^2 - d_1^2}.$$

Consequently,

$$[W_{xz}]_{\max} + [W_{xz}]_{\min} = W_{xz}(0), \quad (V, 170)$$

whence follows simple graphic rule of determination of point  $x=0$ , arranged/located above middle of bed: we build ordinates  $AA_1$  and  $BB_1$  of maximum and minimum of curve  $W_{xz}$  (Fig. 179); we find ordinate  $A_1C$ , equal to their algebraic sum, and point  $x=0$ , which lies between apexes of curve, whose ordinate is equal to  $A_1C$ .

Exactly the same condition occurs also for  $W_{yz}$ , precisely

$$[W_{yz}]_{\max} + [W_{yz}]_{\min} = W_{yz}(0), \quad (V, 170a)$$

whence emerges analogous indicated method of determining point  $x=0$  from curve  $W_{yz}$ .

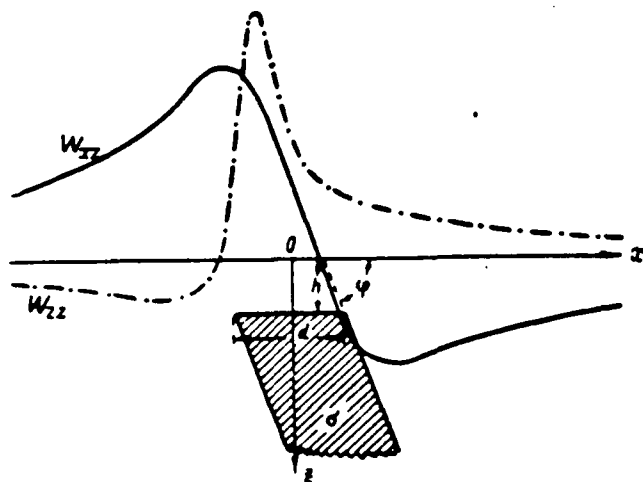


Fig. 178. Curves  $W_{zz}$  and  $W_{zz}$  for case of sloping bed.



Page 343.

Knowing position of origin of coordinates, it is possible to decompose curves  $W_{xz}$  and  $W'_{xz}$  into component curves:  $W_{xz}$  on  $L(x)$  and  $A(x)$ ;  $W'_{xz}$  — on  $L_1(x)$  and  $A_1(x)$ . Let us look how this is done based on example  $W_{xz}$ .

From formula (V, 170) it follows that

$$L(-x) = -L(+x),$$

$$A(-x) = A(+x).$$

Hence

$$\left. \begin{aligned} L(+x) &= \frac{1}{2} [W_{xz}(+x) - W_{xz}(-x)], \\ A(-x) &= \frac{1}{2} [W_{xz}(+x) + W_{xz}(-x)], \\ L(-x) &= \frac{1}{2} [W_{xz}(-x) - W_{xz}(+x)], \\ A(+x) &= \frac{1}{2} [W_{xz}(-x) + W_{xz}(+x)], \end{aligned} \right\} \quad (V, 171)$$

i.e.  $L(x)$  and  $A(x)$  can be constructed graphically according to half-sums and half-differences of ordinates of curve  $W_{xz}$ , that correspond to abscissas  $+x$  and  $-x$ , counted from previously fixed point  $x=0$ , arranged/located above middle of upper edge of bed.

Analogous decomposition can be carried out, also, on curve  $W'_{xz}$ .

On component curves —  $L(x)$  and  $A(x)$  in the case  $W_{xz}$ ,  $L_1(x)$  and  $A_1(x)$  in the case  $W'_{xz}$  — are determined horizontal thickness of layer  $d$  and depth of upper edge  $h$ . For this serve the corresponding formulas

of the solution of the inverse problem of interpretation for the vertical bed on  $W_{xz}$  and  $W_{zz}$ , given in §42.

It remains to determine  $\varphi$  and  $\sigma$ . Let us show how this is possible to do in the case  $W_{xz}$ . Instead of  $\sigma$  on  $L(x)$  and  $A(x)$  it is possible to compute the following values:

$$\sigma_L = \sigma \sin^2 \varphi \text{ по формуле (V, 149),}$$

$$\sigma_A = \sigma \sin 2\varphi \text{ по формуле (V, 156).}$$

Key: (1). according to the formula.

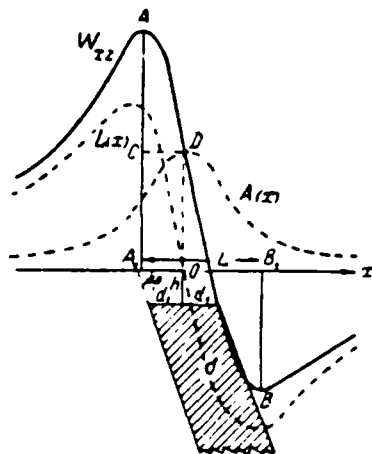


Fig. 179. For determination of middle of upper edge of sloping bed from curve  $W_{zz}$ .

Page 344.

After finding them, we determine

$$\text{ctg } \varphi = \text{arc ctg } \frac{\sigma_A}{2\sigma_L}, \quad (\text{V.172})$$

and then

$$\sigma = \frac{\sigma_L}{\sin^2 \varphi} = \frac{\sigma_A}{\sin 2\varphi}. \quad (\text{V.173})$$

Analogous calculations can be led, also, on  $W_{zz}$ .

Analysis of curves  $L(x)$  and  $A(x)$  for sloping bed makes it possible to use other methods of determining parameters  $\varphi$  and  $\sigma$  of bed. Thus, P. M. Nikiforov brought out the following formulas for determining these elements from curve  $W_{zz}$ :

$$\varphi = \frac{\pi}{2} - \operatorname{arctg} \frac{\sqrt{\left(\frac{l}{2}\right)^2 - x_m^2}}{h}, \quad (\text{V, 174})$$

$$\sigma = \frac{L(x)_{\max}}{f \sin^2 \varphi \ln \frac{|x_m| + d_1}{|x_m| - d_1}}, \quad (\text{V, 175})$$

where  $l$  - distance between the points of maximum and minimum of curve  $W_{xx}$ ;

$x_m$  - the abscissa of maximum  $L(x)$ ;

$h$  - depth of the upper edge of bed;

$d_1$  - half of horizontal thickness of layer;

$f$  - gravitational constant.

FOOTNOTE 1. Formula for the determination  $\varphi$  we give in somewhat changed form. ENDFOOTNOTE.

Application of methods described above of interpretation of anomaly for case of sloping bed is limited to those cases, when these anomalies are well "isolated/insulated" from adjacent anomalies, i.e., when these associated anomalies do not complicate by noticeable form anomaly being investigated. It is necessary to recognize that in practice the number of such favorable cases is limited. Their number can be substantially spread, after developing the analogous analytical methods of interpretation for localized variation anomalies  $\Delta W_{xx}$  and  $\Delta W_{yy}$ , but this problem is not thus far solved. In such cases, when the anomaly being investigated, obtained during variometric or gradiometric photographing, is caused by the effect/action of several sloping (or vertical) beds, already long ago extensively is used the

graphic method of interpretation, with the utilization of atlas of the theoretical curves of gradient  $W_{xx}$ .

For construction of atlas of curves  $W_{xx}$  special nomograms, proposed by K. A. Kirillov (1926), are used. The same nomograms can be applied, also, for the plotting of curves  $W_{xx}$ .

Page 345.

In the method of Kirillov formulas (V, 169) are used in a somewhat different form, which we will obtain, after replacing in the formula (V, 169)  $x$  by  $x+d$ , that is equipollent to the transfer of the origin of coordinates into the point, arranged/located above the right edge of the horizontal edge of bed, and introducing the following designations:

$$\begin{aligned} \frac{x}{h} &= z; & \frac{d}{h} &= a; \\ f\sigma \cos^2 \varphi &= C; & f\sigma \sin 2\varphi &= S; \\ \ln \frac{z^2+1}{(a+z)^2+1} &= \xi, & \operatorname{arctg} \frac{a}{z(a+z)+1} &= \eta. \end{aligned}$$

Then formulas (V, 168) are rewritten in the following form:

$$\left. \begin{aligned} W_{xx} &= C\xi + S\eta, \\ W_{xx} &= \frac{1}{2}S\xi - 2C\eta. \end{aligned} \right\} \quad (\text{IV, 176})$$

For coefficients  $C$  and  $S$  can be constructed tables with two entrances, giving values of these quantities in dependence on given values  $\varphi$  and  $\sigma$ .

If we assign specific values of  $a$ , then for each of these values  $\xi$  and  $\eta$  will be functions only of one variable  $z = \frac{x}{h}$ . This dependence is depicted graphically in Fig. 180 and 181 for the following values of  $a$ :

$$a = 1, 2, 3, \dots, 20.$$

Putting to use these graphs, it is easy to construct theoretical curves  $W_{xx}$  and  $W_{xz}$  for given values of parameters of sloping bed  $d$ ,  $h$ ,  $\phi$  and  $\sigma$ . The plotting of curves is produced as follows. According to the given values  $\phi$  and  $\sigma$  we calculate or find according to tables the appropriate values of coefficients  $C$  and  $S$  and calculate value of  $a = d/h$ . Further we find according to graphs either directly or by interpolation, for the fraction values of  $a$ , values  $\xi$  and  $\eta$  for the specific values of  $z$  and for each of them we calculate  $W_{xx}$  and  $W_{xz}$  according to the formulas (V, 176). Thus can be constructed curves  $W_{xx}$  and  $W_{xz}$  in the function of argument  $z$ . With the plotting of curves it is necessary to keep in mind that value  $z=0$  corresponds to projection on the profile of the right edge of bed, since at this point was selected the origin of coordinates during the derivation of formulas (V, 176).

With interpretation they usually put to use atlases of  $W_{xx}$  theoretical curves of gradient constructed in manner described above for following values  $\phi$ ,  $\sigma$  and  $a$ :

$$\phi = 90^\circ, 80^\circ, 70^\circ, 60^\circ, 50^\circ, 40^\circ, 30^\circ, 20^\circ, 10^\circ; \sigma = 0.5 \text{ g/cm}^3, \\ a = 1, 2, 3, 4, 5, \dots, 15.$$

Page 346.

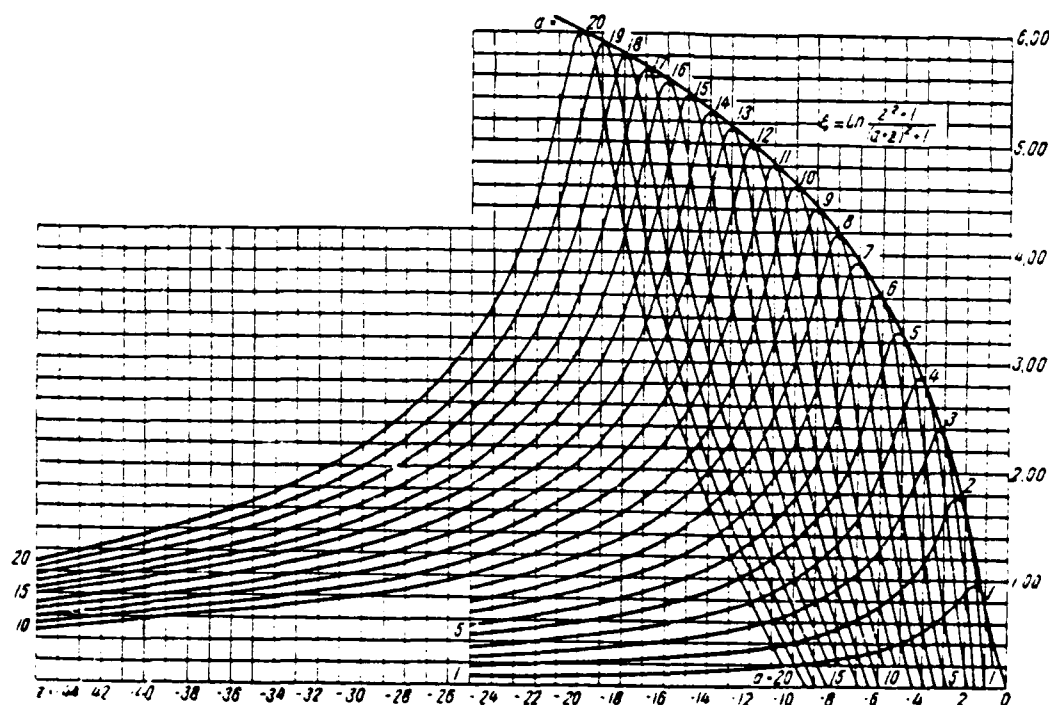


Fig. 180. K. A. Kirillov's nomogram for calculating function

$$\phi = \ln \frac{z^2 - 1}{(a^2 - z^2) - 1}$$

Page 347.

Along horizontal axis are deposited values  $z=x/h$ , i.e., curves, as in the case of sloping step, are built to scale of depth of upper edge of bed  $h$ . Curves are grouped for one and the same values  $\phi$ . On each graph the corresponding values  $\phi$  are inscribed, while in each separate curve - the corresponding value  $a$ .

Fig. 182 depicts atlas of theoretical curves  $W_{12}$  for values

$\varphi = 90^\circ, 70^\circ, 50^\circ$  and  $30^\circ$ .

Curves  $W_{xx}$  in essence are characterized by following parameters:  
1, i.e., with distance between points of maximum and minimum, value of  
summary amplitude  $A = |W_{xx}|_{\max} - |W_{xx}|_{\min}$  and, finally, absolute value of  
relation of minimum and maximum ordinates  $\left| \frac{|W_{xx}|_{\min}}{|W_{xx}|_{\max}} \right|$ , which characterizes  
degree of asymmetry of curves relative to zero line.



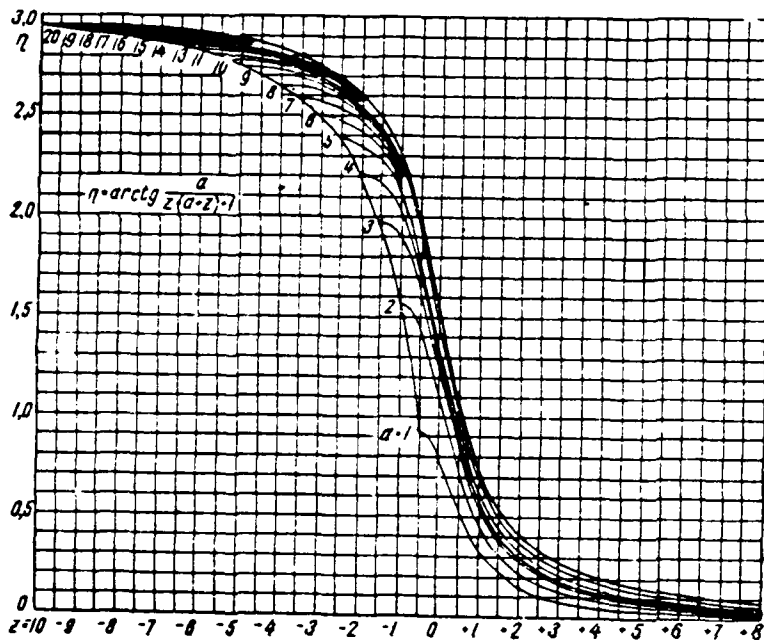


Fig. 181. K. A. Kirillov's nomogram for calculating function

$$\eta = \arctg \frac{a}{z(a+z)+1}$$

Pages 348-349.

Characteristic elements of curves indicated differently are changed in dependence on change in elements of bedding of bed  $d$ ,  $h$ ,  $\phi$  and its excess density  $\sigma$ . From the formulas (V, 168) and (V, 169) and Fig. 182 it is possible to make the following conclusions with respect to the effect of the values indicated on the character of curves  $\eta_{\text{v}}$ .

With increase in thickness of layer  $d$ , and consequently, parameter  $a$  simultaneously are increased  $A$  and  $I$ .

With increase in angle  $\phi$  relation  $\left| \frac{W_{xz}|_{\min}}{W_{xz}|_{\max}} \right|$  is increased, moreover at  $\phi=90^\circ$  this relation becomes equal to one.

With increase in depth of layer  $h$  is increased distance  $l$  (in connection with increase in graphic scale of curve) and simultaneously is reduced amplitude  $A$  as a result of decrease of relation  $a=d/h$ . With the simultaneous and identical increase in  $h$  and  $d$  occurs only an increase of  $l$  without change of  $A$ .

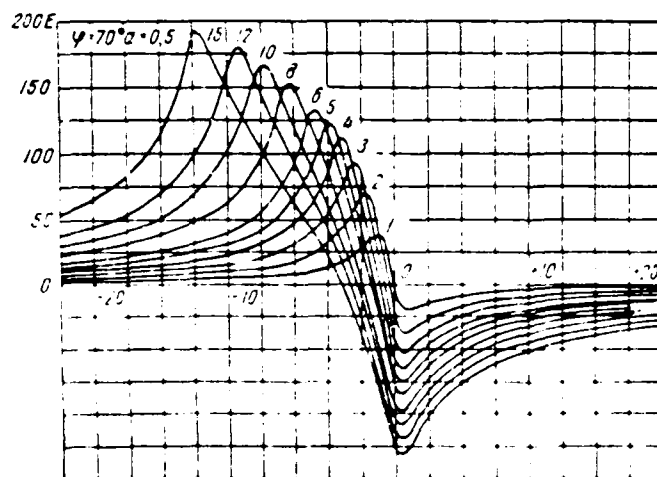
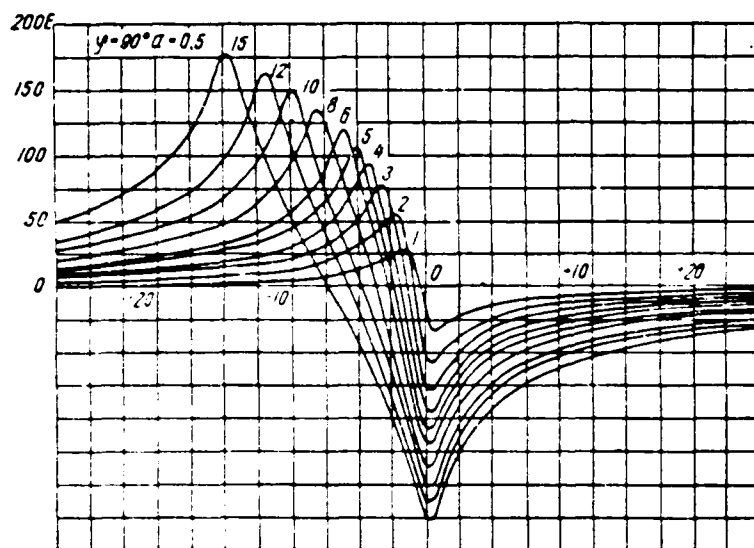
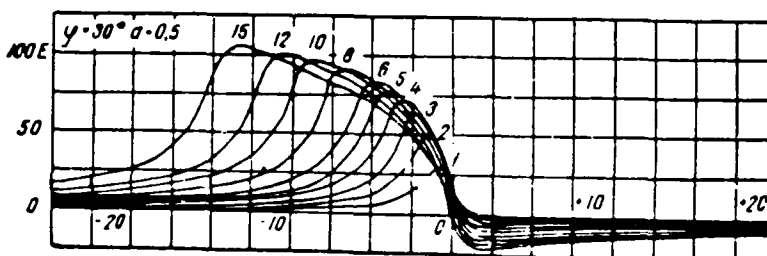
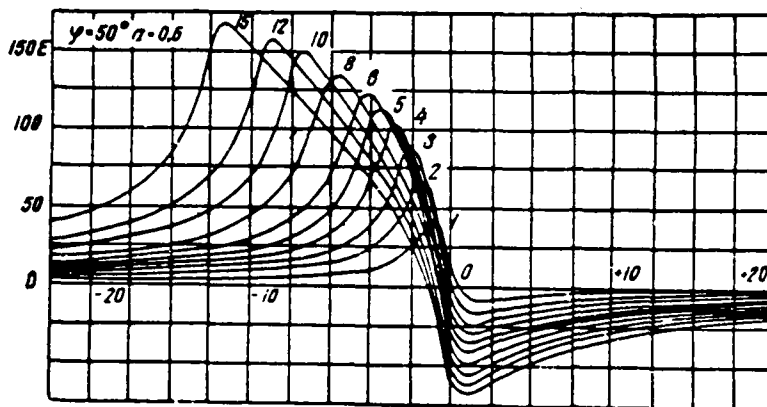


Fig. 182. Theoretical curves  $w_{\dots}$  for sheetlike bodies.



Continuation, Fig. 182.

Page 350.

Finally, increase  $\sigma$ , as in all other cases, conditions proportional increase in all ordinates of curve, and consequently, amplitude  $A$ , without change in its other parameters, since  $\sigma$  enters as constant multiplier into all formulas of gravitation effect.

Thus, we come to conclusion that change in different elements of layer brings to different character to changes in curves  $W_z$ . This fact greatly helps with the interpretation in the case of structures of the type of sloping layer, making it possible to obtain sufficiently

simple results in the majority of the cases.

Below, in description of results of gravitation prospecting works, we will see, that in number of cases during investigation of structures of type of sloping layer depth  $h$  of layers, comprising suite for separate profiles or sections, can be known to us from other data and is accepted as constant value. This fact also substantially facilitates interpretation. The latter in this case can be carried out as follows.

Curve of gradient  $W_{\Sigma}$  obtained as a result of observations along profile, which goes transversely to course/strike of suite being investigated, is built to scale of depth  $h$ , the same precisely, which is accepted during construction of atlas of theoretical curves. If, for example, scale unit  $z$  in the atlas is accepted equal to 1 cm, and depth  $h$  is actually equal to 50 m, then the horizontal scale of the observed curve must be taken 1:5000, i.e., 1 cm - 50 m. Curve in the case of laminated structure will take the complex form, since it is vector sum of several curves, corresponding to the effect/action of several different beds, comprising suite. The example of this curve is given in Fig. 183. Interpretation is reduced to the separation of suite to the separate beds and the determination of the elements of their bedding.

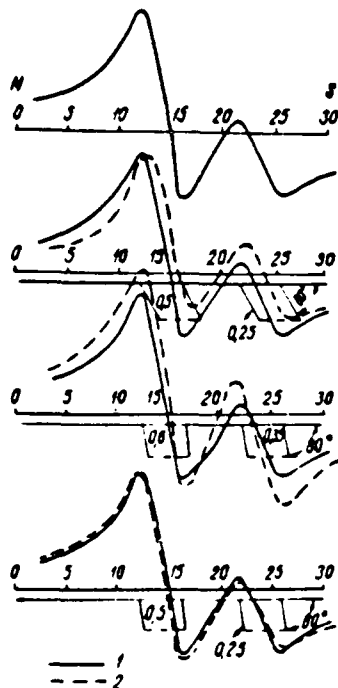


Fig. 183. Example of laminated curve of gradient  $u_x$ , and its interpretation by trial and error by successive approximations of sheet section/cut and corresponding to it summary theoretical curve  $u_x$ . 1 - observed curve; 2 - curve, which corresponds to section/cut.

Page 351.

This is done as follows: according to the character of curve  $u_x$ , is planned the position of the basic beds, comprising suite, moreover the elements of their bedding in the first approximation, are assigned arbitrarily, but after conforming to the character of curve in the individual sections, taking into account, in particular, those observations, which are made above with respect to the connection of change of the elements of the bedding of layer with a change in the

parameters of curves. For the assigned theoretical section/cut summary theoretical curve is built, moreover the latter is obtained as vector sum of the components of the curves, which correspond to the separate beds, assigned in the section/cut. The comparison of this curve with that observed indicates those changes, which must be introduced into the section/cut in order to obtain better approximation/approach to the observed curve. After introducing these changes, are built the second version of theoretical section/cut and the curve corresponding to it and they continue this process until theoretical curve coincides with that observed. The described methodology of interpretation extensively is used with the gravitation prospecting works on the sheet iron-ore deposits of the type KMA and Krivoy Rog (see Chapter IX). Application of this methodology usually gives good results, but for obtaining them is necessary the observance of a series/number of conditions, number of which includes:

- 1) the possibility of the intersection with the interpretive profiles of the entire suite of the causing anomaly beds transversely of the course/strike of this suite;

- 2) the consistency of beds on the course/strike, i.e., the observance of the conditions, required by the two-dimensional task of interpretation.

Two conditions indicated are not always observed in actuality. Thus, with the works on the sheet iron-ore deposits is sometimes difficult or even is impossible intersection with the profiles of entire iron-ore suite due to the presence of banks, quarries/open

pits, different buildings, etc., and sometimes it is necessary to study the structure of the beds, broken by faults or which sharply vary their course/strike, for example on the periclinal sections, etc. Under such conditions quantitative interpretation although complicated, proves to be nevertheless possible during the utilization of the proposed by the author atlas of theoretical curves  $\delta W_{xx}$  (Andreyev, 1948). Curves  $\delta W_{xx}$  are built graphically on curves  $W_{xx}$ . The parameter  $l$  at the plotting of curves  $\delta W_{xx}$  as shows experiment, is expedient to take equal to  $5h$ , where  $h$  - depth of the bedding of the upper edge of beds. The examples of curves  $\delta W_{xx}$  for the sloping beds and the example of the section/cut, constructed according to curve  $\delta W_{xx}$ , are given in Fig. 184 and 185. In spite of the "polyconic" character of these curves in comparison with curves  $W_{xx}$ , their utilization in the practice of interpretation proves to be completely possible and worthwhile.

Page 352.

The same author (Andreyev, 1950) proposed the following method, which can be used for interpretation of variation anomaly  $\delta W_{xx}$  for case of sloping bed. Above we indicated (see pg. 343), how it is possible from curve  $W_{xx}$  to find point  $x=0$ , arranged/located above the middle of the upper edge of bed. The essence of method consists in the investigation of the following dependence:

$$\delta W_{xx}(0, l) = f(l). \quad (V.177)$$

Taking into account formula (V, 169), it is possible to write



DOC = 88020218

PAGE

✓ 633

$$\delta W_{zz}(0, l) = \delta L_1(0, l) + \delta A_1(0, l).$$

Since  $L(x) + L(-x) = L(0) = 0$ , then, obviously,  $\delta L_1(0, l) = 0$  and

$$\delta W_{zz}(0, l) = \delta A_1(0, l). \quad (V, 178)$$

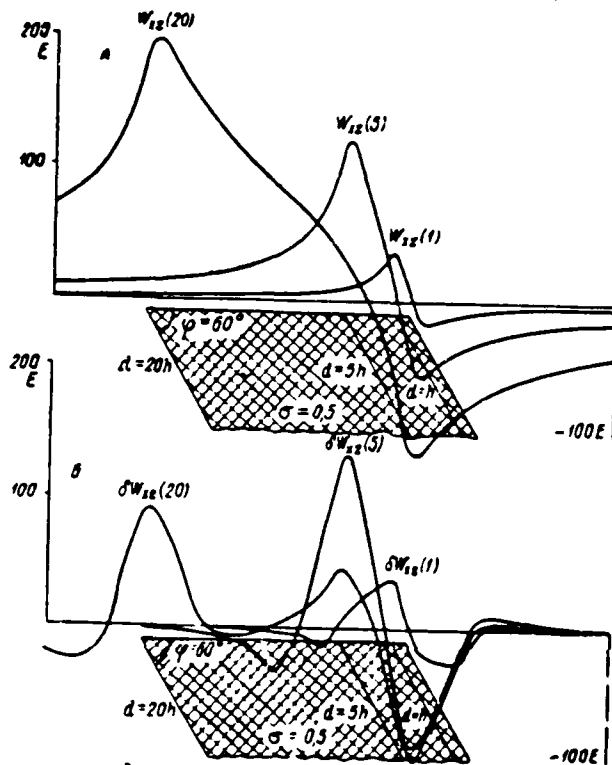


Fig. 184. Comparison of curves  $W_{xz}$  and  $\delta W_{xz}$  for sloping beds.

Page 353.

This dependence for different values  $d_1/h$  is shown in Fig. 186 on double logarithmic scale with  $2f$  from  $\sin^2 \phi = 1$ . The asymptotic branches of the curve, which correspond to the value

$$\lim_{l \rightarrow \infty} \log \delta W_{xz}(0, l) = \log A_1(0, l), \quad (V, 179)$$

on the graph for convenience are combined, since with the use of logarithmic scale we cannot be interested in absolute value  $\delta W_{xz}$ . Value  $h$  is determined on the average/mean horizontal line template  $l=h$ , and ratio  $d_1/h$  - on the index of the corresponding curve. Values  $\sigma$  and  $\mu$

in this case are not determined.

Advantage of method is the fact that we put to use localized form of anomaly  $\delta W_{xx}$  for which makes special sense application of logarithmic templates. On  $\delta W_{xx}$  (with  $l$  sufficiently small) the lower edge of bed virtually does not have an effect.

In such cases, when curve  $W_{xx}$  can to be considered (at least in the first approximation) caused by effect/action of one sloping bed, for its interpretation can be successfully applied described above method of P. M. Nikiforov. Let us examine numerical example for the application of this method. The curve of gradient  $W_{xx}$  given in Fig. 187, if it somewhat is smoothed out (smoothed part is shown by dotted line), can be considered caused by the effect/action of one sloping bed.

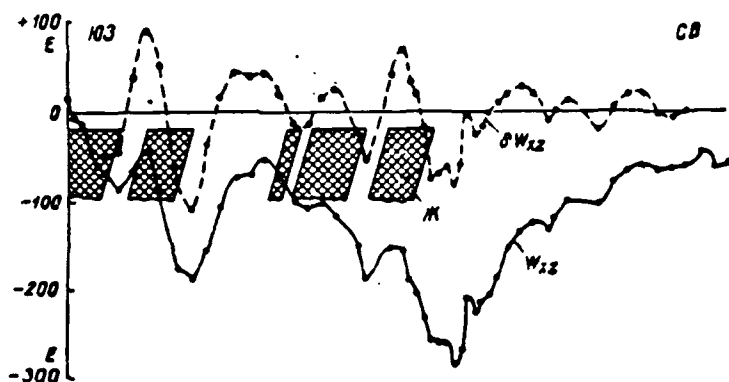


Fig. 185. Example to curve  $W_{zz}$ , complicated by effect of beds, which are located beyond limits of profile. Corresponding curve  $\delta W_{zz}$  and sheet section/cut, constructed according to this curve, is here shown. Zh - ferruginous quartzite.

Page 354.

In described above manner we find point  $x=0$ , arranged/located above the middle of bed, and we separate/liberate the logarithmic curve  $L(x)$ , through which we find

$$x_m = 320 \mu = 3.2 \cdot 10^4 \text{ CFC}; \quad x_{1/2} = 140 \mu = 1.4 \cdot 10^4 \text{ CFC}.$$

Key: (1). CGS.

We calculate according to formula (V, 146)

$$a = \frac{x_m^2 + x_{1/2}^2}{2|x_{1/2}|} = 4.38 \cdot 10^4$$

and further we find through formula (V, 147)

$$d = 2|V^{-a(a+2|x_m|)}| = 5.8 \cdot 10^4 = 580 \mu$$

and according to formula (V, 148)

$$h = \sqrt{x_m^2 - d_1^2} = 135 \mu.$$

Through curve  $W_{xx}$  we find  $l=650$   $m=6.5 \cdot 10^4$  and further according to formula (V, 174)

$$\varphi = \frac{\pi}{2} - \arctg \frac{\sqrt{\left(\frac{l}{2}\right)^2 - x_m^2}}{h} = 65^\circ$$

and according to formula (V, 175), taking into account that

$$L(x)_{\max} = 122 \cdot 10^{-8} \text{ CGS},$$

$$\sigma = \frac{L(x)_{\max}}{l \sin^2 \varphi} \cdot \frac{1}{\ln \frac{|x_m| + d_1}{|x_m| - d_1}} = 0.7 \text{ g/cm}^2.$$

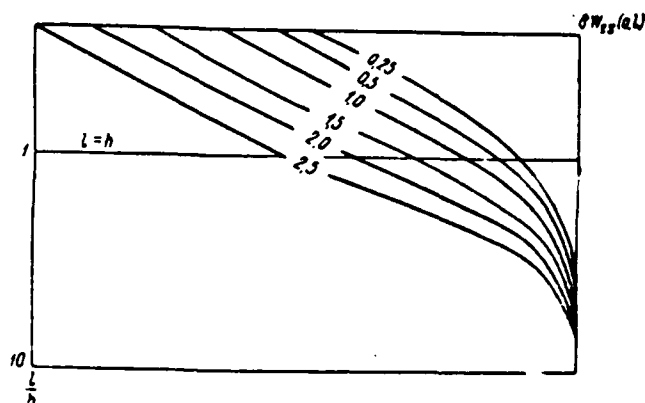


Fig. 186. Template for interpretation of curves  $\delta W_{zz}(0, l) = f(l)$  for sloping bed. According to B. A. Andreyev.

Page 355.

Section of anomaly is in detail developed. Comparison with the data of drilling shows following. Source of anomaly - powerful/thick bed of ferruginous quartzite, which slopes among the gneiss. The upper edge of bed is located at the average depth of 125 m from the surface, i.e.,  $h$  is determined with the error 10 m (8%). Thickness of layer - 550 m, i.e.,  $d$  is determined with the error 30 m (5%). The density of ferruginous quartzite comprises on the average 3.3 g/cm<sup>3</sup>, and gneiss - 2.7 g/cm<sup>3</sup>, i.e.,  $\sigma$  is determined with the error ~0.1 g/cm<sup>3</sup> (20%).

§44. Other cases of two-dimensional problem.

We examined above methods of solving direct and reverse problems for two-dimensional bodies of correct geometric form, which have

primary meaning during geologic interpretation of gravity anomalies. In this case took into consideration the basic forms of presentation/concept or the elements of the anomalous field: anomaly  $\Delta g$ , second derivatives  $W_{xx}$  and  $W_{yy}$  (for the two-dimensional bodies). For the individual cases we examined the localized forms of anomalous elements -  $\delta \Delta g$  and  $\delta W_{xx}$ .

Task of this paragraph - short enumeration of some other, not examined above, versions of solution of direct and reverse problems for two-dimensional bodies of correct geometric form.

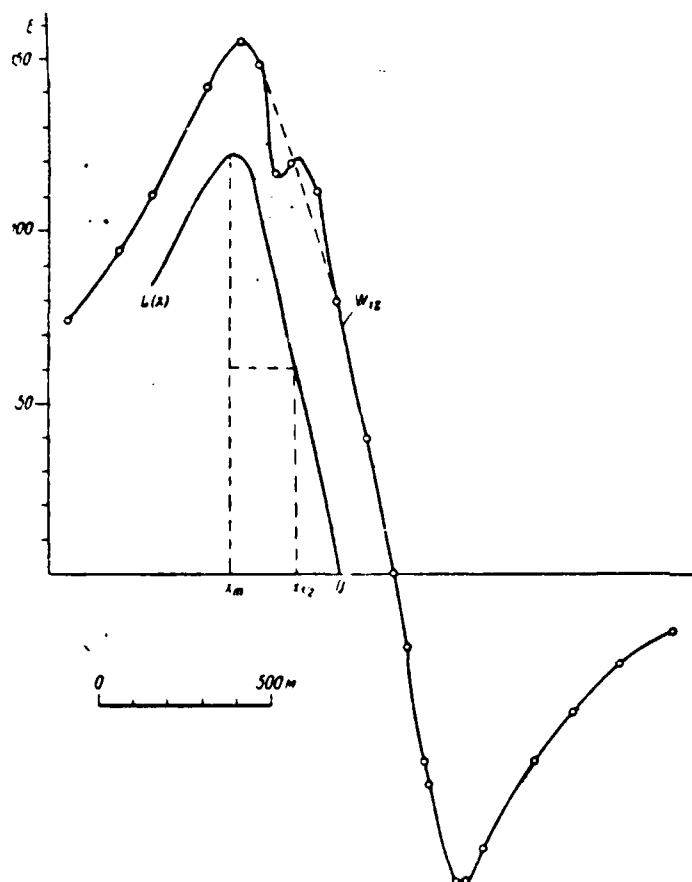


Fig. 187. Example of interpretation of curve  $w_{12}$  by method of P. M. Nikiforov for sloping bed.

Page 356.

There is method of solving direct and reverse problems for sloping layer with arbitrarily arranged/located upper edge and set of two layers. which generate in section body, close to anticlinal fold (Fig. 188). During the solution of inverse problem for these cases are used in the set derivatives  $w_{12}$  and  $w_{11}$ . The method of interpretation



for this case is proposed by N. N. Mikhaylov; his presentation is in the monograph of O. A. Shvank and Ye. N. Lyustikh (1947). A special case of problem of this type represents the problem about the sloping step, whose solution also by the combination of curves  $w_{xz}$  and  $w_{yz}$  is published by A. A. Yun'kov (1937).

Another analog of anticline in the form of triangular prism with excess density, constant or varying with depth according to linear law, is examined for  $w_{xz}$  and  $w_{yz}$  by A. Ya. Jaros (1951), and for anomaly  $\Delta g$  - G. I. Karatayev (1960). The tables of calculations  $\Delta g$ ,  $w_{xz}$  and  $w_{yz}$  for the case of triangular prism with the constant excess density were already long ago published by B. V. Numerov (1931).

One additional analog of anticline in the form of parabolic cylinder is examined in works of A. I. Gavrilov (1945) and A. A. Yun'kov (1959). In the latter works indicated give (on the logarithmic scale) templates for the interpretation of curves  $w_{xz}$  and  $w_{yz}$  caused by the effect/action of body in the form of parabolic cylinder.

A. A. Yun'kov, N. L. Afanas'yev and N. A. Fedorova (1961) published templates of theoretical curves  $w_{xz}$ ,  $w_{yz}$  and  $\Delta g$  for case of sloping step (on semilogarithmic scale).

By A. A. Yun'kov (1940) is published analytical method of solution of direct and reverse problems for infinitely long horizontal

beam with rectangular cross section by curves  $w_{xz}$  and  $w_{yz}$ .

Large atlas of theoretical curves  $w_{xz}$  and  $w_{yz}$  for series/number of cases of two-dimensional bodies of correct geometric form is published by D. S. Mikov (1956).

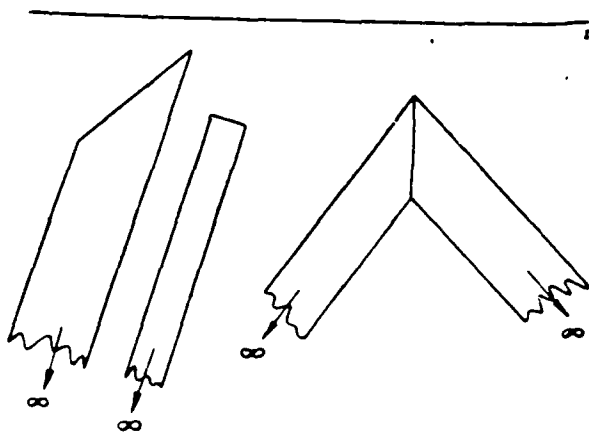


Fig. 188. Beds with arbitrarily arranged/located upper edge and approximate presentation/concept of anticline in the form of set of two such beds.

Page 357.

A. F. Jaros (1950) published method of solving inverse problem for vertical step and vertical bed by derivatives  $\frac{\partial W_{xz}}{\partial x}$  and  $\frac{\partial W_{yz}}{\partial x}$ , whose values it is proposed to determine according to approximation Stirling formula

$$\frac{dU}{dx}(0) = \frac{1}{\Delta x} \left\{ \frac{1}{2} [U(-1) + U(+1)] - \frac{1}{12} [2U(+1) - 2U(-1) - U(+2) + U(-2) + \dots] \right\}. \quad (V.180)$$

where numerals in parentheses represent numbers of points, considered to the right with plus and to the left with minus from initial (zero) point through interval of  $\Delta x$  along  $x$  axis.

To D. Miklovyan (1957) are given formulas for anomaly  $\Delta g$  and

lapses  $g$  of the first, the second and higher orders, caused by effect/action of bodies, whose section formed by chord and by circular arc or represents sector of circle. By him the indicated question is examined for the case of sloping step.

V. L. Gul'nitskiy (1960) brought out formulas, which express values of derivative  $\frac{\partial^2 g}{\partial x^2} = W_{xx}$  for two-dimensional body with section in the form of polygon and for its particular cases - sloping step, bed, etc. The excess density of body is received as constant or it is considered as the linear function of vertical coordinate.

Page 358.

Chapter VI.

INTERPRETATION OF GRAVITY ANOMALIES FOR THE BODIES OF ARBITRARY FORM.

§45. Generalities.

In Chapter V are in detail dismantled/selected methods of quantitative interpretation of gravity anomalies for those cases, when it is possible to make assumption about the fact that the causing anomaly being investigated geologic body (or group of bodies) has correct and besides simple geometric form, which is assigned with interpretation. In this case is obtained the possibility of determination from the gravity anomalies of the depth of bedding, sizes/dimensions, and sometimes also the excess density of such bodies.

Quantity of cases, when with interpretation of gravity anomalies it is possible to make assumptions indicated, is relatively small: roughly speaking, this is approximately half of those cases, when interpretation of anomalies is generally possible. In such remaining cases the interpretation is conducted without the assignment of the shape of the body causing anomaly; these cases are examined in this chapter.

Assignment of shape of body with interpretation is possible with sufficiently good knowledge of geologic conditions of region being investigated. Interpretation under the assumption of the arbitrary shape of body is actually possible also only with the presence of significant geologic information about the region being investigated or the section. This information must concern the following three questions:

- 1) the possible and probable shapes of surface of the geologic body, which causes the anomaly being investigated;
- 2) density distribution of the rocks;
- 3) the partial characteristic of the position of body, which causes anomaly (data of drilling and other geophysical methods, etc.).

In presence of indicated data and with utilization of considered/examined below methods proves to be possible approximate determination of shape of surface of causing anomaly body, judgment about possible and probable depth of its bedding, about its volume and mass, etc.

Page 359.

546. Graphic method of the interpretation of gravity anomalies for the bodies of arbitrary form.

Graphic method of geologic interpretation of gravity anomalies is based on property, which author once named (Andreyev, etc., 1941) property of additivity of gravitational field. This concept, borrowed

from mathematics and formed from additio (Lat.) - addition, expresses the following fact. If we decompose the attracting/tightening body into the individual parts, then, independent of the form of body and method of its laying out, component of attraction along any axis will be equal to the algebraic sum of all its individual parts composing attractions.

If we decompose body into such parts, effect/action of each of which on attracted/tightened point is equal, for example, to one milligal, then determination of gravitation effect, connected with body, obviously, will be reduced to calculation of number of such resulting parts, which will present gravitation effect, expressed in milligals. Laying out in the sections of the equal effect/action is done for entire space, which surrounds the attracting/tightening point. In this case depending on in what part of the space the body is located, the latter proves to be decomposed to different number of sections of the equal effect/action, and consequently, the gravitation effect, caused by it, will be different.

Diagrams, utilized during calculation of gravitation effect, are distinguished depending on the determined with their help derivatives of gravitational potential, and also on coordinate system, in which is determined arrangement of sections of different action. In accordance with this during solution of two-dimensional problem are used following forms of diagrams: for calculation  $\Delta g$  - polar, right angled, oblique-angled; for  $W_{xx}$ ,  $W_{yy}$  - polar and right angled.

FOOTNOTE 1. By some authors is recommended also calculation and utilization of interpretation of values  $\Delta H$  - of the horizontal component of the force of gravity (Tyapkin, 1960). Furthermore, is possible the construction of diagrams for localized anomalies  $\delta \Delta g, W_{xz}$  and so forth. ENDFOOTNOTE.

Page 360.

Most useful are polar diagrams, whose calculation is simplest and is reduced to following. After introducing the polar coordinates ( $\rho, \theta$ ) and after doing in the formulas (III, 9) the substitution:

$$\begin{aligned}x &= \rho \cos \theta, \\z &= \rho \sin \theta, \\dS &= dx dz = \rho d\rho d\theta,\end{aligned}$$

we obtain the following initial formulas for the derivatives of the gravitational potential:

$$\left. \begin{aligned}\Delta g &= 2f\sigma \int d\rho \int \sin \theta d\theta, \\W_{xz} &= 2f\sigma \int \frac{d\rho}{\rho} \int \sin 2\theta d\theta, \\W_{xx} &= -2f\sigma \int \frac{d\rho}{\rho} \int \cos 2\theta d\theta.\end{aligned} \right\} \quad (VI, 1)$$

Gravitational effect/action of body of infinite course/strike, limited in normal section by sector area/site (Fig. 189), we will obtain producing in formula (VI, 1) integration in limits on  $\rho$  from  $\rho_1$  to  $\rho_2$  and on  $\theta$  from  $\theta_1$  to  $\theta_2$ :

$$\left. \begin{aligned}\Delta g &= -2f\sigma (\cos \theta_2 - \cos \theta_1) (\rho_2 - \rho_1), \\W_{xz} &= f\sigma (\cos 2\theta_2 - \cos 2\theta_1) \ln \frac{\rho_2}{\rho_1}, \\W_{xx} &= -f\sigma (\sin 2\theta_2 - \sin 2\theta_1) \ln \frac{\rho_2}{\rho_1}.\end{aligned} \right\} \quad (VI, 2)$$



According to these formulas are determined position, sizes/dimensions and form of areas/sites of equal effect/action, if we assume in them, for example,  $\Delta g = 1 \text{ mgl}$ , and  $W_{xx}$  and  $W_{yy} = 1E$ . Obtained in this case equations will contain two unknowns - difference in the corresponding trigonometric functions of angles  $\theta^1$  and  $\theta^2$  and difference or the relation of radii  $\rho_1$  and  $\rho_2$ .

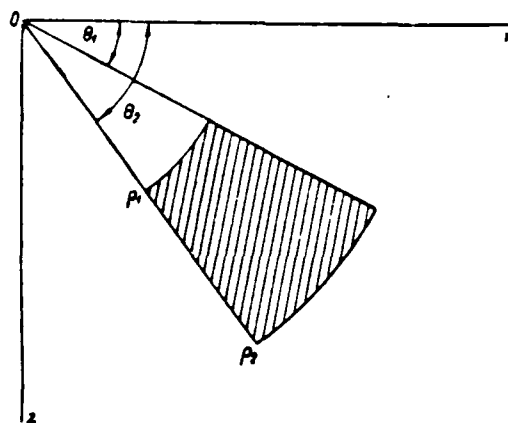


Fig. 189. For determination of areas/sites of equal effect/action.

Page 361.

Therefore we have the capability to each of the equations (VI, 2) to add the proposed by N. N. Samsonov (1931) equation

$$\varrho_2 - \varrho_1 = (\theta_2 - \theta_1) \frac{\varrho_2 + \varrho_1}{2}, \quad (\text{VI}, 3)$$

with observance of which the form of areas/sites will be maximally close to the square. With the observance of this condition our diagram gives minimum error during the calculation of a number of areas/sites, which fill the outline of the section of body, and to interpolation connected with this calculation. During the utilization of equations (VI, 2) and (VI, 3) the system of radii and rays/beams, which determine the boundaries of the areas/sites of the equal effect/action, is determined unambiguously.

Comparing the second and third of formulas (VI, 2) and noting

that  $\cos 2(\theta - 45^\circ) = \sin 2\theta$ , it is possible to ascertain that for calculation  $W_{xx}$  can be used the same diagram, as for  $W_{yy}$ . For the appropriate transition it is necessary to only turn coordinate axes on  $45^\circ$  with respect to the system of the areas/sites of the equal effect/action. In both cases in the adjacent quadrants of point are counted with different signs in accordance with the formulas (VI, 2). These signs are indicated on the diagram (Fig. 190). Instead of the sector areas/sites of the equal effect/action on the diagram usually indicate the points, which correspond to the centers of the areas/sites indicated, which facilitates the use of diagram.

K. F. Tyapkin (1961) recommends on diagram for  $\Delta g$  indicating not geometric centers of areas/sites of equal effect/action, but centers of their effects, whose coordinates  $(q_c, \theta_c)$  to determine from following conditions:

$$\left. \begin{aligned} q_c &= \frac{1}{2} (q_1 + q_2), \\ \cos \theta_c &= \frac{1}{2} (\cos \theta_1 + \cos \theta_2). \end{aligned} \right\} \quad (\text{VI, 4})$$

Under this condition diagram for anomaly  $\Delta g$  becomes somewhat more accurate. The application of analogous rule to the construction of diagram for  $W_{xx}$  and  $W_{yy}$  is inconvenient, since for each of these values different equations are obtained.

Diagram for calculation  $\Delta g$  for case of two-dimensional problem is given in Fig. 191.

Diagrams, given in Fig. 190 and 191, are constructed with value of excess density  $\sigma$ , equal to 1.0 g/cm<sup>3</sup>. If real  $\sigma$  differs from the value indicated, then this is considered as a final result.

Page 361A.

Fig. 190. Top left.

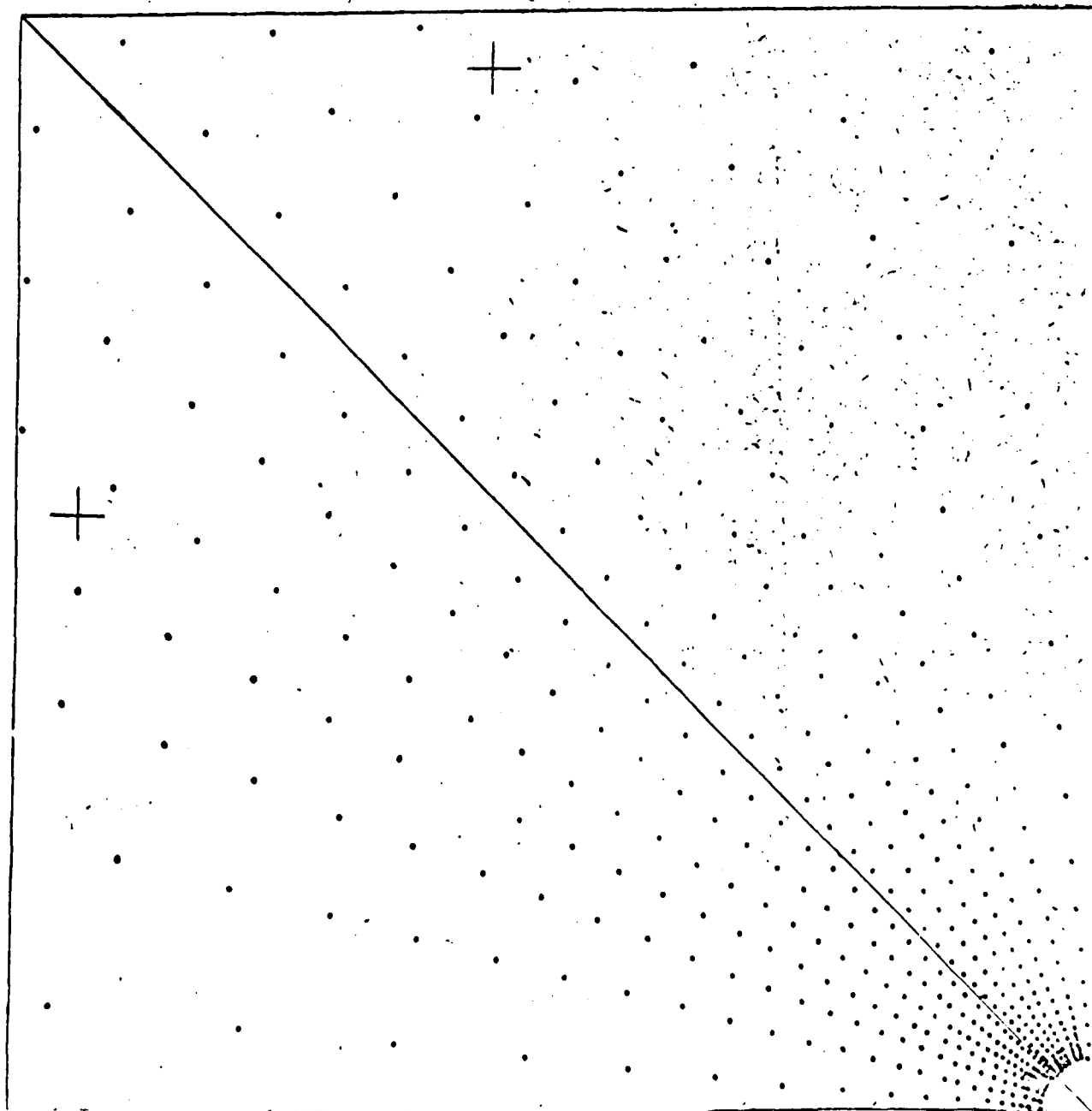


Fig. 190. Top right.

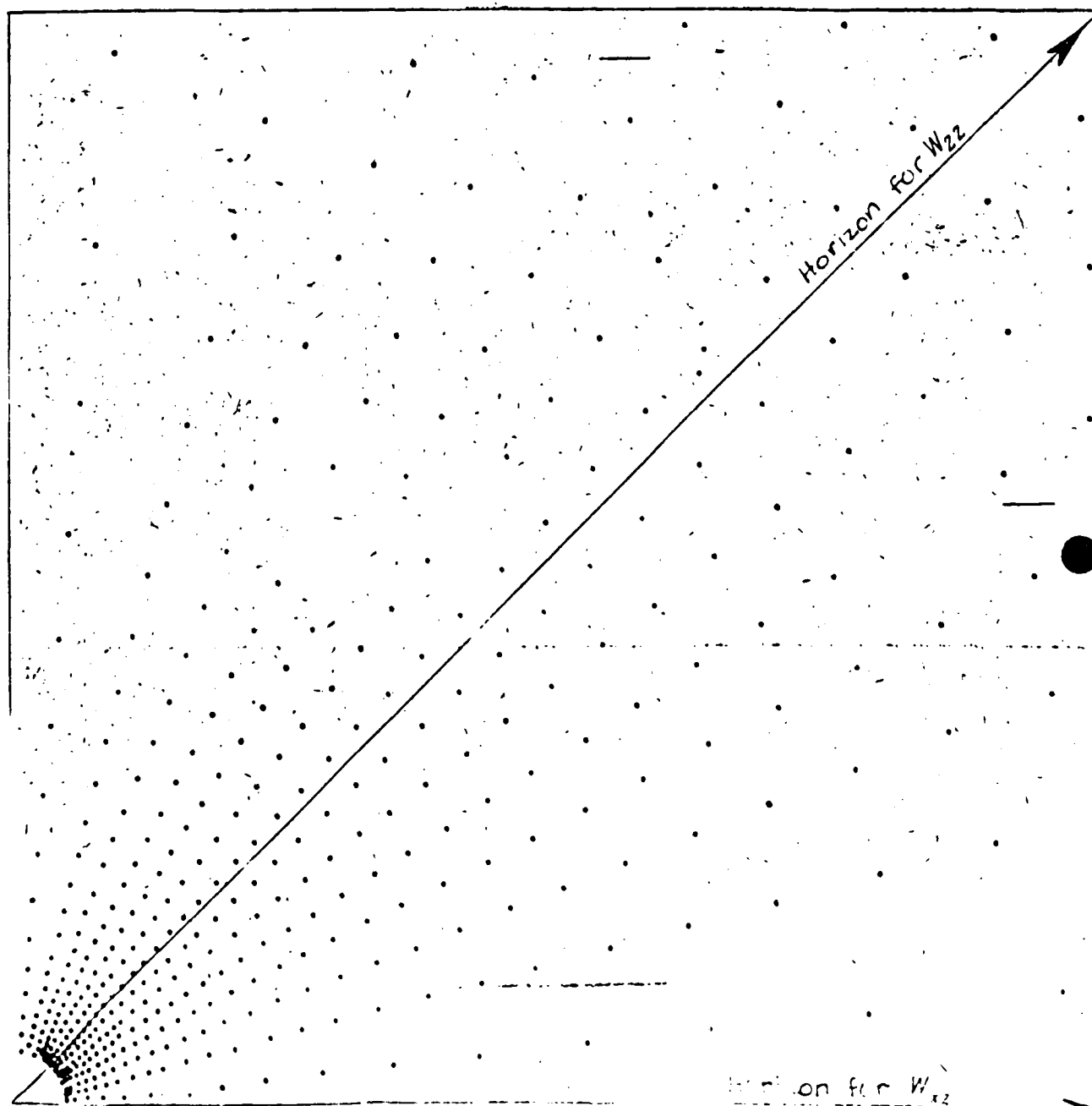


Fig. 190. Bottom left.

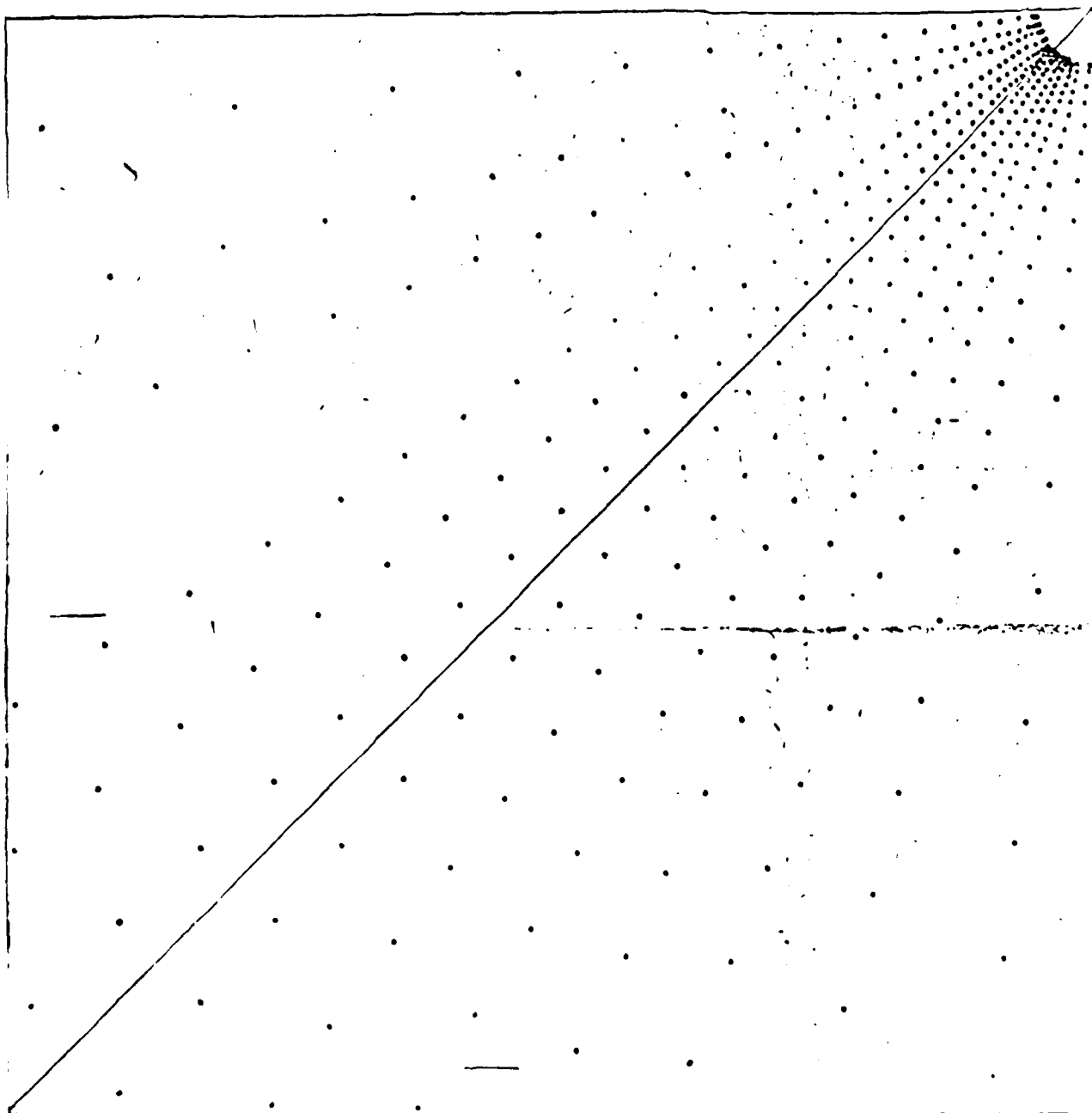


Fig. 190. Bottom right.

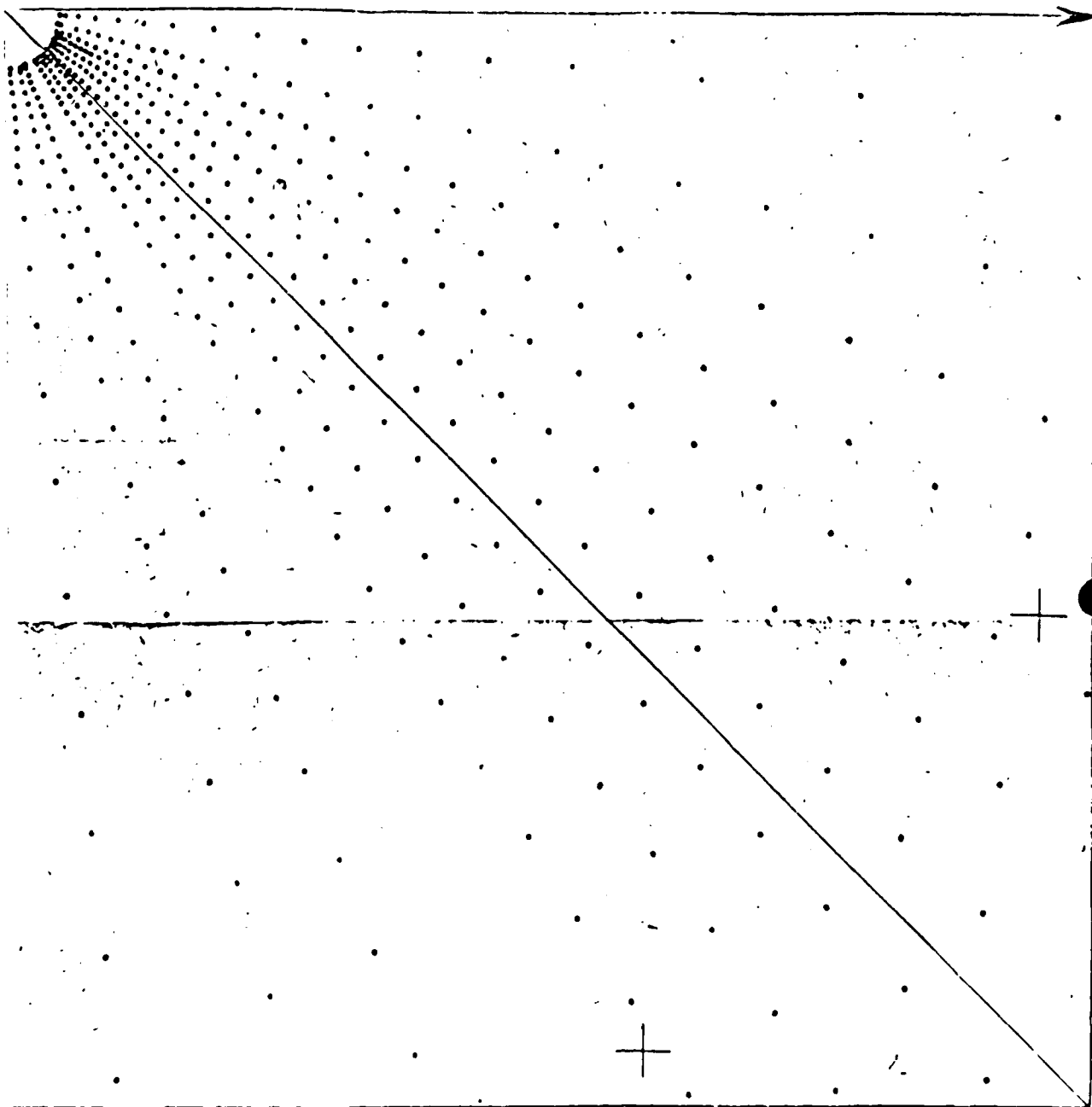


Fig. 190. Polar diagram for calculation  $w_{11}$  and  $w_{12}$ .



Page 361B.

Fig. 191. Left.

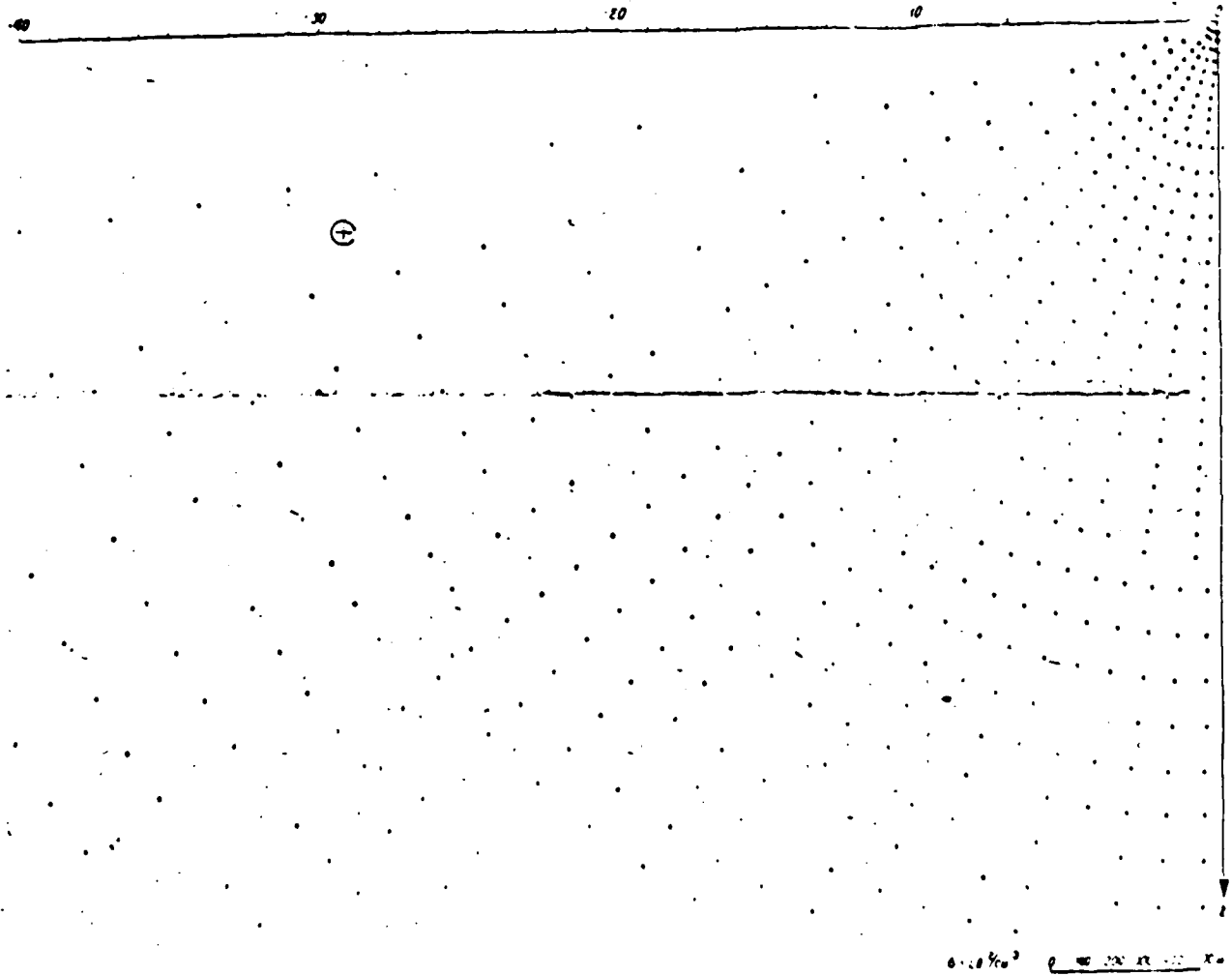
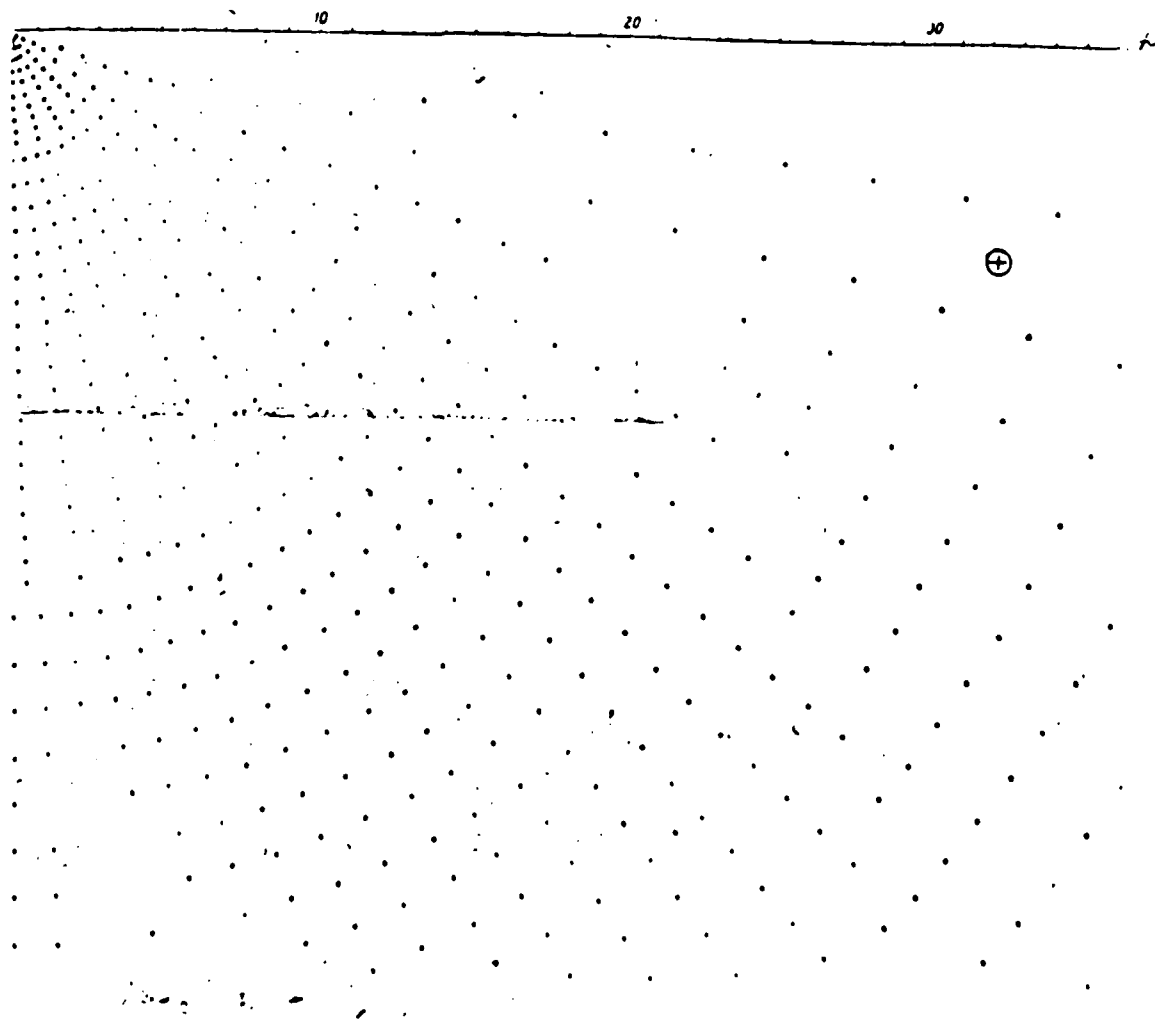


Fig. 191. Right.

Fig. 191. Polar diagram for calculation of anomaly  $\Delta g$ .

Page 362.

If, for example, specific according to the diagram gravitation effect is 5.0 mgal (Fig. 192), and actual value  $\sigma$  is equal to 0.5 g/cm<sup>3</sup>, then

the magnitude of gravitation effect must be taken equal to

$$0,5 \cdot 5,0 = 2,5 \text{ mg/}$$

Essential difference in diagram for  $\Delta g$  and for second derivatives is the fact that for the first of them construction is done on specific graphic scale, which is indicated on diagram, and second diagram - scaleless, i.e., suitable for any picture scale of cross section of body (in both cases, however, is required equality of horizontal and vertical scales). The difference in the diagrams indicated is caused by a difference in the corresponding equations (VI, 2): into the equation for  $\Delta g$  enters a difference in the radii  $\rho_2 - \rho_1$ , and into equations for  $W_{xx}$  and  $W_{yy}$  - their ratio  $\rho_2 / \rho_1$ .

Does arise this question: is it possible to determine magnitude of gravitation effect in anomaly  $\Delta g$  with noncoincidence of scale of diagram and drawing, on which is depicted cross section of body? In order to answer this question, let us focus attention on corresponding formula (VI, 2). Into this formula  $(\rho_2 - \rho_1)$ , as  $\sigma$ , enters by prime factor, consequently, with the nonconformity of scales one should enter just as with the nonconformity of values  $\sigma$ . Let us allow, for example that the scale of the section/cut of body is two times larger than scale of diagram. From the aforesaid above it is clear that in this case the value of anomaly specific according to the diagram will be exaggerated two times and during the calculation of the actual value of gravitation effect one should the value, determined according to the diagram, multiply by the relation of the scales of diagram and

section/cut of body, i.e., by 1/2.

K. F. Tyapkin (1961) recently published polar diagrams for  $\Delta g$  in the case of cylindrical bodies of finite course/strike. The first of the formulas (VI, 1) in this case is substituted by the following:

$$\Delta g = 2f\sigma \int \frac{dq}{\sqrt{q^2 + b^2}} \int \sin \theta d\theta, \quad (\text{VI.5})$$

where  $b$  - half of the length of the body (it is assumed that the profile passes through its middle).

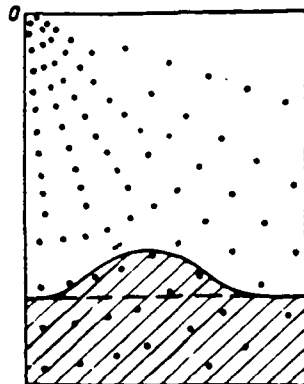


Fig. 192. Example of calculation of gravitation effect of body according to diagram. 1 - interface; 2 - initial horizon/level; 3 - outline of disturbing body.

Page 262A.

[illegible]

**Page 262B.**

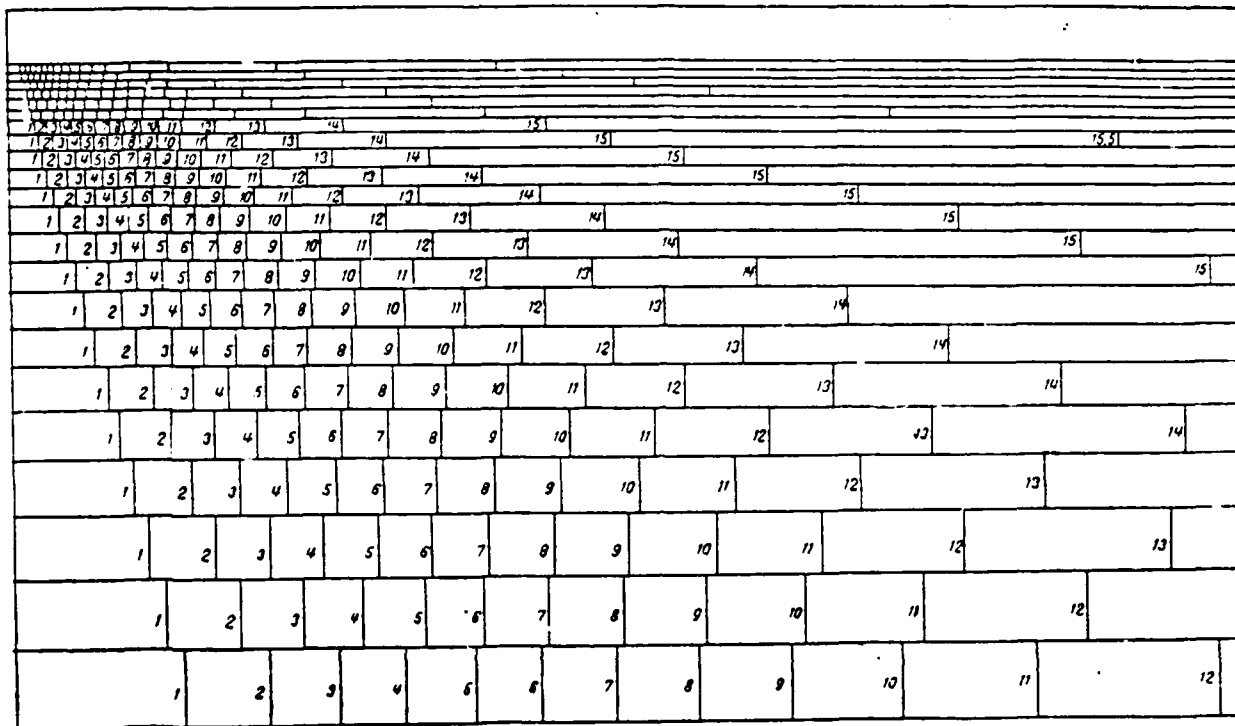


Fig. 193. Right angled diagram for calculation  $W_{\text{st}}$ . According to D. Barton and N. N. Cherepanov.

Page 363.

After integration for area of sector area/site in this case we obtain instead of the first of formulas (VI, 2) the following:

$$\Delta g = 2f\sigma \ln \frac{q_2 + \sqrt{q_2^2 + b^2}}{q_1 + \sqrt{q_1^2 + b^2}} (\cos \Theta_2 - \cos \Theta_1). \quad (\text{VI.6})$$

Based on this equation, by K. F. Tyapkin are constructed and calculated diagrams for values of  $b=1, 2, 3, 4, 5, 6, 7, 8, 9, 10, 12,$

15 and 20 units of scale and  $\sigma=1.0$  g/cm<sup>3</sup>. With the high values of  $b$  the corresponding diagrams barely differ from that given in Fig. 191 for two-dimensional problem, whereas with the low values of  $b$  the differences become substantial.

For second derivatives  $W_{xx}$  and  $W_{yy}$  finiteness of sizes/dimensions of body on course/strike is manifested much more weakly than for  $\Delta g$  (see §38) and for them the construction of special diagrams for finite bodies is little justified. Such diagrams, however, are published in the press (Shvank and Lyustikh, 1947). By their construction/design these diagrams are different; the area/site of the equal effect/action in them have right angled form.

During calculation of right angled diagrams are used formulas for rectangular prism with infinite and finite course, brought out and examined by us in §36 and 42. Fundamental special features these calculations and construction do not present; they are in detail examined in the work of O. A. Shvank and Ye. N. Lyustikh (1947). Here we on this question do not stop, we will be bounded only to the reduction of right angled diagram for calculation  $W_{xx}$  (Fig. 193). The difference of this diagram from those examined above is not only in the form of areas/sites, but also in the fact that the areas/sites are numbered for facilitating the corresponding calculations.

It is of interest to examine one additional construction/design of diagram for calculating anomaly  $\Delta g$ , proposed by G. A. Gamburtsev



(1936) (it is called sometimes "template of Gamburtsev"). Its calculation and construction are characterized by large originality and simplicity; its certain deficiency is the complex form of the areas/sites of the equal effect/action and error in interpolation connected with this during determination of  $\Delta g$  for the body of arbitrary form, somewhat greater than with the use of polar template.

Page 364.

Formula for  $\Delta g$  (VI, 1) can be subjected to following conversion. It is possible to write out

$$\sin \theta dq = dz,$$

whence follows (Fig. 194)

$$\Delta g = 2f \sigma \int dz \int d\theta \quad (\text{VI. 7})$$

or, changing from the differentials to the finite differences,

$$\Delta g \approx 2f \sigma \sum \sum \Delta z \Delta \theta. \quad (\text{VI. 7a})$$

From this relationship/ratio following method of construction of diagram ensues. We select certain  $\Delta \theta = \frac{180^\circ}{n}$ , where  $n$  - integer. Through the origin of coordinates we conduct the system of the rays/beams through the angular interval, equal to  $\Delta \theta$ , evenly distributed in the lower half-plane. We further build the system of straight lines, parallel to the horizontal axis  $x$  and located in the lower half-plane at depths  $\Delta z$ ,  $2\Delta z$ , ... and so forth. In the intersection of contiguous rays/beams and straight lines are formed bevel squares, representing, according to (VI, 7a), the area/site of the equal effect/action of diagram (Fig. 195). As we see,

construction of diagram is exceptionally/exclusively simple: any person, armed with rule and protractor, can prepare it in 5-10 min.

Let us select now value  $\sigma$  (for example,  $1.0 \text{ g/cm}^3$ ), and also scale of diagram, i.e., value  $\Delta z$  in metric measure. Then immediately is determined the "scale value" of diagram, i.e., value  $\Delta g$ , which corresponds to the effect/action of the body of infinite course/strike with the section, which coincides with the area/site of the equal effect/action. Actually, the gravitational effect/action of the plane-parallel plate, whose section is placed between the contiguous horizontal lines of diagram, in accordance with the formula (V, 30) will be equal to

$$2\pi/\sigma \Delta z.$$

In this strip is arranged/located  $n$  areas/sites of equal effect/action, consequently, on one pad falls value

$$\Delta g = \frac{2\pi/\sigma \Delta z}{n}. \quad (\text{VI.8})$$

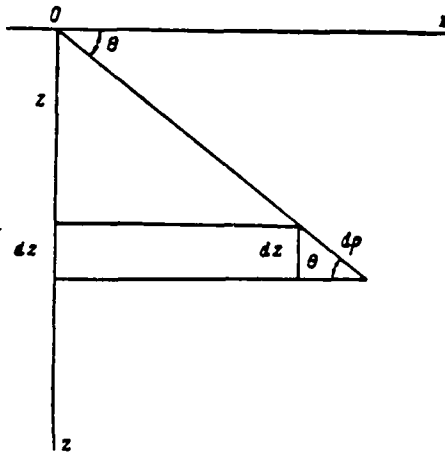


Fig. 194. For calculation of G. A. Gamburtsev's diagram.

Page 365.

In conclusion let us examine one additional diagram for calculating gravitational effect/action of three-dimensional bodies, which have form of vertical cylinders with arbitrary horizontal section. <sup>1</sup> As the geologic analogs of this type of bodies can serve intrusion bodies of the type of the so-called central intrusions with the steep contacts, which slope within the basement, diamond-bearing kimberlitic volcanic pipes in the sedimentary rocks, ore shoots of tube-shaped form, etc.

FOOTNOTE <sup>1</sup>. Proposition of K. F. Tyapkin (1961). ENDFOOTNOTE.

For calculation and construction of corresponding diagrams it is possible to use formula, which expresses gravitational effect/action of vertical circular cylinder on point, arranged/located on its axis

above center of upper basis/base (formula, V, 29),:

$$\Delta g = 2f_0\pi \left[ z_2 - z_1 - \sqrt{z_2^2 + R^2} + \sqrt{z_1^2 + R^2} \right],$$

where  $z_1$  and  $z_2$  - respectively values of depth of upper and lower bases.

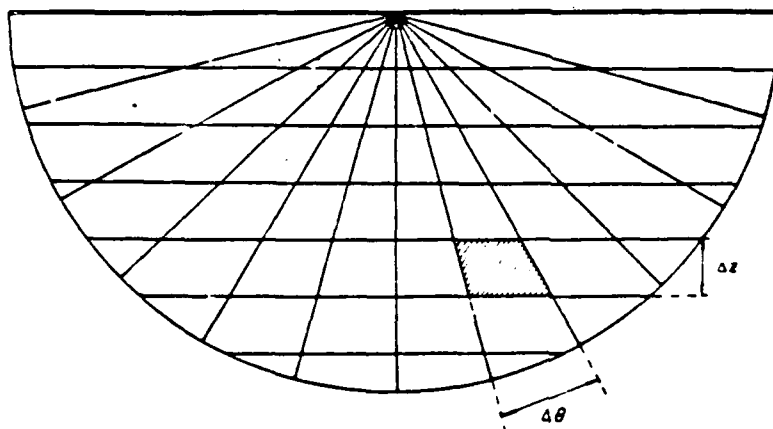


Fig. 195. G. A. Gamburtsev's diagram for calculation  $\Delta g$ .

Page 365.

From this formula directly ensues formula for vertical annulus, limited to radii  $R_1$  and  $R_2$  (Fig. 196a).

$$\Delta g = 2f\sigma\pi \left[ \sqrt{z_1^2 + R_2^2} - \sqrt{z_1^2 + R_1^2} + \sqrt{z_2^2 + R_1^2} - \sqrt{z_2^2 + R_2^2} \right] \quad (\text{VI.9})$$

and for the sector of vertical circular cylindrical ring (Fig. 196b)

$$\Delta g = \frac{2f\sigma\pi}{n} \left[ \sqrt{z_1^2 + R_2^2} - \sqrt{z_1^2 + R_1^2} - \sqrt{z_2^2 + R_1^2} + \sqrt{z_2^2 + R_2^2} \right] \quad (\text{VI.10})$$

Here  $n$  is determined by relationship/ratio

$$n = \frac{2\pi}{\alpha},$$

where  $\alpha$  - angle of visibility of sector from center of upper base (see Fig. 196b).

Putting to use formula (VI, 10) and assuming/setting in it, for

86

example,  $\Delta g = 1$  mgal and  $\sigma = 1.0$  g/cm<sup>3</sup>, it is possible to calculate and to construct diagram for calculating gravitational effect/action of vertical cylinders of arbitrary horizontal section. This section for executing corresponding calculations is approximately the system of the sections of the ring sectors of equal effect/action, as shown in Fig. 197.

Diagram examined above of calculations relates to anomaly  $\Delta g$ . If we in the formula (VI, 10) replace  $z$ , and  $z$ , respectively through  $z_1 - z$  and  $z_1 + z$  and produce differentiation with respect to  $z$ , then are obtained the corresponding formulas for

$$W_{II} = \frac{\partial g}{\partial z}, \quad W_{III} = \frac{\partial^2 g}{\partial z^2}.$$

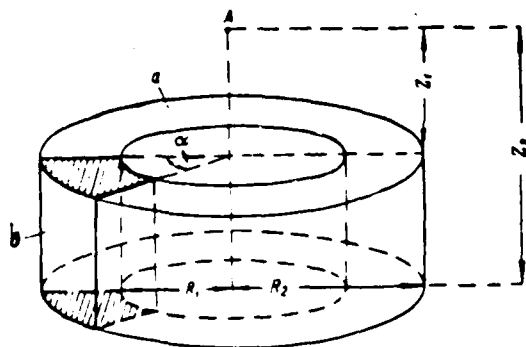


Fig. 196. Vertical circular cylindrical ring (a) and sector of vertical circular cylindrical ring (b). A - observation point.

Page 367.

Utilization of these latter/last formulas gives possibility to calculate and to construct analogous diagrams also for these derivatives. The same system of calculations can be used for determining the gravitational effect/action of three-dimensional bodies with the variable/alternating horizontal section, by assuming that the latter can be represented in the form of the system of sufficiently thin material disks (Fig. 198), moreover the effect/action of each of the disks is determined by method described above.

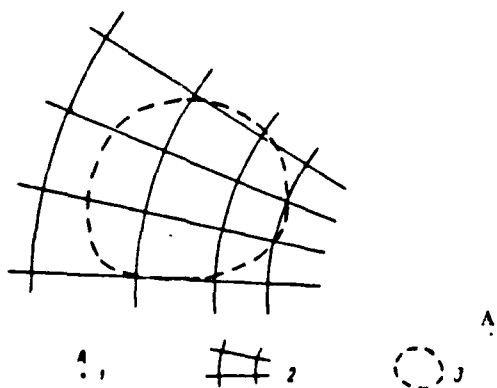


Fig. 197. Approximate presentation/concept of horizontal section of vertical cylindrical body by system of sector areas/sites of equal effect/action. 1 - observation point; 2 - area/site of the equal effect/action; 3 - horizontal section of cylindrical body.

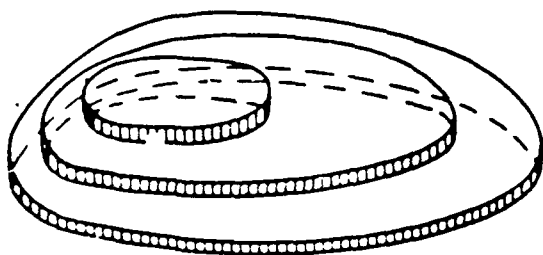


Fig. 198. For calculation of gravitational effect/action of three-dimensional body with variable/alternating horizontal section.

Page 368.

Another system of calculation of gravitational effect/action of three-dimensional body, recently proposed and developed/processed by foreign geophysicists (Talvani and Ewing, 1960; Goguel, 1961), consists in replacement of three-dimensional body by system of polygonal material disks.



In all cases of this type calculations require compiling sufficiently significant quantity of auxiliary diagrams for example, in case examined above - for different depths  $z_1$  and  $z_2$  of bedding of sector of vertical circular cylindrical ring.

#### §47. Ways of mechanizing the calculation.

Compiling diagrams significantly simplifies problem of calculating gravitation effect for bodies of arbitrary form. Repeatedly and already long time are made attempts at further simplification and mechanization of the corresponding calculations by the creation of different auxiliary computers. Wide industrial utilization these devices thus far did not obtain; therefore we are limited below only to short description of the basic idea of some such devices.

Integrating gears, which determine magnitude of gravitation effect (on  $\Delta g$  or on second derivatives) for three-dimensional or two-dimensional bodies, compose basic group of this type of devices. Obtaining these values is reduced to the calculation of integrals with the outline of the cross section of body (for the two-dimensional bodies) or along the system of the horizontals, which characterize the surface of three-dimensional body; this calculation is performed by the automatically appropriate device.

Integrating gears for three-dimensional problem were in different versions designed and prepared, also, in USSR and abroad; however, apparently, none of them showed good results in sense of high productivity and accuracy. Matter concerning the integrators for the two-dimensional problem is another: among similar prepared devices some proved to be sufficiently effective and subsequently they can obtain practical application. In a number of latter focuses attention by its simple and ingenious device G. A. Gamburtsev's integrator (1926), whose short description is given below.

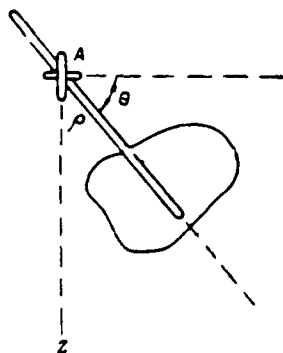


Fig. 199. Schematic of G. A. Gamburtsev's integrator.

Page 369.

Schematic of this integrator is shown in Fig. 199. Rule with the tracer is reinforced in such a way that its axis in any position would pass through point A, for which is calculated value  $\Delta g$ . With the rule is connected the calculating small wheel, the rotational axis of which is fastened motionlessly in parallel to z axis. If with the bypass of the elementarily small arc of the outline of the section of body the rule with the pin moves along its axis up to distance  $d\rho$ , then small wheel in this case will be turned to arc  $\cos \theta d\rho$ . With the bypass of entire outline calculating small wheel will be turned to the arc, numerically equal (see first of the formulas II: , 20)

$$\int \cos \theta d\rho = \frac{\Delta g}{2/a}.$$

whence value  $\Delta g$  is obtained.

It is possible to construct instrument, which makes it possible to obtain immediately curve of anomaly  $\Delta g$  for entire profile with one

bypass of outline. System composes the basis of this instrument from several (up to ten) integrators of Gamburtsev, fastened/strengthened in such a way that the axes of their calculating small wheels, each of which represents "observation point", are arranged/located through certain distances on one horizontal axis (the "line of observations"), and the rules of all integrators are attached to the general/common tracer. This instrument, also proposed by G. A. Gamburtsev, was named multigravimeter (from the the Lat. multi - multiple).

Idea of photo-integrator for calculating anomaly  $\Delta g$ , proposed as early as 1935 by V. V. Fedynskiy (Shvank and Lyustikh, 1947, pg. 187-188), is very interesting. This instrument is based on the following principle. Anomaly of force of gravity  $\Delta g$  caused by the attraction of mass point M, arranged/located at depth h at distance r from observation point, is expressed by the appropriate formula (V, 2):

$$\Delta g = fM \frac{h}{r^3}$$

(f - gravitational constant).

On the other hand, as is known from optics (see, for example, "Course of physics" edited by Papaleksi, 1948, Vol. 2, pg. 339-340), illumination E of element of flat surface  $z=0$  by point source with luminous intensity I, arranged/located at depth h at distance g from element of plane, is expressed formally by analogous relationship/ratio:

$$E = \frac{I \cos(\alpha)}{r^2} = I \frac{h}{r^3},$$

i.e.  $E = \Delta g$ , if  $I = fM$ .

Page 370.

Let us replace attracting/tightening body with system of foci, evenly distributed in its volume, and plane of observation - by photographic plate. Then measuring photometrically the degree of blackening of plate in different places, it is possible to obtain immediately the distribution of anomaly  $\Delta g$ , caused by the effect/action of body on the plane of observations. It is possible to determine the gravitation effect of body in parts, for example, dividing/marking off body into the plane-parallel layers. Unfortunately, until now, this valuable idea is not in practice realized due to the discovered technical difficulties of this type of "thermo-optical modeling".

General conclusion/derivation on problem in question is such: there are many good ideas of mechanization of calculations, connected with calculation of gravity anomalies, but in production of this type mechanizing devices are not thus far introduced.

More detailed survey/coverage of question see of O. A. Shvank and Ye. N. Lyustikh (1947).

548. Determination of the form of interface (contact surface).

In this section we will examine important in theory and practice

of gravitational prospecting problem, which can be formulated as follows: below plane  $z=0$  (plane of observations) is arranged/located of arbitrary form surface, which separates upper and lower thicknesses of rocks, which have different density; determine anomaly of gravitational force, caused by effect/action of indicated interface of density (contact surface). The described model directly corresponds to many real boundaries of heterogeneous lithologic-stratigraphic thicknesses, because of this the problem in the setting examined is encountered very frequently in the practice of geophysicist-pro prospector.

Let us designate density of upper thickness of rocks through  $\sigma_1$ , lower - through  $\sigma_2$ , and density variation on interface we will characterize by value  $\sigma = \sigma_2 - \sigma_1$ .

During this determination and with  $\sigma > 0$  to uplift of interface will correspond positive increase  $\Delta g$ , while in  $\sigma < 0$  - decrement  $\Delta g$ .

On the basis of formula (III, 8), anomaly  $\Delta g$ , caused by effect/action of interface, it is possible to write in the form

$$\Delta g = -f\sigma \int_0^{2\pi} d\alpha \int_0^l dl \int_0^z \frac{z dz}{(z^2 + l^2)^{3/2}}, \quad (VI.11)$$

where introduced by us polar coordinates are connected with right angled relationships/ratios:  $x=l \cos \alpha$ ,  $y=l \sin \alpha$ ,  $dx dy = l d\alpha$ , and vertical coordinate  $z$  characterizes depth of bedding of interface at flowing point  $(l, \alpha)$ .

Let us designate depth of investigated surface in the beginning of coordinates through  $h$  (Fig. 200).

Page 371.

Minus sign in formula (VI, 11) is written from the consideration, that we would have zero value of anomaly in such a case, when interface being investigated would coincide with plane of observations, i.e., entire lower half-space would have uniform density, equal to  $\sigma_0$ .

Formula (VI, 11) can be written in a somewhat different form. Let us lead horizontal plane at depth  $z=h$  (see Fig. 200). It is possible to visualize that the anomaly is caused by the effect/action of the plane-parallel infinite plate, arranged/located between planes  $z=0$  and  $z=h$  with the density -  $\sigma$ , plus a certain correction term ( $u$ ), depending on the relief of interface with the excess density  $\sigma$ , whose excesses are counted off from plane  $z=h$ . Then it is possible to write

$$\Delta g = -2f\sigma\pi h + u, \quad (\text{VI.12})$$

where

$$u = -f\sigma \int_0^{2\pi} d\alpha \int_0^\infty l dl \int_h^z \frac{z dz}{(z^2 + l^2)^{3/2}} \quad (\text{VI.12a})$$

After integration for  $z$  expression  $u$  will be written in the form

$$u = -f\sigma \int_0^{2\pi} d\alpha \int_0^\infty \left( \frac{l}{1 + l^2 + h^2} - \frac{l}{1 + l^2 + z^2} \right) dl.$$

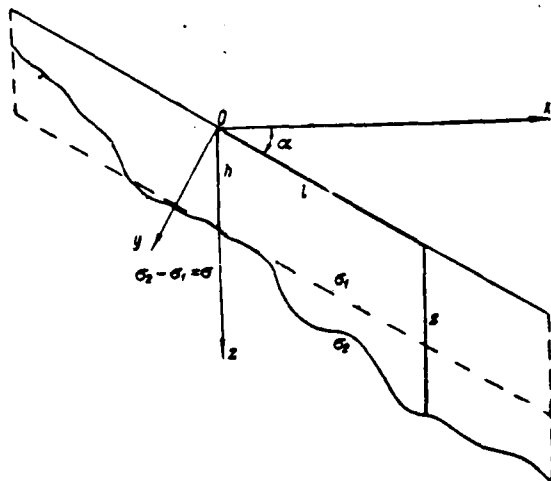


Fig. 200. For determination of gravitational effect/action of interface.

Page 372.

With  $z=h$ , obviously,  $u=0$ .

Approximate value  $u$  can be determined, if we consider that relation

$$\frac{h-z}{l} = \frac{\Delta z}{l}$$

is small value <sup>1</sup>.

FOOTNOTE <sup>1</sup>. The condition indicated is justified in the case of the gently sloping relief of interface. We take  $\Delta z=h-z$  so that the positive values  $\Delta z$  would answer uplifts, and negative - subsidences of relief. ENDFOOTNOTE.



Under this assumption with the utilization of Taylor's formula the integrand is expanded into series

$$\frac{l}{\sqrt{l^2+h^2}} - \frac{l}{\sqrt{l^2+z^2}} = \frac{hl \Delta z}{(l^2+h^2)^{3/2}} + \frac{1}{2} \cdot \frac{l(l^2-2h^2)(\Delta z)^2}{(l^2+h^2)^{5/2}} + \dots$$

If we are bounded in this expansion by first term and substitute it into expression for  $u$ , then latter can be represented in the form

$$u = f \sigma \int_0^{2\pi} d\alpha \int_0^\infty \frac{hl \Delta z dl}{(l^2+h^2)^{3/2}} = \frac{h}{2\pi} \int_S \frac{2\pi f \sigma \Delta z dS}{r^3}.$$

Comparing this formula with Poisson's formula (II, 27)

$$U(0, 0, -h) = \frac{h}{2\pi} \int_S \frac{U dS}{r^3}.$$

we come to following conclusion: determination of  $u$  on  $\Delta z$  in the first approximation is analogous with determination of harmonic function  $U$  at external point  $P$  at height  $h$  by its distribution on plane  $z=0$  or, that is the same, determination  $U$  on plane  $z=0$  from its distribution on plane  $z=h$ , if we count function assigned at flowing point of initial plane in the form

$$U = 2f \sigma \pi \Delta z. \quad (VI, 12b)$$

To this formal analogy we will repeatedly turn later.

Introducing now new variable  $\phi$  from relationship/ratio

$$l = h \operatorname{tg} \phi,$$

it is possible to write

$$u = f\sigma \int_0^{2\pi} d\alpha \int_0^{\frac{\pi}{2}} \Delta z \sin \varphi d\varphi.$$

Page 373.

Constant part in value  $\Delta g$  is equal to  $-2f\sigma\pi\Delta z$ , consequently, with an accuracy to the constant

$$u = \frac{1}{2\pi} \int_0^{2\pi} d\alpha \int_0^{\frac{\pi}{2}} \Delta g \sin \varphi d\varphi = \frac{1}{2\pi} \int_0^{2\pi} d\alpha \int_0^{\frac{\pi}{2}} \Delta g d(\cos \varphi). \quad (VI, 13)$$

Or, changing to finite differences,

$$u \approx \frac{1}{\pi n} \sum \sum \Delta g \Delta (\cos \varphi), \quad (VI, 13a)$$

where  $m=2\pi/\Delta\alpha$  (number of radii);

$$n = \frac{1}{\Delta(\cos \varphi)} \text{ (number of divisions of cosine of angle).}$$

With the help of this relationship/ratio is determined  $u$  according to distribution  $\Delta g$  on plane  $z=0$ .

If  $\sigma$  is known, then relief of interface in the first approximation can be investigated, assuming/setting in formula (VI, 12) correction term  $u=0$ , from relationship/ratio

$$\Delta g = -2/\sigma\pi h.$$

Under actual conditions (since there is always regional background) connection of  $\Delta g$  and  $h$  it is necessary to accept in more general form  $\Delta g=a+bh$ , and for determining constant  $a$  it is necessary

to know factual value of  $h$  for any point in territory of photographing.

For obtaining second approximation/approach it is necessary to use formula (VI, 13) and to determine at each point value of correction term  $u$ , and value  $h$  to determine from formula (VI, 12), taking it in the form

$$\Delta g = -2f\sigma\pi h + u.$$

Method presented above of determination of  $u$  is described by B. V. Numerov (1930).

Is known also other, considerably more complex in sense of computing system, method of removal of refined dependence of  $\Delta g$  on  $h$ , based on noted above formal analogy of determination of  $u$  with case of analytical continuation, published by A. K. Malovichko (1956).

Let us examine analogous two-dimensional problem, assuming infinite course/strike of structural forms of relief in parallel to  $y$  axis.

Page 374.

Then

$$\Delta g = -2f\sigma \int_{-\infty}^{+\infty} dx \int_0^z \frac{z dz}{x^2 + z^2} = -2f\sigma\pi h + u, \quad (\text{VI, 14})$$

where

$$u' = -f\sigma \int_{-\infty}^{+\infty} \ln \frac{x^2+z^2}{x^2+h^2} dx. \quad (\text{VI.14a})$$

Or, being limited as before during expansion of integrand into series by first order of magnitude <sup>1</sup>

$$\frac{h-z}{l} = \frac{\Delta z}{l},$$

it is possible to obtain

$$u' = 2f\sigma \int_{-\infty}^{+\infty} \frac{h \Delta z}{x^2+h^2} dx = \frac{h}{\pi} \int_{-\infty}^{+\infty} \frac{2f\sigma\pi \Delta z}{x^2+h^2} dx. \quad (\text{VI.15})$$

FOOTNOTE <sup>1</sup>. Here is also taken  $\Delta z = h-z$  from consideration indicated above (see pg. 372). ENDFOOTNOTE.

If we compare this expression with appropriate Poisson's formula for two-dimensional problem

$$U_p = \frac{h}{\pi} \int_{-\infty}^{+\infty} \frac{U}{x^2+h^2} dx,$$

then, just as in the case of three-dimensional problem. The formal analogy of determination  $u$  on  $\Delta z$  with determination  $U_p$  from  $U$  is revealed, if we  $u$  again take in the form (VI, 12b).

If we now introduce new variable

$$\varphi = \arctg \frac{x}{h},$$

$u'$  it is possible to express in the form

$$u' = 2f\sigma \int_{-\frac{\pi}{2}}^{\frac{\pi}{2}} \Delta z d\varphi = \frac{2}{\pi} \int_{-\frac{\pi}{2}}^{\frac{\pi}{2}} \Delta g d\varphi.$$

$$u' \approx \frac{1}{n} \sum \Delta g(\varphi). \quad (\text{VI.16})$$

Or, in the finite differences,

where  $n = \pi / \Delta \varphi$  - number of divisions of semicircumference.

Page 375.

L. V. Petrov (1957) published comparison of results of determining subterranean relief for theoretical example, calculated for case of sloping step with angle of slope of lateral face in  $11^\circ 19'$  according to formula

$$\Delta g = -2/\sigma \pi h$$

and by refined formula

$$\Delta g = -2/\sigma \pi h + u,$$

using described above method of B. V. Numerov. The results of calculations were compared with the factual data about the depth of the bedding of interface. Errors in the calculations using the first method reached 25%, on the second - did not exceed 11%. Thus, the application of B. V. Numerov's method contributes to a rather substantial increase in the accuracy of interpretation.

In practice extensively is used already indicated above elementarily simple approach to interpretation of gravity anomalies, caused by effect/action of interface of density, when simple proportionality between changes in anomalies and depths is assumed.

In the geologically studied regions this proportionality can be

checked, moreover during this check it often with the satisfactory accuracy is confirmed - precisely in such cases, when interface is placed at the relatively small depth from the earth's surface.

This fact will be fully coordinated with following theoretical consideration. Let us examine a special case of relief in the form of vertical step, in detail examined in §40 of Chapter V. On x axis, i.e., on the line of observations, which goes transversely of the course/strike of step, we take two points with coordinates  $x_1$  and  $x_2$ , one of which is arranged/located to the left, and another to the right of the boundary of step, i.e., point  $x=0$  (see Fig. 137); the depths of interface at these points will be  $z_1$  and  $z_2$ , and anomaly value, respectively,  $\Delta g(x_1)$  and  $\Delta g(x_2)$ . The difference in the values of anomaly  $\Delta g$  at these points will be the value of variable, which is increased with an increase in distance between the points to the limiting value

$$\Delta g(+\infty) - \Delta g(-\infty) = 2/\sigma\pi (z_1 - z_2).$$

With sufficiently high finite values of  $x_1$  and  $x_2$ , it is possible to take approximately

$$\Delta g(x_2) - \Delta g(x_1) \approx 2/\sigma\pi (z_1 - z_2). \quad (VI.17)$$

i.e. already familiar to us condition of proportionality of values of anomalies and depths, expressed in difference form.

Page 376.

If we now fix/record points  $x_1$  and  $x_2$ , but examine ledged interface at

different average depth

$$\frac{z_1 + z_2}{2},$$

then it is clear that most accurate the relationship/ratio (VI, 17) will be with the minimum average depth of the bedding of interface, since under this condition anomaly  $\Delta g$  above the step varies most sharply and most rapidly it approaches its limiting values with the removal/distance from the edge of step. With an increase in the average depth change of  $\Delta g$  above the step becomes ever smoother and difference  $\Delta g(x_2) - \Delta g(x_1)$  begins ever more to differ from a difference in the limiting values  $\Delta g(+\infty) - \Delta g(-\infty)$  to the side of underestimation, i.e., always

$$\Delta g(x_2) - \Delta g(x_1) < \Delta g(+\infty) - \Delta g(-\infty).$$

With shallow bedding of interface proportionality of anomalies and depths, as already said, is developed sufficiently clearly: map/chart of isoanomalies in this case reproduces even in fine details map/chart, which shows hypsometry of relief of interface. This fact especially clearly illustrates the comparison of the results of the experimental gravitation prospecting works (with the variometers) on ice of lake, represented by the map/chart of the vectors of gradient and isoanomalies of the force of gravity (Fig. 201) and results of the detailed measurements of the depths of the bottom of lake, represented by the hypsometric map/chart (Fig. 202). To the shiny conformity of these maps/charts, which was used at the end of the Thirties of our century the business of the propaganda of the possibilities of gravitational prospecting among our geologists and geophysicists,

contributed the following facts:

1. Presence of the very sharp density boundary (water - bottom depositions of the lake:  $\sigma$  about 1 g/cm<sup>3</sup>), which slopes at the very small depth (1-13 m).

2. Very thick network/grid of variometric observations (through 25 m, sometimes through 12.5 m), because of which by integration obtained very detailed picture of distribution of anomaly  $\Delta g$ .

3. Thorough exception/elimination of regional background: dependence of  $\Delta g$  on  $h$  was assumed in the form

$$\Delta g = a + bh + cx + dy.$$

where  $a$ ,  $b$ ,  $c$ ,  $d$  - constant coefficients, determined via comparison of depths of bottom of lake  $h$  (determined by way of direct measurements in each of observation points) with values of  $\Delta g$  with known values of  $x$  and  $y$  (horizontal coordinates of observation points) from method of least squares.

Regional component of field

$$\Delta g = a + cx + dy$$

was eliminated from directly specific values of anomaly  $\Delta g$ .



Page 377.

With all indicated conditions and precautions, as we see, conformity of anomalous gravitational field with relief of its conditioning interface can be very distinct and developed even in parts.

As we already noted, small depth of bedding of interface is most important condition for similar conformity. If the depth of interface is increased, then the conformity of structural and gravitational maps/charts is disturbed: the latter already ceases to just as distinctly repeat all parts of structural map/chart, these parts are lost, are smeared, as image details are smeared, if focusing/induction to the focus of camera was brought down.

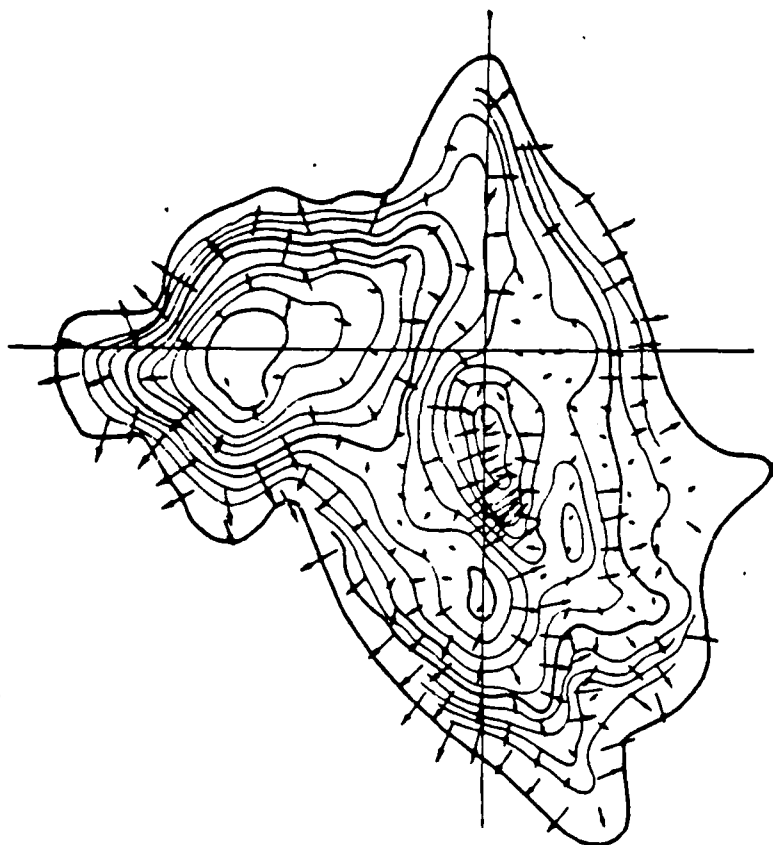


Fig. 201. Vector diagram of horizontal gradients and plan/layout of isoanomalies of gravitational force on lake. Isoanomalies - through  $5 \cdot 10^{-4}$  CGS=0.05 mgl. According to B. V. Numerov (1931).

Page 378.

This figurative analogy belongs to American geophysicist S. Pearson (1945), who proposed the calculating operation, named it "gravitational focusing", target of which is to improve the conformity of gravitational and structural maps/charts with a deep bedding of interface. Essence of this operation - analytical continuation of

anomalous field to a certain auxiliary horizontal plane, situated between the plane of observations and the interface, which conditions the presence of the gravity anomalies (Fig. 203) being investigated. With respect to this auxiliary plane the interface will lie on respectively smaller depth than with respect to the plane of observations, and, consequently, the analytically continued values of anomaly  $\Delta g$  must be better correlated with the behavior of interface.

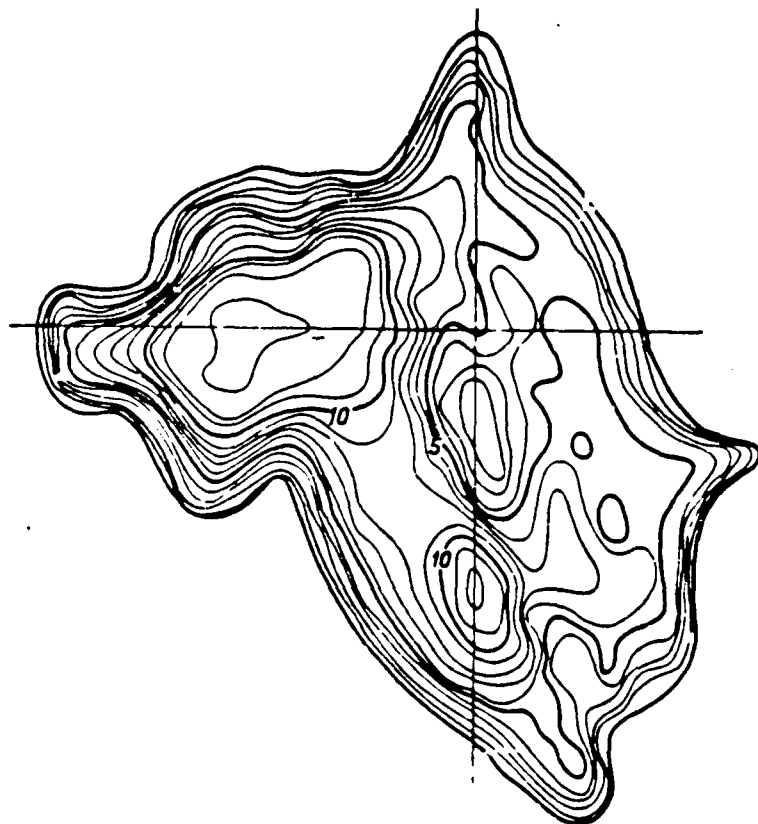


Fig. 202. Plan/layout of isohypses of bottom of lake. Isobaths - through 1 m. According to B. V. Numerov (1931).

Page 379.

Analytical continuation from the initial plane  $z=0$  to S. Pirsno's plane  $z=z_0$  was recommended to realize by the easiest method, on the basis of the approximate relationship/ratio

$$\Delta g|_{z=z_0} \approx \Delta g|_{z=0} + z_0 V_{zz}.$$

As we know (see Chapter IV), the same problem it is possible to solve by more accurate, but also by more complex methods. However, in

this case during the analytical continuation are unavoidable the errors, which with the poor accuracy and the insufficient detail of initial data can be significant. Furthermore, as we know, the operation of analytical continuation downward is sufficiently work consuming, especially in the three-dimensional case. All this in practice limits the possibility of "gravitational focusing", although in certain cases it is unconditionally justified.

Deficiency of usual approach to interpretation, when is allowed simple proportional dependence of change in anomalies and depths up to interface, caused only by value of excess density on this boundary, is revealed especially clearly in the case, when anomaly is caused by effect/action of several interfaces, situated on different average depth. As the example let us examine the case of density section/cut, occurred in Fig. 204, two similarly arranged/located density boundaries  $+\sigma$  and  $-\sigma$ , which generate in the set positive structure with the approximation/approach to surface of the compact rocks. Without any calculations it is obvious that if this uplift/rise has significant amplitude and thickness relative to the compact rocks with the density  $\sigma_1$ , that slope between the upper and lower density boundaries, it has significant thickness, i.e. above the structure must be observed noticeable positive gravity anomaly, in spite of the presentation/concept, that the gravitation effect from lower density boundary must in this case compensate effect from upper bound and summary effect from the structure must be equal to zero.

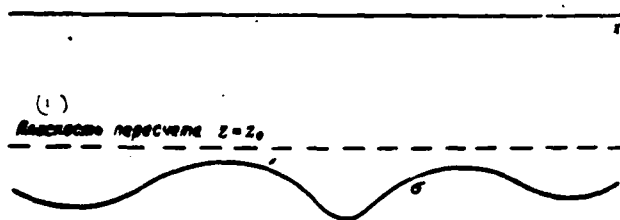


Fig. 203. Explanation to idea of "gravitational focusing".

Key: (1). Plane of scaling  $z=z_0$ .

Page 380.

This example shows that the gravitation effect on the density boundary must, in the more accurate examination, depend not only on relief, but also on the average depth of the bedding of interface: precisely for this reason in the example examined the effect/action of two similarly arranged/located interfaces is not compensated, but prevails the effect/action of upper density bound, situated on the smaller average depth from the plane of observations.

It proves to be possible sufficiently simply to obtain refined version of formula of type (VI, 17), into which in explicit form will enter value of average depth of bedding of interface of density. This question we now will examine.

We will be bounded in this case only to examined above first approximation, when for appropriate computations can be used formal analogy of problem in question with problem of analytical continuation of harmonic function (VI, 12b)

$$U = 2/\sigma\pi \Delta z$$

$$\Delta z = h - z$$

from level  $z=h$  in lower half-space (average depth of interface) to level  $z=0$  (plane of observations).

Let us allow now (being limited to case of two-dimensional problem) that along line, parallel to  $x$  axis, which goes transversely of course/strike of interface being investigated, relative change in depth of bedding of this boundary

is characterized by circular harmonic function of form  $\Delta z = \cos kx$  or by linear combination of functions of this form, for example,

$$\Delta z = e^{ikx} = \cos kx + i \sin kx.$$

Page 381.

The gravitational effect/action of this boundary in accordance with the presented above (pg. 373-374) consideration with an accuracy to constant will be reduced to the calculation of the integral of Poisson of the form

$$U = \frac{h}{\pi} \int_{-\infty}^{+\infty} \frac{e^{ikhx} dx}{(x-x')^2 + h^2} = e^{-kh} e^{ikhx'}. \quad (VI, 18)^*$$

FOOTNOTE \*. See, for example, G. A. Greenberg (1948, pg. 322). The excellent presentation of the methods of calculating such type of integrals see P. F. Chebyshev (1936, pg. 11-20). ENDFOOTNOTE.

Hence, taking into account expression  $e^{ikx}$  written above through trigonometric functions, we come to following conclusion: if relief of interface along x axis is characterized by circular harmonic function, then anomaly  $\Delta g$ , caused by effect/action of interface, along the same axis when making these assumptions is also analogous harmonic function of coordinate x with the same frequency and phase, moreover, if  $\sigma > 0$ , then they will answer maximum uplifts of boundary maximums, and downwarps/troughs - minima of anomaly  $\Delta g$  (Fig. 205). It is important to focus attention on the fact that the coordination of anomaly  $\Delta g$  indicated with the relief of interface on the frequency and the phase occurs with any average depth h of interface and is observed only in the case of the periodically varying relief and field: in the case of the separate localized form of relief the corresponding anomaly  $\Delta g$  with increase in h will be increased always and in the cross sizes/dimensions with the simultaneous decrease of its intensity.



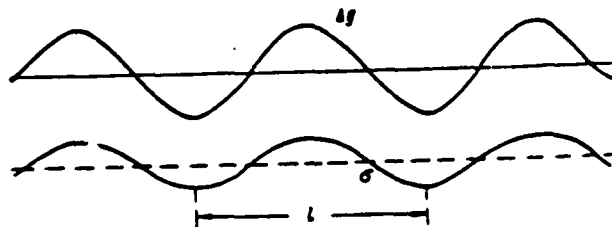


Fig. 205. Case of interface, represented by circular harmonic function.

Page 382.

Taking into account formulas (VI, 12b) and (VI, 18), we can write following approximation for  $\Delta g$  in the case, when

$$\Delta z = z - h = A \cos kx.$$

Then

$$\begin{aligned} \Delta g &= 2f\sigma\pi A e^{-kh} \cos kx = 2f\sigma\pi A e^{-\frac{2\pi h}{l}} = \\ &= 2f\sigma\pi e^{-\frac{2\pi h}{l}} (h - z). \end{aligned} \quad (\text{VI.19})$$

where  $k$  - frequency;

$l$  - period of curve;

$\Delta z = f(x)$  - curve of section of relief.

Taking now two values of  $x$ , equal to  $x_1$  and  $x_2$ , and designating those corresponding to them values of depth  $z$  of surface through  $z_1$  and  $z_2$ , we find from formula (VI, 19)

$$\Delta g(x_2) - \Delta g(x_1) \sim 2f\sigma\pi e^{-\frac{2\pi h}{l}} (z_1 - z_2). \quad (\text{VI.20})$$

Formula (VI, 20) can be considered as refinement to formula (VI, 17). As we see, they are completely of the same type and their difference only in the presence in right side to the formula (VI, 20) of additional multiplier  $e^{-\frac{2\pi h}{l}}$ . With condition  $\frac{h}{l} \rightarrow 0$ ,  $e^{-\frac{2\pi h}{l}} \rightarrow 1$ , the formula (VI, 20) changes in (VI, 17), i.e., (VI, 17) represents a special case (VI, 20). The condition indicated is equivalent to two following:  $h \rightarrow 0$  or  $l \rightarrow \infty$ .

Sense of first condition is clear; it expresses already noted above fact: increase in accuracy of formula (VI, 17) with decrease of average depth  $h$  of interface. With  $h$  sufficiently small the formula (VI, 17) becomes equivalent to formula (VI, 20), generally more accurate. The second condition becomes also clear, if we take into account real sense  $l$  (period of curve): this parameter, obviously, characterizes the cross sizes/dimensions of the structures, intersected by profile ( $x$  axis), for example anticlinal and synclinal folds. Transition  $l \rightarrow \infty$  designates transition to the relief, being structures "infinite width", namely similar is the structure of the step, from the formula for case of which we brought out formula (VI, 17).

Formula (VI, 20) is instructive even in that sense, that "gravitational efficiency" of deep structural relief, i.e., relation

$$\frac{\Delta g(x_2) - \Delta g(x_1)}{x_2 - x_1},$$

expressed, let us say, in milligals to kilometer, proves to be

proportional not simply to excess density  $\sigma$ , but to product

$$S = \sigma e^{-\frac{2\pi h}{T}},$$

which can be in this case named effective excess density.

Page 383.

With the designation indicated we have from the formula (VI, 20)

$$\Delta g(z_2) - \Delta g(z_1) \approx 2fS \pi (z_1 - z_2), \quad (\text{VI, 20a})$$

i.e.  $S$  in the formula (VI, 20a) plays the same role, as  $\sigma$  in the formula (VI, 17).

As can be seen from Table 24, values  $S$  can be much less than value  $\sigma$ .

Given above consideration, and data from Table 24 also elucidate to interpreter many questions, directly connected with examined/considered by us problem and which were remaining to recent of times far from clear, in spite of their large practical importance. Below we stop on the elucidation of these questions.

First of all it proves to be that gravitational effect/action of interface can be any actually evaluated, if is known not only excess density on this boundary, but also average depth  $h$  of its bedding and its "frequency characteristic", i.e. order of magnitude of period  $T$  of harmonic functions, which characterize relief of interface. The "sphere of the activity" of the generally accepted formula (VI, 17), as it proves to be, is limited to the very low values of relation

In other cases the gravitation effect of boundary is much less than determined according to the formula (VI, 17). Thereby is completely elucidated the considered/examined above (pg. 379, Fig. 204) example with the gravitational effect/action of the structure, which presents the combination of two similarly arranged/located interfaces with the excess density of upper  $+\sigma$  and lower  $-\sigma$ . If these two boundaries are arranged/located on different average depth, then their effective density is completely different. If the period of the harmonic characterizing relief in both cases is equal to  $l$ , and the average depth of the bedding of interface is distinguished, for example, 2.5 times and for the upper surface  $(h/l)=20$ , i.e. (from Table 24)  $(S/\sigma)=0.284$ , then for lower boundary it will be  $(h/l)=0.50$ ,  $(S/\sigma)=0.043$ , the gravitational effect/action of upper bound exceeds the effect/action of lower boundary 6.6 times.

--

Table 24. Relationship/ratio of the values of effective  $S$  and the excess  $\sigma$  density during the determination of the gravitational effect/action of interface.

$\frac{h}{l}$	$\frac{S}{\sigma} = e^{-\frac{2\pi h}{l}}$
0.00	1.00
0.05	0.730
0.10	0.534
0.20	0.284
0.50	0.043
1.00	0.002

Page 384.

Real estimation of gravitational effect/action of structure, which presents combination of several similarly arranged/located interfaces, is possible only from point of view of similar "spectrum" presentations/concepts. Designating the values of the average depth of the bedding of the interfaces indicated through  $h_1, h_2, \dots, h_n$  and the values of excess density on these boundaries through  $\sigma_1, \sigma_2, \dots, \sigma_n$  and the period of the harmonic function, which characterizes the structural relief of interfaces, through  $l$  (Fig. 206), we can, on the basis of the formula (VI, 20), write for the present instance the analogous relationship/ratio

$$\Delta g(x_2) - \Delta g(x_1) = 2f\pi S(x_1 - x_2), \quad (\text{VI, 21})$$

where

$$S = \sum_{k=1}^n e^{-\frac{2\pi h_k}{l}} \sigma_k. \quad (\text{VI, 21a})$$

Here  $z_1$  and  $z_2$  represent values of depth of bedding at points  $x_1$

and  $x$ , of any of indicated interfaces, and  $S$  - total effective density of laminated structure.

Below, in Chapter VII, we give example of utilization of formula (VI, 21) with interpretation of regional gravity anomalies.

Page 385.

Let us note now following essential moment: upon transfer from formula (VI, 17) to formula (VI, 20) completely remains valid proportionality of change in anomaly  $\Delta g$  and depth  $z$  of bedding of interface; is made more precise only value of proportionality factor, precisely, it proves to be that this coefficient, as a rule, is less than  $2f\sigma\pi$ .

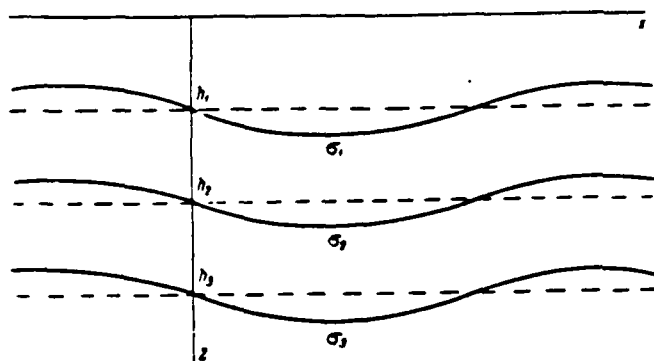


Fig. 206. Case of several accordingly consisting interfaces, whose section is characterized by circular harmonic function.

Page 385.

Practical conclusion/derivation is hence such: with the interpretation of gravity anomalies  $\Delta g$ , caused by the effect/action of the interface, the depth of bedding  $z$  of which at some points of the region being investigated is known (for example, from the data of drilling or seismic survey), should be, first of all, examined the correlation graph/diagram of the dependence between  $\Delta g$  and  $z$  and, if this graph is close to the linear, to deduce from it the value of proportionality factor. In this case one should assume that this coefficient is less (possibly, very considerably) than value  $2f\sigma\pi$ .

From examination made by us ensues possibility of following approach to interpretation of gravity anomalies, caused by effect/action of arbitrary interface (we will be bounded for simplicity to two-dimensional problem, although in principle the said

can below be generalized, also, in case of three-dimensional problem).

From analysis it is known that many functions, assigned analytically or graphically, can be expanded in Fourier series of form

$$f(x) = A_0 + \sum_{k=1}^{\infty} A_k \cos kx + B_k \sin kx.$$

Let us allow (virtually this can be done without any tension) that expansion can be made for curve of anomaly  $\Delta g$ , assigned along line of observations (x axis), and for corresponding curve, representing section of relief surface on average level  $z=h$ , by effect/action of which is caused anomaly being investigated. Let us allow further that this expansion is actually carried out for anomaly  $\Delta g$ . Then, obviously, by each of the harmonics of the obtained expansion, for example  $A_k \cos kx$ , corresponds harmonic in the expansion of the curve of relief  $\Delta z=f(x)$  of form  $a_k = \cos kx$ . moreover for the amplitudes of these harmonics on the basis of formula (VI, 19) it is possible to write the relationship/ratio

$$A_k = 2/\sigma\pi e^{-kh} a_k.$$

Concerning coefficient  $a_0$  in expansion  $\Delta z$ , then, as it is known from theory of Fourier series, this coefficient represents simply average/mean value of  $\Delta z$ , which in this case is equal to zero, consequently, and  $a_0=0$ .

If  $\sigma$  and  $h$  to us from any data are known, then it will prove to



be possible to determine all coefficients of expansion

$$\Delta z = \sum_{k=1}^{\infty} (a_k \cos kx + b_k \sin kx)$$

and, consequently, to obtain and to construct function  $\Delta z = f(z)$  of curve of section of interface.

Page 386.

To this direction in region of interpretation of gravity anomalies is dedicated number of significant investigations (Tsuboi and Fuschida, 1938; Shvank and Lyustikh, 1947; Tsuboi, 1956, etc.). In the latter of the works indicated Japanese geophysicist Tsuboi uses the following presentation/concept of anomaly  $\Delta g(x)$  (two-dimensional task):

$$\Delta g(x) = b \frac{\sin x}{x} = b \int_0^1 \cos kx dk, \quad (VI, 22)$$

leading to considerably simpler computing system, than the previously examined by him expansion into Fourier series.

Value  $b$  in formula (VI, 22) - certain constant, and variable part

$$f(x) = \frac{\sin x}{x}$$

represents clear alternating sign decreasing in terms of absolute value with increase in  $x$  function, represented graphically in Fig. 207. The possibility of the integral transform  $f(x)$  to the form, shown in the right side of the formula (VI, 22), allow, on the basis of the formula (VI. 20, to immediately obtain the appropriate excess

of the subterranean relief of interface in the form

$$\begin{aligned}\Delta z = h - z &= \frac{b}{2f\sigma\pi} \int_0^1 \cos kxe^{hx} dx = \\ &= \frac{b}{2f\sigma\pi(x^2 + h^2)} [(h \cos x + x \sin x) e^h - h] \quad (\text{VI}, 23)\end{aligned}$$

or with  $x=n\pi$ ,

$$\Delta z(n\pi) = \frac{bh}{2f\sigma\pi[(n\pi)^2 + h^2]} (\pm e^h - 1), \quad (\text{VI}, 24)$$

where plus sign is taken for the even, and minus - for the odd values of half-life.

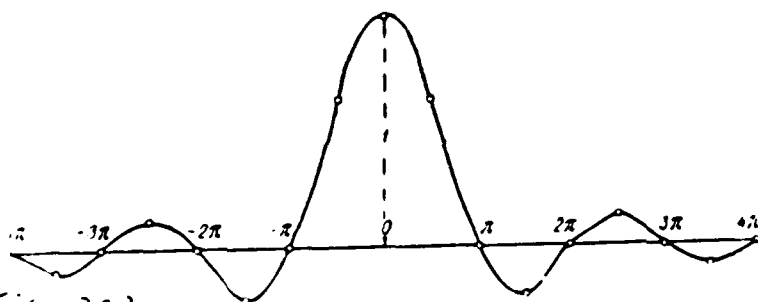


Fig. 207.

Graphic . . . . .  $\sin x/x$ .

Page 387.

If we x count not in fractions/portions of half-life, but fractions/portions of average depth h (is assumed that it is known), i.e., to assume  $x=nh$ , then

$$\Delta z = (nh) = \frac{b}{\sigma} \cdot \frac{(\pm e^{\pi} - 1)}{2f \pi^2 (n^2 + 1)} = \frac{b}{\sigma} \varphi(n), \quad (\text{VI, 25})$$

where values  $\varphi(n)$  are given in Table 25.

If we designate values of anomaly of gravitational force with  $x=nh$  through  $b$ , when  $x=(n+1)h$  - through  $b_1$ , with  $x=(n-1)h$  - through  $b_{-1}$ , and so forth, then

$$\Delta z(nh) = b_0 \varphi(0) + (b_1 + b_{-1}) \varphi(1) + \dots \quad (\text{VI, 25a})$$

During practical application of method indicated its author recommends assigning probable value of average depth  $z=h$  and the counting of average value of anomaly  $\Delta g$  along interpretive profile; this average/mean value to consider corresponding to depth  $z=h$  of interface. Relative to this level the relative deflections of the relief of surface with respect to the formula (VI, 25a) are determined.

Table 25. Values of auxiliary function  $\varphi(n)$  in the method of Tsuboi.

$n$	$\varphi(n) \cdot 10^7$ CFC	$n$	$\varphi(n) \cdot 10^7$ CFC
0	1.6819	$\pm 10$	0.0166
$\pm 1$	-0.9167	$\pm 11$	-0.0150
$\pm 2$	0.3363	$\pm 12$	0.0118
$\pm 3$	-0.1834	$\pm 13$	-0.0108
$\pm 4$	0.0990	$\pm 14$	0.0086
$\pm 5$	-0.0760	$\pm 15$	-0.0081
$\pm 6$	0.0454	$\pm 16$	0.0066
$\pm 7$	-0.0367	$\pm 17$	-0.0062
$\pm 8$	0.0254	$\pm 18$	0.0052
$\pm 9$	-0.224	$\pm 20$	0.0042

Page 388.

Method presented, as we see, is very simple according to computing system. It is at the same time necessary to recognize that the function

$$f(x) = \frac{\sin x}{x}$$

approximates subterranean relief with no smaller accuracy, than Fourier series

$$f(x) = \sum_{k=1}^{\infty} (a_k \cos kx + b_k \sin kx).$$

In the literature attempts at practical utilization of method of Tsuboi (Tatevosyan, 1958) are described.

549. Direct methods of interpretation. General estimated formulas.

Methods, which make it possible to find some parameters of geologic bodies forming anomalies without introduction of special assumptions about their form and attitude, are called direct methods

of interpretation. In the theory of gravitational potential (Zamorev, 1939-1941) is proven, that according to the potential distribution and its derivatives assigned on the surface of the Earth are uniquely determined the following parameters:

- 1) mass M of disturbing body.
- 2) the coordinate ( $x_0$ ,  $y_0$ ,  $z_0$ ) of the center of gravity.
- 3) the relationship/ratio between the moments of different order.

Methods of determining these values are developed by G. A. Gamburtsev (1936), A. A. Zamorev (1939), N. R. Malkin (1930) and other scientists.

At basis of determination of enumerated parameters lies/rests known from theory of potential (Idel'son, 1936) Green's formula:

$$\int_S \left( U \frac{\partial W}{\partial n} - W \frac{\partial U}{\partial n} \right) dS = -4\pi \int_V U dm, \quad (VI, 26)$$

where S - closed surface, which surrounds anomalous masses.

W - gravitational potential.

U - certain function, harmonic within surface of S.

n - external normal to the surface of S.

V - region, occupied with disturbing bouy.

m - mass.

Let us assume that surface S is vertical circular cylinder of radius R, limited by planes  $z=0$  and  $z=z_1$ , perpendicular to axis of cylinder. Under this condition surface S can be decomposed into three

parts; upper ( $S_1$ ) and lower ( $S_2$ ) "covers/caps" and lateral surface ( $S_3$ ). Taking into account relationship/ratio in the direction of standard/normal  $n$  and  $z$  axis, let us find that the formula (VI, 26) will take the form

$$-\int_{S_1} \left( U \frac{\partial W}{\partial z} - W \frac{\partial U}{\partial z} \right) dx dy + \int_{S_2} \left( U \frac{\partial W}{\partial z} - W \frac{\partial U}{\partial z} \right) dx dy + \\ + \int_{S_3} \left( U \frac{\partial W}{\partial R} - W \frac{\partial U}{\partial R} \right) dS = -4\pi \int_V U dm,$$

Page 389.

With increase of radius  $R$  to infinity integral on  $S_3$  will vanish. Taking into account, that areas  $S_1$  and  $S_2$  are equal in the form and the value (only one of them is arranged/located above anomalous masses, and another - below), and taking into account that the integrands are identical, we will obtain

$$\int_{-\infty}^{+\infty} \int_{-\infty}^{+\infty} \left( U \frac{\partial W}{\partial z} - W \frac{\partial U}{\partial z} \right) dx dy = 2\pi \int_V U dm. \quad (VI, 27)$$

In the particular case, with  $U \equiv 1$ ,

$$\int_{-\infty}^{+\infty} \int_{-\infty}^{+\infty} \frac{\partial W}{\partial z} dx dy = 2\pi \int_V dm.$$

Integral in right side of equality represents total anomalous mass  $M$ , and vertical derivative of potential  $\partial W / \partial z$  corresponds to gravitational force. Finally

$$\int_{-\infty}^{+\infty} \int_{-\infty}^{+\infty} \Delta g(x, y) dx dy = 2\pi fM. \quad (VI, 28)$$

Assigning function  $U=x$  and  $U=y$ , let us find by analogous manner relationships for determining horizontal coordinates  $(x_0, y_0)$  of center of gravity of disturbing body

$$\int_{-\infty}^{+\infty} \int_{-\infty}^{+\infty} \Delta g(x, y) x dx dy = 2\pi f \int_V x dm = 2\pi fMx_0. \quad (VI, 29)$$

$$\int_{-\infty}^{+\infty} \int_{-\infty}^{+\infty} \Delta g(x, y) y dx dy = 2\pi f \int_V y dm = 2\pi fMy_0. \quad (VI, 30)$$

Vertical coordinate of center of gravity more complicatedly is calculated. Using a basic formula (VI, 26) and combining the results, which correspond to different presentation/concept of function  $U$ ,  $G$ .

A. Gabburtsev derived relationships/ratios (VI, 31-32):

$$\begin{aligned} & \int_{-\infty}^{+\infty} \int_{-\infty}^{+\infty} \left( W - 2x^2 \frac{\partial^2 W}{\partial z^2} \right) dx dy = \\ & - \int_{-\infty}^{+\infty} \int_{-\infty}^{+\infty} \left( W - 2y^2 \frac{\partial^2 W}{\partial z^2} \right) dx dy = 6\pi fMz_0. \quad (VI, 31) \end{aligned}$$

$$\begin{aligned} & \int_{-\infty}^{+\infty} \int_{-\infty}^{+\infty} \left( x \frac{\partial W}{\partial x} - x^2 \frac{\partial^2 W}{\partial z^2} \right) dx dy = \\ & = \int_{-\infty}^{+\infty} \int_{-\infty}^{+\infty} \left( y \frac{\partial W}{\partial y} - y^2 \frac{\partial^2 W}{\partial z^2} \right) dx dy = -2\pi fMz_0. \quad (VI, 32) \end{aligned}$$

Page 390.

Horizontal derivatives of potential  $\partial W/\partial x$  and  $\partial W/\partial y$  are found just as in magnetic prospecting according to distribution  $Z$ , they determine  $H$ . (see, for example, Tyapkin, 1961). The method of

determination  $(\partial^2 W / \partial z^2) = \partial g / \partial z$  from specified distribution  $\Delta g$  was described in §25.

A. A. Zamorev (1939) established somewhat distinct relationship/ratio for calculation  $z$ .

$$\int_{-\infty}^{+\infty} \int_{-\infty}^{+\infty} \left( W - \frac{fM}{r \sqrt{x^2 + y^2}} \right) dx dy = -2\pi fMz_0. \quad (VI, 32a)$$

Formulas (VI-31, 32a) require preliminary determination from anomaly  $\Delta g$  of anomalous potential  $W$ . Values  $W$  are calculated with the aid of equality (VI, 33), which also follows from Green's formula

$$W = \frac{1}{2\pi f} \int_{-\infty}^{+\infty} \int_{-\infty}^{+\infty} \Delta g(x, y) \frac{1}{r \sqrt{x^2 + y^2}} dx dy. \quad (VI, 33)$$

If excess density  $\sigma$  is known and value of it is constant, then throughout mass of body  $M$  it is easy to determine its volume, and thereby also probable linear dimensions. Knowing the center-of-gravity location and roughly considering the linear dimensions of body, it is possible to indicate the probable depth of the bedding of the upper edge of the body

The calculation of mass and coordinates of the center of gravity of disturbing body on anomalies  $W_{xx}$  and  $W_{yy}$  is realized with the help of the equalities (VI, 34-36)



$$\int_{-\infty}^{+\infty} \int_{-\infty}^{+\infty} x W_{xx} dx dy = \int_{-\infty}^{+\infty} \int_{-\infty}^{+\infty} y W_{yy} dx dy = -2f \pi M, \quad (\text{VI}, 34)$$

$$\int_{-\infty}^{+\infty} \int_{-\infty}^{+\infty} xy W_{xx} dx dy = -2f \pi M y_0, \quad (\text{VI}, 35)$$

$$\int_{-\infty}^{+\infty} \int_{-\infty}^{+\infty} \frac{1}{2} (x^2 - y^2) W_{xx} dx dy = -2f \pi M x_0. \quad (\text{VI}, 36)$$

Page 391.

In the case of bivariate distribution of masses, when course/strike of geologic objects in parallel to y axis, occur analogous relationships/ratios:

$$\int_{-\infty}^{+\infty} \Delta g dx = 2f \pi \lambda, \quad (\text{VI}, 37)$$

$$\int_{-\infty}^{+\infty} x \Delta g dx = 2f \pi \lambda x_0, \quad (\text{VI}, 38)$$

$$-\int_{-\infty}^{+\infty} x (W_x - x W_{xx}) dx = -\int_{-\infty}^{+\infty} x (W_x + x W_{xx}) dx = 2f \pi \lambda z_0, \quad (\text{VI}, 39)$$

where  $\lambda$  - mass of geologic body, per unit of length.

Cross section of body to us is unknown.

$$\lambda = \int_S \sigma(x, z) dx dz, \quad (\text{VI}, 40)$$

where S - cross-sectional area.

In such a case, when excess density  $\sigma$  is constant and value of it is known, cross-sectional area S can be determined according to gravitational observations:

$$S = \frac{\lambda}{\sigma}. \quad (\text{VI}, 41)$$

In order to determine not only area, but also form of cross section, additional information, for example coordinate of some points of outline, which limits cross section of body, is necessary. Most frequently the form of cross section is defined by the method of selection with the help of the templates after in a straight/direct manner is established cross-sectional area.

Let us pause at some questions of practical determination of integrals (VI, 27-29) and (VI, 37-38). It is easy to show the difficulties, which appear with the interpretation, based on the example of the determination of the mass, per unit of the length of two-dimensional body. Formula for the determination  $\lambda$  takes the form

$$\lambda = \frac{1}{2\pi} \int_{-\infty}^{+\infty} \Delta g(x) dx.$$

Page 392.

Equality (VI, 37) is extremely simple according to its structure; however, its utilization is complicated by the fact that integration should be fulfilled in infinite limits. Let us expand integral (VI, 37) into two terms

$$\int_{-\infty}^{+\infty} \Delta g(x) dx = \int_a^R \Delta g(x) dx + I, \quad (\text{VI, 42})$$

Remainder  $I$  is determined as follows:

$$I = \int_{-\infty}^{-R} \Delta g(x) dx + \int_R^{+\infty} \Delta g(x) dx. \quad (VI, 43)$$

Let us consider value I in the particular case of circular horizontal cylinder, which slopes at depth z,

$$\Delta g(x) = 2f\lambda \frac{z}{x^2 + z^2}. \quad (VI, 44)$$

According to equality (VI, 37)

$$\begin{aligned} \int_{-\infty}^{+\infty} \Delta g(x) dx &= 2f\lambda \int_{-\infty}^{+\infty} \frac{z}{x^2 + z^2} dx = 2f\pi\lambda, \\ \int_{-R}^{+R} \Delta g(x) dx &= 2f\lambda \int_{-R}^{+R} \frac{z}{x^2 + z^2} dx = 4f\lambda \operatorname{arctg} \frac{R}{z}. \end{aligned} \quad (VI, 45)$$

Consequently,

$$\begin{aligned} I &= 2f\pi\lambda - 4f\lambda \operatorname{arctg} \frac{R}{z} = 2f\lambda \cdot \\ &\times \left[ \pi - 2\operatorname{arctg} \frac{R}{z} \right]. \end{aligned} \quad (VI, 46)$$

Relative value of residual integral let us find from equality (VI, 47):

$$\begin{aligned} I_{\text{res}} &= I : \int_{-\infty}^{+\infty} \Delta g(x) dx = \\ &= \frac{\pi - 2\operatorname{arctg} \frac{R}{z}}{\pi} = 1. \end{aligned} \quad (VI, 47)$$

Table 26 gives values  $I_{\text{res}}$  as function of relationship/ratio  $R/z$ . For the comparison the values of anomaly  $\Delta g(R)$ , expressed in the fractions/portions of its maximum value  $\Delta g_{\text{max}} = \Delta g(0)$  are indicated also.

Table 26. Relationship/ratio of residual and calculated integrals during the determination of the mass of body.

$\frac{\Delta g(R)}{\Delta g_{\max}}$	$\frac{R}{z}$	$I_{\text{corr.}} \%$
0.03	5.69	12
0.05	4.35	17
0.07	3.65	20
0.10	3.00	25
0.15	2.36	34
0.20	2.00	42
0.25	1.73	50

Page 393.

As we see, residual integral  $I$  has very significant magnitude even in such cases when anomaly decreases to one tenth of maximum value. D. S. Mikov (1954) calculated the special graphs (Fig. 208), which can be used for the approximate separation of residual integral in the case, when body has approximately isometric form and it is possible to liken it to sphere, and in the case of the two-dimensional body, close to the horizontal cylinder. With the help of the correcting graphs it is possible to improve the result of calculations, but in this case somewhat is disturbed the basic idea of the method: to determine mass  $M$ , assigning no assumptions about the shape of body and the distribution of excess density. Actually, if 30-50% of effect depend on correction, which is calculated for the regular bodies, to speak about the complete independence of result from the assumptions is no longer necessary.

Significant errors in determination of mass  $M$  can be connected

with incorrect selection of "normal field". If the value of anomaly decreased to 0.10-0.15 maximum value, its further decrease occurs very gradually. It is difficult to separate the smoothly changing part of the anomaly from the regional background. It is possible to avoid the significant error, caused by this reason, calculating the integrals of the form

$$\int_{-\infty}^{+\infty} \Delta g(x) \cos ax \, dx = A_1(a), \quad (\text{VI. 48})$$

$$\int_{-\infty}^{+\infty} \Delta g(x) \sin ax \, dx = A_2(a). \quad (\text{VI. 49})$$

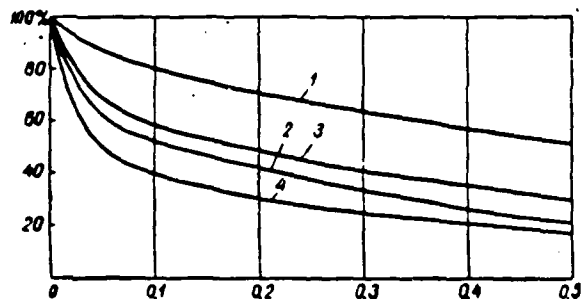


Fig. 208. Graph for evaluating residual integral during determination of mass of body. According to D. S. Mikov (1954). 1 -  $\Delta g$  for the cylinder; 2 -  $\Delta g$  for the sphere; 3 -  $w_{xx}$  for the cylinder; 4 -  $w_{xx}$  for the sphere.

Page 394.

Function  $B(a) = \sqrt{A_1^2(a) + A_2^2(a)}$  in limit with  $\alpha \rightarrow 0$  coincides with integral (VI, 37) (Fig. 209). At the same time, its value does not depend on errors in the selection of "normal field".

Difficulties, which appear during calculation of coordinates of center of gravity, the same order as during determination of mass  $M$ . In this case coordinate  $z$ , is determined only very approximately - much worse than  $x$ , and  $y$ .

In number of cases for checking interpretation of gravity anomalies special criteria can prove to be useful.

Let us examine anomaly  $\Delta g$ , caused by horizontally sloping

cylinder of small cross section  $dS$ . The curve  $\Delta g(x)$  along the profile, which intersects the bodies transversely of course/strike, will be expressed by the equality

$$\Delta g(x, 0) = 2f \sigma(\bar{x}, \bar{z}) dS \frac{\bar{z}}{\bar{z}^2 + (x - \bar{x})^2}, \quad (\text{VI.50})$$

where  $\bar{x}, \bar{z}$  - coordinates of the center of the section of cylinder.

Integral of anomaly  $\Delta g$ , taken on certain part of profile from point  $a$  to point  $b$ , is equal to

$$\begin{aligned} \int_a^b \Delta g(x) dx &= 2f \sigma(\bar{x}, \bar{z}) dS \int_a^b \frac{\bar{z}}{\bar{z}^2 + (x - \bar{x})^2} dx = \\ &= 2f \sigma(\bar{x}, \bar{z}) dS \left[ \text{arctg} \frac{b - \bar{x}}{\bar{z}} - \text{arctg} \frac{a - \bar{x}}{\bar{z}} \right]. \end{aligned} \quad (\text{VI.51})$$

Expression in brackets corresponds to angle  $\varphi$ , at which is visible from point  $(\bar{x}, \bar{z})$  segment of profile  $[a, b]$ . Hence

$$\int_a^b \Delta g(x) dx = 2f \sigma(\bar{x}, \bar{z}) \varphi(\bar{x}, \bar{z}) dS. \quad (\text{VI.52})$$

In the case of body, whose cross section has arbitrary form, we obtain analogously

$$\int_a^b \Delta g(x) dx = 2f \iint_S \sigma \varphi dS = 2f \iint_S \sigma(\bar{x}, \bar{z}) \varphi(\bar{x}, \bar{z}) d\bar{x} d\bar{z}. \quad (\text{VI.53})$$

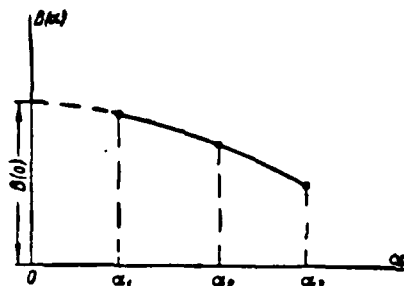


Fig. 209. For determination of mass of body on  $\Delta g$  with utilization of integral transforms.

Page 395.

So-called criterion of A. A. Lyapunov (1955) expresses equality (VI, 53). Let, for example, segment  $[a, b]$  be equal to 10 km. Integral of the anomaly on it is equal to 25 mg/  $\cdot$  km =  $2.5 \times 10^3$  cgs. On the basis of equality (VI, 53)

$$2.5 \cdot 10^3 \text{ cgs} = 2 \cdot \frac{2}{3} \cdot 10^{-7} \sigma_{cp} \varphi_{cp} \cdot S \text{ cgs.}$$

Hence, assigning some parameters, it is possible to find others. When  $\sigma_{cp} = 0.5 \text{ g/cm}^3$ ,  $\varphi_{cp} = \frac{\pi}{2}$  we obtain, that  $S = 2.5 \text{ km}^2$ .

Similar criterion is established/installed by Kh. L. Smolitskiy (1956). In the latter case the anomalous masses of finite length and arbitrary form are examined. It is analogous with the formula (VI, 53)

$$\iint_{\theta} \Delta g(x, y) dx dy = f \iiint_V \sigma(\bar{x}, \bar{y}, \bar{z}) \tau(\bar{x}, \bar{y}, \bar{z}) dV, \quad (\text{VI.54})$$

where  $\theta$  - part of plane  $z=0$ , on which is produced the integration of



anomaly  $\Delta g$ .

$V$  - volume, occupied by body.

$\phi$  - solid angle, at which is visible from each internal point of body the region  $\theta$ .

In the case, if integration is produced only on segment of profile, following relationship/ratio occurs:

$$\int_a^b \Delta g(x, c, o) dx = f \iiint_V \sigma(\bar{x}, \bar{y}, \bar{z}) \psi(\bar{x}, \bar{y}, \bar{z}) dV, \quad (\text{VI.55})$$

where

$$\psi(\bar{x}, \bar{y}, \bar{z}) = \frac{\bar{z}^3}{(\bar{y}-c)^2 + \bar{z}^2} \left[ \frac{\bar{x}-a}{R(a, c)} - \frac{\bar{x}-b}{R(b, c)} \right], \quad (\text{VI.56})$$

$$R(a, c) = \sqrt{(\bar{x}-a)^2 + (\bar{y}-c)^2 + \bar{z}^2}. \quad (\text{VI.57})$$

Together with strict formulas for determining center of gravity of body calculations according to those more approximated, that make it possible to find position of point, close sometimes are led to center of body. These formulas are usually obtained by generalizing the formulas, brought out for special cases of the bodies of spherical and cylindrical form. Putting to use the property of the additivity of the gravitational field (see 546), is found the expression of the anomaly, caused by the set of such bodies, and on the basis of the law of mean - formula for determining the unknown depth. The actually determined depth is close to the depth up to the center of gravity, if the horizontal sizes/dimensions of the body of the same order, that also vertical, or smaller than them. But if horizontal sizes/dimensions considerably exceed vertical, the determined point

can prove to be lower than the center of gravity.

Page 396.

N. L. Afanas'yev (1950) obtained formulas (VI, 60-63) in the manner described above.

In three-dimensional case

$$z_{cp}^2 = \frac{1}{8\pi} \cdot \frac{\left| \int_{-\infty}^{+\infty} \int_{-\infty}^{+\infty} \Delta g \, dx \, dy \right|^2}{\int_{-\infty}^{+\infty} \int_{-\infty}^{+\infty} (\Delta g)^2 \, dx \, dy}, \quad (\text{VI}, 58)$$

$$z_{cp} = \frac{1}{2\pi} \int_{-\infty}^{+\infty} \int_{-\infty}^{+\infty} \frac{\Delta g}{\Delta g_{\max}} \, dx \, dy. \quad (\text{VI}, 59)$$

In two-dimensional case

$$z_{cp} = \frac{1}{2\pi} \cdot \frac{\left| \int_{-\infty}^{+\infty} \Delta g \, dx \right|^2}{\int_{-\infty}^{+\infty} (\Delta g)^2 \, dx}, \quad (\text{VI}, 60)$$

$$z_{cp} = \frac{1}{\pi} \int_{-\infty}^{+\infty} \frac{\Delta g}{\Delta g_{\max}} \, dx. \quad (\text{VI}, 61)$$

In conclusion let us examine some estimated formulas (of type of inequalities) for determining depth of bedding of perturbing masses of more or less arbitrary form, based on joint utilization of values of anomaly  $\Delta g$  and its horizontal gradient at some characteristic points of curve. American geophysicist Fisher's formula, which makes it possible to find the maximum depth of the bedding of the upper part of the fold of the subterranean relief (it has already been discussed in

S40) is most known and in practice widely utilized.

Flexure-shaped folds of subterranean relief different in slope/transconductance can correspond to assigned curve  $\Delta g$  (Fig. 210). The case of vertical step/stage (step) is limiting case in the sense of the maximum value of the corresponding value  $z_1$ , examined in S40 Chapter V. Hence for the arbitrary flexure-shaped fold we obtain

$$z_1 \leq \frac{\Delta g_{\max}}{2/\pi\sigma \left[ e^{\frac{|W_{xz}|_{\max}}{2/\sigma}} - 1 \right]}. \quad (\text{VI.62})$$

Taking into account expansion  $e^x$  into series according to degrees of  $x$  and being limited to three first terms, it is possible to obtain more simplified expression

$$z_1 \leq \frac{\Delta g_{\max}}{\pi \left[ 1 + \frac{(W_{xz})_{\max}}{4/\sigma} \right] (W_{xz})_{\max}}. \quad (\text{VI.63})$$

Page 397.

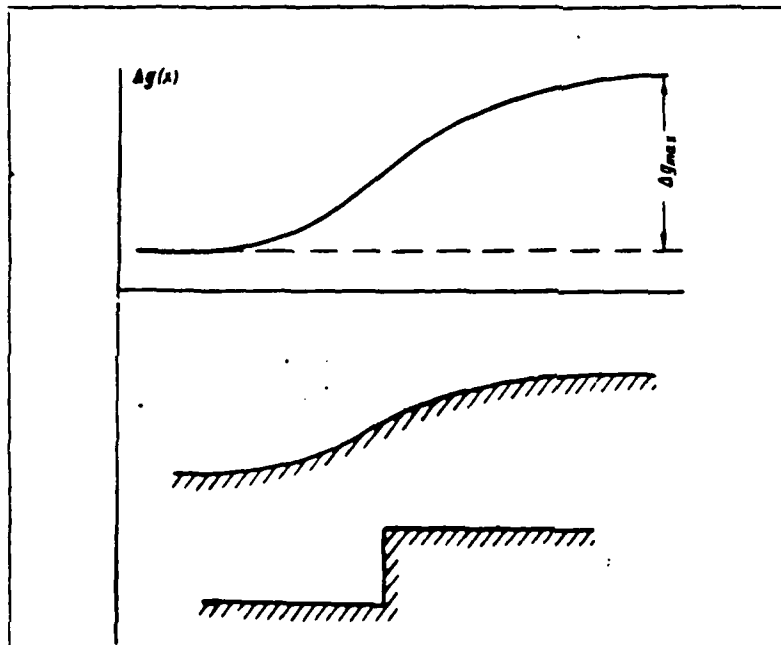
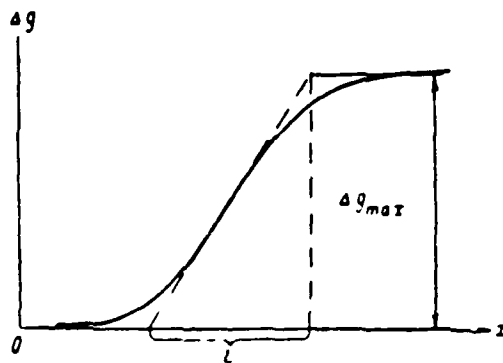


Fig. 210. To Fisher's inequality.

Fig. 211. To determination  $(W_{12})_{\max}$  in Fisher's formula.

Page 398.

Value of maximum gradient (see 540) can be determined graphically (Fig. 211):

$$|W_{12}|_{\max} = \frac{\Delta g_{\max}}{L} \quad (VI.64)$$

Hence

$$z_1 < \frac{L}{\pi \left[ 1 + \frac{(W_{xz})_{max}}{4/\sigma} \right]}. \quad (VI, 65)$$

Even more approximate value of depth  $z_1$  we will obtain from formula (VI, 66) when value of excess density  $\sigma$  is unknown:

$$z_1 \approx \frac{L}{4.5}. \quad (VI, 66)$$

Formulas similar by construction for calculating maximum depth  $h$  of bedding of body, which causes gravity anomaly, are proposed by foreign geophysicists Bottom and Smith (1958). In the case of the three-dimensional body

$$h < \frac{3A(x)}{2 \left| \frac{\partial A}{\partial x} \right|}. \quad (VI, 67)$$

In two-dimensional case

$$h < \frac{A(x)}{\left| \frac{\partial A}{\partial x} \right|}. \quad (VI, 68)$$

where  $A(x)$  - maximum value of anomaly.

$\frac{\partial A}{\partial x}$  - maximum horizontal gradient.

Page 399.

Chapter VII.

GEOLOGIC INTERPRETATION OF THE RESULTS OF REGIONAL GRAVITATIONAL PHOTOGRAPHINGS.

§50. Special features of problem.

By regional gravitational photographings we imply photographings, conducted on large territories on thin networks/grids of observations (through distances, expressed by several kilometers, sometimes by many kilometers), which give characteristic of general/common regional special features of distribution of anomalous gravitational field. Here are involved strip surveys of maritime and almost inaccessible continental territories, area photographings of scales 1:500000 - 1:1000000, partly and larger/coarser.

Before regional gravitational photographings are placed different geologic problems, from which basic are the following:

1) general/common conclusions about investigated region: explanation of degree of its isostatic steadiness, estimation of probable average/mean power coefficient of crust and so forth;

2) tectonic zoning of geosynclinal regions;

3) tectonic zoning of platform regions.

During solution of these problems most important value has qualitative geologic interpretation of gravity anomalies. The quantitative interpretation of separate anomalies is produced rarely, since usually there is no one of its basic prerequisites/premises - sufficient denseness of the network/grid of observations. During the solution of some examination the statistical analysis of gravitational field is used.

Page 400.

Besides general geologic information about region being investigated and data about other geophysical works (if latter were conducted) for more complete and more correct interpretation of gravitational data very vital importance can have reference geological-geophysical profiles, which intersect characteristic large structures, according to which there is not only contemporary geologic section/cut, but can be comprised also more or less reliable paleotectonic (paleogeographic) sections/cuts. Of interest are also the data about the contemporary tectonic motions in the region being investigated, about its seismicity, etc.

Wide application of geophysical methods, and in particular gravitational prospecting, in regional geology was begun considerably later than during searches for local structures and ore deposits, it composes period only 10-15 years. By this is explained that to the question indicated is devoted comparatively few published works and

some positions relative to the geologic interpretation of geophysical, in particular gravitational data, still they require check and refinement. For us it is necessary subsequently to touch on some debatable positions of this type.

§51. General estimations of the regions (isostatic steadiness, thickness of the Earth's crust) being investigated.

Conclusion about isostatic steadiness of one or the other region can be done by calculating for it isostatic anomalies (see §11). If these anomalies as a whole are small, and their average/mean value is close to zero, then this gives grounds to draw a conclusion about the presence in the region of isostatic compensation being investigated. Otherwise it is possible to tell about the isostatic lack of balance of region - to its overload (positive isostatic anomalies) or underloading (negative isostatic anomalies).

Such conclusions can be drawn on isostatic anomalies, calculated according to different systems (Pratt-Hayford, Erie-Heiskanen, Vening-Meinesz), since it proves to be that, in spite of entire difference in isostatic hypotheses, utilization of each of them gives values of isostatic anomalies, close in value both for isolated points, and in particular for points average/mean on group. Essential is another moment - sizes/dimensions of region. The regional character of isostatic compensation now is already universally recognized; therefore conclusions about its presence or absence sense



has to make for the territories of significant area sizes/dimensions (thousand of kilometers in all directions) and besides having any single morphological special features - affiliation with one and the same continental block or maritime tank, comparative uniformity of relief, etc.

Page 401.

As example let us examine gravitational profile through Pacific Ocean, given in Fig. 2.12. As we see, entire/all abyssal basin of Pacific Ocean is characterized by the high positive (200-400 mgal) gravity anomalies, which almost completely disappear during the introduction of isostatic correction; hence it is possible to arrive at the conclusion that the Pacific Ocean basin/depression in the first approximation, can be considered as isostatically balanced. The same conclusion proves to be possible to make, also, for many other territories of both ocean and continental; exception is only geosynclinal regions and the so-called activated/promoted sections within the limits of platforms: intensive isostatic anomalies are specific to them, moreover in their limits the sections of negative anomalies frequently are alternated with the sections of the positive anomalies (this is characteristic for the geosynclinal regions).

Calculation of isostatic anomalies - complex business and not always virtually realized. Therefore frequently conclusions about the isostatic steadiness of one or the other region are made in the average/mean intensity of the anomaly of Faye, considering that it

corresponds to the average/mean intensity of isostatic anomalies. This conclusion, as we saw in §11 of Chapter II, is possible to consider valid only for the regions with specific medium altitude (about 1.3 km) or depth of two seas (about 2.0 km); in all remaining cases it is necessary to consider the presence of systematic, sometimes very significant differences in the average/mean values of the anomalies of Faye and isostatic.

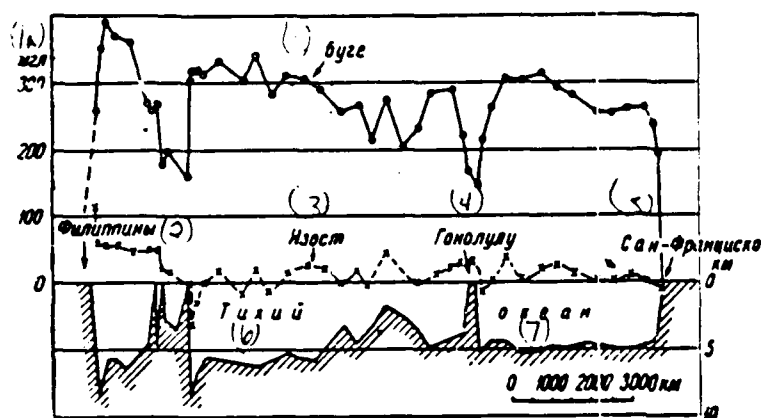


Fig. 212. Curve of Bouguer's anomaly along profile through Pacific Ocean. According to F. Vening-Meinesz (1940).

Key: (1). Bouguer. (1a). mgal. (2). Philippines. (3). Isost. (4). Honolulu. (5). San Francisco. (6). Pacific. (7). ocean.

Page 402.

We consider it necessary to give here example, which shows very clearly possibility of erroneous conclusions during estimation of isostatic equilibrium of region being investigated on gravitation anomalies. Fig. 213 gives anomaly curve of gravitational force in the reductions of Faye and Bouguer along the profile in East Antarctica region. On the basis of the fact that the values of the anomaly of Faye in the profile are close to zero, a number of the authors (see for example, Sorokhtin, Kondratyev, Avsyuk, 1960) made a conclusion about the isostatic steadiness of the continent of East Antarctica. Meanwhile, if we take into account that the profile indicated passes over the surface of the ice dome of Antarctica at an altitude of

several kilometers (to 3-4 km) above sea level and take into account conclusions about the relationship/ratio of the anomalies of Faye and isostatic, made by us above in §11 of Chapter II (see, in particular, Fig. 17), then is obtained conclusion, completely reverse led: about the probable presence here of intensive negative isostatic anomalies, i.e., about the large isostatic deficiency of masses in the region of the continent of East Antarctica. In more detail about this see the works of B. A. Andreyev (1961).

It is necessary to also have following in mind: isostasy plays known role as peculiar "regulator" of tectonic processes, but its role in total balance of tectonic forces, apparently, never is main thing, which determines summary result of effect of these forces. Absence of isostatic compensation testifies about the tectonic activity of one or the other region - this fact is indisputable, but over this we usually have no concrete ways and means to the more specific interpretation of the geologic sense of isostatic gravity anomalies.

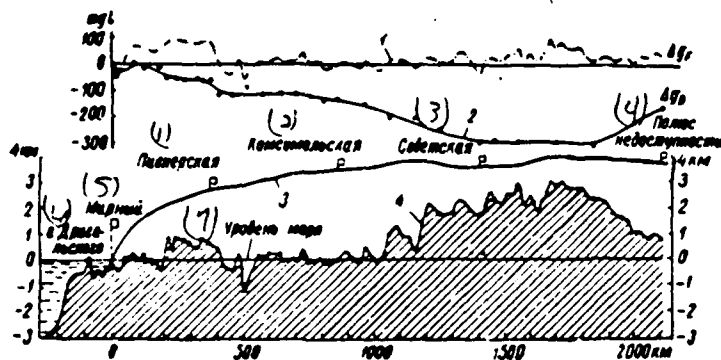


Fig. 213. Gravitational profile in East Antarctica region. From the work of O. G. Sorokhtin, O. K. Kondratyev, Yu. I. Avsyuk (1960). 1 - curve of anomaly  $\Delta g$  in the reduction of Faye; 2 - the same in the reduction of Bouguer; 3 - surface of glacier; 4 - under-ice relief of the bedrocks (according to seismic data).

Key: (1). Pioneer. (2). Komsomol. (3). Soviet. (4). Pole of inaccessibility. (5). Peaceful. (6). Drigol'skiy. (7). Sea level.

Page 403.

In particular, usually are entirely unfounded attempts at the connection of the sign of the oscillatory motions of one or the other regions with the sign of isostatic anomalies (Andreyev, 1960). It is not excluded, however, that the ways of the more specific interpretation of isostatic anomalies will be planned as a result of accumulation and analysis of the new facts, which relate to the problem indicated.

Let us turn now to another question, which recently is placed and is solved during analysis of results of regional gravitational photographs - about determination of probable power/thickness of crust. Premise to solution of this question gives comparison of gravitational data with seismological. For the first time in 1943 by the work of B. Gutenberg in the region of mountains Sierra Nevada (USA) was confirmed via the analysis of seismological data the real presence of the "root of mountains" - a deep downwarp/trough of the surface of the subcrustal layer, the so-called boundary of Mohorovicic, which previously was assumed in connection with the detection here of the large/coarse (to - 300 mgal in the reduction of Bouguer) minimum of gravitational force. This gave basis for G. Woollard (1943) to assume the direct connection of regional gravity anomalies with the thickness of the Earth's crust and the depth of up to Mohorovicic's boundary, and, based on this, to make an attempt at the joint interpretation of gravitational and seismic data along the regional profile through North America.

Joint interpretation of gravitational and seismic data with construction of sections/cuts of earth's crust produced Yu. N. Godin (1957, 1959) for Zakaspiy, B. K. Balavadze for Caucasus (1957) and other authors. In this case the relief of the deep boundaries of the earth's crust was determined on the basis of predicted density distribution in the layers of the earth's crust and the subcrustal layer (see S3, Chapter I), with the utilization of templates or the simple linear dependence between a change in the gravity anomaly and

change in the depths of form  $\Delta g(x_1) - \Delta g(x_2) = 2f\sigma\pi(z_1 - z_2)$  (see Chapter VI).

B. A. Andreyev (1958) proposed to use correlation graph/diagram of dependence between averaged value of Bouguer's anomaly according to data of gravimetry and depth of up to Mohorovicic's boundary, determined according to seismological data, for this joint interpretation and did first attempt at composition of this type of graph for continental regions. Subsequently such kind graphs/curves were composed by R. M. Demenitskaya (1958, 1961) for the earth's surface, Ye. D. Karyakin (1959) for Atlantic Ocean, G. Woollard<sup>1</sup> (1959) for the territory of the USA and some oceanic regions.

FOOTNOTE<sup>1</sup>. Graph, published by Woollard in 1959, - of nonlinear type. In the recently published articles of Steinhard and Woollard (1961) and Sazhina (1952) are indicated the presence of linear correlation between anomaly  $\Delta g$  and thickness of the Earth's crust for the continents. ENDFOOTNOTE.

Page 404.

The report of these graphs is given in Fig. 214 and 215 - separately for the continental and for the oceanic regions. As we see, the regularities, brought out by each of the researchers indicated, do not completely coincide, which seems completely natural, if we take into account the limitedness of the number of sections, for which the most

reliable possible comparison of gravitational and seismic data in the sense of appropriate quality and authenticity of those and others, and also some other facts.

Worthiest on completeness of scope/coverage of material is unconditionally investigation, carried out by R. M. Demenitskaya (about 280 sections of comparison of gravitational and seismic data), but it is possible to dispute it from other positions: from point of view of quality of some materials (in number of cases were used determinations of thickness of crust by teleseismic method, results of prewar determinations, etc.).



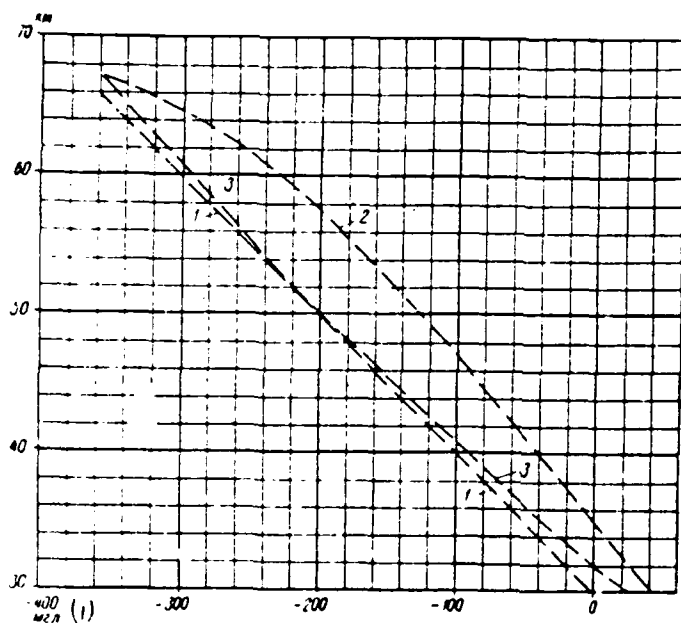


Fig. 214. Graph/diagram of dependence of intensity of anomalies of force of gravity (Bouguer) on thickness of the Earth's crust for continental regions. 1 - according to B. A. Andreyev (1958); 2 - according to R. M. Demenitskaya (1958); 3 - according to G. Woollard (1959).

Key: (1). mg/.

Page 405.

Doubtful methodic moment in the investigations of both R. M. Demenitskaya and G. Woollard, from our point of view, is their attempt to deduce the single regular connection of the intensity of gravity anomalies and power/thickness of earth crust for the continents, the oceans and the littoral zones, although all these regions are distinguished between themselves not only by power/thickness, but also

by composition of the earth's crust. During this association/unification of diverse regions the connection of the intensity of anomalies with the thickness of crust proves to be complex, nonlinear form, and it is determined according to the correlation diagram less reliably than in the case of the simple character of the connection of linear type '.

FOOTNOTE '. This shows, in particular, the comparison of the graphs of R. M. Demenitskaya and G. Woollard. ENDFOOTNOTE.

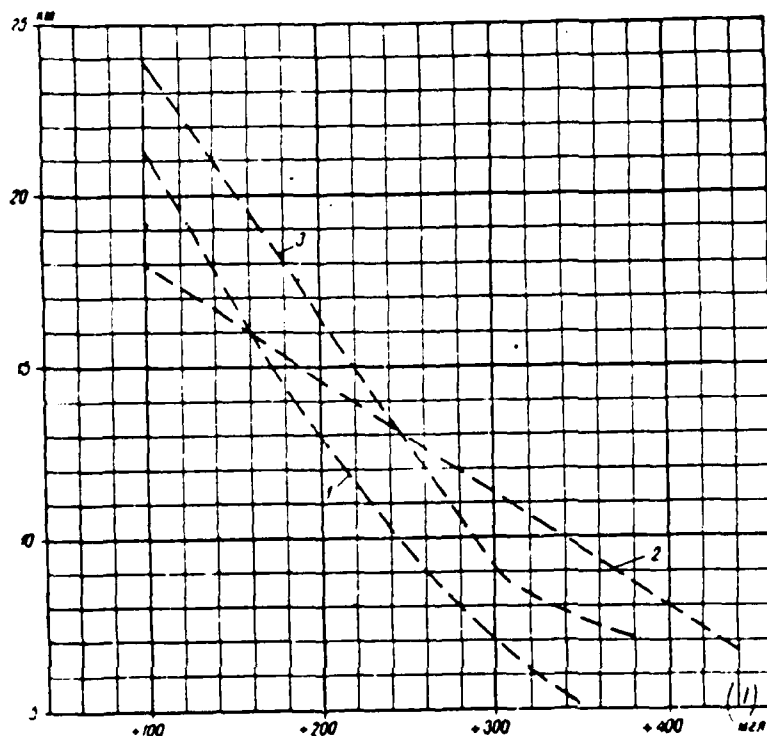


Fig. 215. Graph/diagrams of dependence of intensity of anomalies of force of gravity (Bouguer) on thickness of the Earth's crust for oceanic regions. 1 - according to R. M. Demenitskaya (1958); 2 - according to Ye. D. Karyakin (1959); 3 - according to G. Woollard (1959).

Key: (1). mg/.

Page 406.

Investigation of B. A. Andreyev concerns only continental regions, but it is based on very small number of sections of comparison of gravitational and seismic data. Finally, common deficiency in all investigations indicated is that during their

conducting was not introduced corrections for the structure of the upper layers of the earth's crust for the gravitational field, and the averaging of gravity anomalies was conducted not always and during its conducting there was an element of arbitrariness in the sense of the selection of the sizes/dimensions of the section of averaging, account or nonaccount of given detailed photographings, etc. Thus, all carried out determinations of the dependence of the intensity of regional gravity anomalies on the thickness of the Earth's crust are still inadequate and require further refinements. At the same time the very presence of the regular connection of the intensity of regional gravity anomalies with the thickness of the Earth's crust does not cause doubts, just as its basic character, which can be determined as follows:

1. Continents. Connection, at least for the usual range of change in the thickness of crust (30-60 km), is close to the linear, moreover a change of the value of gravitational field on the average on the order of 10-12 mgal corresponds to a change in the thickness of crust on 1 km. The thickness of crust on the order of 30-35 km corresponds to zero anomalous gravitational field.

2. Oceans. For the usual range of a change in the intensity of the gravity anomalies, characteristic for the oceans (from +200 to +350 mgal), the connection in question is also close to the linear, moreover the effect of changes in the thickness of crust to the gravitational field here is incomparably stronger than on the

continents: 1 km change in the thickness of crust corresponds to a change of the intensity of gravitational field in the average/mean order 30 mgal, i.e., 2.5-3.0 times more than on the continents.

Given regularities it proves to be possible substantiate theoretically, if we make assumption that surface of basalt layer and its basis/base, i.e., Mohorovicic's boundary, will lie in majority of regions accordingly, having uplifts and depressions in some places and approximately one and the same amplitude; this assumption in majority of regions satisfactorily will agree with seismic data. During calculations of the gravitation effect of deep layers we will use B. A. Andreyev's formula for case of  $n$  accordingly sloping interfaces (see formula VI, 21)

$$\Delta g(x_2) - \Delta g(x_1) \approx 2f\pi \sum_{k=1}^n e^{\frac{-2\pi h_k}{l}} \sigma_k (z_1 - z_2) = 2f\pi S(z_1 - z_2),$$

where  $\sigma_1, \dots, \sigma_k, \dots, \sigma_n$  - excess densities on the boundaries;

$h_1, \dots, h_k, \dots, h_n$  - the average depths of the bedding of these boundaries.

Page 407.

$l$  - period of harmonic curve, which represents (in the first approximation) curve of section of structural relief in vertical plane, passing through axis  $x$  (line of observations);

$z_1$  and  $z_2$  - values of depths to one of interfaces at points  $x_1$  and  $x_2$ .

If we examine case of two interfaces with values of  $\sigma_1 = +0.2$  g/cm<sup>3</sup>,  $h_1 = 15$  km (surface of basalt layer) and  $\sigma_2 = +0.4$  g/cm<sup>3</sup>,  $h_2 = 45$  km (Moho surface) and to take into account that cross sizes/dimensions of deep structures of earth's crust are 100-200 km (typical cross size/dimension of regional gravity anomalies, and also mountain ranges), then it is possible in given formulas to assume  $l = 200$  and 400 km, which gives

$$S = 0.12 + 0.10 = 0.22 \text{ g/cm}^3 \text{ for } l = 200 \text{ km,}$$

$$S = 0.16 + 0.20 = 0.36 \text{ g/cm}^3 \text{ for } l = 400 \text{ km.}$$

First term in written sums presents gravitational influence of surface of basalt layer, and the second - boundaries of Mohorovicic. As we see, the fraction/portion of effect of first boundary with the relatively low value  $\sigma$ , which slopes sufficiently close to surface, with  $l = 200-400$  km is almost identical to the effect of the second deep boundary with the high value  $\sigma$ .

It is interesting that with  $l = 100$  km, i.e., roughly speaking, for anomalies with diameter on the order of 50 km, is obtained  $S = 0.8 + 0.2 = 0.10$  g/cm<sup>3</sup>, i.e., sharply prevails effect of basalt layer. Hence, among others, it follows that during the study of the deep structure of the earth's crust it follows to compulsorily put to use the averaged values of the gravitation anomalies, and the system of averaging must be such that the effect of the anomalies of relatively

small cross sizes/dimensions (first tens of kilometers) would be eliminated or would be reduced to the minimum.

Let us return to case in question. Let us take average/mean value of  $S$  for  $l$ , equal to 200 and 400 km; it is equal to  $0.29 \text{ g/cm}^3$ . Substituting this value into the basic formula and assuming/setting in it  $z_1 - z_2 = 1 \text{ km}$ , we obtain

$$\Delta g(x_2) - \Delta g(x_1) = 12 \text{ mg/},$$

which, as we see, closely corresponds to reality.

Let us turn now to case of oceans. According to seismic data here the typical section/cut of the earth's crust schematically it is possible to present in the following form: the layer of sea water ( $\sigma = 1.03 \text{ g/cm}^3$ ) with power/thickness of 4-5 km, the layer of the unconsolidated and consolidated precipitation and volcanogenic rocks ( $\sigma = 2.2-2.6 \text{ g/cm}^3$ ) usually of the very small power/thickness (less than 1 km), the basalt layer ( $\sigma = 2.9 \text{ g/cm}^3$ ) with a thickness of 5-10 km, subcrustal layer ( $\sigma = 3.3 \text{ g/cm}^3$ ).

Page 408.

If we take into account that during the introduction of the correction of Bouguer for the oceanic stations the layer of maritime baude is substituted by medium with a density of  $2.7 \text{ g/cm}^3$  and disregard/neglect the relatively weak effect/action of the layer of the unconsolidated precipitation, then it is possible the density

section/cut of the oceanic earth's crust to schematically represent then just as for the continents, in the form of two density interfaces - on the surface of basalt layer ( $\sigma=+0.2$  g/cm<sup>3</sup>), also, on Mohorovicic's boundary ( $\sigma=+0.4$  g/cm<sup>3</sup>). However, the values of the average depths of these interfaces we must take different, than for the continent, precisely,  $h_1=5$  km and  $h_2=12$  km. The values  $l$ , which characterize the cross sizes/dimensions of deep structure, let us take the same as for the continent, i.e.,  $l=200$  and  $400$  km. Making calculation, analogous to given above for the continents, we obtain

$$S=0.17+0.27=0.44 \text{ g/cm}^3 \text{ for } l=200 \text{ km,}$$

$$S=0.18+0.33=0.51 \text{ g/cm}^3 \text{ for } l=400 \text{ km.}$$

Average/mean value  $S$  is  $0.47$  g/cm<sup>3</sup>, i.e. it proves to be almost two times more than continent. A change in anomalies  $\Delta g$  about  $20$  mg/g on  $1$  km of a change in the thickness of the Earth's crust corresponds to this value. Thus, and for the oceans, true less accurately than for the continent, calculation confirms the actually observed connection of the intensity of regional gravity anomalies with the thickness of the Earth's crust. It is necessary in this case to have in mind that above we sufficiently arbitrarily took for the oceans the same value  $l$  as for the continents. It is possible that for the oceanic regions as a whole are typical the deep structures of crust with larger, than for continents, cross sizes/dimensions. In that case it is necessary during calculation value  $l$  to take more than for the continents, and this gives the high value of change  $\Delta g$  and better



approximation/approach to the actually observed relationships/ratios.

Given above data and considerations testify that regional gravity anomalies can be considered caused either completely or to a considerable extent by deep structure of earth's crust. Some geologists and geophysicists, however, consider that important role in the formation of regional gravity anomalies must play super-deep subcrustal processes and connected with them changes of the density in the shell of the Earth (Subbotin 1955; Fotiadi, 1955; Borisov, 1959). The final explanation of this question requires further investigations; however, given above data and considerations speak that deep subcrustal changes in the density, apparently, only very weakly are developed in the gravitational field.

Page 409.

The basic factor, which determines intensity and character of regional gravity anomalies, is the structure of the earth's crust undoubtedly.

Were made attempts at establishment of connection of thickness of the Earth's crust not only with intensity of regional anomalies of gravitational force, but also with relief of surface of lithosphere (Demenitskaya, 1958; Woollard, 1959). The authors consider these attempts, based on the presentation/concept about the general/universal almost ideal isostatic compensation for the earth's crust, considerably less substantiated than the described above investigations, since many regions with different hypsometric special

features (high mountains, abyssal basins) in actuality are usually distant from compensation state. As we saw above, the connection of gravity anomalies with the power/thickness of crust can be established/installed and theoretically substantiated without the utilization of hypothesis of isostasy.

In mathematical language position of matter it is possible to express so: existence of isostatic equilibrium of earth's crust is sufficient, but by no means necessary condition for existence of regular connection of intensity of gravity anomalies and thickness of crust.

American researchers Werzel and Sherbet (1957) for studying earth's crust recommended utilization of standard sections/cuts ("columns") of earth's crust, constructed via comparison of data, which correspond to zero value of gravity anomaly - for continent in reduction of Bouguer and for ocean in reduction of Faye. This approach did not obtain further development.

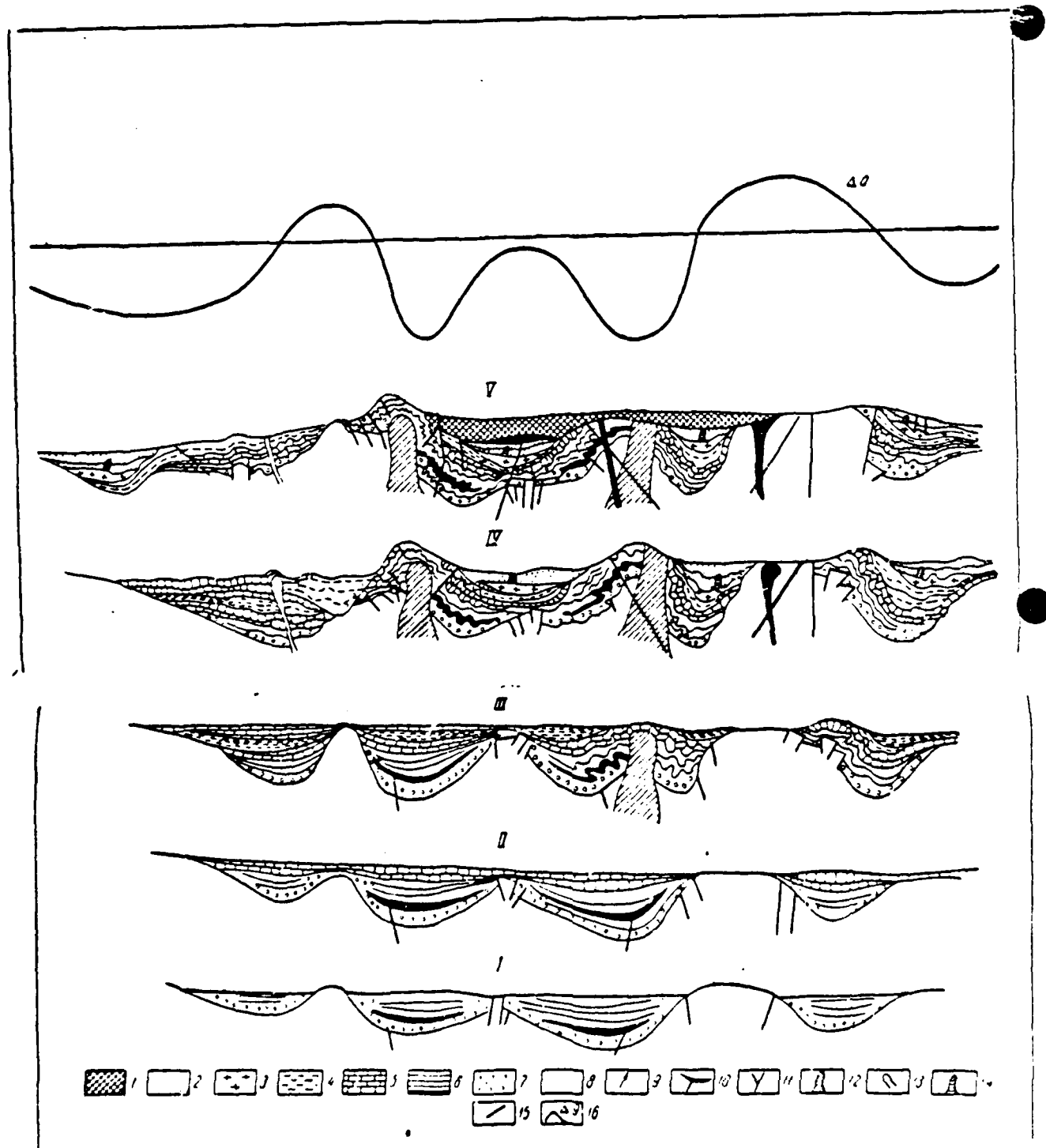
For studying relief of Moho surface was used also method of interpretation, described in §48 of Chapter VI (Tsuboi, 1956).

§52. Tectonic zoning of geosynclinal regions.

Tectonic zoning - most important component part of geologic mapping/charting, which is "classification of sections of earth's crust according to signs of their structure and history of structural

development" (Belousov, 1953, pg. 521). These sections of the earth's crust, which are distinguished by their structure and history of development, are named regional structures; for them are characteristic large horizontal sizes/dimensions (many tens, hundreds, sometimes thousands of kilometers) and the large depth of laying, manifestation not only in the upper layers, but also deep horizons/levels of the earth's crust. In the rocks of sedimentary cover regional structures are developed not only in the relief of the stratigraphic horizons/levels, but also in facial-lithologic special features of these rocks.

Page 410-411.



F 3 216

Fig. 216. Diagram of development of geosynclinal region (according to V. V. Belousov) and the typical distribution of the anomalies of gravitational force above the regional structures. The stages of the development of geosynclinal region; I, II, III - before the inversion, IV, V - after inversion; 1 - formation of internal basins/depressions; 2 - molasse formation; 3 - lagoon formation; 4 - flyschoid caustobiolith formation; 5 - limestone formation; 6 - lower terrigenous formation; 7 - coarsely fragmental depositions; 8 - formation of the preceding cycles; 9 - volcanos; 10 - effusions and sheet intrusions; 11 - interstitial intrusions; 12 - batholites; 13 - small intrusions; 14 - diapirs; 15 - tectonic faults; 16 - anomaly curve of gravitational force.

Page 412.

With the breakdown dislocations in the limits of one or the other regional structures the numerous bodies of the magmatic rock are connected. To the concluding results of zoning is tectonic map/chart with the indication on it not only of near-surface, but also deep elements of regional structures.

Geosynclinal regions are characterized by high mobility, intensive manifestation in their limits of Alpine folding of young (Mesozoic, cenozoic) magmatic rock, development of intensively rugged relief, high seismicity. The regional structures of geosynclinal regions, usually expressed (directly or indirectly) in their relief, present edge/boundary and intermountain downwarps/troughs, mega-anticlinorium, and in the limits of the latter - separate large/coarse anticlinorium and synclinorium, zones of faults and separate large/coarse faults, magmatic complexes, etc.

In gravitational field geosynclinal regions are developed by intensive (the first hundreds milligal) regional gravity anomalies both negative, characteristic for large uplifts/rises and positive, characteristic for basins/depressions, represented frequently by contemporary maritime tanks.

With tectonic zoning of geosynclinal regions geophysical methods, including gravitational prospecting, participate in solution of following problems: 1) explanation of history of geologic development and general/common structural plan/layout of territory being investigated; 2) establishment of location and interrelation of regional structures; 3) study of character of separate large/coarse structures.

Gravitational prospecting has important value during solution of

these problems. It proves to be that the regional gravity anomalies of geosynclinal regions have the specific historico-geologic value. In general form this fact was established already long ago in the work of V. V. Veber and V. V. Fedynskiy (1947), but in more detail explained in the work of the author (Andreyev, 1960).

In order to explain this question, let us pause very briefly at basic laws governing history of geologic development of geosynclinal regions. Each geosynclinal region in its development usually passes two stages: the first, during which predominate the depressions, and the second, during which predominate the uplifts/rises; transition from the first stage to second V. V. Belousov names total reversal or total inversion of geotectonic conditions. During the inversion the redistribution of the zones of uplift/rise and depression occurs: among the pre-inversion downwarps/troughs the central uplifts/rises, which are gradually expanded and which seize entire territory of downwarps/troughs, are formed, and pre-inversion uplifts/rises partially or completely are converted into the downwarps/troughs (Fig. 2.16).

Page 413.

At the second stage of the development of geosynclinal region folding motions are very intensively developed. In the zones of the conjugation of the differing structures of geosynclinal region and in other places tectonic gaps repeatedly are formed; on these gaps the magmatic rocks migrate to the surface.

Comparison of gravitational data on geosynclinal regions with paleogeographic maps/charts and sections/cuts shows following: regional gravity anomalies usually correspond on location to most intensively shown regional structures of pre-inversion stage of development of geosynclinal region. This conformity is straight line, i.e., gravitational minima correspond on the location to pre-inversion downwarps/troughs, and maximums - to pre-inversion uplifts/rises, more accurately to those sections, where these structures were located in the period of their greatest development.

We know, at the same time, that type indicated regional anomalies are directly connected with now existing deep structures of earth's crust: minima - with downwarps/troughs, maximums - with uplifts/rises of Mohorovicic's boundary. Hence it emerges as result that also the deep structures of the earth's crust of geosynclinal regions, isolated on the basis of the regional gravity anomalies, in their origin are connected, apparently, with the pre-inversion cycle of development of these regions. It is possible to assume that the structures of pre-inversion cycle were most intensively expressed in deep layers of the earth's crust and were not converted as a result of the inversion, which changed the sign of the majority of structures in the upper levels. Consequently, the "roots of the mountains" and the uplift/rise of deep layers under the contemporary basins/depressions can be, in all likelihood, considered as the relicts of pre-inversion structural relief.



As classical example to connection of gravity anomalies with pre-inversion structures can serve large Caucasus region, above which is placed regional minimum of force of gravity (Fig. 2.17). The detailed study of facies and power/thicknesses of the rocks of meso-Cenozoic era of this region, carried out by V. V. Belousov (1938- 1940), V. Ye. Khain, and then by number of other researchers (Kirillova, Lyustikh, Rastvorova, Sorokin, Khain, 1960), showed that the contemporary structure of mega-anticlinorium of the large Caucasus is converted, that arose during the upper Neogene and the quaternary period on the spot of at no time existed here deep (many kilometers) geosynclinal basin/depression, which was caving in most intensively in the Lower Jurassic time (see Fig. 217).

Page 414.

Such is the situation also in East Carpathians, where gravitational minimum and pre-inversion downwarp/trough are placed on northeastern slope of contemporary Carpathian mountain range.

Arrangement of deep structures of earth's crust, adjusted on gravity anomalies, determines general/common structural plan/layout of geosynclinal regions. If the character of isoanomaly of gravitational force, and, consequently, deep structures has the exposed linear-strip-like character, then the same course/strike have the separate structures, which are placed usually in an echelon-like structure along the strip of gravity anomalies (Fig. 218). It is a different matter on the "periclinal" of gravitational anomalous zones or in those places, where these zones in the plan/layout have approximately isometric form: in such cases of the axis of structures they have the secant almost a normal position with respect to the isoanomalies of the force of gravity (see gravitational to Minin, in the middle part of Fig. 218).

During more detailed gravitational photographing in geosynclinal regions are frequently noted by local anomalies of the separate structure of these anticlinorium, synclinorium, large zones of fault, etc. In a number of cases foothill downwarps/troughs on the boundary of geosynclinal regions with the adjoining platform (Fig. 219) are separated/liberated well by the gravitational minima of the moderate intensity (-40, -60 mgal). In such cases when anticlinorium of

folding region proves to be that moved to the region of foothill downwarp/trough, above them general/common minimum with the axis, which is placed in the edge/boundary part of the moved anticlinorium, usually is observed.

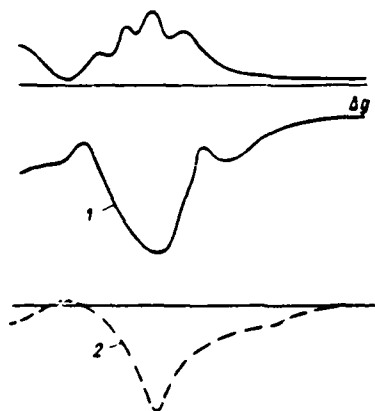


Fig. 217. Conformity of location of regional gravitational minimum (1) and Lower Jurassic pre-inversion downwarp/trough (2) for regions of large Caucasian ridge/spine.

Page 415.

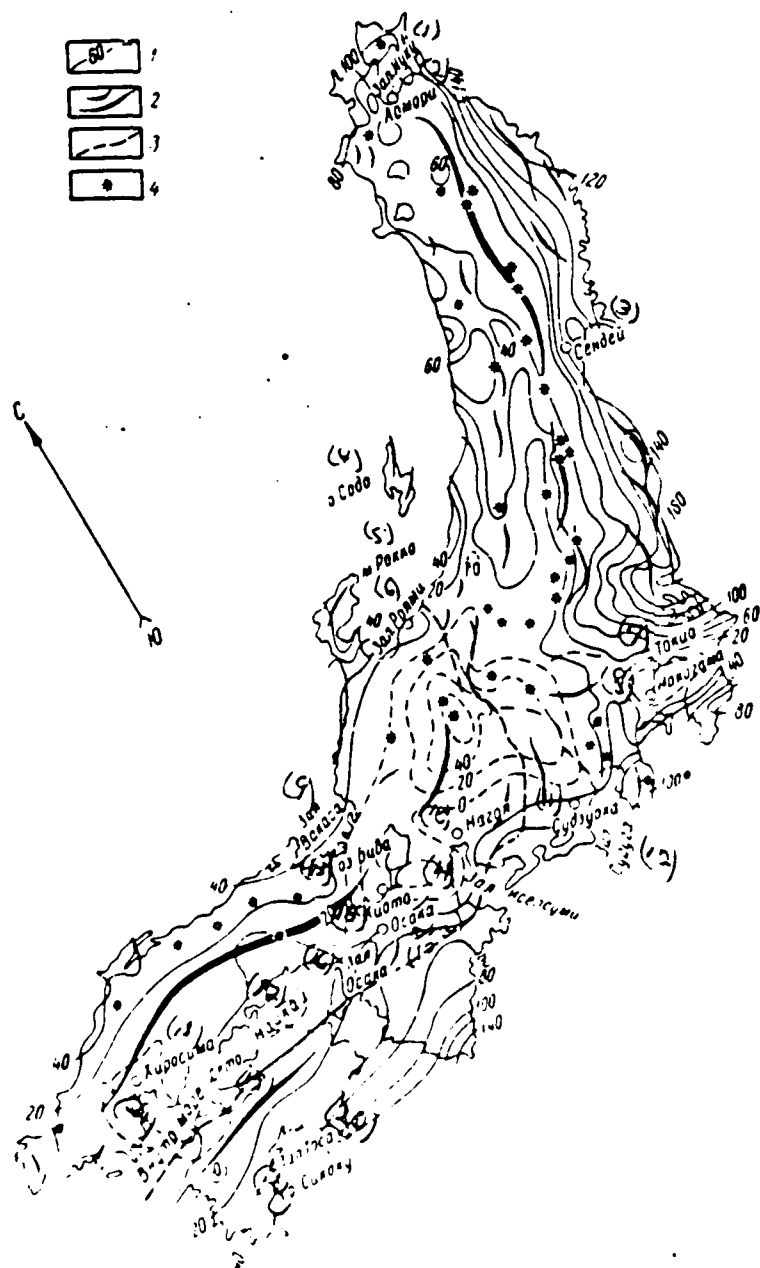


Fig. 218. Schematic gravitational map of Japan (according to Tsuboi, et al, 1956), combined with tectonic map/chart (on Shatskiy, et al, 1956). 1 - isoanomalies; 2 - anticlinorium and anticlines; 3 -

tectonic breaks; 4 - volcanos.

Key: (1). Iuku Bay [Mutsu Bay]. (2). Aomori. (3). Sendai. (4). Sado Island. (5). Cape Rokko. (6). Toyama Bay. (7). Tokyo. (8). Yokohama. (9). Wakasa Bay. (10). Nagoya. (11). Shizuoka. (12). Suruga Bay. (13). Lake Biwa. (14). Ise-shima. (15). Kyoto (15a). Osaka. (16). Osaka Bay. (17). Setonaikai. (18). Hiroshima. (19). [same as (17)]. (20). Tosa Bay. (21). Inland sea. (22). Shikoku.

Page 416.

The author (Andreyev, 1958) discovered that plutonic structures of mezo-Cenozoic age, isolated in geosynclinal regions on gravitational anomalies, can have sufficiently defined value for metallogenic zoning: to zones of gravitational maximums (i.e. to uplifts/rises of deep layer earth's crust) gravitates in essence mesocratic type mineralization, connected with ultrabasic and basic magma (chromium, nickel, copper, gold and silver, pyritic lead - zinc, mercury), and to minima (i.e. to downwarps/troughs of deep layers) - leucocratic type mineralization, connected predominantly with acid magma (lead - zinc vein, molybdenum, tungsten, tin).

FOOTNOTE<sup>1</sup>. We put to use here terminology and classification of V. K. Tschaikovskiy (1956). ENDFOOTNOTE.

Soon then with a number of the authors (Kazanli, Popov, Antonenko, 1959; Moisenko, 1959; Khalevin, 1960; Shcherb, 1960) it was explained

that the analogous regularities occur in Kazakhstan and in Urals, i.e., they are not limited to the youngest folding regions, but they are developed also in the ore provinces, connected with the Hercynian, but possibly, and more ancient structures.

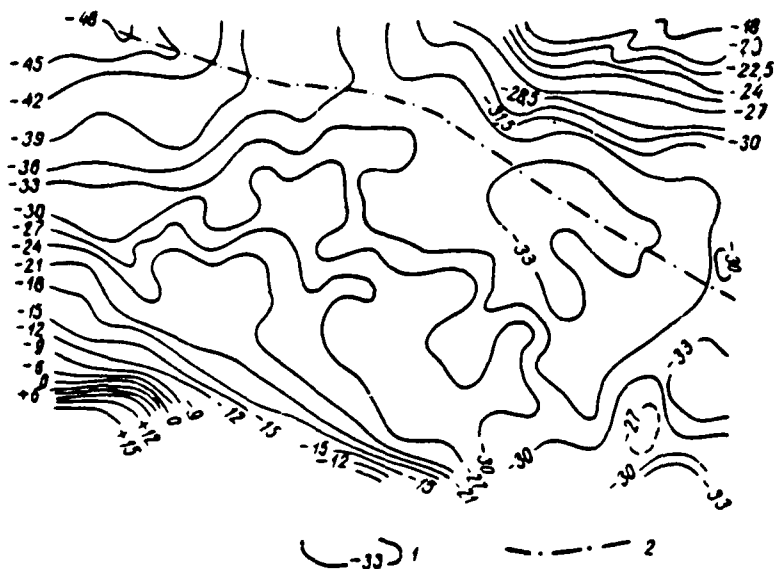


Fig. 219. Gravitational minimum above foothill downwarp/trough. 1 - isoanomalies of gravitational force; 2 - axis of downwarp/trough.

Page 417.

The similar to those indicated associations of structural-metallogenic zones of folding regions with regional gravitational anomalies noted V. S. Mironov for Rudnyy Altai and Kalby: "... the polymetallic belt of Rudnyy Altai, limited by the Irtysh and Northeastern zones of warping, is confined to the zone of the positive anomalies of the gravitational force. The Kalby rare-metal belt is confined to the narrow negative anomaly, which extends along the left bank of the Irtysh and Irtysh zone of warping... the gold-ore belt/zone, which is placed west of rare-metal and in parallel to it, it is characterized by an increase in the gravitational field" (Mironov, 1959). In this case to the zones of the warping of the ore Altai, as it proved to be,



correspond to an anomaly of the type of "gravitational step/stage", i.e., the zones of transition from the positive anomalies to the negative<sup>1</sup>.

FOOTNOTE<sup>1</sup>. Most recently appeared the indications (Fotiadi, 1961) to the analogous bonds of metallogenic and gravitational zonality for the northeast of the USSR. ENDFOOTNOTE.

The facts given here signify/mark the new important direction in the metallogenic investigations, in which, true, until only very first steps/pitches are done.

As we see, in this paragraph for us it was necessary very to rapidly and briefly touch many important and interesting questions. This style of presentation, naturally, is predetermined by program and ultimate purpose of this book, it is preserved also in this entire chapter. The more detailed presentation of some of these questions is contained in another work of B. A. Andreyev (1960).

#### § 53. Tectonic zoning of platform regions.

By platform regions here and subsequently are implied regions, in which are absent intensive manifestations of Alpine folding. Depending on the age of metamorphic basement we will distinguish Hercynian, Caledonian and Precambrian platforms.

Weak manifestation of the contemporary and relatively recent tectonic movements of platforms affects not only on their external appearance (gently sloping relief, gently sloping forms of bedding of upper layers of depositions), but, most of all, on their deep structure. For the typical consolidated platform regions the characteristically almost horizontal bedding of the deep layers of the earth's crust, what indicates weak manifestation of regional gravity anomalies and seismic data. Regional platform structures are manifested also in the bedding of the deep layers of bark, but in contrast to geosynclinal regions this conformity is usually not a reverse but a straight line, i.e., upper layers repeat the structure of deep layers. The leading process of the structural development on the platforms is not inversion, but an inheritance of the ancient structural forms. This is manifested, in particular, in the fact that the internal structure and the relief of the surface of basement has very close connection with the structure of the thickness of sedimentary rocks covering basement.

Page 418.

With tectonic zoning are investigated following large/coarse structural elements of platform regions: 1) inside the basement - boundary of unequal-age shields and blocks, within latter - folding zones, regional zones of faults, magmatic complexes; 2) on stratigraphic boundaries within thickness of sedimentary rocks, and also on surface of basement - uplift/rise and first-order downwarps/troughs (anticlinal and synclinal, according to N. S.

Shatskiy), linear uplifts/rises and the downwarps/troughs of the second order (rises/ramparts and trenches, according to A. D. Arkhangel'), large zone of faults. As let us see below, gravitational prospecting actively participates and gives valuable results during the solution of the problems indicated.

Metamorphic and magmatic rock, which form part of basement of platform regions, as we saw in § 10 of Chapter II, are sufficiently considerably distinguished by its density. The separate structural elements and the blocks of basement, which are distinguished in composition and density of species/rocks, have the large sizes/dimensions, which are expressed by ten (sometimes hundred) kilometers on the horizontal and several kilometers on the vertical line. These structural elements of basement are developed by sufficiently intensive (milligals, ten milligal) gravitational anomalies. If such anomalies are observed on the crystalline shields, then their geologic nature usually is sufficiently easily explained in by the utilization of the given geological survey works, taking into account data about the density of outgoing on the surface species/rocks (Fig. 220). In a somewhat weakened form of this type of anomaly are noted also in the regions, where the basement occurs under a layer of sedimentary rocks, moreover if the the thickness of this layer does not exceed 2-3 km, then the type indicated anomalies are unconditionally prevailing above all remaining so that all the remaining anomalous factors (for example, the relief of the surface of basement), actually, barely are developed against their background.

On configuration in plan/layout and by geologic nature gravity anomalies connected with internal structure of the basement, it is possible to subdivide into following three typical varieties (Fig. 221): 1) strip-like linear anomalies (positive or negative), connected usually with folding structures, and also sometimes with sheet intrusions within basement; 2) anomaly of type of "gravitational step/stage", that characterizes increase or decrease in the gravitational force in determinate direction and connected with normal or tectonic contacts of species/rocks of different density within basement; 3) anomalies, which have form, close to isometric, observed usually above intrusion masses, which slope within basement.

Page 419.

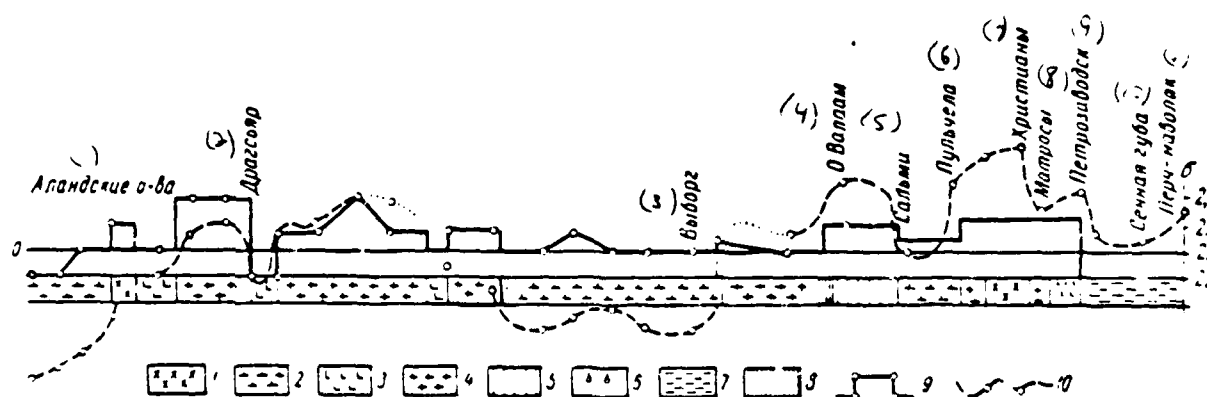


Fig. 220. Gravitational anomalies and density of species/rocks along profile in southern part of Baltic shield. On 1 - Archean gneissoids; 2 - granites of Rapakivi; 3 - migmatites; 4 - post-Bothnian granites; 5 - diabase; 6 - quartzite and sandstones; 7 - suite of dolomite and quartz effusions; 8 - phyllite; 9 - density curve of the crystalline rocks; 10 - curve  $\Delta g$ .

Key: (1). Aland Islands. (2). Dragsfjord. (3). Vyborg. (4). Valaam Island. (5). Sal'mi. (6). Pul'chela. (7). Christiany. (8). Matrosy. (9). Petrozavodsk. (10). Sennaya guba [bay]. (11). Perch-navolak.

The great experiment of gravitation prospecting works on Precambrian shields, carried out in the USSR and abroad, shows that virtually all intensive clearly localized gravity anomalies with a horizontal gradient from 1 mg/ per 1 km and higher prove to be connected with rocks which emerge on surface of basement, i.e., with structural magmatic complexes, which can be established/installed during geologic mapping/charting of basement on sufficiently large/coarse scale. Is explained this fact, apparently, by the fact that the Precambrian metamorphic rock usually are sharply dislocated, up to the formation of isoclinal folds, and also with the very large depth of the erosion shear/section, to which fall all or almost all metamorphic and magmatic rock, which form part of basement. The same occurs also for the magnetic anomalies. This gives the possibility to claim that the quantitative interpretation of gravitational and magnetic anomalies in the platform regions gives depths of the bedding of the perturbing masses, which with the high fraction/portion of probability can be identified with the depth of the surface of basement.

FOOTNOTE'. This identification is most reliable for the regions of ancient (Precambrian) platforms.

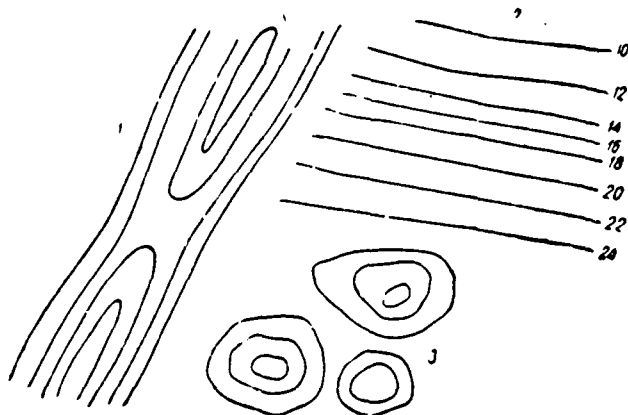


Fig. 221. Arrangement of the isoanomaly above typical gravity anomalies of platform regions, connected with internal structure of basement. 1 - strip-like linear anomalies; 2 - "gravitational of step/stage"; 3 - isometric ("mosaic") anomalies.

Page 421.

This approach to task of studying relief of the surface of basement recently became generally accepted during utilization of magnetic anomalies (Andreyev, 1954; Simonenko, 1956; Fotiadi, 1958). Analogous approach is subsequently used by I. G. Klushin (1958, 1960) also for the gravity anomalies. Calculations were performed for the southeastern regions of Russian platform by the method of the integral transforms (see § 40, Chapter V) on intensive on the order of 10 mgal and higher) anomalies of the type of "gravitational step/stage". Anomalies were removed from the gravitational maps/charts of scale 1:200000.

Fig. 222 shows comparison of depths of bedding of anomalous

DOC = 88020222

PAGE

~~18~~ 768

masses, calculated according to data of gravitational prospecting, with depths of bedding of surface of basement in appropriate sections, determined by drilling and seismic survey. The close cross correlation of each values of the depths (calculation it gives the value of the coefficient of correlation  $\sim 0.7-0.8$ ) is undoubted.



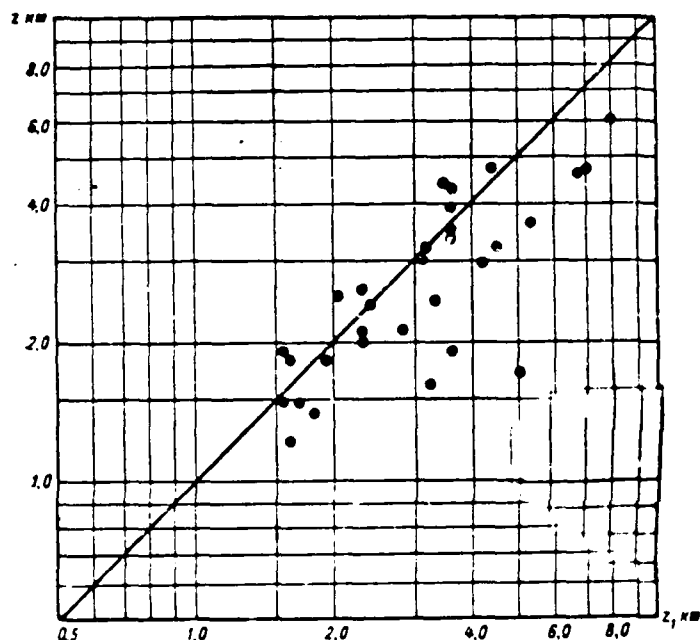


Fig. 222. Comparison of values of depths of up to  $L_{\text{sement}}$  calculated on gravity anomalies by method of integral trans.  $z_1$ ) and of those determined by drilling or by seismic survey ( $z$ ) for southeastern regions of Russian platform. According to I. G. Klushin (1960).

Page 422. <sup>17</sup> The root-mean-square error in the determination of the depth from the unitary anomalies proves to be order 25%; it is possible to decrease it, neutralizing results along several profiles in the limits of zones with the identical structure of the anomalous field<sup>1</sup>.

FOOTNOTE <sup>1</sup>. This indication, on the basis of experiment of the interpretation of magnetic anomalies, was for the first time made by

B. A. Andreyev (1954). ENDFOOTNOTE.

It was subsequently explained that the same results can be obtained for the anomalies of the type of "gravitational step/stage", using method of G. D. Managadze in the modification of B. A. Andreyev, described in §40 of Chapter V. Subsequently on anomalies of the strip-like type there should be tested also method of Ye. A. Mudretsova or diverse variants of the method of limiting distributions for  $W_{12}$  in the case of vertical bed, described in §§42-43 of Chapter V. It is highly probable that these methods will also prove to be those applied during the determination of the relief of the surface of basement from to gravity anomalies.

Large platform basins/depressions, in limits of which surface of basement is omitted at significant depth (many kilometers), and gravitational forces are noted by minima. The side parts of these basins/depressions are frequently complicated by faults and very clearly they are expressed for the gravitational maps/charts (Fig. 223).

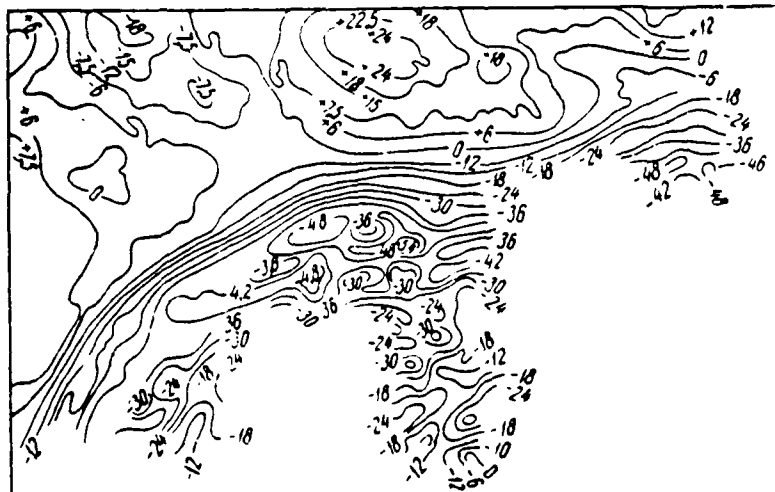


Fig. 223. Gravity anomaly above onboard part of large/coarse platform basin/depression.

Page 423.

Gravitational minima above the basins/depressions are caused by the effect of the relief of the surface of the basement, composed by more compact rocks than the covering basement sedimentary rocks, and also frequently and by a change in a facies-lithologic composition of sedimentary rocks: by an increase in the power/thickness of lighter sandy-clay species/rocks, by appearance in the section/cut of the halogen rocks, etc. In certain cases, for example, when basement is comparatively uniform paleozoic species/rocks, and sedimentary cover - relatively by the lungs by sandy-clay rocks, approximate judgment about the relief of the surface of basement proves to be possible to obtain, assuming the linear bond of anomalies  $\Delta g$  with the depth of the bedding of basement, confirmed via the comparison of data of

DOC = 88020222

PAGE

~~15~~ 772

gravitational photographing and seismic survey (Fig. 224). A question about the possibility of this type of assumption by us is in detail examined in § 48 of Chapter VI.

Structures of second order of type of rises/ramparts in such cases, when they have large amplitude and steep/abrupt onboard parts and are composed in yard by species/rocks, sharply distinct in density from cap rock, which is also directly manifested on gravitational map/chart by anomalies of sufficiently high intensity (Fig. 225).

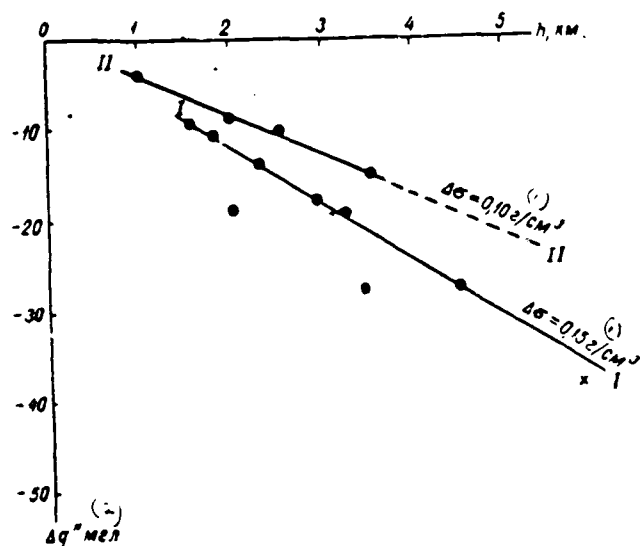


Fig. 224. Dependence between intensity of anomaly  $\Delta g$  and depth  $H$  of surface of basement for region of the Southern Minusinsk basin/depression. According to A. P. Tarkov (1953). I - western part of the basin/depression; II - eastern part of the basin/depression.

Key: (1).  $\text{g/cm}^3$ . (2).  $\text{mg/l}$ .

Page 424.

However, the majority of platform archlike structures are characterized by a comparatively small amplitude and are very gently sloping, with the angles of the slope of limbs of the order of tens of minutes or first degrees of an arc; such structures are not directly expressed by noticeable gravity anomalies. Nevertheless and in these cases it proves to be that usually there is a sufficiently specific conformity in the arrangement of structures and gravity anomalies; the structures are placed either in the outlines of the zones of linear

strip-like anomalies - sometimes positive, sometimes negative, or in the edge/boundary parts of such anomalous zones, i.e. they coincide with anomalies of the type "gravitational step". In this case, which especially clearly confirms not direct, but indirect coupling of gravity anomalies with the structures, the arrangement of structures is linked also with the arrangement of the magnetic anomalies, clearly caused not by the structure of the sedimentary thickness, virtually nonmagnetic, but, in all likelihood, by the structure of crystalline basement (Fig. 226).

This conformity is observed for many structures of second order of Russian platform, western-Siberian lowland, midcontinent (USA) and other regions, and, moreover not only for gravitational, but also for magnetic anomalies.

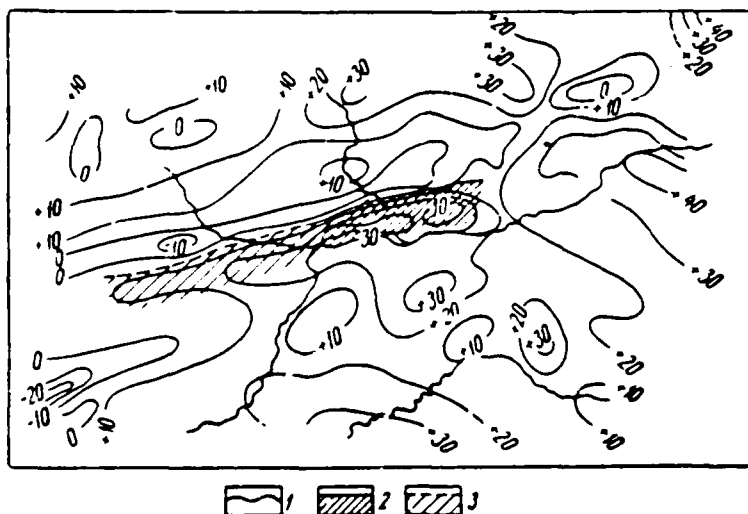


Fig. 225. Gravity anomaly above structure of second order. Northern steep/abrupt part of structure is directly expressed by an anomaly of the type of "gravitational step". 1 - isoanomalies; 2 - position of steep side of structure according to geologic data; 3 - western continuation of structure according to data of gravitational prospecting.

Page 425.

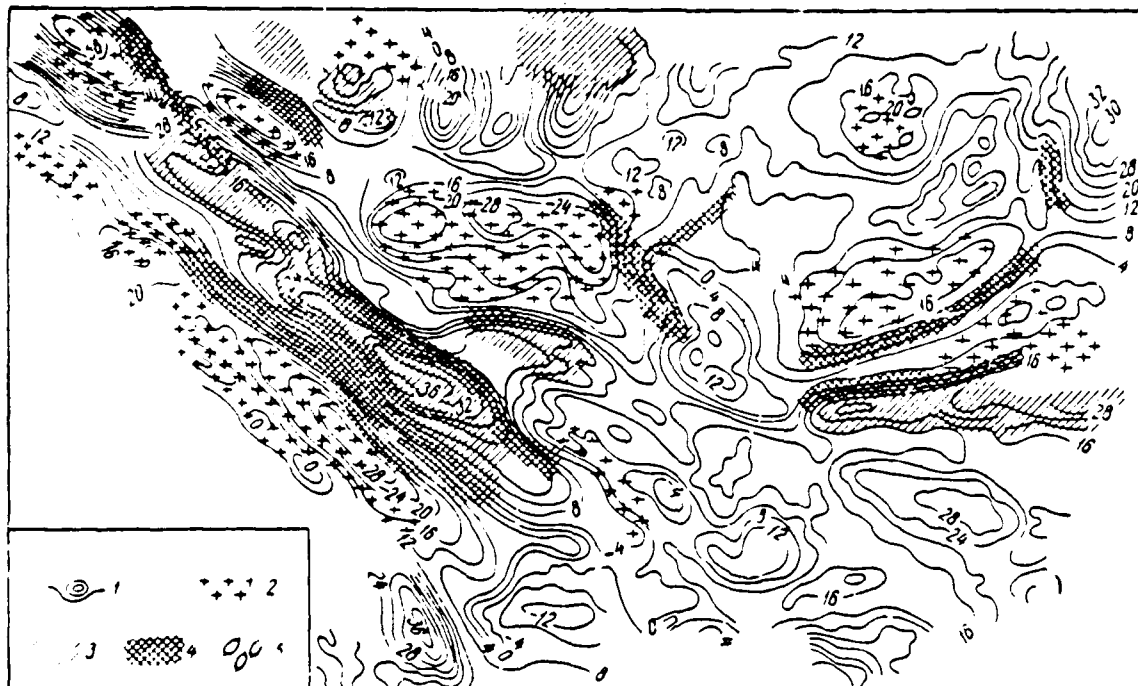


Fig. 226. Diagram of comparison of results of gravitational prospecting, magnetic prospecting and structural geologic photographings. According to A. Sh. Faytel'son. 1 - isoanomalies of gravitational force; 2 - region of the propagation of positive magnetic anomalies; 3 - region of the propagation of negative magnetic anomalies; 4 - linear structures; 5 - separate uplifts/rises.

Page 426.

This fact was noted for the Russian platform already by A. D. Arkhangel'skiy (1940), who put forth the following assumption for the explanation of a similar conformity of anomalies and structures: "we assume that at the basis of rises/ramparts and trenches, which characterize our basins/depressions, lie/rest the dislocations of



basement. They appear as its gently sloping inflations/bulgings or the fold of very large diameter, agreeing in their course/strike with the elements of tectonics of basement. A deficiency in the plasticity in the species/rocks rapidly leads to formation in these folds after cleaving, shifts/shears and especially the overthrusts. These dislocations of the basement, being transmitted by that covering the latter to plastic sedimentary rocks, cause the different disturbances/breakdowns, which in the form can very sharply differ from folds and overthrusts of their underlying gneissic masses" here. In other words, the magnetic and gravity anomalies of platform regions reflect the internal structure of basement, and the dislocations of basement, connected with its internal structure, condition location and character of the structures of sedimentary cover.

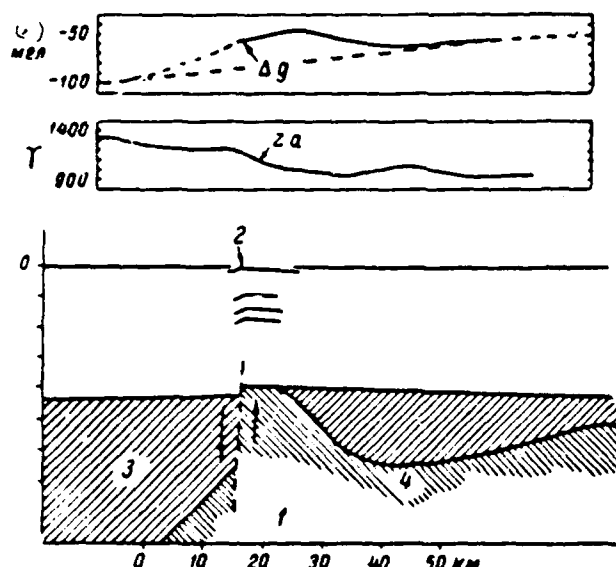


Fig. 227. Geological-geophysical section/cut (according to boring and seismic data), which shows bond of internal structure of basement, fault in it (1), flexure-shaped structure in sedimentary cover (2) with gravitational and magnetic anomalies; 3, 4 - variety of crystalline schists. According to Kornfeld (Kornfeld, 1954).

Key: (1). mg/.

Page 427.

The fact that the faults of basement are formed in accordance with its internal structure, following the contacts of species/rocks, can be seen based on numerous examples on the Precambrian shields, one of which we give in Fig. 227. If above the basement the thickness of sedimentary rocks is located, then with the shifts of the separate lumps/blocks of basement in the layers of sedimentary rocks are formed tensile strains, and then, with the repeated shifts of opposite sign,

archlike structures (Fig. 228). Reality of this type of the diagram, formulated by I. K. Zerkhaninov (1954), are confirmed by the fact of the increased tectonic susceptibility to cracking of sedimentary rocks in the crest parts of the structures of platform regions, about which narrower we mentioned in § 5 of Chapter I. All this confirms hypothesis of A. D. Arkhangel'skiy.

Indirect conformity of linear gravitational and magnetic anomalies indicated with structures of second order extensively is used with tectonic zoning of platform regions and has great practical value during searches for deposits of useful minerals, whose arrangement is controlled by regional structures - first of all of local oil and gas-bearing platform structures, with which discussion will deal in following chapter.

Study of internal structure and relief of surface of crystalline basement frequently has very high value for searches for ore deposits. The structural elements of basement are, in particular, the iron-ore tanks of type of KMA and Krivoy Rog (see § 60 of Chapter IX), intrusion complexes, for example ultrabasic intrusions with the deposits of chromium, nickel, etc. (see § 51 of Chapter IX). with the zones of fault in the basement and the covering thicknesses of sedimentary rocks are connected many magmatic formations, which carry valuable useful minerals: kimberlitic tubes with the diamonds (for example, in East Siberia), vein bodies with the deposits of rare, noble, radioactive metals, etc. In the investigation of structural

DOC # 88020222

PAGE

~~27~~ 780

elements indicated above gravitational prospecting usually participates very actively and successfully in the complex with magnetic prospecting and other geophysical methods.

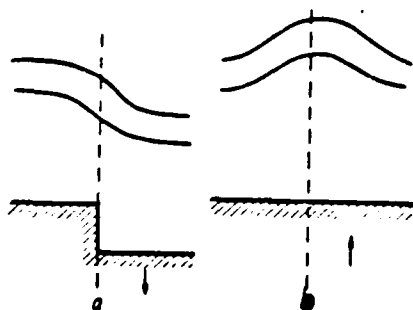


Fig. 228. Diagram of formation of platform structure according to I. K. Zerchaninov (1953). a) the stretching of layer with the relative vertical movement of blocks of the basement; b) the formation of anticlinal structure with the reverse vertical movement of blocks of the basement.

Page 428.

Chapter VIII.

## SEARCHES AND PROSPECTING OF OIL- AND GAS-BEARING STRUCTURES.

### § 54. General comments.

During searches for oil bearing and gasiferous structures of 20-30 years ago gravitational prospecting was a very popular geophysical method; they tried it to use also during prospecting of such structures. Salt domes were the usual objects of gravitation prospecting works at that time, large anticlinal folds so forth - structures, which are usually developed by the very intensive anomalies, detection and geologic interpretation of which is sufficiently light and simple task. Only as an exception of gravimetric prospecting sometimes collided then with the more difficult for the searches types of the oil bearing uplifts/rises, with which to it several it was necessary to deal, also, subsequently, for example concerning the searches for rip masses in the Ural downwarp/trough. Subsequently, with the gradual changeover of the basic volume of oil prospecting works in Volga-Urals province, into the western-Siberian lowland, etc., the main object of these works become the gently sloping dome- shaped folds, typical for the internal regions of platform regions. The gravitation effect, caused by the effect of interfaces in the thickness of sedimentary rocks in the sections of the manifestation of such structures, as show appropriate calculations, it is very weak (usually the fraction/portion of

milligal on anomaly  $\Delta g$ ), based on this for a long time it was considered that these structures virtually are not developed in the gravity anomalies. This view was strengthened still and because into postwar period in petroleum geology the application of unproductive gravitational variometers was interrupted, but the first of the used types of gravimeters did not reach the accuracy, required in the majority of the cases while performing of work in connection with the searches for petroleum and gas fields. This fact, and also sufficiently successful application of a method of the waves reflected during the searches for dome-shaped platform structures, led to the fact that in the postwar period almost they ceased to consider gravitational prospecting in petroleum geology, giving up to this method only the solution of the problems of tectonic zoning.

Page 429.

In actuality, as we will see below, account of factor of laminar zonality of density, connected with platform structures, and also new possibilities, caused by application during the photographing of gravimeters of increased accuracy, make it possible to express confident judgment about worthwhileness of utilization of gravitational prospecting on new ideological and new technical basis for searches for local platform oil and gas-bearing structures. The account of the factor of the laminar zonality of density proves to be in a number of cases necessary for the correct interpretation of data of gravitational prospecting also in the geosynclinal regions during the searches for oil and gas-bearing structures.

In view of the great variety of conditions and possibilities of applying gravitational prospecting during searches for oil and gas we examine below this question separately for following types of oil and gas-bearing uplifts/rises: 1) salt/hydrochlovic domes; 2) anticlinal folds; 3) rip masses; 4) dome-shaped platform structures.

#### § 55. Salt domes.

Rock salt, as we already know, has virtually a constant density ( $2.15 \text{ g/cm}^3$ ), frequently less in value than density of enclosing rocks, which conditions the presence of negative anomalies connected with salt domes of gravitational force. As a result of the significant dimensions of domes in the plan/layout and in particular on the vertical lines, connected with them negative gravity anomalies have, as a rule significant intensity (many milligals, ten milligal) and large cross sizes/dimensions (kilometers, tens of kilometers). These anomalies usually are well localized and they are sharply pronounced, in particular for the shallow sloping domes.

In some salt dome regions gravitational minima above domes are observed in simple nonfolded form (Caspian basin in the USSR, Rumania, Iran). In other regions the gravitational minima above the domes are complicated by the additional maximums, caused either by the presence above the domes of the powerful/thick gypsum anhydrite cap of "cap rock" (Nordvik-Khatanga region in the USSR, Gulf of Mexico in the



USA), or the dense breccia-like species/rocks, which slope above the dome and carried out to the surface from the depth in the process of an increase in the salt/hydrochloric domes (Dnieper-Donets basin/depression). The types of the gravity anomalies above the salt/hydrochloric domes are shown in Fig. 229 and 230. In all salt dome regions gravitational prospecting is basic method during the searches for domes.

Page 430.

The anomalies above the domes take this characteristic form that their geologic nature does not usually cause doubts.

For domes, which slope at relatively small depth from surface (less than their cross sizes/dimensions), according to gravitational data in majority of cases sufficiently confidently is fixed the position of steep/abrupt part of dome, and also its sizes/dimensions and planform - on outline of zone of maximum horizontal gradients of gravitational force, which borders crest part of dome. This zone is directly defined according to data of variometric photographing, with the help of which in the prewar period were investigated our salt dome regions. In the postwar years, with the transition for gravimetric photographing, the productivity of works increased, but the interpretation of their results was complicated.

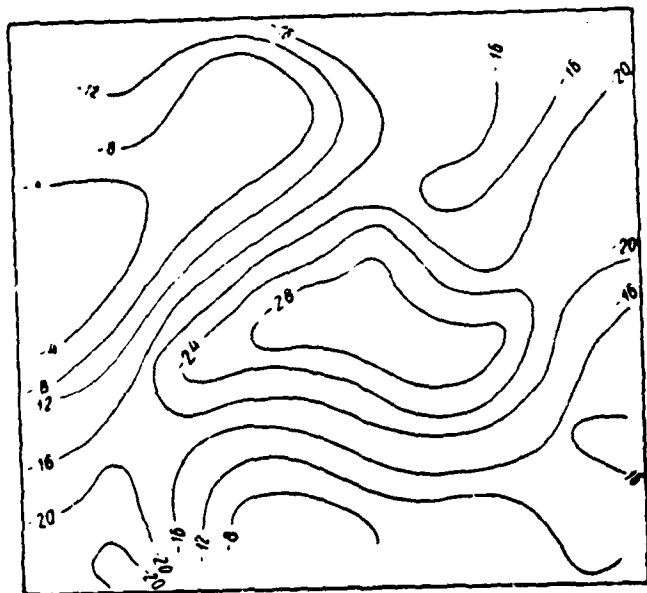


Fig. 229. Gravitational map/chart of salt dome structure, expressed by simple minimum of gravitational force.

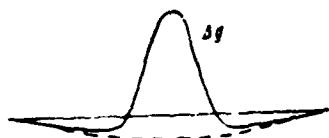


Fig. 230. Example to complex gravity anomaly of salt dome structure: combination of maximum, caused by cap rock, and minimum, caused by salt/hydrochloric nucleus of dome. On Nettleton (1948).

Page 431.

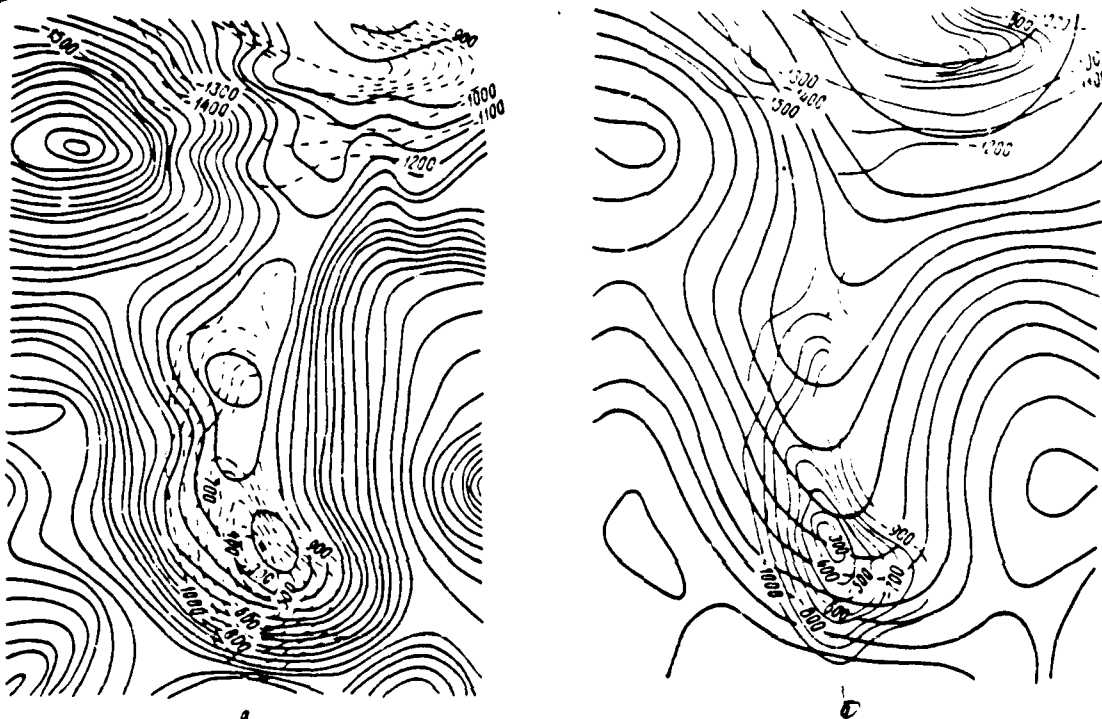


Fig. 231. Isoanomalies of the force of gravity (a) and vertical gradient of force of gravity (b) above salt dome structure. According to B. V. Kotlyarevskiy (1958). Heavy unnumbered lines - isoanomalies; thin lines - isohypses of roof of salt according to data of seismic survey (marks - in meters).

Page 432.

In the relatively small dimensions of domes, their close arrangement, presence of regional background, the judgment about the location, the sizes/dimensions and the form of separate dome is far from always confident, as can be seen from the example given in Fig. 231a. In such cases for refining the outlines of anomalies it is expedient to

use one of the methods of their localization, described in chapter IV, for example by the recount of anomalies  $\Delta g$  and  $\delta \Delta g$  or in  $W_n$  (Fig. 231b).

Study of form of onboard parts of domes is a complex, but important task during prospecting of salt domes. Difficulties for gravitational prospecting during the solution of this problem consist not only in the presence of the disregarded effect of adjacent domes, regional background, etc., but also in the "3-dimensional nature" of domes, which impedes application with the interpretation of the anomalies of templates for the two-dimensional task. At present in the Ural-Emba region for prospecting the steep/abrupt bort of domes the complex of gravimetric photographing and drilling seismic survey (with the study of direct waves, which arrive to the drilling seismic receiver and which intersect the boundary of the salt dome) is used.

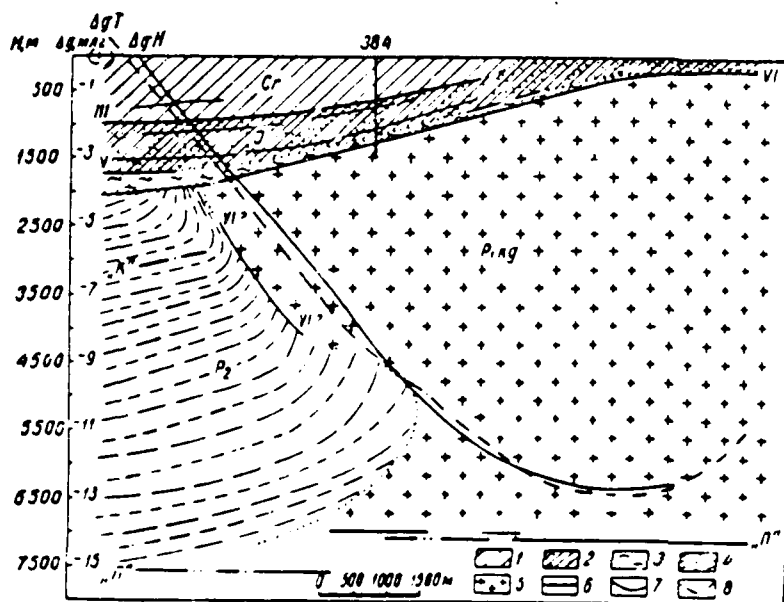


Fig. 232. Determination of position in section of steep side of salt dome structure with utilization of gravimetric prospecting and seismic survey. 1 - Cretaceous; 2 - Jurassic; 3 - triassic; 4 - upper Permian; 5 - lower Permian; 6 - reference seismic horizons/levels III, VI, II; 7 - observed curve of the anomalies of gravitational force; 8 - theoretical curve of the anomalies of gravitational force.

Key: (1). mg/.

Page 433.

The selection of the section/cut of the dome, which gives the theoretical curve  $\Delta g$  along the profile through the dome, similar to the observed curve, is produced with the help of the template for the two-dimensional task; the selection of section/cut is corrected taking into account data of drilling seismic survey. The example of this

section is given in Fig. 232. It is necessary to keep in mind that the most confident results in the case indicated could be obtained during the utilization of gravity anomalies in the localized form of ( $\delta\Delta g$  or  $W_m$ ), with construction and utilization for them of templates, similar themes, such as are used for anomaly  $\Delta g$ , or during the joint utilization of data of gravimetric and variometric photographings.

#### § 56. Anticlinal folds.

Large anticlinal folds in tectonically active oil bearing regions in majority of cases are very well mapped with the application of gravitational prospecting. Under such conditions we usually deal concerning great (several kilometers) thickness of the sedimentary rocks, the significant part of section/cut of which, especially in the upper levels, usually present terrigenous, in particular clay rocks, whose density increases/grows with the depth. Denser carbonate rocks in the majority of regions predominate only in the lower horizons of the section. Therefore, with the anticlinal folds in many instances the maximums the force of gravity (Fig. 233 and 234) are connected.

The indicated gravitational characteristic of anticlinal folds was never considered the rule, and all the remaining - rare exception. However, with the development of gravitation prospecting works it seemed that the examples, which confirm this rule, apparently, not more than the examples reverse, which indicate the bond with the anticlinal folds not of maximums, but, conversely, the minima of gravitational force.

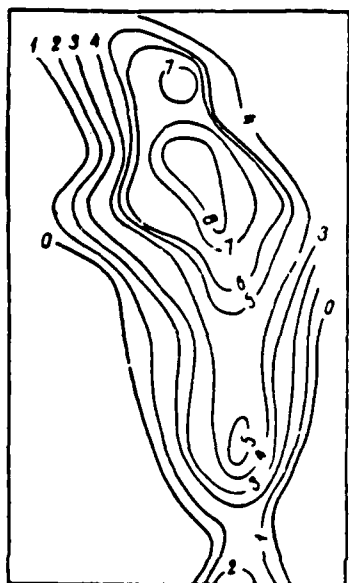


Fig. 233. Gravity anomaly above anticlinal fold in one of Far East regions. According to V. V. Fedynskiy (1956).

Page 434.

In a number of cases of the reasons for this effect are explained, and they prove to be sufficiently different in the character.

1. Reverse by usually observed sequence of distributing density section/cut (more compact rocks on top, lighter - from below).

Examples: a) in foothill zone of Fergana depression upper level relative to compact rocks - conglomerates of Neogene - sharply it is reduced in power/thickness in arches/summaries of anticlines; b) in intermountain basin of San Joaquin (California, USA), in nucleus of anticlinal fold will lie powerful/thick layer of diatomaceous slates

of extremely high porosity and very low density ( $\sigma=0.9$  g/cm<sup>3</sup>)<sup>1</sup> (Fig. 235).

FOOTNOTE <sup>1</sup>. See D. Barton's article in the collection "Geophysical Case Histories" (1948, vol. 1, p. 515). ENDFOOTNOTE.

2. Laminar zonality of density, caused or by change in lithofacies composition of rocks (relative increase in total power of sandy interlayers against total power of clayey in crest parts folds, composed by sandy-clayey stratum), by tectonic factor (shattering and increased tectonic susceptibility to cracking of species/rocks in crest parts of folds).



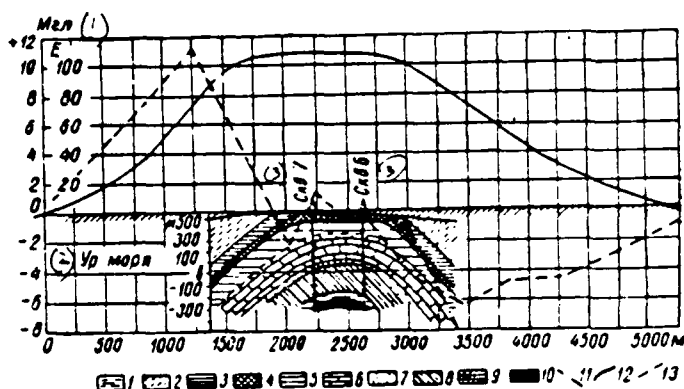


Fig. 234. Gravity anomaly above anticlinal fold in one of Central Asia regions. According to Yu. N. Godin and N. P. Tuayev. The oligocene: 1 - arenaceous thickness; 2 - clayey thickness. Eocene: 3 - green earth of Fergana/Fergan tier; 4 - L horizon/level; 5 - green clays of the Suzak horizon/level. Paleocene period: 6 - limestone. The Senonian: 7 - sandstones; 8 - clay; 9 - sandy-clay thickness; 10 - clay; 11 - fault; 12 - anomaly  $\Delta g$ ; 13 - gradient of force of gravity.

Key: (1). Mg/l. (2). Sea level. (3). borehole.

Page 435.

Both these factors are established in the region of the Apsheronsk peninsula, where above the anticlinal folds the minima of the force of gravity (Fig. 236) are noted. The same nature, apparently, have the minima of gravitational force above anticlinal structures of Western Ciscaucasia, (Sazhina, 1957) and Carpathian downwarp/trough (Antipov, 1960). The decrease of the density of species/rocks in the crest part of some structures of subcarpathia is proved experimentally (Subbotin,

1949). In some regions, for example in the Ararat valley of Armenia, the part of the anticlinal folds is noted by maximums, and another part - by minima of gravitational force.

Thus, we can state/establish that as a result of diversity of physico-geologic factors, which condition gravity anomalies above anticlinal folds of oil bearing regions, these anomalies prove to be into some conditions positive in others - negative, moreover in total set quantity of those and other cases, apparently, is approximately equal. It is understood, in certain cases this creates known difficulties during the qualitative geologic interpretation of gravity anomalies in the folding oil bearing regions. As far as the quantitative interpretation of the gravity anomalies above the anticlinal structures is concerned, for its execution rarely there are sufficiently favorable conditions in the sense of a good study of the density of species/rocks and other factors, which influence gravitational field.

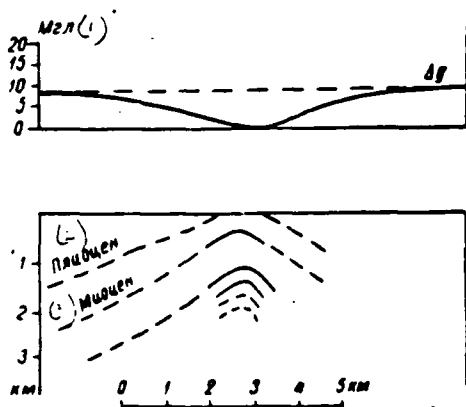


Fig. 235. Gravity anomaly above the anticline of San Joaquin (California, USA). According to D. Barton (1948).

Key: (1). Mg/. (2). Pliocene. (3). Mioxene.

Page 436.

Nevertheless, if above the anticlinal fold the gravity anomaly of symmetrical form is noted, then it is possible to try to determine the depth of the bedding of the reference level, which creates anomaly (with the known density characteristic of species/rocks), for example, using the method, described by us based on theoretical example in § 35 of Chapter V, or by by of trial and error of the section/cut of fold with the help of the template, described in § 46 of Chapter VI.

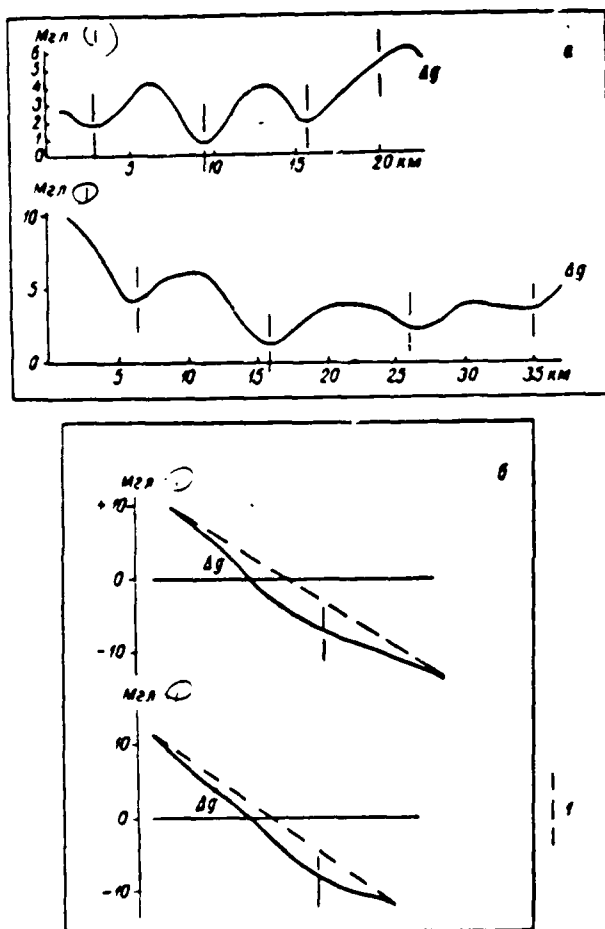


Fig. 236. Gravity anomalies above anticlinal folds of Apsheronsk peninsula. 1 - position of the axes of anticlinal folds.

Key: (1). Mg/.

Page 437.

§ 57. Reef masses.

Reef masses are peculiar and difficult subject of investigation

for geophysical methods, including for gravitational prospecting. Their peculiarity consists in the fact that these are tectonic structural forms, but the facies isolations, frequently only complicated by secondary tectonics, but the difficulty of their detection is connected with the fact that the rip masses are developed in the complex physico-geologic situation, which it is necessary to decipher while performing of prospecting and prospecting work. The at the same time practical value of reefs in petroleum geology of our sharply increases/grows, about which is indicated the discovery in recent years of a number of the new rip deposits of oil and gas in the southern part of the Ural downwarp/trough, and also recent data about the presence in limits of the Volga-Ural province of platform type rip petroleum deposits. Platform type reefs are already familiar in the USA; it is possible that they will be discovered in the series/number of the regions of our country.

In region of Ural downwarp/trough gravitational prospecting together with electrical prospecting very actively participates in stage of liberation/precipitation of promising sections, in territory of which is probable detection of rip masses. Searches and prospecting reefs in the limits of these sections is realized by a complex of seismic survey (KMPV [correlation method of refracted waves], RNP) and drilling operations. Above the separation of anomalous gravitational field to regional and local components plays the most important role during the utilization of data of gravitational prospecting during the solution of problem indicated,

moreover particularly interesting the fact that in this case none of these components does not go into the "production wastes", but each of them expediently is used subsequently.

In structure of Ural downwarp/trough there participates thick and different in composition complex of sedimentary rocks of Permian age, represented by the Ufa tier (terrigenous rocks), the Kungursk tier (hydrochemical precipitation: anhydrite, gypsum, rock salt), Sakmarsk and Artinsk tiers (carbonate rocks). Reef masses are placed in the roof of carbonate Sakmarsk-Artinsk deposits, in the edge/boundary part of the downwarp/trough, near its boundary with the Russian platform. For the map/chart of the regional (averaged) anomalies of gravitational force platform bort of Ural downwarp/trough is expressed by the zone of "gravitational step/stage", by the width only of 8-12 km, which presents transition from the weakly negative field above the platform to the intensively lowered/reduced field of downwarp/trough (Fig. 237). Thus, on the regional gravity anomalies is very clearly contoured entire/all as a whole rip zone of Ural downwarp/trough.

Page 438.

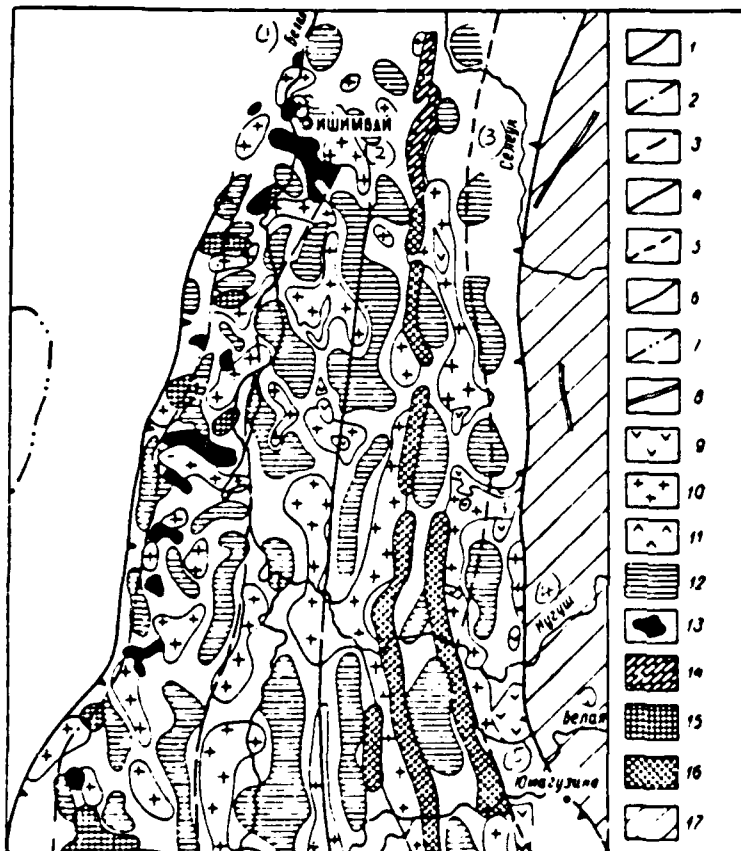


Fig. 237. Geological-geophysical tectonic diagram of southern part of Ural downwarp/trough. According to F. I. Khat'yany (1959). 1 - western boundary of the Cis-Ural downwarp/trough along Kungur; 2 - western boundary of Cis-Ural downwarp/trough on the Sakmarsk-Artinsk deposits; 3 - eastern band edge of reefs; 4 - the centerline of Cis-Ural downwarp/trough; 5 - boundary of the steep climb of Sakmarsk-Artinsk deposits; 6 - eastern boundary of Cis-Ural downwarp/trough; 7 - outlines of archlike uplifts/rises over the surface of halide Kungur; 8 - tectonic breaks; 9 - outcrop of Kungur gypsum to the topographic surface; 10 - s. t Kungur uplifts; 11 -

anhydrite gypsum Kungur uplifts; 12 - Kungur downwarps/troughs, carried out by Permian-Triassic deposits; 13 - rip masses; 14 - anticlinal folds; 15 - zone highly promising for the searches for rip masses; 16 - zone highly promising for the searches for anticlinal folds; masses; 16 - zone highly promising for the searches for anticlinal folds; 17 - region of the western slope of the folding Urals.

Key: (1). White. (2). Ishimbay. (3). Seleuk. (4). Nugushch. (5). Yumaguzino.

Page 439.

In limits of the reef zone indicated promising sections for searches for reefs are separated/liberated on basis of several direct and indirect signs.

1. From limits of rip zone are eliminated as all unpromising sections, which are characterized by coincidence of uplifts/rises of supporting/reference electric horizon/level (corresponding to roof of Kungur) and local minima gravitational forces.





under center section of which the roof of Sakmar-Artinsk rocks usually forms downwarps/troughs and does not contain rip masses, correspond to these zones.

2. As promising are separated/liberated sections, in limits of which uplifts of roof of Kungur are characterized by local maxima of the force of gravity. According to the work experience, such sections answer the nonsalt uplifts of Kungur, which present in a number of cases of the structure of veiling above the reef masses occurring below. In the southern part of the downwarp/trough the sections of the local maximums gravitational force, which are placed on the periphery of salt Kungur uplifts, are considered as the most promising, this is explained by "creep" of salt observed in this region in the form of separate tongues to the rip masses, which played the role of rigid limit stop with the tectonic shifts of plastic salt masses (Fig. 238).

3. Sections promising for searches for reef masses in majority of cases are placed perpendicularly to external edge of downwarp/trough. In this direction an increase in the majority of rip stands occurred.

For separation of local anomalies in this region different methods, described in Chapter IV, were tested. Sufficient to effective was acknowledged simplest of them - the method of variations  $\delta\Delta g$  (Khat'yanov, 1960; Khat'yanov and Nasyrov, 1960).

In press/printing there is a report about successful utilization of gravitational prospecting for searches for reefs abroad - in province of Ontario (Canada), in region of Great Lakes, in which are several favorable prerequisites/premises for searches for rip masses; latter will lie not very deeply from surface (500-600 m), but on the side from them will lie saliferous species/rocks of considerably less density (density of salt 2.2 g/cm<sup>3</sup>, but carbonate rocks of reef - 2.5 g/cm<sup>3</sup>). Nevertheless, for the separation of reef masses there is required detailed photographing by high-accuracy gravimeter, thorough account and exception/elimination of regional background and i.e. new rip mass was discovered on an isolated thus local ("remaining") anomaly by an intensity of only 0.4 mgal (Pohly, 1956).

§ 58. Dome-shaped platform uplifts/rises.

Dome-shaped platform uplifts/rises are characterized by small amplitude (first tens of meters) and small angles of inclination/slope of wings (several degrees of arc). If we moreover, supplement that the oil bearing horizons/levels will lie on the significant depth from the surface (1-2 km, sometimes more), then there becomes obvious the extreme difficulty of the search for such structures by any geophysical methods.

Page 441.

At the same time, platform structures in the oil bearing regions

present basic resource/lifetime in the petroleum industry at present: in our country in 1959 80% of reserves of oil it was concentrated in the Volga-Ural province, and according to the seven-year plan/layout 1959-1965 in this province fit about 65% of preparation for the industrial reserves of oil.

Gravitational prospecting for a long time was considered inapplicable for searches for platform structures, and this task was laid exclusively on seismic survey by method of the waves reflected. However, the difficulties, which arose before this method during the solution of the problem indicated, proved to be such significant that the efficiency of method, in spite of its very large technical refinements, it proves to be thus far completely insufficient. Conclusion about the inapplicability of gravitational prospecting for the searches for gently sloping platform structures was done on the basis of the assumption about the fact that their gravitation effect was caused only by the structural relief of interfaces between the layers of constant density (model of "laminated medium"). During such a calculation it is obtained, that the gravitation effect, caused by the effect/action of platform structure, has very low value. If we, for example, approximately represent this structure in the form of the vertical circular cylinder with a height of 50 m, with a radius of 5 km, sloping at the depth 1 km, then the maximally possible gravitational effect according to the formula (V, 29) will be

with  $\sigma = +0.5 \text{ g/cm}^3$   $\Delta g_{\max} = +0.8 \text{ mg/}$

with  $\sigma = 0.3 \text{ g/cm}^3$   $\Delta g_{\max} = +0.5 \text{ mg/}$

If we take into account that anomaly of this order will be developed in accompaniment of different kind of associated anomalies, from which some (connected, for example, with nonhomogeneous structure of the basement) can be significant in value, then it is clear that to reveal/detect this anomaly, apparently, practical is impossible. To this conclusion us it leads in this case utilization during appropriate calculation of the model of "laminated medium".

Let us allow, however that with local structure being investigated is connected zonal change of density in thickness of sedimentary rocks, caused either by facies-lithologic or tectonic factor, or summary effect of both these factors. This change in the density can be very small in the value, but if it is developed in the thickness of the species/rocks of large thickness, then its gravitation effect can prove to be sufficiently large - in any case much larger (in terms of the absolute value) of values  $\Delta g_{max}$  corrected above.

Page 442.

Let us allow further that this change in density will be only  $-0.1 \text{ g/cm}^3$  and it occurs in volume of vertical circular cylinder with radius of 5 km, with height of 1 km (i.e. is such power/thickness of thickness, in which zonal change in density is developed).

FOOTNOTE'. Accepting here minus sign, we consider that the zonal

changes in the density, connected with the structures, are most frequently negative (see § 11 of Chapter II). ENDFOOTNOTE.

The depth of the bedding of the upper end/face of cylinder let us conditionally assume to be equal to zero. Then the maximum (in terms of the absolute value) value gravitation effect according to the formula (V, 29) will be  $\Delta g = -3.8$  mg/.

As we see, the anomaly, which in absolute value considerably exceeds the anomaly caused directly by the structure, is obtained. Algebraic sum of both anomalies comprises in this case:  $-3.8 + 0.8 = -3.0$  mgal or  $-3.8 + 0.5 = -3.3$  mgal. This anomaly, certainly, it is possible to reveal/detect during gravimetric photographing.

Actually whether, however, presence of laminar zonality of density in platform regions can it condition noticeable gravitation effects? To both these of a question at present it is possible to give affirmative response/answer for this most important oil bearing region as Volga-Ural province.

For the Volga-Ural province presence in section/cut of sedimentary rocks of very powerful/thick (1000-1500 m) thickness of carbonate rocks (limestone, dolomite), which relate on age to Carboniferous period and Devon is characteristic. It is established by many researchers and described in detail is the intensively marked tectonic susceptibility to cracking of the carbonate rocks of the

province indicated, the expressed by the presence both macro- and the microcracks, from which only part is closed with cement, and another part is filled with water, air or "living oil". The maximum development of tectonic susceptibility to cracking is observed in the arches/summaries and on the steep/abrupt wings of platform structures (permiaks, 1949; London, 1950; Mileschina, 1953; Nalivkin, 1955, etc.). This gives grounds to assume that with the platform structures of Volga-Ural province the zones of an increase in porosity and corresponding reduction of the density of the carbonate rocks must be regular connected.

This decrease of density of carbonate rocks is established on many structures by immediate determination. Density variation reaches  $-0.3 \text{ g/cm}^3$  in the carbonate rocks of Permian age (roses, 1949; Andreev, 1957) and  $-0.1$ ,  $-0.2 \text{ g/cm}^3$  in the carbonate rocks of the Carboniferous period (Boronin, 1959).

Page 443.

By indirect, but very convincing confirmation of decrease of density of species/rocks on structures is fact of decrease of average speed of elastic waves, established/installed via analysis of seismic given in whole series prospecting areas S. V. Krylov (Andreyev, Boronin, Krylov, 1961). The average speed was determined to deep reference horizons in the Carboniferous period and the Devon (1200-1800 m); its relative changes on the structures reach 2-6%.

On the basis of all these data it is possible to assume that with dome-shaped uplifts/rises in series/number of regions of Volga-Ural province local minima of gravitational force are connected.

Indication about the bond of some structures with the gravitational minima has already sufficiently long ago been done E. N. Fotiadi (1955).

Late by V. P. Boronin for the territory of the Tatar ASSR were comprised detailed compound gravitational and magnetic cards and maps/charts of the localized gravity anomalies  $\delta\Delta g$ . The analysis of these materials made by it showed that with many dome-shaped structures of the Tatar ASSR the local minima of the force of gravity of weak intensity (Fig. 239) were connected. These minima, as a rule, are not repeated in the magnetic field, i.e., they, in all likelihood, are connected not with the structure of basement, but with the structure the thickness of sedimentary rocks they reflect the zones of the reduction of the density of the carbonate rocks, confined to the dome-shaped structures.

Gravitational characteristic of structures is naturally dissimilar in limits of entire vast Volga-Ural province.



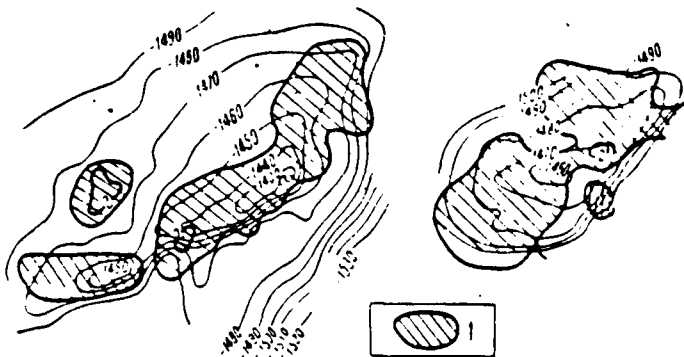


Fig. 239. Local minima of force of gravity (1) above dome-shaped oil bearing structures of Tatarya. According to V. P. Boronin (1959). Enumerated lines - stratoisohypses; 1 - local minima of gravitational force.

Page 444.

In its southern regions, which are characterized by the shallow bedding of the carbonate rocks, by the large amplitude and by the definition of the manifestation of dome-shaped uplifts/rises, the prevailing value in the formation of gravitation effect has already directly structural relief of density interfaces, but not the laminar zonality of density, connected with the structures. In accordance with this in these regions large/coarse dome-shaped uplifts/rises are expressed no longer by minima, but by the maxima of the force of gravity (Fig. 240). This once more proves the dialectics of prospecting work.

However, on the whole gravitational prospecting unconditionally has prospects for application during searches for oil bearing

structures of Volga-Ural province. It is obvious that in different regions of this province the approach to the interpretation of the probable geologic value of gravity anomalies must be different. Prospecting gravitation prospecting works must be produced by the complex of the methods of seismic survey (in essence by the method of the reflected waves) and gravitational prospecting with the gravimeters of high accuracy. It is necessary to keep in mind that the results given above were established/installed via the analysis of gravimetric photographings, which were being produced with the instruments of the type of GAK and SN-3. It is clear that an increase in the accuracy of photographing must increase substantially the efficiency of the utilization of a method.

Let us examine question about possibility of applying gravitational prospecting during searches for local structures in other platform region - western-Siberian lowland. Gravimetric-prospecting works to the searches for structures at the proper methodic and technical level here barely it was conducted, and the conclusions/derivations given below and consideration carry preliminary character. From the point of view of gravitational prospecting, the fact that in the thickness of the sedimentary terrigenous rocks of this region there are no sharp density boundaries, is a special feature of western-Siberian lowland: density in them gradually increases with the depth. The surface of more compact rocks of premesozoic basement presents the density boundary; this boundary is expressed in the near-rim parts of the

basin/depression, where the power/thickness and the density of sedimentary rocks is small, and it is weakly expressed in the internal part of the basin/depression, and sedimentary rocks, beginning from the depths of 2-3 km even more, are diagenetically condensed and little distinct in the density from the species/rocks of basement.

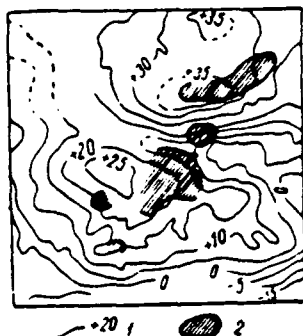


Fig. 240. Results of gravitation prospecting and electro-prospecting works in one of Saratov Volga Region regions. According to O. A. Swank. 1 - isoanomalies of gravitational force; 2 - region of uplifts/rises according to the data of electrical prospecting.

Page 445.

In the near-rim parts of the basin/depression the structures are developed by the sufficiently sharp maximums gravitational force. Relative to the structures of the internal parts of the basin/depression until recently there was an opinion that they are not separated/liberated by gravitational prospecting, whereas the searches for these structures were produced exclusively by the method of the waves reflected.

Recently in work of D. F. Umantsev (1958), a number of data which that show presence of lowland connected with local structures and very sharply pronounced laminar zonality of density of species/rocks of Eocene is given: above structures average density of these species/rocks is reduced on 0.2-0.5 g/cm<sup>3</sup> (Fig. 241). In the

work indicated it is not communicated, which a physico-geologic nature of this phenomenon, but it can be established in the following way. Fig. 242 gives (according to the data of D. F. Umantsev) the distribution of the average density of the rocks on stratigraphic horizons of the lowland. As we see, in this curve, besides the general/common tendency of the rise in density with the stratigraphic depth, four local minima are planned. Comparison of these data with the results of the detailed lithofacies analysis of different stratigraphic horizons/levels of lowland, made by V. P. Kazarinov (1958), show that each of the minima of density indicated corresponds to the periods of the breaks of steeling-accumulation and formation of the formation of the bark of wind erosion with the development, in particular, silicon opoka-like differences in the species/rocks; the latter, as is known, are characterized by high porosity and respectively low density. In the same direction, as a rule, act other geochemical and mechanical conversions of the rocks, connected with the wind erosion, and the summary expression of entire this process are minima in the density curve Fig. 242. The most intensive and prolonged process of shaping of the crust of wind erosion was (according to data of V. P. Kazarinov) in the Eocene-Pliocene, moreover the sharpest and deep minimum in the density curve corresponds to this period.

Structures of western-Siberian lowland are typically consedimentary, i.e., arisen in process of forming their component/term species/rocks; in this case younger horizons/levels

inherited structural forms of more ancient horizons/levels. The rocks in the limits of the uplifts/rises, which were being constantly renewed in the process of oscillatory motions, naturally, it had to to the greater degree undergo the effect of wind erosion, siliconization and other processes, which lead to their intensive reduction of the density. It was explained that on those structures, where D. F. Umantsev discovered the minima of the density of the species/rocks of Eocene, this horizon/level was clays with the intensive development in them of silicon opoka-like differences in the crest parts of the uplifts/rises (Andreev, 1959).

Page 446.

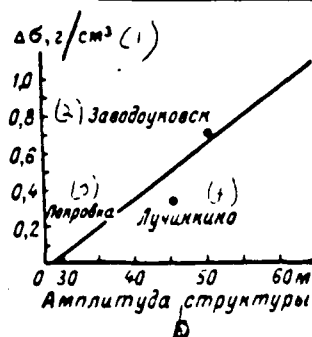
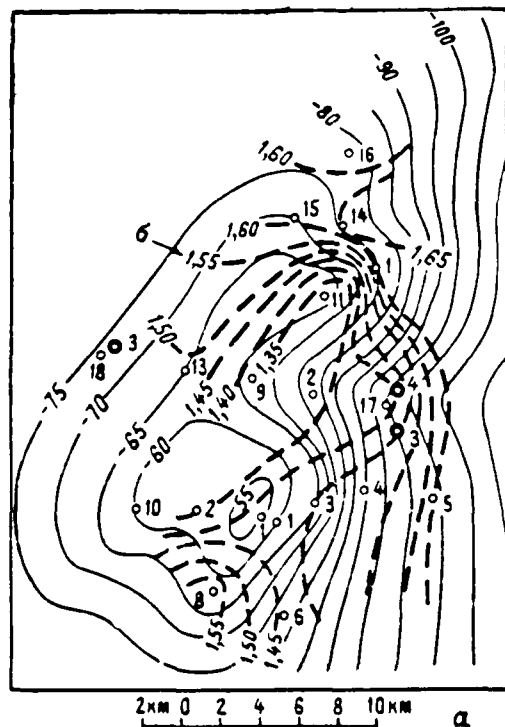


Fig. 241. Change in average density of species/rocks of Eocene on local structures of western-Siberian lowland. According to D. F. Umantsev.(1957). a) Luchinsk structure. Thin lines - stratoisohypses on the roof of Eocene (sign in the meters), heavy dashed lines - isoline of density (sign in  $\text{g/cm}^3$ ); b) change ( $\Delta\delta$ ) of the density of the species/rocks of Eocene in the dependence on the

amplitude of structures.

Key: (1). g/cm<sup>3</sup>. (2). Zavodoukovsk. (3). Pokrovka. (4).  
Luchinkino. (5). Amplitude of structure.

Page 447.

Thus, there was made clear the physico-geologic nature of laminar zonality of density of species/rocks of Eocene, connected with local structures of western-Siberian lowland. From the aforesaid, it is clear that a zonality of the type examined above must be multistage - in accordance with the presence in this territory of several breaks of sedimentation and periods corresponding to them of shaping of the bark of wind erosion. Thus, even if we take into calculation only one factor - the effect/action of wind erosion under the conditions for the development of consedimentary structures, then it is possible to arrive at the conclusion that the laminar zonality of density, apparently, must seize many sections of the stratigraphic section/cut of lowland, that, as it proves to be, is confirmed in actuality.



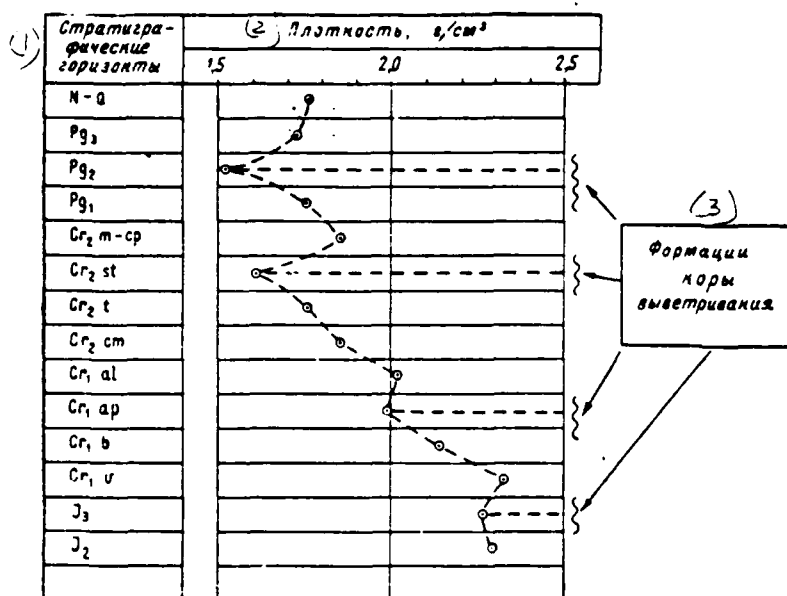


Fig. 242. Distribution of average density of species/rocks on stratigraphic horizons/levels of western-Siberian lowland (according to Umantsev, 1958) and position in stratigraphic section/cut of periods of crusting of wind erosion. According to Kazarinov (1958). Key: (1). Stratigraphic horizons/levels. (2). Density,  $g/cm^3$ . (3). Formations of crust of wind erosion.

Page 448.

In work of N. A. Tuyezova (1959) there are given data of determination of physical property from series/number of blowholes of Tatar and Sargatsk prospecting areas of western-Siberian lowland, which show to significant decrease of density, increase in porosity and decrease of coefficient of rebound upon transfer from wings to arch/summary of structures of II order. This decrease most

considerably for it is sandstone, but it is developed also in other types of species/rocks, reaching (over the Tatar area) for the Cretaceous species/rocks -  $0.28 \text{ g/cm}^3$ , and for the Jurassic -  $0.14 \text{ g/cm}^3$ . The crest part of the Tatar structure is characterized by the considerable development of the coarse-grained rocks, in comparison with the pericline and the wings. It is possible to say thus that the laminar zonality of the density of species/rocks in this case is caused by a whole series of lithofacies factors.

All this gives grounds to hope for the fact that subsequently gravitational prospecting with utilization of high-accuracy gravimeters must obtain application during searches for structures in western-Siberian lowland. In this case it is possible to rely on the fact that in the internal regions the basins/depressions of structure will be developed by the local minima of gravitational force.

Abroad idea about existence of laminar zonality of physical properties of sedimentary rocks, its bond with structures also of account of this zonality with interpretation of results of gravitation prospecting works is not thus far still completely realized. Meanwhile, is a series/number of the facts, which speak, that this idea is confirmed by the practice of foreign works. We already gave above example to the gravity anomaly above the anticlinal fold in California (USA), which is undoubtedly connected with the laminar zonality of the density of facies nature (appearance in the section/cut of great thickness of siliceous schists); there the

discussion dealt with the large/coarse anticline of young folding region.

In platform regions gravitational prospecting frequently gives results, which most plausibly and simply can be interpreted taking into account possible presence of laminar zonality of density of species/rocks. As the example let us point out the work of L. Spencer and D. Peters (1948), where the local negative gravity anomaly of small intensity (about 0.5 mgal) above the gently sloping anticlinal fold, composed in the upper (studied by drilling) part of the section/cut with a schist-carbonate thickness; with the fold there is connected large petroleum deposit "Magnolia field" in the region of midcontinent (USA). For the explanation to anomaly the authors had to do an assumption about the probable presence in the lower (not studied by drilling, investigated only by seismic survey) part of the section/cut of the fold of the powerful/thick saliferous horizon/level with the low density, whose uplift/rise, on their assumption, and conditions the appearance of a gravitational minimum.

Page 449.

It is much more natural, however, to assume that the gravitational minimum is connected with the zone of the increased susceptibility to cracking in crest fold.

The same type negative gravity anomaly, judging by article of R. Rayk and D. Walton (1956), is discovered in section of the largest

petroleum deposit "Parensis" of the Aquitaine basin (France), which is located in the crest part of a large anticlinal fold, composed by strongly fissure cavernous limestone; it is completely probable that origin and this anomalies has reason, analogous indicated above.

Thus, it is possible to assume that study and account of phenomenon of laminar zonality of density must contribute to considerable increase in efficiency of gravitational prospecting during searches for petroleum and gas fields, connected with dome-shaped platform structures. It also denotes some prospects for the utilization of a method during the searches for the lithologic-stratigraphic beds of oil and gas.

Page 450.

Chapter IX.

SEARCHES AND PROSPECTING OF THE DEPOSITS OF ORE AND NONMETALLIFEROUS  
USEFUL MINERALS.

§59. Generalities.

Gravitational prospecting enters into complex of geophysical works during searches and prospecting of many ore and nonmetalliferous useful minerals. In this case it is assigned to the solution of the different geologic problems:

- 1) large-scale geologic mapping in connection with the searches for those or other useful minerals;
- 2) the straight/direct searches for deposits;
- 3) prospecting deposits.

If we examine entire set of problems indicated, then enumeration of types of deposits, on which sufficiently extensively is used gravitational prospecting, is sufficiently vast (Table 27). From their number we will be bounded only to those objects and problems, during investigation of which the utilization of gravitation prospecting is, according to the work experience, most complete and effective. In the examination of this type of objects and problems we barely touch on methodic and technical questions of the application of gravitational prospecting and we give entire attention to questions of the geologic interpretation of gravity anomalies in connection with

these objects and problems.

If we compare petroleum and ore gravitational prospecting, then between them it is possible to perceive following essential differences.

1. Petroleum gravitational prospecting is usually limited to photographings of sufficiently small scale (rarely larger/coarser than 1:200000); ore gravitational prospecting requires, as a rule, large-scale photographings (1:25000 - 1:5000, sometimes 1:2000 - 1:1000).

2. Exceptionally/exclusively gravimetric photographing composes basis of petroleum gravitational prospecting (postwar period), while in many ore regions variometric or gradiometric photographing composes basic (on labor inputs and resources) volumes of gravitation prospecting works.

Page 451.

3. Petroleum gravitational prospecting usually comes forward in complex with seismic survey; ore gravitational prospecting usually is matched with magnetic prospecting, electrical prospecting, sometimes with metallometry.

4. Petroleum gravitational prospecting is frequently limited to qualitative geologic utilization of anomalies, ore gravitational

---

prospecting frequently puts to use different methods of quantitative interpretation of anomalies.

5. If petroleum gravitational prospecting is occupied actually by problems of geologic mapping in connection with searches for deposits of oil and gas, then ore gravitational prospecting in many instances deals concerning useful minerals, frequently solving problems of straight/direct searches, and sometimes also prospectings of deposits - up to calculation of reserves.

Table 27. Objects and the problems, investigated with the wide utilization of gravitation prospecting works during the searches and prospecting of ore and nonmetalliferous useful minerals (besides oil and gas).

Объекты (1)	Крупномасштабное геологическое картирование (2)	Поиски месторождений (3)	Разведка месторождений (4)
(5) А. Рудные месторождения:			
(6) Железо . . . . .	○	○	+
(7) Хром . . . . .	+	○	○
(8) Никель . . . . .	+	+	○
(9) Медь . . . . .	+	○	○
(10) Полиметаллы . . . . .	+	○	
Б. Нерудные месторождения:			
(11) Апатит . . . . .	+	+	
(12) Корунд . . . . .	+	+	
(13) Барит . . . . .		+	
(14) Сера . . . . .	+	○	
(15) Соли . . . . .	○	○	○
(16) Бораты . . . . .		+	
(17) Угли . . . . .		+	

Note: + - wide utilization of gravitational prospecting; ○ - wide utilization of gravitational prospecting with the high industrial effect.

Key: (1). Objects. (2). Large-scale geologic mapping/charting. (3). Searches for deposits. (4). Prospecting deposits. (5). A. Ore deposits. (6). Iron. (7). Chromium. (8). Nickel. (9). Copper. (10). Polymetals. (11). B. Nonmetalliferous deposits. (12). Apatite. (13). Corundum. (14). Barite. (15). Sulfur. (16). Salts. (17). Borates. (18). Carbons/coals.



Page 452.

6. Usual object of petroleum gravitational prospecting - deep structures. Ore gravitational prospecting usually deals concerning the objects, which slope comparatively shallow from the surface. Furthermore, in certain cases ore gravitational prospecting actively "goes to the approach" with object being investigated, coming forward in the role not only of ground-based, but also subterranean photographing (in mine workings), for example within the ore field being investigated.

These characteristic features of ore gravitational prospecting will be clearly visible, also, in subsequent presentation. This presentation is limited by framework and goals of the book; therefore it does not apply to all 12 useful minerals, enumerated in Table 27, but it is limited in essence only to the most mastered by gravitational prospecting types of deposits. At conclusion of chapter we briefly stop on some problems of the interpretation of the results of the subterranean gravitation prospecting works, & recently begin to play role during the searches for different useful minerals.

560. Iron-ore deposits of type KMA and Krivoy Rog.

As already mentioned above, iron-ore deposits of type KMA and Krivoy Rog present classical object of gravitation prospecting works, on which application of this method proved to be very effective. To the successful application of gravitational prospecting in this case

contribute favorable physico-geological conditions, and also the 40-year "industrial length of service" of method on the iron-ore deposits (in KMA - since 1921, in Krivoy Rog - since 1925). For a large part of this prolonged period the application of gravitational prospecting was very intensive, moreover the results of the interpretation of gravity anomalies underwent systematic check and utilization in the process of geological exploration works.

Basic goals, to solution of which was assigned gravitational prospecting, were following:

- 1) study of general/common structure of iron-ore basin;
- 2) mapping/charting iron-ore thickness;
- 3) searches for rich iron ores.

Let us examine application of gravitational prospecting during solution of each of goals indicated.

Page 453.

Study of general/common structure of iron-ore basin. Thicknesses of crystalline schists of Precambrian, including ferruginous quartzite (see §4 of Chapter I), differ as a whole in the density from those accomodating from gneissoids; the excess density of entire iron-ore suite proves to be equal to approximately 0.15-0.20 g/cm<sup>3</sup>, if it is considered with the help of the formula

$$\sigma = \frac{\sum_{k=1}^n \sigma_k d_k}{\sum_{k=1}^n d_k} - \sigma_{av}$$

where  $\sigma_k$  and  $d_k$  — value of density and thickness of the separate horizons/levels of iron-ore suite;

$\sigma_{av}$  — average density of the enclosing rocks.

Synclitorium of iron-ore thickness are noted usually by sufficiently intensive (ten milligal) positive gravity anomalies; they are accompanied by positive magnetic anomalies. In this case, however, it proves to be that those and other anomalies, which have general/common geologic reason, are distinguished by nature: the maximums of gravitational force are placed above the center sections of synclinal structures, and magnetic maximums ( $Z_s$  or  $T_s$ ) — above the emergences/outcrop of the separate beds of iron-ore rocks to the surface of basement (Fig. 243). This nonconformity of the location of gravitational and magnetic maximums is caused by a difference in analytical nature of the anomalies: analog  $Z_s$  (in the two-dimensional goal) is not  $\Delta g$ , but lapse  $W_{ss} = \frac{\partial g}{\partial s}$  (see §16 of Chapter I).

Joint examination and analysis of gravitational and magnetic anomalies give very distinct picture of arrangement of structural elements of iron-ore suite in plan/layout. Besides this analysis of gravity anomalies gives the possibility on the separate profiles, which intersect iron-ore suite, to construct for it schematic diagrams and to approximately consider the probable propagation of suite at the depth; the example of this type of constructions for one of the iron-ore regions is given in Fig. 244. Calculations it is desirable

to conduct for the profiles, investigated by detailed variometric (see below) and magnetic survey, and also by drilling, which makes it possible during the selection of section/cut to immediately assign horizontal sizes/dimensions and basic elements of synclinal structure. Selection is conducted with the utilization of the templates (see §46 of Chapter VI). It is useful to also consider area  $S$  of the section of iron-ore suite according to A.G. Gamburtsev's formula (see VI, 37 and VI, 41):

$$S = \frac{\int_{-\infty}^{+\infty} \Delta g dr}{2/\sigma\pi}.$$

Page 454.

Before production of this type of calculations it is frequently necessary to produce localization of gravity anomaly being investigated, that in presence of profile of sufficient extent in majority of cases it is possible to do by simplest graphic method, by considering that regional background and effect/action of accompanying anomalies on the interesting us section of gravitational profile are expressed by sloping straight line (Fig. 245). If regional background with the interpretation is not excluded, then large errors during the determination of the depth of the propagation of iron-ore synclinal structure are possible. These errors can be substantially reduced with the exception/elimination of regional background even by the described elementary approximate method.

Mapping/charting iron-ore thickness. This problem is solved with the utilization as the basic method - variometric (or gradiometric) photographing, auxiliary - magnetic survey. Scale and detail of photographing depend on the depth of the bedding of iron-ore suite.

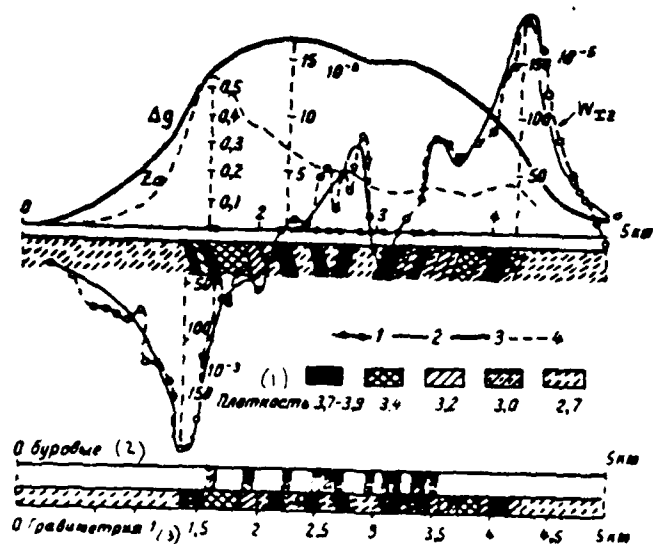


Fig. 243. Gravitational and magnetic anomalies along profile through folding iron-ore basin. Anomaly curves: 1 -  $\Delta g$ ; 2 - gradient  $W_{xz}$  of observation; 3 - gradient  $W_{xz}$  theoretical, that corresponds to sheet section/cut; 4 - component  $z_1$  of magnetic field.

**Key: (1). Density. (2). Boring. (3). Gravimetry.**

Page 455.

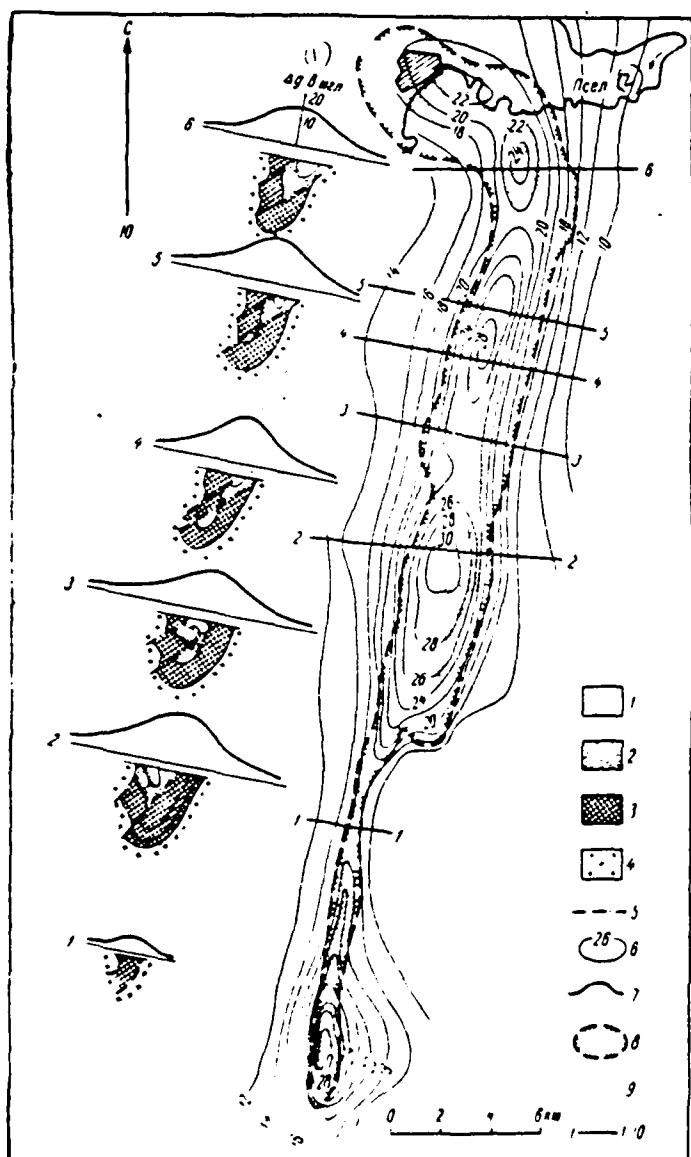


Fig. 244. Plan/layout of gravity anomaly above iron-ore basin, gravitational profiles and corresponding to them geologic sections/cuts. 1 - sandstones, micro-quartzite and dolomite ( $\sigma_{\text{avg}} = 0,1-0,2 \text{ g/cm}^3$ ); 2 - lower and middle thicknesses of upper section ( $\sigma_{\text{avg}} = 0,5-0,6 \text{ g/cm}^3$ ); 3 - whole ferruginous quartzite and slates of middle

and lower sections ( $\sigma_{\text{дог}} = 0,35-0,70 \text{ g/cm}^3$ ); 4 - granites, gneiss; 5 - faults; 6 - isoanomalies of gravitational force; 7 - calculated curve  $\Delta g$ ; 8 - outline of magnetic anomaly on isodynamic line 1000  $\gamma$ ; 9 - outlines of ore body; 10 - line of profiles.

Key: (1). In mgal. (2). Psel.

Page 456.

Practice developed the following rule: observations along the profiles, assigned transversely of the course/strike of suite, are conducted through the interval, whose value is taken one order with the average depth of the bedding of iron-ore suite in the region being investigated; the distance between the profiles is taken several times steeper pitch along the profile. In the sections with an intensive change in the gradient of gravity force the additional observations are placed. Usually adopted picture scales of the results of photographings - from 1:5000 to 1:25000.

During designing and interpretation of results of gravitation prospecting works it is necessary to know hypsometry of surface of basement in region being investigated. For its characteristic are used data of drilling according to the blowholes available in the region, data of electro-prospecting and seismic survey works, and also calculations of the depths of the bedding of iron-ore suite on the magnetic anomalies (Andreyev, 1955; Krutikhovskaya and Kuzhelov, 1960).



Methodology of interpretation of curves of gradient of force of gravity, used in iron-ore basins for sheet structures with selection of sheet section/cut and summation of corresponding theoretical curves, in general form was described in §43 of Chapter V. With the help of this methodology according to the data of variometric photographing it is possible to carry out construction of the sheet sections/cuts of iron-ore suite with the large detail and the sufficiently high accuracy. This can seem surprising, if we have in mind the ambiguity of the solution of the inverse problem of interpretation. Matter here is the fact that physico-geologic conditions of iron-ore basins are favorable for obtaining with the interpretation of sufficiently simple results in view of the fact that with the upper edges of beds the singular points of anomalous field are connected, and this gives the possibility of sufficiently confident construction of sheet section/cut. For the beds with the ratio of the horizontal thickness  $d$  to depth  $h$  of the upper edge

$$\frac{d}{h} > 1$$

the horizontal thickness  $d$  and excess density  $\sigma$  (with assigned  $h$ ) usually are determined with the error not more than 20-30%. With an increase in the relation indicated the accuracy of interpretation increases/grows, with the decrease - it falls.

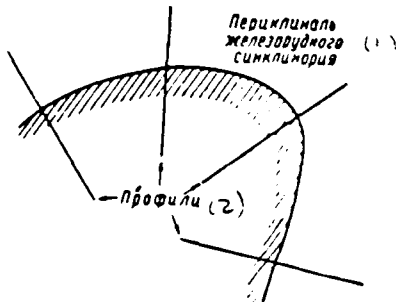


Fig. 246. Worthwhile arrangement of profiles on pericline of iron-ore structure.

Key: (1). Pericline of iron-ore synclorium. (2). Profiles.

Page 458.

Having series/number of this type of sections/cuts along system of profiles, it is possible to construct sheet map/chart of investigated section, which is basis for construction of geologic map/chart of iron-ore thickness. One should indicate that the composition of such geologic maps/charts without the utilization of gravitation prospecting data is in many instances very complex problem even when a large number of the exploration wells is present. Work experience shows the modern need for the utilization of gravitation prospecting (variometric) works during mapping/charting of iron-ore regions.

Besides establishment of location and elements of bedding of beds of ferruginous quartzite and other rocks, on sheet map/chart is fixed the position of waste disturbances/breakdowns, which are set to

systematic shift of beds on contiguous profiles (Fig. 247), and also with respect to abrupt change in sense of the vector of horizontal gradient of gravitational force.

Searches for rich iron ores. With the iron-ore formations of type KMA and Krivoy Rog are connected the deposits of the rich iron ores of two types: 1) residual hematite-martite - in the crust of the wind erosion of basement; 2) endogenic magnetite-martite - within the beds of ferruginous quartzite. First type ores have basic practical value.

Finally developed methodology of searches for rich iron ores with application of gravitational prospecting and other geophysical methods is not thus far developed, but is explained series/number of prospecting geophysical signs, which considerably facilitate solution of problem indicated and in number of cases of deposits of rich ores directly led to detection.

Detection of deposits of residual type rich iron ores in certain cases proved to be possible during drilling in limits of propagation of iron-ore suite of sections, statistics of following geophysical signs:

- 1) on gravitational prospecting - presence of intensive maximum force of gravity, and also increased excess density of beds, isolated via interpretation of gravity anomalies;

- 2) on magnetic prospecting - lowered/reduced intensity of

anomalous magnetic field;

3) on seismic survey (KMPV [correlation method of refracted waves]) - presence of dip of horizon of high boundary speed, which corresponds to surface of invariable crystalline rocks of basement; appearance of new horizon/level with boundary speed, which corresponds to surface of crust of wind erosion.

As example Fig. 248 gives results of gravitation prospecting, magnetic prospecting and seismic survey works on one of sections of development of iron-ore formation.

Page 459.

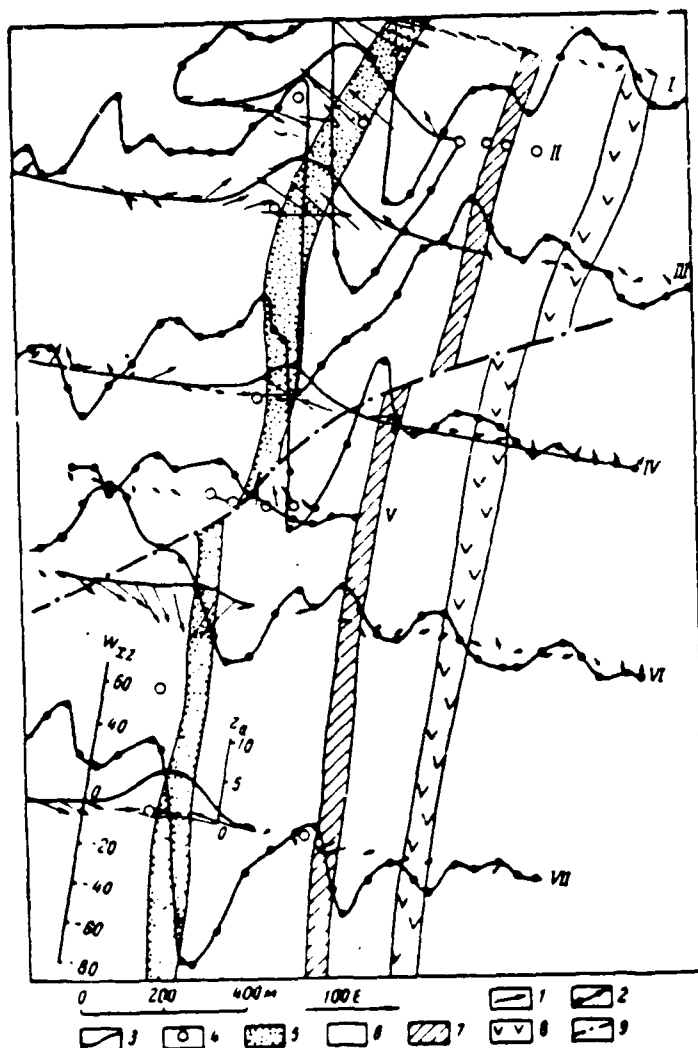


Fig. 247. Sheet map/chart of iron-ore region. According to K. V. Klimova. 1 - vectors of the horizontal gradient of gravitational force; 2 - curve of horizontal gradient of gravitational force,  $W_{22}$  in gauss; 3 - curve of vertical component of magnetic field  $Z_v$  in thousand of gammas; 4 - blowhole; 5 - ferruginous quartzite; 6 - slates; 7 - different gneiss; 8 - metabasic materials of greenstone strip; 9 - predicted line of fault.

Page 460.

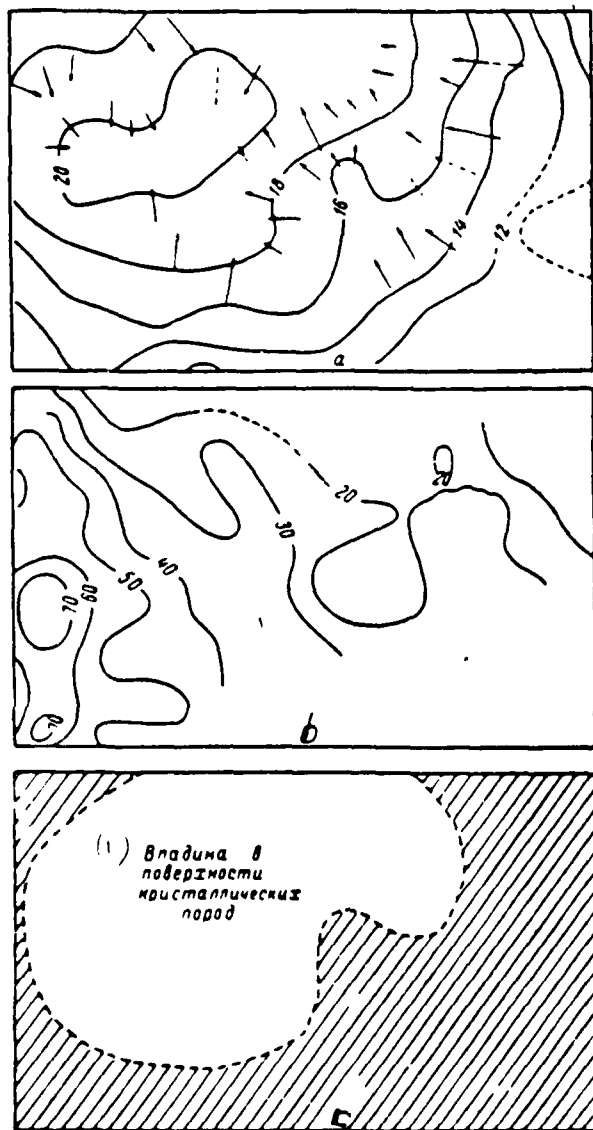


Fig. 248. Results of gravitation prospecting (a), magnetic prospecting (b) and seismic survey (c) works on deposit of residual type rich hematite-martite ores.

Key: (1). Basin/depression in the surface of the crystalline rocks.

Page 461.

As we see, in this section is observed the combination of positive gravity anomaly, relative to the lowered/reduced (slightly anomalous) magnetic type, that slopes in the depression in the roof of the beds of ferruginous quartzite and their accomodating slates.

#### §61. Chromites.

On deposits of chromites method of gravitational prospecting is used for: 1) mapping of masses of ultrabasic rocks, with which are connected these deposits; 2) searches for chromite ore bodies; 3) prospecting chromites.

Mapping/charting masses of ultrabasic rocks. The masses of the ultrabasic rocks (serpentinous peridotite, dunite) will lie among the sedimentary or acid igneous rocks and they are usually separated among the latter by low positive excess density. Because of this above the masses are observed positive gravity anomalies, in certain cases sufficiently intensive, in others - weak, up to the fact that some contacts of ultrabasic mass with the enclosing rocks almost not at all are separated or are separated not by positive, but negative excess density. The latter fact stands in connection with the differentiation of density within the enclosing rocks and the rocks of mass, and also with the more intensive serpentinization of the ultrabasic rocks. As we already noted above (§4 Chapter I), the serpentinous ultrabasic rocks have low density and noticeably do not

differ in this parameter from the acid and sedimentary rocks. Therefore during mapping/charting of the ultrabasic rocks gravitational prospecting should be compulsorily used in the complex with magnetic prospecting, keeping in mind, that in the magnetic field even the intensively serpentinous ultrabasic rocks are expressed by positive anomalies.

Fig. 249 gives example to gravity anomaly above Kempersayskiy mass of ultrabasic rocks according to data of variometric photographing. As we see, the vectors of the horizontal gradient of gravitational force note the boundaries of mass with the enclosing rocks, but usually are not directed perpendicularly to contact as a result of the systematic increase of gravitational forces from the north to the south. The executor/performer of works A. A. Nepomnyashchikh (1959) explained this special feature by the fact that in the southern part of the mass its vertical thickness is increased in connection with the possible presence here of feeding channel of intrusion. On the greater part of the area of mass, in accordance with the produced interpretation of anomaly, the latter has flat/plane platelike form with the significant preponderance of the horizontal sizes/dimensions above the vertical.

Page 462.

In some places the position of the contacts of mass with the enclosing rocks as a result of geophysical works underwent significant changes in comparison with the results of previously carried out geological



surveying works (Fig. 250).

Searches for chromite ores. Gravitational prospecting is usually the only geophysical method, whose application during the searches for chromite ores in many instances is possible and worthwhile. The first discoveries of chromite ore bodies with the application of variation gravitational prospecting were done in 1933 by us in USSR (Andreyev, 1937). Subsequently the same method was with great success used for the searches and prospecting of chromites in the territory of the largest Kempersayskiy chromite deposit; in its honor were named on this deposit ore bodies "Geophysical I" and "Geophysical II", mentioned in the courses of ore deposits (Tatarinov, et al, 1947).

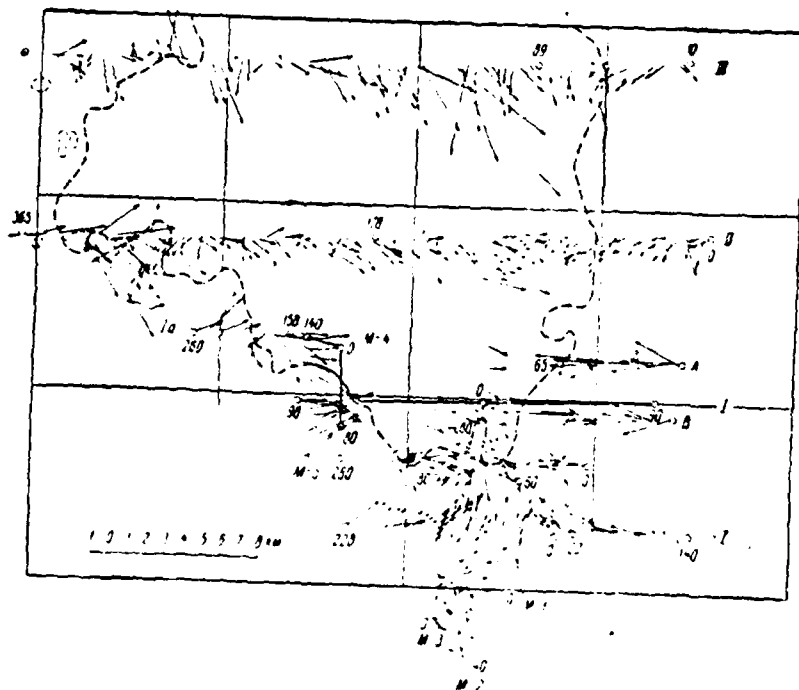


Fig. 249. Gravity anomaly above chromite mass of ultrabasic rocks. According to A. A. Nepomnyashchikh (1959).

Page 463.

Ore bodies, composed by massive chromite and sloping in serpentinous peridotite (serpentines) are separated by significant excess density (on the order of 1.2-1.5 g/cm<sup>3</sup>) and they are characterized by gravity anomalies of positive sign, which during detailed prospecting photographing in many instances are completely distinctly caught in measurements with gravitational variometers (Fig. 251) or high-accuracy gravimeters (Fig. 252). During the searches for chromites the very thick network/grid of observations (through 20-25 m) and the very thorough elaboration of anomalous sections with

thickening of observations to 2-5 m is required. Usually, together with the ore anomalies, is revealed a significant quantity of anomalies of barren, caused by the density heterogeneity of enclosing rocks (serpentine), by the inclusions in them of the vein rocks, etc. Separation of ore and nonmetalliferous anomalies frequently proves to be possible to produce with the utilization in the complex with gravitational prospecting of magnetic prospecting (see Andreyev, 1937), and also chromometric photographing.

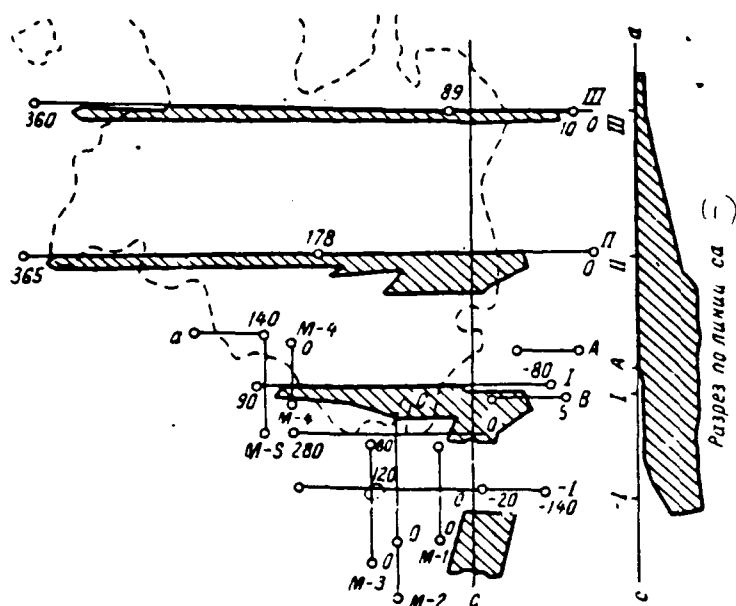


Fig. 250. Sections/cuts and plan/layout of mass of ultrabasic rocks. Results of the interpretation of the gravity anomaly, given in Fig. 249. According to A. A. Nepomnyashchikh (1959).

Key: (1). Section/cut along the line ca.

Page 464.

Thus, the zones of the condensed serpentines are usually developed not only by gravitational maximums, but also by maximums of component of magnetic field, and furthermore, at the low thickness of drifts in the form of the small uplifts/rises of relief, but above the vein bodies of microdiorites, which are developed by gravitational  $Z_1$  maximums, are observed reductions in component  $Z_2$  of magnetic field.

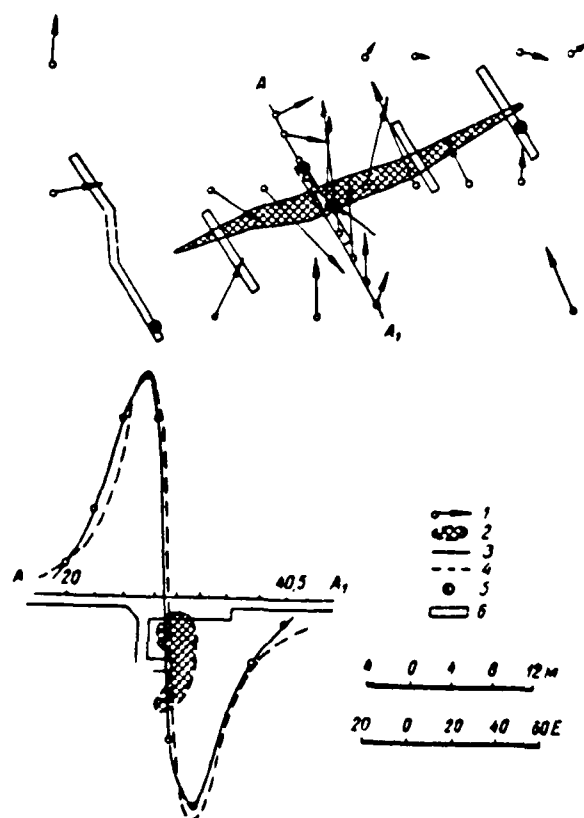


Fig. 251. Results of variometric gravitational photographing above deposit of chromite. According to B. A. Andreyev, (1937). 1 - vectors of gradient; 2 - outline and the section/cut of ore body; 3 - curve of the gradient of observation; 4 - curve of gradient theoretical (corresponding to section/cut); 5, 6 - untimbered shaft and furrow.

Page 465.

On the other hand, the gravitational maximums of ore nature in instances must be accompanied by the increased concentration of

chromium in the eluvium - rock waste. Chromite presents the mineral, stable in the zone of wind erosion, and chromite ores are accompanied by the aureoles of mechanical type scattering.

Appropriate calculations show (Andreyev, 1937) that with production of prospecting variometric photographing with interval between observation points 20-25 m and subsequent thorough elaboration of anomalous zones it is possible to rely on detection of chromite ore bodies with thickness of 2-5 m, which slope at depths from 1 to 13 m from surface. These calculations are confirmed by the practice of prospecting variometric works.

Prospecting ore bodies. As a result of the high value of excess density and sufficiently significant sizes/dimensions of ore bodies in comparison with the depth of their bedding, ore gravity anomalies usually are clearly expressed and have high intensity. If average density values of chromites and enclosing rocks for the region being investigated are sufficiently reliably known, then ore anomalies frequently can be subjected to the quantitative interpretation, whose results will have a value with the prospecting works. These will be, first of all, those cases, when ore anomalies have a course/strike in the direction, perpendicular to the line of observations, and to their interpretation it is possible to apply formulas and methods of two-dimensional goal.

Form and sectional area of ore body can be selected with the help

of template for bodies of arbitrary form (see §46 Chapter VI). This method is especially convenient and reliable, if the position of ore body in the upper levels partially is already established by prospecting works.

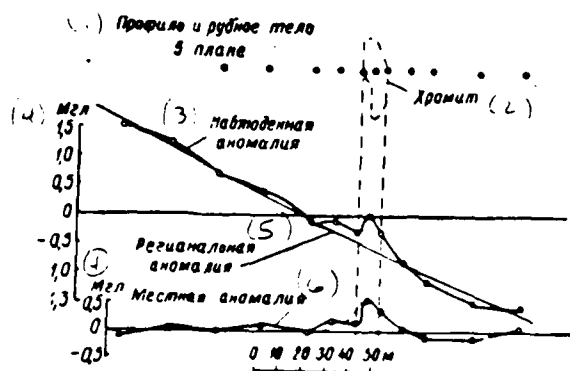


Fig. 252. Results of gravimetric photographing above deposit of chromite.

Key: (1). Profile and ore body in the plan/layout. (2). Chromite. (3). Observed anomaly. (4). Mgal. (5). Regional anomaly. (6). Local anomaly.



Page 466. <sup>π</sup> If along the profile the distribution of anomaly  $\Delta g$ , expressed by the clearly localized maximum (Fig. 253) is known, then it is possible to determine the cross-sectional area of body S, using the formula of G. A. Gamburtsev mentioned above. The comparison of data of similar calculation with the data of prospecting, carried out by the author for one of the deposits (Andreyev, 1937), showed that virtually in this case calculation determines only the sectional area of ore bodies to the level, which corresponds to the approximately triple horizontal thickness of ore bodies, since the lower parts of these bodies according to gravitational data are determined unstably. Data of calculations it proves to be possible to use during the calculation of the reserves of chromite ores on the lowest categories ( $C_2$  and  $C_3$ ).

#### 562. Pyritic ores (copper, sulfur).

Among copper-ore and sulfuric deposits pyritic deposits have high value. During the searches and prospecting of pyritic deposits usually are used the complex of geophysical methods - magnetic prospecting, electrical prospecting, gravitational prospecting. The first two methods are used for the preliminary investigation of promising areas and usually is separated a large quantity of anomalous zones, from which ore are only some, comparatively scarce. These anomalous zones are in turn investigated by gravitational prospecting, which frequently makes it possible to definitely solve a question about their ore or nonmetalliferous nature before setting of testing

mine-drilling works. Furthermore, in certain cases gravitational prospecting makes it possible to make conclusions about sizes/dimensions and shape of ore bodies, that have value during prospecting of the latter.

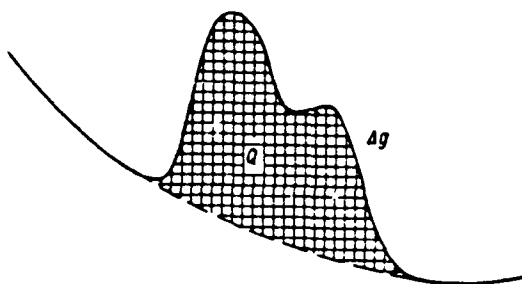


Fig. 253. Determination of "anomalous area" during calculation of cross-sectional area of chromite ore bodies by G. A. Gamburtsev's method.

Page 467.

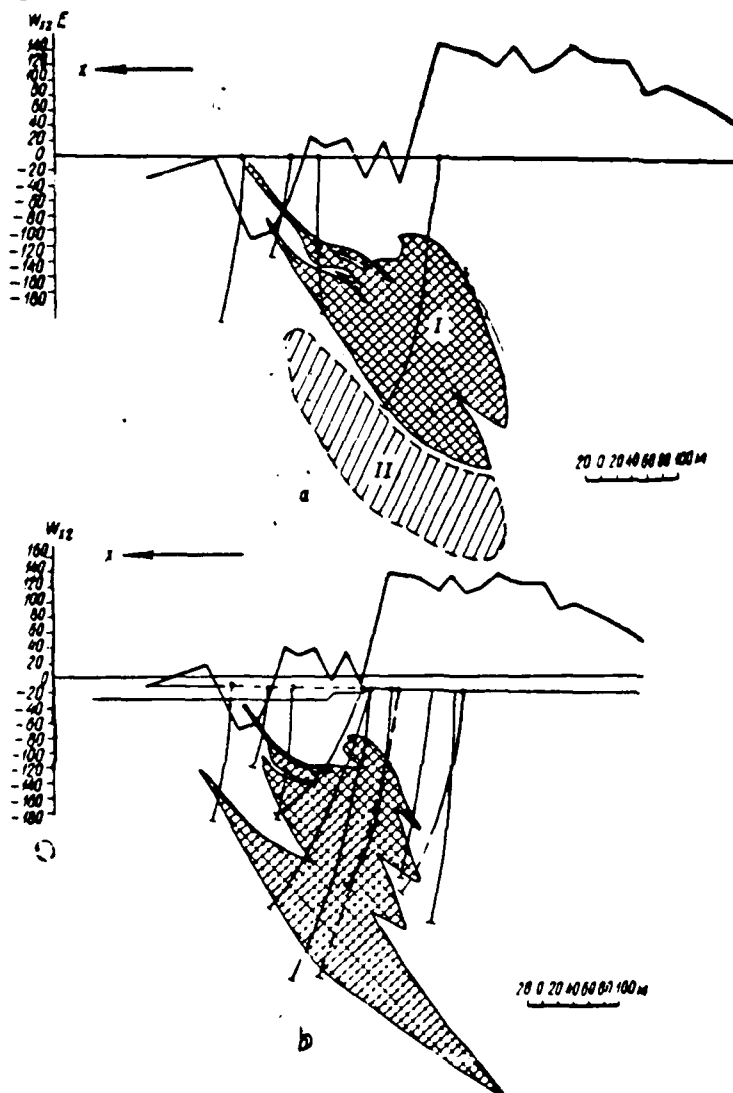


Fig. 254. Results of interpretation of materials of gravitation prospecting works on deposit of copper pyrites of South Urals. According to A. Ya. Jaros, et al (1957). a) the geologic section/cut of deposit according to the data of the prospecting works, carried out before setting of gravitational prospecting; I - ore body, known; II - new ore block, predicted according to the data of gravitational prospecting. b) the new geologic section/cut of deposit, which

) confirms the conclusions, made on the interpretation of gravitation prospecting data.

Page 468.

With beds of pyritic ores are connected intensive gravitation anomalies, in particular on gradient of gravity force, which is explained by high excess density of ores with respect to surrounding rocks ( $1.0-1.8 \text{ g/cm}^3$ ) and by significant sizes/dimensions of ore bodies in comparison with depth of their bedding. By us in the USSR gravitational prospecting successfully was used on the deposits of pyritic ores in Urals (Andreyev, etc., 1941; Jaros, Ansimov and Polyakov, 1957), also, in Karelia (Katskov, 1957).

) Interesting example, which shows possibility of gravitational method during prospecting of pyritic ores, is given in Fig. 254, where results of variometric and gravimetric works and section/cut are shown according to data of drilling on one of deposits of copper pyrites of South Urals. The excess density of pyritic ores with respect to the enclosing rocks (albitophyres, porphyrite), determined on the cores of the exploration wells, proved to be equal to  $1.7 \text{ g/cm}^3$ . The calculation of gravitation effect from the ore body, produced on the template for the section of body, determined by drilling, showed that the theoretical anomaly proves to be noticeably less in the intensity of the observed anomaly. During the selection of the section/cut, which corresponds to the observed anomaly, it was necessary to make an assumption about the presence at the depth of new large/coarse ore

body or about the propagation of known body at the large depth. Produced on the basis of these data additional reconnaissance of deposit with the depression of existing and the additive of new drill holes, confirmed the conclusion, made via the analysis of gravity anomaly, and led to the discovery of the new ore horizon/level (Fig. 254b) and to an increase in the reserves of deposit by 70%.

### 563. Deposits of mineral salts.

We already stopped (in §55) on analysis of salt dome structures with application of gravitational prospecting. Another object of this method, connected with the searches for mineral salts, is saliferous formations of some internal platform regions, including powerful sheet bodies of the halogen rocks. Before gravitational prospecting and other geophysical methods (seismic survey, electrical prospecting) is posed the problem of studying hypsometry of the surface of this type of sheet beds, which is coordinated with the general character of the bedding of the covering and basement rocks, but usually complex fine/small dome-shaped forms (Fig. 255).

Page 469.

If thickness of halide thickness is significant (more than depth of its upper surface) and at isolated points of territory being investigated this thickness opened by drill holes, then, as shows experiment, for interpretation of gravity anomalies in section being investigated it is expedient to attempt to use graph/diagram of

dependence of value of gravity anomalies from depth of occurrence of surface of salt, taking anomalies from gravitational map/chart for points of arrangement of blowholes, and depth of salt - according to data of drilling. If graph proves to be close to rectilinear, then we are right to allow that anomalous field is caused in essence by the effect/action of the upper surface of salt thickness, which usually has negative excess density  $\sigma$  with respect to the persalt thickness, so that decreases correspond to uplifts of salt, and to subsidences - increases in anomaly  $\Delta g$  (Fig. 256). The angular coefficient of straight-line relationship  $\Delta g = f(z)$ , where  $z$  - depth up to the interface being investigated, can be determined on the basis of formula (VI, 17):

$$\begin{aligned}\Delta g(x_2) - \Delta g(x_1) &\approx \\ &\approx 2f\sigma\pi(z_1 - z_2),\end{aligned}$$

whence

$$b = 2f\sigma\pi.$$

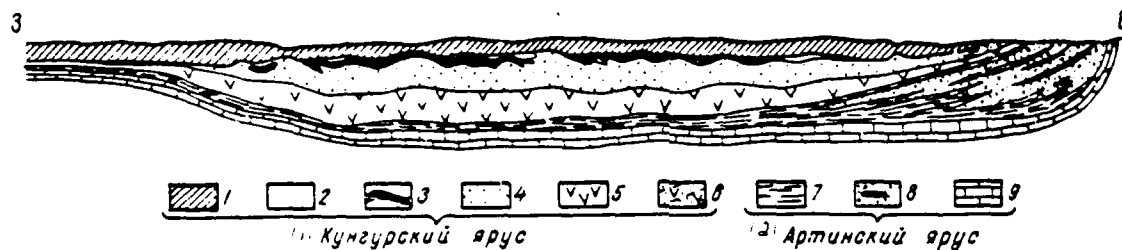


Fig. 255. Typical section of salt deposit of platform region. According to A. A. Ivanov (1953). 1 - cover rocks: gypsiferous clays, marls, limestone, sandstones; 2 - cover rock salt; 3 - thickness of guelder rose-magnesium salts; 4 - underlying rock salt; 5 - clayey-anhydrite thickness; 6 - saliferous clays and marls with the gypsum and the anhydrite; 7 - clay, limestone and dolomite; 8 - sandstones, marls, clay and conglomerates; 9 - limestone.

Key: (1). Kungur stage. (2). Artinskiy stage.

Page 470.

If  $\sigma$  is more or less constant in value and is reliably known and characteristic cross dimension  $l$  of separate uplifts/rises and downwarps/troughs of surface being investigated satisfies condition  $l \gg \sigma$ , then values of coefficient  $b$ , determined from indicated relationship/ratio and according to correlation graph, must be numerically close or equal. This type of correlation graph can be used for the conversion of values  $\Delta g$  into approximate values of  $z$ , that also was done in some saliferous regions.

General/common expression of coefficient of linear dependence is



given in formula (VI, 20).

#### S64. Deposits of carbons/coals.

Application of gravitational prospecting in carboniferous basins encompasses many-year period - more than 30 years. By us in USSR this type works were begun in 1929 on the outskirts of Donets basin and subsequently is undergone in this region considerable development in connection with the solution of structural-geologic problems. In the same direction gravitational prospecting obtained application, also, in a series/number of other carboniferous basins - in particular in lignitic basins of Urals, Kazakhstan and Middle Asia. Was used gravitational prospecting in some coal fields and abroad. It is explained that in certain cases gravitational prospecting can be applicable, also, for the liberation/precipitation of productive carboniferous suites and even separate large/coarse coal seams.

For illustration of application of gravitational prospecting in coal fields let us examine application of this method with resolution of problem of large Donbass. Essence of this problem, advanced by the important geologist Academician P. I. Stepanov in 1929, consists of the following. Donbass is half-open type folding coal field: in its central part the carboniferous depositions of the Donets Carboniferous period are bared and accessible to direct development, and on the periphery of basin these depositions are almost everywhere hidden under younger depositions of the Mesocenozoic. Primary task in the

problem of large Donbass consisted in the explanation of the actual outlines of the basin, within limits of which carboniferous depositions are located at the depth, accessible for the development (first hundreds of meters). In the solution of this problem, at present in essence completed, the most important role played geophysical methods and, in particular, gravitational prospecting.

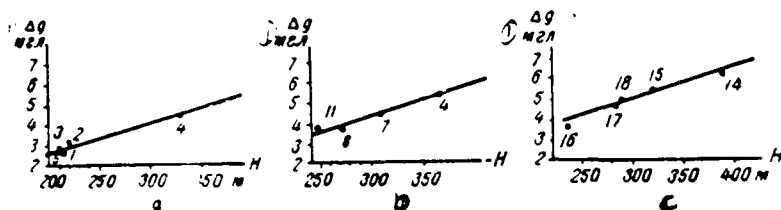


Fig. 256. Dependence  $\Delta g = f(H)$  for three regions (a, b, c) of deposits of potassic salts.  $H$  - depth to the roof of salt.

Key: (1). mg/.

Page 471.

Method was used, first, for explaining region of propagation of paleozoic geosyncline, with which was connected Donets carboniferous basin. This region, as now it is explained, passes through uncovered Donbass approximately to latitudinal direction, to the west from it it is wedged in between Kursk-Voronezh and Ukrainian Precambrian masses of Russian platform, and to the east it is continued by broad band between the Russian platform and the region of the Alpine folding of Caucasus up to the West coast of the Caspian sea (Fig. 257). The region of the propagation of the folding Paleozoic era is developed as the zone of the vast regional maximum gravitational force, whose position was established by conducting in the territory of area gravitational photographings indicated with the pendulums and by gravimeters. The maximum indicated can be explained by an increase in the density of great thickness of paleozoic rocks in the center section of the Donets geosynclinal zone, connected with the intensive manifestation here of folding.

410

Gravitational prospecting in complex with electrical prospecting and seismic prospecting was used also for studying hypsometry of surface of carbonaceous rocks of middle Carboniferous period on periphery of Donbass. This surface is structural-erosion, moreover central strip relative to the shallow bedding of rock of the carboniferous Carboniferous period proves to be limited from north and south by sharp ledged reductions in the roofs of the Carboniferous period, beyond limits of which carboniferous depositions usually are located at the depth, no longer accessible for performing of operational work. These ledged reductions in the surface of the Carboniferous period, which represent in many instances of the border of industrial Donbass, were revealed well with variometric photographing. The interpretation of the curves of the horizontal gradient of gravitational force was produced either by the method of P. M. Nikiforov, described in §43 Chapter V or by selecting the section/cut according to the diagram for the bodies of the arbitrary form, described in §46 Chapter V.

Example of this type of construction for one of regions is given in Fig. 258. Variometric photographing was conducted through the profile, whose northern end is passed along the section, where the rocks of the carboniferous Carboniferous period ( $\sigma=2.6$  g/cm<sup>3</sup>) outcrop on the surface, and remaining part - on the territory, where the surface of the Carboniferous period is hidden under the thickness of the depositions of the Mesocenozoic ( $\sigma=2.0$  g/cm<sup>3</sup>).

Page 472.

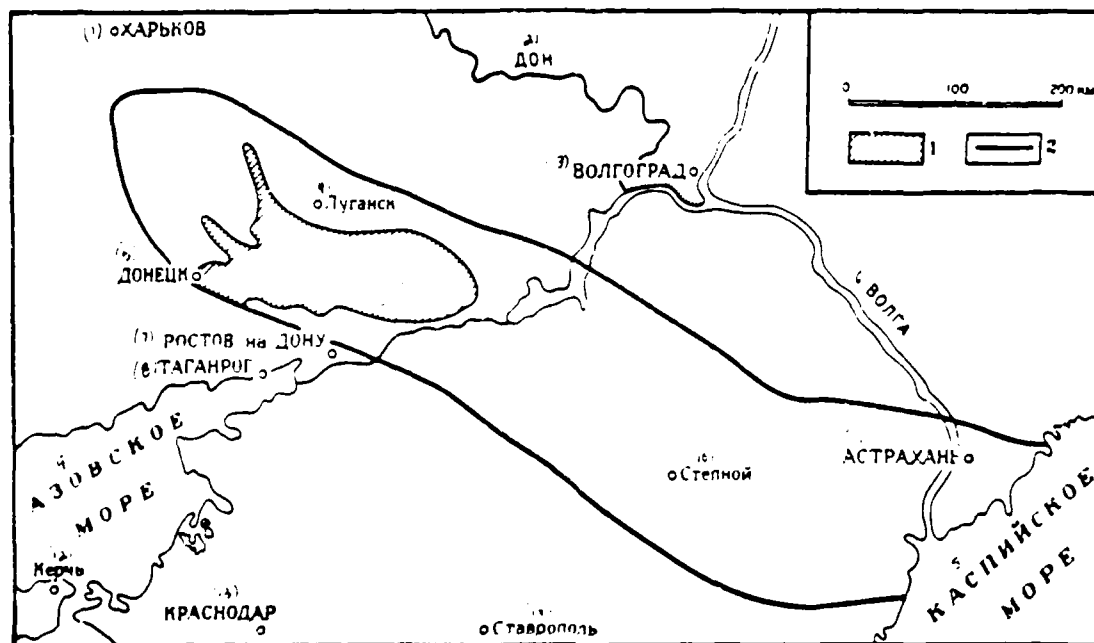


Fig. 257. Regional structure of Donbass and lying regions. According to N. S. Shatskiy et al. (1956). 1 - uncovered part of the Donets basin; 2 - outlines of large Donbass.

Key: (1). Kharkov. (2). Don. (3). Volgograd. (4). Lugansk. (5). Donetsk. (6). Volga. (7). Rostov on Don. (8). Taganrog. (9). Sea of Azov. (10). Steppe. (11). Astrakhan. (12). Kerch'. (13). Krasnodar. (14). Stavropol'. (15). Caspian Sea.

Page 472.

On the curve of horizontal gradient clearly are drawn two ledged subsidences of the horizon/level of positive excess density, which corresponds to the surface of the Carboniferous period, south of the section, in which the Carboniferous period is bared, and the

uplift/rise of this surface at the southern end of the profile. The curve of anomaly  $\Delta g$ , obtained by integrating the curve of gradient, is here given. The given section/cut of surface of carbon is constructed according to the curve of gradient by selection with the help of the template. the correctness of the construction of section/cut was subsequently with high accuracy confirmed by boring and seismic survey works.

In certain cases gravitational prospecting found use during straight/direct searches and prospecting of beds of brown coal, which considerably differ in their density from enclosing rocks and having sufficiently large thickness, in consequence of which caused by them gravitation effect sometimes proves to be significant in value. Fig. 259 shows results on profile of variometric photographing on "Jeliondel' deposit" (Australia), that intersects the edge/boundary part of the thick (more than 100 m) bed of brown coal ( $\rho=1.1 \text{ g/cm}^3$ ), which slopes in the tertiary sandy-clay depositions ( $\rho=1.9 \text{ g/cm}^3$ ), which in turn fill basins/depressions in the surface of Jurassic sandstones ( $\rho=2.4 \text{ g/cm}^3$ ).

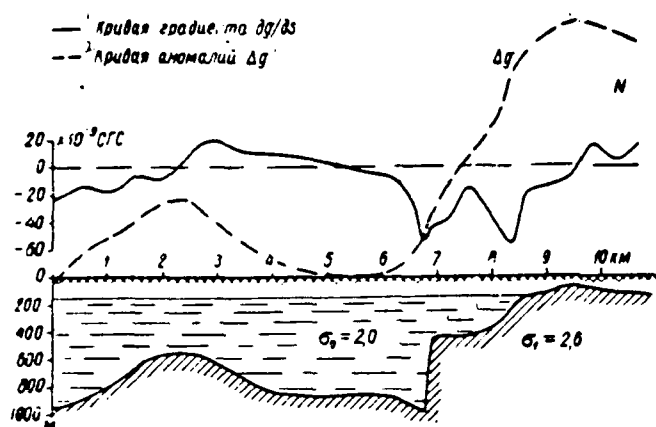


Fig. 258. Study of relief of surface of carboniferous Carboniferous period of Donbass with application of gravitation prospecting works. According to N. N. Samsonov.

Key: (1). Curve of gradient  $dg/ds$ . (2). Curve of anomalies  $\Delta g$ .

Page 474.

Gravitation effect basic in the value in this case is caused directly by the bed of brown coal. Of this it is possible to be convinced, if we take formula (V, 106) for the case of the vertical step

$$|W_{xz}|_{\max} = 2f\sigma \ln \frac{z_2}{z_1}$$

and substitute into it the appropriate values for the contact carbon/coal - sandy-clay rocks:  $\sigma = 1.1 - 1.9 = -0.8 \text{ g/cm}^3$  and, on the section/cut in Fig. 259,  $z_2/z_1 \approx 5.0$ , which gives

$$|W_{xz}|_{\max} \approx 171 \cdot 10^{-4} \text{ CGU} = 171E.$$

Respectively for contact sandy-clay rocks - sandstones we have:  $\sigma = 1.9 - 2.4 = -0.5$ ;  $z_2/z_1 \approx 3.2$ , which gives

$$|W_{xz}|_{\max} \approx 77 \cdot 10^{-4} \text{ CGU} = 77E.$$

i.e. anomaly is less in value than in first case, 2.2 times.

Prevailing effect of quite carbon bed on anomalous gravitational field one can see well also from given in Fig. 259 schematic diagram, obtained on curve of gradient  $W_{\alpha}$  by selection with utilization of template: maximum of curve corresponds to edge of bed.

In USSR gravitational prospecting on basis of variometric photographing was used for liberation/precipitation of productive carboniferous thicknesses on lignitic basins of eastern slope of Urals (Jaros, 1961).



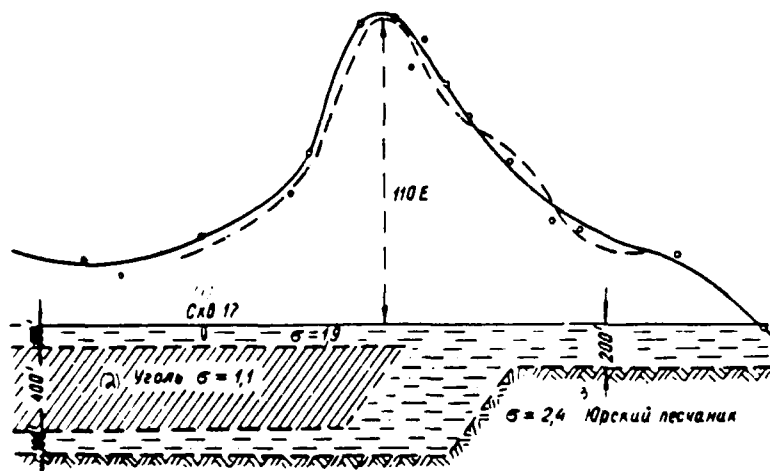


Fig. 259. Results of gravitation prospecting works on lignitic deposit "Jeliondel" (Australia). According to Edzy and Laby (1932).

Key: (1). Hole. (2). Coal. (3). Jurassic sandstone.

Page 475.

#### 565. Subterranean (mine/shaft) gravitational prospecting.

Subterranean (mine/shaft) gravitational prospecting is developed in essence in connection with searches for ore deposits: copper, polymetals, iron, etc. In certain cases they tried to use it (abroad) also on the deposits of carbon/coal and salt. Works were produced both with variometers and with gravimeters. The works, carried out by underground gravitational prospecting, have experimental or experimental-production character mainly. In this sense, and also according to the planned positive results, these works determine prospects, in a number of cases completely determined, of important

region of the future industrial utilization of gravitational prospecting.

Slow development and introduction of subterranean gravitational prospecting is explained by complexity of goals, which it is necessary to solve in connection with conducting, processing/treatment and geologic interpretation of results of gravitational measurements, conducted in mine workings. We will pause here only at the special features of the goal of the interpretation of the results of this type of photographings.

The fact is limitation of subterranean gravitational prospecting that object (usually ore body itself, sometimes ore-bearing structure) proves to be arranged/located very differently with respect to production/consumption, in which are produced observations. How this complicates the interpretation of the results of these observations, is evident at least from the fact that one and the same ore body, for example spherical form, arranged/located under the production/consumption, causes maximum, and arranged/located above the production/consumption - minimum of anomaly  $\Delta g$ , and with the arrangement of this body on the side from the production/consumption, in the plane of observations, its gravitation effect can be equal to zero (§34 Chapter V).

Conditions of interpretation, however, substantially are facilitated, if about possible arrangement of object being

investigated is any additional information (for example, data of prospecting), and gravitational measurements are made not on one, but at several horizons/levels. With the interpretation it is necessary to have in mind those laws governing spatial distribution of the anomalous elements of the gravitational field, which were in detail investigated by us for different bodies of correct geometric form in Chapter V.

Is most elaborated procedure and interpretation of results of subterranean gravitation prospecting works for conditions for searches and prospecting chalcopyrite deposits Central Urals, established as a result of multi-flight experimental field works, carried out by department of exploration geophysics MGRI under management of Ye. A. Mudretsova (Mudretsova, 1958; 1960).

Page 476.

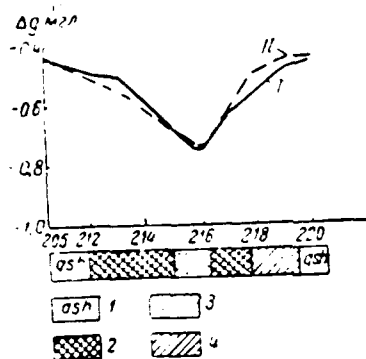


Fig. 260. Results of subterranean gravimetric works on chalcopyrite deposit. According to Ye. A. Mudretsova (1960). I - observed curve  $\Delta g$ ; II - calculated curve  $\Delta g$ ; 1 - chlorite-sericitic slates; 2 - sulfuric pyrite; 3 - copper impregnation; 4 - copper pyrite.

Key: (1). mg/.

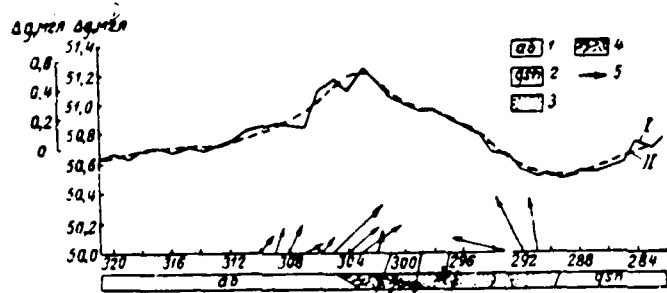
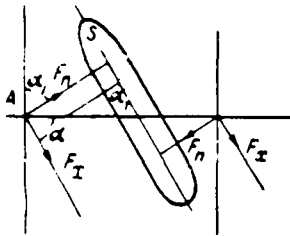


Fig. 261. Results of subterranean variometric works on chalcopyrite deposit. According to Ye. A. Mudretsova (1960). I - observed curve  $\Delta g$ ; II - calculated curve  $\Delta g$ ; 1 - albitophyres; 2 - chlorite-sericitic slates; 3 - copper impregnation; 4 - sulfuric pyrite; 5 - vector of total horizontal gradient.

Key: (1). mg/.



Page 477.

These works showed worthwhileness of the industrial introduction of gravitational prospecting together with other geophysical methods during the searches for blind ore bodies and during the detailed prospecting of the ore bodies, discovered by productions/consumptions under indicated deposit conditions. Work should be performed by the complex of high-accuracy gravimetric and variometric photographings, moreover the first is placed in the entire inspected territory, and the second - in the separate small sections for the purpose of the elaboration of the structure of anomalous field.

Fig. 260 gives example of study of ore zone by gravimetric photographing. Profile intersects ore lens for its entire extent, beginning from picket 212. Anomaly  $\Delta g$  is obtained of negative sign in connection with the fact that the base mass of bed is arranged/located above the investigated working. As we see, anomaly has the small intensity (about 0.4 mgal). Fig. 261 shows the results of the elaboration of ore anomaly by subterranean variometric photographing.

For quantitative interpretation of anomalies  $\Delta g$  under Ye. A. Mudretsovoy's indicated conditions is developed special method, with which ore body is substituted by flat/plane material leaflet, which coincides with section/cut of body in incidence/drop. This replacement is possible, since the thickness of lenticular chalcopyrite ore bodies is usually small (5-10 m) in comparison with the sizes/dimensions of these bodies in the course/strike and in the incidence/drop. Are calculated normal and tangential components of the attraction of material leaflet (Fig. 262) with the help of the special templates, whose description is in the work of Ye. A. Mudretsova (1958).

Page 478.

#### CONCLUSION.

Let us bring short total carried out above detailed examination of all aspects of complex problem of geologic interpretation of gravity anomalies. Achievements in the solution of this problem in many respects determine the prospects for further development of gravitational prospecting; they substantially affect also the development of other geophysical methods, for example magnetic prospecting. The essential progress in the business of the geologic interpretation of gravity anomalies was reached and will be reached subsequently on the basis of the deepened analysis of all geological-geophysical conditions of applying of gravitational prospecting and those mathematical problems, which directly ensue from the essence of the geologic goals, placed before this method.

Both geological, and corresponding to them mathematical problems gradually are complicated, moreover in specific development stage of gravitational prospecting they require qualitative renovation and refinement of the developed earlier approaches and methods during geologic interpretation of data. Development in estimation and interpretation of data of the method of conditionally-probabilistic criteria (this is characteristic as a whole for the contemporary natural science and technology) can serve as the index of the occurring now qualitative change in the interpretation of data of

gravitational prospecting. Specifically, this approach will make it possible to draw and to together analyze scalene on their physical bases materials, in each specific case not very sharp and clear, but united under sameness places and the geologic history, whose separate aspects they reflect.

Actively is penetrated in practice of interpretation and will be further developed analysis of three-dimensional/space picture of distribution of anomalous fields, especially in connection with application of rapidly moving computer technology. Computers will find use, also, during the solution of the complex logical problems of interpretation.

Page 479.

Will be also subsequently continued occurring in recent years critical review of "canonical" models of geologic media, like model of laminated medium, essential refinement of latter in concept of laminar zonality of density and other physical properties. Increasing development will undergo the methods of the quantitative systematization of the virtually observed anomalies above the known geologic structures and the deposits of useful minerals. This will make it possible to quantitatively consider the degree of the conformity of the studied anomalies to the specific geologic forms.

Imperative attempts to increase depth of penetration of geologic conclusions/derivations, extracted via analysis of gravity anomalies,



DOC = 88020225

PAGE

~~28~~ 875

will be continued.

Development of enumerated questions, on our deep conviction, undoubtedly will increase role of gravitational prospecting and its value in general complex of geological-geophysical methods.

Page 480.

#### REFERENCES.

- B. A. Andreyev. Application of geophysical methods during the searches and prospecting of chromite deposits. Transactions of TsNIGRI, Iss. 100, 1937.
- B. A. Andreyev. On calculation of the network/grid of observations with the gravitation prospecting works. Materials of TsNIGRI, Geophysics, Coll. 5, 1938.
- B. A. Andreyev. Goals of exploration geophysics, connected with the Dirichlet's problem. Materials of the AUGRI, Geophysics, Coll. 13, 1948.
- B. A. Andreyev. The question about the geologic interpretation of the results of gravitation prospecting works on the deposits of the type KMA. Prospecting material resources, No 6, 1949.
- B. A. Andreyev. Two methods of determining the elements of the bedding of the steep beds from magnetic anomalies. Transactions of VIRG, Iss. 2, Gosgeolizdat [State Publishing House of Geological Literature], 1950a.
- B. A. Andreyev. About the applicability of the formulas of two-dimensional problem with the interpretation of gravitational and magnetic anomalies. Transactions of VIRG, Iss. 3, 1950b.
- B. A. Andreyev. Simple method of calculating the geophysical anomalies at the height. Transactions of VIRG, Iss. 3, 1950c.
- B. A. Andreyev. Calculations of spatial distribution of potential

fields and their utilization in exploration geophysics. Izv. of the AS USSR, ser. of geogr. and geophysics, No 1, 1947 (P I); No 3, 1949 (P II); the ser. of geophysics, No 2, 1952 (P III); No 1, 1954 (P IV).

B. A. Andreyev. Determination of the depth of the surface of crystalline basement from the magnetic anomalies. Applied geophysics, Iss. 13, Gostoptekhizdat [ T T [ T - State Scientific and Technical Publishing House of Petroleum and Mineral Fuel Literature], 1955.

B. A. Andreyev. On the calculation of the vertical gradient of force of gravity. Coll. applied geophysics, Iss. 17, Gostoptekhizdat, 1957a.

B. A. Andreyev. Laminar zonality of the physical properties of sedimentary rocks and its bond with the structures of platform regions. Sov. geology, Coll. 61, Gosgeoltekhizdat [State Scientific and Technical Publishing House For Literature on Geology, Geodesy, and the Conservation of Mineral Resources], 1957b.

B. A. Andreyev. Gravity anomalies and the thickness of the Earth's crust of continental regions. DAN USSR, Vol. 119, No 2, 1958a.

B. A. Andreyev. Gravity anomalies and structural-metallic zones. DAN USSR, Vol. 121, No 6, 1958b.

B. A. Andreyev. On the prospects for the development of structural geophysics. Sov. geology No 6, 1959a.

Page 481.

B. A. Andreyev. Relationship/ratio between the gravity anomalies and the structural relief in the case of several interfaces of density. DAN USSR, Vol. 124, No 2, 1959b.

B. A. Andreyev. Characteristic and classification of the geologic goals, solved by the method of gravitational prospecting. Collection of production-tech. information on the geophysical instrument manufacture, Iss. 3, 1959c.

B. A. Andreyev. Geophysical methods in regional structural geology. Gosgeoltekhizdat, 1960a.

B. A. Andreyev. Development and introduction of the methods of processing/treatment and interpretation of data of gravitational prospecting. Coll. geophysical prospecting, Iss. 2, Gostoptekhizdat, 1960b.

B. A. Andreyev. The gravity anomalies of Faye and isostasy. DAN USSR, Vol. 139, No 1, 1961.

B. A. Andreyev, V. P. Boronin, S. V. Krylov. Geophysical special features of the oil bearing structures of Volga-Ural province. Sov. geology, No 7, 1961.

K. N. Ansimov. Template  $\mu$  for the bodies of arbitrary form. Transactions of Irkutsk mining and smelting institute, ser. general, Iss. 11, 1956.

V. I. Antipov. Geologic results of geophysical works in Ciscarpathia and in the limits of the southwestern outskirts of Russian platform. Questions of searches, prospecting and extracting of oil and gas on the territory of UkrSSR [- Ukrainian SSR] (collection of articles), Gostoptekhizdat, 1960.

A. D. Arkhangel'skiy. On the structure of Russian platform. Bull. Moscow Is. of exper. nature, section of geology, Vol. XVIII (3-4), 1940.

- A. K. Auzin. Some results of geophysical works on the copperpolymetal deposit in central Kazakhstan. In the book: State and the long term for the development of exploration geophysics. Gostoptekhizdat, 1961.
- M. S. Bartlett. Theory of random functions. M., IL., 1958.
- D. Barton. Calculations with the interpretation of observations with the torsion balance of Eotvos. Russ. translation. Ser. tech.-inf., Coll. TsISON of Glavneft' [Main Administration of the Petroleum Industry], Iss. 15, Baku-Moscow, 1935.
- V. V. Belousov. Basic questions of geotectonics. Gosgeolizdat, 1953.
- I. S. Berzon. Gravitational field above the vertical step/stage in the case of a linear change in the difference in the densities with the depth. Transactions of VKGR, Iss. 13 (20), 1938.
- F. Birch, D. Scheurer and G. Spicer. Handbook for the geologists on the physical constants. IL, 1949.
- M. S. Vykova and D. N. Kazanli. Bond of the structure of the gravimetric field of central Kazakhstan with the Early Hercynian lithofacies regions. Izv. AN of the Kazakh USSR, ser. geolog., Iss. 2 (27), 1957.
- K. Ye. Veselov. Application of the second vertical derivative of the gravitational potential during the geologic interpretation of gravimetric photographing. Coll. applied geophysics, Iss. 11, Gostoptekhizdat, 1954.
- F. Vening-Meinesz. Gravimetric observations at sea. Geodezizdat [геодезия и - Publishing House of Geodetic and Cartographic Literature], 1940.

Page 482.

Questions of contemporary foreign tectonics (collection of articles). IL, 1960.

G. A. Gamburtsev. Geologic interpretation of gravitational and magnetic observations with the help of instruments for the mechanical calculations. Applied physics. Vol. V, Iss. 3-4, 1928.

G. A. Gamburtsev. Geologic interpretation of gravitational and magnetic observations with the help of instruments for the mechanical calculations (communication/report II). Applied physics, Vol. VI, Iss. 1, 1929.

G. A. Gamburtsev. Determination of excess or defect of subterranean masses on the basis of magnetic and gravitational observations. Applied physics, Vol. 7, Iss. 5 M., 1930.

G. A. Gamburtsev. Methods of the interpretation of gravitational observations. Applied geophysics, Iss. 1, ONTI, 1936.

G. A. Gamburtsev. Determination of the center of gravity of perturbing body from the gravitational observations. Izv. of the AS USSR, M., 1938.

I. S. Gelfand. Direct and inverse problems of the potential of attraction for the hemisphere. Sverdlovsk mountain institute, transactions and materials, Iss. V, 1940.

K. V. Gladkiy. Separation of summary gravitational fields as the process of frequency filtration. Coll. applied geophysics, Iss. 25, Gostoptekhizdat, 1960.

K. V. Gladkiy. Relationship/ratio between the averaging and analytical continuation into the upper half-space of gravity

anomalies. Izv. of VUZ [Institute of Higher Education], ser. geology and prospecting, No 5, 1961.

Yu. N. Godin. Regional geophysical investigations. Geology of oil, No 6, 1957.

Yu. N. Godin. Comprehensive geophysical investigations of the southeast of Russian platform. Geology of oil, No 5, 1958.

Yu. N. Godin. To a question about the searches for oil bearing structures. Coll. geophysical prospecting for oil and gas.

Gostoptekhizdat, 1959.

S. Goldman. Information theory. M., IL, 1957.

F. M. Holzman, B. T. Kalinina. Simple methods of frequency analysis and synthesis and their application to the solution of some geophysical problems. Coll. applied geophysics, Iss. 21, Gostoptekhizdat, 1958.

G. A. Greenberg. Questions of the mathematical theory of electric and magnetic phenomena. Ed. of the AS USSR, 1948.

V. L. Gul'nitskiy. Direct problem of the field of second normal derivative of vertical component of gravity force in the case of two-dimensional body with faces and other simpler bodies. Izv. of AN of Kav. SSR, ser. geolog., Iss. 1 (39), 1960.

R. M. Demenitskaya. Planetary structures of the earth's crust and their representation in anomalies of Bouguer. Sov. geology, No 6, 1958.

R. M. Demenitskaya. The basic features of the structure of crust of the Earth according to geophysical data. Gostoptekhizdat, 1961.

G. Jeffreys. Earth, its origin, history and structure. IL, 1960.

Page 483.

V. A. Ditkin and A. P. Prudnikov. Integral transforms and operational calculus. Fizmatgiz, 1961.

G. N. Duboshin. Theory of attraction. Fizmatgiz, 1961.

L. N. Yelanskiy, S. V. Pavel'yev. On the third vertical derivatives of the potential of the physical fields of the Earth. Coll. applied geophysics, Iss. 24. Gostoptekhizdat, 1960.

N. Ye. Zhukovskiy. Mechanics. GTTI, 1950.

A. I. Zaborovskiy. Methodology of the interpretation of magnetic and gravity anomalies. Transactions of MGRI, Vol. XXVIII, 1955.

A. A. Zamorev. On the determination of derivatives and relationships/ratios between the moments/torques of the perturbing masses from the derivative, assigned on the plane. Izv. of the AS USSR, ser. geograph. and geophys., No 3, 1939.

A. A. Zamorev. Investigation of the two-dimensional inverse problem of potential. Izv. of the AS USSR, ser. of geogr. and geophysics, No 4-5, 1941.

I. K. Zerchaninov. On the transformation of platform type structures in the process of their formation and reflection of this process on the beds of oil confined to them. Oil economy, No 12, 1953.

N. I. Idel'son. Theory of potential. ONTI, 1936.

A. A. Ivanov. Bases of geology and the methodology of searches, prospecting and evaluating the deposits of salts. Gosgeolizdat, 1953.

V. K. Ivanov. Distribution of the special features of potential and three-dimensional/space analog of Polya's theorem. Mathematical collection, 40 (82), No 3, 1956.



D. N. Kazanli, A. A. Popov, A. I. Antonenko. Deep seismic sounding in central Kazakhstan. Messenger of AN of the Kazakh USSR, No 4, (169), 1959.

A. P. Kazanskiy. On the determination of the elements of the bedding of useful minerals according to the data of gravimetry. Izv. of the AS USSR, ser. of geogr. and geophysics, No 2-3, 1938a.

A. P. Kazanskiy. Determination of the basic elements of the bed of large extent into the depth according to the data of gravimetry and magnetometry. Izv. of the AS USSR, ser. geograph., and geophysics, No 2-3, 1938b.

V. P. Kazarinov. Formations of Mesozoic and cenozoic of western-Siberian lowland in connection with the searches for oil and gas. Sov. Geology, No 12, 1958.

V. A. Kazinskiy. Bases of the theory of subterranean gravimetry. DAN USSR, Vol. 109, No 5, 1956.

V. N. Kalashnikov. Application of theory of random functions during the solution of some problems of gravitational prospecting.

Transactions of MINKh and GP im. academician Gubkina, Iss. 25, 1959.

O. A. Kalinina. Reference data about density and porosity of the rocks and experiment of their geologic interpretation. Geology and the oil content of Timan-Pechersk region. Transactions of VNIGRI

[ - All-Union Petroleum Scientific Research Institute of Geological Exploration (Moscow) ], Iss. 133, Gostoptekhizdat, 1959.

L. V. Kantorovich, V. I. Krylov. The approximation methods of the highest analysis GITTL, 1st ed., 1941; 2nd ed., 1947; 3rd Izv., 1952.

- G. I. Karatayev. Calculation of the components of the potential of attraction for horizontal triangular prism of infinite course/strike. Materials on geology, hydrogeology, geophysics and useful minerals of Western Siberia. Transactions of SNIIGGIMS, Iss. 9, 1960.
- Ye. D. Karyakin. Dependence between the gravity anomalies of Bouguer and the thickness of the Earth's crust in the region of Atlantic Ocean. DAN USSR, 129, No 6, 1959.
- K. A. Kirillov. Method of accelerated calculation  $V_x$  and  $V_y$  in the case of sloping layer. Izv. IPG, Iss. 2, 1926.
- A. I. Kitov, N. A. Krinitskiy. Electronic digital computers and programming. M., State Publishing House of physico-mathematical lit., 1961.
- I. G. Klushin. On the liberation/precipitation of the geophysical anomalies smaller than the root-mean-square error of measurement. Izv. of the AS USSR, ser. of geophysics, No 2, 1959.
- I. G. Klushin. On transformations of gravity anomalies. Coll. applied geophysics, Iss. 24, Gostoptekhizdat, 1960.
- I. G. Klushin, Yu. I. Nikol'skiy. Separation of gravitational field to regional and local components with the help of the computer. Coll. applied geophysics, iss. 22, Gostoptekhizdat, 1959.
- I. G. Klushin and I. N. Tolstikhin. Liberation/precipitation of linear tectonic dislocations on the geophysical maps/charts. Geology and geophysics, No 6, Izd. SO AN SSSR [ - Siberian Department of the Academy of Sciences of the USSR], 1961.
- A. N. Kolmogorov. Interpolation and the extrapolating of stationary

random sequences. Izv. of the AS USSR, ser. of math., No 5, 1941.  
N. G. Komardintseva, YU. A. Pryakyuina, I. A. Konyukhov. Study of fissure collectors/receptacles and their value for the searches for oil and gas in Daghestan. Prospecting and the conservation of mineral resources, No 3, 1961.

V. Yu. Kondrachuk. On the density of the crust of erosion of Volynskiy gabbro-labradorite mass. Transactions of the institute of geolog. sciences of the AS USSR, ser. of geophysics, Iss. 2, 1958.  
V. A. Kotelnikov. On the capacity of "ether/ester" and wire in the electrical communication. Materials for I All-Union congress, VEK, 1933.

B. V. Kotlyarevskiy. Calculation of templates and tables, which are used with the interpretation of gravimetric observations.  
Transactions of VKGR, Iss. 3. GONTI, 1938.

B. V. Kotlyarevskiy. Utilization of vertical gradients of gravity force for the geologic interpretation. Exploration and trade geophysics, Iss. 21, 1958.

R. S. Krasovitskaya. Geologic efficiency of regional gravimetric works on KMA. Coll. materials on geology and useful minerals of the central regions of the European USSR Iss. 1, 1958.

P. N. Kropotkin, Ye. N. Lyustikh, N. N. Povalo-Shvayko. Anomalies of gravitational force on the continents and the oceans and their value for geotectonics. Ed. of MGU, 1958.

Page 485.

Z. A. Krutikhovskaya, G. K. Kuzhelov. Application of geophysical

methods for studying the iron-ore formation of Ukrainian crystalline shield. Gosgeoltekhizdat, 1960.

A. N. Krylov. Lectures about the approximate calculations. M., GITTL, 1954.

Course of physics edited by academician N. D. Papaleksi. Vol. I and II. Gostoptekhizdat, 1948.

O. K. Litvinenko. Application of computers for the separation of the local and regional anomalies. Coll. applied geophysics, Iss. 25. Gostoptekhizdat, 1960.

A. A. Logachev. Course of magnetic prospecting, Gosgeolizdat, 1951.

A. A. Logachev. Methodic management/manual on aeromagnetic photographing. M., Gosgeoltekhizdat, 1955.

P. I. Lukavchenko. Table and nomogram for calculating the corrections of gravitational force for area relief during the photographing with the gravimeters. Gostoptekhizdat, 1951.

Ye. N. Lyustikh. Isostasy and isostatic hypotheses. Transactions of the geophysical institute of the AS USSR, No 38 (165), 1957.

Ye. N. Lyustikh. Selection of the reduction of gravitational force in connection with the solution of geologic questions. Izv. of the AS USSR, ser. geology, No 4, 1958.

V. A. Magnitskiy. Bases of physics of the Earth. Geodezizdat, 1953.

N. R. Malkin. Dependence between the gradients of Newtonian potential on the plane in application to the investigation of gravity anomalies. Izv. of the AS USSR, VII, series of section of physico-mathematical sciences, No 8, 1930.

N. R. Malkin. Integrators of gravitational force on the assigned in

the horizontal relief of the perturbing masses. DAN USSR, series A, No 13, 1932.

N. R. Malkin. On a change in the elements of terrestrial magnetism with the height. Transactions GGO, Vol. I (No. 3). Ed. Main geophysical observatory, 1934.

N. R. Malkin. On the determination of the vertical derivative of gravity force from the observations with the torsion balance. Astronomical journal, Vol. XIII, Iss. 5, 1936.

A. K. Malovichko. On the interpretation of gravimetric observations in connection with the searches for the structures, promising to the oil and gas. Coll. applied geophysics, Iss. 13. Gostoptekhizdat, 1955.

A. K. Malovichko. Methods of the analogous continuation of the anomalies of the force of gravity and their application to the goals of gravitational prospecting. Gostoptekhizdat, 1956.

A. K. Malovichko, O. L. Tarunina. To the methodology of the development/detection of the anomalous fields, commensurate with the observation errors. Coll. geophysical prospecting, No 4, Gostoptekhizdat, 1961.

G. D. Managadze. Interpretation of the anomaly of gravitational force above the vertical step with the help of the variation function. Communications/reports of AN of Gruz. SSR, Vol. XX, No 6, 1958.

*Page 486*  
G. D. Managadze. Interpretation of the variation anomaly of gravitational force above the horizontal circular cylinder of infinite course/strike. Transactions of Tbilisi State university, Vol. 68, 1959a.

G. D. Managadze. To the determination of the elements of the bedding of vertical step by curve  $\Delta g$ . Exploration and trade geophysics, Iss. 33, 1959b.

G. D. Managadze. On one analytical method of solving the inverse problem of gravimetry. Transactions of Tbilisi State university. vol. 68, 1959c.

G. D. Managadze. On the graphic method of interpretation of the variation anomaly of gravitational force. Transactions of Tbilisi State university, Vol. 68, 1959d.

Sh. Ye. Mikeladze. Numerical methods of mathematical analysis. M., GITTL, 1953.

D. S. Mikov. Atlas of theoretical curves for interpretation of magnetic and gravity anomalies. Gosgeoltekhizdat, 1956.

A. G. Mileschina. On the study of susceptibility to cracking in carbonate type rocks. Geochemical methods of the searches for oil and gas, Iss. 1, 1953.

A. A. Mikhaylov. Course of gravimetry and the theory of the figure of Earth. M., 1939.

F. M. Morse, D. Ye. Kimbell. Operations research (translation). Soviet radio, 1956.

F. S. Moiseyenko. Some lines of the deep structure of central Kazakhstan and the arrangement/position of ore deposits. DAN USSR, 127, No 5, 1959.

Ye. A. Mudretsova. Determination of the elements of the bedding of the steep bed by the curve of anomaly of gravitational force. Prospecting and the conservation of mineral resources, No 5, 1956.

Ye. A. Mudretsova. To the interpretation of the anomalies of gravitational force in the subterranean gravimetric measurements. Transactions of MGRI, Vol. 36, 1958.

A. A. Nepomnyashchikh. Logarithmic gravitational templates. Izv. of the AS USSR, ser. of geophysics, No 1, 1952.

A. A. Nepomnyashchikh. Study of form and sizes/dimensions of Kempersay ultrabasic mass. Sov. geology, No 9, 1959.

L. Ya. Nesterov. Physical properties of sandstone, limestone and slates. Materials of AUGRI, geophysics, Coll. 9, 1940.

L. Ya. Nesterov and M. A. Nesterova. Comparative study of some physical properties of the igneous rocks of north-eastern Azov region and Karelia. Materials of the AUGRI, geophysics, Coll. 9, 1940.

P. A. Nikifor. Physical basis of the gravitational method of mountain prospecting. Izv. IPG, Iss. 1, 1925 and Iss. 2, 1926.

Yu. I. Nikol'skiy. Some questions of the methodology of the interpretation of gravity anomalies in the limits of the geologically closed territories of the west of Central Asia. Coll. problems of the oil and gas-bearing capacity of Central Asia, Iss. 1, Gostoptekhizdat, 1960.

P. S. Novikov. On the uniqueness of the solution of the inverse problem of potential. DAN USSR, XVII, No 3, 1938.

B. V. Numerov. Theoretical bases of the application of gravitational methods in geology. Effect of external masses on the gravitational observations in the case of infinite course/strike. Transactions of GGRU, Iss. 36, 1931.

M. L. Ozerskaya. Experiment of the laboratory of the elastic

properties of rocks. Applied geophysics, Iss. 12, Gostoptekhhizdat, 1955.

Page 487.

M. L. Ozerskaya. Physical properties of rocks of crystalline basement. Applied geophysics, Iss. 13. Gostoptekhhizdat, 1955.

A. P. Ochkur. Logging of density. Coll. Questions of ore geophysics. Gosgeoltekhizdat, 1957.

N. N. Pariyskiy. Vertical component of the attraction of hyperbolic dome. Transactions of the geophysical institute of the AS USSR, No 12, 1950.

Ye. N. Permyakov. Tectonic susceptibility to cracking of Russian platform. Ed. MOIP, 1949.

B. D. Poletayev. Determination of the densities of the rocks by observations with the gravimeter in the mines/shafts. Prospecting and the conservation of mineral resources, No 2, 1954.

I. A. Poletayev. Signal (about some basic concepts of cybernetics). Soviet radio, 1958.

E. A. Prozorovich. To a question about the factors of the consolidation of sedimentary rocks. Transactions of the Azerb. scientific-research institute for the extraction of oil, Iss. IV, 1956.

N. I. Puzyrev. Interpretation of the data of seismic prospecting by the method of reflected waves. Gostoptekhhizdat, 1959.

O. M. Raspopov. Calculation of the vertical gradient of gravity force according to the known distribution of the anomalies of



gravitational force on the surface of any form. Sci. W. of LGU, No 278, 1959.

G. Renbou. Interpretation of readings/indications of torsion balance. Central office of petroleum technical information VNTS (TsBNTI [- Central Office of Scientific and Technical Information]). Foreign petroleum technology, Iss. 145, 1934.

G. Reykh. Geologic bases of applied geophysics. Russian translation. Applied geophysics, Iss. 1, Ed. by G. A. Gamburtsev, ONTI, 1936.

L. N. Rozanov. On the bond of the densities of rocks with tectonics of Buguruslan region. Applied geophysics, Iss. 3. Gostoptekhizdat, 1947.

U. Ross-Ashby. Introduction to cybernetics. IL, 1959.

N. B. Sazhina. Thickness of the Earth's crust and its bond with the relief and the anomalies of gravitational force. Soviet geology, No 8, 1962.

F. A. Sludskiy. On the investigations of the local anomalies of the force of gravity and terrestrial magnetism. Izv. Russ. geogr. Is., Vol. XXXII, 1896.

V. I. Smirnov. Geologic bases of searches and prospectings of ore deposits. Ed. of MGU, 1957.

V. I. Smirnov. Course of higher mathematics. Vol. I-V, GTTI, 1960-1961.

Contemporary mathematics for the engineers. IL, 1958.

State and the prospect for the development of exploration geophysics. Materials of scientific-technical conference. Edited by V. V.

Fedynskiy. Gostoptekhizdat, 1961.

L. V. Sorokin. Gravimetry and gravimetric prospecting. Gostoptekhizdat, 1953.

Handbook of geophysics. Vol. 1. Gostoptekhizdat, 1960.

V. N. Strakhov. On the analytical continuation of two-dimensional magnetic fields. DAN USSR, Vol. 126, Iss. 5, 1959.

Page 488.

V. N. Strakhov. Experiment of interpretation of the magnetic anomalies of KMA by the construction of isolines  $\Delta Z$  in the vertical plane. Applied geophysics, Iss. 27. Gostoptekhizdat, 1960.

S. I. Subbotin. Geologic interpretation of this geophysical investigations in the western regions of Ukrainian SSR. Transactions of scientific-geologic conference on oil, ozocerite and combustible gases of Ukrainian SSR. Ed. of AS of Ukr. SSR, 1949.

S. I. Subbotin. Some results of studying the density of the rocks of Ukrainian crystalline massif. Scientific entries of L'vov polytech institute, Iss. XVI, 1949.

S. I. Subbotin. On the bond of the anomalies of gravitational force with the vertical motions of the earth's crust. Izv. of the AS USSR, ser. geophysics No 4, 1955.

D. B. Tal'virskiy, Ye. M. Khakhalev. Structure of the surface of pre-Jurassic basement in the lower current r. Yenisey according to the data of seismic survey. Geology and geophysics, No 6. Ed. of SO AN SSSR, 1961.

A. G. Tarkhova, A. A. Sidorov. On mathematical processing of geophysical data. Izv. of the AS USSR, ser. geophysics No. 10, 1960.

P. M. Tatorinov, A. G. Betekhtin. Course of the deposits of useful minerals. Gostoptekhizdat, 1946.

Tectonic map/chart of the USSR scale 1:4000000 for the schools of higher learning. Editor in chief academician N. S. Shatskiy. The main administration of geodesy and cartography with the Council of Ministers of the USSR, institute of geolog. sciences of the AS USSR M., 1952.

N. A. Tuyezova, D. F. Umantsev. Some laws governing the distribution of the physical properties of the Mesocenozoic depositions of the west of Siberian lowland. State and the prospect for the development of exploration geophysics (collection of reports). Gostoptekhizdat, 1961.

K. F. Tyapkin. On the correction of the results of variometric observations under the conditions of sheet type deposits due to the effect of the finiteness of beds. Izv. DGI, Vol. 36. Dnepropetrovsk, 1958.

K. F. Tyapkin. Templates for calculation  $\Delta g$  and  $\Delta H$ , caused by finite on the course/strike cylindrical bodies, Kiev, 1959.

K. F. Tyapkin. Interpretation of the gravity anomalies, caused by finite on the course/strike geologic objects. Part I. Gosgeoltekhizdat, 1961.

E. Whittaker and G. Robinson. Mathematical processing of the results of observations. ONTI, 1935.

D. F. Umantsev. Density characteristic of the geologic section/cut of the Mesocenozoic of the western part of the western-Siberian lowland. Applied geophysics, Iss. 18. Gostoptekhizdat, 1958.

D. G. Uspenskiy. Ways of the development of the gravitational method of searches and prospecting the ore deposits. Sov. geology, No 2, 1958.

D. L. Uerzel and G. L. Sherbet. Interpretation of the anomaly of gravitational force on the basis of the standard columns of the earth's crust for the oceans and the continents. Coll. The earth's crust. IL, 1957.

Page 489.

A. Sh. Faytel'son. Some positions of the geologic interpretation of the results of gravitation prospecting. Exploration and trade geophysics, Iss. 8. Gostoptekhizdat, 1954.

V. V. Fedynskiy. Geophysical prospecting for oil and gas in Soviet Union. The IV international petroleum congress. Vol. II. Gostoptekhizdat, 1956.

E. E. Fotiadi. Geologic structure of Russian platform according to the data of regional geophysical studies and supporting/reference drilling. Tr. of VNIIGeofiziki, Iss. IV, Gostoptekhizdat, 1958.

E. E. Fotiadi. The basic features of the tectonic structure of Siberia and Far East in light of the regional geological and geophysical investigations. Geology and geophysics, No 10, Novosibirsk, 1961.

N. I. Khalevin. Structure of Urals in light of geophysical data. Sov. geology, No 12, 1960.

L. A. Khalfin. Informational theory of the interpretation of geophysical investigations. DAN USSR, Vol. 122, No 6, 1958.

Z. Khammer. Contemporary methods of the interpretation of the materials of gravimetric and magnetic prospectings. International oil congress, IV session, Vol. II, Geophysical methods of prospecting. Gostoptezizdat, 1956.

A. A. Charkevich. Theoretical bases of radio communication. GTTI, 1957.

F. I. Khat'yanov. Experiment of the liberation/precipitation of regional and local gravity anomalies in the Ural downwarp/trough. News of petroleum technology, No 2, 1960.

F. I. Khat'yanov, A. V. Amirova, Z. S. Ivanova. Laminar zonality of the speed of seismic waves within the limits of some oil bearing platform structures of Bashkirya. Sov. geology, No 3, 1961.

F. I. Khat'yanov and S. S. Nasyrov. Methodology of searches for gas and petroleum-bearing structures in Bashkir-Orenburg Ural region. Ufa, 1960.

I. O. Tsimel'zon. On nature of the local anomalies of the force of gravity of Apsheronsk peninsula. Applied geophysics, Iss. 14, Gostoptekhizdat, 1956.

P. L. Chebyshev. Theory of probability. Ed. of the AS USSR, 1936.

S. V. Shalayev. On the quantitative geologic interpretation of complex magnetic anomalies in the electronic digital computers. Coll. Applied geophysics, Iss. 31. Gostotekhizdat, 1961.

S. V. Shalayev. Experiment of the calculation of potential function in the lower half-plane in terms of its values, measured on the surface of the Earth. DAN USSR, Vol. 117, No 3, 1957.

S. V. Shalayev. Application in geophysics of the analytical

continuation of potential function into the lower half-plane. W. of LGI, Vol. XXXVI, Iss. 2, Geology, 1959.

S. V. Shalayev. Application of complex variable functions during the geologic interpretation of gravitational and magnetic data. Tr. of the institute of geology and geophysics of SO AN SSSR, questions of prospecting geophysics, Iss. 1, 1960.

Page 490.

O. A. Shvank. Calculation of the first and second vertical derivatives of anomalies of gravitational force. Coll. applied geophysics, Iss. 27. Gostoptekhizdat, 1960a.

O. A. Shvank. Determination of the character of geologic fault according to gravimetric data. Exploration and trade geophysics, Iss. 36, Gostoptekhizdat, 1960b.

O. A. Shvank and Ye. N. Lyustikh. Interpretation of gravimetric observations. Gostoptekhizdat, 1947.

A. S. Shirokov, V. I. Fedyuk. On the applications of geophysical methods during prospecting of ore deposits. Prospecting and the conservation of mineral resources, No 3, 1960.

O. Yu. Schmidt. Mathematical determination of heavy subterranean masses from the observations by variometer of Eotvos'. Transactions of OKKMA, Iss. VI, GIZ, 1925.

S. S. Schulz and Ye. P. Bruns. Structural-facies analysis of the separate sedimentary folds. Questions of geology of Asia, Vol. II. Ed. of the AS USSR, 1955.

G. N. Shcherb. To the problem of rare-metal belts/zones. Laws

governing the arrangement/position of useful minerals (collection of articles). Vol. 3. Izd. of the AS USSR, 1960.

Eczh and Laby. Bases/bases and the methods of geophysical prospecting. Gravimetric methods. Translation of duplicating machine. Ed. BITOR TsNIGRI, 1932.

R. Eotvos. On the geodetic works in Hungary, in particular about the observations with the torsion balance. Appendix to part XIV, W. of VTP, Spb., 1912.

A. A. Yun'kov. Determination of the depths of upper and lower bound, slope angle and excess density of oblique step/stage according to the observations with the gravitational variometer. Transactions of Sverdlovsk mining institute, Iss. 3, 1937.

A. A. Yun'kov. Searches for the chromite by the method of gravimetry. ONTI, 1937.

A. A. Yun'kov. Determination of depths, width and excess of the density of infinitely long horizontal beam with the rectangular cross section from the observations with the gravitational variometer. Sverdlovsk mining institute, transactions and materials, Iss. VI, 1940.

A. A. Yun'kov. Determination of depth and elements of the bedding of anticline. Izv. Dnepropetrovsk mining institute, Iss. 36, 1958.

A. A. Yun'kov, N. L. Afanas'yev, N. A. Fedorova, N. K. Stupak, K. F. Tyapkin, V. P. Telezhenko. Collection of articles. Proceedings of Dnepropetrovsk mining institute, Vol. XXII. Ugletekhizdat [глетехиздат - State Scientific and Technical Publishing House of Literature on the Coal Industry], 1952.

A. A. Yun'kov, N. L. Afanas'yev, N. A. Fedorova. Interpretation of anomalies above contacts and faults: 1)  $\Delta g$ ; 2)  $V_{xx}$  and  $H$ ; 3)  $V_{\Delta}$ ,  $V_{\Sigma}$ . (three albums). Gostoptekhizdat, 1961.

A. Ya. Jaros. Solution of direct problem for the anticlinal fold, covered with rocks with the variable/alternating density. Theory and the practice of the interpretation of geophysical anomalies (collection of articles). Gosgeoltekhizdat, 1951.

A. Ya. Jaros. Detailed gravitational prospecting in Urals. State and the prospect for the development of exploration geophysics. Gostoptekhizdat, 1961.

A. Ya. Jaros, K. N. Anisimov, A. B. Polyakov. Experiment of the application of gravitational prospecting for studying deep horizons/levels of pyritic deposit. Transactions of Sverdlovsk mining institute, Iss. XXX, Gostoptekhizdat 1957.



## Page 491.

Barton D. C. Lost Hills, California — an antiklinal minimum. *Geophysical case histories*. Soc. Expl. Geophys., vol. 1, 1948.

Bode H. W., Shannon C. E. A simplified derivation of linear least square smoothing and prediction theory. *PIRE*, vol. 38, No 4, 1950.

Bott M. H. P., Smith R. A. The estimation of the limiting depth of gravitating bodies. *Geophys. prospecting*, vol. 6, No 1, 1958.

Celmius A. Direkte Verfahren zur Auswertung von Schweremessungen bei Zweidimensionale Massenverteilung. *Geofis. pura et appl.*, v. 38 (1967/111).

Dean W. C. Frequency analysis for gravity and magnetic interpretation. *Geophys.*, vol. XXIII, No 1, 1958.

Elcius T. A. The second derivation method in gravity interpretation. *Geophys.*, vol. XVI, No 1, 1951.

Fajkiewicz Z. The use of cracovian computation in estimating the regional gravity. *Geophys.*, 24, No 3, 1959.

Goetz J. A gravity investigation of a sulfid deposit. *Geophys.*, 23, No 3, 1958.

Goguel J. Calcul de l'attraction d'un polygone horizontal de densite uniforme. *Geophys. prospecting*, vol. 9, No 1, 1961.

Griffin W. Residual gravity in theory and practice. *Geophys.*, vol XIV, No 1, 1949.

Heap W. O. Electronic calculators speed up analysis of complex geophysical computation. *Oil & Gas J.*, No 4, 1955.

Heiland C. A. *Geophysical exploration*. Prentice-Hall, N. Y., 1946.

Heiskanen W. A., Vening-Meinesz F. A. *The Earth and its gravity field*. McGraw-Hill Book Comp., 1958.

Henderson R. G. Comprehensive system of automatic computation in magnetic and gravity interpretation. *Geophys.*, vol. XXV, No 3, 1960.

Hughes D. The analytic basis of gravity interpretation. *Geophys.*, vol. VII, 1942.

Jung K. *Schwerkraftverfahren in der angewandten geophysic*. Leipzig, 1961.

Kogbetliantz E. G. Electronic computers aid geophysical interpretation. *Oil & Gas J.*, vol. 54, No 67, 1956.

Kornfeld J. A. Seismic problem in Williston basin. *Oil & Gas J.*, 52, No 50, 1954.

Milicoveanu D. Noi formule de calcul penetra interpreare masurator gravimetrice in prospectiunile geofizice. *Petrol si Gaze*, 8, No 12, 1958; 9, No 1, 1958.

Nettleton L. *Geophysical prospecting for oil*. N. Y., 1940.

Nordund N. *Differenrechnung*. Berlin, 1924.

Oldham C. H. The correlation between pre-cambrian rock densities and bouguer gravity anomalies near Parry Sound, Ontario. *Geophys.*, vol. XIX, No 1, 1954.

Pohly B. A. Gravity case history: Dawn No 156, Pool, Ontario. *Geophys.*, vol. 19, No 1, 1954.

Purson S. I. Quantity interpretation of gravity meters surveys. *The oil weekly*, vol. 117, No 7, 1945.

Page 492.

Rosenbach O. A contribution to the computation of the second derivation from gravity data. *Geophys.*, vol. XVIII, No 1, 1953.

Roy A., Burman S. D. Application of relaxation method to upward continuation of gravity and magnetic data. *Geophys. pura et appl.*, 45, No 1, 1960.

Saxov S., Nygaard K. Residual anomalies and depth estimation. *Geophys.*, vol. XVIII, No 4, 1953.

Siebert A. A mechanical integrator for the computation of gravity anomalies. *Geophys.*, No 4, 1942.

Soliani L. Considerazioni interpretative sopra un rilievo gravimetrico. *Rivista geofis. appl.*, anno XV, No 2, 1954.

Spencer L. and Peters J. Geophysical case history of the Magnolia field, Columbia county, Arkansas. *Geophys. case histories.*, vol. 1, Publ. Soc. expl. geophys., 1948.

Steinhard J. S., Wollard G. P. Linear analysis of the results of explosion seismic measurements on the continents. *J. geophys. res.*, vol. 66, No 8, 1961.

Talvani M., Fasing M. Rapid computation of gravitational attraction of three-dimensional bodies of arbitrary shape. *Geophys.*, vol. XXV, No 1, 1960.

Talvani M., Sutton G. H., Worzel L. A crustal section across the Puerto-Rico trench. *J. geophys. res.*, vol. 64, No 10, 1959.

Tsuboi Ch. Crustal structure in northern and middle California from gravity pendulum data. *Bull. Geol. soc. Amer.*, vol. 67, No 12, pt. 1, 1956.

Tsuboi Ch., Fuschida T. Relation between gravity values and corresponding subterranean mass distribution. *Bull. Earthquake Res. inst.*, Tokyo Imp. univ., 15, pt. 3, 1937.

Tsuboi Ch., Jitsukawa A., Tajima H. Gravity measurement along the lines of precise levels over whole Japan by means of a Worden gravimeter. *Proc. Japan Acad.*, vol. XXIX, No 6, 7, 9, 19, 1953.

Tsuboi Ch., Tomoda J. The relation between the Fourier series method and the  $\frac{g_{\text{po}}}{x}$  method for gravity interpretation. *J. phys. earth*, 6, No 1, 1958.

Vaick R. Bouguer corrections with varying surface density. *Geophys.*, vol. XXI, No 4, 1956.

Vaick R. and Walton G. Parentis oil field, France. *Geophys. case histories.* Vol. II. Publ. Soc. expl. geophys., 1956.

Wiener N. *The extrapolation, interpolation and smoothing of stationary series.* N. Y., 1949.

Wollard G. P. Transcontinental gravitational and magnetic profile on North America and its relation to geologic structure. *Bull. Geol. soc. Amer.*, 54, No 6, 1943.

Wollard G. P. Crustal structure from gravity and seismic measurements. *J. geophys. res.*, 64, No 10, 1959.

Zagorac Z. Contribution to the method of torsion balance surveying in underground. *Geophys.*, 18, No 2, 1953.

Pages 493-495.

No Typing.